Acta Ichthyologica et Piscatoria 54, 2024, 1–11 | DOI 10.3897/aiep.54.109601

ACTA
ICHTHYOLOGICA
ET PISCATORIA

Feeding habits of Pacific anchovy, *Engraulis japonicus* (Actinopterygii: Clupeiformes: Engraulidae), captured off the southern coasts of Korea

Seong Yong MOON[1], Heeyong KIM[2]

1 *South Sea Fisheries Research Institute, National Institute of Fisheries Science, Yeosu, Republic of Korea*
2 *Research and Development Planning Division, National Institute of Fisheries Science, Busan, Republic of Korea*

https://zoobank.org/B1EF93E0-61B6-441B-A4D3-79814B2C0BA5

Corresponding author: Heeyong Kim (heeyongkim@korea.kr)

Academic editor: Ken Longenecker ♦ **Received** 15 July 2023 ♦ **Accepted** 14 November 2023 ♦ **Published** 18 January 2024

Citation: Moon SY, Kim H (2024) Feeding habits of Pacific anchovy, *Engraulis japonicus* (Actinopterygii: Clupeiformes: Engraulidae), captured off the southern coasts of Korea. Acta Ichthyologica et Piscatoria 54: 1–11. https://doi.org/10.3897/aiep.54.109601

Abstract

Understanding the feeding ecology of anchovies in the southern waters of Korea is crucial for improving ecosystem management. However, to date, few studies have examined seasonal changes in the diet of Pacific anchovy, *Engraulis japonicus* Temminck et Schlegel, 1846, in Korean waters, with the majority of these focusing on the larval and adult stages. The presently reported study provides updates on the feeding habits of *E. japonicus* off the southern coast of Korea. We analyzed 347 individuals. One-way analysis of similarity was performed to evaluate the differences in diet composition among size classes and seasons of *E. japonicus*, and correspondence analysis was conducted using the matrix of the percentage by number (%N) data for prey with occurrence of less than 10% to determine the distribution of prey across all size classes and each season. The diet of *E. japonicus* was investigated according to season and four size classes. The fork length of these specimens ranged from 5.4 to 14.1 cm. A total of 55 prey taxa of varying sizes between 0.33 mm (diatom *Coscinodiscus* spp.) and 5.8 mm (fish larvae) were recorded. Anchovies were exclusively planktivorous, and copepods were the most common prey, comprising 82.1% of the identified food items and 84.3% of anchovy stomach contents analyzed. However, their occurrence and abundance varied according to season and Pacific anchovy size class. According to the percentage of the index of relative importance (%IRI), the most important prey items were the copepods *Calanus sinicus* (48.0%), *Paracalanus orientalis* (31.7%), bivalve larvae (5.8%), *Ditrichocorycaeus affinis* (4.2%), and calanoid copepods (2.4%). Analysis of similarities and similarity percentage analysis indicated that a distinct diet of Pacific anchovy in the southern waters of Korea is potentially driven by differences in hydrological conditions. Correspondence analysis revealed that anchovies had the most significant impact on the differences between size classes. The results deepen our understanding of prey species diversity and intraspecific food competition off the southern coast of Korea.

Keywords

copepods, diet, Pacific anchovy, southern waters of Korea

Introduction

The Pacific anchovy, *Engraulis japonicus* Temminck et Schlegel, 1846, is a widely distributed pelagic fish abundant in the coastal and offshore waters of the western North Pacific (Zenitani and Kimura 1997; Kim and Lo 2001; Wan and Bian 2012; Yamamoto et al. 2018). This anchovy is one of the commercially most important fish species present in Korean waters, where it is exploited using anchovy drag and offshore stow nets (Kim and Lo 2001). The total annual catch of *E. japonicus* was 209 102 to 250 106 tonnes from 2003 to 2013, and almost 187

849 tonnes from 2014 to 2021 from Korean waters (KOSIS 2023). The majority of the catch is taken from the southern coast of Korea, which occupies approximately 87% of Korean waters (KOSIS 2023). Pacific anchovies are an important intermediate link between zooplankton and higher-level fish species in marine food webs, and they are one of the main keystone species within the marine ecosystem (Tang et al. 2005; Wan and Bian 2012; Shin et al. 2021).

Studies on the feeding habits of fish may play a key role in understanding resource partitioning between and within species (Harmelin-Vivien et al. 1989; Wu et al. 2018), prey selection (Takasuka et al. 2003), predator–prey size relations (Scharf et al. 2000; Jin et al. 2010), distribution of feeding patterns with latitude (Pauly and Christensen 2000), ontogenetic diet shift (Jin et al. 2010), and habitat selection (Labropoulou et al. 1999; Zhang et al. 2007). They are also particularly important when establishing fishery management plans for exploited species that are important for their economic value (Lassalle et al. 2011; Bachiller and Irigoien 2015).

The fundamental publication on fish feeding was that by Hyslop (1980) who reviewed, summarized, and critically analyzed the methods used in studies on fish stomach contents. Hyslop (1980) divided the “objective” methods into four categories: 1) occurrence methods, 2) numerical methods, 3) volumetric methods, and 4) gravimetric methods. Among “subjective” methods he listed the index of relative importance (IRI).

The trophic ecology of *E. japonicus* has been studied to understand the functional ecology of the pelagic ecosystem (Ma et al. 2019). This is particularly subject to highly variable recruitment success, and therefore, environmental variability causes substantial stock fluctuations (Takasuka and Aoki 2006; Wang et al. 2021a). *Engraulis japonicus* is one of the most important small pelagic species in Korean waters, with respect to biomass and commercial interest (Kim and Lo 2001; Kim et al. 2005). The diet and recruitment of *E. japonicus* are affected by variations in the environmental processes governing plankton abundance (Uotani et al. 1978; Tanaka et al. 2006; Kim et al. 2013). However, most of these studies have been conducted in Japanese waters (Uotani et al. 1978; Aoki and Miyashita 2000; Islam and Tanaka 2009; Yasue et al. 2010) and the Yellow Sea (Wang et al. 2021b). To date, few studies have examined seasonal changes in the diet of *E. japonicus* in Korean waters, with most of these focusing on the larval (Park and Cha 1995; Kim et al. 2005; Yoo and Jeong 2016) and adult stages (Chang et al. 1980; Kim et al. 2013). *Engraulis japonicus* predominantly feeds on plankters, such as the diatoms such as *Coscinodiscus* spp. (Bacillariophyta) and copepods, such as *Calanus sinicus*, *Ditrichocorycaeus affinis*, and *Paracalanus orientalis* (= *Paracalanus parvus* sensu lato) along the southern coast of Korea (Kim et al. 2013). Understanding the feeding ecology of anchovies in the southern waters of Korea is crucial for improving ecosystem management.

Hence, in the presently reported study, the feeding habits of Pacific anchovy, *E. japonicus*, were studied in terms of size and seasonally in Korean waters. This is the first study to analyze annual dietary changes of Pacific anchovy off the southern coast of Korea. We aimed to provide feeding data of *E. japonicus* regarding the important ecological and economic role of pelagic fish. These data can contribute to the already emphasized need for the development of ecosystem-based fishery management.

Material and methods

Sample collection. The specimens of Pacific anchovy, *Engraulis japonicus*, were collected monthly from November 2020 to October 2021 using a set net, anchovy boat seine, and bottom trawl in the southern waters of Korea during daylight hours (Fig. 1; Table 1). The stomachs of 347 *E. japonicus* individuals were analyzed. The anchovies were measured to the nearest 0.1 cm (FL, fork length), and their stomachs were immediately preserved in 10% formalin. All stomach contents were washed out onto a Petri dish, and aliquots comprising 20~100% of the total volume of each pool were taken to be examined under the Olympus SZX10 (Tokyo, Japan) stereomicroscope at 100× magnification. The stomach contents were identified to the lowest feasible taxonomic level, and prey items were counted and measured under the stereomicroscope. All the prey items in the aliquots were counted and identified up

Table 1. Sampling information of Pacific anchovy, *Engraulis japonicus*, from the southern waters of Korea.

Date	Depth [m]	Fishing gear	Sample number	Sample size (FL) [cm]
27 Nov 2020	18	Anchovy boat seine	20	7.1–13.8
23 Dec 2020	23	Anchovy boat seine	30	5.4–9.2
12 Jan 2021	28	Anchovy boat seine	25	6.9–12.7
19 Feb 2021	20	Bottom trawl	30	5.5–13.0
23 Mar 2021	27	Anchovy boat seine	30	8.0–14.1
13 Apr 2021	17	Set net	30	7.7–11.4
21 May 2021	19	Set net	30	8.9–13.0
17 Jun 2021	16	Set net	30	7.4–11.5
29 Jul 2021	24	Anchovy boat seine	30	7.3–11.4
20 Aug 2021	16	Bottom trawl	30	6.2–10.8
9 Sep 2021	28	Anchovy boat seine	30	8.0–11.5
14 Oct 2021	15	Set net	32	9.6–11.2

FL = fork length.

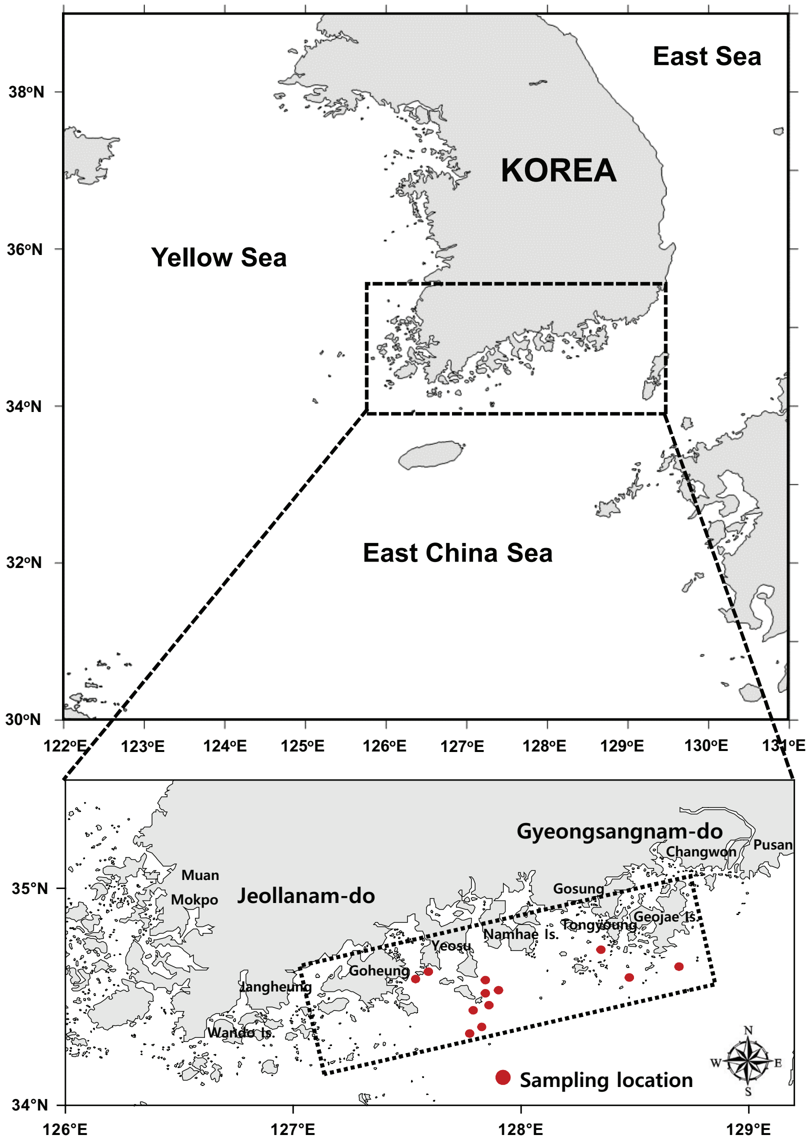

Figure 1. Map of the sampling area (dotted line) of the Pacific anchovy, *Engraulis japonicus*, in the southern waters of Korea. Note: East Sea is otherwise known as the Sea of Japan.

to the lowest possible taxa, and their widths and lengths were measured [µm], if distinguishable, using the software ImageJ (Abràmoff and Magalhães 2004). Prey dry weight (DW) [µg] was obtained from estimations by James (1987), Uye (1982), Pinchuk and Hopcroft (2007), and Borme et al. (2009). The diet was described using the relative contribution of a food item to total stomach content.

Feeding habits. To examine the ontogenetic variations in the feeding ecology of Pacific anchovy, individuals were divided into the following four FL classes

- <6 cm (group 1),
- 6.0–8.9 cm (group 2),
- 9.0–11.9 cm (group 3), and
- ≥12.0 cm (group 4).

The size groups were analyzed in accordance with the standard by establishing the maturing size of anchovies (Moon et al. 2022b) in 2-cm increments. The diet of *E. japonicus* was investigated according to season and the four size classes. The qualitative importance of each prey item in the *E. pacificus* diet was described using the relative frequency of occurrence (%F), the percentage by number (%N), and the percentage by (dry) weight %W_D (Hyslop 1980). We define the relative frequency of occurrence (%F) as the percentage of stomachs containing one or more individuals of a given food category; the percentage by number (%N)—as the percentage of the total individuals in all food categories; and the percentage by (dry) weight %W_D—as the percentage of the (dry) weight of total individuals in all food categories.

These indies were then integrated into the index of relative importance (IRI) modified by Borme et al. (2009) (based on Pinkas et al. 1971)

$$\mathrm{IRI} = (\%N + \%W_D) \times \%F$$

where %IRI$_i$ is the percentage of the index of relative importance, i is the number of a specific food category, and n is the total number of food categories.

For comparison, the IRI values calculated for each prey item were transformed to its percentage (%IRI) values using the following equation by Cortés (1999)

$$\%\,\text{IRI} = \text{IRI}_i / \sum_{i=1}^{n} \text{IRI}_i \times 100$$

To assess the feeding strategy of *E. japonicus*, we used the graphical analysis described by Amundsen et al. (1996). In mathematical terms, the prey-specific abundance is calculated as

$$P_i = 100\Sigma S_i \times \Sigma S_{ti}^{-1}$$

where P_i is equal to the prey-specific abundance of prey *i*, S_i is the weight of prey *i* in stomachs, and S_{ti} is the total weight of prey in the stomachs of predators that contain prey *i*.

Statistical analysis. One-way analysis of similarity (ANOSIM) was performed to evaluate the differences in diet composition among size classes and seasons of *E. japonicus*. Typifying and distinguishing the prey for each size class were performed using the similarity-percentages procedure (SIMPER). This procedure was established by the average contribution of each prey item to the similarity and dissimilarity among size classes and seasons. Correspondence analysis (CA) was conducted using the matrix of the percentage by number (%*N*) data for prey with an occurrence of less than 10% to determine the distribution of prey across all size classes and each season. Sea water temperatures in the southern sea of the Korean Peninsula show distinct seasonal patterns (Kim et al. 2011; Han and Lee 2020), so we analyzed data from winter (December to February), spring (March to May), summer (June to August), and autumn (September to November). PRIMER software package (Version 6.1.9) (Clarke and Warwick 2001) was used to perform cluster, SIMPER, and ANOSIM analyses. CA was performed using CANOCO software (Version 4.5).

Results

A total of 347 specimens of Pacific anchovy, *Engraulis japonicus*, measuring between 5.4 and 14.1 cm FL were examined for diet composition. Overall, 15.7% of stomachs were empty, and prey items included one phytoplankter, 50 crustaceans, one chaetognath, two mollusks, and two vertebrates (Table 2). The dominant zooplankton prey groups included calanoid copepods (%*F* = 59.1, %*N* = 60.0, %IRI = 82.8) and cyclopoid copepods (%*F* = 29.7, %*N* = 10.6, %IRI = 5.1). The abundant prey items were *Calanus sinicus* (%*F* = 19.9, %*N* = 30.8, %IRI = 48.0), *Paracalanus orientalis* (%*F* = 28.0, %*N* = 22.8, %IRI = 31.7), bivalve larvae (%*F* = 17.9, %*N* = 7.7, %IRI = 5.8), *Ditrichocorycaeus affinis* (%*F* = 14.1, %*N* = 7.5, %IRI = 4.2), other calanoid copepods (%*F* = 11.8, %*N* = 2.2, %IRI = 2.4), and copepods eggs (%*F* = 7.5, %*N* = 6.2, %IRI = 1.5).

Diet composition in relation to fish size and season. The diet composition for size classes concerning the cumulative percentage IRI is depicted in Fig. 2A. A total of 5 stomachs from the group with a fish length below 6 cm (FL) were examined, revealing 4 prey items. According to the %IRI, the most significant prey items in this group were diatoms *Coscinodiscus* spp. (44.3%), copepods *Ditrichocorycaeus affinis* (35.4%), and Harpacticoida (8.9%). For group 2 (6.0–8.9 cm FL), comprising 156 stomachs, 28 prey items were identified. The primary prey consisted of copepods *Paracalanus orientalis* (46.1%), *Ditrichocorycaeus* spp. (20.4%), *D. affinis* (11.7%), and other calanoid copepods (11.1%). Group 3 (9.0–11.9 cm FL) included 172 stomachs with 47 prey items. The dominant prey items were the copepods *Calanus sinicus* (44.9%), *P. orientalis* (42.9%), *D. affinis* (4.4%), and diatoms *Coscinodiscus* spp. (1.9%). Finally, in group 4 (≥12.0 cm FL), 14 stomachs were analyzed, and 17 prey items were found. The most important prey items were the copepods *P. orientalis* (43.3%) and *C. sinicus* (43.1%).

The variations in diet composition according to size class were determined using ANOSIM, which showed that the diets differed significantly in prey number between the size classes (Table 3). The SIMPER analysis showed that *P. orientalis*, bivalve larvae, *Ditrichocorycaeus* spp., *C. sinicus*, and *D. affinis* were the prey items that contributed the most to discriminating the size classes (Table 3).

A total of 90, 90, 82, and 85 stomachs from the spring, summer, autumn, and winter seasons, respectively, were analyzed (Fig. 2B). According to %IRI, the most important prey items in each season were the copepods *C. sinicus* (67.9%), *D. affinis* (16.0%), *P. orientalis* (10.3%), and the euphausiid *Euphausia pacifica* (3.8%) in spring; *C. sinicus* (37.8%), *Ditrichocorycaeus* spp. (11.7%), calanoid copepods (7.1%), and *D. affinis* (5.5%) in summer; *C. sinicus* (41.2%), *P. orientalis* (36.6%), *D. affinis* (4.7%), and copepod eggs (4.1%) in autumn; and *Coscinodiscus* spp. (48.7%), *C. sinicus* (18.7%), *P. orientalis* (9.8%), *Ditrichocorycaeus* spp. (6.6%), and bivalve larvae (3.9%) in winter. ANOSIM showed that there were no significant differences between the seasons for stomach content (Table 4). According to SIMPER analysis, the stomach contents that contributed the most to the diet were *C. sinicus*, copepods eggs, *D. affinis*, *P. orientalis*, and *Coscinodiscus* spp.

The relative prey importance of *E. japonicus* is graphically represented in Fig. 3, where prey-specific abundance (P_i) is plotted against the frequency of occurrence. *Calanus sinicus* is situated in the upper right corner of the diagram for the spring, summer, and autumn seasons. It constitutes the dominant prey item, making up more than

Table 2. Stomach contents (and associated parameters) of Pacific anchovy, *Engraulis japonicus*, from the southern waters of Korea.

Taxon	Prey items	%*F*	%*N*	IRI	%IRI
Bacillariophyta	*Coscinodiscus* spp.	7.5	7.5	56.4	1.8
Cladocera	*Pseudevadne* spp.	0.9	0.0	0.0	1.8
	Pseudevadne tergestina	0.3	0.0	0.0	0.0
	Podon polyphemoides	0.6	0.0	0.0	0.0
Copepoda	Total	71.5	82.1	11 005.7	98.1
Calanoida	Total	59.1	60.0	7654.4	82.8
	Acartia omorii	0.9	0.1	0.1	0.0
	Acartia pacifica	0.9	0.2	0.2	0.0
	Acartia erythraea	0.9	0.8	1.2	0.0
	Acartia sp.	2.9	0.5	1.7	0.1
	Calanus sinicus	19.9	30.8	1648.8	48.0
	Candacia bipinata	1.2	0.5	3.8	0.1
	Candacia sp.	0.3	0.0	0.0	0.0
	Centropagus dorsispinatus	4.3	0.8	11.0	0.4
	Centropagus furcatus	1.7	0.2	0.5	0.0
	Centropages abdominalis	0.3	0.0	0.0	0.0
	Centropages sp.	0.3	0.0	0.0	0.0
	Clausocalanus furcatus	0.0	0.0	0.0	0.0
	Euchaeta rimana	0.3	0.7	1.5	0.0
	Labidocera sp.	0.3	0.0	0.1	0.0
	Paracalanus orientalis	28.0	22.8	969.4	31.7
	Paracalanus sp.	1.2	0.1	0.2	0.0
	Pseudodiaptomus marinus	0.3	0.0	0.0	0.0
	Temora discaudata	0.9	0.1	0.3	0.0
	Temora turbinata	1.2	0.2	0.5	0.0
	Tortanus forcipatus	0.3	0.0	0.0	0.0
	Other calanoid copepods	11.8	2.2	74.1	2.4
Cyclopoida	Total	29.7	10.6	372.0	5.1
	Oithona similis	0.9	0.1	0.1	0.0
	Oithona sp.	2.3	0.2	0.6	0.0
	Oncaea sp.	2.3	0.2	0.5	0.0
	Oncaea venella	0.6	0.1	0.0	0.0
	Oncaea venusta	0.9	0.3	0.3	0.0
	Triconia sp.	1.4	0.1	0.2	0.0
	Ditrichocorycaeus affinis	14.1	7.5	128.0	4.2
	Ditrichocorycaeus spp.	11.2	2.1	26.0	0.9
Harpacticoida	Total	9.2	5.2	51.4	1.0
	Microsetella sp.	4.9	1.6	8.5	0.3
	Unidentified harpacticoids	5.8	3.6	22.2	0.7
Copepoda larvae	Total	8.1	6.3	51.0	1.5
	Unidentified copepodids	0.9	0.1	0.1	0.0
	Calanus nauplii	0.6	0.0	0.0	0.0
	Copepod eggs	7.5	6.2	46.7	1.5
Cirripedia	Total	6.9	0.6	4.1	0.1
	Cirripedia nauplii	2.6	0.2	0.6	0.0
	Cirripedia cyprii	4.0	0.3	1.4	0.0
Decapoda	Total	6.6	0.8	15.8	0.0
	Decapod zoea and mysis	3.7	0.4	4.7	0.0
	Crab megalopa	2.3	0.1	0.4	0.2
	Decapod eggs	0.3	0.0	0.0	0.0
	Unidentified Decapoda	0.3	0.3	0.3	0.0
Ostracoda	Ostracoda	0.9	0.1	0.1	0.0
Cumacea	Cumacea	2.0	0.2	1.1	0.0
Euphausiacea	Total	1.2	0.3	23.4	0.8
	Euphausia pacifica	1.2	0.3	19.9	0.7
	Euphausia sp.	0.6	0.1	1.8	0.1
Amphipoda	Total	1.4	0.1	0.5	0.0
	Unidentified gammarids	1.4	0.1	0.4	0.0
	Unidentified hyperiids	0.3	0.0	0.0	0.0
Chaetognatha	*Adianosagitta* sp.	0.3	0.0	0.0	0.0
Mollusca	Total	18.4	7.7	184.1	6.0
	Gastropod larvae	0.6	0.0	0.0	0.0
	Bivalve veliger	17.9	7.7	177.7	5.8
Fishes	Total	2.0	0.3	4.7	0.2
	Unidentified fish eggs	1.2	0.2	0.8	0.0
	Unidentified fish larvae	0.9	0.2	1.4	0.0
Other items	Total	13.5	0.2	24.8	0.8

%*F* = the relative frequency of occurrence of each food item, %*N* = the percentage by number of each food item, IRI = index of relative importance, %IRI = the percentage of the index of relative importance.

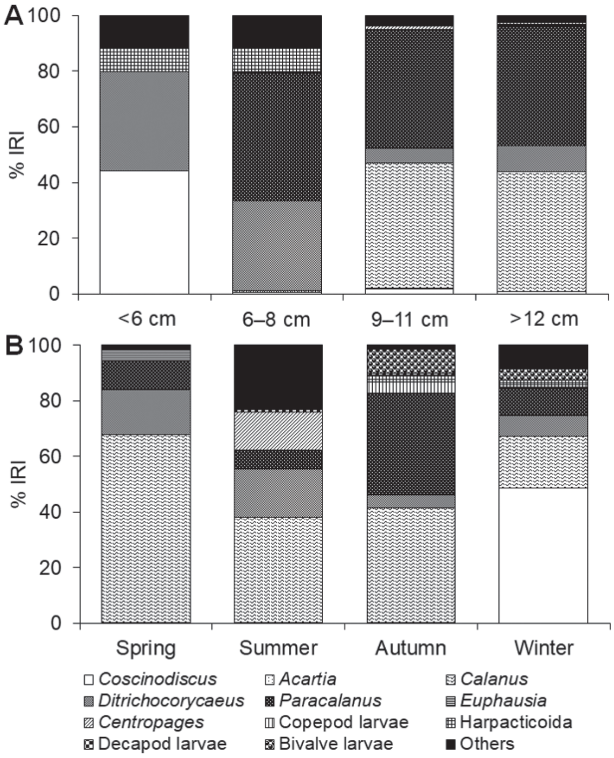

Figure 2. Changes in composition of stomach contents by %IRI of Pacific anchovy, *Engraulis japonicus*, in the southern waters of Korea: (**A**) size classes, (**B**) seasons.

40% by P_i and 20% by FO (frequency of occurrence) of the stomach contents. In contrast, *Acartia* sp., decapod larvae, cirriped larvae, and Harpacticoida were infrequent prey items for all seasons. *Euphausia pacifica* (spring and summer) and *P. orientalis* (autumn) are positioned in the upper left and right parts of the graph, respectively.

Canonical analysis (CA) of *N*% (number percentage) of prey items identified groups of prey species that were discriminated between each season with ontogenetic variation (Fig. 4A). Ontogenetic changes in the diet were investigated in the Pacific anchovy (*E. japonicus*) collected. Copepods were the most frequently observed prey item across all fish sizes. CA analysis of *N*% of prey items showed the groups of prey that distinguished each ontogenetic variation. Factors 1 and 2, illustrated by the eigenvalues on the first and second axes, explained 0.185 and 0.092 of the variance, respectively. The size of all groups was clearly apparent on the CA graph. Group 1 was distinctly separated into the positive part of Axis 1, distinguished by diatoms *Coscinodiscus* spp. Groups 2 and 4 were separated into the negative part of Axis 3, distinguished by copepod larvae, *Centropages*, *Paracalanus*, and *Ditrichocorycaeus*. Group 3 was separated into the positive part of Axis 2, distinguished by *Acartia* and decapod larvae. The data according to season are shown in the CA graphs (Fig. 4B). Spring was separated into the positive part of Axis 1, showing the consumption of Euphausiids, *Euphausia*, *Ditrichocorycaeus*, copepods, and *Calanus*. Summer was separated into the positive part of Axis 2, showing the consumption of *Centropages* and decapod larvae. Autumn was separated into the negative part of Axis 3, owing to the consumption of *Acartia* and bivalve larvae. Winter was separated into

Table 3. Comparison of diet composition of Pacific anchovy, *Engraulis japonicus*, from the southern waters of Korea among size classes by one-way ANOSIM (*R* and *P* value) and SIMPER. Global $R = 0.277$, $P < 0.001$.

Model	Parameter	Length class [cm]		
		<6 vs. 6.0~8.9	6.0~8.9 vs. 9.0~11.9	9.0~11.9 vs. ≥12
One-way ANOSIM	*R* value	0.417	0.269	0.330
	p value	0.002	0.001	0.002
SIMPER	Discriminating food item 1	Calanoid copepods	*Calanus sinicus*	*Euphausia pacifica*
	Contribution [%]	24.75	16.19	17.17
	Discriminating food item 2	Cirripedia larvae	*Euphausia pacifica*	*Calanus sinicus*
	Contribution [%]	16.22	13.83	15.80
	Discriminating food item 3	*Paracalanus orientalis*	Calanoid copepods	Calanoid copepods
	Contribution [%]	13.09	11.36	12.21

Table 4. Comparison of diet composition of Pacific anchovy, *Engraulis japonicus*, from the southern waters of Korea among seasons by one-way ANOSIM (R and *p* values) and SIMPER. Global $R = -0.059$, $P > 0.001$.

Model	Parameter	Season			
		Spring vs. summer	Summer vs. autumn	Autumn vs. winter	Winter vs. spring
One-way ANOSIM	*R* value	–0.259	–0.259	–0.148	0.222
	p value	ns	ns	ns	ns
SIMPER	Discriminating food item 1	*Calanus sinicus*	*Calanus sinicus*	*Calanus sinicus*	*Calanus sinicus*
	Contribution [%]	42.49	36.40	35.08	46.59
	Discriminating food item 2	*Eurytemora pacifica*	Fish larvae	Fish larvae	*Eurytemora pacifica*
	Contribution [%]	24.59	10.14	12.63	19.42
	Discriminating food item 3	*Centropages abdominalis*	*Paracalanus orientalis*	Bivalvia larvae	*Euchaeta rimana*
	Contribution [%]	6.94	8.61	8.92	19.42

ns = not significant.

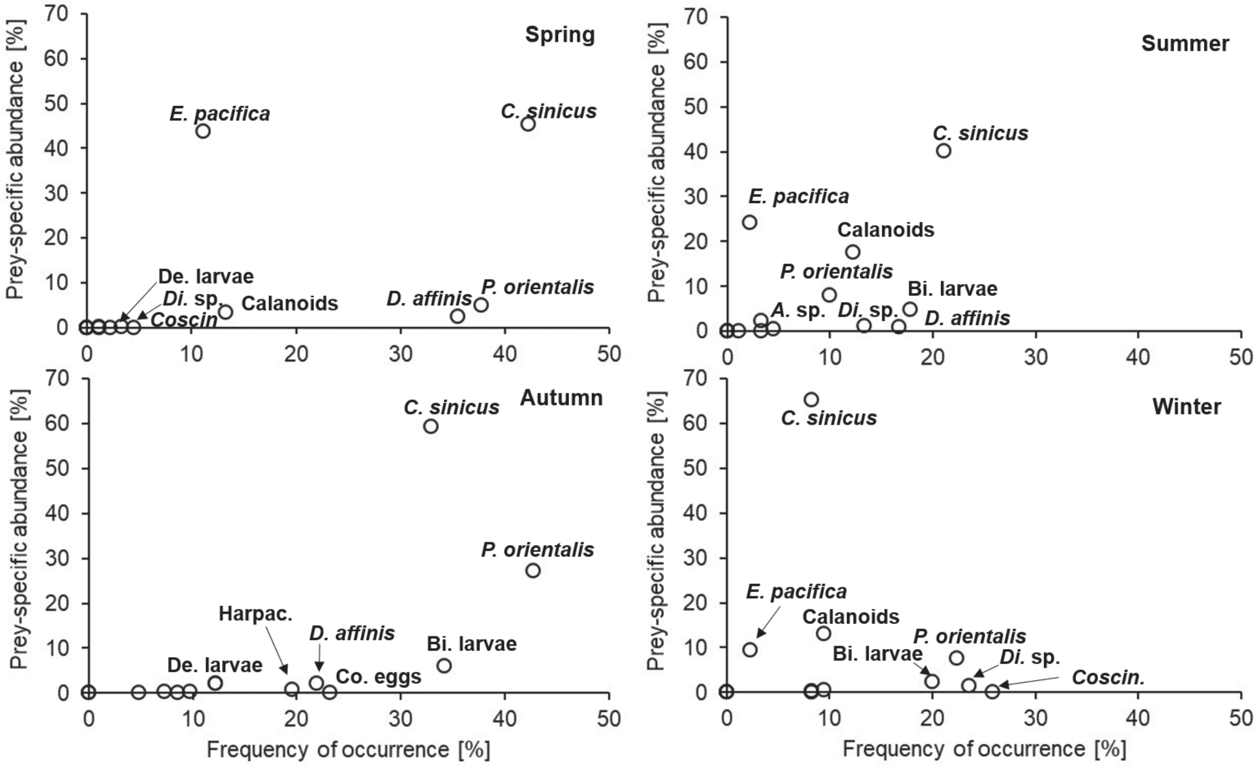

Figure 3. Seasonal changes of percent prey-specific abundance ($\%P_i$) versus the relative frequency of occurrence ($\%F$) for Pacific anchovy, *Engraulis japonicus*, from the southern waters of Korea. Abbreviations: *Coscin.* = *Coscinodiscus*, *C. sinicus* = *Calanus sinicus*, *P. orientalis* = *Paracalanus orientalis*, *D. affinis* = *Ditrichocorycaeus affinis*, Harpac. = harpacticoid copepods, *Di*. sp. = *Ditrichocorycaeus* sp., Calanoids = calanoid copepods, Bi. larvae = bivalve larvae, Co. eggs = copepod eggs, *E. pacifica* = *Euphausia pacifica*, De. larvae = decapod larvae.

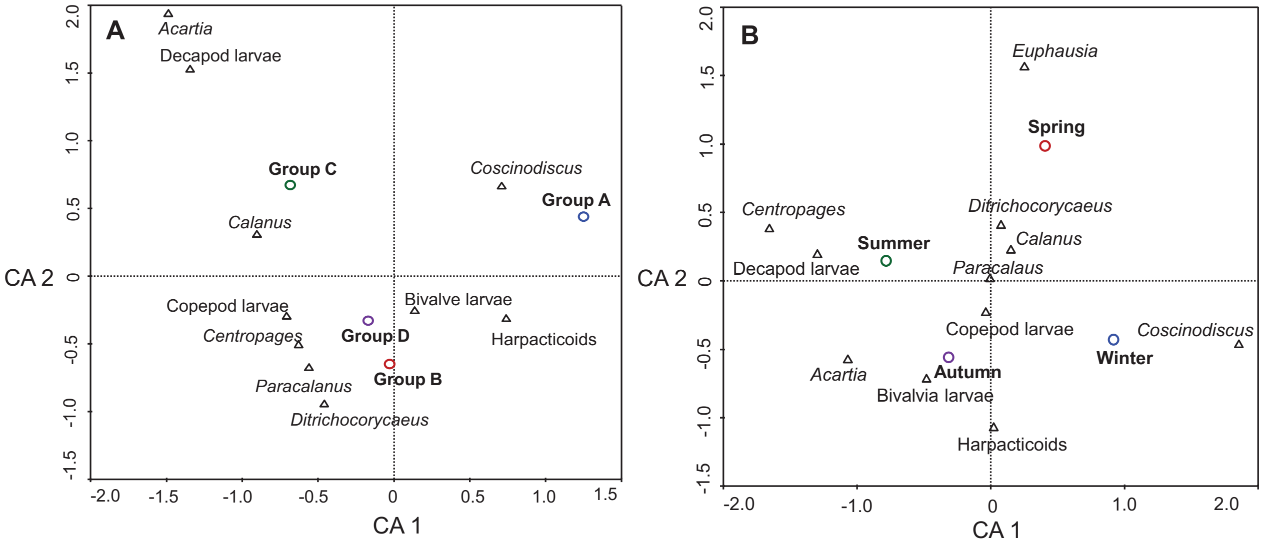

Figure 4. Correspondence analysis biplot for prey items of Pacific anchovy, *Engraulis japonicus*, from the southern waters of Korea, based on the percentage numerical frequency ($\%N$). (**A**) size classes, (**B**) season. Abbreviations: Group A = fork length < 6 cm, Group B = fork length 6–8.9 cm, Group C = fork length 9–11.9 cm, Group D = fork length ≥ 12 cm.

the negative part of Axis 4 owing to the consumption of the phytoplanktonic *Coscinodiscus* spp. (Bacillariophyta). The other prey items are halfway between the four groups, which comprise general prey that were consumed in similar proportions in all seasons.

Discussion

Several studies have reported the feeding habits of Pacific anchovy, *Engraulis japonicus*, at various locations (Uotani et al. 1978; Aoki and Miyashita 2000; Yasue et al.

2010; Kim et al. 2013; Wang et al. 2021b). In this study, we found that anchovies were exclusively planktivorous, and the primary prey items were copepods, diatoms (such as *Coscinodiscus* spp.), and to a lesser extent mollusk larvae. The main prey items for anchovy were *Calanus sinicus*, *Paracalanus orientalis*, bivalve larvae, *Ditrichocorycaeus affinis*, and copepod eggs. The food items of Pacific anchovy were not only small and medium prey (<2 mm, such as *Coscinodiscus* spp., *P. orientalis*, and *D. affinis*), but also large prey (>2 mm, such as *C. sinicus* and bivalve larvae). Some individuals contained relatively large prey (>4 mm, such as decapod larvae, amphipods, and *Euphausia pacifica*) along with much smaller prey. Graphical analysis of the diet composition showed that *E. japonicus* is an opportunistic and specialized predator characterized by strong individual feeding specialization. *Engraulis japonicus* from the southern coast of Korea employs two feeding modes: selective feeding on large prey or filter feeding on small prey, as suggested for Pacific anchovy of Sagami Bay (Mitani 1988), *Engraulis encrasicolus* (Linnaeus, 1758) in the Gulf of Lions (Mediterranean Sea) (Plounevez and Champalbert 2000), and Cape anchovy, *Engraulis capensis* Gilchrist, 1913 (see James 1987). According to Kim et al. (2013), Cirripedia larvae and *C. sinicus* were present during summer, with large phytoplankters (such as *Coscinodiscus* spp.) and *Pseudodiaptomus marinus* present during autumn. In particular, *C. sinicus* is situated in the upper right corner of the diagram for the spring, summer, and autumn seasons, indicating specialization within the *E. japonicus* population. *C. sinicus* has been previously described as particularly important for the Pacific anchovy diet (Islam and Tanaka 2009; Kim et al. 2013; Yoneda et al. 2022). In the southern waters of Korea, the abundance of bivalves is very important, as is evident from the abundance of bivalve larvae presented in the results on the zooplankton community by Moon et al. (2010, 2022a). In this study, prey items of anchovies showed no significant difference between the seasons of the stomach contents by performing an ANOSIM test. These results showed that the dominant prey items according to the season in this study were *C. sinicus*, *E. pacifica*, *P. orientalis*, bivalve larvae, and *D. affinis.*

The diet of *E. japonicus* from the southern coast of Korea differed from that of previous studies in Japanese waters (Yasue et al. 2010; Islam and Tanaka 2009), Chinese waters (Wang et al. 2021b), and Korean waters (Chang et al. 1980; Kim et al. 2013). Phytoplankters are generally known to contribute only sporadically to the diet of Pacific anchovy (Bulgakova 1993; Kim et al. 2013). The copepods used as the primary prey in this study are consistently dominant on the southern coast of Korea throughout the year. However, their species composition undergoes seasonal changes, as documented by Moon et al. (2010, 2022a). The prevalent copepod species include *P. orientalis*, *D. affinis*, and *C. sinicus*, as reported by Moon et al. (2010, 2022a) and Shin et al. (2022). In particular, *C. sinicus*, which was abundant in anchovies larger than 9 cm FL, showed high occurrence on the southern coast of Korea from winter to spring (Shin et al. 2022). The calanoids, including the genera *Calanus* and *Paracalanus*, have been previously described as a major for anchovy diets (Uotani et al. 1978; Mitani 1988; Takasuka and Aoki 2006; Kim et al. 2013). In addition, diatoms *Coscinodiscus* spp. also occurred highly in the winter of Korean waters (Park and Lee 1990), and Japanese waters (Nishikawa et al. 2000; Fukao et al. 2012). Diatoms *Coscinodiscus* spp. are predominantly found on the southern coast of Korea during the winter season (Park and Lee 1990), so it is believed that anchovies are utilized along with other prey items. Bivalve and decapod larvae were present in the anchovy diets, as shown by %IRI in all anchovy size classes (see Table 2; Fig. 2). The prey items of *E. japonicus*, which generally comprise zooplanktonic prey, may also be of importance in the species composition and community structure of zooplanktons in the southern coast of Korea (Kim et al. 2013). Off the southern coast of Korea, the spatial and temporal variability of zooplankton populations was associated with changes in phytoplankton composition and density and with the combined effects of regional climatology and local hydrography (Moon et al. 2022a; Shin et al. 2022). These findings deepen our knowledge on the feeding plasticity of *E. japonicus* (see Mitani 1988; Tanaka et al. 2006).

Investigation of the feeding behavior of the Pacific anchovy indicates that raptorial feeding is dominant over filter feeding and that prey appears to be selected primarily based on size. Anchovies selectively fed on phytoplankton (*Coscinodiscus* spp.) and zooplankton, especially calanoid copepods (Uotani et al. 1978; Takasuka and Aoki 2006; Kim et al. 2013). As the anchovies grew, calanoid copepods were steadily substituted by large crustaceans, such as euphausiids and bivalve larvae, which became more frequent in the diets of group 2 (6.0–8.9 cm) and group 3 (9.0–11.9 cm). The increase in the abundance of potentially important prey species is suggested by James (1987) and Plounevez and Champalbert (2000). The southern waters of Korea are temperate and highly productive, and due to seasonal changes in water quality, hydrodynamics, nutrients, and phytoplankton primary productivity change strongly (Park and Lee 1990; Yang and Kim 1990; Baek et al. 2010); zooplankton abundance also varies (Moon et al. 2010; 2022a; Shin et al. 2022). The abundance and distribution of zooplankton were correlated with phytoplankton composition and density (Zenitani et al. 2011). In particular, phytoplankton can be consumed by zooplankton, which is the primary food item for most marine fish larvae and small pelagic fish, such as anchovies. In the southern waters of Korea, the abundance and distribution of zooplankton were strongly associated with environmental factors, such as sea temperature, salinity, and chlorophyll-a concentration (Moon et al. 2022a). Copepods were the dominant prey of anchovies during all seasons, but there was no significant difference between seasons. Notably, anchovies exhibited similar diets in winter and spring, including *C. sinicus* and *E. pacifica*. This selectivity for larger nutrient-rich prey can be explained by the energy requirements of *E. japonicus* for successful reproduction. Our results suggest that *E. japonicus* has a narrow food niche and is a specialized feeder, with copepods being the dominant prey for all seasons.

Pacific anchovies are an essential link between primary production and energy transfer to higher trophic levels (Zenitani and Kimura 1997). The majority of studies of the population dynamics of larvae, juvenile, and adults of *E. japonicus* confirm the important role of copepods as the main link between phytoplankters and anchovy production (Zenitani and Kimura 1997; Takasuka and Aoki 2006).

Conclusions

Through this study, we found that anchovies inhabiting the southern coast of Korea are phyto- and zooplankton-feeders and have the flexibility to utilize various prey depending on prey availability, which may vary depending on the size of the anchovies. However, this study did not include larval stages of *E. japonicus* off the southern coast of Korea, and studies of the diet of anchovy larvae are needed to understand the overall diet of anchovies. The relation between various environmental influences and anchovy population dynamics in this study emphasizes the need to increase our understanding of the feeding ecology of *E. japonicus* off the southern coast of Korea in relation to plankton dynamics and environmental factors.

Acknowledgments

This research was supported by a grant from the National Institute of Fisheries Science (NIFS) of Korea (R2024010).

References

Abràmoff M, Magalhães P, Ram S (2004) Image processing with ImageJ. Biophotonics International 11(7): 36–42.

Amundsen PA, Gabler HM, Staldvik FJ (1996) A new method for graphical analysis of feeding strategy from stomach contents data. Journal of Fish Biology 48(4): 607–614. https://doi.org/10.1111/j.1095-8649.1996.tb01455.x

Aoki I, Miyashita K (2000) Dispersal of larvae and juvenile of Japanese anchovy *Engraulis japonicus* in the Kuroshio extension and Kuroshio–Oyashio transition regions, western North Pacific Ocean. Fisheries Research 49(2): 155–164. https://doi.org/10.1016/S0165-7836(00)00197-1

Bachiller E, Irigoien X (2015) Trophodynamics and diet overlap of small pelagic fish species in the Bay of Biscay. Marine Ecology Progress Series 534: 179–198. https://doi.org/10.3354/meps11375

Baek SH, Shin K, Hyun B, Jang PG, Kim HS, Hwang OM (2010) Distribution characteristics and community structure of phytoplankton in the different water mass during early summer of southern sea of Korea. Ocean and Polar Research 32(1): 1–13. https://doi.org/10.4217/OPR.2010.32.1.001

Borme D, Tirelli V, Brandt SB, Umani SF, Arneri E (2009) Diet of *Engraulis encrasicolus* in the northern Adriatic Sea (Mediterranean): Ontogenetic changes and feeding selectivity. Marine Ecology Progress Series 392: 193–209. https://doi.org/10.3354/meps08214

Bulgakova Y (1993) Daily feeding dynamics of the Black Sea anchovy, *Engraulis encrasicolus*. Journal of Ichthyology 33(7): 78–88.

Chang SD, Hong SY, Park CK, Chin P, Lee B, Lee TY, Kang YJ, Gong Y (1980) Studies on the migration of anchovy *Engraulis japonica* in Korean waters. Publications of the Institute of Marine Science Fisheries University Busan 12: 1–38.

Clarke KR, Warwick RM (2001) Change in marine communities: an approach to statistical analysis and interpretation. 2nd edn. Primer-E, Plymouth, UK, 172 pp.

Cortés E (1999) Standardized diet compositions and trophic levels of sharks. ICES Journal of Marine Science 56(5): 707–771. https://doi.org/10.1006/jmsc.1999.0489

Costello MJ (1990) Predator feeding strategy and prey importance: A new graphical analysis. Journal of Fish Biology 36(2): 261–263. https://doi.org/10.1111/j.1095-8649.1990.tb05601.x

Fukao T, Kimoto K, Kotani Y (2012) Effect of temperature on cell growth and production of transparent exopolymer particles by the diatom *Coscinodiscus granii* isolated from marine mucilage. Journal of Applied Phycology 24(2): 181–186. https://doi.org/10.1007/s10811-011-9666-3

Han IS, Lee JS (2020) Change the annual amplitude of sea surface temperature due to climate change in a recent decade around the Korean Peninsula. Journal of the Korean Society of Marine Environment and Safety 26(3): 233–241. https://doi.org/10.7837/kosomes.2020.26.3.233

Harmelin-Vivien ML, Kaim-Malka RA, Ledoyer M, Jacob-Abraham SS (1989) Food partitioning among scorpaenid fishes in Mediterranean seagrass beds. Journal of Fish Biology 34(5): 715–734. https://doi.org/10.1111/j.1095-8649.1989.tb03352.x

Hyslop EJ (1980) Stomach contents analysis—A review of methods and their application. Journal of Fish Biology 17(4): 411–429. https://doi.org/10.1111/j.1095-8649.1980.tb02775.x

Islam MS, Tanaka M (2009) Diet and prey selection in larval and juvenile Japanese anchovy *Engraulis japonicus* in Ariake Bay, Japan. Aquatic Ecology 43(2): 549–558. https://doi.org/10.1007/s10452-008-9207-6

James AG (1987) Feeding ecology, diet and field-based studies on feeding selectivity of the Cape anchovy *Engraulis capensis* Gilchrist. South African Journal of Marine Science 5(1): 673–692. https://doi.org/10.2989/025776187784522784

Jin X, Zhang B, Xue Y (2010) The response of the diet four carnivorous fishes to variations in the Yellow Sea ecosystem. Deep Sea Research Part II: Topical Studies in Oceanography 57(11–12): 996–1000. https://doi.org/10.1016/j.dsr2.2010.02.001

Kim JY, Lo NCH (2001) Temporal variation of seasonality of egg production and the spawning biomass of Pacific anchovy, *Engraulis japonicus*, in the southern waters of Korea in 1983–1994. Fisheries Oceanography 10(3): 297–310. https://doi.org/10.1046/j.1365-2419.2001.00175.x

Kim JY, Kang YS, Oh HJ, Suh YS, Hwang JD (2005) Spatial distribution of early life stage of anchovy (*Engraulis japonicus*) and hairtail (*Trichiurus lepturus*) and their relationship with oceanographic features of the East China Sea during the 1997–1998 El Niño Event. Estuarine, Coastal and Shelf Science 63(1–2): 13–21. https://doi.org/10.1016/j.ecss.2004.10.002

Kim MJ, Youn SH, Kim JY, Oh CW (2013) [Feeding characteristics of the Japanese anchovy, *Engraulis japonicus* according to the distribution of zooplankton in the coastal water of southern Korea.] Korean Journal of Environmental Biology 31(4): 275–287. [In Korean with English abstract] https://doi.org/10.11626/KJEB.2013.31.4.275

Kim SJ, Woo SH, Kim BM, Hur SD (2011) [Trends in sea surface temperature (SST) change near the Korean peninsula for the past 130 years.] Ocean Polar Research 33(3): 281–290. [In Korean with English abstract] https://doi.org/10.4217/OPR.2011.33.3.281

KOSIS (2023) Fishery: Fishery production survey. Korean Statistical Information Service. [English version] [Accessed 2023 February 28] http://kosis.kr/eng

Labropoulou M, Machias A, Tsimenides N (1999) Habitat selection and diet of juvenile red porgy, *Pagrus pagrus* (Linnaeus, 1758). Fish Bulletin 97(3): 495–507.

Lassalle G, Lobry J, Le Loc'h F, Bustamante P, Certain G, Delmas D, Dupuy C, Hily C, Labry C, Le Pape O, Marquis E, Petitgas P, Pusineri C, Ridoux V, Spitz J, Niquil N (2011) Lower trophic levels and detrital biomass control the Bay of Biscay continental shelf food web: Implications for ecosystem management. Progress in Oceanography 91(4): 561–575. https://doi.org/10.1016/j.pocean.2011.09.002

Ma S, Cheng J, Li J, Liu Y, Wan R, Tian Y (2019) Interannual to decadal variability in the catches of small pelagic fishes from China Seas and its responses to climatic regime shifts. Deep Sea Research Part II: Topical Studies in Oceanography 159: 112–129. https://doi.org/10.1016/j.dsr2.2018.10.005

Mitani I (1988) [Food habits of Japanese anchovy in the Shirasu fishing ground within Sagami Bay.] Nippon Suisan Gakkaishi 54(11): 1859–1865. [In Japanese with English abstract] https://doi.org/10.2331/suisan.54.1859

Moon SY, Oh HJ, Soh HY (2010) Seasonal variation of zooplankton communities in the southern coastal waters of Korea. Ocean and Polar Research 32(4): 411–426. https://doi.org/10.4217/OPR.2010.32.4.411

Moon SY, Lee MH, Jung KM, Kim H, Jung JH (2022a) [Spatial and temporal distribution and characteristics of zooplankton communities in the southern coast of Korea during the spring to summer period.] Korean Journal of Fisheries and Aquatic Science 55(2): 154–170. [In Korean with English abstract] https://doi.org/10.5657/KFAS.2022.0154

Moon SY, Baeck GW, Lee MH, Kim H, Jung KM (2022b) [Reproductive characteristics of Pacific anchovy *Engraulus japonicus* from the southern waters of Korea.] Korean Journal of Fisheries and Aquatic Science 55(6): 927–937. [In Korean with English abstract] https://doi.org/10.5657/KFAS.2022.0927

Nishikawa T, Miyahara K, Nagai S (2000) [Effects of temperature and salinity on the growth of the giant diatom *Coscinodiscus wailesii* isolated from Harima-Nada, Seto Inland Sea, Japan.] Nippon Suisan Gakkaishi 66(6): 993–998. [In Japanese with English abstract] https://doi.org/10.2331/suisan.66.993

Park KJ, Cha SS (1995) [Food organisms of postlarvae of Japanese anchovy (*Engraulis japonicus*) in Kwangyang Bay.] Korean Journal of Fisheries and Aquatic Science 28(3): 247–252. [In Korean with English abstract]

Park JS, Lee SG (1990) [Distribution and species composition of phytoplankton in the southern water of Korea and their relation to the character of water masses.] Korean Journal of Fisheries and Aquatic Science 23(3): 208–214. [In Korean with English abstract]

Pauly D, Christensen V (2000) The Ecopath modelling approach and FishBase. In: Froese R, Pauly D (Eds.) FishBase 2000: Concepts, Design and Data Sources. ICLARM, Manila, 177.

Pinchuk AI, Hopcroft RR (2007) Seasonal variations in the growth rates of euphausiids (*Thysanoessa inermis*, *T. spinifera*, and *Euphausia pacifica*) from the northern Gulf of Alaska. Marine Biology 151(1): 257–269. https://doi.org/10.1007/s00227-006-0483-1

Plounevez S, Champalbert G (2000) Diet, feeding behavior and trophic activity of the anchovy (*Engraulis encrasicolus* L.) in the Gulf of Lions (Mediterranean Sea). Oceanologica Acta 23(2): 175–192. https://doi.org/10.1016/S0399-1784(00)00120-1

Scharf FS, Juanes F, Rountree RA (2000) Predator size–prey size relationships of marine fish predators: Interspecific variation and effects of ontogeny and body size on trophic niche breadth. Marine Ecology Progress Series 208: 229–248. https://doi.org/10.3354/meps208229

Shin D, Park TH, Lee CL, Hwang K, Kim DN, Lee SJ, Kang SK, Park HJ (2021) Characterization of trophic structure of fish assemblages in the east south seas of Korea based on C and N stable isotope ratios. Water 14(1): 58. https://doi.org/10.3390/w14010058

Shin SS, Choi SY, Seo MH, Lee SJ, Soh HY, Youn SH (2022) Spatiotemporal distribution characteristics of copepods in the water masses of the northeastern East China Sea. Journal of Marine Science and Engineering 10(6): 754. https://doi.org/10.3390/jmse10060754

Takasuka A, Aoki I (2006) Environmental determinants of growth rates for larval Japanese anchovy *Engraulis japonicus* in different waters. Fisheries Oceanography 15(2): 139–149. https://doi.org/10.1111/j.1365-2419.2005.00385.x

Takasuka A, Aoki I, Mitani I (2003) Evidence of growth-selective predation on larval Japanese anchovy *Engraulis japonicus* in Sagami Bay. Marine Ecology Progress Series 252: 223–238. https://doi.org/10.3354/meps252223

Tanaka H, Aoki I, Ohshimo S (2006) Feeding habits and gill raker morphology of three planktivorous pelagic fish species off the coast of northern and western Kyushu in summer. Journal of Fish Biology 68(4): 1041–1061. https://doi.org/10.1111/j.0022-1112.2006.00988.x

Tang QS, Su JL, Sun S, Zhang J, Huang DJ, Jin XS, Tong L (2005) [A study of marine ecosystem dynamics in the coastal ocean of China.] Advances in Earth Science 20(12): 1288–1299. [In Chinese with English Abstract]

Uotani I, Izuha A, Asai K (1978) [Food habits and selective feeding of anchovy larvae (*Engraulis japonica*).] Nippon Suisan Gakkaishi 44(5): 427–434. [In Japanese with English abstract] https://doi.org/10.2331/suisan.44.427

Uye SI (1982) Length–weight relationships of important zooplankton from the Inland Sea of Japan. Journal of the Oceanographical Society of Japan 38(3): 149–158. https://doi.org/10.1007/BF02110286

Wan R, Bian X (2012) Size variability and natural mortality dynamics of anchovy *Engraulis japonicus* eggs under high fishing pressure. Marine Ecology Progress Series 465: 243–254. https://doi.org/10.3354/meps09795

Wan R, Bian X (2012) Size variability and natural mortality dynamics of anchovy *Engraulis japonicus* eggs under high fishing pressure. Marine Ecology Progress Series 465: 243–254. https://doi.org/10.3354/meps09795

Wang Y, Liang C, Chen Z, Liu S, Zhang H, Xian W (2021a) Spring ichthyoplankton assemblage structure in the Yangtze Estuary under environmental factors. Frontiers in Marine Science 8: e806096. https://doi.org/10.3389/fmars.2021.806096

Wang J, Jiang RJ, Hu CL, Li Z, Xiao Y, Xu YJ, He ZT, Xu HX (2021b) [Feeding ecology of *Engraulis japonicus* based on stomach contents and stable isotope.] Chinese Journal of Applied Ecology 32(6): 2035–2044. [In Chinese with English abstract] https://doi.org/10.13287/j.1001-9332.202106.029

Wu ZW, Zhang X, Dromard CR, Tweedley JR, Loneragan NR (2018) Partitioning of food resources among three sympatric scorpionfish (Scorpaeniformes) in coastal waters of the northern Yellow Sea. Hydrobiologia 826(1): 331–351. https://doi.org/10.1007/s10750-018-3747-0

Yamaguchi A, Taniuchi T (2000) Food variations and ontogenetic dietary shift of the starspotted-dogfish *Mustelus manazo* at five locations in Japan and Taiwan. Fisheries Science 66(6): 1039–1048. https://doi.org/10.1046/j.1444-2906.2000.00166.x

Yamamoto K, Saito M, Yamashita Y (2018) Relationship between the daily growth rate of Japanese anchovy *Engraulis japonicus* larvae and environmental factors in Osaka Bay, Seto Inland Sea, Japan. Fisheries Science 84(2): 373–383. https://doi.org/10.1007/s12562-018-1178-5

Yang HS, Kim SS (1990) A study on sea water and ocean current in the sea adjacent to Korea Peninsula 1. Physical processes influencing the surface distributions of chlorophyll and nutrient in the Southern Sea of Korea in summer. Korean Journal of Fisheries and Aquatic Sciences 23(6): 417–424.

Yasue N, Doiuchi R, Yoshimoto Y, Takeuchi T (2010) Diet of late larval Japanese anchovy *Engraulis japonicus* in the Kii Channel, Japan. Fisheries Science 76(1): 63–73. https://doi.org/10.1007/s12562-009-0181-2

Yoneda M, Fujita T, Yamamoto M, Tadokoro K, Okazaki Y, Nakamura M, Takahashi M, Kono N, Matsubara T, Abo K, Xinyu G, Yoshie N (2022) Bottom-up processes drive reproductive success of Japanese anchovy in an oligotrophic sea: A case study in the central Seto Inland Sea, Japan. Progress in Oceanography 206: 102860. https://doi.org/10.1016/j.pocean.2022.102860

Yoo JT, Jeong JM (2016) [Gut composition of postlarval and juvenile anchovy *Engraulis japonicus* in the coastal waters of Yeosu, Korea.] Korean Journal of Fisheries and Aquatic Science 49(5): 642–647. [In Korean with English abstract] https://doi.org/10.5657/KFAS.2016.0642

Zenitani H, Kimura R (1997) [Increase in late winter egg production of the Japanese anchovy as related to recovery of the stock size along the Pacific coast of Japan.] Nippon Suisan Gakkaishi 63(5): 665–671. [In Japanese with English abstract] https://doi.org/10.2331/suisan.63.665

Zenitani H, Kono N, Tsukamoto Y (2011) Simulation of copepod biomass by a prey-predator model in Hiuchi-nada, central part of the Seto Inland Sea: Does copepod biomass affect the recruitment to the shirasu (Japanese larval anchovy *Engraulis japonicus*) fishery? Fisheries Science 77: 455–466. https://doi.org/10.1007/s12562-011-0343-x

Zhang B, Tang Q, Jin X (2007) Decadal-scale variations of trophic levels at high trophic levels in the Yellow Sea and the Bohai Sea ecosystem. Journal of Marine Systems 67(3–4): 304–311. https://doi.org/10.1016/j.jmarsys.2006.04.015

Acta Ichthyologica et Piscatoria 54, 2024, 13–20 | DOI 10.3897/aiep.54.105627

PENSOFT.

ACTA ICHTHYOLOGICA ET PISCATORIA

Genetic diversity of three consecutive selective breeding generations in *Pseudobagrus vachellii* (Actinopterygii: Siluriformes: Bagridae)

Huan WANG[1,2], Guoqing DUAN[1,2], Huaxing ZHOU[1,2]

1 *Institute of Fisheries Science, Anhui Academy of Agricultural Sciences, Hefei, Anhui, China*
1 *Anhui Province Key Laboratory of Aquaculture and Stock Enhancement, Hefei, Anhui, China*

https://zoobank.org/32F3DC73-E260-4939-AF92-196F602111E2

Corresponding author: Guoqing Duan (duangq2010@126.com)

Academic editor: Jolanta Kiełpińska ♦ **Received** 28 April 2023 ♦ **Accepted** 21 December 2023 ♦ **Published** 29 January 2024

Citation: Wang H, Duan G, Zhou H (2024) Genetic diversity of three consecutive selective breeding generations in *Pseudobagrus vachellii* (Actinopterygii: Siluriformes: Bagridae). Acta Ichthyologica et Piscatoria 54: 13–20. https://doi.org/10.3897/aiep.54.105627

Abstract

Pseudobagrus vachellii (Richardson, 1846) is a commercially important freshwater fish species in China. To understand the effects of artificial breeding on the genetic diversity of three consecutive *P. vachellii* breeding populations (F1, F2, and F3) since 2012, a genetic analysis was conducted using polymorphic microsatellite markers. The mean allele number, expected heterozygosity, observed heterozygosity, and the polymorphic information content from generation F1 to F3 decreased from 7.75 to 5.63, from 0.77 to 0.63, from 0.83 to 0.77, and from 0.72 to 0.58, respectively. Analysis of molecular variance showed greater genetic divergence within the three generations (93.67%) than that among the generations (6.33%), and the overall differentiation level was moderate. Additionally, the lowest genetic differentiation was between F2 and F3 ($F_{st} = 0.0484$), and the highest was between F1 and F3 ($F_{st} = 0.12864$). Inbreeding occurred in each generation and was the highest in generation F3. Structural analysis showed that the three *P. vachellii* generations were most likely divided into two different genetic clusters. Although genetic diversity declined slightly in the mass selection lines after three breeding generations, overall genetic diversity was maintained at a relatively high level. To minimize the loss of genetic diversity and inbreeding in the subsequent breeding process, a moderate number of parents can be used for each generation. Information regarding the genetic diversity and structure of the selective *P. vachellii* breeding generations obtained in this study will be useful for future broodstock management and selective breeding programs.

Keywords

genetic diversity, genetic structure, microsatellites, *Pseudobagrus vachellii*, selective breeding

Introduction

Pseudobagrus vachellii (Richardson, 1846) represents the family Bagridae and is an endemic freshwater fish species widely distributed in China. However, wild populations have rapidly declined owing to habitat destruction, water pollution, and overfishing. As an edible fish, it has the largest body size and is the fastest-growing group in the genus *Pseudobagrus*. Moreover, it is the male parent of the hybrid yellow catfish "Huangyou 1" (GS-02-001-2018). *Pseudobagrus vachellii* possesses high nutritional value and has a great taste, with low bone amounts in the muscle (Zheng et al. 2021). However, long farming periods can result in problems such as slow growth rate, differences in morphological traits, mottling of body color, short and thick body shapes (Fig. 1), and decreased stress resistance in the retained population. These problems greatly affect the market value of *P. vachellii*.

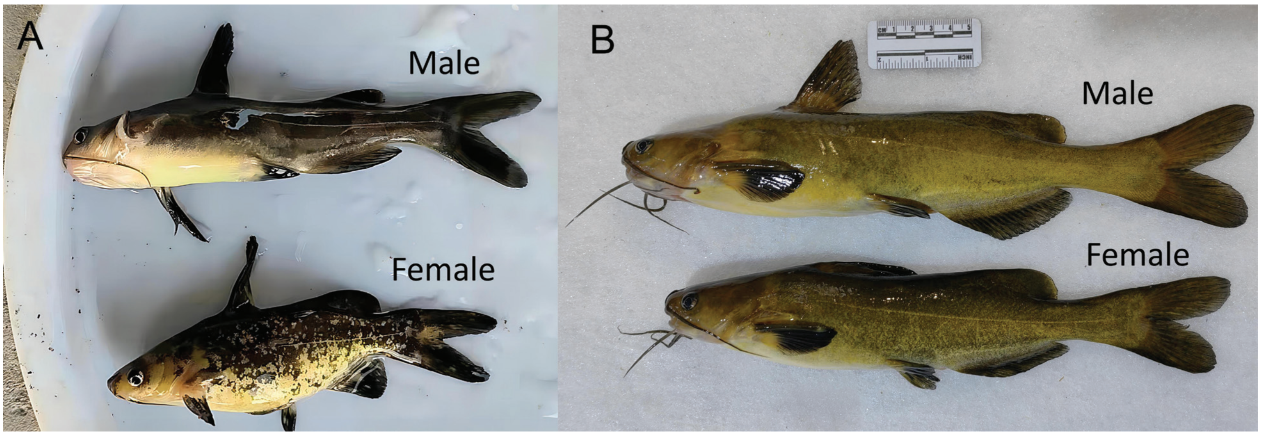

Figure 1. Comparison between *Pseudobagrus vachellii* populations. **(A)** Poor germplasm population and **(B)** mass-selected population by our project team.

Artificial selective breeding is an effective way to improve performance traits, breed excellent aquatic varieties, and increase productivity; however, it also decreases genetic diversity in breeding populations (Gjedrem et al. 2012; Chen et al. 2017; Phuc et al. 2021; Swain et al. 2022). As a raw material, for artificial selection in captive populations, maintaining the genetic diversity of the breeding population is a prerequisite for the continuous utilization of aquatic germplasm resources, and genetic assessments should be conducted periodically (Diyie et al. 2021). For many fish species, usually in the late stages of artificial selection breeding, the number of breeding individuals gradually decreases, which leads to increased inbreeding, decreased population genetic diversity, and loss of genetic variability in artificially bred seed populations. This eventually leads to the loss of product development and utilization (Ortega-Villaizan et al. 2011; Liu et al. 2018).

Because of the long-term artificial breeding of *Pseudobagrus vachellii*, nonstandard conservation, and germplasm degradation have occurred in nursery farms. The mass selection program of *P. vachellii* derived from the wild Huai River and Yangtze River populations for growth traits and morphological characteristics has been conducted since 2012 for three generations. Compared with that of the unselected *P. vachellii*, the growth rate increased by 15 percentage points, which showed obvious advantages (Duan et al. 2023). However, the changes in the genetic variation and diversity among these three breeding generations are unknown.

The microsatellite marker technique is a sensitive, simple, and efficient method for studying the genetic diversity of aquatic animals (Fu et al. 2017). Some microsatellite markers have been successfully developed for the genetic analysis of *P. vachellii* (see Wang et al. 2021; Zheng et al. 2020). Eight polymorphic microsatellite loci were used to monitor changes in genetic diversity and structure during the selection process in this study. This useful information can be used to evaluate whether the levels of variation are appropriate for a long-term selective breeding program. Moreover, it provides guidelines for avoiding genetic variation loss and inbreeding for future *P. vachellii* selective breeding programs and promotes the sustainable and healthy development of the *P. vachellii* industry.

Materials and methods

Mass selection process and pond culture management. In our selective breeding program, three generations of *Pseudobagrus vachellii* were produced between 2012 and 2021 at the Fishery Research Institute of the Anhui Academy of Agricultural Sciences in Hefei, Anhui, China (Fig. 2). From the founder group comprising more than 800 *P. vachellii* individuals, 80 individuals with large sizes and similar morphological traits were screened as breeding parents. The female-to-male ratio was approximately 1:1, and they were artificially bred in May 2014. Approximately 300 000 F1-generation hatchlings, which were cultivated using natural bait in the ponds (rotifers, branchiostomatids, copepods, etc.) for one week, were fed compound feed powder (with a protein content of

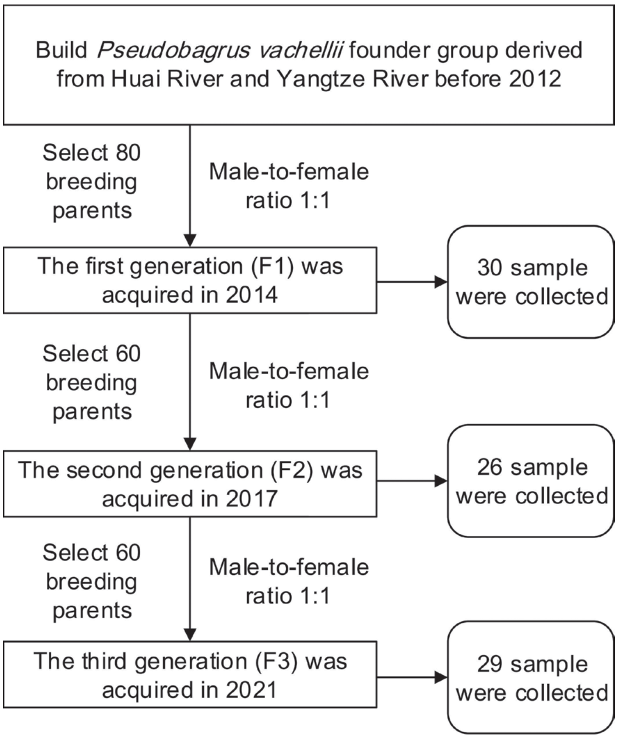

Figure 2. Mass selection of *Pseudobagrus vachellii* and sample collection.

45%) for cultivation and then changed to compound feed granules (with a protein content of 40%–45%). When the fish were half a month old, they were fed compound feed pellets (protein content of 40%–45%), and selection was carried out at 1 month, 12 months, and 32 months of age, respectively, using growth rate and morphological traits as the main selection indexes. Healthy and disease-free individuals with fast growth rates and similar morphological traits were selected and retained for cultivation. In June 2017, 60 breeding parents with a good degree of sexual maturity and morphology were selected from the F1 generation at a male-to-female ratio of approximately 1:1. They were then artificially inseminated to obtain approximately 220 000 F2 generation first hatchery fry. The fry were bred in the same way as the F1 generation and were selected at one, 12, and 32 months of age, using growth rate and morphological traits as the selection indices. In June 2021, 60 breeding parents with a good degree of sexual maturity and morphology were selected from the F2 generation at a female-to-male ratio of approximately 1:1. Artificial insemination was then performed to obtain approximately 220 000 fry in the F3 generation. The fry cultivation method was the same as that of the F1 generation, and selection was carried out at 1 month and 12 months of age, respectively, using growth rate, morphological traits, and hypoxia tolerance as selection indices. The number of individuals in the selection group was then approximately 7500. The female breeding parents of the F1, F2, and F3 generation all weighed over 150 g and the males weighed not less than 250 g. During breeding, oxytocin was injected artificially, and after the effect time was reached, insemination was performed by squeezing the eggs artificially, and the fertilized eggs were incubated on a mesh. Each female fish produced 6000~9000 eggs.

Fish materials and sample collection. The care and use of experimental animals in this study complied with the guidelines and policies approved by the Experimental Animal Welfare and Ethical Committee of the Anhui Academy of Agricultural Sciences. Twenty-six to thirty individuals from each generation were sampled randomly, and 85 unrelated individuals were randomly selected from each generation (Fig. 2). The fish body length was 31.77 ± 9.99 cm and the body weight was 434.24 ± 291.48 g. Muscle tissue samples were quickly removed, cleaned with 0.70% physiological saline, and stored at 4°C in 95% ethanol for subsequent experiments.

Table 1. Summary of microsatellite loci details for *Pseudobagrus vachellii*.

Locus	Primer sequence (5′→3′)	Motif	Size range [bp]	Reference
PV1	TAATGCATTTTCTGCTGCCA CACACGGGGGATGAATTAAG	AGATG	127–152	Wang et al. 2021
PV2	GAAACCCGACTCTGTCAAGG TGAGGGCTAGAAAGGGACAA	TGA	226–283	Wang et al. 2021
PV4	CAGAGGCATTTCTCAGAGGC CAGGTTGCAGGTACTGTCCA	CAAT	168–208	Wang et al. 2021
PV6	TTGCCGTAGTATCGGCTACC TAAGGGGTTCGGATGTGAAG	ATTG	160–192	Wang et al. 2021
PV7	TCGACTGCTGTTTATCCGTCT CGATAAACTTTCGCAGACCC	AAC	248–275	Wang et al. 2021
PV9	AGTCAGGTTGTATGCCCACC ACAGGGAAAGAGACGTGCAT	GAAT	183–215	Wang et al. 2021
PV12	TAATGCATTTTCTGCTGCCA CACACGGGGGATGAATTAAG	AGATG	127–152	Wang et al. 2021
Y73	GCTTTCTTGATGCAACCCAG TGGATATTGACGAGTTCCATGT	CATA	118–138	Zheng et al. 2020

DNA extraction and genotyping. Genomic DNA was extracted using a DNeasy Blood and Tissue Kit (Tiangen, Beijing, China) following the manufacturer's instructions. A panel of eight microsatellite markers previously developed for *Pseudobagrus vachellii* were amplified using polymerase chain reaction (PCR) at annealing temperatures (Zheng et al. 2020; Wang et al. 2021) (Table 1). The PCR reactions were conducted using a Peltier thermal cycler using a 30 µL reaction mixture. Each reaction mixture contained 3 µL of 10× PCR buffer, and final concentrations of 2.5 µL (2.5 mmol · L^{-1}) deoxynucleotide triphosphates, 1 µL (10 µmol · L^{-1}) of each forward and reverse primer, 0.3 µL (5 U · $µL^{-1}$) of Taq DNA polymerase (Transgen, Beijing, China), and 1–2 µL (50 ng · $µL^{-1}$) of template DNA that was added to 30 µL double-distilled H_2O. Temperature profiles for the PCR consisted of an initial denaturation at 94°C for 5 min, 31–34 cycles of 94°C for 30 s, annealing at primer-specific temperatures (53–60°C) for 40 s, extension at 72°C for 50 s, and a final extension at 72°C for 10 min (Wang et al. 2022). The PCR products were separated and sized on an ABI 3730xl automated sequencer with a ROX 500 size standard, and the resulting genotype traces were scored in GeneMapper 3.7 (all Applied Biosystems). The presence of null alleles, large allele dropouts, scoring of stutter peaks, and typographic errors were assessed using a micro-checker (Van Oosterhout et al. 2004).

Data analysis. The microsatellite data were analyzed using web-based Genepop software (http://genepop.curtin.edu.au/), with Markov chain parameters of 10 000 dememorizations, 500 batches, and 5000 iterations per batch to determine whether each locus deviated from the Hardy–Weinberg equilibrium and to test the linkage equilibria. The number of alleles (N_a), number of effective alleles (N_e), observed heterozygosity (H_o), expected heterozygosity (H_e), Shannon diversity index (I), and Nei's genetic distance (D_a) values were calculated using Popgene 1.32, respectively (Nei 1972; Yeh et al. 1997). The genetic differentiation coefficient (F_{st}) is one of the most widely used descriptive statistics for evaluating genetic differentiation between and among populations and can provide important insights into the evolutionary processes that influence genetic variation among populations (Holsinger and Weir 2009). According to the rule by Wright (1965), an F_{st} value of 0.000–0.049 represents low differentiation, values of 0.05–0.25 indicate moderate differentiation and values higher than 0.25 indicate high differentiation among populations. The F_{st} and genetic variation were analyzed using analysis of molecular variance (AMOVA) with Arlequin 3.5 software (Excoffier and Lischer 2010). An unweighted pair group method with arithmetic mean (UPGMA) phylogenetic tree based on Nei's genetic distance was constructed using MEGA software (version 7.0) (Kumar et al. 2016). The polymorphism information content (PIC) of each locus and population was calculated using Cervus 3.0 (Kalinowski et al. 2007). The genotypes determined using COANCESTRY (V1.0.1.1; Wang 2011) were used to measure relatedness estimates (*R*) between generations and within-generation genotypes as described by Wang (2002), and the inbreeding coefficient (*F*) was determined as described by Ritland (1996). Microsatellite data were also analyzed using the STRUCTURE 2.3.3 program and the admixture model was used to estimate population genetic structure among and within species (Evanno et al. 2005). We conducted an analysis with ten iterations for each population size (*K*) of one–eight, and with the Markov chain Monte Carlo running for 500 000 iterations and an initial burn-in of 100 000 iterations. The *K* values described by Evanno et al. (2005) were calculated to identify the most reasonable *K* using the Structure Harvester program (Earl and vonHoldt 2012). The runs were averaged using CLUMPP version 1.1.2 (Jakobsson and Rosenberg 2007), and the results were visualized using DISTRUCT version 1.1 (Rosenberg 2004).

Results

Summary statistics. No evidence of allelic stutter or large allele dropouts was found in the dataset, and no null alleles were detected at any of the eight loci. Almost all eight loci were highly polymorphic (PIC > 0.5) (Botstein et al. 1980). In this study, microsatellite markers were used for the genetic analysis of three consecutive *P. vachellii* selective breeding generations. The genetic indicators of the eight microsatellite loci are listed in Table 2. The mean observed H_o was 0.80, the mean expected H_e was 0.7506, the mean N_a per locus was 8.625, the effective N_e was 4.448, and *I* was 1.6396. A comparison of the genetic information of three consecutive selective breeding generations of *P. vachellii* is shown in Table 3. A relatively high level of overall genetic diversity was observed (H_e = 0.6323–0.7663, PIC = 0.5754–0.7183), whereas the number of microsatellite alleles (N_a, N_e), heterozygosity (H_o, H_e), and PIC decreased slightly in the mass selection lines.

Genetic variation and differentiation among generations. AMOVA revealed that the variation among populations was only 6.33%, whereas the variation within populations was 93.67%. Wright (1965) proposed that $F_{st} < 0.05$ indicated low differentiation, $0.05 < F_{st} <$

Table 2. Genetic information of three consecutive *Pseudobagrus vachellii* selective breeding generations based on microsatellite markers.

Locus	Generation	H_o	H_e	PIC	N_a	N_e	I	P_{HW}
PV1	F1	0.8667	0.7701	0.7196	6	4.1190	1.5634	0.8594
	F2	0.8846	0.7006	0.6389	5	3.1962	1.3135	0.2015
	F3	0.5172	0.4398	0.5753	6	1.7613	0.9377	1.0000
	Total	0.7529	0.6788	0.6340	6	3.0751	1.3707	0.7430
PV2	F1	0.8667	0.8582	0.8274	12	6.4057	2.0987	0.0453^{P1}
	F2	0.7692	0.8303	0.7901	10	5.3865	1.8958	0.4104
	F3	1.0000	0.8234	0.4121	8	5.2399	1.7889	0.0817
	Total	0.8824	0.8940	0.8790	15	8.9863	2.3666	0.0433^{P1}
PV4	F1	0.8000	0.7989	0.7573	9	4.6632	1.7798	0.6263
	F2	0.6923	0.7504	0.7061	8	3.7871	1.6194	0.2022
	F3	0.7586	0.6479	0.7827	4	2.7529	1.1643	0.2692
	Total	0.7529	0.7513	0.7130	9	3.9513	1.6352	0.3439
PV6	F1	0.8000	0.7797	0.7340	8	4.2857	1.6859	0.2693
	F2	0.9615	0.8499	0.8138	9	6.0089	1.9566	0.9566
	F3	0.9655	0.8088	0.5814	7	4.8754	1.7118	0.0036^{P2}
	Total	0.9059	0.8315	0.8040	10	5.7662	1.9079	0.0303^{P1}
PV7	F1	0.9667	0.7073	0.6456	7	3.2847	1.4120	0.0170^{P1}
	F2	1.0000	0.6350	0.5457	4	2.6510	1.0729	0.0000^{P3}
	F3	1.0000	0.5420	0.7647	3	2.1399	0.8192	0.0000^{P3}
	Total	0.9882	0.7477	0.7000	8	3.8959	1.5027	0.0000^{P3}
PV9	F1	0.7333	0.7062	0.6587	8	3.2727	1.5158	0.4576
	F2	0.6154	0.6719	0.6279	8	2.9328	1.4405	0.2814
	F3	0.7931	0.7060	0.4230	6	3.2660	1.4314	0.8142
	Total	0.7176	0.7009	0.6690	9	3.2983	1.5740	0.6080
PV12	F1	0.8667	0.7701	0.7196	6	4.1190	1.5634	0.8605
	F2	0.8846	0.7014	0.6399	5	3.2038	1.3152	0.1813
	F3	0.5172	0.4398	0.6566	6	1.7613	0.9377	1.0000
	Total	0.7529	0.6797	0.6360	6	3.0837	1.3733	0.7151
Y73	F1	0.7000	0.7401	0.6842	6	3.6735	1.4767	0.8230
	F2	0.6538	0.6900	0.6187	5	3.0938	1.2538	0.6961
	F3	0.5862	0.6503	0.4121	5	2.7710	1.1687	0.5595
	Total	0.6471	0.7208	0.6640	6	3.5278	1.3864	0.8927
Mean ± SD		0.8000 ± 0.1062	0.7506 ± 0.0713	0.7124 ± 0.0810	8.625 ± 2.826	4.4481 ± 1.8974	1.6396 ± 0.3223	/

H_o = observed heterozygosity, H_e = expected heterozygosity, PIC = mean polymorphism information content per locus, N_a = number of alleles, N_e = effective allele number, I = Shannon diversity index, P_{HW} = Hardy–Weinberg probability test; SD = standard deviation; $^{P1} = P < 0.05$, $^{P2} = P < 0.01$, $^{P3} = P < 0.001$.

Table 3. Comparison of genetic information of three consecutive *Pseudobagrus vachellii* selective breeding generations.

Parameter	Generation		
	F1	F2	F3
n	30	26	29
N_a	7.750 ± 2.053	6.750 ± 2.25	5.625 ± 1.598
N_e	4.2279 ± 1.0049	3.7825 ± 1.2355	3.0709 ± 1.3356
I	1.6370 ± 0.2197	1.4835 ± 0.3146	1.2449 ± 0.3647
H_o	0.8250 ± 0.085	0.8077 ± 0.1454	0.7672 ± 0.2091
H_e	0.7663 ± 0.05	0.7287 ± 0.0761	0.6323 ± 0.1492
PIC	0.7183 ± 0.0542	0.6728 ± 0.0851	0.5754 ± 0.1425

n = number of fish specimens studied, N_a = number of alleles, N_e = effective allele number, I = Shannon diversity index, H_o = observed heterozygosity, H_e = expected heterozygosity, PIC = mean polymorphism information content per locus.

0.15 indicated moderate differentiation and $F_{st} > 0.15$ indicated high differentiation. The overall F_{st} value was 0.06329, which indicated a moderately differentiated degree ($0.05 < F_{st} < 0.15$) (Table 4). The F_{st} values for the three generations ranged from 0.0484–0.1286. The lowest genetic differentiation was observed between F2 and F3 ($F_{st} = 0.0484$) with the smallest genetic distance ($D_a = 0.142$), whereas the highest genetic differentiation was observed between F1 and F3 ($F_{st} = 0.1286$) with the largest genetic distance ($D_a = 0.4373$) (Table 5). The UPGMA phylogenetic tree based on Nei's genetic distance (Nei 1972) indicated that the three generations could divide the population into two clades. The analysis revealed that F2 and F3 formed sister relations and were clustered with F1 (Fig. 3). Structural analysis showed that $K = 2$ was the ideal number of subtypes; that is, three consecutive *Pseudobagrus vachellii* selective breeding generations were most likely to be divided into two different genetic clusters (Fig. 4). Different colors represent different genetic clusters in the figure, and the degree of gene purification increased with the development of breeding.

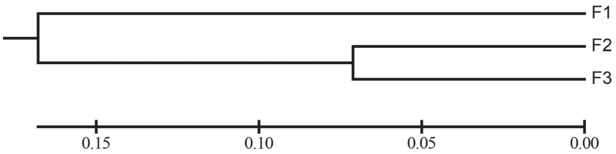

Figure 3. Nei's unweighted pair group method with arithmetic mean (UPGMA) tree of three consecutive *Pseudobagrus vachellii* selective breeding generations of based on microsatellites. Note: Scale bar denotes genetic distance.

Table 4. Analysis of molecular variance (AMOVA) results for three consecutive *Pseudobagrus vachellii* selective breeding generations using eight microsatellite loci.

Source of variation	DF	Sum of squares	Variance component	Percentage
Among populations	2	33.741	0.1934	8.26
Within populations	167	646.792	2.8619	91.74
Total	169	688.700	3.0553	100.00

Genetic differentiation (F_{st}) = 0.06329, DF = degrees of freedom.

Table 5. Genetic differentiation (F_{st}) values and Nei's genetic distance among three consecutive *Pseudobagrus vachellii* selective breeding generations.

Generation	F1	F2	F3
F1		0.05372	0.12864
F2	0.2336		0.04840
F3	0.4373	0.14210	

Note: Nei's genetic distance (below diagonal) and F_{st} (above diagonal).

Partner relatedness and inbreeding coefficient analysis. The results showed that the relation (R) and inbreeding coefficient (F) within each generation had positive values and were the largest in generation F3; the relatedness increased in succeeding generations (Table 6). The R value between generations was negative, except for in F2 and F3, which were positive. Although the F value among all three generations was negative compared to the relatedness between F1 and F2 (−0.08417), the relatedness between F1 and F3 decreased (−0.13296) (Table 7).

Table 6. Relation (R) and inbreeding coefficients (F) within each *Pseudobagrus vachellii* generation.

Coefficient	Generation		
	F1	F2	F3
R	0.01879	0.10225	0.28897
F	0.06303	0.01196	0.07394

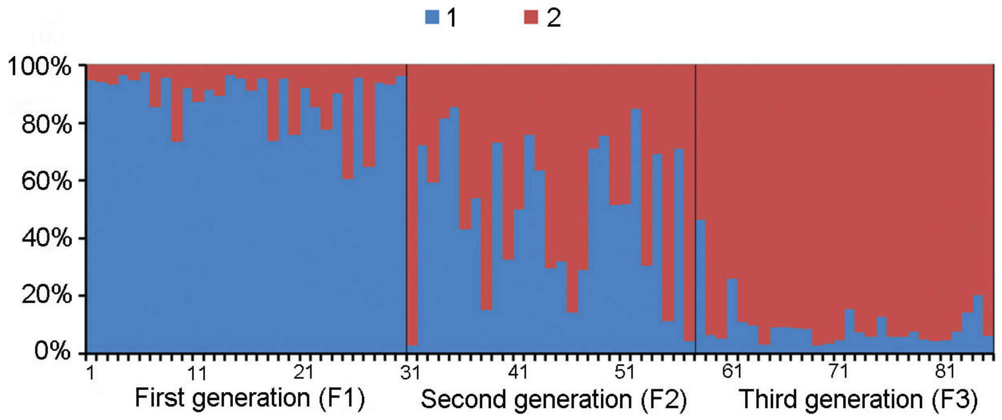

Figure 4. Population genetic structure of the three consecutive *Pseudobagrus vachellii* generations. The assignment results show that $K = 2$ (parameter introduced by Evanno et al. 2005). The two colors represent two different genetic clusters. The Y-axis denotes the proportion of ancestral components in an individual relative to other populations.

Table 7. Relation (*R*) and inbreeding coefficient (*F*) among three *Pseudobagrus vachellii* generations.

Generation	F1	F2	F3
F1		–0.08417	–0.13296
F2	–0.03138		0.09238
F3	–0.07943	–0.01061	

Note: The inbreeding coefficient (*F*) is below the diagonal, and the relation (*R*) is above the diagonal.

Discussion

Selection quickly improves certain traits, but the genetic diversity is usually lower than that of founder populations (Zhang et al. 2010). Many fish species have high fecundity and require relatively few parents to produce offspring; therefore, maintaining genetic diversity over successive generations is a recognized challenge for aquaculture breeding programs (Zhang et al. 2010; Ortega-Villaizan et al. 2011; Liu et al. 2018; Varney and Wilbur 2020). The presently reported study revealed that the genetic diversity of *Pseudobagrus vachellii* declined slightly after three generations of breeding. These results are similar to those obtained from other artificial breeding of aquatic animals. For example, a report showed that even when using a relatively large number of banana shrimp (*Penaeus merguiensis* De Man, 1888) broodstocks, a substantial loss of allelic diversity within lines over 14 generations is still observed (Knibb et al. 2014). Li et al. (2018) found a slight decrease in genetic diversity over three successive generations of early- and late-maturing strains of the Chinese mitten crab (*Eriocheir sinensis* Milne Edwards, 1853). In cultured silver-lipped pearl oysters, *Pinctada maxima* (Jameson, 1901), genetic diversity decreased, and the effective population size was reduced (Lind et al. 2009). High genetic diversity was observed among generations of Nile tilapia, *Oreochromis niloticus* (Linnaeus, 1758), in Ghana (Diyie et al. 2021), and Wang et al. (2022) reported that the genetic diversity of cultured *Procambarus clarkii* (Girard, 1852) tends to decline. These studies are important for ensuring the sustainability of the aquaculture industry.

Generally, $0.25 < \text{PIC} < 0.50$ meant that the single sequence repeat (SSR) loci were moderately polymorphic, and $\text{PIC} > 0.50$ meant that the SSR loci were highly polymorphic (Botstein et al. 1980). In the presently reported study, with an increase in breeding generations, the genetic diversity of the three artificially selected populations gradually decreased, and the PIC values were 0.7183, 0.6728, and 0.5754, respectively, indicating that the SSR loci were highly polymorphic. The overall number of alleles declined from 7.75 to 5.63, and a similar decline in the number of alleles was reported in previous studies (Zhang et al. 2018; Varney and Wilbur 2020). A study of three successive selection lines of Pacific abalone showed that the mean H_o and H_e values decreased from 0.679 to 0.622 and 0.756 to 0.649, respectively (Chen et al. 2017). These results were similar to those of the presently reported study in that after three consecutive *P. vachellii* selective breeding generations, the mean H_o and H_e values from the F1 generation to the F3 generation decreased from 0.8250 to 0.7672 and from 0.7663 to 0.6323, respectively. These results revealed a high level of genetic diversity in the three successive generations of breeding populations.

In the presently reported study, the F_{st} among the various generations of *P. vachellii* was 0.06329, indicating a moderate degree of differentiation. Additionally, the lowest genetic differentiation was observed between F2 and F3 ($F_{st} = 0.0484$), whereas the highest genetic differentiation was observed between F1 and F3 ($F_{st} = 0.12864$), indicating that the genetic similarity of the selected offspring increased gradually. However, the genetic structure of F3 changed significantly compared to that of F1.

In terms of successive generations of mass selection, strategies to avoid inbreeding are of critical concern (Fu et al. 2017). Inbreeding depression, through the loss of genetic variation, can ultimately limit long-term genetic progress through selective breeding (Evans et al. 2004; Varney and Wilbur 2020). The presently reported study showed that there was no inbreeding among the three generations; however, inbreeding occurred in each generation, and the largest inbreeding occurred in generation F3. These results are consistent with those of previous studies on long-term artificial selection, as genotypes become more homogeneous, leading to inbreeding depression (Zhang et al. 2010; Chen et al. 2017). Therefore, in the subsequent breeding process, pooling of fertilized eggs from multiple crosses to create cohorts and moderate numbers of parents for each generation (at least 30 pairs) can be used to minimize the loss of genetic diversity and inbreeding depression.

In conclusion, the presently reported study revealed that the genetic similarity of the offspring increased gradually by artificial selection, and the genetic diversity of *P. vachellii* declined slightly after three generations of breeding. However, the level of genetic diversity was still high, which has the potential for further breeding. To minimize the negative influence of inbreeding, new strains can be bred by appropriately increasing the number of breeding parents in the subsequent breeding process, thereby reducing the probability of inbreeding and adopting high selection pressure.

Acknowledgments

This work was financially supported by the Young Talent Program of Anhui Academy of Agricultural Sciences (2023–2027) and the Wuhu City Science and Technology Planning Project (No. 2022ly15).

References

Botstein D, White RL, Skolnick MH, Davis R (1980) Construction of a genetic linkage map in man using restriction fragment length polymorphisms. American Journal of Human Genetics 32(3): 314–331. https://doi.org/10.1017/S0016672300034467

Chen N, Luo X, Lu C, Ke C, You W (2017) Effects of artificial selection practices on loss of genetic diversity in the Pacific abalone, *Haliotis discus hannai*. Aquaculture Research 48(9): 4923–4933. https://doi.org/10.1111/are.13311

Diyie RL, Agyarkwa SK, Armah E, Amonoo NA, Owusu-Frimpong I, Osei-Atweneboana MY (2021) Genetic variations among different generations and cultured populations of Nile tilapia (*Oreochromis niloticus*) in Ghana: Application of microsatellite markers. Aquaculture 544: 737070. https://doi.org/10.1016/j.aquaculture.2021.737070

Duan G, Zhou H, Wang H, Ling J, Hu Y, Pan T, Yang M, Wu L, Jiang H (2023) [Analysis of the morphological traits effects on body weight of 60 days old breeding groups of *Pelteobagrus vachelli* [sic].] Anhui Nongye Daxue xuebao—Journal of Anhui Agricultural University 50: 78–85. [In Chinese]

Earl DA, vonHoldt BM (2012) STRUCTURE HARVESTER: A website and program for visualizing STRUCTURE output and implementing the Evanno method. Conservation Genetics Resources 4(2): 359–361. https://doi.org/10.1007/s12686-011-9548-7

Evanno G, Regnaut S, Goudet J (2005) Detecting the number of clusters of individuals using the software STRUCTURE: A simulation study. Molecular Ecology 14(8): 2611–2620. https://doi.org/10.1111/j.1365-294X.2005.02553.x

Evans F, Matson S, Brake J, Langdon C (2004) The effects of inbreeding on performance traits of adult Pacific oysters (*Crassostrea gigas*). Aquaculture 230(1–4): 89–98. https://doi.org/10.1016/j.aquaculture.2003.09.023

Excoffier L, Lischer HEL (2010) Arlequin suite ver 3.5: A new series of programs to perform population genetics analyses under Linux and Windows. Molecular Ecology Resources 10(3): 564–567. https://doi.org/10.1111/j.1755-0998.2010.02847.x

Fu J, Lü W, Li W, Shen M, Luo X, Ke C, You W (2017) Comparative assessment of the genetic variation in selectively bred generations from two geographic populations of ivory shell (*Babylonia areolata*). Aquaculture Research 48(8): 4205–4218. https://doi.org/10.1111/are.13241

Gjedrem T, Robinson N, Rye M (2012) The importance of selective breeding in aquaculture to meet future demands for animal protein: A review. Aquaculture 350–353: 117–129. https://doi.org/10.1016/j.aquaculture.2012.04.008

Holsinger K, Weir B (2009) Genetics in geographically structured populations: Defining, estimating and interpreting FST. Nature Reviews. Genetics 10(9): 639–650. https://doi.org/10.1038/nrg2611

Jakobsson M, Rosenberg NA (2007) CLUMPP: A cluster matching and permutation program for dealing with label switching and multimodality in analysis of population structure. Bioinformatics 23(14): 1801–1806. https://doi.org/10.1093/bioinformatics/btm233

Kalinowski ST, Taper ML, Marshall TC (2007) Revising how the computer program CERVUS accommodates genotyping error increases success in paternity assignment. Molecular Ecology 16(5): 1099–1106. https://doi.org/10.1111/j.1365-294X.2007.03089.x

Knibb W, Whatmore P, Lamont R, Quinn J, Powell D, Elizur A, Anderson T, Remilton C, Nguyen NH (2014) Can genetic diversity be maintained in long term mass selected populations without pedigree information?—A case study using banana shrimp *Fenneropenaeus merguiensis*. Aquaculture 428–429: 71–78. https://doi.org/10.1016/j.aquaculture.2014.02.026

Kumar S, Stecher G, Tamura K (2016) MEGA7: Molecular evolutionary genetics analysis version 7.0 for bigger datasets. Molecular Biology and Evolution 33(7): 1870–1874. https://doi.org/10.1093/molbev/msw054

Li Q, Wu X, He J, Liu Q, Cheng Y (2018) Can genetic diversity be maintained during mass selection of the Chinese mitten crab, *Eriocheir sinensis*? Aquaculture Research 49(4): 1606–1615. https://doi.org/10.1111/are.13616

Lind CE, Evans BS, Knauer J, Taylor JJ, Jerry DR (2009) Decreased genetic diversity and a reduced effective population size in cultured silver lipped pearl oysters (*Pinctada maxima*). Aquaculture 286(1–2): 12–19. https://doi.org/10.1016/j.aquaculture.2008.09.009

Liu D, Zhou Y, Yang K, Zhang X, Chen Y, Li C, Li H, Song Z (2018) Low genetic diversity in broodstocks of endangered Chinese sucker, *Myxocyprinus asiaticus*: Implications for artificial propagation and conservation. ZooKeys 792: 117–132. https://doi.org/10.3897/zookeys.792.23785

Nei M (1972) Genetic distance between populations. American Naturalist 106(949): 283–292. https://doi.org/10.1086/282771

Ortega-Villaizan M, Noguchi D, Taniguchi N (2011) Minimization of genetic diversity loss of endangered fish species captive broodstocks by means of minimal kinship selective crossbreeding. Aquaculture 318(1/2): 239–243. https://doi.org/10.1016/j.aquaculture.2011.04.047

Phuc TH, Vu NT, Nga N, Ky N, Nguyen NH (2021) Assessment of a long-term selective breeding program for giant freshwater prawn *Macrobrachium rosenbergii* since 2007. Aquaculture 541: e736745. https://doi.org/10.1016/j.aquaculture.2021.736745

Ritland K (1996) Estimators for pairwise relatedness and individual inbreeding coefficients. Genetical Research 67(2): 175–185. https://doi.org/10.1017/S0016672300033620

Rosenberg NA (2004) DISTRUCT: A program for the graphical display of population structure. Molecular Ecology Notes 4(1): 137–138. https://doi.org/10.1046/j.1471-8286.2003.00566.x

Swain SK, Sahu BP, Das SP, Sahoo L, Das PC, Das P (2022) Population genetic structure of fringe-lipped carp, *Labeo fimbriatus* from the peninsular rivers of India. 3 Biotech 12(11): e300. https://doi.org/10.1007/s13205-022-03369-y.

Van Oosterhout C, Hutchinson WF, Wills DP, Shipley P (2004) MICRO-CHECKER: Software for identifying and correcting genotyping errors in microsatellite data. Molecular Ecology Notes 4(3): 535–538. https://doi.org/10.1111/j.1471-8286.2004.00684.x

Varney RL, Wilbur AE (2020) Analysis of genetic variation and inbreeding among three lines of hatchery-reared *Crassostrea virginica* broodstock. Aquaculture 527: e735452. https://doi.org/10.1016/j.aquaculture.2020.735452

Wang Q, Guo W, Cheng W, Deng G, Xu H, Xia R (2021) Isolation of microsatellite markers for *Pelteobagrus vachellii* based on RAD sequencing. Fisheries Science and Technology Information 48(5): 250–254. https://doi.org/10.16446/j.fsti.20200700123

Wang H, Jiang H, Duan G, Song G, Ling J, Pan T, Hu Y, Zhou H, Yang M (2022) The genetic diversity of the rice-crayfish eco-farming *Procambarus clarkii* in Anhui Province, China. Turkish Journal of Fisheries and Aquatic Sciences 22(1): TRJFAS19904. https://doi.org/10.4194/TRJFAS19904

Wang J (2002) An estimator for pairwise relatedness using molecular markers. Genetics 160(3): 1203–1215. https://doi.org/10.1093/genetics/160.3.1203

Wang J (2011) COANCESTRY: a program for simulating, estimating and analysing relatedness and inbreeding coefficients. Molecular Ecology Resources 11(1): 141–145. https://doi.org/10.1111/j.1755-0998.2010.02885.x

Wright S (1965) The interpretation of population structure by F-statistics with special regard to systems of mating. Evolution; International Journal of Organic Evolution 3(3): 395–420. https://doi.org/10.2307/2406450

Yeh FC, Yang RC, Boyle TBJ, Ye ZH, Mao JX (1997) POPGENE, the user-friendly shareware for population genetic analysis. Molecular Biology and Biotechnology Center, University of Alberta, Canada.

Zhang T, Kong J, Wang W, Wang Q (2010) Genetic variability assessed by microsatellites in the breeding populations of the shrimp *Penaeus* (*Fenneropenaeus*) *chinensis* in China. Aquaculture 310(1–2): 229–233. https://doi.org/10.1016/j.aquaculture.2010.07.025

Zhang J, Li Q, Wang Q, Cong R, Ge J, Kong L (2018) The impact of successive mass selection on population genetic structure in the Pacific oyster (*Crassostrea gigas*) revealed by microsatellite markers. Aquaculture International 26(1): 113–125. https://doi.org/10.1007/s10499-017-0196-0

Zheng X, Xu J, Zhang J, Wang T, Yin S (2020) [Genetic diversity analysis in four different geographical populations of yellow catfish *Pelteobagrus vachelli* [sic] by microsatellite markers.] Shuichan kexue—Fishery Sciences 39(5): 657–668. [In Chinese] https://doi.org/10.16378/j.cnki.1003-1111.2020.05.003

Zheng X, Fu D, Cheng J, Tang R, Yin S (2021) Effects of hypoxic stress and recovery on oxidative stress, apoptosis, and intestinal microorganisms in *Pelteobagrus vachelli* [sic]. Aquaculture 543: e736945. https://doi.org/10.1016/j.aquaculture.2021.736945

Acta Ichthyologica et Piscatoria 54, 2024, 21–25 | DOI 10.3897/aiep.54.115071

PENSOFT.

ACTA
ICHTHYOLOGICA
ET PISCATORIA

First record of Triacanthidae Bleeker, 1859 (Actinopterygii: Tetraodontiformes) from the Red Sea

M. P. GOUTHAM-BHARATHI[1], T. K. SIRAJUDHEEN[1], Ronald Grech SANTUCCI[1], Ronald FRICKE[2], Mark DIMECH[1]

1 *KAUST—Beacon Development, King Abdullah University of Science and Technology, Thuwal, Jeddah, Saudi Arabia*
2 *Staatliches Museum für Naturkunde, Stuttgart, Germany*

https://zoobank.org/C37C2967-7411-4BDF-A8BD-1B291EFEB80B

Corresponding author: M. P. Goutham-Bharathi (goutham.muthupalani@kaust.edu.sa)

Academic editor: Adnan Tokaç ♦ **Received** 1 November 2023 ♦ **Accepted** 17 December 2023 ♦ **Published** 29 January 2024

Citation: Goutham-Bharathi MP, Sirajudheen TK, Santucci RG, Fricke R, Dimech M (2024) First record of Triacanthidae Bleeker, 1859 (Actinopterygii: Tetraodontiformes) from the Red Sea. Acta Ichthyologica et Piscatoria 54: 21–25. https://doi.org/10.3897/aiep.54.115071

Abstract

The Tetraodontiform family Triacanthidae Bleeker, 1859 is recorded for the first time from the Red Sea. Fishing experiments employing a commercial shrimp trawler off Jizan, Saudi Arabia, revealed species occurrences of short-nosed tripodfish, *Triacanthus biaculeatus* (Bloch, 1786) at depths ranging from about 11 to 34 m. Currently, this species has only been found in shallow sandy/muddy habitats in the southern Red Sea. Further surveys are imperative to demonstrate the actual distribution of short-nosed tripodfish across a wider range of environmental gradients along the Red Sea.

Keywords

marine record, Saudi Arabia, short-nosed tripodfish, trawl, *Triacanthus biaculeatus*

Introduction

The Tetraodontiform fish family Triacanthidae Bleeker, 1859, commonly known as triplespines or tripodfishes, are found on continental shelves in the Indo–West Pacific, usually just below the sea surface down to the depth of 60 m (Tyler 1968). These small-sized fishes (>30 cm TL) are benthic, usually inhabiting sandy or weed-covered bottoms in shallow coastal waters (Heemstra et al. 2022). Seven species in four genera viz., *Pseudotriacanthus* Fraser-Brunner, 1941 (one species), *Triacanthus* Oken, 1817 (two species), *Tripodichthys* Tyler, 1968 (three species), and *Trixiphichthys* Fraser-Brunner, 1941 (one species) are recognized globally (Tyler 1968; Matsuura 2015; Heemstra et al. 2022). Recent fishing experiments off Jizan, Saudi Arabia, revealed occurrences of the short-nosed tripodfish, *Triacanthus biaculeatus* (Bloch, 1786) at depths ranging from about 11 to 34 m, constituting the first documented record of the family Triacanthidae from the Red Sea.

Materials and methods

Fishing experiments employing a commercial shrimp trawler were carried out as part of stock assessment and selectivity studies during May–August 2023 off Jizan in the southern Red Sea coast of Saudi Arabia. Species occurrences of short-nosed tripodfish ($n = 19$) were recorded from seven hauls at depths ranging from about 11 to 34 m (Table 1; Fig. 1). Three voucher specimens were collected as part of faunal surveys, fixed in 10% formalin and then later transferred to 70% ethanol for further analysis. Fishing experiments were conducted employing an authorized fishing vessel operating along the southern

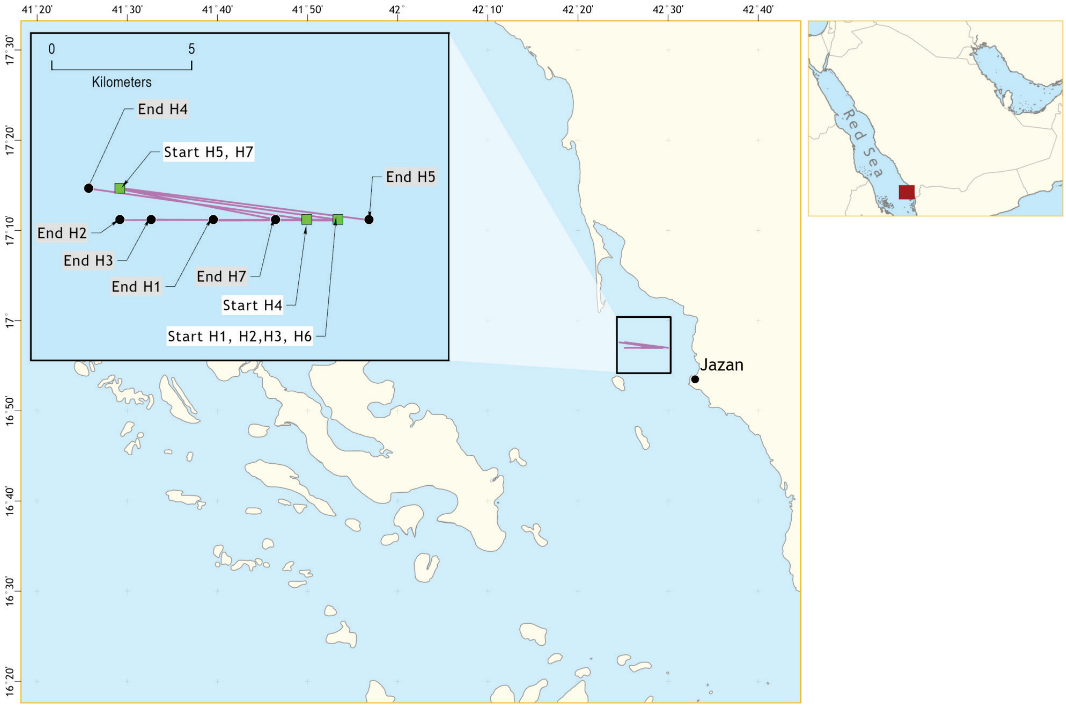

Figure 1. Map of the Red Sea showing experimental fishing hauls ($n = 7$) where species occurrences of *Triacanthus biaculeatus* (Bloch, 1786) were recorded.

Table 1. Geographic coordinates of the experimental fishing hauls ($n = 7$) where species occurrences of *Triacanthus biaculeatus* (Bloch, 1786) were recorded (southern Red Sea coast of Saudi Arabia; 2023).

Haul No.	Date	GPS coordinates		Depth [m]		*N*
		Start	End	Start	End	
H1	31 May	16°56.013′N, 042°29.248′E	16°56.908′N, 042°27.058′E	23.4	26.7	1
H2	20 Jun	16°56.968′N, 042°29.447′E	16°56.880′N, 042°25.405′E	24.3	34	1
H3	20 Jun	16°56.921′N, 042°29.409′E	16°56.763′N, 042°26.010′E	23.7	34	1
H4	15 Aug	16°56.922′N, 042°29.091′E	16°57.480′N, 042°24.689′E	13.3	20.9	3
H5	15 Aug	16°57.340′N, 042°25.119′E	16°57.003′N, 042°29.740′E	20.9	11.4	4
H6	15 Aug	16°57.022′N, 042°29.561′E	16°57.456′N, 042°24.939′E	20.9	20.9	4
H7	15 Aug	16°57.730′N, 042°25.122′E	16°56.845′N, 042°28.363′E	19	13.3	5

N = number of specimens recorded.

Red Sea coast of Saudi Arabia. All three specimens were already dead when collected. *Triacanthus biaculeatus* is currently not listed as threatened according to the IUCN Red List of Threatened Species (Matsuura and Motomura 2015).

Species identification followed Carpenter et al. (1997), Matsuura (2001), and Heemstra et al. (2022). Genus and species classifications followed Fricke et al. (2023a); family authorship followed van der Laan et al. (2014). Morphometrics were measured to the nearest 1 mm using a fish ruler and a digital Vernier caliper to the nearest 0.1 mm. The specimens were deposited to the faunal collections of Beacon Development—King Abdullah University of Science and Technology, Saudi Arabia. A short taxonomic description is provided based on the voucher specimens from the Red Sea along with a note on their geographical distribution in the Indo–Pacific. Data on the distribution of *T. biaculeatus* (map was generated using SimpleMappr; Shorthouse 2010) is based on published literature and it does not represent exhaustive inventories. Abbreviated synonymies include original descriptions and key references.

Results

Family Triacanthidae Bleeker, 1859
Genus *Triacanthus* Oken, 1817

Triacanthus biaculeatus (Bloch, 1786)

English vernacular name: short-nosed tripodfish

(Fig. 2; Table 2)

Balistes biaculeatus Bloch, 1786.—Bloch (1786): 17, pl. 148 (2) [type locality: “Ostindien” (Indonesia)].

Triacanthus biaculeatus (Bloch, 1786).—Carpenter et al. (1997): 235.—Matsuura (2001): 3908.—Heemstra et al. (2022): 414, pl. 105, 106.

Material examined. SAUDI ARABIA, southern Red Sea, Jizan; three specimens were trawled from a sandy/muddy habitat between 16°56.922′N, 042°29.091′E and 16°57.480′N, 042°24.689′E; 15 Aug. 2023; M.P. Goutham-Bharathi leg., BD/KAUST-0823-003 (155 mm TL); BD/KAUST-0823-004 (180 mm TL); BD/KAUST-0823-005 (200 mm TL); 13.3–20.9 m.

Figure 2. *Triacanthus biaculeatus* (Bloch, 1786) [BD/KAUST-0823-004]; 180 mm TL; Jizan, southern Red Sea, Saudi Arabia.

Table 2. Morphometric and meristic data of *Triacanthus biaculeatus* (Bloch, 1786) collected from the southern Red Sea coast of Saudi Arabia in 2023.

Character	Specimen number		
	BD/KAUST-0823-003	BD/KAUST-0823-004	BD/KAUST-0823-005
Morphometrics			
Total length [mm]	155	180	200
Standard length (SL) [mm]	120	137	154
Head length [mm]	33.9	39.9	43.7
Pre-dorsal length [mm]	45.5	52.3	59.1
Body depth [mm]	42.9	50.7	55.0
Snout length [%SL]	16.1	18.8	16.2
Second spine of dorsal fin [%SL]	7.0	7.8	5.6
Post orbital length [%SL]	6.9	8.1	7.1
Meristics			
Dorsal fin spines	5	5	5
Dorsal fin rays	24	24	25
Anal fin rays	21	20	20
Pectoral fin rays	16	14	15

Description. Body moderately elongated, strongly compressed, head profile from above eye to first dorsal-fin spine base slightly convex to straight; skin moderately thick with minute scales, upright spinules on each scale producing rough shagreen-like appearance; mouth small, terminal, snout moderately acute; five dorsal spines; anterior dorsal fin membrane black, spiny dorsal-fin membrane very dark between first and third spines, equally dark between third and fifth spines; caudal peduncle tapering distinctly, wider than deep.

Color. The coloration of the freshly collected specimens was silvery, upper half of body dusky and pale below with indistinct pale mid-lateral stripe; large dark blotch on dorsum beneath spiny dorsal fins; soft dorsal, anal and pectoral fins yellowish; caudal fin dark yellow.

Discussion

Triacanthus biaculeatus is differentiated from its congener, *Triacanthus nieuhofii* Bleeker, 1852 by the first dorsal fin coloration (spiny dorsal-fin membrane very dark between first and third spines, and usually equally dark between third and fifth spines vs. very dark between first and second spines, slightly to less dark between second and third spines, and pale between third and fifth spines) and the outline of head from base of first dorsal-fin spine to above eye (slightly convex or almost a straight line vs. convex in front of spine and then straight or slightly concave over eye) (Matsuura 2015; Mohanty et al. 2018).

Triacanthus biaculeatus is widespread across the whole Indo–West Pacific (Matsuura 2001; Santini and Tyler 2002; Fricke et al. 2023a), ranging from the Persian/Arabian Gulf to South Africa (Eastern Cape) and India and Sri Lanka, and Mauritius; elsewhere to Bay of Bengal (India), Indonesia, Taiwan, Philippines, China, Korea, central Japan, Western Australia and Queensland (Australia) (Bishop 2003; Heemstra et al. 2022; Fricke et al. 2023a). *Triacanthus biaculeatus* is hitherto unknown from the Arabian coasts and Madagascar (Santini and Tyler 2002; Fricke et al. 2018); the presently reported study constitutes the first documented record of this species for the Red Sea from Jizan, Saudi Arabia (Fig. 3).

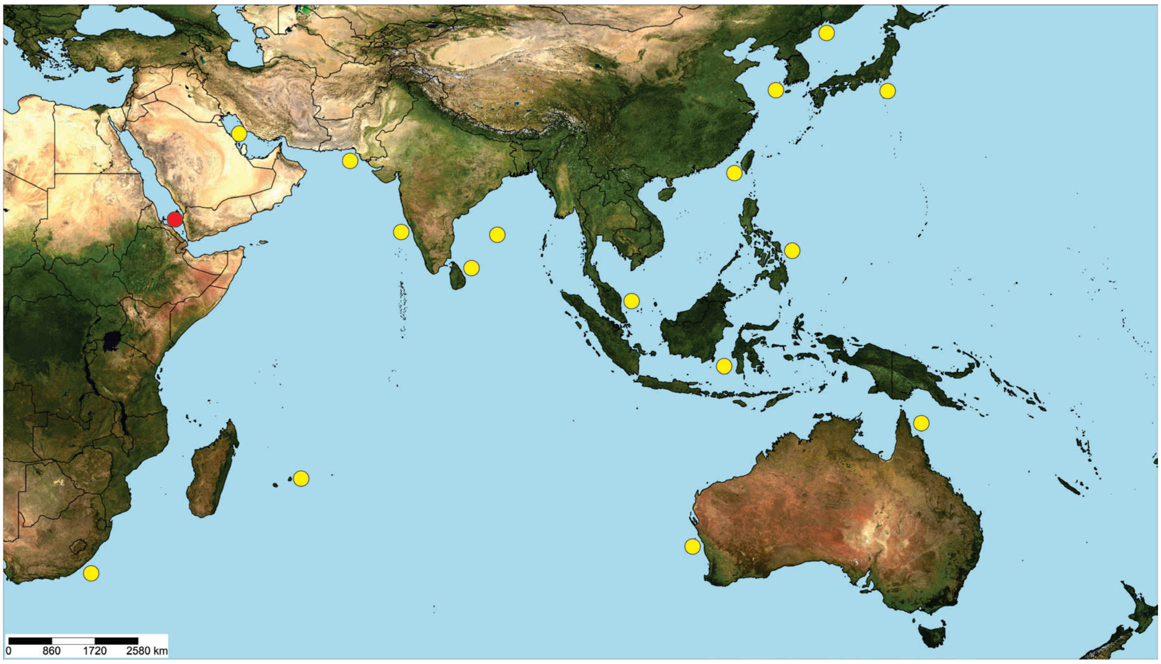

Figure 3. Distribution of *Triacanthus biaculeatus* (Bloch, 1786) in the Indo–West Pacific. Yellow closed circles = previous records; red closed circle = presently reported record (the map was generated using SimpleMappr; Shorthouse 2010).

A total of ten extant Tetraodontiform fish families are recognized globally (Matsuura 2015; Fricke et al. 2023b) of which, six are known from the Red Sea: Balistidae Rafinesque, 1810, Diodontidae Bonaparte, 1835, Molidae Bonaparte, 1835, Monacanthidae Nardo, 1843, Ostraciidae Rafinesque, 1810, and Tetraodontidae Bonaparte, 1831 (see Golani and Bogorodsky 2010; Golani and Fricke 2018). Including the presently reported new record, the Tetraodontiform fish fauna of the Red Sea now comprises 48 species distributed among seven families (Golani and Bogorodsky 2010; Golani and Fricke 2018; Matsuura et al. 2020).

Currently, *T. biaculeatus* seems restricted to shallow sandy/muddy habitats in the southern Red Sea. According to Bogorodsky et al. (2014), the increased number of new records from the southern Red Sea could be attributable to the recent expansion of fish populations from the Gulf of Aden or other parts of the northwestern Indian Ocean. Based on its wider geographic distribution in the Indo–Pacific (Matsuura 2001) and its abundance in the trawling grounds along the Persian/Arabian Gulf (Carpenter et al. 1997), it is highly likely that *T. biaculeatus* could have naturally expanded its distribution and a breeding population already exists regionally in the southern Red Sea. Further surveys are imperative to demonstrate the actual distribution of this species across a wide range of environmental gradients along the Red Sea.

Acknowledgments

The authors thank the Ministry of Environment, Water and Agriculture, Saudi Arabia, for funding the research project on the Assessment of the major fish stocks in the Red Sea waters of the Kingdom. We thank Dia A. Elbashier and Badraldinn K. Albashier, Fisheries Field Specialists, and the trawler crew for their support during the fishing experiments and sampling. Abhishekh P. Vijayan is acknowledged for his assistance in the preparation of the map of the Red Sea showing experimental fishing hauls.

References

Bishop JM (2003) History and current checklist of Kuwait's ichthyofauna. Journal of Arid Environments 54(1): 237–256. https://doi.org/10.1006/jare.2001.0874

Bloch ME (1786) Naturgeschichte der ausländischen Fische. Band 2. Berlin, i–viii + 1–160, pls. 145–180.

Bogorodsky SV, Alpermann TJ, Mal AO, Gabr MH (2014) Survey of demersal fishes from southern Saudi Arabia, with five new records for the Red Sea. Zootaxa 3852(4): 401–437. https://doi.org/10.11646/zootaxa.3852.4.1

Carpenter KE, Krupp F, Jones DA, Zajonz U (1997) FAO species identification field guide for fishery purposes. The living marine resources of Kuwait. Eastern Saudi Arabia, Bahrain, Qatar, and the United Arab Emirates, FAO, Rome, 293 pp.

Fricke R, Mahafina J, Behivoke F, Jaonalison H, Léopold M, Ponton D (2018) Annotated checklist of the fishes of Madagascar, southwestern Indian Ocean, with 158 new records. FishTaxa: Journal of Fish Taxonomy 3(1): 1–432.

Fricke R, Eschmeyer WN, van der Laan R (Eds.) (2023a) Eschmeyer's catalog of fishes: Genera, species, references. Online version, updated 2 Oct. 2023. Internet publication, California Academy of Sciences, San Francisco, CA, USA. http://research.calacademy.org/research/Ichthyology/Catalog/fishcatmain.asp

Fricke R, Eschmeyer WN, Fong JD (2023b) Genera/species by family/subfamily in Eschmeyer's Catalog of Fishes. Online version, updated 2 Oct. 2023. Internet publication, California Academy of Sciences, San Francisco, CA, USA. http://researcharchive.calacademy.org/research/ichthyology/catalog/SpeciesByFamily.asp

Golani D, Bogorodsky SV (2010) The fishes of the Red Sea—Reappraisal and updated checklist. Zootaxa 2463(1): 1–135. https://doi.org/10.11646/zootaxa.2463.1.1

Golani D, Fricke R (2018) Checklist of the Red Sea fishes with delineation of the Gulf of Suez, Gulf of Aqaba, endemism and Lessepsian migrants. Zootaxa 4509(1): 1–215. https://doi.org/10.11646/zootaxa.4509.1.1

Heemstra PC, Heemstra E, Ebert DA, Holleman W, Randall JE (2022) Coastal fishes of the western Indian Ocean. Vol. 5. South African Institute for Aquatic Biodiversity, 491 pp.

Matsuura K (2001) Triacanthodidae, Triacanthidae, Balistidae, Ostraciidae, Aracanidae, Triodontidae, Tetraodontidae. Pp. 3902–3928, 3948–3957. In: Carpenter KE, Niem VH (Eds) FAO species identification guide for fishery purposes. The living marine resources of the Western Central Pacific. Vol 6. Bony fishes part 4 (Labridae to Latimeriidae). FAO, Rome.

Matsuura K (2015) Taxonomy and systematics of tetraodontiform fishes: A review focusing primarily on progress in the period from 1980 to 2014. Ichthyological Research 62(1): 72–113. https://doi.org/10.1007/s10228-014-0444-5

Matsuura K, Motomura H (2015) *Triacanthus biaculeatus* (Persian Gulf assessment). The IUCN Red List of Threatened Species 2015: e.T193795A57283390. [Accessed on 13 January 2024].

Matsuura K, Bogorodsky SV, Mal AO, Alpermann TJ (2020) Canthigaster aziz, a new deep-dwelling toby fish (Tetraodontiformes: Tetraodontidae) from the Red Sea. Zootaxa 4834(1): 81–95. https://doi.org/10.11646/zootaxa.4834.1.5

Mohanty SR, Mohapatra A, Mishra SS (2018) First record of Triacanthus nieuhofii Bleeker, 1852 (Tetraodontiformes: Triacanthidae) from northern east coast of India. Records of the Zoological Survey of India 118(3): 310–313. https://doi.org/10.26515/rzsi/v118/i3/2018/118502

Santini F, Tyler JC (2002) Phylogeny and biogeography of the extant species of triplespine fishes (Triacanthidae, Tetraodontiformes). Zoologica Scripta 31(4): 321–330. https://doi.org/10.1046/j.1463-6409.2002.00097.x

Shorthouse DP (2010) SimpleMappr, an online tool to produce publication-quality point maps. [Accessed 16 October 2023] https://www.simplemappr.net

Tyler JC (1968) A monograph on plectognath fishes of the superfamily Triacanthoidea. Monographs—Academy of Natural Sciences of Philadelphia 16: 1–364.

van der Laan R, Eschmeyer WN, Fricke R (2014) Family-group names of recent fishes. Zootaxa 3882(1): 1–230. https://doi.org/10.11646/zootaxa.3882.1.1

Acta Ichthyologica et Piscatoria 54, 2024, 27–36 | DOI 10.3897/aiep.54.114014

PENSOFT.

ACTA
ICHTHYOLOGICA
ET PISCATORIA

Relations between morphological traits and body weight of shortbelly eel, *Dysomma anguillare* (Actinopterygii: Anguilliformes: Synaphobranchidae), from coastal waters of Zhoushan, East China Sea, determined by multivariate analyses

Ziyan ZHU[1], Tianyan YANG[1], Sige WANG[1]

1 *Fishery College, Zhejiang Ocean University, Zhoushan, China*

https://zoobank.org/14728E68-E38F-4B9A-BD32-DABBAD698B52

Corresponding author: Tianyan Yang (hellojelly1130@163.com)

Academic editor: Sanja Matić-Skoko ◆ **Received** 11 October 2023 ◆ **Accepted** 5 December 2023 ◆ **Published** 31 January 2024

Citation: Zhu Z, Yang T, Wang S (2024) Relations between morphological traits and body weight of shortbelly eel, *Dysomma anguillare* (Actinopterygii: Anguilliformes: Synaphobranchidae), from coastal waters of Zhoushan, East China Sea, determined by multivariate analyses. Acta Ichthyologica et Piscatoria 54: 27–36. https://doi.org/10.3897/aiep.54.114014

Abstract

The shortbelly eel, *Dysomma anguillare* Barnard, 1923, is an essential component in the food chain of the marine ecosystem and plays an important role in nearshore fisheries and biodiversity in the East China Sea. In order to provide theoretical support for fishery resource assessment and sustainable utilization of *D. anguillare*, an important bycatch in the offshore area of China, the relations between morphological traits and body weight were investigated based on the measurement of 28 metric traits for the first time. The correlation analysis showed that 25 morphological traits were significantly ($P < 0.05$) correlated with the logarithm of body weight ($\lg X_0$), in which the correlation coefficient of the total length (X_1) was the largest with the extremely high significance ($P < 0.01$). The optimum multiple regression equation of morphological traits was constructed after deleting redundant independent variables: $\lg X_0 = 0.367 + 0.003X_1 + 0.010X_7 - 0.010X_8 + 0.011X_{10} + 0.042X_{14} + 0.006X_{15} + 0.024X_{19} - 0.004X_{23}$. The total length ($X_1$) had the highest positive direct relation with $\lg X_0$ (0.699), which was in accordance with the results of determinate coefficient analysis, while the indirect effect of body height (X_7) through lower jaw length (X_{19}) to $\lg X_0$ was the greatest. The gray correlation analysis indicated that body length (X_2) and distance from snout to dorsal fin origin (X_{22}) were the most closely related to body weight. The comprehensive comparison showed that X_1, X_2, and X_{22} should be used as the ideal morphometric traits for measuring the body weight of *D. anguillare*, and the conclusions obtained from this study will provide valuable references for fishery resource management of this commercial fish species.

Keywords

body weight, *Dysomma anguillare*, gray relational analysis, morphological traits, path analysis

Introduction

The shortbelly eel, *Dysomma anguillare* Barnard, 1923, belonging to the order Anguilliformes and family Synaphobranchidae, is a demersal fish species that is widely distributed in the tropical Indian and western Pacific oceans (Nelson et al. 2016). In China, *D. anguillare* mainly inhabits the nearshore waters and estuaries of the South China Sea and the southern East China Sea (Chen and Zhang 2015). As one of the few widespread species of the genus *Dysomma*, it is also an important bycatch during bottom trawling off the southeastern coasts of China (Zhang 2010). Gradual research progress on ecology, population structure, and molecular genetics of this fish species has been made in recent years (Zhang and Tang 2003; Du et al. 2018; Wang et al. 2019; Yang et al. 2022), but fundamental information on fishery resources biology is still very limited. Ascertaining the biological and genetic backgrounds of target species is the prerequisite and basis for scientific fishery management and biodiversity conservation (Gulland and Carroz 1969).

Body weight is an essential trait for growth and a direct reflection of production performance, which is correlated with various morphological traits. By analyzing the relations between the morphological traits and body weight of economic fishes, ichthyologists can provide reliable suggestions for population resource assessment and the optimum catchable size (William 2011). However, body weight is susceptible to genetic variation, pleiotropy, and the complicated changing environment, and it is inconvenient and imprecise to determine their body weight while fish are still alive. Therefore, the measured values available from other morphological traits are needed to acquire the body weight indirectly.

Recently, published studies have already demonstrated that the correlations between morphological traits and body weight can be clarified by multivariate analysis in many aquatic animals, such as fishes (He et al. 2017; Uiuiu et al. 2017; Yang et al. 2020), crustaceans (Ma et al. 2013; Jiang et al. 2017; Zou et al. 2017), cephalopods (Chen et al. 2012), gastropods (Zhao et al. 2014), and bivalves (Zhang et al. 2018; Guo et al. 2021). Until now, however, there have been no reports on the morphology of *D. anguillare.* Existing research results of the trophic niche and population dynamics of *D. anguillare* have shown a sign of resource decline in the East China Sea since 2018 (Du et al. 2018; Yang et al. 2022), which might be related to the long-term fishing pressure, as well as climate change. In practice, understanding the correlation between morphological traits and body weight of fishery species contributes to formulating mesh size and minimum landing allowable catch size, and then helps to maintain the proper population size to achieve sustainable utilization of the fishery resources. Thus, in this study, correlation analysis, regression analysis, path analysis, determination analysis, and gray correlation analysis were comprehensively applied to characterize the morphological traits and ascertain their effects on the body weight of *D. anguillare*. The main purpose of this study was to fill the gaps of basic biological data on *D. anguillare* and to better understand the dominant shape traits that influence body weight, to lay a foundation for sustainable exploitation and utilization of commercial eels in the future.

Materials and methods

A total of 85 specimens of *Dysomma anguillare* were collected by trawling in the coastal waters of the Zhoushan Archipelago, East China Sea in October 2022. Frozen fish individuals were transported to the Fishery Ecology and Biodiversity Laboratory (FEBL) of the Zhejiang Ocean University of China for further analysis. The body weight (X_0), was obtained by an electronic balance to the nearest 0.01 g, and the measurable characters were determined by a digital vernier caliper and a ruler with the accuracies of 0.01 mm and 1 mm, respectively. Twenty-seven measurable parameters are depicted in Fig. 1.

Microsoft Excel 2019 was used for calculating the path coefficients and determination coefficients. Multivariate analyses such as correlation analysis, regression analysis, and path analysis are conducted to reveal the direct and indirect effects of morphological traits on body weight by using SPSS 26.0 software (Field 2005).

Kolmogorov–Smirnov test (K–S test) and Shapiro–Wilk test (S–W test) are two commonly used normal test methods, and are suitable for statistical analysis with large samples ($n > 50$) and small samples ($n \leq 50$), respectively (Shapiro and Wilk 1965; Tikhomirov 1993). The P-value lower than the significance level of 0.05 implies the null hypothesis is rejected and it is assumed that the data is non-normally distributed (Tong 1990). Only data meeting the normal distribution can be used for the subsequent correlation analysis and regression analysis, and conversion can be applied if the raw data cannot satisfy the condition.

Correlation analysis can be performed through the software SPSS 26.0 after confirming the normal distribution of the data. It can be distinguished whether the two morphological traits are related to the analysis of the significance level (Singh and Chaudhary 1979). The two morphological traits are related or extremely related if the significance is at 0.05 level ($P < 0.05$) or at 0.01 level ($P < 0.01$), respectively. Otherwise, they have no relation ($P > 0.05$).

The aim of multiple regression analysis is to find out the linear relation between body weight and the related morphological traits. After removing the morphological traits unrelated to the body weight based on correlation analysis, the effects of morphological traits on the body weight are studied by stepwise multiple regression analysis (Wittink and Heights 1988). The significance test (T-test) is performed on the partial regression coefficient (B), or non-standardized regression coefficient for each independent variable to verify the validity of the established regression equation. Furthermore, the F-test is used to check the significance of the multiple regression equation.

The path analysis reflects the effects of the independent variables on the dependent variable, and it can be divided into parts: the direct effects of each trait on body weight and the indirect effects of each trait on body weight through other traits (Sheng and Wu 1999). These two effects can be assessed by the direct and indirect path coefficients, respectively. The direct path coefficient, also named the path coefficient, is the same as the standardized regression coefficient obtained directly from multiple regression analysis. And the indirect path coefficient ($P_{X_iX_j}$) can be calculated from the formula [1] below.

$$P_{X_iX_j} = r_{X_iX_j} \times P_{X_j} \qquad [1]$$

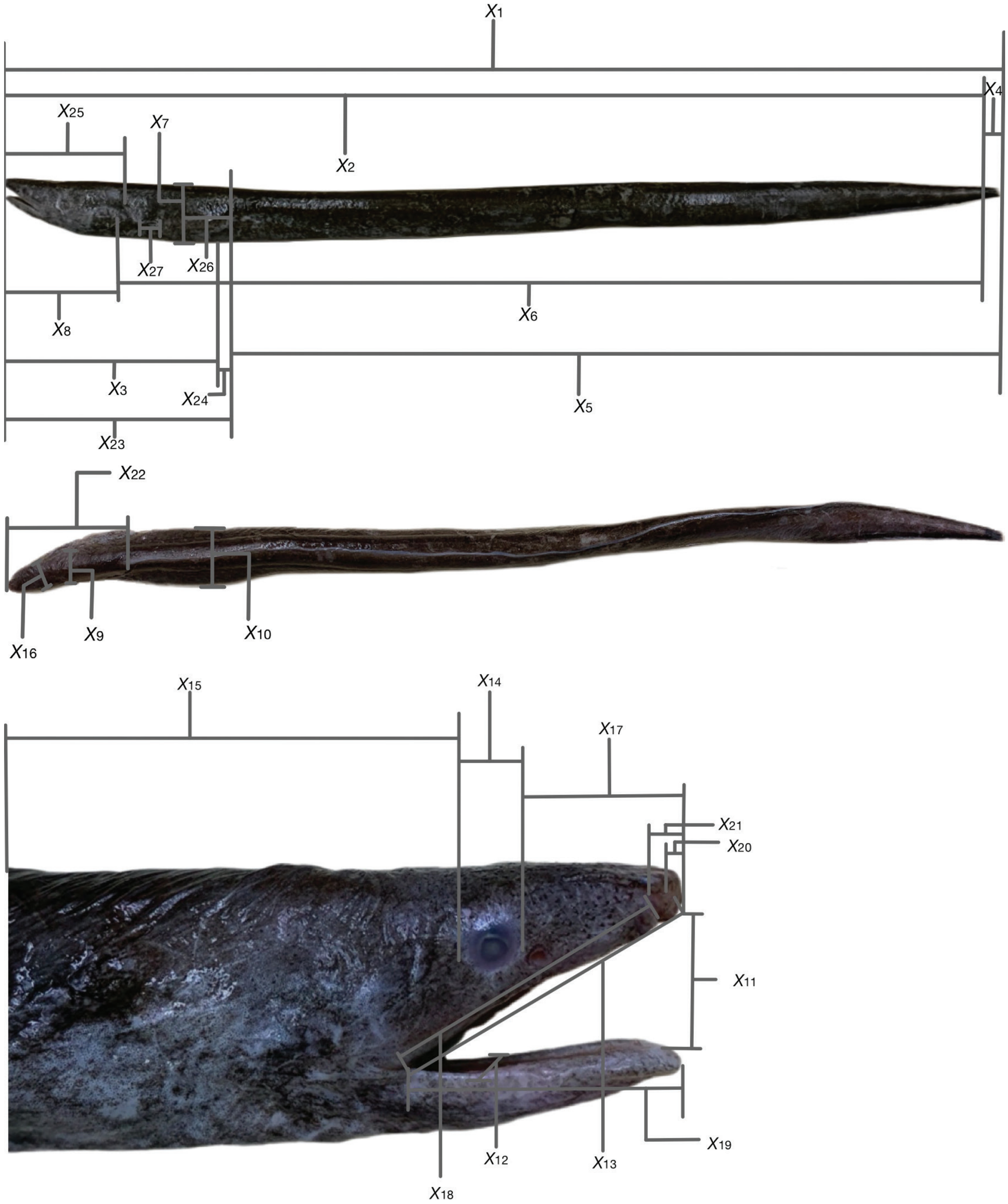

Figure 1. Diagrams of morphometric measurements of *Dysomma anguillare.* (**A**) Lateral view (**B**) Dorsal view (**C**) Head view. Abbreviations: X_1 = total length, X_2 = body length, X_3 = anal length, X_4 = tail length, X_5 = postanal length, X_6 = trunk length, X_7 = body height, X_8 = head length, X_9 = head breadth, X_{10} = body width, X_{11} = oral fissure height, X_{12} = oral fissure width, X_{13} = oral fissure length, X_{14} = eye diameter, X_{15} = head length after eye, X_{16} = interocular distance, X_{17} = snout length, X_{18} = upper jaw length, X_{19} = lower jaw length, X_{20} = distance from snout to anterior nostril, X_{21} = distance from snout to posterior nostril, X_{22} = distance from snout to dorsal fin origin, X_{23} = distance from snout to anal fin origin, X_{24} = distance from the anal fin origin to the anus, X_{25} = distance from the first aperture of lateral line to snout, X_{26} = distance from dorsal fin origin to anal fin origin, X_{27} = pectoral fin length.

The coefficient of determination (CD) is a measure of how well a linear regression model fits the data and is calculated as the square of the correlation between the dependent variable and the predicted values from the regression model (Nagelkerke 1991). The determination coefficient (d_{X_i}) shows the direct effects that the independent variables have on the dependent variables, while the co-determination coefficient ($d_{X_iX_j}$) shows the indirect effects accordingly. The determination coefficient and co-determination coefficient are concluded from the following formulas [2] and [3], respectively (Wright 1921).

$$d_{X_i} = P^2_{X_i} \quad [2]$$

$$d_{X_iX_j} = 2 \times r_{X_iX_j} \times P_{X_i} \times P_{X_j} \quad [3]$$

In the above three formulas, $r_{X_iX_j}$ means the correlation coefficient between morphological traits X_i and X_j. P_{X_i} and P_{X_j} mean the direct path coefficients of the morphological traits X_i and X_j on body weight, respectively.

The gray system theory (GST) was first proposed by a Chinese scholar, professor Julong Deng in 1982, and it has become an effective tool for studying the uncertainty of a small sample and limited information (Deng 1982). As an important part of GST, gray relational analysis (GRA) or gray box analysis utilizes the correlation order to express the relations of various factors, and it is suitable for solving problems with complicated interrelations between multiple factors and variables (Kuo et al. 2008). According to this theory, body weight (X_0) and 27 morphological traits (X_1–X_{27}) of *D. anguillare* are taken as a gray system, with the former as reference data and the latter as comparative data. For comparison purposes, the dimensionless treatment method in formula [4] is applied to solve the problem of dimensional inconsistency among different traits. Formula [5] is used to calculate the correlation coefficients between X_i and X_0, while formula [6] is used to obtain the correlation degree between X_i and X_0.

$$X_i'(K) = \frac{X_i(K) - \overline{X_i}}{S_i} \quad [4]$$

$$\xi i\,(K) = \frac{min Vi(K) + \rho\; max Vi(K)}{Vi(K) + \rho\; max Vi(K)} \quad [5]$$

$$\gamma_i = \frac{1}{n}\sum\nolimits_{k=1}^{n} \xi i\,(K) \quad [6]$$

In the formula [4], $X_i'(K)$ is the dimensionless data, $X_i(K)$ is the original data, $\overline{X_i}$ is the mean value of X_i, and S_i is the standard deviation of X_i. In the formula [5], $Vi\,(K)$is the absolute difference between X_i and X_0 at a point K that denotes as $Vi\,(K) = |X_0'\,(\mathrm{K}) - X_i'\,(K)|$, ρ is the gray resolution coefficient (ρ = 0.5), as well as *max Vi* (*K*) and *min Vi* (*K*) represent the absolute values of the secondary maximum difference and the secondary minimum difference, respectively. In the formula [6], γ_i is the correlation degree between X_i and X_0, and n is the sample size ($n = 85$).

Results

Descriptive statistics of morphometric traits. The statistical data on 28 morphometric parameters of *Dysomma anguillare* are shown in Table 1. The coefficient of variation (CV) is a normalized measure of dispersion of a probability distribution. The CV of X_4 (50.61%) was the greatest, followed by X_{11} (46.68%) and X_0 (40.12%), but the CV of X_{13} (11.00%) was the lowest. The standard deviation (SD) ranged from 0.57 to 48.46, showing an obvious fluctuation in the total length of different samples.

Normal distribution test and correlation analysis. In the K–S test and S–W test, the *P*-value lower than the significance level of 0.05 implies the null hypothesis is rejected and it is assumed that the data is non-normally distributed (Tong 1990). The logarithmic conversion was performed on the body weight to satisfy the normal distribution (Zhan et al. 2019), and the converted data were subjected to the K–S test considering the sample size of this study. The results showed the significance value was 0.100, which followed the normal distribution and could be used for regression analysis subsequently. Phenotypic correlations of 27 morphological traits (X_i) and logarithmic body weight ($\lg X_0$) were analyzed. As shown in Suppl. material 1, 21 morphological traits measured in this study had extremely significant correlations with $\lg X_0$ ($P < 0.01$), and four (X_4, X_{12}, X_{20}, and X_{27}) were significantly correlated with $\lg X_0$ ($P < 0.05$). Only two morphological traits including X_{11} and X_{25} did not correlate with $\lg X_0$ ($P > 0.05$), indicating that these traits were stable and not affected by environment or growth stage. The correlation coefficients ranged from –0.603 (X_{11} versus X_{20}) to 0.996 (X_1 versus X_2), which suggested that the total length (X_1) was strongly associated with the body length (X_2). While the oral fissure height (X_{11}) was the least relevant with distance from the snout to the anterior nostril (X_{20}).

Table 1. The descriptive statistics of phenotypic parameters for *Dysomma anguillare* from the East China Sea.

Trait	*N*	Value			Standard deviation (SD)	Coefficient of variation (CV) [%]
		Min.	Max.	Mean		
X_0	68	27.20	145.50	63.54	25.49	40.12
X_1	85	301.00	557.00	396.55	48.46	12.22
X_2	85	296.00	540.00	388.00	46.82	12.07
X_3	85	38.20	82.00	61.53	9.04	14.69
X_4	85	3.50	38.60	8.56	4.33	50.61
X_5	84	218.00	461.00	334.79	45.37	13.55
X_6	84	261.80	533.88	345.09	47.22	13.68
X_7	84	12.30	32.30	19.22	3.81	19.83
X_8	85	34.20	65.60	49.10	7.42	15.11
X_9	82	6.10	16.50	9.39	1.76	18.71
X_{10}	85	7.00	23.60	14.22	3.67	25.79
X_{11}	68	6.08	33.60	14.01	6.54	46.68
X_{12}	68	3.20	11.70	6.32	1.79	28.35
X_{13}	68	15.58	24.90	19.60	2.16	11.00
X_{14}	85	2.10	5.30	3.46	0.57	16.46
X_{15}	84	22.60	47.70	35.12	0.63	16.44
X_{16}	85	5.10	14.80	8.07	1.83	22.71
X_{17}	84	6.60	20.80	10.50	1.97	18.81
X_{18}	84	8.40	30.00	18.99	2.89	15.22
X_{19}	84	12.00	26.30	16.63	2.45	14.74
X_{20}	84	1.70	5.00	2.47	0.57	23.12
X_{21}	84	6.00	13.00	8.65	1.05	12.08
X_{22}	84	32.10	63.00	44.37	5.62	12.68
X_{23}	84	44.70	94.20	70.96	10.90	15.37
X_{24}	84	5.40	11.30	8.66	1.17	13.51
X_{25}	84	10.76	87.18	31.81	8.24	25.92
X_{26}	85	11.20	32.40	23.68	4.06	17.15
X_{27}	84	5.20	32.78	9.49	2.79	29.43

N = number of measurements. X_0 is the body weight. All other variables are morphometric characters defined in Fig. 1.

Multiple regression analysis. The results of stepwise multiple regression analysis are presented in Table 2. When the number of independent variables increased from 1 to 8, the correlation coefficient of each regression model also gradually increased from 0.865 to 0.959. In the meantime, the estimated standard error decreased from 0.083 to 0.050. The results indicated that the accuracy of the regression model kept increasing during the above process. The corrected coefficient of determination reached 0.909, which meant that a 90.9% variation of the dependent variable could be attributed to independent variables. Therefore, these 8 morphological traits (X_1 = total length; X_7 = body height; X_8 = head length; X_{10} = body width; X_{14} = eye diameter; X_{15} = head length; X_{19} = lower jaw length; X_{23}= distance from snout to anal fin origin) brought into the regression equation had a great determining relation with lgX_0. The results of the T-test for each independent variable in the regression equation are shown in Table 3. The non-standardized regression coefficients of 6 variables (X_1 = total length; X_7 = body length; X_8 = head length; X_{10} = body width; X_{14} = eye diameter; X_{19} = lower jaw length) and 2 variables (X_{15} = head length after eye; X_{23} = distance from the first aperture of lateral line to snout) achieved extremely significant level ($P < 0.01$) and significant level ($P < 0.05$), respectively, demonstrating that the established regression equation was valid. Besides, the potential collinearity problems were diagnosed using the variance inflation factor (VIF) test that measured the correlation among independent variables (Wesolowsky 1976). None of the VIF values were above the threshold level of 10, which meant fewer effects of multicollinearity were detected among independent variables (O'Brien 2007). Furthermore, the results of the F-test were also summarized in Suppl. material 2. The F value of 80.447 ($P = 0.000$) declared that the regression equation reached a very significant level ($P < 0.01$), and the independent variable could effectively explain the variation of the dependent variable. That is, the regression equation had statistical significance. Therefore, a multiple regression equation was established as follows: $\lg X_0 = 0.367 + 0.003X_1 + 0.010X_7 - 0.010X_8 + 0.011X_{10} + 0.042X_{14} + 0.006X_{15} + 0.024X_{19} - 0.004X_{23}$.

Path analysis. The path analysis revealed the effects of the independent variable (X_i) on the dependent variable (lgX_0). The results showed that the sum of each indirect relation to body weight was greater than that of the direct effects (Table 4). The direct effects of each trait on lgX_0 in the established regression equation are presented in descending order as: X_1 (total length) > X_8 (head length) > X_{19} (lower jaw length) > X_{10} (body width) > X_{23} (distance from snout to anal fin origin) > X_{15} (head length after eye) > X_7 (body height) > X_{14} (eye diameter), wherein X_8 and X_{23} negatively impacted lgX_0. Among all indirect effects, the indirect effect of X_7 through X_{19} to lgX_0 was in the first place (IP = 0.554), followed by the indirect effect of X_7 through X_1 to lgX_0 (IP = 0.489), while, X_{15} had the least indirect relation with lgX_0 through X_{14} (IP = 0.028). VIF values were between 1.6 and 8.7, lower than the empirical value (VIF = 10), indicating the collinearity effects were eliminated and the analysis results were reliable.

Determination coefficient analysis. In this study, the sum of the determination coefficients was calculated to be 0.920 (Table 5), fulfilling the criterion for screening the main independent variables with this value of no less than 0.850 according to Wang et al. (2021). It was indicated that these eight traits introduced by the model had a great determining relation with lgX_0, which was in consistence with the conclusion of path analysis. X_1 had the largest determinant relation with lgX_0 (0.489), while X_{14} had the least determinant relation with lgX_0 (0.022). X_1 and X_8 had the greatest negative co-determining relation with lgX_0 (–0.475), but the smallest positive co-determi-

Table 2. The regression model summary for *Dysomma anguillare* from the East China Sea.

Model	Correlation coefficient (R)	Coefficient of determination (R^2)	Corrected coefficient of determination (Adjusted R^2)	Standard error (SE)
1	0.865[a]	0.748	0.744	0.083
2	0.900[b]	0.810	0.804	0.073
3	0.919[c]	0.844	0.836	0.067
4	0.927[d]	0.860	0.851	0.064
5	0.942[e]	0.888	0.878	0.058
6	0.950[f]	0.903	0.893	0.054
7	0.955[g]	0.912	0.901	0.052
8	0.959[h]	0.920	0.909	0.050

[a] = predictor: (constant), X_{19}
[b] = predictor: (constant), X_{19}, X_1
[c] = predictor: (constant), X_{19}, X_1, X_{14}
[d] = predictor: (constant), X_{19}, X_1, X_{14}, X_{10}
[e] = predictor: (constant), X_{19}, X_1, X_{14}, X_{10}, X_8
[f] = predictor: (constant), X_{19}, X_1, X_{14}, X_{10}, X_8, X_6
[g] = predictor: (constant), X_{19}, X_1, X_{14}, X_{10}, X_8, X_7, X_{23}
[h] = predictor: (constant), X_{19}, X_1, X_{14}, X_{10}, X_8, X_7, X_{23}, $X_{15.}$
Variables X_1 through X_{23} are morphometric characters defined in Fig. 1.

Table 3. The results of regression coefficient for *Dysomma anguillare* from the East China Sea.

Variable	Partial regression coefficient (B)	Standard error (SE)	Standardized regression coefficient (β)	T-statistics	P value	Variance inflation factor (VIF)
Constant	0.367	0.064	—	5.758	0.000	—
X_1	0.003	0.000	0.699	6.267	0.000	8.698
X_7	0.010	0.003	0.194	3.314	0.002	2.394
X_8	–0.010	0.002	–0.418	–4.409	0.000	6.288
X_{10}	0.011	0.002	0.227	4.722	0.000	1.613
X_{14}	0.042	0.014	0.149	3.054	0.003	1.661
X_{15}	0.006	0.003	0.199	2.356	0.022	4.981
X_{19}	0.024	0.006	0.303	4.140	0.000	3.747
X_{23}	–0.004	0.001	–0.226	–2.596	0.012	5.320

Variables X_1 through X_{23} are morphometric characters defined in Fig. 1.

Table 4. Effects of eight morphometric traits on body weight of *Dysomma anguillare* from the East China Sea.

Trait	Correlation coefficient (*R*)	Path coefficient (*P*)	Indirect path coefficient (IP)									Variance inflation factor (VIF)
			Total	X_1	X_7	X_8	X_{10}	X_{14}	X_{15}	X_{19}	X_{23}	
X_1	0.825	0.699	1.469		0.212	0.246	0.187	0.121	0.193	0.251	0.259	8.698
X_7	0.771	0.194	2.474	0.489		0.392	0.376	0.380	0.372	0.554	0.400	2.394
X_8	0.571	–0.418	0.549	0.121	0.083		0.098	0.036	0.106	0.096	0.129	6.288
X_{10}	0.553	0.227	0.712	0.140	0.122	0.149		0.046	0.113	0.135	0.147	1.613
X_{14}	0.538	0.149	0.765	0.167	0.227	0.100	0.084		0.061	0.218	0.074	1.661
X_{15}	0.384	0.199	0.642	0.123	0.103	0.138	0.097	0.028		0.113	0.161	4.981
X_{19}	0.865	0.303	0.862	0.187	0.179	0.146	0.135	0.118	0.132		0.151	3.747
X_{23}	0.579	–0.226	0.749	0.170	0.114	0.173	0.129	0.035	0.166	0.132		5.320

Variables X_1 through X_{23} are morphometric characters defined in Fig. 1.

Table 5. Determination coefficients of eight morphometric traits on body weight of *Dysomma anguillare* from the East China Sea.

Trait	X_1	X_7	X_8	X_{10}	X_{14}	X_{15}	X_{19}	X_{23}
X_1	0.489							
X_7	0.190	0.038						
X_8	–0.475	–0.091	0.175					
X_{10}	0.196	0.047	–0.125	0.052				
X_{14}	0.083	0.031	–0.030	0.014	0.022			
X_{15}	0.177	0.041	–0.119	0.045	0.009	0.040		
X_{19}	0.350	0.093	–0.164	0.082	0.047	0.071	0.092	
X_{23}	–0.270	–0.050	0.164	–0.067	–0.012	–0.075	–0.091	0.051
SDC				0.920				
RCD				0.080				
e				0.392				

SDC = sum of determination coefficient, RCD = residual coefficient of determination, *e* = residual factor ($= \sqrt{1 - R^2}$). Variables X_1 through X_{23} are morphometric characters defined in Fig. 1.

nation coefficient appeared between X_{14} and X_{15} (0.009). The residual factor (*e*) was determined to be 0.392, which reflected that perhaps certain factors were not taken into account, and the relation among different traits should be further considered.

Gray relational analysis. The mean values of gray relational coefficients between different morphological traits and body weight were different, ranging from 2.466 to 396.522 (Table 6). Meanwhile, the standard deviation of the correlation coefficient of each morphological trait was calculated to analyze the dispersion degree among samples. The gray correlation degree represented the mean value of the relational coefficient between X_i and $\lg X_0$, and it was sorted from the largest to the smallest in order: X_2 (body length) > X_{22} (distance from snout to dorsal fin origin) > X_{18} (upper jaw length) > X_5 (postanal length) > X_{23} (distance from snout to anal fin origin) > X_7 (body height) > X_8 (head length) > X_{17} (snout length) > X_1 (total length) > X_{20} (distance from snout to anterior nostril) > X_{26} (distance from dorsal fin origin to anal fin origin) > X_6 (trunk length) > X_9 (head breadth) > X_{25} (distance from the first aperture of lateral line to snout) > X_4 (tail length) > X_{24} (distance from the anal fin origin to the anus) > X_{21} (distance from snout to posterior nostril) > X_{16} (interocular distance) > X_{15} (head length after eye) > X_{10} (body width) > X_{19} (lower jaw length) > X_{12} (oral fissure width) > X_3 (anal length) > X_{27} (pectoral fin length) > X_{13} (oral fissure length) > X_{14} (eye diameter) > X_{11} (oral fissure height).

Discussion

The linear body measurements have been widely applied to evaluate body demission to an animal's overall body size, and the prediction of body weight using morphometric features is very practical in aquaculture breeding programs and fishery management (Gjedrem 2005; William 2011). Herein, the relation between 27 morphological traits and the body weight of *Dysomma anguillare* was first established. In the case of morphological traits, the CV values for tail length (X_4) varied greatly, compared with those measured for other morphological traits. Unlike the standard deviation that must always be considered in the context of the mean of the data, the CV provides a relatively simple and quick tool to com-

Table 6. The gray relational coefficients and gray relational degrees of each trait of *Dysomma anguillare* from the East China Sea.

Traits	Gray relational coefficient			Gray correlation degree	Gray correlation order
	Min.	Max.	Mean ± SD		
X_1	301.000	557.000	396.552 ± 48.460	0.918	9
X_2	296.000	540.000	388.004 ± 46.824	0.937	1
X_3	38.200	82.000	61.531 ± 9.039	0.893	23
X_4	3.500	38.600	8.560 ± 4.332	0.907	15
X_5	218.000	461.000	334.792 ± 45.375	0.936	4
X_6	261.800	533.880	345.091 ± 47.220	0.909	12
X_7	12.300	32.300	19.220 ± 3.810	0.925	6
X_8	34.200	65.600	49.099 ± 7.419	0.921	7
X_9	6.100	16.500	9.389 ± 1.756	0.908	13
X_{10}	7.000	23.600	14.225 ± 3.668	0.897	20
X_{11}	6.080	33.600	14.014 ± 6.541	0.840	27
X_{12}	3.200	11.700	6.323 ± 1.792	0.894	22
X_{13}	15.580	24.900	19.600 ± 2.155	0.883	25
X_{14}	2.100	5.300	3.461 ± 0.570	0.865	26
X_{15}	0.000	47.700	34.711 ± 6.890	0.900	19
X_{16}	5.100	14.800	8.070 ± 1.833	0.900	18
X_{17}	6.600	20.800	10.496 ± 1.974	0.920	8
X_{18}	8.400	30.000	18.994 ± 2.892	0.936	3
X_{19}	12.000	26.300	16.629 ± 2.452	0.894	21
X_{20}	1.700	5.000	2.466 ± 0.570	0.915	10
X_{21}	6.000	13.000	8.655 ± 1.045	0.901	17
X_{22}	32.100	63.000	44.370 ± 5.625	0.937	2
X_{23}	44.700	94.200	70.956 ± 10.903	0.925	5
X_{24}	5.400	11.300	8.661 ± 1.170	0.904	16
X_{25}	10.760	87.180	31.809 ± 8.244	0.908	14
X_{26}	11.200	32.400	23.679 ± 4.062	0.909	11
X_{27}	5.200	32.780	9.491 ± 2.794	0.888	24

Variables X_1 through X_{27} are morphometric characters defined in Fig. 1.

pare different data series (Field 2005). For the majority of Anguilliformes species, it is difficult to measure the tail length (total length) precisely because the extended dorsal fin and anal fin are usually connected to the caudal fin. Perhaps it was the main reason for the greatest variation of this phenotypic feature in the study. Furthermore, all the CVs were larger than 10%, which indicated there were individual differences in growth rate and it was an important prerequisite for size-selective fishing.

The correlation analysis results showed that 25 traits were positively correlated with the logarithm of body weight, except for the oral fissure height (X_{11}) and distance from the first aperture of the lateral line to the snout (X_{25}). The top 3 phenotypic correlation coefficients of morphological traits were lower jaw length (X_{19}), total length(X_1), and body height (X_7), which were quite different from other bony fishes, such as *Larimichthys polyactis* (Bleeker, 1877) (see Liu et al. 2016), *Lates calcarifer* (Bloch, 1790) (see Yang et al. 2020), and *Amphiprion ocellaris* Cuvier, 1830 (see Wang et al. 2021), implying that the relation between morphological traits and body weight of different fishes was species-specific, and it might be also related to the living environment and whether the research object was a cultivated species.

Only using correlation coefficients can't adequately explicate all aspects of the relations among all variables and will be misleading when investigating causal effects (Falconer and Mackay 1996). Conversely, path analysis can effectively compensate for these shortcomings because of providing an algorithm to understand the direct, indirect, and total effect of one variable on another in a hypothesized model, and can therefore accurately reflect the relative importance of the results (Baloch et al. 2001). Our results showed that total length (X_1) was estimated to have the largest direct relation with the body weight, which was consistent with the results of *Misgurnus anguillicaudatus* (Cantor, 1842) (see Wang et al. 2011), *Anguilla reinhardtii* Steindachner, 1867 (see An et al. 2012), and *Lethenteron reissneri* (Dybowski, 1869) (see Ma et al. 2018). The phenotypic traits occupying a large geometric space for organisms are just the primary factors that cause changes in body weight (Chen and Liu 2022). The energy obtained by feeding mainly provides an increase in body length and body weight. The ample geometric space for longitudinal growth will be conducive to accumulate nutrients such as lipids and proteins, conforming to the regular growth pattern of rod-shaped fishes.

The conclusion of determinant coefficients analysis generally agreed with that of path analysis, with total length (X_1) having the largest determinant relation with the body weight. The total coefficient of determination was higher than the critical value of 0.850, which manifested that 92% of the variation came from eight independent variables, and the selected morphological traits could reflect the variation of body weight to a large extent. The multiple regression equation constructed based on these 8 parameters reached a very significant level ($P < 0.01$), reconfirming the accuracy of prediction to the body weight through morphological traits aforesaid. Nevertheless, the correlation coefficients of the retained eight morphological traits disaccorded with their direct effects on body weight, indicating that correlation analysis could not bespeak the true relations among variables (An et al. 2013). Moreover, the larger residual factor insinuated that some other morphometric traits acting on body weight still had not been found. In future studies, it is necessary to take both the external and internal characteristics into consideration.

GST is proved to be useful for dealing with poor, incomplete, and uncertain information (Deng 2005). Compared to conventional mathematical statistics such as correlation analysis, regression analysis, and path analysis, this geometry-based method does not require strict compliance with certain statistical laws or linear relations among objects. Nowadays, it has been widely applied in the fields of industry, agriculture, finance, and environmental science (Wang et al. 2000; Pai et al. 2007; Lai et al. 2009; Zhang and Qi 2011; Xia et al. 2016), and has gradually been used in quantitative analysis of morphological traits in *Paralichthys olivaceus* (Temminck et Schlegel, 1846) (see Liu et al. 2014), *Pinctada fucata* (Gould, 1850) (see Tan et al. 2015), *Siganus guttatus* (Bloch, 1787) (see Huang et al. 2019), and *Trachysalambria curvirostris* (Stimpson, 1860) (see Zhang and Cheng 2022). In the presently reported study, the gray correlation degree showed that X_2 and X_{22} had equal importance to the body weight. The results of the path analysis and gray correlation analysis were not exactly the same for how to determine the importance of independent variables. The former focused on the direct and indirect relations between dependent and independent variables, but the latter only brought independent variables into consideration (Wright 1921; Deng 2005). Consequently, a combination of two methods needed to be adopted to identify the key factors influencing the target traits.

Conclusion

In the presently reported study, a multivariable statistic method including correlation analysis, regression analysis, path analysis, and gray correlation analysis was applied to evaluate the morphological influence on body weight for *Dysomma anguillare* in the coastal waters of China for the first time. Integrated research findings suggested that the three metric traits representing the longitudinal growth of the fish body could be regarded as suitable indicators for formulating mesh size and minimum landing allowable catch size during the fishery resource management of *D. anguillare*.

Certainly, the correlations between the morphological traits of fishes and their body weight were also related to growth stage, sex, habitat environment, nutritional condition as well as genetic regulation. Hence, we should comprehensively deliberate the influence of multiple factors and increase the sample size as much as possible to make the results more reliable.

Acknowledgments

We are grateful to Dr Wei Meng and Dr Rijin Jiang of Zhejiang Marine Fisheries Research Institute for sample collection. This research was funded by the Technology Planning Project of Zhoushan (No. 2022C41022), the Innovation and Entrepreneurship Training Program for College Students (No. 202310340056), and the Science and Technology Innovation Project of College Students in Zhejiang Province (No. 2023R411005).

References

An L, Meng QL, Dong XS, Li X, Yang L, Liu YQ, Zhang ZS, Zhu YA (2012) [Mathematical analysis of effects of morphometric attributes on body weight for *Anguilla reinhardtii*.] Zhongguo Nongxue Tongbao—Chinese Agricultural Science Bulletin 28(2): 60–64. [In Chinese with English abstract] https://doi.org/10.11924/j.issn.1000-6850.2011-2133

An L, Zhu YA, Fu PS, Zhang LG, Li X, Dong XS, Yang PF, Meng QL (2013) [Mathematical analysis of effects of morphometric attributes on body weight in Sutchi catfish *Pangasius sutchi*.] Shuichanxue Zazhi—Chinese Journal of Fisheries 26(1): 5–9. [In Chinese with English abstract] https://doi.org/10.3969/j.issn.1005-3832.2013.01.002

Baloch MJ, Lakho AR, Bhutto H, Solangi MY, Sola MY (2001) Path coefficient analysis for assessing direct and indirect effects of yield components on seed cotton yield in *Gossypium hirsutum* L. Journal of Biological Sciences 1(5): 354–355. https://doi.org/10.3923/jbs.2001.354.355

Chen XJ, Liu BL (2022) [Fishery resources biology.] Science Press, Beijing, China, 248 pp. [In Chinese]

Chen DG, Zhang MZ (2015) [Marine fishes of China. Volume 1.] China Ocean University Press, Qingdao, China, 743 pp. [In Chinese]

Chen XJ, Lu HJ, Liu BL, Fang Z (2012) Relationship between beak morphological variables and body size and mantle length of male and female Argentine shortfin squid (*Illex argentinus*). Journal of Ocean University of China 11(4): 539–546. https://doi.org/10.1007/s11802-012-2080-x

Deng JL (1982) Control problems of grey systems. Systems and Control Letters 5(1): 288–294. https://doi.org/10.1016/S0167-6911(82)80025-X

Deng JL (2005) [Primary methods of grey system theory.] 2nd edn. Huazhong University of Science and Technology Press, Wuhan, China, 169 pp. [In Chinese]

Du XX, Tian SQ, Wang JQ, Wang ZH, Gao CX (2018) [Spatial and temporal characteristics of fish community structure in coastal waters of southern Zhejiang.] Dalian Haiyang Daxue Xuebao—Journal of Dalian Ocean University 33(4): 522–531. [In Chinese with English abstract] https://doi.org/10.16535/j.cnki.dlhyxb.2018.04.018

Falconer DS, Mackay TFC (1996) Introduction to quantitative genetics. Longman Group, Essex, UK.

Field A (2005) Discovering statistics using SPSS (2nd edn.). Sage Publications, London, UK.

Gjedrem T (2005) Selection and breeding programs in aquaculture. Springer, Dordrecht, Netherlands. https://doi.org/10.1007/1-4020-3342-7

Gulland JA, Carroz JE (1969) Management of fishery resources. Advances in Marine Biology 6: 1–60, 62–71. https://doi.org/10.1016/S0065-2881(08)60437-X

Guo D, Chen J, Zhai ZQ, Ren TT, Wang JJ, Bai LR, Yu DH (2021) [Analysis on the effects of morphological traits of *Lutraria sieboldii* on its body mass trait.] Agricultural Biotechnology 10(4): 71–76. [In Chinese]

He J, Zhao YF, Zhao JL, Gao J, Han DD, Xu P, Yang RQ (2017) Multivariate random regression analysis for body weight and main morphological traits in genetically improved farmed tilapia (*Oreochromis niloticus*). Genetics, Selection, Evolution 49(1): 80. https://doi.org/10.1186/s12711-017-0357-7

Huang XL, Zhang DG, Lin HZ, Yang SS, Yu W, Yang YK, Huang Z, Li T (2019) [Gray incidence degree analysis of relationship between morphometric traits and body weight in speckled spinefoot *Siganus guttatus* cultured in a cage.] Fisheries Science 38(1): 61–66. [In Chinese with English abstract] https://doi.org/10.16378/j.cnki.1003-1111.2019.01.009

Jiang S, Zhou FL, Yang QB, Yang LS, Li T, Jiang SG, Huang JH (2017) Correlation and path coefficient analyses of the morphological characteristics and body weight of *Penaeus monodon* (Crustacea, Decapoda, Penaeidae). Insights in Aquaculture and Biotechnology 1(2): e6.

Kuo Y, Yang T, Huang GW (2008) The use of grey relational analysis in solving multiple attribute decision-making problems. Computers and Industrial Engineering 55(1): 80–93. https://doi.org/10.1016/j.cie.2007.12.002

Lai YP, Li J, Zhang ZQ, Dong XF, Liu XC, Wei HT, Hu XR, Peng ZS, Yang WY (2009) [Grey correlation analysis of morphological traits related to drought tolerance of wheat at seedling stage.] Mailei Zuowu Xuebao—Journal of Triticeae Crops 29(6): 1055–1059. [In Chinese with English abstract]

Liu YX, Liu YJ, Zhou Q, Gao L, Fang H, Han G, Wang YF, Jiang XF, Liu HJ (2014) [Grey relational analysis between main growth traits and body weight in Japanese flounder (*Paralichthys olivaceus*).] Journal of Fishery Sciences of China 21(2): 205–213. [In Chinese with English abstract]

Liu F, Chen L, Lou B, Zhan W, Chen RY, Xu DD, Wang LG, Xu QX, MA T, Mao GM (2016) [Correlation and path coefficient analysis on body weight and morphometric traits of small yellow croaker *Pseudosciaena polyactis*.] Oceanologia et Limnologia Sinica 47(3): 655–662. [In Chinese with English abstract]

Ma HY, Ma CY, Ma LB, Xu Z, Feng NN, Qiao ZG (2013) Correlation of growth-related traits and their effects on body weight of the mud crab (*Scylla paramamosain*). Genetics and Molecular Research 12(4): 4127–4136. https://doi.org/10.4238/2013.October.1.3

Ma QH, Li J, Xu L, Liu HX, Liu X, Pang Y, Han YL, Li QW (2018) [Mathematical analysis of effects of morphometric attributes on body weight of Asiatic brook lamprey *Lampetra reissneri* and gender distinguish.] Shuichanxue Zazhi—Chinese Journal of Fisheries 31(5): 19–28. [In Chinese with English abstract] https://doi.org/10.3969/j.issn.1005-3832.2018.05.006

Nagelkerke NJD (1991) A note on a general definition of the coefficient of determination. Biometrika 78(3): 691–692. https://doi.org/10.1093/biomet/78.3.691

Nelson JS, Grande TC, Wilson VH (2016) Fishes of the world. 5th edn. John Wiley and Sons, Hoboken NJ, USA, 386 pp. https://doi.org/10.1002/9781119174844

O'Brien RM (2007) A caution regarding rules of thumb for variance inflation factors. Quality and Quantity 41: 673–690. https://doi.org/10.1007/s11135-006-9018-6

Pai TY, Hanaki K, Ho HH, Hsieh CM (2007) Using grey system theory to evaluate transportation effects on air quality trends in Japan. Transportation Research Part D: Transport and Environment 12(3): 158–166. https://doi.org/10.1016/j.trd.2007.01.007

Shapiro SS, Wilk MB (1965) An analysis of variance test for normality (complete samples). Biometrika 52(3–4): 591–611. https://doi.org/10.1093/biomet/52.3-4.591

Sheng ZL, Wu CX (1999) [Quantitative genetics.] China Agriculture Press, Beijing, China, 176 pp. [In Chinese]

Singh RK, Chaudhary BD (1979) Biometrical methods in quantitative genetic analysis. Haryana Agriculture University Press, Hissar, India, 303 pp.

Tan CG, Liu BS, Zhang DL, Niu ZK, Zhang B, Chen MQ, Fan SG, Jiang S, Huang GJ, Li YN, Chen SW, Yu DH (2015) [Analysis of grey relationship between morphological traits and body weight of pearl oyster (*Pinctada fucata*).] Nanfang Shuichan Kexue—South China Fisheries Science 11(2): 35–40. [In Chinese with English abstract] https://doi.org/10.3969/j.issn.2095-0780.2015.02.005

Tikhomirov VM (1993) ε-entropy and ε-capacity of sets in functional spaces. Pp. 86–170. In: Shiryayev AN (Ed.) Selected Works of A. N. Kolmogorov. Volume III. Information theory and the theory of algorithms. Part of book series: Mathematics and its applications. Vol. 27. Springer, Dordrecht, Netherlands. https://doi.org/10.1007/978-94-017-2973-4_7

Tong YL (1990) The multivariate normal distribution. Springer, New York, NY, USA. https://doi.org/10.1007/978-1-4613-9655-0

Uiuiu P, Laţiu C, Popescu F, Constantinescu R, Coroian CO, Ihuț A, Cocan DI, Mireșan V (2017) Morphological traits of brown trout (*Salmo trutta fario*) from Fiad trout farm, Bistrița-Năsăud County. Bulletin of the University of Agricultural Sciences and Veterinary Medicine Cluj-Napoca. Animal Science and Biotechnologies 74(2): 194–196. https://doi.org/10.15835/buasvmcn-asb:0029

Wang J, Hou YS, Li WL, Cheng WH (2000) Application of grey system theory to tree growth prediction. Journal of Forestry Research 11(1): 34–36. https://doi.org/10.1007/BF02855492

Wang L, Ling QF, Hao XF, Yu LY, Liu Y (2011) [Analysis of effects of morphological traits on body weight for 4-month aged of *Misgurnus anguillicaudatus*.] Shuishengtaixue Zazhi—Journal of Hydroecology 32(4): 97–102. [In Chinese with English abstract] https://doi.org/10.3969/j.issn.1003-1278.2011.04.018

Wang YM, Zhang FY, Zhao M, Ma CY, Zhang LZ, Ma LB (2019) The complete mitochondrial genome of *Dysomma anguillare* (Anguilliformes, Synaphobranchidae) with phylogenetic consideration. Mitochondrial DNA. Part B, Resources 4(1): 1688–1689. https://doi.org/10.1080/23802359.2019.1604103

Wang HS, Ye L, Hu QY, Fu MH, Xiao ZH (2021) [Correlation between morphological traits and body mass and path analysis of *Amphiprion ocellaris*.] Nanfang Nongye Xuebao—Journal of Southern Agriculture 52(1): 221–227. [In Chinese with English abstract] https://doi.org/10.3969/j.issn.2095-1191.2021.01.027

Wesolowsky GO (1976) Multiple regression and analysis of variance: An introduction for computer users in management and economics. Wiley, New York, NY, USA.

William HI (2011) Fisheries management and conservation. Taylor and Francis, London, UK.

Wittink DR, Heights N (1988) The application of regression analysis. Allyn and Bacon, Boston, MA, USA.

Wright S (1921) Correlation and causation. Journal of Agricultural Research 20(7): 557–585.

Xia XF, Sun Y, Wu K, Jiang QH (2016) Optimization of a straw ring-die briquetting process combined analytic hierarchy process and grey correlation analysis method. Fuel Processing Technology 152: 303–309. https://doi.org/10.1016/j.fuproc.2016.06.018

Yang R, Hu J, Zhao W, Zhou SJ, Yu G, Yang QB, Ma ZH (2020) [Correlation analysis of morphological attributes effects on body weight of *Lates calcarifer* cultured in indoor and outdoor rearing system.] Shui Chan Yan Jui—Open Journal of Fisheries Research 7(1): 48–57. [In Chinese with English abstract] https://doi.org/10.12677/OJFR.2020.71008

Yang R, Han DY, Gao CX, We XJ, Zhao J, Ye S (2022) [Change of trophic niche of *Dysomma anguillare* in the offshore waters of southern Zhejiang by stable isotope analysis.] Acta Ecologica Sinica 42(23): 9796–9807. [In Chinese with English abstract] https://doi.org/10.5846/stxb202112073477

Zhan YY, Zhang WJ, Ge C, Lin K, Li G, Song J, Chang YQ (2019) Relationships between body weight and other morphological traits in young sea cucumbers *Apostichopus japonicas*. Journal of Oceanology and Limnology 37(2): 759–766. https://doi.org/10.1007/s00343-019-7255-5

Zhang CG (2010) [Fauna Sinica: Osteichthyes, Anguilliformes, Notacanthiformes.] Science Press, Beijing, China, 453 pp. [In Chinese]

Zhang XM, Cheng SF (2022) [Path analysis and gray correlation analysis of morphological traits to body weight of *Trachypenaeus curvirostirs*.] Yuye Kexue Jinzhan—Progress in Fishery Sciences 43(1): 153–162. [In Chinese with English abstract] https://doi.org/10.19663/j.issn2095-9869.20200806001

Zhang XF, Qi YB (2011) [The grey correlation analysis on the relationship between the rural finance and the rural economic growth in Sichuan Province.] Yazhou Nongye Yanjiu—Asian Agricultural Research 3(1): 77–79. [In Chinese with English abstract]

Zhang B, Tang QS (2003) [Feeding habits of six species of eels in East China Sea and Yellow Sea.] Shuichan Xuebao—Journal of Fisheries of China 27(4): 307–314. [In Chinese with English abstract] https://doi.org/10.3321/j.issn:1000-0615.2003.04.004

Zhang AG, Wang LL, Yang XL, Hu XC, Fu YB, Li CH, Chen AH, Yuan XT (2018) Relationship between shell morphological traits and body weight in two estuarine clams, *Meretrix meretrix* and *Cyclina sinensis* in Shuangtaizi estuary, Bohai Sea in China. Journal of Shellfish Research 37(5): 989–996. https://doi.org/10.2983/035.037.0509

Zhao LQ, He YY, Yang F, Nie HT, Yan XW (2014) Correlation and path analysis of morphological and weight traits in marine gastropod *Glossaulax reiniana*. Chinese Journal of Oceanology and Limnology 32(4): 821–827. https://doi.org/10.1007/s00343-014-3290-4

Zou X, Ma HY, Lu JX, Gong YY, Xiao LJ (2017) Mathematical analysis of morphological traits and their effects on body weight in the red crab (*Charybdis feriata*). African Journal of Agricultural Research 12(6): 429–434. https://doi.org/10.5897/AJAR2016.11060

Supplementary material 1

Correlation analysis of morphological traits for *Dysomma anguillare*

Authors: Ziyan Zhu, Tianyan Yang, Sige Wang

Data type: docx

Link: https://doi.org/10.3897/aiep.54.114014.suppl1

Supplementary material 2

Variation analysis of multiple regression equations

Authors: Ziyan Zhu, Tianyan Yang, Sige Wang

Data type: docx

Link: https://doi.org/10.3897/aiep.54.114014.suppl2

Acta Ichthyologica et Piscatoria 54, 2024, 37–41 | DOI 10.3897/aiep.54.113513

PENSOFT.

ACTA
ICHTHYOLOGICA
ET PISCATORIA

First Southern Hemisphere record of the longnosed stargazer, *Ichthyscopus lebeck* (Actinopterygii: Perciformes: Uranoscopidae)

Gino V. LIMMON[1,2,3], Kunto WIBOWO[4], Teguh PERISTIWADY[5], Ruby V. KUSUMAH[6], Muhammad AFRISAL[4,7]

1 *Fisheries and Marine Science Faculty, Pattimura University, Ambon, Indonesia*
2 *Maritime and Marine Science Center of Excellence, Pattimura University, Ambon, Indonesia*
3 *Center for Collaborative Research on Aquatic Ecosystem in Eastern Indonesia, Ambon, Indonesia*
4 *Museum Zoologicum Bogoriense, Research Center for Biosystematics and Evolution, National Research and Innovation Agency, Cibinong, Indonesia*
5 *Research Center for Oceanography, National Research and Innovation Agency, Jakarta Utara, Indonesia*
6 *Research Center for Fishery, National Research and Innovation Agency, Cibinong, Indonesia*
7 *Capture Fisheries Department, Indonesia Defense University, Belu, Indonesia*

https://zoobank.org/83CFFDC6-4EE8-4EFE-9A83-FB9A2D5E982B

Corresponding authors: Gino V. Limmon (gino.limmon@gmail.com); Kunto Wibowo (kunt003@brin.go.id)

Academic editor: Ronald Fricke ◆ **Received** 30 September 2023 ◆ **Accepted** 7 January 2024 ◆ **Published** 5 February 2024

Citation: Limmon GV, Wibowo K, Peristiwady T, Kusumah RV, Afrisal M (2024) First Southern Hemisphere record of the longnosed stargazer, *Ichthyscopus lebeck* (Actinopterygii: Perciformes: Uranoscopidae). Acta Ichthyologica et Piscatoria 54: 37–41. https://doi.org/10.3897/aiep.54.113513

Abstract

Two specimens (290.2 and 309.5 mm in standard length) of the longnosed stargazer, *Ichthyscopus lebeck* (Bloch et Schneider, 1801), were recently collected from Jakarta Bay, Jakarta, Indonesia. Described more than two centuries ago, *I. lebeck* has hitherto been documented exclusively from the Northern Hemisphere, encompassing the Arabian Sea, southern coastal India, the Bay of Bengal, the Andaman Sea, and Singapore. The present paper documents the first record of the species in the Southern Hemisphere. Detailed descriptions of these specimens are provided, contributing valuable insights into the characteristics of *I. lebeck* in the newly reported locality.

Keywords

distribution, Indonesia, morphology, Southern Hemisphere

Introduction

The genus *Ichthyscopus* Swainson, 1839, family Uranoscopidae, includes eight valid species, i.e. *Ichthyscopus barbatus* Mees, 1960; *Ichthyscopus fasciatus* Haysom, 1957; *Ichthyscopus insperatus* Mees, 1960; *Ichthyscopus lebeck* (Bloch et Schneider, 1801); *Ichthyscopus nigripinnis* Gomon et Johnson, 1999; *Ichthyscopus pollicaris* Vilasri, Ho, Kawai et Gomon, 2019; *Ichthyscopus sannio* Whitley, 1936; and *Ichthyscopus spinosus* Mees, 1960 (see Vilasri et al. 2019). The genus is distinguishable from other genera by the following external morphological characters: lateral lines on each side of body joined dorsally midway along caudal peduncle; cleithral spine embedded in dermal fringed flaps; upper and lower lips with developed compressed cutaneous cirri; and pectoral fin blade-shaped, upper rays longer than middle ray (Kishimoto 2001; Vilasri 2013). *Ichthyscopus lebeck* and the recently described new species *I. pollicaris* have both been reported as having a restricted distribution in the Northern Hemisphere, ranging from the Arabian Sea, southern coastal India, the Andaman Sea, Singapore, and east Asian waters, whereas the other six species are allopatrically distributed in waters off Australia and New Guinea (Vilasri et al. 2019).

Two specimens of *Ichthyscopus lebeck*, caught as bycatch by fishermen from Jakarta Bay, Jakarta, Indonesia, were obtained at the Tanjung Pasir Fish Landing Port, Banten. They are described herein, being the first records of *I. lebeck* from waters off Indonesia and in the Southern Hemisphere.

Methods

Counts and measurements followed Gomon and Johnson (1999) and Vilasri et al. (2019). Standard and head lengths are abbreviated as SL and HL, respectively. The vertebral number was counted from a radiograph of MZB.26859, 309.5 mm SL, and the morphological description based on both specimens collected from Jakarta Bay. Curatorial procedures for the specimens, deposited at the Museum Zoologicum Bogoriense, Indonesia (MZB), followed Motomura and Ishikawa (2013).

Results

Family Uranoscopidae Bonaparte, 1831
Ichthyscopus Swainson, 1839

Ichthyscopus lebeck (Bloch et Schneider, 1801)

English common name: longnosed stargazer

Fig. 1; Table 1

Material examined. MZB.26859, 309.5 mm SL, MZB.26860 mm SL, 290.2 mm SL, Jakarta Bay, 5°57′S, 106°42′E, Jakarta, Indonesia (purchased at the Tanjung Pasir Fish Landing Port, Banten, Indonesia, 3 Nov. 2022, by K. Wibowo; see Fig. 2 for the collection site).

Description. Meristic and morphometrics shown in Table 1. Body elongated, progressively compressed posteriorly, moderately deep, its depth 2.7–3.2 in SL. Head large, slightly convex dorsally, mostly encased in irregular low vermiculated bone. Interorbital fossa rounded posteriorly, extending well beyond posterior margin of orbits, its mid-longitudinal length shorter than interorbital width. Orbit oval, its diameter noticeably greater than that of eyes. Nostrils with short, stiff, densely branched fimbriate edges; anterior nostril circular, distinctly shorter than eye diameter; posterior nostril circular, elongated, its length about equal to longitudinal orbit diameter; its posterior margin about level with posterior margin of eye. Mouth large, opening prominently upward; both lips with single row of long compressed fimbriae. Upper jaw with dense band of minute villiform teeth. Lower jaw with sharp uniserial spaced canines. Chin smooth, lateral surface without barbels. Opercular margin distinctly fimbriate dorsolaterally, weakly crenulated ventrally. Cleithral spine short, with sharp tip, covered by fleshy skin flap; tip of spine at about middle of skin flap. Cleithral flap fimbriated ventrally, posterior tip of flap reaching level with middle of pectoral fin. Narrow, low fleshy groove from inside opercular opening to about one-fourth to one-third length of uppermost pectoral fin ray; tiny fimbriae present on ventral margin of groove; posterior end of groove with small flap. Preopercle, opercle, and subopercle without spines. Dorsal fin with 2 approximately equal length spines, and 17–18 rays, becoming progressively longer posteriorly; origin of dorsal fin about level with origin of anal fin; posterior end of dorsal fin base slightly anterior to posterior end of anal fin base. Anal fin with 18 soft rays, first ray short, length of fourth to fifteenth ray about equal; membrane between rays (except three posteriormost rays) relatively deeply concave. Pectoral fin with 18 rays, blade-like and rounded posteriorly, fifth ray longest. Pelvic fin large, with small skin-covered spine and 5 branched rays; posterior tip of depressed fin distinctly beyond posterior margin of opercle. Caudal fin somewhat rounded, tips of branched rays extending slightly beyond surrounding membrane. Ventral surface of abdomen with three developed skin flaps; medial flap longest, extending from anteriormost of isthmus to anterior margin of anus; lateral flaps located on each side of medial flap, on posterior two-thirds of abdomen and extending to middle of second or third anal-fin ray. Third or fourth to eighteenth rays associated with short oblique skin flaps on each side; flaps lowering progressively posteriorly. Small rectangular posteroventrally oblique cycloid scale rows on body (some rows anteroventrally oblique on midlateral body surface in smaller specimen). Anterodorsal and ventral surfaces of body and lateral surface behind pectoral fin base naked. Vertebrae 9 + 16 (Fig. 1D).

Color when fresh. (Fig. 1A–C). Head pinkish to white laterally, brown dorsally. Nape uniformly brown without distinct white blotches. Upper portion of body dark brown, with ca. 2 or 3 rows of white blotches, from slightly less to larger than eye diameter, running from above cleithral flap to caudal peduncle. Lower and ventral portions of body white. Dorsal fin dark, with a series of white blotches near base and outer edge. Pectoral fin dark yellowish, pinkish or whitish distally, with a large white transverse blotch anteriorly. Pelvic and anal fins yellowish to pinkish-white. Upper portion of caudal fin dark with ca. two pale white blotches; lower portion yellowish to pinkish.

Discussion

The data on Indonesian specimens agreed closely with the diagnosis of *Ichthyscopus lebeck* given by Vilasri et al. (2019), e.g. number of caudal vertebrae 16; number of upper lip fimbriae 29 or 30; posterior nostril longitudinally elongated, its posterior margin well beyond center of orbit; ventral surface of abdomen with three developed skin flaps, i.e. medial flap, extending from anteriormost of isthmus to anterior margin of anus, and lateral flaps on each side of medial flap, on posterior

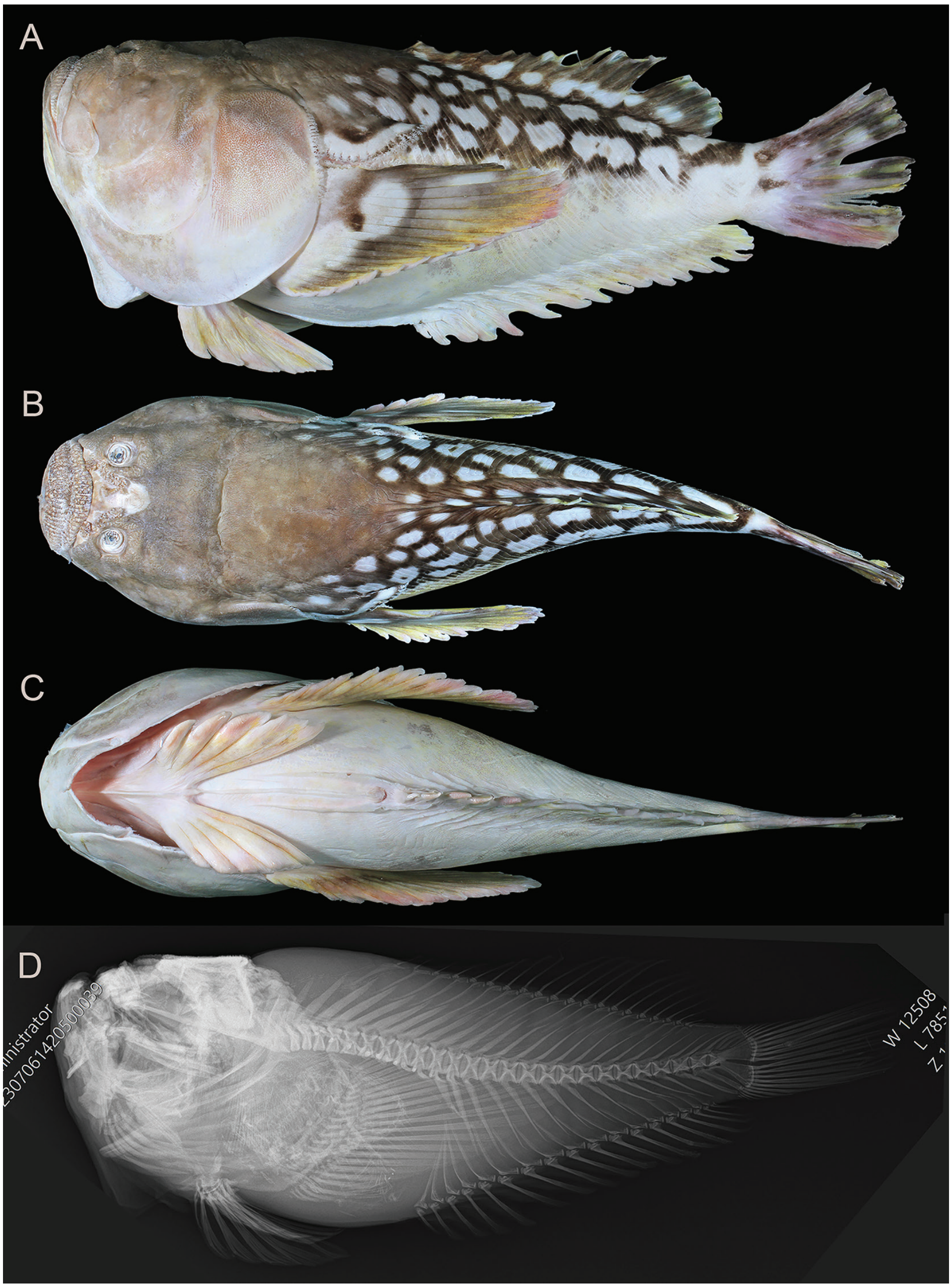

Figure 1. Fresh specimen of *Ichthyscopus lebeck* from Indonesia; MZB.26859, 309.5 mm SL. (**A**) lateral view; (**B**) dorsal view; (**C**) ventral view; (**D**) radiograph.

Figure 2. Collection site (star) of the specimens of *Ichthyscopus lebeck* from Indonesia; examined in this study.

Table 1. Counts and measurements (expressed as percentages of standard and head lengths) of *Ichthyscopus lebeck* from Indonesia.

Parameter	This study		Vilasri et al. 2019
	Southern Hemisphere		Northern Hemisphere
	MZB.26859	MZB.26860	*n* = 11
Standard length (SL) [mm]	309.5	290.2	191–368
Counts			
Dorsal fin rays	II, 18	II, 17	II, 17.5–19
Anal fin rays	18	18	17–19
Pectoral fin rays	18	18	18–19
Pelvic fin rays	I, 5	I, 5	—
Vertebrae (abdominal + caudal)	9 + 16	—	9 + (16–17)
Upper lip fimbriae (both sides)	30	29	25–34
Lower lip fimbriae (both sides)	48	46	43–53
Opercular fimbriae	20	16	15–22
Cleithral flap fimbriae	19	19	17–22
Scale rows	60	55	50–61
Measurements [%SL]			
Body depth	37.0	31.3	29.8–36.6
Head length (HL)	40.9	42.2	39.7–43.3
Head width	32.6	33.3	29.3–34.3
Pectoral fin length	31.0	29.3	26.4–33.3
Pelvic fin length	24.4	26.2	21.6–28.1
Measurements [%HL]			
Orbital diameter longitudinal	11.7	10.7	10.1–13.6
Orbital diameter transverse	10.1	9.4	9.1–10.6
Eye diameter	6.8	7.5	6.4–9.1
Interorbital distance	21.1	21.6	20.2–24.5
Interorbital fossa width	16.9	17.5	14.9–19.5
Cleithral spine length	24.1	22.8	16.0–27.4

two-thirds of abdomen and extending to middle of second or third anal-fin ray; dorsolateral surface of body dark brown with distinct white blotches, without dark saddles; no distinct notch separating anterior and posterior portions of dorsal fin; cirri present on anteroventral opercular margin; large white transverse blotch on pectoral fin base; uppermost pectoral ray with uniformly dusky hue, without obvious spots. Although Vilasri et al. (2019) noted that the posterior ends of the lateral skin flaps on eleven examined individuals of *I. lebeck* had been consistently attached to the middle of the second anal fin ray, those of the presently reported specimens were attached to the middle of the third anal fin ray (in the larger specimen) and asymmetrically to the middle of the second and third anal fin rays in the left and right sides of the body, respectively (in the smaller specimen). Additionally, a yellowish coloration had been evident on the head, body, and all fins in Vilasri et al. (2019: fig. 6), while the specimens examined here (Fig. 1A) had only a very faint yellowish hue, limited primarily to the fins. All other morphological characters, including morphometrics and meristics, of the presently reported specimens agreed closely with those of *I. lebeck* given by Vilasri et al. (2019), except body depth of MZB.26859 37.0% of SL (vs. 29.8–36.6, in the latter). The minor differences are herein regarded as intraspecific variations of *I. lebeck*.

Ichthyscopus lebeck shares similarities with the east Asian species *I. pollicaris* and Australian species *I. sannio* in having three skin flaps developed on the ventral surface of abdomen, the upper half of the body dark brown with white blotches, and lacking transverse bands. However, *I. lebeck* is distinct from both in several aspects, including some morphological features, meristics, and coloration, as detailed by Gomon and Johnson (1999) and Vilasri et al. (2019).

Since its original description in Bloch and Schneider (1801), *Ichthyscopus lebeck* has only been reported from the Northern Hemisphere [e.g., Arabian Sea, southern coast of India (Kishimoto 2001; Vilasri et al. 2019), western Bay of Bengal, India (Velamala and Naranji 2018; Chakraborty et al. 2020), northern Bay of Bengal, Bangladesh (Habib and Islam 2020), and Andaman Sea and Singapore. The southernmost record at latitude 1°N, was based on a single specimen (Kishimoto 2001; Vilasri 2019; Vilasri et al. 2019)]. In addition, from 2005 to 2019, multiple additional reports of the species in Singapore waters were documented (Tan and Lim 2013; Tan and Chan 2019), one specimen having been collected from Changi Beach and deposited in the Zoological Reference Collection of the Lee Kong Chian Natural History Museum, National University of Singapore (Tan and Chan 2019). Accordingly, the presently reported specimens collected from Jakarta Bay (at a latitude of 5°–6°S), represent the southernmost records of the species and first confirmed occurrence of the species in the Southern Hemisphere.

Ichthyscopus lebeck is known to inhabit sandy or muddy habitats in the intertidal zones of seagrass ecosystems in Singapore (Tan and Lim 2013; Tan and Chan 2019), estuarine areas near mangrove ecosystems in India (Chakraborty et al. 2020), and depths of 15–20 meters (this study). The species has the habit of waiting for its prey by burying into the substrate, leaving only its eyes and mouth visible. Fishermen in Jakarta Bay have also noted that the species is often caught using drift gillnets operated at night, indicating its tendency for increased activity during nighttime.

Because there are no significant natural geographical barriers that separate waters off Singapore (southern South China Sea) and Jakarta Bay (Java Sea), as well as coastal areas of the Arabian Sea, Indian Ocean, Andaman Sea, and Singapore, it is likely that *I. lebeck* is distributed along these coastlines where suitable habitats occur. The paucity of reports of the species' presence in some areas may be due either to its secretive behavior, resulting in less common sightings, or to the population not being particularly abundant.

Acknowledgments

We are especially grateful to S. Sauri (MZB, Indonesia) for his efforts in cataloging the specimens and to Dr G. S. Hardy (Ngunguru, New Zealand) for assisting with the English text and valuable input in reviewing the manuscript. This study was supported by "Program Pendanaan Riset dan Inovasi untuk Indonesia Maju (RIIM) and Lembaga Pengelola Dana Pendidikan (LPDP), Kementerian Keuangan Republik Indonesia".

References

Bloch ME, Schneider JG (1801) M. E. Blochii, Systema Ichthyologiae Iconibus cx Ilustratum. Post obitum auctoris opus inchoatum absolvit, correxit, interpolavit Jo. Gottlob Schneider, Saxo. Sumtibus Auctoris Impressum et Bibliopolio Sanderiano Commissum, Berolini, i–ix + 584 pp. https://doi.org/10.5962/bhl.title.5750

Chakraborty P, Yardi K, Mukherjee P, Das S (2020) First record of two species of fishes from West Bengal, India and additional new ichthyofaunal records for the Indian Sundarbans. International Journal of Fisheries and Aquatic Studies 8(2): 6–10.

Gomon MF, Johnson JW (1999) A new fringed stargazer (Uranoscopidae: *Ichthyscopus*) with descriptions of the other Australian species of the genus. Memoirs of the Queensland Museum 43(2): 597–619.

Habib KA, Islam MJ (2020) An updated checklist of marine fishes of Bangladesh. Bangladesh. Journal of Fisheries 32(2): 357–367. https://doi.org/10.52168/bjf.2020.32.40

Haysom NM (1957) Notes on some Queensland fishes. Ichthyological Notes Queensland 1(3): 139–144.

Kishimoto H (2001) Uranoscopidae. Pp. 3519–3531. In: Carpenter KE, Niem VH (Eds.) FAO species identification guide for fisheries purposes. The living marine resources of the western Central Pacific. Vol. 6. Bony fishes, part 4. (Labridae to Latimeriidae). FAO, Rome.

Mees GF (1960) The Uranoscopidae of Western Australia (Pisces, Perciformes). Journal of the Royal Society of Western Australia 43(2): 46–58.

Motomura H, Ishikawa S (Eds.) (2013) Fish collection building and procedures manual. English edition. Kagoshima University Museum, Kagoshima and the Research Institute for Humanity and Nature, Kyoto, Japan, 70 pp.

Swainson W (1839) On the natural history and classification of fishes, amphibians, and reptiles, or monocardian animals. Spottiswoode, London, i–vi + 452 pp. https://doi.org/10.5962/bhl.title.62140

Tan HK, Chan SY (2019) A longnose stargazer at Changi Beach. Singapore Biodiversity Records 2019: 8–9.

Tan R, Lim KKP (2013) Long-nosed stargazers at Changi. Singapore Biodiversity Records 2013: 90–91.

Velamala GR, Naranji MK (2018) On the occurrence of the rare long-nosed Stargazer *Ichthyscopus lebeck* (Bloch et Schneider, 1801) (Uranoscopidae) in the coastal waters off Visakhapatnam, India. Journal of Threatened Taxa 10(5): 11697–11700. https://doi.org/10.11609/jott.3520.10.5.11697-11700

Vilasri V (2013) Comparative anatomy and phylogenetic systematics of the family Uranoscopidae (Actinopterygii: Perciformes). Memoirs of the Faculty of Fisheries Sciences. Hokkaido University 55: 1–106. https://doi.org/10.11646/zootaxa.3366.1.1

Vilasri V (2019) Uranoscopidae. Pp. 534–537. In: Psomadakis PN, Thein H, Russell BC, Tun MT (Eds.) FAO species identification guide for fisheries purposes. Field identification guide to the living marine resources of Myanmar. FAO Species Identification Guide for Fishery Purposes. FAO and MOALI, Rome.

Vilasri V, Ho HC, Kawai T, Gomon MF (2019) A new stargazer, *Ichthyscopus pollicaris* (Perciformes: Uranoscopidae), from East Asia. Zootaxa 4702(1): 49–59. https://doi.org/10.11646/zootaxa.4702.1.10

Whitley GP (1936) More ichthyological miscellanea. Memoirs of the Queensland Museum 11(1): 23–51.

Acta Ichthyologica et Piscatoria 54, 2024, 43–48 | DOI 10.3897/aiep.54.117547

PENSOFT.

ACTA
ICHTHYOLOGICA
ET PISCATORIA

Evaluation of large-scale marking with alizarin red S in different age rainbow trout fry for nonlethal field identification

Jan TUREK[1], Pavel LEPIČ[1], Adam BOŘÍK[1], Petra GALICOVÁ[1], Petra NOVÁKOVÁ[1], Mladen AVRAMOVIĆ[1], Tomáš RANDÁK[1]

1 *Faculty of Fisheries and Protection of Waters, University of South Bohemia in Ceske Budejovice, South Bohemian Research Center of Aquaculture and Biodiversity of Hydrocenoses, Vodnany, Czech Republic*

https://zoobank.org/DF7772FE-CD35-48C8-A0E4-91C0D1DE9B56

Corresponding author: Jan Turek (turek@frov.jcu.cz)

Academic editor: Predrag Simonović ♦ **Received** 18 December 2023 ♦ **Accepted** 10 January 2024 ♦ **Published** 13 February 2024

Citation: Turek J, Lepič P, Bořík A, Galicová P, Nováková P, Avramović M, Randák T (2024) Evaluation of large-scale marking with alizarin red S in different age rainbow trout fry for nonlethal field identification. Acta Ichthyologica et Piscatoria 54: 43–48. https://doi.org/10.3897/aiep.54.117547

Abstract

Fry of rainbow trout, *Oncorhynchus mykiss* (Walbaum, 1792), was subjected to one-hour and four hours immersion in Alizarin red S (ARS) bath 150 $mg \cdot L^{-1}$. The experiment involved seven age groups (40, 50, 60, 70, 80, 90, and 100 days) and was conducted to estimate the minimal age of salmonids for mass marking with ARS bath enabling subsequent effective, simple field nonlethal identification, based on fin rays checking. The fish were examined at the ages of 200 and 300 days. The results showed a high retention level of ARS traces in caudal fin rays ensured satisfactory visibility and quick detection. A success rate of marking detection was >90% at 200 and 300 days of age and the fish were immersed in ARS solution from 60 days of age (685°D). This treatment provided better results in fish bathed for four hours. Recognition of marks using a laser pointer and protective glasses was successful even in fish, with a 3.5–5.0 times length increase compared to the marking time. The results indicate a high potential for ARS marking and its field identification for juvenile salmonids, which can significantly expand the possibilities of field experiments.

Keywords

Actinopterygii, alizarin red S, chemical marking, fin rays, Salmonidae, 532 nm laser pointer detection

Introduction

Fish marking is a powerful tool in fisheries science (Thorsteinsson 2002). It is possible to obtain a wide range of information by marking fish. Methods based on the re-capturing of marked fish provide information on the composition of populations in open waters, as well as the growth and survival of stocked fish in natural conditions.

The use of farmed and restocked fish for different goals, including conservation efforts, is growing at a rapid rate. Yet, monitoring the benefits of using hatchery-raised fish for supplementation is often lacking, often due to hatcheries not marking or tagging all fish before release (Warren-Myers et al. 2018). Effective mass marking of early-age categories of fish is particularly problematic. Simultaneously, there is broad agreement among scientists that fish generally have to be stocked in their early life stages if stocking aims to support natural populations (Järvi 2002; Metcalfe et al. 2003). Typically, salmonids in captivity develop reared-related traits that diverge them from wild conspecific in feeding behavior, response to predators, and habitat use (Einum and Fleming 2001). This phenomenon substantially reduces their fitness in wild environments (Fraser et al. 2011).

Although the use of natural or chemical marks (e.g., tetracycline, calcein, and alizarin red), like exposure to stable isotopes via egg immersion or vaccination, involves no or no extra handling, subsequent analysis may require killing the fish after catch (Thorsteinsson 2002; Uglem et al. 2020). In the case of efforts to restore and strengthen weakened populations, especially of salmonid fish, the necessity of killing individuals to identify the origin is counterproductive, because it also includes the killing of wild fish offspring. Bath marking of fish in ARS uses the ability of ARS to bind to calcareous structures in organisms (bone, scale, otolith) (Puchtler et al. 1968) has been known for a long time and is described for various species of salmonid fish, published studies used identification based on otolith analysis (Baer and Rösch 2008; Caudron and Champigneulle 2009; Unfer and Pinter 2013; Lejk and Martyniak 2018; Lejk and Radtke 2021). For this identification method, it is necessary to kill the examined fish. However, several studies mention the possibility of identifying ARS markings using fin-ray analysis in cyprinids (Lü et al. 2015, 2016). For pike, *Esox lucius* Linnaeus, 1758, this procedure has been verified, including the possibility of field identification (Halačka et al. 2018a). Ossification of the fin rays is essential for the success of such marking. Therefore, it is necessary to verify the minimum age and size of individuals of various fish species for marking ARS baths, enabling the subsequent simple and effective field identification of marked fish.

The first purpose of the presently reported study was to investigate the possibility of a simple field nonlethal method of identification ARS marked salmonid fish based on fin rays checking. The second aim was a preliminary estimate of the minimal age of salmonid fish for mass marking with ARS bath enabling subsequent effective field identification with rainbow trout as model species.

Materials and methods

Experimental fish and marking procedure. One thousand juvenile rainbow trout, *Oncorhynchus mykiss* (Walbaum, 1792), aged 30 days (after hatching), weighing 0.45 ± 0.13 g (mean weight ± standard deviation) were purchased from a local producer (Vladimír Šefl, Bušanovice, Czech Republic) where they were reared in a recirculation system (plastic trough) with water temperature 11.0 ± 0.1°C and fed commercial pellets (INICIO Plus, 0.5 mm; Biomar). Fish were randomly divided and stocked in three aquariums (volume 300 L) at the Faculty of Fisheries and Protection of Waters (FFPW) in Vodňany, Czech Republic. Aquaria were filled with tap water filtered through an active carbon filter. Each aquarium was aerated and connected to an individual external filter (Eheim professional 4+, EHEIM GmbH, Germany). Fish excrement and other sediments were drained daily at 12:00 h including 30% water change. Every 10 days, at 40, 50, 60, 70, 80, 90, and 100 days of fish age, 100 fish were randomly chosen, divided into two groups and placed in smaller aquariums with 10 L of ARS solution (alizarin red S, Carl Roth GmbH + Co. KG, Germany) in a concentration of 150 mg · L^{-1}. One group was always bathed for one hour, the other for four hours. Experimental groups were labelled 40/1, 50/1, 60/1, 70/1, 80/1, 90/1, 100/1 or 40/4, 50/4, 60/4, 70/4, 80/4, 90/4, 100/4 according to age of marking and duration of immersion. During the bath, the aquariums were aerated, and the mortality of fish was recorded. After the bath, fish were measured (standard length, SL and total length, TL; mm) and weighed individually (Table 1), and each group was stocked to separate sections of aerated aquariums (water volume 50 L) connected to an individual external filter (see above). During the experiment, fish were fed by commercial pellets of a reasonable size (INICIO Plus, 0.8 mm, and 1.1 mm; Biomar) at 2% of the stock weight daily, divided into three rations. The mortality of fish in each group was recorded daily. Every 10 days the total weight of the stock in each aquarium/section was detected due to the specification of the feed ration. During this part of the experiment (age of fish 30–100 days), the mean water temperature was 14.3 ± 1.2°C, oxygen content 10.1 ± 1.0 mg · L^{-1}, and pH 7.2 ± 0.7. Based on temperature measurements, it was possible to calculate degree-days (°D) for a certain age of fish as the multiplication product of the mean daily water temperature (°C) and the number of days after hatching.

Table 1. Biometric data for fry of rainbow trout, *Oncorhynchus mykiss* (*n* = 50 for each group) at times of the marking immersion.

Age [day]	Cumulative D° [°C]	SL [mm]	TL [mm]	W [g]
40	438	33.9 ± 1.2	38.8 ± 1.6	0.57 ± 0.06
50	562	37.2 ± 2.4	43.1 ± 2.9	0.81 ± 0.08
60	685	40.1 ± 3.1	48.1 ± 3.6	1.08 ± 0.12
70	833	45.1 ± 3.6	54.2 ± 4.3	1.55 ± 0.18
80	966	50.4 ± 6.5	60.3 ± 7.1	2.04 ± 0.32
90	1109	57.6 ± 8.6	67.6 ± 9.2	3.03 ± 0.53
100	1262	61.3 ± 8.9	72.1 ± 9.6	4.14 ± 0.89

D° = degree day (mean daily water temperature × number of days after hatching), SL = standard length, TL = total length, *W* = weight. Values of SL, TL, and *W* are mean ± standard deviation.

At the age of 100 days, the experimental fish groups and control group (250 ind.) were stocked separately into the flow-through circular 500-L tanks filled with river water from the Blanice (Vodňanská) River, at the experimental facility of the FFPW. Fish were reared for 100 days and fed by commercial pellets of a reasonable size (INICIO Plus, 1.5 mm, and 2.0 mm; EFICO Enviro 921, 3 mm; Biomar) at 2% of the stock weight daily. Mortality was recorded for each experimental group and control group. Based on the obtained results of the first evaluation, six groups of fish were selected (marked one and four hours at 60, 80, and 100 days of age), which were further reared to evaluate the visibility of markings at the age of 300 days.

Evaluation of marking visibility. After they were reared for another 100 days (i.e., until the age of 200 days), 20 randomly chosen fish from each group were removed for the analysis of fin rays. The marking detectability was checked and viewed using a green laser pointer (100 mW power; OEM) emitting light of wavelength 532 nm. The evaluators were equipped with protective glasses (SOH, Prague) for working with the laser, preventing the passage of light with a wavelength of 190–540 nm but allowing to observe light with a wavelength of 580 nm, which is the emission value for the given ARS excitation. In the fin rays of the marked fish, the induced fluorescence of the fiery-red tissue can be observed (Fig. 1). During checking, the fish were placed on a damp, black plastic mat, protected from direct sunlight (the evaluation took place in a shade). The evaluation at the 300 days of fish age was provided for groups of fish marked at 60, 80, and 100 days of age. The presence of marks was verified on the fin rays of the caudal and/or anal fin. Randomly chosen marked and control fish was anesthetized with clove oil ($0.03\ \mathrm{mL \cdot L^{-1}}$) and given to two trained examinators for evaluation. All fish were individually measured (SL and TL, mm) and weighted (g) before evaluation. Both examiners checked 10 fish from each marked group, randomly interspersed 80 unmarked control fish, without prior information about the belonging of a specific fish to one of the groups. Detectability of the mark was defined as either "marked" or "unmarked". After marking evaluation and recovery from anesthesia, the fish were returned to the appropriate tank.

Statistical analyses. A one-way analysis of variance (ANOVA) was used to assess differences in weight and length, among fish groups at both mark evaluation times. Post hoc comparisons were made by Tukey's honest significant difference test. Student's *t*-test was used to test for weight and length differences among marked fish with detected and undetected markings. Marking recognition rates were compared with the Pearson and maximum likelihood χ^2 test. Significance was accepted for values of $P < 0.05$.

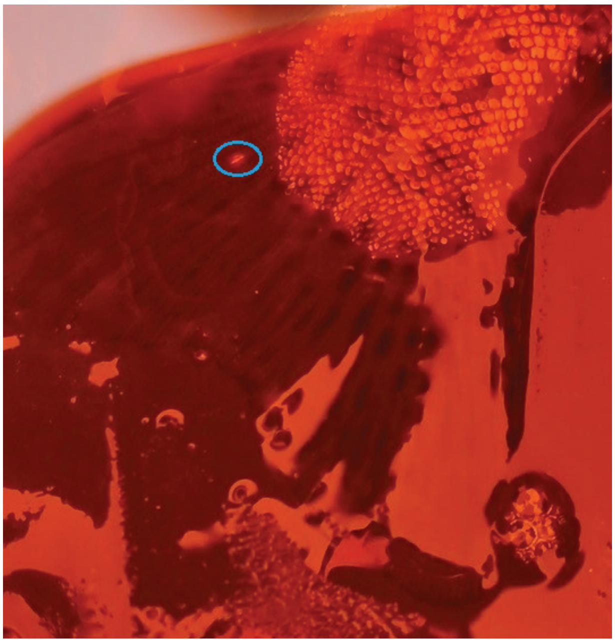

Figure 1. Visible marking in the fin ray of rainbow trout, *Oncorhynchus mykiss* stained with alizarin red S. In the blue circle, a part of the marked fin ray activated by the laser pointer is visible (photo taken through protective glasses).

Results

No effect of the marking procedure on the mortality of rainbow trout fingerlings was found. During the immersion of the fish in the alizarin solution, only two fish deaths were recorded, in groups 60/4 and 90/1. The survival rate in 14 experimental groups during subsequent rearing was 94%–100% at 200 days of age vs. 95.6% in control group. At 300 days of age, survival in the experimental 6 groups was 90%–98% vs. 93.6% in control group. No differences in weight ($F = 0.53$; $P = 0.883$), SL ($F = 0.46$; $P = 0.907$), and TL ($F = 0.37$; $P = 0.968$) were recorded between experimental and control fish at 200 days or 300 days ($F = 1.02$; $P = 0.417$ for SL; $F = 1.11$; $P = 0.356$ for TL, and $F = 2.12$; $P = 0.054$ for weight) of age (Table 2).

The detectability of marking was significantly different at both checking times (Fig. 2). At 200 days of age the mark

Table 2. Biometric data for experimental and control (C) groups of rainbow trout, *Oncorhynchus mykiss* ($n = 20$ for marked groups, $n = 160$ for control group) in marking check times.

Group	Age 200 days			Age 300 days		
	SL [mm]	TL [mm]	*W* [g]	SL [mm]	TL [mm]	*W* [g]
40/1	165.7 ± 12.6	187.7 ± 13.0	73.3 ± 12.5	—	—	—
40/4	163.3 ± 18.0	183.3 ± 18.8	74.3 ± 16.1	—	—	—
50/1	161.0 ± 20.2	182.9 ± 22.1	71.5 ± 21.6	—	—	—
50/4	167.3 ± 14.2	188.5 ± 15.6	74.8 ± 16.2	—	—	—
60/1	163.6 ± 18.1	184.8 ± 19.4	69.4 ± 17.7	248.7 ± 20.2	277.7 ± 21.0	249.5 ± 55.5
60/4	166.8 ± 18.5	189.0 ± 19.6	77.0 ± 21.1	249.9 ± 19.6	279.0 ± 20.5	263.3 ± 50.4
70/1	164.6 ± 16.2	186.3 ± 16.5	77.6 ± 17.4	—	—	—
70/4	175.1 ± 14.2	196.9 ± 15.4	88.7 ± 17.3	—	—	—
80/1	158.7 ± 15.9	180.3 ± 17.6	69.8 ± 20.6	235.8 ± 27.4	264.5 ± 30.2	229.0 ± 71.5
80/4	164.0 ± 15.4	185.4 ± 17.3	75.6 ± 18.1	251.2 ± 22.7	279.9 ± 26.1	286.6 ± 53.7
90/1	164.4 ± 15.8	184.7 ± 16.2	73.7 ± 19.1	—	—	—
90/4	168.6 ± 17.0	189.1 ± 15.7	79.9 ± 17.0	—	—	—
100/1	163.1 ± 20.6	183.8 ± 22.6	78.3 ± 24.0	250.8 ± 21.4	279.5 ± 24.3	272.9 ± 62.9
100/4	165.7 ± 12.5	187.2 ± 14.6	74.5 ± 21.3	251.5 ± 36.5	281.2 ± 39.1	290.4 ± 99.6
Control	162.8 ± 15.3	182.1 ± 16.5	71.5 ± 19.2	244.9 ± 26.5	271.5 ± 27.7	254.5 ± 68.7

Values are mean ± standard deviation, *n* = number of fish, SL = standard length, TL = total length, *W* = weight. In SL, TL, and *W*, no significant ($P < 0.05$) differences between groups according to ANOVA in both checking times were found.

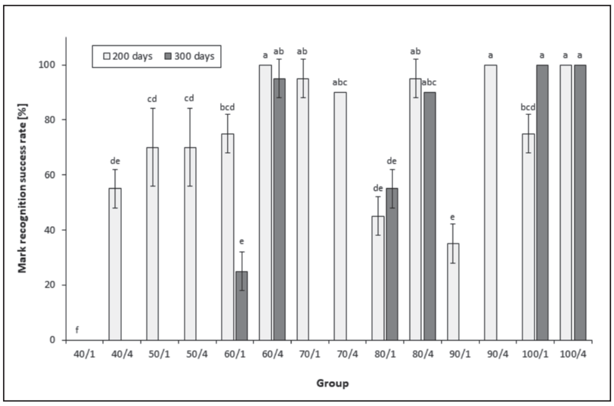

Figure 2. Alizarin red S marking recognition rate in fin rays of experimental groups of rainbow trout, *Oncorhynchus mykiss*, at 200 and 300 days of age. Different letters indicate significant differences ($P < 0.05$) between groups according to Pearson and maximum likelihood χ^2 test.

recognition success rate was from 0% (group 40/1) to 100% (groups 60/4, 90/4, and 100/4). Except for fish tagged at 50 and 70 days of age, the mark recognition was always higher in the four-hour immersion group than the one-hour immersion one, with the difference being statistically significant in some groups. When evaluated at 300 days of age, there was a significant decrease in the detectability of marking in the 60/1 group and an increase in the 100/1 group compared to the evaluation at 200 days. For the other groups, the detectability of marking changed but not statistically significantly. At both evaluation times, no significant differences in weight ($F = 1.35$; $P = 0.657$ for 200 days evaluation; $F = 2.55$; $P = 0.244$ for 300 days evaluation), SL ($F = 1.45$; $P = 0.905$ for 200 days evaluation; $F = 2.18$; $P = 0.982$ for 300 days evaluation), and TL ($F = 1.45$; $P = 0.995$ for 200 days evaluation; $F = 2.52$; $P = 0.275$ for 300 days evaluation), were recorded between the fish of the experimental groups with successful and unsuccessful marking detection (Table 3).

Table 3. Biometric data for marked rainbow trout, *Oncorhynchus mykiss*, with detected and undetected marks in marking check times.

	Age 200 days		Age 300 days	
	Detected	**Undetected**	**Detected**	**Undetected**
n	197	83	93	27
SL [mm]	165.2 ± 17.4	164.9 ± 14.5	246.5 ± 27.3	253.0 ± 17.1
TL [mm]	186.4 ± 18.6	186.4 ± 15.4	275.5 ± 29.5	282.0 ± 18.6
W [g]	75.9 ± 19.7	74.9 ± 17.1	265.0 ± 74.3	266.2 ± 51.2

Values are mean ± standard deviation, *n* = number of fish, SL = standard length, TL = total length, *W* = weight. In SL, TL, and *W*, no significant ($P < 0.05$) differences between groups according to Student's *t*-test in both checking times were found.

Discussion

During the experiment, there was no negative effect of immersion in 150 mg · L^{-1}ARS solution on the survival and growth of marked fish in both duration time one and four hours. The observed death of two fish during the immersion in our experiment can probably be attributed to stress or injury during handling. Concentration ARS immersion up to 300 mg · L^{-1} is published as safe for different fish species by many studies (Lü et al. 2015; Lü et al. 2016), although Unfer and Pinter (2013) recorded increased mortality in brown trout fry and alevin at three-hour duration immersion in ARS concentrations of 150 and 300 mg · L^{-1} compared to control fish. Jurgelėnė et al. (2022) point out the possibility of different toxicity of alizarin red S produced by different manufacturers. Baer and Rösch (2008) recorded more than 95% mortality of 20-day-old brown trout (TL 25–29 mm) immersed for three hours in ARS 300 mg · L^{-1} bath with added 10 g · L^{-1} sodium chloride (NaCl) for the possibility to increase the marking efficiency. Immersion in 50 and 150 mg · L^{-1} ARS was found to be safe, with or without NaCl added. Halačka et al. (2018b) found 100% mortality in a 72-h toxicity test on zebra fish, *Danio rerio* (Hamilton, 1822), in 150, 300, and 600 mg · L^{-1} ARS immersions if NaCl (10 g · L^{-1}) was added compared to zero mortality in the same without NaCl. Due to these inconsistent results, NaCl was not used in the marking immersion in the presently reported experiment to reduce the risk of experimental fish mortality, which could compromise the evaluation of the experiment.

Our experiment demonstrated the possibility of using ARS immersion for mass marking of young age categories of salmonid fish with minimal losses of fish. When followed by simple non-lethal mark detection in the field this approach is a suitable choice for monitoring the stocking programs with young salmonids. The majority of the study results published so far, which have focused on the possibility of non-lethal detection of chemical marking of fish, state the necessity of tissue sampling and detection of the marking in the laboratory using a special microscope (Lü et al. 2015; Lü et al. 2016), although Mohler (2003) describes the possibility of using a hand-held calcein mark detector to immediately discern between marked and non-marked fish by the presence or absence of a visible green fluorescence in the fin rays and other calcified structures. The possibility of field identification of fluorescent markers is also mentioned by Uglem et al. (2020). The method of detection of ARS marking, used in the presently reported study, was described in the methodology of Halačka et al. (2018a) for pike. Its main advantage is the possibility of identifying the marked fish directly in the field, which minimizes the stress of the researched fish and the time and personnel requirement of the research.

The second important goal of the study was to determine the minimum age (size) of the fish, necessary for the formation of a sufficiently distinct mark. The principle of the method namely requires the calcification of the fin rays; they enable the establishment of ARS. To achieve high mark detection rate (90% +) in rainbow trout in the presently reported study, the minimum age of tagged fish for mark application was 60 days (685°D, SL 48.1 ± 3.6 mm), while better results were achieved in fish with immersion duration of four hours compared to those immersed for one hour. In contrast, Halačka et al. (2018a) did not find a significant difference in the identifiability of tags between fish immersed for one or three hours in 150 mg · L^{-1} ARS solution for pike fry.

The results of our study also demonstrate a good detectability of marking even in the case of significant length growth of marked fish. Deterioration of marking identifiability at 300 days of age compared to 200 days was noted only in the 60/1 group, which proves the already mentioned advantage of a longer duration of the marking bath. Fish checked at 300 days of age had 3.7–5.0 times longer body length than at the time of marking. It is the growth of the fish and possible changes in the color and physiological changes of the fish tissues that are mentioned as a frequent reason for the deterioration of the detectability of internal tags (e.g., Halačka et al. 2018b; Thorsteinsson 2002). Thus, it seems that the increase in length of the marked fish does not significantly reduce the identifiability of the ARS markings in rainbow trout, and thus in salmonid fish in general. The final size of the fish in the presently reported experiment corresponded to the size of wild adult brown trout found by Turek et al. (2010) during local mark–recapture experiments in the Blanice (Vodňanská) River. Considering the lower growth rate of stocked salmonid fish in nature, it can be assumed that the presented method of marking and identification will make it possible to recognize fish stocked as fed fry even several years after stocking.

In conclusion, a four-hour duration ARS immersion (150 mg · L^{-1}) is suitable for marking the juveniles salmonids from 60 days of age (685°D) for later nonlethal field identification, based on fin rays checking by 532 nm laser pointer using protective glasses preventing the passage of light with a wavelength of 190–540 nm. The use of the presented marking and identification methods can significantly improve and simplify the implementation of mark-recapture experiments in salmonids in open waters.

Acknowledgments

The study was financially supported by the Ministry of Agriculture of the Czech Republic, NAZV project No. QK23020064 and by the Ministry of Education, Youth, and Sports of the Czech Republic, project PROFISH (CZ .02.1.01/0.0/0.0/16_019/0000869).

References

Baer J, Rösch R (2008) Mass-marking of brown trout (*Salmo trutta* L.) larvae by alizarin: Method and evaluation of stocking. Journal of Applied Ichthyology 24(1): 44–49. https://doi.org/10.1111/j.1439-0426.2007.01038.x

Caudron A, Champigneulle A (2009) Multiple marking of otoliths of brown trout, *Salmo trutta* L., with alizarin redS to compare efficiency of stocking of three early life stages. Fisheries Management and Ecology 16(3): 219–224. https://doi.org/10.1111/j.1365-2400.2009.00661.x

Einum S, Fleming IA (2001) Implications of stocking: Ecological interactions between wild and released salmonids. Nordic Journal of Freshwater Research 75: 56–70.

Fraser DJ, Weir LK, Bernatchez L, Hansen MM, Taylor EB (2011) Extent and scale of local adaptation in salmonid fishes: Review and meta-analysis. Heredity 106: 404–420. https://doi.org/10.1038/hdy.2010.167

Halačka K, Poštulková E, Kopp R, Mareš J (2018a) Možnost využití značení štik pomocí Alizarinové červeně a způsob terénní detekce značených ryb. [The possibility of using the marking of pike using alizarin red and the method of field detection of marked fish.] Mendelova univerzita v Brně Ústav biologie obratlovců AV ČR v.v.i. Ověřená technologie, Technologie R18/2018, 16 pp. [In Czech]

Halačka K, Poštulková E, Kopp R, Mareš J (2018b) Alternativní značení vysazovaných ryb pro umožnění jejich následného sledování. [Alternative marking of stocked fish to enable their follow-up.] Mendelova univerzita v Brně Ústav biologie obratlovců AV ČR v.v.i. Ověřená technologie, Technologie R17/2017, 18 pp. [In Czech]

Järvi T (2002) Performance and ecological impacts of introduced and escaped fish: Physiological and behavioural mechanisms–AQUAWILD. Final report to: European Commission EC Contract No. FAIR CT, 97-1957. National Board of Fisheries, Institute of Freshwater Research, Sweden.

Jurgelėnė Ž, Montvydienė D, Stakėnas S, Poviliūnas J, Račkauskas S, Taraškevičius R, Skrodenytė-Arbačiauskienė V, Kazlauskienė N (2022) Impact evaluation of marking *Salmo trutta* with alizarin red S produced by different manufacturers. Aquatic Toxicology 242: 106051. https://doi.org/10.1016/j.aquatox.2021.106051

Lejk AM, Martyniak A (2018) Low temperature effect on multiple alizarin immersion mass-marking of juvenile sea trout *Salmo trutta* m. *trutta* L. otoliths. Turkish Journal of Fisheries and Aquatic Sciences 18(5): 747–752. https://doi.org/10.4194/1303-2712-v18_5_10

Lejk AM, Radtke G (2021) Effect of marking *Salmo trutta lacustris* L. larvae with alizarin red S on their subsequent growth, condition, and distribution as juveniles in a natural stream. Fisheries Research 234: e105786. https://doi.org/10.1016/j.fishres.2020.105786

Lü HJ, Fu M, Xi D, Yao WZ, Su SQ, Wu ZL (2015) Experimental evaluation of using calcein and alizarin red S for immersion marking of bighead carp *Aristichthys nobilis* (Richardson, 1845) to assess growth and identification of marks in otoliths, scales and fin rays. Journal of Applied Ichthyology 31(4): 665–674. https://doi.org/10.1111/jai.12778

Lü HJ, Fu M, Dai S, Xi D, Zhang ZX (2016) Experimental evaluation of calcein and alizarin red S for immersion marking of silver carp *Hypophthalmichthys molitrix* (Valenciennes, 1844). Journal of Applied Ichthyology 32(1): 83–91. https://doi.org/10.1111/jai.12981

Metcalfe NB, Valdimarsson SK, Morgan IJ (2003) The relative roles of domestication, rearing environment, prior residence and body size in deciding territorial contests between hatchery and wild juvenile salmon. Journal of Applied Ecology 40(3): 535–544. https://doi.org/10.1046/j.1365-2664.2003.00815.x

Mohler JW (2003) Producing fluorescent marks on Atlantic salmon fin rays and scales with calcein via osmotic induction. North American Journal of Fisheries Management 23(4): 1108–1113. https://doi.org/10.1577/M02-143

Puchtler H, Meloan SN, Terry MS (1968) On the history and mechanism of alizarin and alizarin red S stains for calcium. Journal of Histochemistry and Cytochemistry 17(2): 110–124. https://doi.org/10.1177/17.2.110

Thorsteinsson V (2002) Tagging methods for stock assessment and research in fisheries. Report of concerted action FAIR CT.96.1394 (CATAG). Marine Research Institute Technical Report (79), Iceland, 179 pp.

Turek J, Horký P, Velíšek J, Slavík O, Hanák R, Randák T (2010) Recapture rate and growth of hatchery-reared brown trout (*Salmo trutta* v. *fario*, L.) in Blanice River and the effect of stocking on wild brown trout and grayling (*Thymallus thymallus*, L.). Journal of Applied Ichthyology 26(6): 881–885. https://doi.org/10.1111/j.1439-0426.2010.01520.x

Uglem I, Kristiansen TS, Mejdell CM, Basic D, Mortensen S (2020) Evaluation of large-scale marking methods in farmed salmonids for tracing purposes: Impact on fish welfare. Reviews in Aquaculture 12(2): 600–625. https://doi.org/10.1111/raq.12342

Unfer G, Pinter K (2013) Marking otoliths of brown trout (*Salmo trutta* L.) embryos with alizarin red S. Journal of Applied Ichthyology 29(2): 470–473. https://doi.org/10.1111/jai.12100

Warren-Myers F, Dempster T, Swearer SE (2018) Otolith mass marking techniques for aquaculture and restocking: Benefits and limitations. Reviews in Fish Biology and Fisheries 28(3): 485–501. https://doi.org/10.1007/s11160-018-9515-4

Acta Ichthyologica et Piscatoria 54, 2024, 49–61 | DOI 10.3897/aiep.54.112465

ACTA ICHTHYOLOGICA ET PISCATORIA

Identification of pen shells (Bivalvia: Ostreida: Pinnidae) collected off northern Iloilo, Philippines using their morphological characters

Cheryl JELA[1,2], Harold M. MONTECLARO[1], Nathaniel C. AÑASCO[1], Gerald F. QUINITIO[1], Ricardo P. BABARAN[1]

1 *Institute of Marine Fisheries and Oceanology, College of Fisheries and Ocean Sciences, University of the Philippines Visayas, Miagao, Iloilo, Philippines*

2 *Northern Iloilo State University, Estancia, Iloilo, Philippines*

https://zoobank.org/09C77EEF-6135-4135-B655-003AC04FA626

Corresponding author: Ricardo P. Babaran (rpbabaran@upv.edu.ph)

Academic editor: Sanja Matić-Skok ♦ **Received** 12 September 2023 ♦ **Accepted** 7 January 2024 ♦ **Published** 19 February 2024

Citation: Jela C, Monteclaro HM, Añasco NC, Quinitio GF, Babaran RP (2024) Identification of pen shells (Bivalvia: Ostreida: Pinnidae) collected off northern Iloilo, Philippines using their morphological characters. Acta Ichthyologica et Piscatoria 54: 49–61. https://doi.org/10.3897/aiep.54.112465

Abstract

This study describes morphological characteristics of pen shells collected along the coast of northern Iloilo, Philippines. A total of 380 pen shell individuals with intact shells and their adductor muscles were carefully examined and measured. Eleven species were studied, namely: *Atrina pectinata* (Linnaeus, 1767), *Atrina inflata* (Dillwyn, 1817), *Atrina vexillum* (Born, 1778), *Atrina seminuda* (Lamarck, 1819), *Atrina rigida* ([Lightfoot], 1786), *Pinna bicolor* Gmelin, 1791, *Pinna atropurpurea* Sowerby, 1825, *Pinna deltodes* Menke, 1843, *Pinna muricata* Linnaeus, 1758, *Pinna incurva* Gmelin, 1791, and *Pinna nobilis* Linnaeus, 1758. The species were identified based on the nine characteristics of the valve for the genus *Pinna* and eight for the genus *Atrina*. These characteristics were then correlated with their adductor muscles' morphology. Analysis of variance revealed that the three most dominant species investigated under genus *Atrina*, namely *Atrina pectinata*, *Atrina inflata*, and *Atrina vexillum*, were found to be significantly different in the eight characters of the valve ($P < 0.05$). Moreover, three representative *Pinna* species, *Pinna bicolor*, *Pinna atropurpurea*, and *Pinna deltodes*, were significantly ($P < 0.05$) different based on shell width, dorsal posterior shell margin, sulcus width, and dorsal posterior margin to dorsal nacreous margin. The observed high correlation ($P < 0.05$) between adductor muscle properties and different shell length characteristics for five dominant species can be used as a predictor of growth and suggests that the increase in the size of adductor muscle correlates to the increase in the size of the mentioned shell characteristics. No previous study of this kind was conducted in the Philippines. This work provides relevant information for related biological research on other pen shell species and for the management of pen shell resources in northern Iloilo and, possibly, other regions in the world.

Keywords

adductor muscle, *Atrina pectinata*, fisheries management, growth predictor, *Pinna bicolor*, taxonomy

Introduction

The family Pinnidae (Order: Ostreida) belongs to the class Bivalvia and is commonly known as pen shell (Deudero et al. 2015). They are large, thin, wedge-shaped shells (Burns and Smith 2011) that are nearly burrowed in soft substrates in shallow waters. A total of 61 species is known worldwide (Deudero et al. 2015). In the Philippines, 15 species occur (Poppe 2010; Schultz and Huber 2013; Lemer et al. 2016), including four species in northern Iloilo (Laureta 2008).

Morphologically, pen shells are cryptic (Lemer et al. 2016) and are extremely prone to breakage, and this makes their identification confusing and challenging (Idris et al. 2008). Although they can repair their damaged shells by themselves, the repaired shells are always different from intact ones in form and sculpture (Rosewater 1982; Idris et al. 2008). Species of the genus *Atrina* have a continuous nacreous area that occupies the entire anterior inner valve surface (Rosewater 1982; Scheltema and Williams 1983). In contrast, species of the genus *Pinna*, another genus of the family Pinnidae, have a nacreous area that is divided into dorsal and ventral lobes by an anteroposteriorly directed sulcus (Souji et al. 2014).

Aside from northern Iloilo, other active fisheries for pen shells are localized in various areas in the Philippines, but the species of interest is always *Atrina pectinata* (Linnaeus, 1767) because of the high demand for its adductor muscle by the export market, particularly in Taiwan. Each year about 20 tonnes of this species are captured by local divers in the southwestern region of the Visayan Sea (Del Norte-Campos et al. 2021) while about 18 tonnes are gathered in the Province of Eastern Samar (Diocton and Adalla 2019). Meanwhile, the mantle of *Atrina pectinata* is consumed locally. Similar practices are noted in Sorsogon Province, in the southeastern region of the main island of Luzon (Amano and Mojados 2020). Pen shell fishery is a major activity in coastal areas throughout the Visayan Sea, but it is rarely documented. In this study area, which forms part of the Visayan Sea, a small number of poor fishers who are mostly educated only up to primary level, conduct gathering operations 20 days per month to support their households mainly from the sales of adductor muscles, but they also land various fin fish species and other bivalve species as bycatch (Jela unpublished*). Due to the high economic value and food value of adductor muscles (Greenwald 1996; Katsanevakis et al. 2011; Leal-Soto et al. 2011; Basso et al. 2015), it is likely that demand for pen shells will continue to increase while a decline in production persists.

Pen shells have a large posterior adductor muscle that is responsible for the opening and closing of the shell. It appears as dark and light phases, which are respectively called blocking and working muscles (Czihak and Dierl 1961). It is the most important energy storage site in many marine bivalves and accumulates mostly protein and carbohydrate reserves to sustain gametogenesis (Saucedo and Southgate 2008). The age of the pen shell can be discerned through the scar created by the posterior adductor muscle (Garcia-March et al. 2011); however, it is difficult to count its early years because of the nacre deposition in later life that conceals the few scars that represent the year of life of the pen shell (Richardson et al. 2004).

In managing wild pen shell resources, it is important to make an accurate identification of species occurring in a certain locality. Previously, Laureta (2008) identified a total of four pen shells of the family Pinnidae in the Visayan Sea off the coasts of northern Iloilo. However, this count is likely low because the Visayan Sea is home to diverse bivalves. Moreover, a preliminary cursory investigation of adductor muscles that are sold in the market revealed varied shapes and forms, suggesting the occurrence of not just four species and that the pen shell fishery is no longer limited to *Atrina pectinata*. However, sorting of the adductor muscles to determine species is difficult because no information is known about the morphological characteristics of collected species of the family Pinnidae in the area.

Obtaining morphological data of pen shells at the landing sites is not possible due to the existing fishing method, which requires underwater extraction of the meat each time a pen shell is encountered. With the aid of a compressor, divers extract individual pen shells from their habitat, shuck all the meat, and leave empty shells at the sea bottom. This method is preferred because more meat can be collected during each dive. Moreover, the shells are no longer loaded on their small boats because of their bulkiness. Also, there is no motivation for landing the shells because there is no market for them. Therefore, categorization of species monitoring based on shell shape and size is not possible. However, it was observed that the adductor muscles landed at local markets with their mantle have different shapes. Thus, an alternative morphological characterization strategy based on the shapes of the adductor muscles can be adopted. The information obtained would provide insights as to which species need to be managed. More detailed measurements of their morphological characteristics would also provide information about pen shell diversity in the area.

This study focuses on species of the family Pinnidae. First, it aims to update the checklist of *Atrina* and *Pinna* species that occur in the coastal waters of the Visayan Sea, off northern Iloilo, in the Philippines. This information is useful for future research related to the taxonomy, morphology, and genetic diversity of pen shell species in the Philippines. The second objective seeks to determine some relations in the characters of landed adductor muscles and the pen shells, which may be used for identifying species for better management.

Materials and methods

Study area. This study was carried out in the coastal waters of northern Iloilo, part of the Visayan Sea, Philippines (Fig. 1A). Pen shells were directly collected by fishers from the seabed during low tide; this corresponds to 0 m depth in our data sheet. Divers were contracted to collect pen shells also at water depths of 5, 10, 15, and 20 m, which were established at each of the designated six sampling stations where they reportedly occur (Fig. 1B).

---

* Jela CB (2023) Taxonomy, ecology and fishery of pen shells and some aspects of the reproductive biology of *Atrina pectinata* in the northern Iloilo, Philippines. Doctoral dissertation, University of the Philippines, Visayas, Miagao, Iloilo, Philippines, 102 pp.

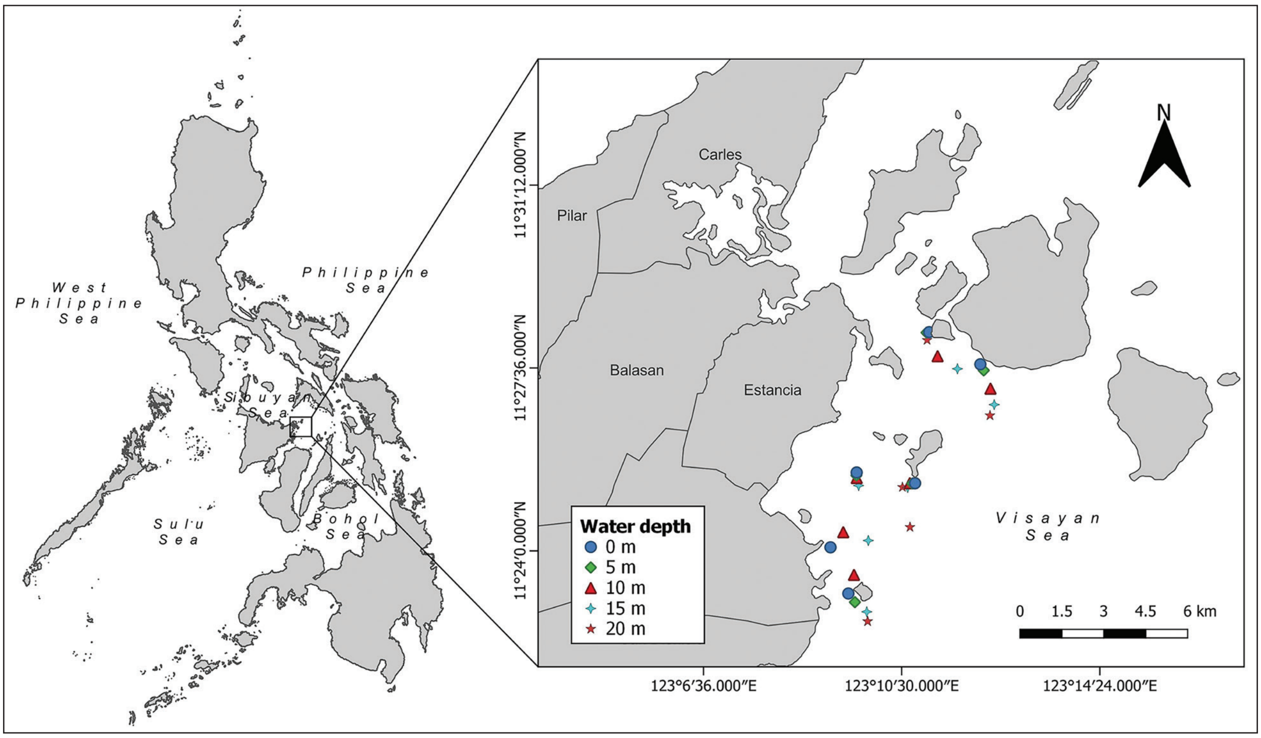

Figure 1. Map of the Philippines showing the province of Iloilo, Philippines (**A**), and location of six sampling stations at five water depths (0 m, 5 m, 10 m, 15 m, and 20 m) (**B**) in the coastal waters of northern Iloilo, part of Visayan Sea, Philippines.

Sample collection and measurements. A total of 380 intact adult individuals of various pen shell species were collected using compressor diving, stored in a styrofoam box, preserved with ice, brought to the biological laboratory of Northern Iloilo State University, and carefully examined for morphological measurements and identification. The specimens were cleaned with a metal knife to remove epibionts and washed with tap water to remove dirt. Shells were carefully shucked individually and flesh was removed. The right valve of each shell was measured using a Vernier caliper to the nearest 0.01 mm following the method of Idris et al. (2008), with emphasis on the following parameters (distances): 1) total shell length (TSL); 2) length of anterior to posterior adductor margin (LAPAM); 3) posterior adductor to posterior shell margin (PAPSM); 4) dorsal posterior shell margin (DPSM); 5) dorsal margin (DM); 6) shell width (ShW); 7) sulcus width (SuW); 8) posterior adductor margin to posterior nacreous margin (PAMPNM); and, 9) dorsal nacreous length (DNL).

The measurements are not the same for all species because of varied morphologies. It is important to note that the dorsal posterior shell margin differs in *Atrina* and *Pinna* species. Measurement of nacreous length started at the end of the muscle scar because the nacreous layer was apparent at the end of the posterior margin of the anterior adductor muscle scar. Moreover, for species of the genus *Pinna*, the sulcus width was also measured (Fig. 2). The dorsal posterior shell margin of different species with different morphologies was identified by dividing the posterior margin into equal parts (dorsal and ventral margin). The dorsal posterior shell margin was then measured. The shell specimens were then photographed, labeled, and stored.

Species identification. The specimens were identified based on their morphological characteristics such as shell structure, specifically in the way the parts are organized, and sculpture, as indicated by length, color patterns, and other related traits. Identification guides include the works of Grave (1911), Winckworth (1929), Butler and Keough (1981); Scheltema and Williams (1983); Poutiers (1998), Leal (2002), Idris et al. (2008), and Laureta (2008).

Data analysis. The mean and standard deviation of the different shell and adductor muscle morphometric characters were calculated for each species. One-way analysis of variance was used to estimate the differences in the means of the different parameters of the shells. Post-hoc tests were subsequently applied to show how the various parameters differed. This analysis was performed using the SPSS package, ver. 20. Before analysis, the normality of data was tested using the Kolmogorov–Smirnov test. Using three dominant species of the two pen shell genera in this study, the relation between shell and adductor muscle morphology was determined by linear regression.

Results

Five species of the genus *Atrina*, namely, *Atrina pectinata*, *Atrina inflata* (Dillwyn, 1817), *Atrina vexillum* (Born, 1778), *Atrina seminuda* (Lamarck, 1819), and *Atrina rigida* ([Lightfoot], 1786) and six species of the genus *Pinna*, namely, *Pinna bicolor* Gmelin, 1791, *Pinna atropurpurea* Sowerby, 1825, *Pinna deltodes* Menke, 1843, *Pinna muricata* Linnaeus, 1758, *Pinna incurva* Gmelin, 1791, and *Pinna nobilis* Linnaeus, 1758 were collected from the

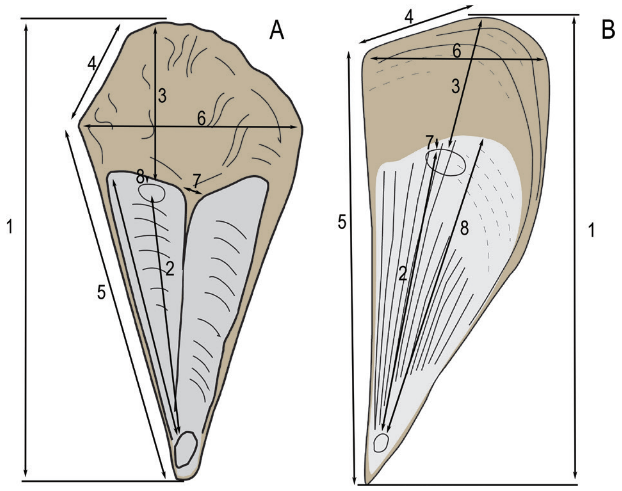

Figure 2. A diagram of the interior right valve of genus *Pinna* (**A**) showing the position of the nacreous layer and 8 characteristics of the shell. 1 = total shell length (TSL); 2 = length of anterior to posterior adductor margin (LAPAM); 3 = posterior adductor to posterior shell margin (PAPSM); 4 = dorsal posterior shell margin (DPSM); 5 = dorsal margin (DM); 6 = shell width (ShW); 7 = sulcus width (SuW); 8 = posterior adductor margin to posterior nacreous margin (PAMPNM) and 9 = dorsal nacreous length (DNL). A diagram of the interior right valve of genus *Atrina* (**B**) showing the position of the nacreous layer and 8 characteristics of the shell. 1 = total shell length (TSL); 2 = length of anterior to posterior adductor margin (LAPAM); 3 = posterior adductor to posterior shell margin (PAPSM); 4 = dorsal posterior shell margin (DPSM); 5 = dorsal margin (DM); 6 = shell width (ShW); 7 = posterior adductor margin to posterior nacreous margin (PAMPNM); and 8 = dorsal nacreous length (DNL).

waters of northern Iloilo. Table 1 summarizes the measurements of shell characteristics of the samples collected while Table 2 provides descriptive characteristics of those species. Figures 3, 4 show the images of the shells of these species. The dominant species were *A. pectinata*, *A. inflata*, *A. vexillum*, *P. bicolor*, *P. atropurpurea*, and *P. deltodes*.

Differences in shell morphology of dominant species. Only the dominant species were used to compare the shell morphology of pen shell species. These include three species of the genus *Atrina*, namely, *A. pectinata*, *A. inflata*, and *A. vexillum*, and three species of the genus *Pinna*, namely, *P. bicolor*, *P. deltodes*, and *P. atropurpurea*. These were subjected to length–length analysis. The other species were not analyzed because the number of specimens for them was inadequate. Figure 5 presents eight morphometric measurements of the three dominant *Atrina* species. They were significantly different in all the characteristics measured in this study (ANOVA, $P < 0.05$). Post-hoc analyses revealed that the total shell length, length of posterior adductor to posterior shell margin, dorsal margin, and dorsal nacreous length of *A. pectinata* was always significantly higher ($P < 0.05$) than their corresponding values in *A. vexillum* and *A. inflata*. The length of its anterior to posterior adductor margin was significantly different relative to *A. inflata* ($P < 0.05$) but was similar to *A. vexillum*. Only *A. pectinata* and *A. inflata* differed in terms of the dorsal posterior shell margin ($P < 0.05$). The shell width of *A. pectinata* was significantly lower than *A. vexillum* ($P < 0.05$) but not different from *A. inflata*. And, the posterior adductor margin to the posterior nacreous margin of *A. pectinata* was significantly higher compared to *A. inflata* and *A. vexillum* due to the 0 value of the posterior adductor margin to posterior nacreous margin of *A. vexillum* ($P < 0.05$). Meanwhile, Figure 6 shows the morphometric characteristics of the three dominant *Pinna* species. These species differed based on the dorsal posterior shell margin, the width of the shell, the sulcus width, and the posterior adductor margin to the posterior nacreous margin (ANOVA, $P < 0.05$). The three species differed only in several characteristics. The dorsal posterior shell margin of *P. deltodes* was significantly higher than those of *P. atropurpurea* and *P. bicolor*, but *P. atropurpurea* and *P. bicolor* also differed ($P < 0.05$). The shell width of *P. bicolor* was significantly different ($P < 0.05$) relative to *P. deltodes* and *P. atropurpurea*, which were similar. The three species had

Table 1. Principal metric shell characters of eleven pen shell species of the genera *Atrina* and *Pinna* (family Pinnidae) based on literature sources.

Species	*n*	Metric shell character [mm]								
		TSL	LAPAM	PAPSM	DPSM	DM	ShW	SuW	PAMPNM	DNL
A. pectinata[1]	55	199.95 ± 47.07	106.57 ± 30.91	72.92 ± 18.75	52.56 ± 33.37	181.40 ± 40.70	93.16 ± 27.27	0.00	8.06 ± 1.51	125.95 ± 27.95
A. inflata[2]	47	164.40 ± 25.27	94.61 ± 14.40	61.08 ± 14.39	92.21 ± 35.40	131.12 ± 20.02	101.54 ± 17.88	0.00	3.11 ± 1.74	107.90 ± 16.94
A. vexillum[2]	17	173.45 ± 33.87	96.37 ± 21.47	55.51 ± 14.57	70.76 ± 24.57	117.66 ± 17.21	115.76 ± 22.09	0.00	0.00	101.55 ± 16.50
A. seminuda[3]	1	274.00	138.00	102.00	29.00	219.00	161.00	0.00	19.00	162.00
A. rigida[3]	1	240.00	140.00	45.00	115.00	160.00	145.00	0.00	0.00	145.00
P. bicolor[2]	43	299.10 ± 50.12	137.30 ± 27.79	122.61 ± 20.95	41.43 ± 5.38	251.37 ± 48.79	98.80 ± 17.35	2.37 ± 0.47	4.73 ± 1.92	157.59 ± 29.25
P. atropurpurea[2]	34	293.87 ± 39.58	135.20 ± 20.97	121.55 ± 15.18	50.54 ± 4.45	248.03 ± 38.11	122.4 ± 7.84	4.94 ± 0.78	7.56 ± 4.49	158.02 ± 31.80
P. deltodes	10	280.18 ± 93.34	142.71 ± 32.36	131.42 ± 18.80	89.58 ± 45.10	269.29 ± 41.35	120.95 ± 15.76	9.10 ± 0.94	9.38 ± 0.67	177.44 ± 49.58
P. muricata[2]	2	225.50 ± 0.71	109.50 ± 9.19	102.00 ± 2.83	54.00 ± 8.49	223.5 ± 4.95	123.50 ± 10.61	4.00 ± 0.00	2.12 ± 0.18	135.50 ± 27.8
P. incurva[5]	1	257.00	93.00	130.00	31.00	240.00	96.00	1.00	5.00	122.00
P. nobilis[6]	1	419.00	172.00	205.00	93.00	365.00	133.00	8.00	14.00	223.00

Values are expressed as mean ± standard deviation. References: [1] = Poutiers (1998), [2] = Winckworth (1929), [3] = Leal (2008), [4] = Scheltema (1983), [5] = Stella et al. (2015), [6] = Basso et al. (2015); *n* = number of specimens; Measurements: TSL = total shell length , LAPAM = length of anterior to posterior adductor margin, PAPSM = posterior adductor to posterior shell margin, DPSM = dorsal posterior shell margin, DM = dorsal margin, ShW = shell width, SuW = sulcus width, PAMPNM = posterior adductor margin to posterior nacreous margin, DNL = dorsal nacreous length.

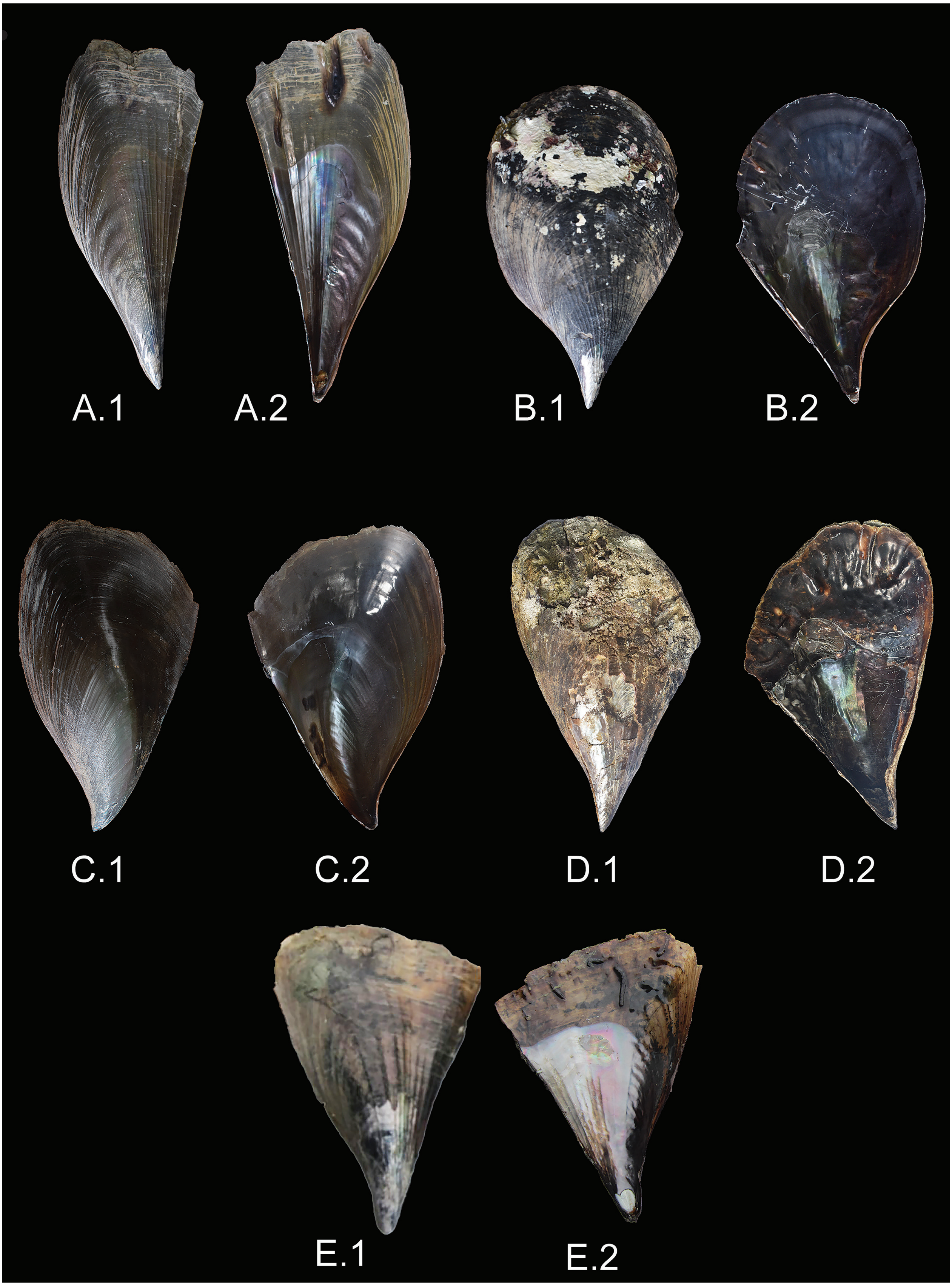

Figure 3. Photographs of selected species of the genus *Atrina* showing the external and internal surface of the right valve collected from northern Iloilo, Philippines. External valve (**A.1**, **B.1**, **C.1**, **D.1**, **E.1**), internal valve (**A.2**, **B.2**, **C.2**, **D.2**, **E.2**). *Atrina pectinata* (A.1–A.2), *A. vexillum* (B.1–B.2), *A. inflata* (C.1–C.2), *A. seminuda* (D.1–D.2), and *A. rigida* (E.1–E.2).

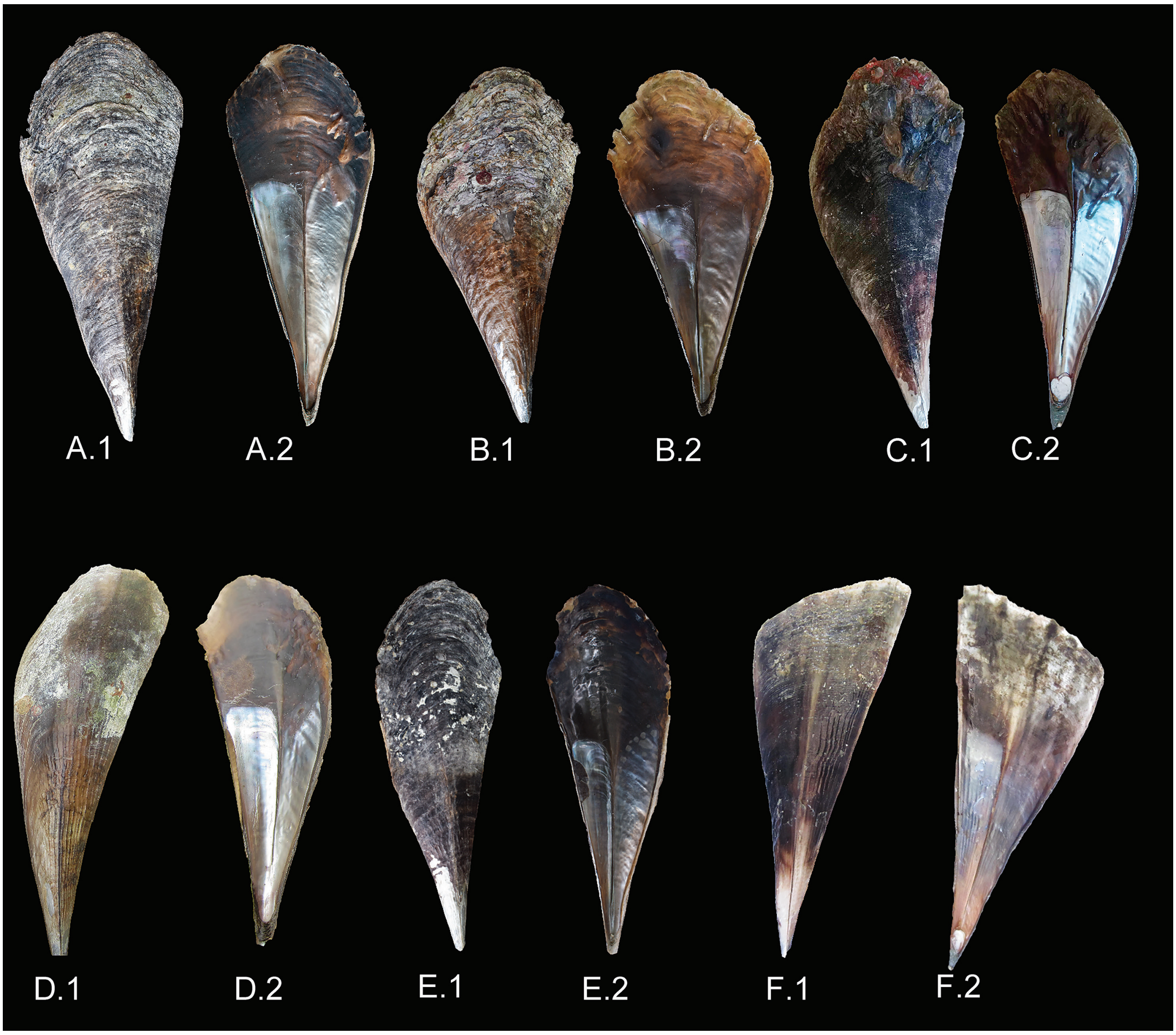

Figure 4. Photographs of selected species of the genus *Pinna* showing the external and internal surface of the right valve collected from northern Iloilo, Philippines. External valve (**A.1**, **B.1**, **C.1**, **D.1**, **E.1, F.1**), internal valve (**A.2**, **B.2**, **C.2**, **D.2**, **E.2, F.2**). *Pinna bicolor* (A.1–A.2), *P. deltodes* (B.1–B.2), *P. atropurpurea* (C.1–C.2), *P. incurva* (D.1–D.2), *P. nobilis* (E.1–E.2), and *P. muricata* (F.1–F.2).

Table 2. Descriptive characters of eleven pen shell species of the genera *Atrina* and *Pinna* (family Pinnidae) based on literature sources.

Species	Description/Comment	Reference
A. pectinata	Large, thin, fragile, and triangularly wedge shaped; shell external surface slightly shiny, light-tannish grey tinged with brownish toward the umbone	Poutiers 1998
A. inflata	Strongly swollen shape shell	Winckworth 1929
A. vexillum	Dark to almost black color of shell	Winckworth 1929
A. seminuda	Large, fan-shaped, and triangular with 15 narrow radial ribs separated by larger interspaces	Leal 2008
A. rigida	Large, triangular in shape, and surface of shell with 15 radial ribs	Leal 2002
P. bicolor	External valve of shell dark purple with nearly straight ventral margin and dorsal margin	Winckworth 1929
P. atropurpurea	External valve of shell dark purple; ventral margin and dorsal margin nearly straight	Winckworth 1929
P. deltodes	Shell length reached up to 370.8 mm; dorsal and ventral regions flared posteriorly and nearly rounded at apex with highest point between dorsal and ventral margins	Scheltema 1983
P. muricata	Triangulated, whitish in color, blotch of dark purple	Winkworth 1929
P. incurva	Narrowly attenuated shell; light yellow at posterior and reddish-brown towards anterior	Stella et al. 2015
P. nobilis	World's largest triangular-shape bivalve	Basso et al. 2015

different sulcus widths ($P < 0.05$). The posterior adductor margin to the posterior nacreous margin of *P. bicolor* was significantly lower ($P < 0.05$) than those of *P. atropurpurea* and *P. deltodes*, which were similar.

Adductor muscle morphology. Representative specimens of the posterior adductor muscles of the most dominant species belonging to the genera *Atrina* (Fig. 7) and *Pinna* (Fig. 8) are illustrated for comparison. Table 3

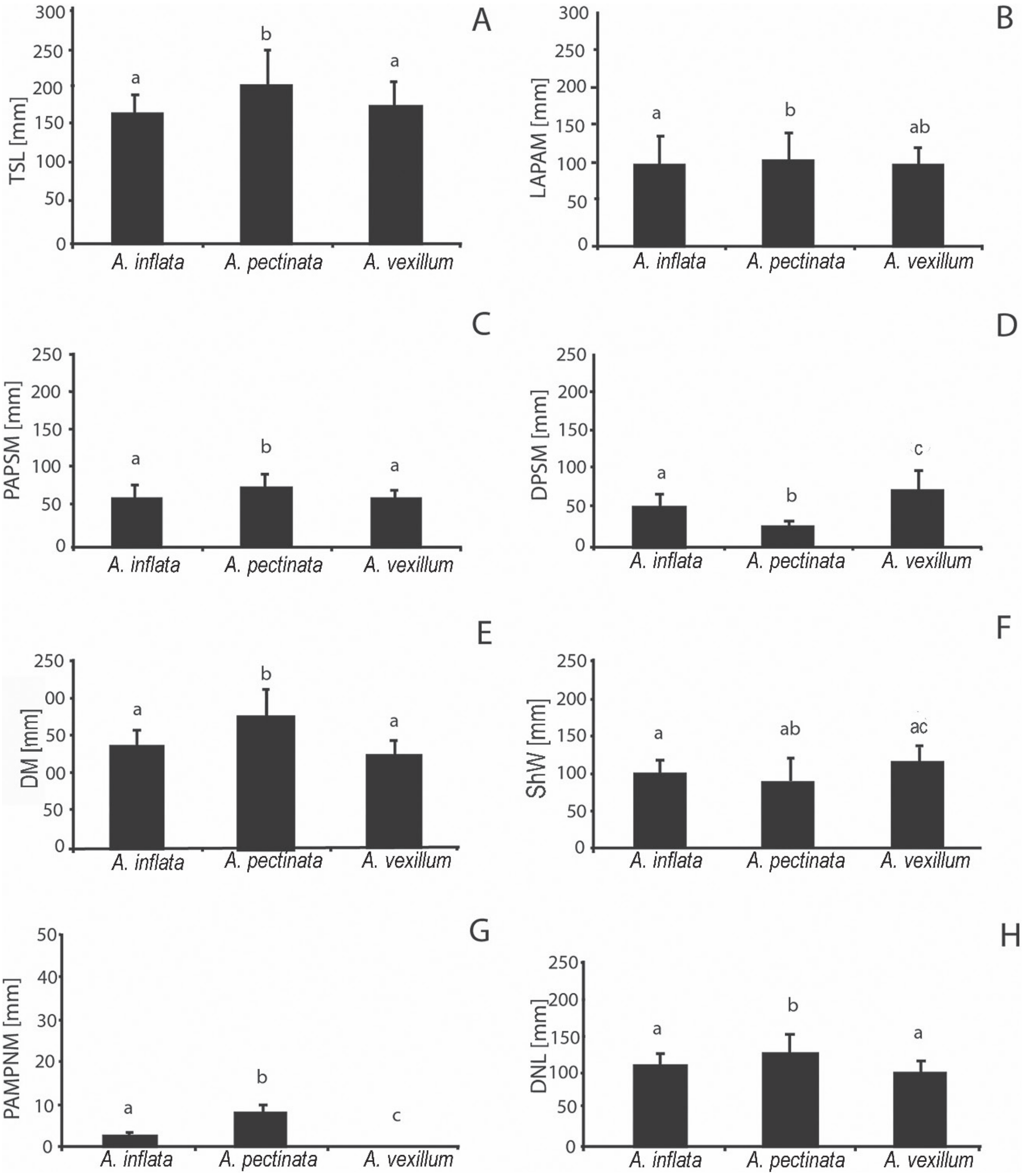

Figure 5. Measurements of eight morphometric characters of *Atrina inflata* (n = 45), *A. pectinata* (n = 231), and *A. vexillum* (n = 17). Values are expressed as the mean ± standard deviation. TSL = total shell length (**A**), LAPAM = length of anterior to posterior adductor margin (**B**), PAPSM = posterior adductor to posterior shell margin (**C**), DPSM = dorsal posterior shell margin (**D**), DM = dorsal margin (**E**), ShW = shell width (**F**), PAMPNM = posterior adductor margin to posterior nacreous margin (**G**), DNL = dorsal nacreous length (**H**). Small letters above the columns indicate the results of post-hoc tests.

presents additional information about the adductor muscles of the five dominant species examined.

Relation between shell length characters and adductor muscles of dominant species. The regression equations between the different length characteristics and their respective adductor length and thickness for five dominant pen shell species (r^2, 0.23–0.94) are shown in Table 4. This procedure was not performed on *P. deltodes* because the number of samples was inadequate. All eight length characteristics of *A. pectinata* and *A. inflata* were all positively significantly correlated ($P < 0.05$) with their adductor muscle length and thickness. In the case of *A. vexillum*, dorsal nacreous

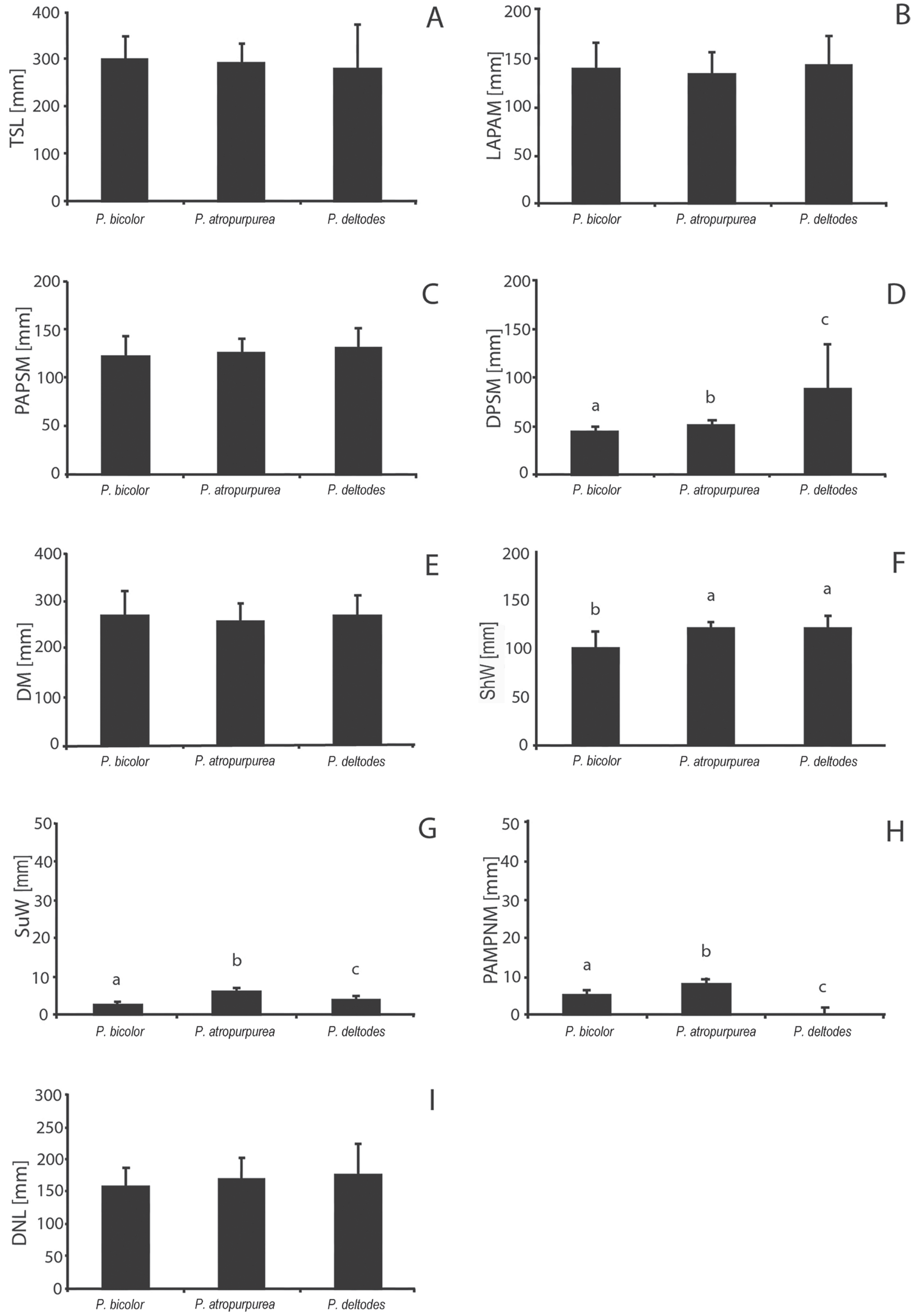

Figure 6. Measurements of nine morphometric characters of the genus *Pinna*: *P. bicolor* (*n* = 43), *P. atropurpurea* (*n* = 34), and *P. deltodes* (*n* = 10). Values are expressed as the mean ± standard deviation. TSL = total shell length (**A**), LAPAM = length of anterior to posterior adductor margin (**B**), LPAPSM = length of posterior adductor to posterior shell margin (**C**), LDPSM = length of dorsal posterior shell margin (**D**), DM = dorsal margin (**E**), ShW = shell width (**F**), SuW = sulcus width (**G**), PAMPNM = posterior adductor margin to posterior nacreous margin (**H**), DNL = dorsal nacreous length (**I**). Small letters above the columns indicate the results of post-hoc tests.

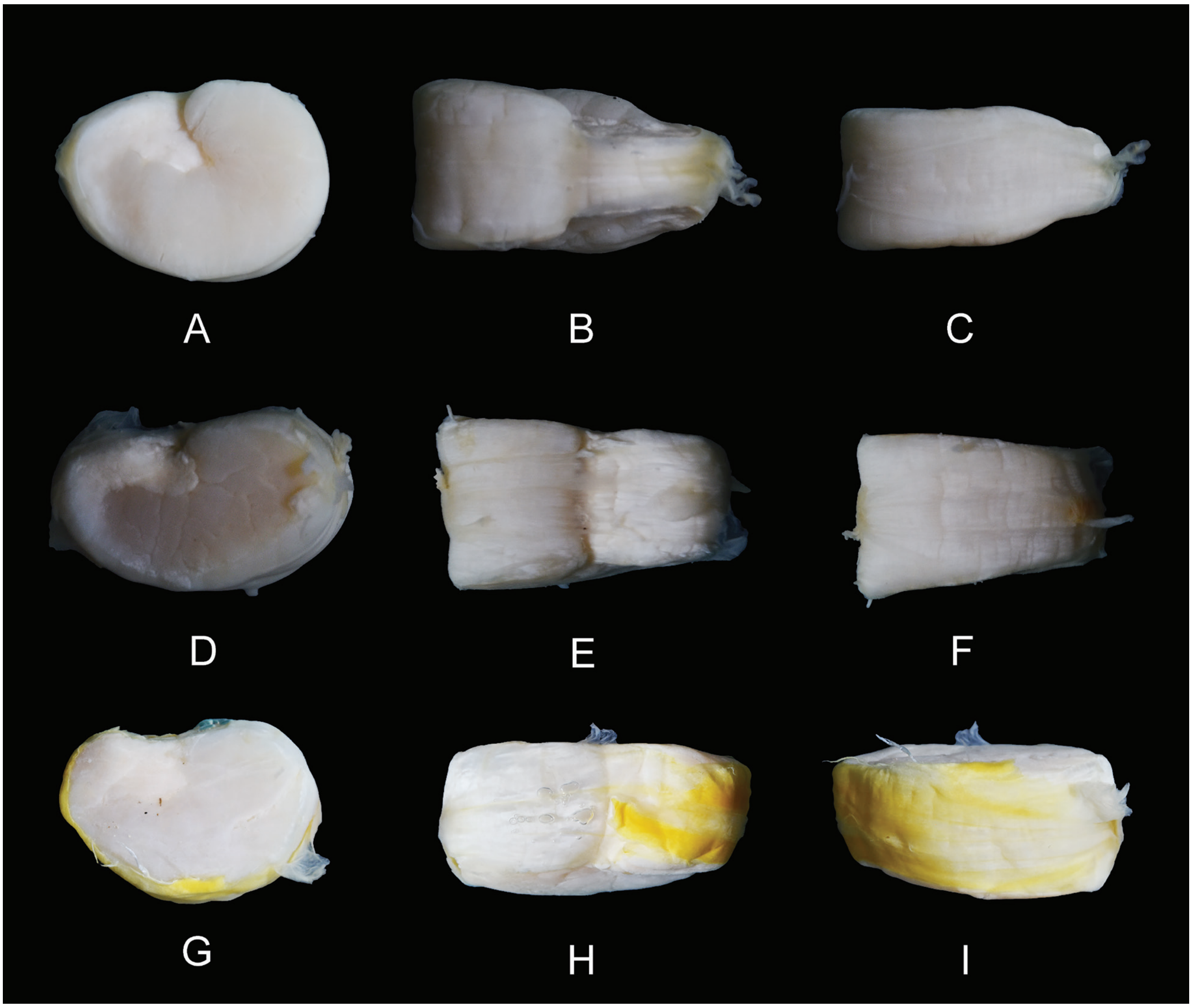

Figure 7. Photographed images of the posterior adductor muscles of *Atrina pectina* (**A**, **B**, **C**), *Atrina inflata* (**D**, **E**, **F**), and *Atrina vexillum* (**G**, **H**, **I**) collected from northern Iloilo, Philippines.

Table 3. Selected biometric characters of the adductor muscle of five pen shell species of the genera *Atrina* and *Pinna* (family Pinnidae) collected from northern Iloilo, Philippines.

Species	*n*	Biometric characters			Descriptive characters
		AMW [g]	AMT [mm]	AML [mm]	
A. pectinata	53	7.99 ± 5.30	13.52 ± 5.68	21.13 ± 8.04	Fibers smooth, packed with epithelial tissue with no fissures and cavities. Most of muscle comprised of dark muscles
A. inflata	47	7.47 ± 4.55	17.30 ± 3.45	24.42 ± 6.31	Tubular-like, asymmetrical, dark muscle 57.14 percentage points thicker than light muscle, light muscle attached to dark muscle by epithelial tissue, longitudinal fissure easily recognizable at external side of surface of adductor muscle
A. vexillum	17	12.61 ± 10.59	14.81 ± 6.26	24.25 ± 9.30	Shape nearly circular, fibers packed with yellow epithelial tissue, comprised of high percentage of dark muscles, fissures, and cavities observed in muscles
P. bicolor	43	11.52 ± 4.35	12 ± 4.57	19.46 ± 8.54	Fibers well packed with thick epithelial tissue.
P. atropurpurea	34	11.82 ± 4.95	14.24 ± 4.81	22.20 ± 4.87	Dark muscle occupying almost half of total area, fissures visible in light muscles

Values are expressed as mean ± standard deviation. *n* = number of specimens, AMW = adductor muscle weight, AMT = adductor muscle thickness, AML = adductor muscle length.

length (DNL) was not correlated with its adductor muscle thickness, whereas DNL and dorsal margin were not correlated with its adductor muscle length. Meanwhile, all nine shell length characteristics of *P. bicolor* were positively correlated with its adductor muscle thickness (r^2, 0.59–0.88) and length (r^2, 0.47–70). The shell length characteristics of *P. atropurpurea* were also positively correlated with its adductor muscle thickness (r^2, 0.40–0.84) and length (r^2, 0.38–0.84). The total shell length and adductor muscle thickness of *P. bicolor* and *P. atropurpurea* exhibited a high correlation ($r^2 = 0.88$ and $r^2 = 0.84$, respectively $P < 0.05$). (Table 4).

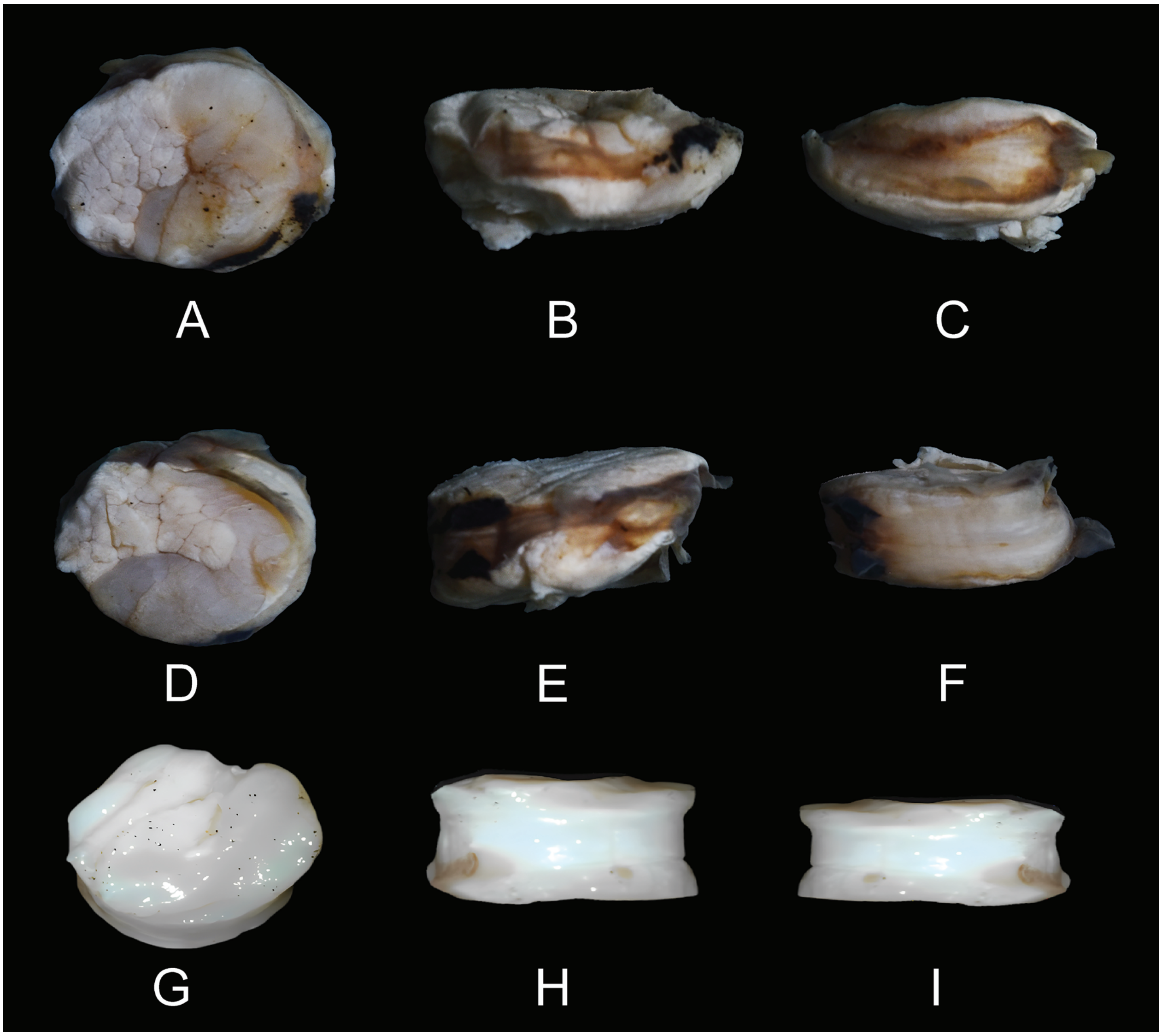

Figure 8. Photographed images of the adductor muscle of *Pinna bicolor* (**A**, **B**, **C**), *Pinna atropurpurea* (**D**, **E**, **F**), and *Pinna deltodes* (**G**, **H**, **I**) collected from northern Iloilo, Philippines.

Discussion

Species of the family Pinnidae are cryptic and can easily adapt to environmental changes (Lemer et al. 2014). The results of the presently reported study revealed that they indeed differ in size, structure, and color. These characteristics can be confusing, especially for early career scientists, as their shells can easily be broken (Idris et al. 2008). Although it is already known that the presence of a longitudinal sulcus separating the dorsal and ventral lobes of the nacreous layer in species of the genus *Pinna* distinguishes them from species of the genus *Atrina* (see Rosewater 1982), the possible presence of species not previously recorded in this area is still worth investigating.

Five species of the genus *Atrina* and six species of the genus *Pinna* representing the family Pinnidae were identified. The number of identified species updates the previous record for this area (Laureta 2008). A comprehensive presentation of the differences in shell morphology of the most abundant species, *A. pectinata*, *A. inflata*, *A. vexillum*, *P. bicolor*, *P. atropurpurea*, and *P. deltodes*, is believed to be the first attempt for these species, which may be useful later for comparative studies when new records are made.

The ecological conditions of the coastal habitats in northern Iloilo apparently define the pen shell species that dominate in an area. For example, many of the six species investigated are different from other areas where pen shells are known to thrive, such as in Sugai Pulai, Malaysia (Idris et al. 2008). The single specimen of *P. nobilis*, which was previously noted to be the largest pen shell species recorded (Basso et al. 2015) and reportedly most dominant in the Mediterranean Sea (Zavodnik et al. 1991; Richardson et al. 1999; Cappello et al. 2019), was also the largest among all the pen shells collected at this study site. Other species that occurred only once, namely, *A. seminuda*, *A. rigida*, and *P. incurva*, are recorded for the first time in this area; this information is important to

Table 4. Relations of thickness (AMT) and length (AML) of adductor muscles with various shell length characters of five pen shell species of the genera *Atrina* and *Pinna* (family Pinnidae) collected off northern Iloilo, Philippines.

Species	Shell length parameter	Regression equation in relation to AMT	r^2	Regression equation in relation to AML	r^2
A. pectinata	TSL	TSL = 118.18 + 6.1775AMT	**0.65**	TSL = 115.12 + 3.6141AML	**0.70**
	LAPAM	LAPAM = 64.95 + 3.7165AMT	**0.68**	LAPAM = 57.0798 + 3.6865AML	**0.53**
	PAPSM	PAPSM = 50.933 + 1.6319AMT	**0.49**	PAPSM = 48.9457 + 1.1068AML	**0.40**
	DPSM	DPSM = 16.455 + 0.5544AMT	**0.53**	DPSM = 15.588 + 0.3827AML	**0.46**
	DM	DM = 113.62 + 5.2092AMT	**0.62**	DM = 102.35 + 3.7313AML	**0.55**
	ShW	ShW = 42.959 + 3.7025AMT	**0.68**	ShW = 38.45 + 2.5204AML	**0.60**
	PAMPNM	PAMPNM = 5.9356 + 0.1743AMT	**0.57**	PAMPNM = 5.6912 + 0.12AML	**0.50**
	DNL	DNL = 79.162 + 3.5137AMT	**0.63**	DNM = 82.243 + 3.4853AML	**0.55**
A. inflata	TSL	TSL = 38.411 + 7.2823AMT	**0.94**	TSL = 77.9 + 3.5417AML	**0.78**
	LAPAM	LAPAM = 32.859 + 3.742AMT	**0.86**	LAPAM = 54.255 + 0.7746AML	**0.68**
	PAPSM	PAPSM = 8.3944 + 0.1451AMT	**0.86**	PAPSM = 13.942 + 0.0216AML	**0.68**
	DPSM	DPSM = –26.772 + 4.2591AMT	**0.81**	DPSM = –5.9699 + 0.1653AML	**0.74**
	DM	DM = 48.778 + 4.9386AMT	**0.80**	DM = 72.092 + 2.5437AML	**0.75**
	ShW	ShW = 24.212 + 0.5108AMT	**0.81**	ShW = 48.975 + 2.1814AML	**0.67**
	PAMPNM	PAMPNM = 1.1411 + 0.1053AMT	**0.79**	PAMPNM = 1.7861 + 0.0482AML	**0.59**
	DNL	DNL = 30.729 + 4.5414AMT	**0.81**	DNL = 56.923 + 0.1445AML	**0.64**
A. vexillum	TSL	TSL = 95.015 + 5.3281AMT	**0.80**	TSL = 91.46 + 3.4011AML	**0.69**
	LAPAM	LAPAM = 57.606 + 2.8578AMT	**0.69**	LAPAM = 55.284 + 1.8414AML	**0.61**
	PAPSM	PAPSM = 30.051 + 0.9754AMT	**0.77**	PAPSM = 33.665 + 0.0576AML	**0.47**
	DPSM	DPSM = 31.616 + 0.3508AMT	**0.40**	DPSM = 16.745 + 2.66AML	**0.53**
	DM	DM = 96.02 + 1.6189AMT	**0.40**	DM = 98.573 + 0.8836AML	0.25
	ShW	ShW = 80.021 + 2.7749AMT	**0.47**	ShW = 70.652 + 2.0813AML	**0.56**
	DNL	DNL = 89.426 + 1.0767AMT	0.23	DNL = 87.379 + 0.7421AML	0.23
P. bicolor	TSL	TSL = 169.58 + 10.566AMT	**0.88**	TSL = 204.44 + 4.7226AML	**0.61**
	LAPAM	LAPAM = 75.166 + 5.314AMT	**0.77**	LAPAM = 86.519 + 2.6928AML	**0.69**
	PAPSM	PAPSM = 80.544 + 3.5058AMT	**0.59**	PAPSM = 87.839 + 1.7866AML	**0.53**
	DPSM	DPSM = 30.323 + 0.9515AMT	**0.66**	DPSM = 31.532 + 0.5245AML	**0.70**
	DM	DM = 160.45 + 9.1931AMT	**0.74**	DM = 177.6 + 4.7868AML	**0.70**
	ShW	ShW = 62.051 + 3.1587AMT	**0.69**	ShW = 66.768 + 1.7051AML	**0.70**
	SuW	SuW = 1.6609 + 0.0812AMT	**0.63**	SuW = 1.901 + 0.0377AML	**0.47**
	PAMPNM	PAMPNM = 3.8235 + 0.1302AMT	**0.65**	PAMPNM = 4.0774 + 0.0672AML	**0.61**
	DNL	DNL = 97.88 + 4.8372AMT	**0.70**	DNL = 106.2 + 2.5549AML	**0.68**
P. atropurpurea	TSL	TSL = 136.44 + 2.654AMT	**0.84**	TSL = 153.29 + 6.7133AML	**0.84**
	LAPAM	LAPAM = –55.099 + 6.4382AMT	**0.78**	LAPAM = 62.818 + 3.4563AML	**0.80**
	PAPSM	PAPSM = 78.469 + 3.7725AMT	**0.51**	PAPSM = 81.516 + 2.0957AML	**0.56**
	DPSM	DPSM = 33.683 + 1.355AMT	**0.77**	DPSM = 36.574 + 0.667AML	**0.66**
	DM	DM = 120.85 + 10.931AMT	**0.68**	DM = 130.25 + 6.0454AML	**0.74**
	ShW	ShW = 99.603 + 1.8321AMT	**0.64**	ShW = 101.38 + 1.0035AML	**0.68**
	SuW	SuW = 3.2058 + 0.2142AMT	**0.40**	SuW = 3.5594 + 0.1104AML	**0.38**
	PAMPNM	PAMPNM = 3.4914 + 0.3815AMT	**0.79**	PAMPNM = 3.9787 + 0.2034AML	**0.79**
	DNL	DNL = 45.005 + 10.03AMT	**0.78**	DNL = 58.218 + 5.3281AML	**0.78**

Pinna deltodes was not included due to insufficient samples for regression analysis. Values in **bold** font represent a significant correlation at 0.05 level. Values are expressed in millimeters. TSL = total shell length, LAPAM = length of anterior to posterior adductor margin, PAPSM = posterior adductor to posterior shell margin, DPSM = dorsal posterior shell margin, DM = dorsal margin, ShW = shell width, SuW = sulcus width, PAMPNM = posterior adductor margin to posterior nacreous margin, DNL = dorsal nacreous length.

note because it can be used to make ecological reports about pen shell diversity in northern Iloilo and can be included in the management plan for these resources. There are now 11 species compared to the previous record for this area (Laureta 2008), and four of these were observed to be rarely occurring (see Tables 1, 2, 3). This strongly suggests that there may still be unrecorded species that could be discovered if a more comprehensive survey covering a larger area including deeper waters is made. This may be the subject of a more comprehensive study worth considering in the future.

The analysis of pen shell morphology relied on nine internal and external characteristics of the valve among species of the genus *Pinna* and eight characteristics among species of the genus *Atrina*. The external surface sculpture of the valves and the size and position of the adductor muscles, which create distinctive scars on the inner side of the valves, were used to define individual species of the family Pinnidae, as suggested by Rosewater (1961). The comparisons made revealed that the three *Pinna* species, *P. bicolor*, *P. atropurpurea*, and *P. deltodes*, were found to be different based on shell width, dorsal posterior shell margin, sulcus width, and dorsal posterior margin to dorsal nacreous margin, similar to the study of Idris et al. (2008). The differences of the adductor muscle scar from the posterior nacreous margin appeared to be influenced by the different positions of the muscle within the shell. Meanwhile, the difference in the length of the dorsal margin was due to the different curvatures of their shell.

Although no new species were identified in this study, following this comprehensive examination of specimens collected with a more comprehensive survey will lead to the generation of a comprehensive checklist of pen shell species in northern Iloilo. The application of this same method to other known pen shell-occurring areas in the Philippines, such as in the Samar Sea, where an active fishery exists (Diocton and Adalla 2019), may also be worth considering.

The considerable size of the adductor muscle and its nutritional value (Wu and Wu 2017) make pen shells of great interest to fisheries. It serves as a source of income (Diocton and Adalla 2019; Del Norte-Campos et al. 2021) and food (Greenwald 1996) for many artisanal fishers. However, in northern Iloilo, only adductor muscles are landed and sold in the market, leaving empty shells scattered in the substrate. This practice by fishers presents challenges in assessing the state of pen shell populations in the area or the management of these resources unless strategies to regulate the resources are introduced soon. Under such conditions, these resources may be overexploited, just like most wild fishery resources (Pauly et al. 1998).

It is important to note that no previous characterization of the adductor muscle was made for pen shells, and the use of this information may give previously unexplored insights about these resources. The linear regression analyses and correlations made with various shell length parameters with adductor muscle thickness and length may enable fishery scientists to determine the impacts of pen shell fisheries on the resources more precisely by closely monitoring the adductor muscles that are sold in the market, but this would even be more realistic if smaller-sized individuals are also represented. With the expected depletion of pen shell resources as harvesting pressure increases, pen shell juveniles may be harvested and secretly sold or brought home for domestic consumption. Perhaps, it is important to include size limitation measures among the strategies to regulate the harvesting of pen shells to ensure the sustainability of this important resource in the area.

Based on the different forms of the marketed adductor muscles, it is evident that species other than *A. pectinata*, which commands the highest value among all pen shell species, are also accepted for general consumption. The linear regression analyses and correlations between various shell characters and several adductor characters of the six dominant species were done to infer the state of wild pen shell populations. Through this, it is evident that certain characteristics can be used to discriminate the different species under *Pinna*. The appropriate procedure to do this is to relate the dimensions of the adductor muscles with various characteristics of their shells. Using extracted information from the dominant species, it seems possible to determine the species of their source organisms.

The described and analyzed morphological characteristics of the adductor muscle of *A. pectinata*, *A. inflata*, *A. vexillum*, *P. bicolor*, and *P. atropurpurea* suggest that the relations of thickness and length of adductor muscles with the various lengths characters of the shell can be used to differentiate the species by looking at the characteristics of the adductor muscles. The high correlations between various adductor muscle characteristics and shell length characters indicate that they could be a good for taxonomic purposes. The specific and distinct identity of each species in this study has provided information on the diversity of pen shells as well as an opportunity for the newly discovered species to be included in the catalog of bivalves in northern Iloilo, Philippines. Also, through the marketed adductor muscles, it is possible to assess the level of pressure posed by fishers on wild pen shells in this area using established modeling methods. Thus, this study may be useful in stock assessment and in monitoring the sizes of shucked pen shells.

Acknowledgments

This study is part of the dissertation of the first author, who is a scholar under the Advanced Science and Technology Human Resource Development (ASTHRD) Program of the Department of Science and Technology (DOST). The conduct of her field research was partially supported by "Marine Fisheries Assessment of Panay: Building Local Fisheries Information through Research Capability Enhancement in HEI's", a research project that was supported by the Commission on Higher Education (CHED). Permits to conduct the study were granted and additional supporting data were provided by the Municipal Mayors of Carles, Estancia, and Batad, all in Iloilo Province.

References

Amano VL, Mojados J (2020) Value chain analysis of pen shell (Baloko) in the Province of Sorsogon, Philippines. Bicol University Research and Development Journal 21(3): 21–33. https://doi.org/10.47789/burdj.mbtcbbgs.20182103.5

Basso L, Garcia-March JR, Vasquez-Luis M, Deudero S (2015) The penshell *Pinna nobilis*: A review of population status and recommended research priorities in the Mediterranean Sea. Advances in Marine Biology 71: 109–160. https://doi.org/10.1016/bs.amb.2015.06.002

Burns JR, Smith SDA (2011) Growth, population dynamics and morphometrics of *Pinna bicolor* (Gmelin, 1791) in Lake Macquarie, New South Wales, Australia. Molluscan Research 31(3): 183–188. https://doi.org/10.11646/mr.31.3.6

Butler AJ, Keough MJ (1981) Distribution of *Pinna bicolor* Gmelin (Mollusca: Bivalvia) in South Australia with observations on recruitment. Transactions of the Royal Society of South Australia 105: 29–39. https://doi.org/10.3923/jbs.2008.882.888

Cappello T, Maisano M, Giannetto A, Natalotto A, Parrino V, Mauceri A, Spanò N (2019) Pen shell *Pinna nobilis* L. (Mollusca: Bivalvia) from different peculiar environments: adaptive mechanisms of osmoregulation and neurotransmission. European Zoological Journal 86(1): 333–342. https://doi.org/10.1080/24750263.2019.1673492

Czihak G, Dierl W (1961) *Pinna nobilis* L.: eine Präparationsanleitung. Gustav Fischer Verlag, Stuttgart, Germany, 40 pp.

Del Norte-Campos A, Lapara SS, Sanchez KAS (2021) Population dynamics of the comb pen shell *Atrina pectinata* (Linnaeus, 1767) (Mollusca, Bivalvia: Pinnidae) collected by diving from shallow areas of the southwest Visayan Sea, northeastern Panay Island, Philippines. Philippine Journal of Science 150(3): 1051–1060. https://doi.org/10.56899/150.03.38

Deudero S, Vázquez-Luis M, Álvarez E (2015) Human stressors are driving coastal benthic long-lived sessile fan mussel *Pinna nobilis* population structure more than environmental stressors. PLoS One 10(7): e0134530. https://doi.org/10.1371/journal.pone.0134530

Diocton RC, Adalla EC (2019) Some aspect on the biology of pen shell *Atrina pectinata* (Linneaus, 1767) in coastal waters of Maqueda Bay, Philippines. Journal of Marine Science Research and Oceanography 2(2): 1–6. https://doi.org/10.33140/JMSRO.02.02.02

Garcia-March JR, Marquez-Aliaga A, Wang YG, Surge D, Kersting DK (2011) Study of *Pinna nobilis* growth from inner record: How biased are posterior adductor muscle scars estimates? Journal of Experimental Marine Biology and Ecology 407(2): 337–344. https://doi.org/10.1016/j.jembe.2011.07.016

Grave BH (1911) Anatomy and physiology of the wing-shell *Atrina rigida*. Bulletin of the Bureau of Fisheries 29: 409–439, pls. XLVIII–L.

Greenwald M (1996) The cruising chef cookbook. Paradise Cay Publication, Arcata, CA, USA, 300 pp.

Idris MH, Arshad A, Bujang JS, Ghaffar MA, Daud SK (2008) Biodiversity and distribution of pen shells (Bivalvia: Pinnidae) from the seagrass beds of Sungai Pulai, Peninsular Malaysia. Research Journal of Fisheries and Hydrobiology 3(2): 54–62.

Katsanevakis S, Poursanidis D, Issaris Y, Panou A, Petza D, Vassilopoulou V, Chaldaiou I, Sini M (2011) "Protected" marine shelled molluscs: Thriving in Greek seafood restaurants. Mediterranean Marine Science 12(2): 429–438. https://doi.org/10.12681/mms.42

Laureta LV (2008) Compendium of the economically important seashells in Panay, Philippines. University of the Philippines Press, Quezon City, 162 pp.

Leal JH (2002) Bivalves. Pp. 25–98. In: Carpenter KE (Ed.) The living marine resources of the western central Atlantic. Volume 1. Introduction, mollusks, crustaceans, hagfishes, sharks, batoid fishes and chimaeras. FAO Identification Guide for Fishery Purposes. FAO, Rome.

Leal-Soto S, Barraza-Guardado R, Castro-Longoria R, Chávez-Villalba J, Hoyos-Cháirez F (2011) Cultivation of pen shells: An Example with *Atrina maura* in northwestern Mexico. Journal of the World Aquaculture Society 42(6): 789–800. https://doi.org/10.1111/j.1749-7345.2011.00528.x

Lemer S, Buge B, Bemis A, Giribet G (2014) First molecular phylogeny of the circumtropical bivalve family Pinnidae (Mollusca, Bivalvia): Evidence for high levels of cryptic species diversity. Molecular Phylogenetics and Evolution 75: 11–23. https://doi.org/10.1016/j.ympev.2014.02.008

Lemer S, David C, Filipina S, Don D, Victor S, Gonzalo G (2016) The family Pinnidae (Bivalvia) in the Philippine archipelago: Observations on its distribution and phylogeography. Nautilus 130(4): 137–145.

Pauly D, Christensen V, Dalsgaard J, Froese R, Torres F Jr (1998) Fishing down marine food webs. Science 279(5352): 860–863. https://doi.org/10.1126/science.279.5352.860

Poppe GT (2010) Philippine marine mollusks Vol. III. ConchBooks, Hackenheim, Germany.

Poutiers JM (1998) Bivalves. Acephala, Lamellibranchia, Pelecypoda. Pp. 123–362. In: Carpenter KE, Niem VH (Eds) FAO species identification guide for fishery purposes. The living marine resources of the western central Pacific. Volume 1. Seaweeds, corals, bivalves, and gastropods. FAO, Rome.

Richardson CA, Kennedy H, Duarte CM, Kennedy DP, Proud SV (1999) Age and growth of the fan mussel *Pinna nobilis* from south-east Spanish Mediterranean seagrass (*Posidonia oceanica*) meadows. Marine Biology 133(2): 205–212. https://doi.org/10.1007/s002270050459

Richardson CA, Peharda M, Kennedy H, Kennedy P, Onofri V (2004) Age, growth rate and season of recruitment of *Pinna nobilis* (L) in the Croatian Adriatic determined from Mg:Ca and Sr:Ca shell profiles. Journal of Experimental Marine Biology and Ecology 299(1): 1–16. https://doi.org/10.1016/j.jembe.2003.08.012

Rosewater J (1961) The family Pinnidae in the Indo–Pacific. Indo–Pacific Mollusca 1(4): 175–226.

Rosewater J (1982) Review of Hawaiian Pinnidae and revalidation of *Pinna exquisita* Dall, Bartsch, and Rehder, 1938 (Bivalvia: Mytiloida). Pacific Science 36(4): 453–458.

Saucedo P, Southgate PC (2008) Chapter 5—Reproduction, development and growth. Pp.131–186. In: Southgate PC, Lucas JS (Eds.) The pearl oyster: A beginner's guide to programming images, animation, and interaction. Elsevier, Oxford, UK. https://doi.org/10.1016/B978-0-444-52976-3.00005-X

Scheltema RS, Williams IP (1983) Long distance dispersal of planktonic larvae and the biogeography and evolution of some Polynesian and western Pacific mollusks. Bulletin of Marine Science 33(3): 545–565.

Schultz PW, Huber M (2013) Revision of the worldwide recent Pinnidae and some remarks of fossil European Pinnidae. Acta Conchyliorum 13: 1–164.

Souji S, Vardhanan Y, Radhakrishnan T (2014) New record of two Pinnidae species (Bivalvia: Pinnidae): DNA barcoding (COI) and morphological analysis. Indian Journal of Scientific Research 8(1): 159–168.

Winckworth RA (1929) Marine Mollusca from south India and Ceylon. III: Pinna. With an index to the recent species of *Pinna*. Journal of Molluscan Studies 18: 276–297. https://doi.org/10.1093/oxfordjournals.mollus.a063990

Wu S, Wu Y (2017) Proximate composition and nutritional evaluation of the adductor muscle of pen shell. 3Biotech 7(3): e160. https://doi.org/10.1007/s13205-017-0840-4

Zavodnik D, Hrs-Brenko M, Legac M (1991) Synopsis on the fan shell *Pinna nobilis* L. in the eastern Adriatic Sea. Pp. 169–178. In: Boudouresque CF, Avon M, Gravez V (Eds.) Les espèces marines à protéger en Méditerranée. GIS Posidonie, Marseille, France.

Acta Ichthyologica et Piscatoria 54, 2024, 63–74 | DOI 10.3897/aiep.54.112995

PENSOFT.

ACTA
ICHTHYOLOGICA
ET PISCATORIA

Reproductive features of data-deficient yellowfin snapper, *Lutjanus xanthopinnis* (Actinopterygii: Eupercaria: Lutjanidae), from east-coast of Peninsular Malaysia: Implications for sustainable fisheries management

Md Moshiur RAHMAN[1,2], Nur Asma ARIFFIN[1], Ying Giat SEAH[1,3],
Tun Nurul Aimi MAT JAAFAR[1], Muhammad Hanif FADZLI[1], Ahasan HABIB[1]

1 *Faculty of Fisheries and Food Science, Universiti Malaysia Terengganu, Kuala Nerus, Terengganu, Malaysia*
2 *Faculty of Fisheries, Sylhet Agricultural University, Sylhet, Bangladesh*
3 *Fish Division, South China Sea Repository and Reference Centre, Institute of Oceanography and Environment, University Malaysia Terengganu, Terengganu, Malaysia*

https://zoobank.org/584584D7-EB3D-4EF8-92D9-508A636CCC39

Corresponding author: Ahasan Habib (a.habib@umt.edu.my)

Academic editor: Ken Longenecker ♦ **Received** 20 September 2023 ♦ **Accepted** 9 November 2023 ♦ **Published** 26 February 2024

Citation: Rahman MM, Ariffin NA, Seah YG, Mat Jaafar TNA, Fadzli MH, Habib A (2024) Reproductive features of data-deficient yellowfin snapper, *Lutjanus xanthopinnis* (Actinopterygii: Eupercaria: Lutjanidae), from east-coast of Peninsular Malaysia: Implications for sustainable fisheries management. Acta Ichthyologica et Piscatoria 54: 63–74. https://doi.org/10.3897/aiep.54.112995

Abstract

Understanding the reproductive biology of fishes is crucial to making accurate and scientifically sound recommendations for fisheries management. The presently reported study is the first to report the reproductive characteristics of the data-deficient and recently described yellowfin snapper, *Lutjanus xanthopinnis* Iwatsuki, Tanaka et Allen, 2015, collected from the eastern South China Sea, Malaysia. A total of 572 fish specimens were sampled monthly from March 2022 to April 2023 using a gillnet and a trawl net. Subsequently, these specimens were measured and weighed. Their total length (TL) ranged from 15.3 to 26.8 cm (19.25 ± 2.04 cm; mean ± SD). Their body weight (W_B) ranged from 53.5 g to 279.7 g (114.5 ± 40.3 g; mean ± SD). For the reproductive biology study, the following parameters were determined: the sex ratio, gonadosomatic index (GSI), hepatosomatic index (HSI), spawning period, fecundity, condition factor (K), length at maturity, and the gonadal maturity stages. In the sex ratio, males (M) were significantly dominant over females (F) (M:F = 1:0.75) ($\chi^2 = 11.18$). Consequently, the monthly mean GSI of pooled sex revealed a consistent trend from January to August, indicating spawning seasons with peak periods in March and April. The batch fecundity of 67 mature females (16.0–25.2 cm TL; 64.5– 279.3 g W), was determined to range from 16 405 to 94 357 oocytes. The fecundity increased with gonad weight in contrast to weight and length. The length at first maturity of females and males was 14.53 and 20.56 cm, respectively. Females matured earlier than males. Macroscopic and histological examination of gonads revealed monthly variation in the ratio of gonad stages for males and females. This study offers crucial data on the reproductive biology of *L. xanthopinnis*, which will help with sustainable fishery management in this area and can be used as a reference for the management of similar fish populations in other regions of the world.

Keywords

east coast of Peninsular Malaysia, fecundity, length at maturity, marine fish, spawning season

Introduction

Fishes of the family Lutjanidae, commonly known as snappers, are ecologically and economically imperative in tropical and sub-tropical regions (Allen 1985; Messias et al. 2019). The majority of species within the family Lutjanidae are represented by the genus *Lutjanus* (see Allen 1985), and species of this genus are highly prized and consumed in numerous countries worldwide (Adibah and Darlina 2014). The yellowfin snapper, *Lutjanus xanthopinnis* Iwatsuki, Tanaka et Allen, 2015, is a small lutjanid species previously misidentified with *Lutjanus madras* extensively distributed through the eastern Indian and western Pacific oceans, ranging from Sri Lanka to the Andaman Sea and the Malay Peninsula, southeast to Bali, Malaysia, Brunei, to the Philippines, north to China and Taiwan, and south to Japan (Iwatsuki et al. 2015). Due to this, relatively little information is available about this species, so it is listed as Data Deficient (IUCN 2019). Nevertheless, this species has also been used for commercial purposes, and its harvest is included in Malaysia's annual fish landing statistics. Species of *Lutjanus* make up a significant share of landings in Malaysia, which have been continuously increasing over the past ten years (2013–2022), with the mean value of 15 391 tonnes per year (DOF 2023).

Fish reproductive biology, including spawning timing and duration, sex ratio, maturity stages, length at maturity, and fecundity, is essential for managing stocks and assessment of fisheries (Tsikliras et al. 2013; Alam et al. 2020). To comprehend the reproductive biology of fishes, many researchers have studied these parameters. For example, Palla and Sotto (2021) studied *Lutjanus vitta*, Araki and Tachihara (2021)—*Lutjanus quinquelineatus* Iwatsuki, Tanaka et Allen, 2015, and Fernandes et al. (2022)—*Lutjanus synagris* (Linnaeus, 1758). Despite the importance of the biology of fish in some nations, the lack or unavailability of fisheries data results in overfishing of the stocks and in some cases, management failure (Kinas 1996; Alves and Minte-Vera 2012). For rendering reliable scientific recommendations in fishery management, the knowledge of species' various reproductive aspects is crucial (Khatun et al. 2019; Longenecker et al. 2022). Fisheries managers must have a thorough knowledge of a species' reproductive biology to provide effective fisheries management to ensure sustainability (Coulson et al. 2019). However, there is a scarcity of comprehensive data pertaining to the biology and ecology of *L. xanthopinnis* globally (Arai et al. 2023). In addition, no published data is hitherto available on the reproductive biology of *L. xanthopinnis* in Malaysia or any other geographical location.

Therefore, this study aims to explore the reproductive aspects of *L. xanthopinnis*, including its sex ratio, gonadosomatic index, spawning season, condition factor, hepatosomatic index, batch fecundity, and length at maturity in the eastern South China Sea, Malaysia. The findings of this study will enhance the existing knowledge referring to this particular species providing valuable insights for the future sustainable management of snapper fisheries. Furthermore, these findings can serve as a model for managing this fish species in other geographic regions, offering guidance and direction for effective fishery management.

Materials and methods

Area of study and sample collection. Fresh specimens of *Lutjanus xanthopinnis* were sampled monthly from March 2022 to April 2023 from commercial fish landing port (Pulau Kambing, eastern South China Sea) (05°19′20.3″N, 103°07′42.6″E), east-coast of Peninsular Malaysia (Fig. 1). A total of 572 specimens (326 males and 246 females) were collected using gillnet and trawl net. Gillnets made of nylon netting with a 45 to 48 mm mesh size were used in water depths of 5 to 20 m, while trawl net with 38 mm codend mesh was used at depths of 20 to 40 m. The obtained samples were stored in ice and transported to the Fisheries Science Laboratory, Universiti Malaysia Terengganu (UMT), for further analysis and identified using multiple systematic morphological features mentioned by Iwatsuki et al. (2015).

Morphometrics, determination of sex, and sex ratio. Each specimen's total length (TL) and standard length (SL) were measured to the nearest 0.1 cm by using an L-shaped board, and an electronic balance was used to record body weight (W_B) to the nearest 0.1 g. All of the fish specimens were dissected, and the sex of each individual was determined visually by examination of the gonads. Subsequently, the gonads of each specimen were removed and weighed using an electronic balance (ATX224 SHIMADZU) to the nearest 0.0001 g. In the presently reported study, the sex ratio was calculated by the proportion of male (M) and female (F) numbers and expressed as M:F ratio. The total number of both sexes was used to calculate monthly variations in sex ratios. The Chi-square (χ^2) test was used to estimate the discrepancies in the expected sex ratio 1:1.

Gonadal histology and identification of maturity stages. Autopsied fish gonad tissue (25 samples per month) was put in a histological cassette and fixed in 10% neutral buffered formalin. After 24 h, fixed gonads are transferred to 70% ethanol and then dehydrated with a series of ethanol dilutions (vacuum automatic tissue processor Leica TP1020). The gonads were embedded in paraffin using Leica HistoCore Arcadia H, cut on 5-µm thick sections with Galileo SEMI Series 2 rotary microtome, and counterstained with hematoxylin/eosin then mounted on a glass slide using cover slip. Then, the histological slides were photographed with Nikon Eclipse 80i. For each individual, the stage of gonad development was identified. Five gonadal maturity stages of *L. xanthopinnis* were distinguished based on

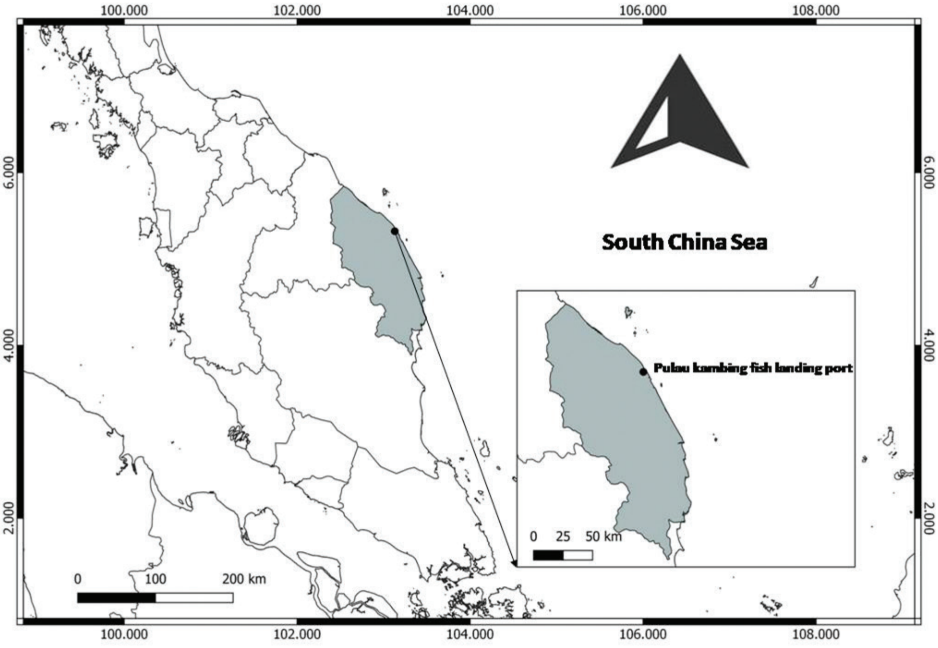

Figure 1. Map depicting the study area (Pulau Kambing Fish Landing Port in Terengganu, east-coast of Peninsular Malaysia).

macroscopic and histological examination of gonads described by Russell et al. (2003), Grandcourt et al. (2006), Brown-Peterson et al. (2011), and Fakoya and Anetekha (2019):

- Immature (stage I),
- Developing/regenerating (stage II),
- Spawning capable (stage III),
- Actively spawning (stage IV), and
- Regressing (stage V).

Gonadosomatic index, hepatosomatic index, and condition factor. The gonadosomatic index (GSI) was assessed monthly for both sexes to understand the spawning season. The mean GSI for each month was calculated using the following formula

$$\mathrm{GSI} = \{W_{\mathrm{G}} \times (W_{\mathrm{B}} - W_{\mathrm{G}})^{-1}\} \times 100,$$

where W_{B} is the body weight [g] and W_{G} is the gonad weight [g] (Pacicco et al. 2023). A line graph was used to display the monthly mean GSI. The increasing peak of the GSI depicts the spawning season for this species. The monthly pattern of the hepatosomatic index (HSI) (Costa 2019; Fadzli et al. 2022) utilizing the following equation

$$\mathrm{HSI} = (W_{\mathrm{L}} \times W_{\mathrm{B}}^{-1}) \times 100,$$

where W_{L} is the liver weight [g]. The relative condition factor (K) for each *L. xanthopinnis* specimen was estimated using the formula developed by Le Cren (1951), which is stated as follows

$$K = (W_{\mathrm{BE}} \times W_{\mathrm{BC}}^{-1}),$$

where W_{BE} is the empirically determined body weight [g] of studied fish and W_{BC} is the calculated body weight resulting from length–weight relations (modified from Rahman et al. 2023).

Length at maturity. We estimated size at maturity as the length predicted to comprise 50% mature individuals (L_{50}). This was calculated based on the percentage of matured individuals (stage III and IV) suggested by Palla and Sotto (2021) of each 2-cm size class. A line drawn against the midpoint of each size class (TL) for matured females (N = 162) and males (N = 132) out of 572 fish was carried out according to (King 2007) utilizing the logistic equation as follows

$$\ln[(1 - R_{\mathrm{M}}) \times R_{\mathrm{M}}] = rL_{50} - rL,$$

where R_{M} is the mature individuals rate, rL_{50} is the intercept a, $-r$ is the slope of line, r is $-b$, and L is the total length of fish. For the calculation of r and L_{50}, values of $\ln[(1 - P) \times \mathrm{P}^{-1}]$ were plotted opposed to the midpoint of each size class as: $L_{50} = a/r$.

Batch fecundity. Batch fecundity (BF) is the number of eggs each fish releases during a single spawning phase (Gonçalves et al. 2009). The oocytes from (stages III and IV) were used to determine the batch fecundity of mature females (BF). The ovary was divided into three sub-samples, taken from the front, center, and back and weighed to the nearest 0.1 g. Oocytes (N_{O} = 67) were separated from the connective tissue and observed under a dissecting microscope (OLYMPUS SZ51) to calculate. Then, BF is estimated by the following (Fry et al. 2009)

$$\mathrm{BF} = (N_{\mathrm{ES}} \times W_{\mathrm{G}}) \times W_{\mathrm{GS}}^{-1},$$

where N_{ES} is the egg count in a subsample, W_G is the weight of the (whole) gonad, and W_{GS} is the weight of the subsample gonad.

Statistical analysis. The data were analyzed using Excel 2010 and PAST 4.09 (Hammer et al. 2001). Chi-Square (χ^2) analysis was used to assess the sex ratio for any variations beyond the expected 1:1. The correlations between BF and body weight, total length, and gonad weight were derived using regression analysis. The analysis also took into consideration a significance level of $P < 0.05$.

Results

Morphometric measurement and sex ratio. The TL for males of *Lutjanus xanthopinnis* varied from 16 to 26.8 cm (19.53 ± 2.28 cm; mean ± SD), and females ranged from 15.3 to 25.2 cm (18.88 ± 1.58 cm). Moreover, the BW for males ranged from 59.5 to 279.7 g (120.5 ± 45.8 g), and females varied between 53.5 and 279.3 g (106.4 ± 29.6 g), respectively. The monthly sex ratio analysis showed that this species favored males over females. An overall sex ratio of 1:0.75 (M:F) was found among the 572 fish examined, with 326 (57%) males and 246 (43%) females (Table 1). Nevertheless, the statistical analysis revealed that the overall population of the monthly sex ratio differed significantly (χ^2 = 11.18) from the expected (1:1) ratio. Additionally, the sex ratio concerning size depicted in Table 2, showed that males dominated over female fish. Females utterly dominated over males in the 14 to 16 cm class range. Overall, statistical analysis shows the sex ratio also significantly varied (χ^2 = 11.18) for size groups.

Gonad development and identification of maturity stages. Five gonad maturation stages were recognized in *L. xanthopinnis* (Figs. 2, 3), which include immature (stage I), developing/regenerating (stage II), spawning capable (stage III), actively spawning (stage IV) and regressing (stage V). The macroscopic and histological investigation of the gonad revealed the monthly ratio of males and females at various gonadal stages off Pulau Kambing Fish Landing Port in Terengganu, as depicted in (Fig. 4). In addition, the reproductively active stages of gonads (spawning capable and actively spawning) for both sexes were observed in January to August as also depicted in (Fig. 4). This finding suggests that the studied fish species has an extended spawning season from January to August.

Gonadosomatic index, hepatosomatic index, and condition factor. The mean GSI values for male and female individuals varied from 0.43 to 2.7 and from 0.95 to 3.9, respectively. However, the monthly GSI trend for both sexes was consistent from January to August (1.14–2.7 in males; 1.8–3.9 in females) with peaks in March and April (Figs. 5A, 5B). On the other hand, the mean monthly GSI for both sexes drastically declined from September to December (0.43–0.96 in males; 0.95–1.16 in females) (Figs. 5A, 5B). In addition, the monthly mean GSI of pooled sex revealed a consistent trend from January to August, indicating this species spawning seasons with peak periods in March and April (Fig. 5C). Conversely, the monthly mean GSI significantly dropped for pooled sex from September to December (Fig. 5C), which corresponds to the specimen resting period. On the contrary, the monthly HSI for males and females ranged from 0.53 to 1.22 (Fig. 5A) and 0.72 to 2.09 (Fig. 5B), respectively. Monthly changes in *K* and HSI were used to analyze the energy consumption patterns of fish during the reproductive phase. Moreover, the monthly mean *K* for both sexes was very consistent, except that it differed slightly in December. The monthly *K* for males and females varied from 1.01 to 1.07 and 1.00 to 1.25 (Figs. 5A, 5B), showing that they are growing in good health. The monthly values of *K* were inversely related to the evolution of GSI. However, a distinct pattern was observed in the relations between GSI and HSI.

Table 1. Sex ratio of *Lutjanus xanthopinnis* by month with consequent Chi-square (χ^2) values from eastern South China Sea, Malaysia.

Month	Total (*N*)	Male (*N*)	Female (*N*)	Male [%]	Female [%]	Sex ratio (M:F)	χ^2
Mar	37	16	21	43.24	56.76	1:1.31	0.67
Apr	47	28	19	59.57	40.43	1:0.67	1.72
May	40	31	9	77.5	22.5	1:0.29	12.1^{s}
June	41	27	14	65.85	34.15	1:0.52	4.12^{s}
July	35	19	16	54.29	45.71	1:0.85	0.26
Aug	45	31	14	68.89	31.11	1:0.45	6.42^{s}
Sep	43	25	18	58.14	41.86	1:0.72	1.14
Oct	42	19	23	45.24	54.76	1:1.21	0.38
Nov	36	20	16	55.56	44.44	1:0.8	0.44
Dec	39	15	24	38.46	61.54	1:1.6	2.07
Jan	42	33	9	78.57	21.43	1:0.28	13.71^{s}
Feb	48	19	29	39.58	60.42	1:1.53	2.08
Mar	34	25	9	73.53	26.47	1:0.36	7.52^{s}
Apr	43	18	25	41.86	58.14	1:1.38	1.13
Total	572	326	246	57.00	43.00	1:0.75	11.18^{s}

^{s} = significant difference at a level of 5%.

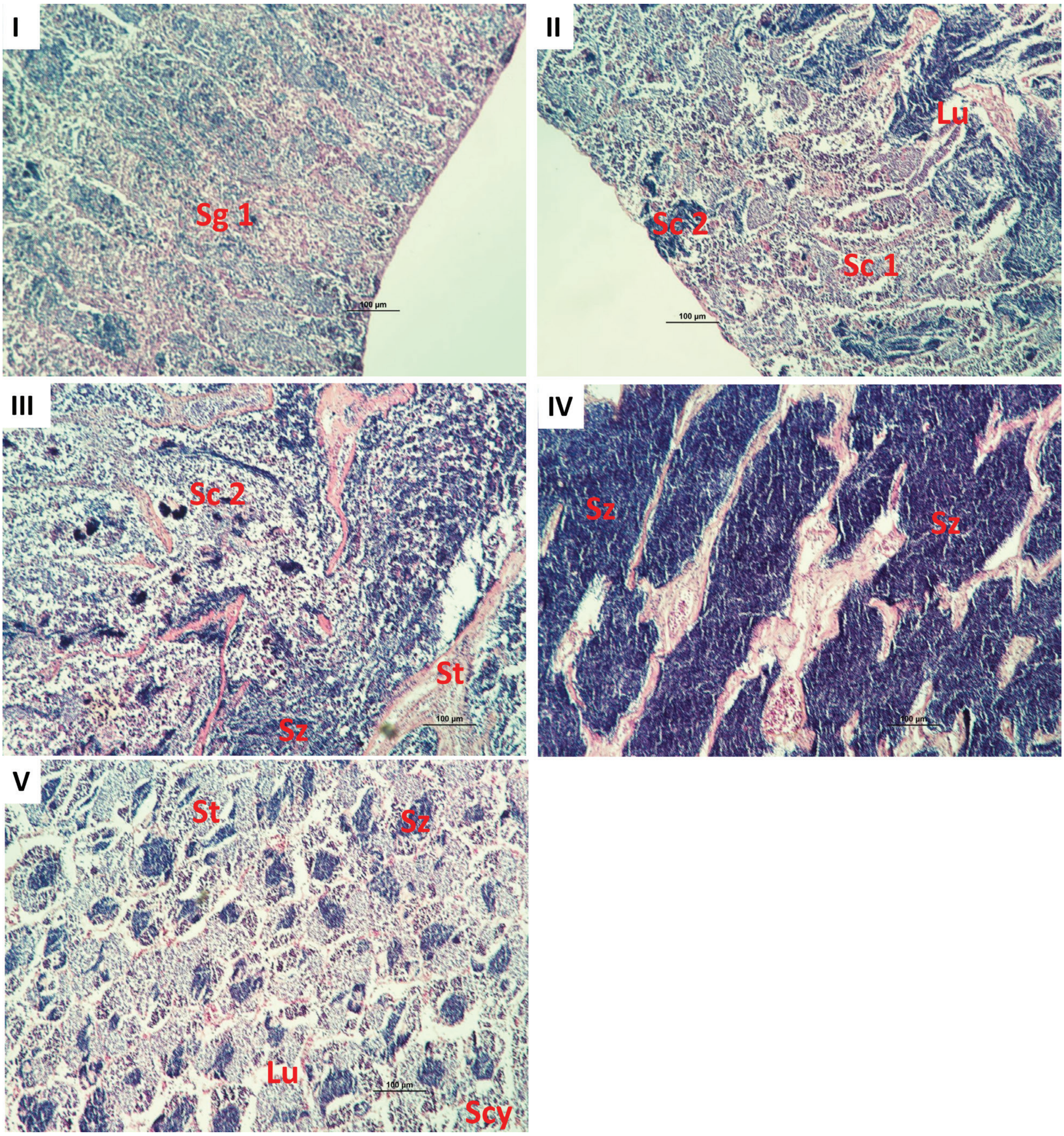

Figure 2. Microphotographs (10 × magnifications) of histological slides for five gonadal maturity stages in male yellowfin snapper, *Lutjanus xanthopinnis*, from eastern South China Sea(Malaysia). (**I**) Immature phase containing spermatogonia (stage I). (**II**) Developing/regenerating phase (stage II); (**III**) Spawning capable phase. (**IV**) Actively spawning phase containing very high numbers of spermatozoa (stage IV). (**V**) Regressing phase (stage V). Abbreviations: Sg1 = primary spermatogonia; Sc1 = primary spermatocyte; Sc2 =secondary spermatocyte; St = spermatid; Sz = spermatozoa, Lu = lumen; Scy = spermatocyst.

Table 2. Sex ratio of *Lutjanus xanthopinnis* by size groups with associated Chi-square (χ^2) values from eastern South China Sea, Malaysia.

Size range [cm]	Total (*N*)	Male (*N*)	Female (*N*)	Male [%]	Female [%]	Sex ratio (M:F)	χ^2
14–16	12	3	9	25	75	1:3	3.00
16–18	171	101	70	59.06	40.94	1:0.69	5.62^{S}
18–20	221	115	106	52.04	47.96	1:0.92	0.37
20–22	117	63	54	53.84	46.16	1:0.85	0.69
22–24	29	24	5	82.76	17.24	1:0.21	12.45^{S}
24–26	17	15	2	88.24	11.76	1:0.14	9.94^{S}
26–28	5	5	0	100.00	0.00	—	5.00^{S}
Total	572	326	246	57.00	43.00	1:0.75	11.18^{S}

^{S} = significant difference at a level of 5%.

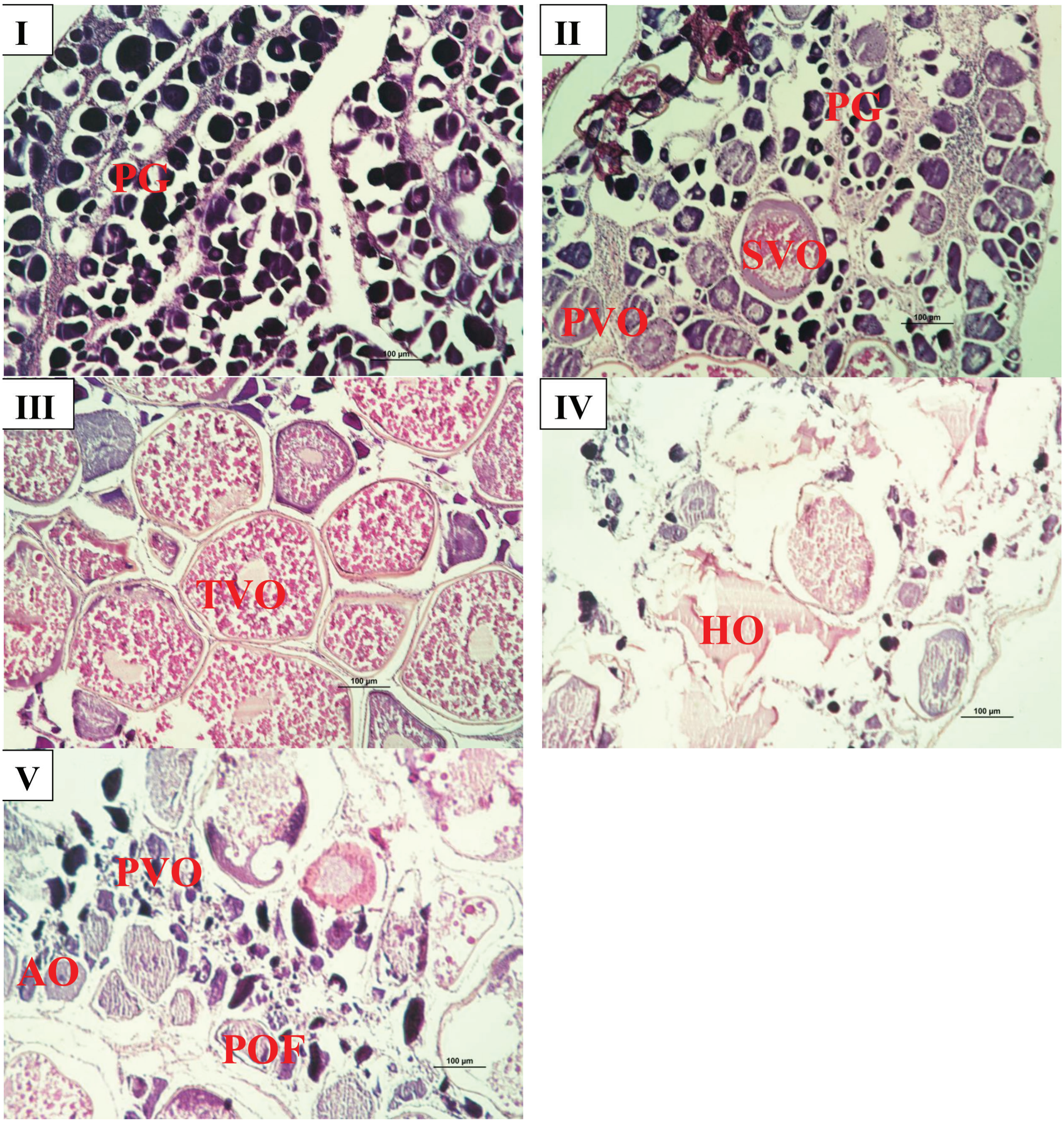

Figure 3. Microphotographs (10 × magnifications) of histological slides for five gonadal maturity stages in female yellowfin snapper, *Lutjanus xanthopinnis*, from eastern South China Sea(Malaysia). (**I**) Immature phase (stage I). (**II**) Developing/regenerating phase (stage II); (**III**) Spawning capable phase. (**IV**) Actively spawning phase (stage IV). (**V**) Regressing phase (stage V). Abbreviations: PG = primary growth of oocytes; PVO = primary vitellogenic oocytes; SVO = secondary vitellogenic oocytes; TVO = tertiary vitellogenic oocytes; HO = hydrated oocytes; AO = atretic oocyte; POF = post-ovulatory follicle.

Length at maturity. Mature male individuals ranged from 16.1 to 26.8 cm (20.64 ± 2.52 cm) in total length while females—15.8 to 25.2 cm (19.03 ± 1.68 cm). Straight-line analysis revealed that female *L. xanthopinnis* in Terengganu waters reached earlier length at first maturity than males. The calculated length at 50% sexual maturity (L_{50}) of *L. xanthopinnis* was 20.56 cm ($N = 132$) for males (Fig. 6A) and 14.53 cm ($N = 162$) for females (Fig. 6B). The association of mature proportion and total had provided a coefficient of determination (R^2) of 0.737 for females and 0.888 for males.

Batch fecundity. For batch fecundity, 67 mature female gonads were evaluated, TL varied from 16 to 25.2 cm (19.4 ± 1.96 cm), the W_B ranged from 64.5 to 279.36 g (118.5 ± 41.48 g), and the W_G ranged from 1.6 to 11.1 g (3.98 ± 2.3 g). The overall quantity of mature oocytes in ovaries ranged from 16 405 to 94 357 oocytes (35 904 ± 19 121 oocytes). In the presently reported study, the fecundity of fish exhibited a positive correlation with gonad weight compared to the length and weight of the fish (Fig. 7). The strongest correlation was found when fecundity was compared with W_G ($R^2 = 0.966$).

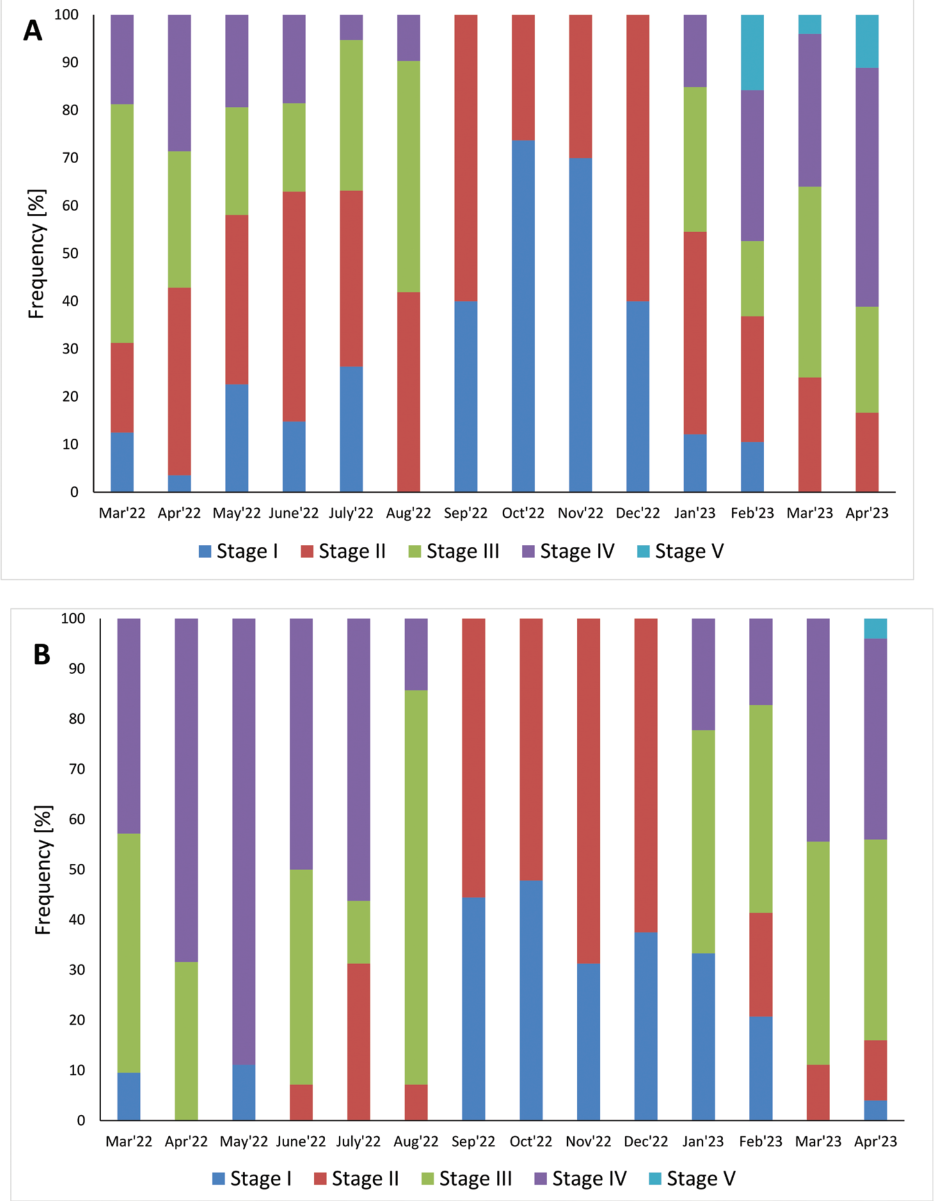

Figure 4. Monthly fluctuations in gonadal developmental stages for males (**A**) and females (**B**) of *Lutjanus xanthopinnis.*

Discussion

The lack of precise fishery and biological data required for fisheries management is common in developing countries. The presently reported study provides first-hand information on the reproductive biology of *Lutjanus xanthopinnis* on the east coast of Peninsular Malaysia. The highest total length of *L. xanthopinnis* was measured in Terengganu waters, Malaysia at 26.8 cm which is considerably longer than the length that Velamala et al. (2020) reported from the Visakhapatnam Coast, India. The higher maximum length observed in this study may be caused by different environmental variables associated with differences in geography (Smoliński and Berg 2022). The presently reported study found that the monthly recorded and size-based sex ratio of *L. xanthopinnis* population was biased towards males and differed from the expected ratio of 1:1. Many researchers have made similar findings about various *Lutjanus* species (Fry et al. 2009; Pradeep 2016; Araki and Tachihara 2021) corroborating the results of the presently reported study. The sex ratio deviates from the expected 1:1 for several reasons, including population adaption, sexual behavior, availability of food, and environmental variables (Brykov et al. 2008; Vandeputte et al. 2012).

The fish spawning season is regulated by an association of the GSI and the pattern of the gonadal development stages, which provides a trustworthy indicator of reproductive activity (Rizzo and Bazzoli 2020). The spawning season was estimated to be protracted from January to August, with a peak period in March and April based on GSI and gonad development stages (Figs. 4, 5). According to Yaakob and Chau (2005), Malaysia's northeast monsoon season continues from November to February. Spawning begins towards the end of the rainy season (January) and continues until mid-summer (August). The majority of tropical lutjanids are serial spawners with prolonged spawning seasons

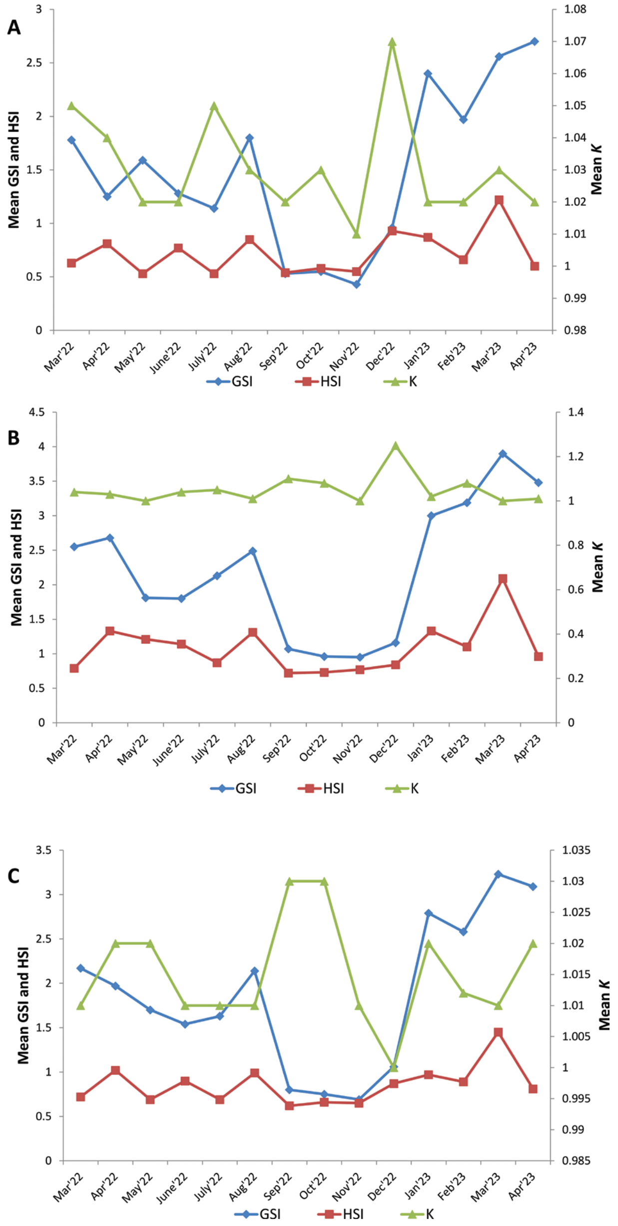

Figure 5. Monthly variations of gonadosomatic index (GSI), hepatosomatic index (HSI) and condition factor (K) of males (**A**), females (**B**), and combined sexes (**C**) of *Lutjanus xanthopinnis* collected at Pulau Kambing Fish Landing Port (Terengganu, Malaysia) eastern South China Sea.

(Kritzer 2004; Shimose and Tachihara 2005; Marriott et al. 2007). Similar findings about the spawning season for *Lutjanus* species were observed in earlier studies conducted in different regions: May to September for *L. quinquelineatus* (see Araki and Tachihara 2021), April to August for *Lutjanus fulviflamma* (Forsskål, 1775) (see Shimose and Nanami 2015), June to September for *Lutjanus fulvus* (Forster, 1801) (see Shimose and Nanami 2014), May to October for *Lutjanus gibbus* (Forsskål, 1775) (see Nanami et al. 2010a), June to October for *Lutjanus decussatus* (Cuvier, 1828) (see Nanami et al. 2010b). While the timing of the spawning season varied, it was observed to be prolonged and coincided with the period of warmest water temperature, which is compatible with the findings of the presently reported study.

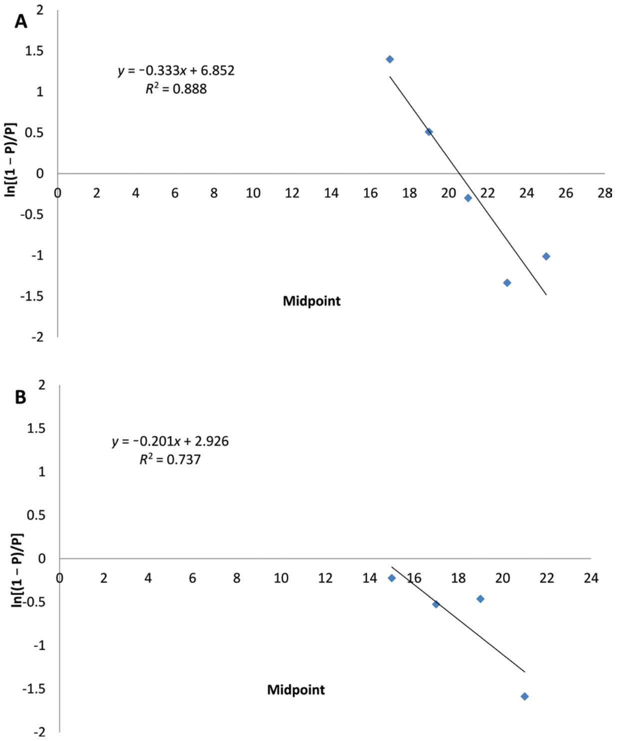

Figure 6. Proportions of mature males (**A**) (n = 132) and females (**B**) (n = 162) of *Lutjanus xanthopinnis* by fitting to a straight line of ln[$(1 - R_M) \times R_M$] against the midpoint of each size class. The fish were collected at Pulau Kambing Fish Landing Port (Terengganu, Malaysia) eastern South China Sea. R_M = mature individuals rate.

Variations in K and HSI were used to evaluate the patterns of energy use in fish during the reproductive phase. In the presently reported study, the mean condition factor (K) was higher than 1 in both sexes, indicating they are physiologically stable. According to Jisr et al. (2018), if a fish species has a K value equal to or very close to 1, we consider that species to have a general fitness level. Muchlisin et al. (2017) claim that when K is 1, there is still a balance between prey and predators, the waterways are in good condition, and fish can flourish. In general, condition factors are typically influenced by several biotic and abiotic factors, such as food availability, water quality, age, size, sex, and stage of gonad development (Kuriakose 2014). The condition factor and its strong opposite relation with GSI show that muscle weight decreases during reproduction due to the mobilization of muscle energy to aid gonad development. These findings were supported by Fadzli et al. (2022), where decreasing condition factors imply rapid growth of gonads. However, the pattern of HSI showed associations with the monthly progression of GSI, indicating that liver lipid storage is not necessary for fish reproduction.

Understanding the length at maturity will help determine the size that should be fished for sustainable fisheries (Thulasitha and Sivashanthini 2013). The calculated length at 50% sexual maturity (L_{50}) of *L. xanthopinnis* was 20.56 cm for males and 14.53 for females (Fig. 6). These length values were higher than those reported for *L. quinquelineatus* from Okinawa, Japan by Araki and Tachihara (2021) and smaller than those reported for

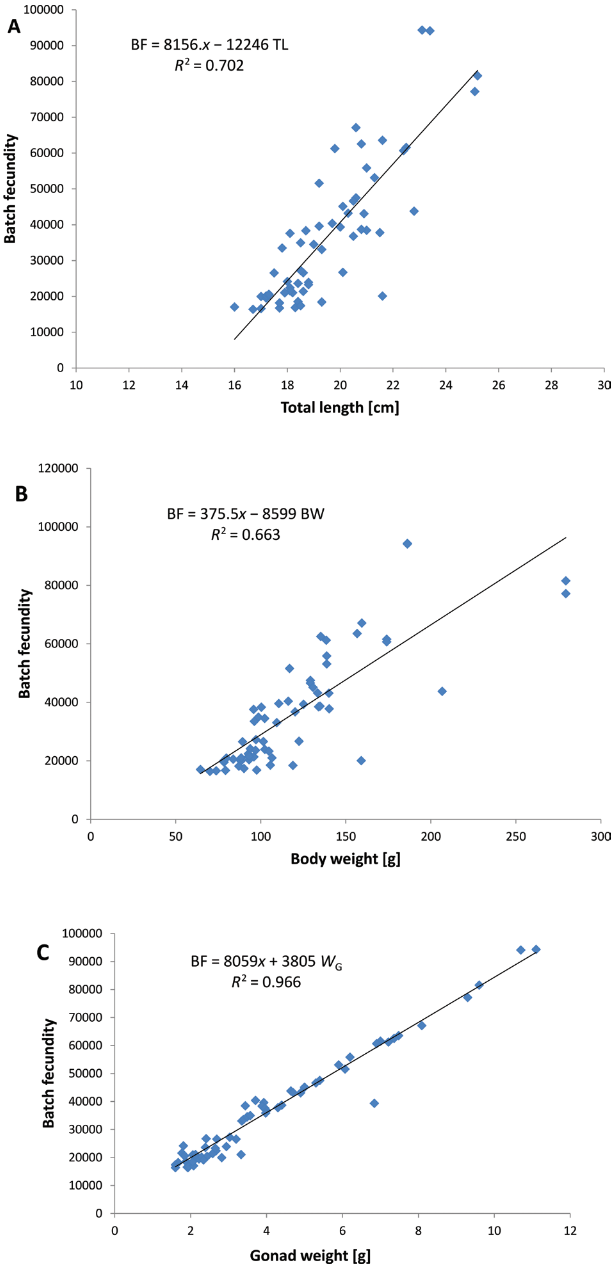

Figure 7. Relations between batch fecundity and total length (**A**), relations between batch fecundity and body weight (**B**), and relations between batch fecundity and gonad weight (**C**) of *Lutjanus xanthopinnis* collected at Pulau Kambing Fish Landing Port (Terengganu, Malaysia) eastern South China Sea. BF = batch fecundity, W_G = gonad weight

L. gibbus from New Caledonia by Moore (2019). Variations in length maturity may be caused by differences in food available in different geographic locations (Oliveira et al. 2017). Tropical marine fish maturity size increases with distance from the distribution center (Trip et al. 2014). Small-size *Lutjanus* species generally mature earlier than the large snapper (Araki and Tachihara 2021). Moreover, the sample size and composition, sampling interval, and diagnostic criteria all influence the length of maturity estimation (Gaspare and Bryceson 2013). In the presently reported study, the early maturity of females is probably due to excessive fishing pressure.

Fecundity is crucial for developing successful fish species recruitment and regulating the fish population (Fernandes et al. 2022). Our study on *L. xanthopinnis* in Terengganu waters revealed that the fecundity varied from 16 405 to 94 357 oocytes and showed a positive relation with gonad weight compared to the length and weight of the fish. The BF value determined in the presently reported was lower than the value reported by Palla and Sotto (2021) and higher than the value reported by Pradeep (2016). In addition, the relations between BF with TL, W_B, and W_G were exponential, which is supported by the findings of Fadzli et al. (2022). Grimes (1987) implied that tropical lutjanids can be very fecund species. The age, the relation of body size, population density, and environmental variability could all contribute to the variation in fecundity (Bradshaw and McMahon 2008).

Management strategies. The purpose of fisheries management is to maximize the benefits of the output unit (fish stock) which has been managed. Based on the findings of our study, a few management strategies are suggested here for the sustainable management of *L. xanthopinnis* in Malaysia and elsewhere. For instance, *L. xanthopinnis* in the eastern South China Sea, Malaysia has an L_{50} of 20.56 for males and 14.53 cm for females, meaning 50% of fish at this length are mature. For sustainable management, we recommend catching fish smaller than the L_{50} be strongly prohibited and that fishing not be allowed during the peak spawning seasons. Some researchers revealed that snapper species exhibit aggregating behavior during spawning season (Claro and Lindeman 2003; Malafaia et al. 2021; Motta et al. 2022), focusing on these aggregations at specific times and locations may lead to overexploitation. Consequently, marine protected areas must be established along with other management and conservation measures to ensure the survival of species and ecosystems. There is a need for improved dissemination of stock status information among state and Commonwealth agencies tasked with overseeing the management of particular fisheries targeting this species. This would facilitate the establishment of collaborative management plans that span multiple jurisdictions.

Conclusion

This study used a multidisciplinary way to understand better the reproductive biology of *Lutjanus xanthopinnis* in the Terengganu waters of the South China Sea, Malaysia, including size structure, sex ratio, gonad maturation stages, gonadosomatic index, spawning season, condition factor, hepatosomatic index, length at first maturity, and fecundity. Knowledge about reproductive biology is essential for sustainable management, especially in rising nations like Malaysia, where managers depend on the maturity length and the reproductive period's start and duration to manage fisheries resources. The presently reported study offers first-hand knowledge of the reproductive biology *L. xanthopinnis*, globally and in Malaysia. These results might be a foundation for managing reef fisheries efficiently and sustainably.

Acknowledgment

The study was funded by the Fundamental Research Grant Scheme (FRGS) with project reference FRGS/1/2021/WAB05/UMT/02/4, and the authors gratefully acknowledge the Malaysian Ministry of Higher Education (MoHE) for their support. We thank Encik Muhammad Haniff Bin Mohd Yusoff, Fisheries Officer at FPSM, UMT, for assistance during histology lab work. We also appreciated the logistical assistance provided by the Faculty of Fisheries and Food Science at Universiti Malaysia Terengganu.

References

Adibah AB, Darlina MN (2014) Is there a cryptic species of the golden snapper (*Lutjanus johnii*)? Genetics and Molecular Research 13(4): 8094–8104. https://doi.org/10.4238/2014.October.7.4

Alam A, Gopinath V, Kumar J, Das SCS, Jha DN, Joshi KD, Srivastava RS (2020) Maturity, breeding cycle, and fecundity of *Mastacembelus armatus* (Actinopterygii: Synbranchiformes: Mastacembelidae) in the sub-tropical waters of the river Ganga. Acta Ichthyologica et Piscatoria 50(2): 191–199. https://doi.org/10.3750/AIEP/02898

Allen GR (1985) FAO species catalogue: Vol. 6. Snappers of the world: An annotated and illustrated catalogue of lutjanid species known to date. FAO, Rome.

Alves DC, Minte-Vera CV (2012) Scientometric analysis of freshwater fisheries in Brazil: Repeating past errors? Reviews in Fish Biology and Fisheries 23(1): 113–126. https://doi.org/10.1007/s11160-012-9282-6

Arai T, Taha H, Alidon N, Jumat J, Azmey S, Zan ND, Jafar TNAM, Habib A (2023) Mitochondrial cytochrome c oxidase subunit I gene analysis of the yellowfin snapper, *Lutjanus xanthopinnis* in the Indo–Pacific region and a note on *Lutjanus lutjanus* population structure. Heliyon 9(9): e19348. https://doi.org/10.1016/j.heliyon.2023.e19348

Araki K, Tachihara K (2021) Age, growth, and reproductive biology of the five-lined snapper *Lutjanus quinquelineatus* around Okinawa-jima Island, southern Japan. Fisheries Science 87(4): 503–512. https://doi.org/10.1007/s12562-021-01520-x

Bradshaw CJA, McMahon CR (2008) Fecundity. Pp. 1535–1543. In: Jorgensen SE, Fath B (Eds.) Encyclopedia of ecology. [Five volume set.] Oxford, UK, Elsevier. https://doi.org/10.1016/B978-008045405-4.00645-5

Brown-Peterson NJ, Wyanski DM, Saborido-Rey F, Macewicz BJ, Lowerre-Barbieri SK (2011) A standardized terminology for describing reproductive development in fishes. Marine and Coastal Fisheries 3(1): 52–70. https://doi.org/10.1080/19425120.2011.555724

Brykov VA, Kukhlevsky AD, Shevlyakov EA, Kinas NM, Zavarina LO (2008) Sex ratio control in pink salmon (*Oncorhynchus gorbuscha* and chum salmon (*O. keta*) populations: The possible causes and mechanisms of changes in the sex ratio. Russian Journal of Genetics 44(7): 786–792. https://doi.org/10.1134/S1022795408070053

Claro R, Lindeman KC (2003) Spawning aggregation sites of snapper and grouper species (Lutjanidae and Serranidae) on the insular shelf of Cuba. Gulf and Caribbean Research 14(2): 91–106. https://doi.org/10.18785/gcr.1402.07

Costa AM (2019) Reproductive cycle of the blue jack mackerel, *Trachurus spicturatus* (Bowdich, 1825), off the Portuguese continental coast. Aquatic Living Resources 32: 14. https://doi.org/10.1051/alr/2019011

Coulson PG, Norriss JV, Jackson G, Fairclough DV (2019) Reproductive characteristics of the fishery important temperate demersal berycid *Centroberyx gerrardi* indicate greater reproductive output in regions of upwelling. Fisheries Management and Ecology 26(3): 236–248. https://doi.org/10.1111/fme.12343

DOF (2023) Annual fisheries statistics 2023. Department of Fisheries. Ministry of Agriculture and Agro-based Industries, Putrajaya, Malaysia. [Accessed 8 April 2023] https://www.dof.gov.my/en/resources/fisheries-statistics-i/

Fadzli MH, Jaafar TNAM, Ali MS, Nur NFM, Tan MP, Piah RM (2022) Reproductive aspects of the coastal trevally, *Carangoides coeruleopinnatus* in Terengganu waters, Malaysia. Aquaculture and Fisheries 7(5): 500–506. https://doi.org/10.1016/j.aaf.2022.04.009

Fakoya KA, Anetekha MA (2019) Macroscopic gonad staging and reproductive seasonality in the Gorean snapper, *Lutjanus goreensis* a gonochoristic west African lutjanid. West African Journal of Applied Ecology 27(1): 1–22.

Fernandes JFF, Freitas J, de Araújo SA, de Santana TC, Lobato RS, Figueiredo MB (2022) Reproductive biology of the lane snapper, *Lutjanus synagris* (Linnaeus 1758) (Perciformes, Lutjanidae), in the Maranhão continental shelf, northeast of Brazil. Environmental Biology of Fishes 105(8): 1033–1050. https://doi.org/10.1007/s10641-022-01310-z

Fry G, Milton DA, Van Der Velde T, Stobutzki I, Andamari R, Badrudin, Sumiono B (2009) Reproductive dynamics and nursery habitat preferences of two commercially important Indo–Pacific red snappers *Lutjanus erythropterus* and *L. malabaricus.* Fisheries Science 75(1): 145–158. https://doi.org/10.1007/s12562-008-0034-4

Gaspare L, Bryceson I (2013) Reproductive biology and fishery-related characteristics of the Malabar grouper (*Epinephelus malabaricus*) caught in the coastal waters of Mafia Island, Tanzania. Journal of Marine Sciences: 2013. https://doi.org/10.1155/2013/786589

Gonçalves P, Costa AM, Murta AG (2009) Estimates of batch fecundity and spawning fraction for the southern stock of horse mackerel (*Trachurus trachurus*) in ICES Division IXa. ICES Journal of Marine Science 66(4): 617–622. https://doi.org/10.1093/icesjms/fsp066

Grandcourt EM, Al Abdessalaam TZ, Francis F (2006) Age, growth, mortality and reproduction of the blackspot snapper, *Lutjanus fulviflamma* (Forsskål, 1775), in the southern Arabian Gulf. Fisheries Research 78(2–3): 203–210. https://doi.org/10.1016/j.fishres.2005.11.021

Grimes CB (1987) Reproductive biology of the Lutjanidae: A review. Pp. 239–294. In: Polovina JJ, Ralston S (Eds.) Tropical snapper and groupers: Biology and fisheries management. Westview Press, Boulder, CO, USA.

Hammer O, Harper DAT, Ryan PD (2001) Past: Paleontological Statistics Software Package for Education and Data Analysis. Palaeontologia Electronica 4: 1–9.

IUCN (2019) The IUCN Red List of Threatened Species. Version 2019-2. [Accessed: 04 July 2019] https://www.iucnredlist.org/

Iwatsuki YUKIO, Tanaka FUMIYA, Allen GR (2015) *Lutjanus xanthopinnis*, a new species of snapper (Pisces: Lutjanidae) from the Indo–west Pacific, with a redescription of *Lutjanus madras* (Valenciennes 1831). Journal of the Ocean Science Foundation 17: 22–42.

Jisr N, Younes G, Sukhn C, El-Dakdouki MH (2018) Length–weight relationships and relative condition factor of fish inhabiting the marine area of the Eastern Mediterranean city, Tripoli-Lebanon. Egyptian Journal of Aquatic Research 44(4): 299–305. https://doi.org/10.1016/j.ejar.2018.11.004

Khatun D, Hossain M, Nawer F, Mostafa AA, Al-Askar AA (2019) Reproduction of *Eutropiichthys vacha* (Schilbeidae) in the Ganges River (NW Bangladesh) with special reference to potential influence of climate variability. Environmental Science and Pollution Research International 26(11): 10800–10815. https://doi.org/10.1007/s11356-019-04523-5

Kinas PG (1996) Bayesian fishery stock assessment and decision making using adaptive importance sampling. Canadian Journal of Fisheries and Aquatic Sciences 53(2): 414–423. https://doi.org/10.1139/f95-189

King M (2007) Fisheries biology, assessment and management. Blackwell Publishing Ltd., Oxford, UK, 382 pp. https://doi.org/10.1002/9781118688038

Kritzer JP (2004) Sex-specific growth and mortality, spawning season, and female maturation of the stripey bass (*Lutjanus carponotatus*) on the Great Barrier Reef. Fish Bulletin 102: 94–107.

Kuriakose S (2014) Estimation of length weight relationship in fishes. Summer School on Advanced Methods for Fish Stock Assessment and Fisheries Management. Reprinted from the CMFRI, FRAD. Training Manual on Fish Stock Assessment and Management, 150 pp.

Le Cren ED (1951) The length–weight relationship and seasonal cycle in gonad weight and condition in the perch (*Perca fluviatilis*). Journal of Animal Ecology 20(2): 201–219. https://doi.org/10.2307/1540

Longenecker K, Franklin EC, Hill-Lewenilovo R, Lalavanua W, Langston R, Mangubhai S, Piovano S (2022) Many immature individuals and largest size classes lacked females for three coral reef fishes (Actinopterygii) in Fiji market surveys: Implications for fishery management. Acta Ichthyologica et Piscatoria 52(1): 53–65. https://doi.org/10.3897/aiep.52.80586

Malafaia PN, França AR, Olavo G (2021) Spawning aggregation sites of the cubera snapper, *Lutjanus cyanopterus*, on the continental shelf of Bahia state, northeastern Brazil. Fisheries Research 242: e106037. https://doi.org/10.1016/j.fishres.2021.106037

Marriott RJ, Mapstone BD, Begg GA (2007) Age-specific demographic parameters, and their implications for management of the red bass, *Lutjanus bohar* (Forsskal 1775): A large, long-lived reef fish. Fisheries Research 83(2–3): 204–215. https://doi.org/10.1016/j.fishres.2006.09.016

Messias MA, Alves TI, Melo CM, Lima M, Rivera-Rebella C, Rodrigues DF, Madi RR (2019) Ethnoecology of Lutjanidae (snappers) in communities of artisanal fisheries in northeast Brazil. Ocean and Coastal Management 181: 104866. https://doi.org/10.1016/j.ocecoaman.2019.104866

Moore BR (2019) Age-based life history of humpback red snapper, *Lutjanus gibbus*, in New Caledonia. Journal of Fish Biology 95(6): 1374–1384. https://doi.org/10.1111/jfb.14142

Motta FS, Freitas MO, Rolim FA, Abilhoa V, Pereira Filho GH (2022) Direct evidence of a spawning aggregation of cubera snapper (*Lutjanus cyanopterus*) in southeastern Brazil and its management implications. Fisheries Research 252: 106339. https://doi.org/10.1016/j.fishres.2022.106339

Muchlisin ZA, Fransiska V, Muhammadar AA, Fauzi M, Batubara AS (2017) Length–weight relationships and condition factors of the three dominant species of marine fishes caught by traditional beach trawl in Ulelhee Bay, Banda Aceh City, Indonesia. Ribarstvo 75(3): 104–112. https://doi.org/10.1515/cjf-2017-0014

Nanami A, Kurihara T, Kurita Y, Aonuma Y, Suzuki N, Yamada H (2010a) Age, growth and reproduction of the humpback red snapper *Lutjanus gibbus* off Ishigaki Island, Okinawa. Ichthyological Research 57(3): 240–244. https://doi.org/10.1007/s10228-010-0160-8

Nanami A, Okuzawa K, Yamada H, Suzuki N, Aonuma Y (2010b) Reproductive activity in the checkered snapper, *Lutjanus decussatus*, off Ishigaki Island, Okinawa. Ichthyological Research 57(3): 314–318. https://doi.org/10.1007/s10228-010-0155-5

Oliveira MR, Nóbrega MF, Oliveira JEL, Chellappa S (2017) Reproductive biology of blue runner, *Caranx crysos* (Mitchell, 1815) from the coastal waters of Rio Grande do Norte, Brazil (Southwest Atlantic Ocean). Journal of Aquaculture and Marine Biology 5(5): e00136. https://doi.org/10.15406/jamb.2017.05.00136

Pacicco AE, Brown-Peterson NJ, Murie DJ, Allman RJ, Snodgrass D, Franks JS (2023) Reproductive biology of yellowfin tuna (*Thunnus albacares*) in the northcentral US Gulf of Mexico. Fisheries Research 261: 106620. https://doi.org/10.1016/j.fishres.2023.106620

Palla HP, Sotto FB (2021) Reproductive biology of brownstripe snapper *Lutjanus vitta* (Quoy and Gaimard, 1824) from West Sulu Sea, Philippines. Egyptian Journal of Aquatic Research 47(1): 67–73. https://doi.org/10.1016/j.ejar.2021.01.001

Pradeep HD (2016) Reproductive biology and histology of female bigeye snapper *Lutjanus lutjanus* (Bloch, 1790) off Madras coast along southeast coast of India. P. 10. In: International Conference on Climate change adaptation and biodiversity: Ecological sustainability and resource management for livelihood security (ASA: ICCB-2016; Vol. 8).

Rahman MM, Ariffin NA, Seah YG, Jaafar TNAM, Habib A (2023) Length–weight relationships and relative condition factors of three coral-associated *Lutjanus* species from Terengganu waters of the South China Sea, Malaysia. Turkish Journal of Zoology 47(4): 216–221. https://doi.org/10.55730/1300-0179.3134

Rizzo E, Bazzoli N (2020) Reproduction and embryogenesis. Pp. 287–313. In: Baldisserotto B, Urbinati EC, Cyrino J (Eds.) Biology and physiology of freshwater neotropical fish. Academic Press. https://doi.org/10.1016/B978-0-12-815872-2.00013-0

Russell DJ, McDougall AJ, Fletcher AS, Ovenden JR, Street R (2003) Biology, management and genetic stock structure of mangrove jack, (*Lutjanus argentimaculatus*) in Australia. Department of Primary Industries, Queensland, Fisheries Research Development Corporation, Project No. 1999/122, DPI QO03003, 189 pp.

Shimose T, Nanami A (2014) Age, growth, and reproductive biology of blacktail snapper, *Lutjanus fulvus*, around the Yaeyama Islands, Okinawa, Japan. Ichthyological Research 61(4): 322–331. https://doi.org/10.1007/s10228-014-0401-3

Shimose T, Nanami A (2015) Age, growth, and reproduction of blackspot snapper *Lutjanus fulviflammus* (Forsskål 1775) around Yaeyama Islands, southern Japan, between 2010 and 2014. Journal of Applied Ichthyology 31(6): 1056–1063. https://doi.org/10.1111/jai.12894

Shimose T, Tachihara K (2005) Age, growth and maturation of the blackspot snapper *Lutjanus fulviflammus* around Okinawa Island, Japan. Fisheries Science 71(1): 48–55. https://doi.org/10.1111/j.1444-2906.2005.00929.x

Smoliński S, Berg F (2022) Varying relationships between fish length and scale size under changing environmental conditions—Multidecadal perspective in Atlantic herring. Ecological Indicators 134: e108494. https://doi.org/10.1016/j.ecolind.2021.108494

Thulasitha WS, Sivashanthini K (2013) Reproductive characteristics of doublespotted queenfish, *Scomberoides lysan* (Actinopterygii: Perciformes: Carangidae), from Sri Lankan waters: Implications for fisheries management. Acta Ichthyologica et Piscatoria 43(1): 7–13. https://doi.org/10.3750/AIP2013.43.1.02

Trip EDL, Clements KD, Raubenheimer D, Choat JH (2014) Temperature-related variation in growth rate, size, maturation and life span in a marine herbivorous fish over a latitudinal gradient. Journal of Animal Ecology 83(4): 866–875. https://doi.org/10.1111/1365-2656.12183

Tsikliras AC, Stergiou KI, Froese R (2013) Editorial note on reproductive biology of fishes. Acta Ichthyologica et Piscatoria 43(1): 1–5. https://doi.org/10.3750/AIP2013.43.1.01

Vandeputte M, Quillet E, Chatain B (2012) Are sex ratios in wild European sea bass (*Dicentrarchus labrax*) populations biased? Aquatic Living Resources 25(1): 77–81. https://doi.org/10.1051/alr/2012002

Velamala GR, Naranji MK, Netto-Ferreira AL, Kondmudi RB (2020) Length–weight relationships for 16 snapper fishes from Visakhapatnam coast, India. Thalassas 36: 75–78. https://doi.org/10.1007/s41208-019-00174-y

Yaakob O, Chau QP (2005) Weather downtime and its effect on fishing operation in Peninsular Malaysia. Jurnal Teknologi 42(A): 13–26. https://doi.org/10.11113/jt.v42.730

Acta Ichthyologica et Piscatoria 54, 2024, 75–86 | DOI 10.3897/aiep.54.112388

PENSOFT.

ACTA
ICHTHYOLOGICA
ET PISCATORIA

Dynamics of fish community structure in the Yeosu Coast, Korea: A comprehensive analysis of daily set-net catch data during 2008–2022

Seong Yong MOON[1], Mi Hee LEE[1], Kyung-Mi JUNG[2], Myung Sung KOO[3]

1 *South Sea Fisheries Research Institute, National Institute of Fisheries Science, Yeosu, Republic of Korea*
2 *Coastal Water Fisheries Resources Research Division, National Institute of Fisheries Science, Busan, Republic of Korea*
3 *Fisheries Engineering Research Division, National Institute of Fisheries Science, Busan, Republic of Korea*

https://zoobank.org/79543B83-63E3-4FED-BE2A-553359D17A14

Corresponding author: Myung Sung Koo (kms2736@korea.kr)

Academic editor: Sanja Matić-Skoko ♦ **Received** 7 September 2023 ♦ **Accepted** 18 December 2023 ♦ **Published** 15 March 2024

Citation: Moon SY, Lee MH, Jung K-M, Koo MS (2024) Dynamics of fish community structure in the Yeosu Coast, Korea: A comprehensive analysis of daily set-net catch data during 2008–2022. Acta Ichthyologica et Piscatoria 54: 75–86. https://doi.org/10.3897/aiep.54.112388

Abstract

This study focuses on the Yeosu Coast, a critical ecological and economic zone on the Korean Peninsula. We conducted a comprehensive analysis of fish data obtained from daily set nets for the period of 2008–2022 (excluding 2017) to investigate variations in fish composition and community structure over a 15-year period. The catches were characterized by a prevalence of warm-water fish species, reflecting the temperate and subtropical character of the Yeosu Coast. The total catch during the study period was 3210.8 tonnes, with 2010 and 2016 registering the highest and lowest catches, respectively. Our analysis identified sea surface temperature as a primary factor correlated with these changes in species composition. The two dominant species, *Scomberomorus niphonius* (Cuvier, 1832) and *Engraulis japonicus* Temminck et Schlegel, 1846 together accounted for a remarkable 78.9% of the total catch. Notably, the Shannon–Weaver diversity index values were lower in 2015 than in 2008, indicating potential shifts in the community structure. Our analysis identified sea surface temperature as the most dominant factor that influenced these changes in species composition. Furthermore, we highlight the significant threats posed by climate change and the increasing number of jellyfish challenging fisheries on the Yeosu Coast. These threats have the potential to result in diminished set-net catches and declining biodiversity within this valuable ecosystem. Our findings underscore the importance of monitoring and addressing these ecological shifts to ensure the long-term sustainability of Yeosu Coast fisheries.

Keywords

climate change, biodiversity, fish composition, sea surface temperature, Shannon–Weaver diversity index

Introduction

The Yeosu Coast, located in the central-southern region of Korea, is a ria-type coast. It has a dynamically diverse marine environment owing to factors such as the Tsushima Warm Current (TWC), the Jeju Warm Current flowing from the West of Jeju Island, and the formation of southern coastal waters during winter, which spread beneath the weak water temperature layer in summer (Lie and Cho 1997; Choo 2002; Chang et al. 2004). These seasonal variations create habitats for both pelagic and coastal settling fish species, creating an essential fishing ground with abundant fish resources (Kim et al. 2003; Hwang et al. 2006; Kim et al. 2013). Notably, different water masses converge at the Yeosu Coast and form a frontal zone that fosters nutrient supply through upwelling, resulting in increased primary production of phytoplankton and zooplankton abundance (Kang and Jeon 1999; Moon et al. 2010, 2022a). This dynamic ecosystem serves as a spawning ground and nursery for small pelagic fish (Yoo et al. 2017; Moon et al. 2022b).

Hence, the Yeosu Coast boasts rich fish resources and supports fishing activities that employ various fishing gear. Among these, the most popular gear is the set net, which is a passive fishing method that intercepts fish schools using nets to guide them into a specific area for capture. While the pelagic and seasonally migratory fish species residing in offshore waters are the primary targets of set nets, catches are typically influenced by fluctuations in sea conditions, such as water temperature, in the deployment area. This attribute enables localized set nets to closely monitor the recruitment and catch trends of pelagic and migratory fish species (Kim et al. 2003; Hwang et al. 2006; Kim et al. 2013). Despite the installation of various set nets along the Yeosu Coast, the larger-scale set nets may be more effective in capturing a comprehensive array of fish species, including pelagic and demersal types (Kim et al. 2003; Hwang et al. 2006). Because of the significant fluctuations experienced by the monthly or seasonal set-net survey data, identifying potential survey periods and increasing sample sizes are necessary to closely analyze the species composition and catch characteristics of demersal fish species in the surveyed area.

Previous studies on set-net fisheries conducted along the Yeosu Coast have been primarily focused on the species composition and quantitative variations in set-net-caught fish (Jeong et al. 2005; Hwang et al. 2008), species composition and quantitative variations in longline-caught fish (Han and Oh 2007; Kim et al. 2017), species richness and quantitative variations in set-net-caught fish (Kim et al. 2003), species richness and quantitative variations in bycatch from set nets (Jeong et al. 2015), and bycatch in general (Yoo et al. 2016). However, these investigations were based on species composition and quantitative variations in fish captured over short timeframes. Remarkably, no study has examined the species composition of set-net catches off the Yeosu Coast using daily catch data for over two decades (Hwang et al. 2006).

Furthermore, the influence of climate change on the composition of marine ecosystems has been documented (Hoegh-Guldberg and Bruno 2010; Doney et al. 2012; Zhang et al. 2020). In recent years, the southern coast of the Korean Peninsula, including the Yeosu area, has witnessed a persistent increase in surface water temperature due to climate change (Han and Lee 2020). This highlights the need for long-term comparative data regarding species richness and fluctuation patterns. Such information is vital for the effective management and preservation of fishery resources in such a region. In this study, daily catch data from set nets along the Yeosu Coast spanning the past 15 years (2008–2022) were collected. The objective of this study was to determine the composition, catch quantities, and attributes of key commercial fish species. These data were then correlated with changes in water temperature. A comparison was also conducted linking these findings to those of studies conducted two decades ago. The overarching goal of this study is to provide foundational data to support the efficient conservation and sustainability of fishery resources off the Yeosu Coast in the context of a rapidly changing climate.

Materials and methods

Data collection. The set-net fishing sites and real-time coastal information system for sea surface temperature (SST) by the Korea Oceanographic Data Center (KODC) in this study were located between Dolsan and Geumo Islands, Yeosu, Jeollanam-do (Fig. 1). The maps were created using the ODV software (Schlitzer 2021). Daily catch data obtained during the set-net fishing season from 2008 to 2022 were scrutinized, excluding 2017 because of missing data. This analysis aimed to assess the catch ratio and variations in major fish species on a monthly and yearly basis. The set net used (750–800 m in length, 30 m in width, with mesh sizes of 120 mm in the leader net and 75 mm in the playground)was a modified hawkbill net set to the mean depth of 25 m near Dolsan Island, Yeosu. It captured small pelagic fish that migrated near the shore from spring to early summer (March–June). Set nets with a mesh size of 0.42 cm were used during spring and early summer, whereas a larger mesh size of 27.55 cm was employed during the late summer and winter fishing seasons (July–December). As the daily catch data were recorded in terms of box counts, the monthly catch for each species was computed by converting the mean box weight into 15 kg during the fishing period. Species that were challenging to identify in the daily catch data, such as sharks and cetaceans, and those with sporadic appearances and significantly higher weights, were excluded from the analysis. The analysis focused on the major commercial fish species. To understand the correlation between the catch of major fish species in set nets and shifts in SST over the past 15 years, daily water temperature data obtained from the KODC (KODC 2023, Fig. 1) of the National Institute of Fisheries Science were used. These real-time marine environment fishery information observations were collected from 2008 to 2022 and transformed into monthly mean data for Hwatae Island (34°35′10″N, 127°43′02″E) in Yeosu, a location proximate to the set-net fishing grounds. Jellyfish data were obtained from the Korean jellyfish monitoring program (KoJeM), operated by the National Institute of Fisheries Sciences (NIFS), South Korea. The KoJeM program was launched in 2006 as a weekly survey to track changes in the ratio of jellyfish occurrences in the coastal waters of South Korea. In this study, we assessed jellyfish data over the period from 2008 to 2022, as these years correspond to the period with the best sampling resolution (NIFS 2023).

Data analysis. To evaluate the species diversity of the captured fishery resources, the species diversity index (H') was calculated using the Shannon–Weaver diversity index (Shannon and Weaver 1963) expressed as follows:

$$H' = \sum_{i=1}^{S} P_i \times \mathrm{Log} P_i$$

where S is the total catch of species and P_i is the relative cover of i_{th} species.

Changes in the fish community across ecological successions along the Yeosu Coast were analyzed over a

15-year study period using non-metric multidimensional scaling (nMDS). The nMDS ordinations were generated from Bray–Curtis similarity matrices calculated using log-transformed catch data for all species (Clarke and Gorley 2014). Species within each nMDS group were compared using similarity analysis (ANOSIM) to identify statistically significant differences among the groups. ANOSIM ranks the similarity between samples within the similarity matrix and tests the null hypothesis that the average rank of the within-group similarity is not significantly different from the average rank of the between-group similarity. Groups found to be significantly different by ANOSIM were further analyzed using the similarity percentage routine (SIMPER) to identify the species or taxa that most contribute to the distinctiveness of each group. SIMPER calculates the average similarity within each group and determines the percentage contribution of each species/taxon to the overall group similarity. These analyses were performed using the PRIMER version 6.0 statistical package (Clarke and Gorley 2014). In addition to the analyses of nMDS and SIMPER, we conducted univariate linear regression analyses to examine the relations between biotic variables (dependent variables) and potential explanatory variables (independent variables). The biotic variables were the abundances of eight fish species: *Scomberomorus niphonius* (Cuvier, 1832), *Engraulis japonicus* Temminck et Schlegel, 1846, *Pampus argenteus* (Euphrasen, 1788), *Trichiurus japonicus* Temminck et Schlegel, 1844, *Lophius litulon* (Jordan, 1902), *Seriola quinqueradiata* Temminck et Schlegel, 1845, *Scomber japonicus* Houttuyn, 1782, and *Trachurus japonicus* (Temminck et Schlegel, 1844). We used two environmental variables as potential explanatory factors: annual mean SST and the ratio of jellyfish occurrences. Both of these variables were available for the entire 15-year study period.

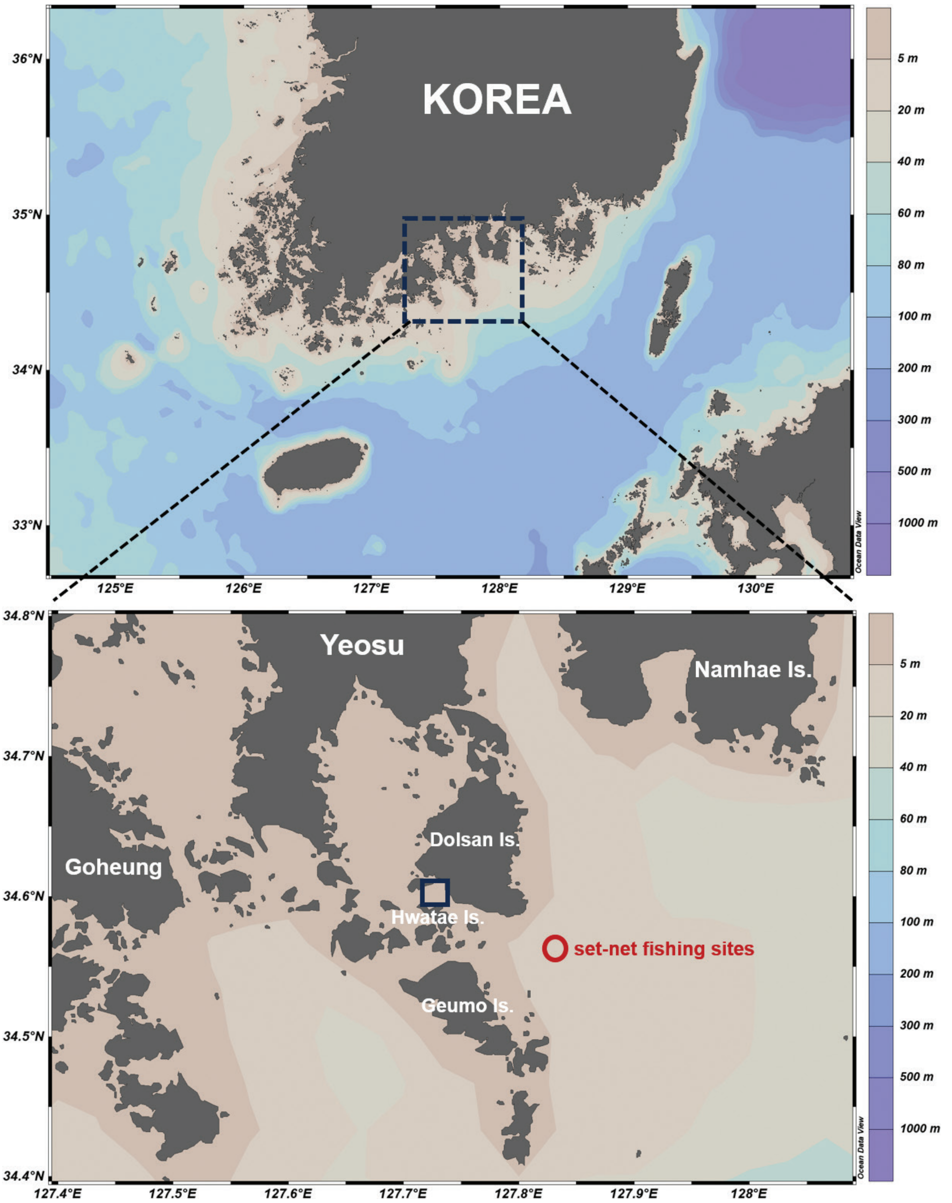

Figure 1. Map showing the set-net fishing sites (red circle) and real-time coastal information system for sea surface temperature by the KODC (Korea Oceanographic Data Center) (black square) at the Yeosu Coast, Korea.

Results

Sea surface temperature. Throughout the survey period, the mean monthly SST near Hwatae Island, near the Yeosu set nets, exhibited typical characteristics of temperate waters with well-defined seasonal shifts ranging from 6.78 to 26.76°C. The lowest SST was recorded in February 2018, whereas the highest was recorded in August 2018. Notably, elevated mean SST of 26.76 and 26.47°C were noted in the summers of 2018 and 2021, respectively, which were primarily attributed to the heightened coastal SST during the summer (Fig. 2A).

Species composition, diversity index, and catch characteristics. The set-net catch during the study period included 15 orders, 49 families, and 84 taxa of fish species. The highest number of species was observed in 2011, whereas the lowest was observed in 2021 (Fig. 2B). The species diversity index (H') of the Yeosu set nets ranged from 0.93 to 1.85 across the years (Fig. 2C), with the lowest and highest values registered in 2015 and 2016, respectively. From 2008 to 2022, the cumulative catch from the Yeosu coastal set nets reached 3210.8 tonnes. The peak catch was recorded at 470.6 tonnes in 2010, whereas the lowest was 75.5 tonnes in 2016 (Fig. 2D). *Scomberomorus niphonius* and *Engraulis japonicus* constituted a substantial proportion, accounting for 78.9% of the total catch. The fishing season for Yeosu's coastal set nets spans from April to December, peaking during the fall months of October and November. The yearly catch rate analysis showed that the catch rate of *Scomberomorus niphonius* exceeded 60% every year, except in 2013 and 2016, which witnessed rates of 55.3% and 32.4%, respectively (Fig. 2E). Conversely, the *Engraulis japonicus* catch rate fluctuated annually, with the highest rate of 34.2% recorded in 2016. *Pampus argenteus* (Euphrasen, 1788) exhibited a declining trend, after increasing from a catch rate of 5.6% in 2008 to 10.9% in 2011, whereas *Trichiurus japonicus* demonstrated average fluctuations. Five additional species, namely *Pampus argenteus*, *Lophius litulon*, *Sarda orientalis* (Temminck et Schlegel, 1844), *Seriola quinqueradiata*, and *Trachurus japonicus* had catch rates exceeding 3%.

Community structure and occurrence of major fish species. Using the fish catch data, cluster analysis was conducted using the Bray–Curtis similarity [%] and the nMDS array method based on a 70% similarity threshold. This analysis yielded Cluster A, comprising four clusters for the period 2008–2011, Cluster B for 2012–2015, and Cluster C for 2016–2022 (Fig. 3). The ANOSIM test, applied to assess the significance of ecological segregation among fish communities near the Yeosu Coast of Korea, confirmed significant differences in the assemblage structure between the three groups identified via set-net sampling (ANOSIM, $P < 0.05$, global $R = 0.773$). SIMPER analysis further explored these differences in mean species abundance across the groups (Table 1). The values in Table 1 represent the average similarities between the communities, as characterized by SIMPER. A large portion of the similarity within each set-net fish community stemmed from species contributing over 3% of the total abundance and commonly found within the pre-defined year groups. Cluster A was dominated by *Scomberomorus niphonius*, *Engraulis japonicus*, *Pampus argenteus*, *Trichiurus japonicus*, *Lophius litulon*, *Cololabis saira* (Brevoort, 1856), *Trachurus japonicus*, and *Seriola quinqueradiata*. Cluster B shared several dominant species with Cluster A, including *Scomberomorus niphonius*, *Engraulis japonicus*, *Pampus argenteus*, *Trichiurus japonicus*, and *Lophius litulon*, but also featured *Nibea albiflora* (Richardson, 1846) prominently. Cluster C, while still containing *Scomberomorus niphonius*, differed more distinctly from the others, with *Pampus argenteus*, *Trichiurus japonicus*, and *Lophius litulon* emerging as key contributors alongside *Pampus punctatissimus* (Temminck et Schlegel, 1845).

Relations between major fish species and environmental factors. The analysis of annual patterns of catch fluctuations among the dominant species in the Yeosu set nets (Fig. 4) revealed consistent annual patterns of increases and decreases. *Scomberomorus niphonius*, primarily caught during the fall, has declined since 2010 and resurged since 2020. *Engraulis japonicus*, which is mainly caught during the spring, has shown a declining catch trend since 2012. The number of *Pampus argenteus* captured from spring to fall has declined since 2013. *Trichiurus japonicus*, typically caught during the summer and fall, has demonstrated an upward trend since 2014; however, *Trichiurus japonicus* catches have remained minimal, except in 2010. *Lophius litulon*, which is often caught during the winter and spring, exhibited a trend of annual increases and decreases in catch. An analysis of the relation between monthly mean SST and the

Table 1. Similarity percentage analysis (SIMPER) list of fish species captured in daily set nets in the Yeosu Coast, Korea during 2008–2022 contributing mostly to similarities within specified periods.

Cluster	Main species	Contribution [%]
Cluster A (2008–2011)	*Scomberomorus niphonius*	5.91
Average similarity: 82.13	*Engraulis japonicus*	4.57
	Pampus argenteus	4.51
	Trichiurus japonicus	4.25
	Lophius litulon	4.15
	Cololabis saira	3.80
Cluster B (2012–2015)	*Scomberomorus niphonius*	6.21
Average similarity: 83.28	*Engraulis japonicus*	5.42
	Pampus argenteus	4.80
	Trichiurus japonicus	4.59
	Lophius litulon	4.28
	Nibea albiflora	3.89
Cluster C (2016–2022)	*Scomberomorus niphonius*	6.60
Average similarity: 76.65	*Pampus argenteus*	5.42
	Trichiurus japonicus	5.15
	Engraulis japonicus	4.94
	Lophius litulon	4.77
	Pampus punctatissimus	4.57

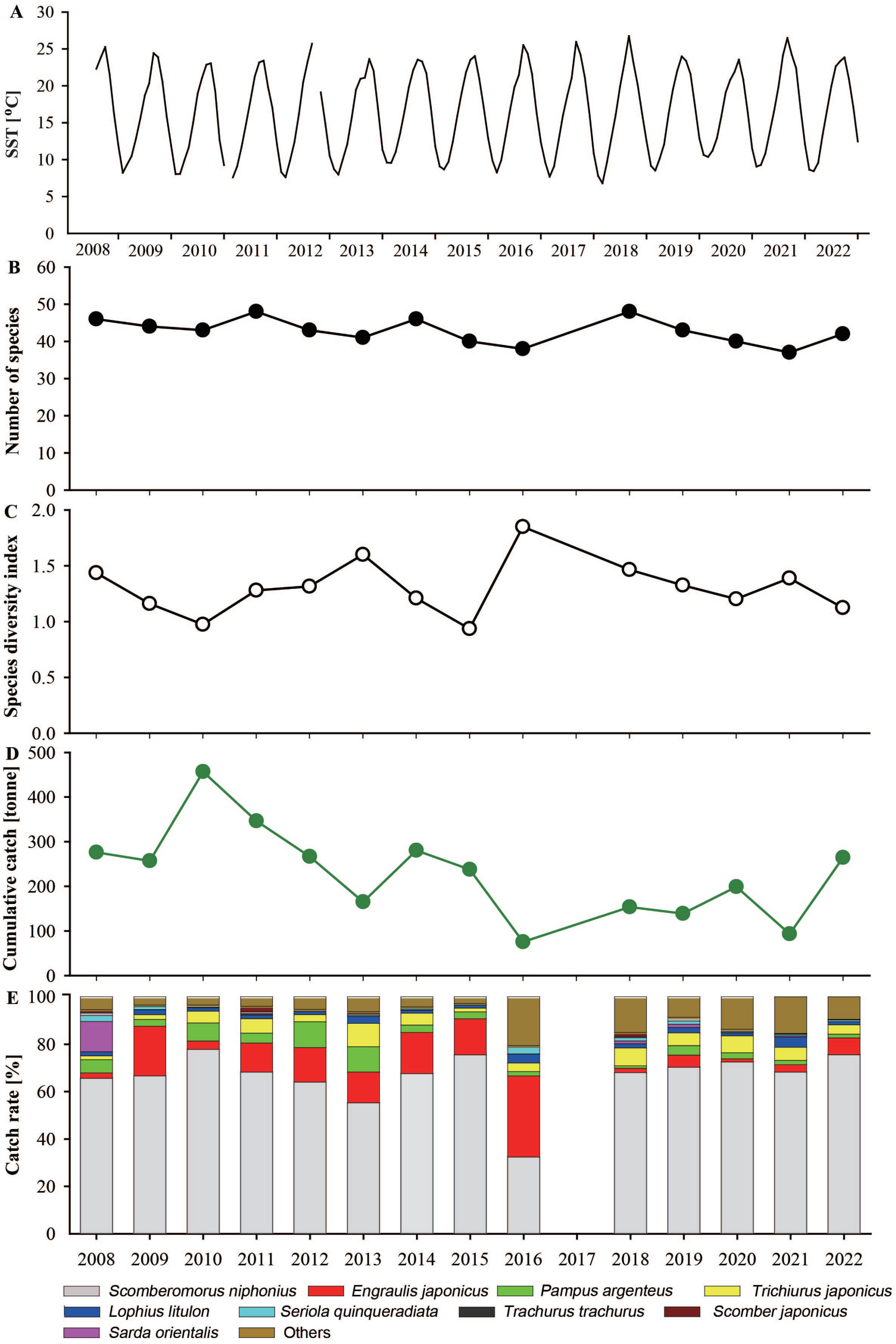

Figure 2. Monthly average variations in sea surface temperature (SST) (**A**), number of fish species (**B**), fish species diversity index (H') (**C**), cumulative catch (**D**), and catch rate (**E**) of daily set-net catch in the Yeosu Coast, Korea during 2008–2022.

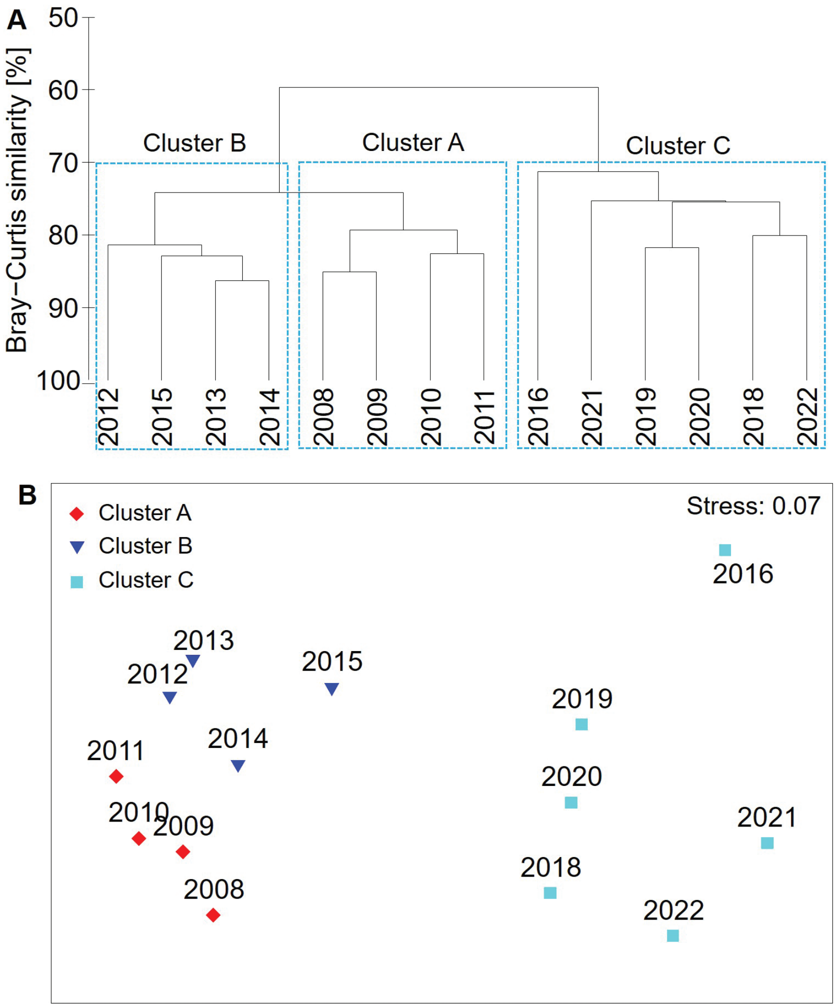

Figure 3. Cluster analysis (**A**) and non-metric multi-dimensional scaling (nMDS) analysis (**B**) of the fish assemblages of daily set-net catch in the Yeosu Coast, Korea during 2008–2022.

log-transformed catches of the top eight species during the survey period revealed that catches of *Scomberomorus niphonius* and *Trichiurus japonicus* significantly increased with increasing SST ($P < 0.05$; Fig. 5). Conversely, catches of *Lophius litulon* declined with increasing SST. However, no significant correlation was found between SST and *Pampus argenteus*, *Seriola quinqueradiata*, *Scomber japonicus*, and *Trachurus japonicus*. Notably, while *Lophius litulon* showed a negative association with warming temperatures *Seriola quinqueradiata*, *Scomber japonicus*, and *Trachurus japonicus* displayed no significant relation with SST. The relation between the monthly catch of set nets in the Yeosu Coast and the frequency of jellyfish outbreaks during the study period was analyzed. The catch of commercial species was affected by the frequency of jellyfish outbreaks. Specifically, *Scomberomorus niphonius* and *Trachurus japonicus* exhibited a pattern where log-transformed catch quantities decreased as the occurrence ratio of jellyfish increased (Fig. 6). SST and the occurrence ratio of jellyfish showed a positive correlation (Fig. 7). The analysis of the annual catch of two subtropical fish species in the set nets in the Yeosu Coast (Fig. 8) revealed an increase in the catch frequency of *Sphyraena pinguis* Günther, 1874 since 2011. Similarly, the catch of *Auxis rochei* (Risso, 1810) was approximately 2.1 tonnes in 2018, but it reached a peak of 6.8 tonnes in 2020.

Discussion

Analysis of species composition and community characteristics. We analyzed fish species composition and community characteristics using daily logbook data collected from March to December, which corresponds to the fishing season of the set nets located off the coast of Yeosu. Data from 2017 were excluded because of unavailability. Over the study period, water temperatures ranged from 6.78 to 26.76°C, with notable peaks in average annual water temperatures observed in 2018 and 2021, particularly during the summer months when they exceeded 25°C. The highest fish species richness was recorded in 2011, totaling 48 taxa, whereas the lowest was recorded in 2021. During this period, changes in the community composition of fish species were observed. Among these changes, the species that contributed to fish communities shifted. For example, *Seriola* spp. was the second most dominant fish taxon two decades ago; however, this position shifted

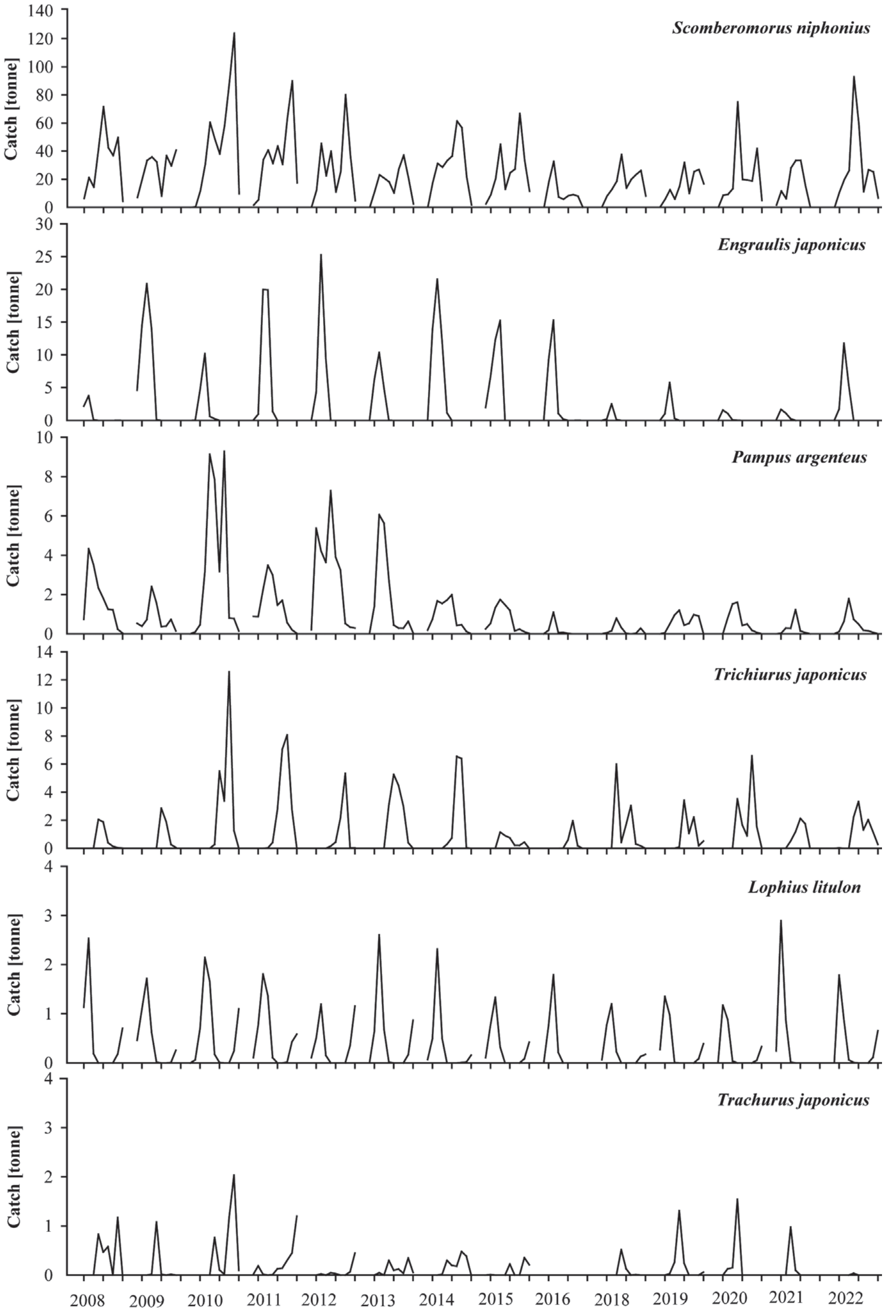

Figure 4. Annual patterns of catch fluctuations among the dominant fish species in daily set-net catch in the Yeosu Coast, Korea during 2008–2022.

to *Engraulis japonicus* after 2013. Based on daily catch data and considering the comparison of the sampling area, period, gear, and dominant species (Table 2), Hwang et al. (2006) stated that *Scomberomorus niphonius*, *Engraulis japonicus*, *Lophius litulon*, and *Trichiurus japonicus* accounted for 51.9% of the total catch two decades ago. In contrast, the presently reported study highlights the most abundant species, in descending order as follows: *Scomberomorus niphonius*, *Engraulis japonicus*, *Pampus argenteus*, *Trichiurus japonicus*, *Pampus punctatissimus*, and *Lophius litulon*. While the sequence of abundance is similar to the findings reported by Kim et al. (2013), notable distinctions include *Pampus argenteus* being the dominant species over *Sarda orientalis*. Notably, the prevalence of *Scomberomorus niphonius* surged to 68.8% while that of *Trichiurus japonicus* decreased to 4.6%. These shifts were particularly pronounced on the southern coast of Korea (KOSIS 2023). This suggests the influence of factors impacting the catch of *Engraulis japonicus*, such as habitat alterations due to long-term climate change (Bang et al. 2022) and closed fisheries seasons.

Community structure and subtropical fish species. Our study confirmed the statistical significance of the annual community structure of the Yeosu coastal set-net catch through cluster analysis. Among the fish species, fluctuations in the catch of *Scomberomorus niphonius*, *Engraulis japonicus*, *Pampus argenteus*, *Trichiurus japonicus*, and *Lophius litulon*, notably contributed to each cluster. Additionally, 11 subtropical fish species were identified.

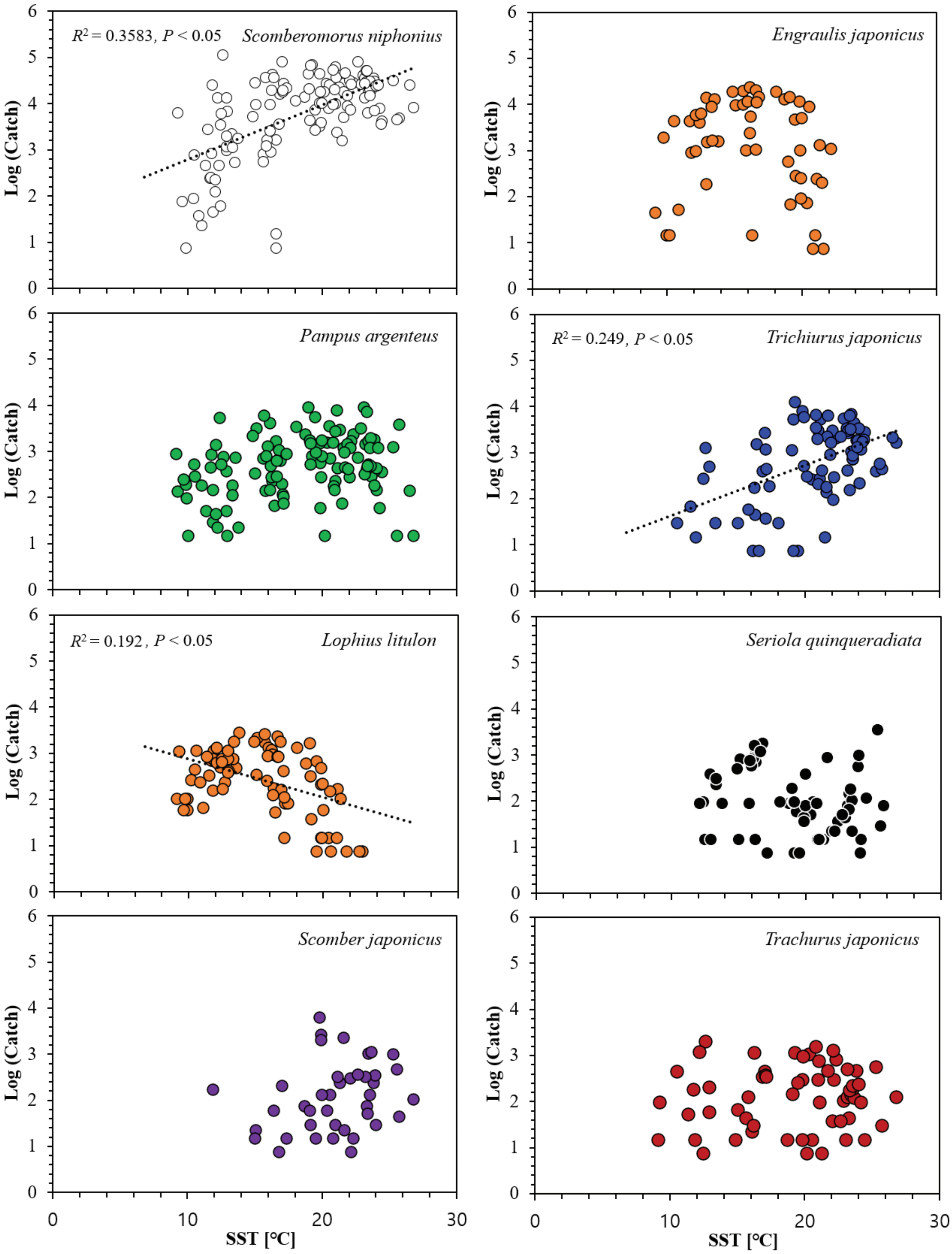

Figure 5. Correlations between monthly mean sea surface temperature (SST) and log-transformed catches of the top eight fish species from daily set nets in the Yeosu Coast, Korea during 2008–2022.

The catch frequencies of temperate and subtropical fish species showed an upward trend, with *Sphyraena pinguis* increasing since 2010, followed by *Auxis rochei* since 2018. Previous studies on the composition and occurrence of subtropical fish species in Korea were primarily conducted in Jeju Island, a region sensitive to subtropical climates. The increasing numbers of subtropical fish species observed over the years (Ko et al. 2015, 2021) are attributed to a surge in surface water temperature of 1.03°C in southern waters over 51 years (Han and Lee 2020). Moreover, daily water temperature observations along the Yeosu Coast, strongly influenced by the TWC during

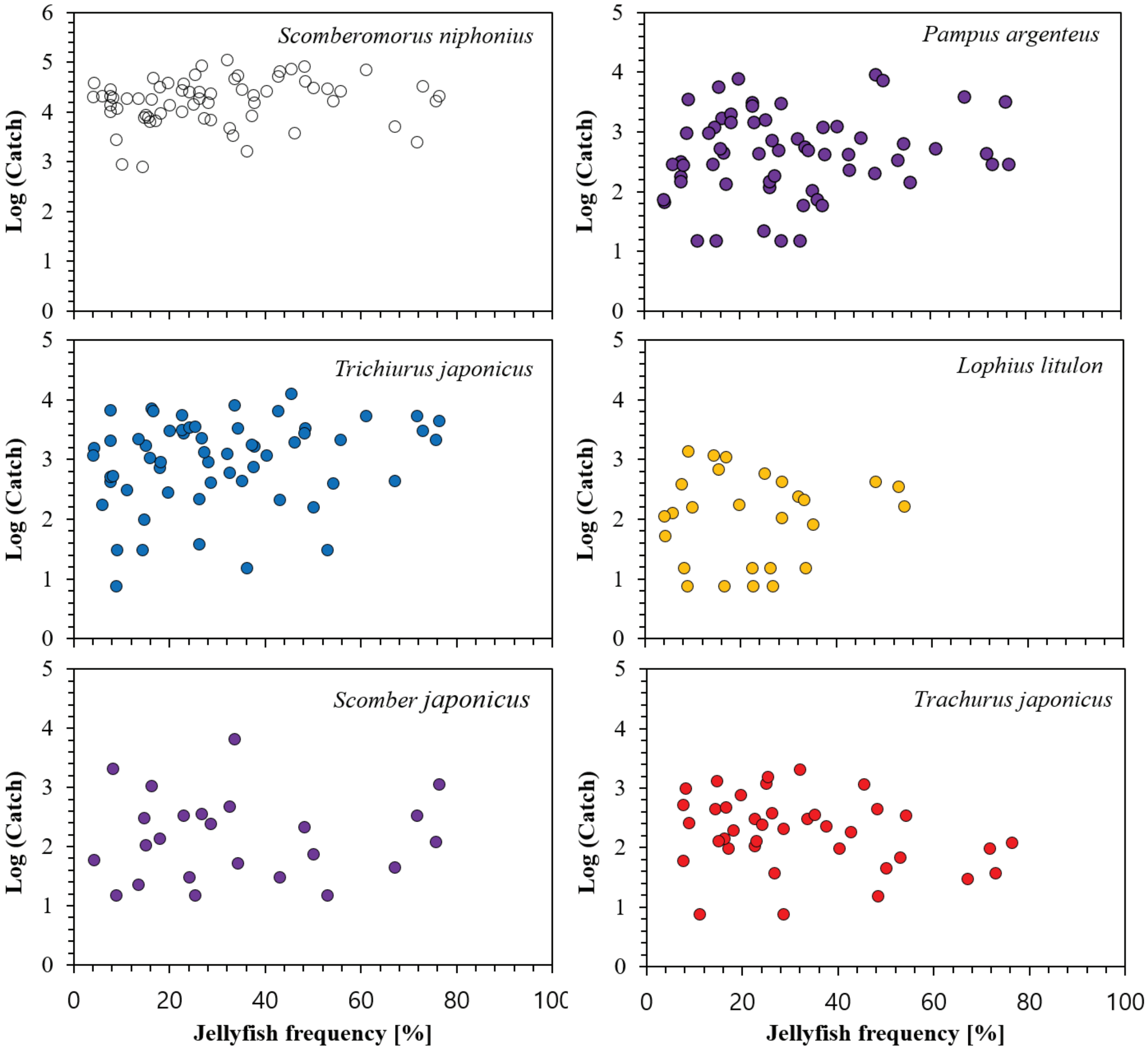

Figure 6. Correlations between monthly occurrence ratios of jellyfish and log-transformed catches of major fish species captured in daily set nets in the Yeosu Coast, Korea during 2008–2022.

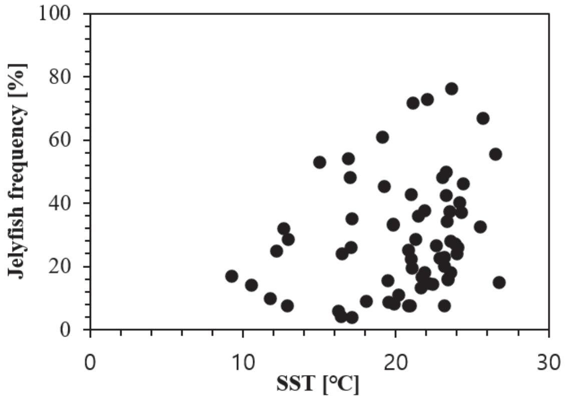

Figure 7. Correlations between monthly mean sea surface temperature (SST) and occurrence ratio of jellyfish from daily set-net catch in the Yeosu Coast, Korea during 2008–2022.

summer, have resulted in water temperatures higher than those previously recorded. This conducive environment facilitated the emergence of subtropical fish species.

Fishing season and impacts of climate change. The fishing season of the Yeosu coastal set nets spans from spring (March and April) to early winter (December), with the peak catch concentrated in the fall months of October and November. Notably, *Engraulis japonicus* emerged as the primary target species at the beginning of the fishing season, extending from April to June. Subsequently, *Scomberomorus niphonius* became the main target species, mirroring the transition observed in the dominant species highlighted by Kim et al. (2013) in their study of the same waterbodies between 2004 and 2011. This shift can be attributed to the increased water temperatures along the southern coast over the last two decades. These elevated temperatures have facilitated the optimum water temperature conducive to supporting warm-water species such as *Scomberomorus niphonius* and *Engraulis japonicus*. Their integration into the coastal set-net fishery may be a response to the TWC inflows from the outer sea (Kim et al. 2013). The relation between fish species composition, catch, and environmental factors was explored in a study

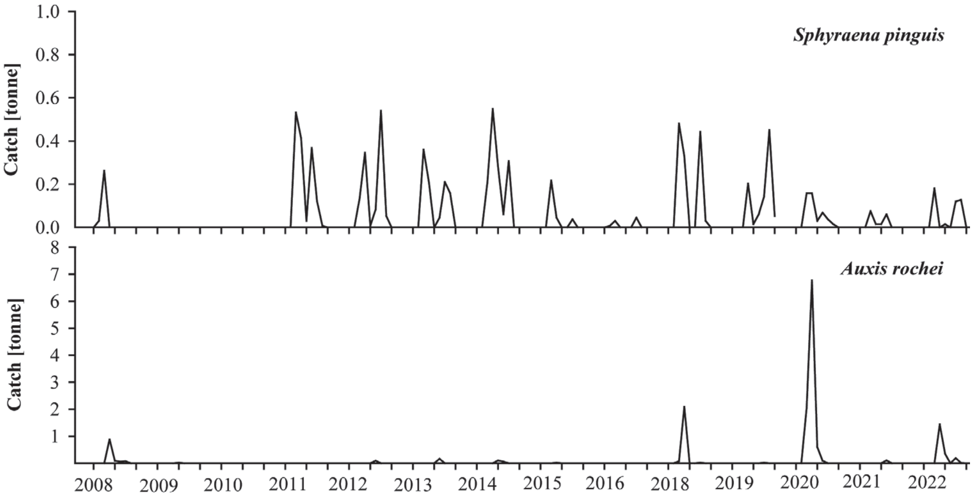

Figure 8. Annual catches of subtropical fishes from daily set-net catch in the Yeosu Coast, Korea during 2008–2022.

Table 2. Comparison of the sampling area, period, gear, and dominant species of fish collected using set nets in the coastal waters of Yeosu, Korea during 2008–2022.

Parameter	Reference		
	This study	**Hwang et al. 2006**	**Kim et al. 2013**
Sampling area	Yeosu coast	Yeosu coast	Yeosu coast
Sampling period	2008–2022	2002–2003	2004–2011
Sampling gear	Large set net	Large set net	Large set net
Dominant species	*Scomberomorus niphonius*	*Scomberomorus niphonius*	*Scomberomorus niphonius*
	Engraulis japonicus	*Seriola* spp.	*Engraulis japonicus*
	Pampus argenteus	*Sarda orientalis*	*Pampus argenteus*
	Trichiurus japonicus	*Engraulis japonicus*	*Trichiurus japonicus*
	Pampus punctatissimus	*Lophius litulon*	*Lophius litulon*
	Lophius litulon	*Trichiurus japonicus*	*Sarda orientalis*

by Kim et al. (2013), who found strong correlations among water temperature, frequency of jellyfish appearance, and species composition of fish joining the Yeosu coastal set-net fishery. Although water temperature and jellyfish frequency showed high correlations, no clear relation was established with the number of fishing days affected by typhoons. Consequently, water temperature evidently exerts the most significant influence on the Yeosu coastal set-net fishery, although the rate of jellyfish emergence may also play a role. Over the past decade, substantial jellyfish outbreaks have negatively affected fishery production in Korea, China, and Japan, which has damaged fishing gear, spoiled fish with jellyfish contamination, and caused predation of fish eggs and larvae. These events contributed to a potential reduction in the abundance of commercial fish species. Rising water temperatures are closely associated with jellyfish outbreaks (Kang et al. 2000; Uye 2008; Kim et al. 2013; Yoon et al. 2014), and large-scale outbreaks have been reported in Korean coastal waters since 2003 (Lee et al. 2008; Oh et al. 2021). Moreover, the increasing frequency and number of jellyfish, along with their earlier emergence and delayed disappearance, can potentially affect fishing operations and commercial fish species abundance by interfering with fixed gear such as set nets. This underscores the importance of developing strategies to mitigate jellyfish damage in set-net fishing areas in the future (Kim et al. 2013; Yoon et al. 2014; Song et al. 2015). *Scomberomorus niphonius*, a prominent catch in the Yeosu coastal set nets, is a migratory fish captured off the South Sea coast. It occupies a significant position in the food chain of this ecosystem as a representative piscivorous fish. Its diet primarily comprises anchovies, hairtails, and mackerel (Huh et al. 2006; Lee et al. 2011). As a pelagic species, the coastal recruitment of *Scomberomorus niphonius* is closely associated with the distribution of its prey species. *Engraulis japonicus* that enter the *Scomberomorus niphonius* spawning grounds on the southern and western coasts in May are crucial prey (Shoji and Tanaka 2005; Kim et al. 2013; Zhang et al. 2022). Additionally, *Trichiurus japonicus*, which prefers anchovies as prey, contributes to the dynamics of the *Scomberomorus niphonius* diet (Huh et al. 2006; Lee et al. 2021a). *Scomberomorus niphonius* catch has two peaks, one in spring and the other in fall, aligning with the timing of *Engraulis japonicus* and *Trichiurus japonicus* recruitment into the set-net fishery. The migration pattern of *Scomberomorus niphonius* from warm outer seawater to the South Sea coast for spring spawning coincides with the inward migration of *Engraulis japonicus*, their primary prey, to the same area. This synchronization highlights the potential importance of *Engraulis japonicus* availability in the recruitment of *Scomberomorus niphonius* to the coast (Kim et al. 2013). Climate change is expected to shift marine biota and fishery ecosystems in South Korea, directly affecting fisheries. Consequently, the importance of assessing the vulnerability to climate change in policy formulation is increasing (Kim et al. 2023). Additionally, fishery production in South Korea has been steadily declining since 1986 and climate change has caused changes in the species composition and communities of fishery resources (Lee et al. 2021b; Song et al. 2022). Therefore, long-term fish catch records from specific waters are essential to develop effective policies that address the impacts of climate changes on marine ecosystems. The changes in catch observed in the set nets off the Yeosu Coast were similar to those reported by Kim et al. (2013), but the species composition differed. They noted that the catch of *Scomberomorus niphonius* varied according to the catch rate, except in 2016. Importantly, the catch rate has been increasing over time, and the species composition has also changed. Set nets offer advantages for quantifying the recruitment and catch of settled pelagic and coastal fish species. The location where the gear is deployed and variations in sea conditions, including water temperature, influence the catch (Kim et al. 2003; Hwang et al. 2006; Kim et al. 2013). Notably, these nets allow effective analysis of the seasonal and annual catch characteristics of commercial fish species. However, in the future, continuous collection of data, such as the occurrence of subtropical fish species, bycatch during fishing, and body composition of commercial fish species through direct engagement with fishing vessels, will provide ecological evidence to conserve and sustain coastal fishery resources of Yeosu under the influence of climate change.

Acknowledgments

This study was supported by a grant from the National Institute of Fisheries Science (NIFS) of Korea (grant number R2024010). This research was supported by the Korea Institute of Marine Science and Technology Promotion (KIMST) and funded by the Ministry of Oceans and Fisheries (20210044).

References

Bang M, Sohn D, Kim JJ, Choi W, Jang CJ, Kim C (2022) Future changes in the seasonal habit suitability for anchovy (Engraulis japonicus) in Korean waters projected by a maximum entropy model. Frontiers in Marine Science 9: e922020. https://doi.org/10.3389/fmars.2022.922020

Chang KI, Teague W, Lyu S, Perkins H, Lee DK, Watts DR, Kim Y-B, Mitchell DA, Lee CM, Kim K (2004) Circulation and currents in the southwestern East/Japan Sea: Overview and review. Progress in Oceanography 61(2–4): 105–156. https://doi.org/10.1016/j.pocean.2004.06.005

Choo HS (2002) [The variations of oceanic conditions and the distributions of eggs and larvae of anchovy in the southern sea of Korea in summer.] Korean Journal of Fisheries and Aquatic Sciences 35(1): 77–85. [In Korean with English abstract] https://doi.org/10.5657/kfas.2002.35.1.077

Clarke KR, Gorley RN (2014) Change in marine communities: An approach to statistical analysis and interpretation. 3rd edn. Primer, Plymouth, UK.

Doney SC, Ruckelshaus M, Duffy JE, Barry JP, Chan F, English CA, Galindo HM, Grebmeier JM, Hollowed AB, Knowlton N, Polovina J, Rabalais NN, Sydeman WJ, Talley LD (2012) Climate change impacts on marine ecosystems. Annual Review of Marine Science 4(1): 11–37. https://doi.org/10.1146/annurev-marine-041911-111611

Han IS, Lee JS (2020) Change the annual amplitude of sea surface temperature due to climate change in a recent decade around the Korean peninsula. Journal of the Korean Society of Marine Environment and Safety 26(3): 233–241. https://doi.org/10.7837/kosomes.2020.26.3.233

Han KH, Oh YS (2007) [Species composition and quantitative fluctuation of fishes collected by gape net in coastal waters of Yeosu, Korea.] Journal of the Korean Society of Fisheries and Ocean Technology 43(4): 261–273. [In Korean with English abstract] https://doi.org/10.3796/KSFT.2007.43.4.261

Hoegh-Guldberg O, Bruno JF (2010) The impact of climate change on the world's marine ecosystems. Science 328(5985): 1523–1528. https://doi.org/10.1126/science.1189930

Huh SH, Park JM, Baeck GW (2006) [Feeding habits of Spanish mackerel (*Scomberomorus niphonius*) in the Southern Sea of Korea.] Korean Journal of Fisheries and Aquatic Sciences 39(1): 35–41. [In Korean with English abstract] https://doi.org/10.5657/kfas.2006.39.1.035

Hwang SD, Kim JY, Kim JI, Kim ST, Seo YI, Kim JB, Kim YH, Hea SJ (2006) [Species composition using the daily catch data of a set-net in the coastal waters off Yeosu, Korea.] Korean Journal of Ichthyology 18(3): 223–233. [In Korean with English abstract]

Hwang JH, Yoo KH, Lee SH, Han KH (2008) [Fluctuation in the abundance and species composition of fishes collected by a fyke net in the coastal waters of Geumo-do, Yeosu.] Korean Journal of Fisheries and Aquatic Sciences 41(1): 39–47. [In Korean with English abstract] https://doi.org/10.5657/kfas.2008.41.1.039

Jeong HH, Han KH, Kim CC, Yoon SM, Seo WI, Hwang SY, Lee SH (2005) [Fluctuations in abundance and species composition of fishes collected by both sides fyke net in Dol-san, Yeosu.] Korean Journal of Ichthyology 17(1): 64–72. [In Korean with English abstract]

Jeong JM, Yoo JT, Kim HY, Lee SK, Go WJ, Kim YH (2015) [Species composition of bycatch fishes collected by a gape net with wings in the coastal waters of Dolsan-do, Yeosu, Korea.] Hangug Susan Haghoi Ji 48(5): 805–809. [In Korean with English abstract] https://doi.org/10.5657/KFAS.2015.0805

Kang YS, Jeon KA (1999) [Biological and chemical characteristics and trophodynamics in the frontal zone in the southern waters of Korea.] Korean Journal of Fisheries Aquatic Sciences 32(1): 22–29. [In Korean with English abstract]

Kang YS, Jo YJ, Go WJ, Kim SS, Jeon KA, Oh HJ (2000) [Swarm of salps (Tunicata: Thaliacea) and its impact on marine ecosystem in the South Sea of Korea.] Journal of the Korean Society of Oceanography 5(1): 47–58. [In Korean with English abstract]

Kim YH, Kim JB, Chang DS (2003) [Seasonal variation of abundance and species composition of fishes caught by a set-net in the coastal waters off Yeosu, Korea.] Hangug Susan Haghoi Ji 36(2): 120–128. [In Korean with English abstract] https://doi.org/10.5657/kfas.2003.36.2.120

Kim HY, Song SH, Lee SK, Kim JB, Yoo JT, Jang DS (2013) [Dominant causes on the catch fluctuation of a set-net fishery in the mid-south sea of Korea.] Journal of the Korean Society of Fisheries and Ocean Technology 49(3): 250–260. [In Korean with English abstract] https://doi.org/10.3796/KSFT.2012.49.3.250

Kim KT, Han KH, Lee SH, Youn BI (2017) [Fluctuations in abundance and species composition of fishes collected by gape net in Dolsan District of Yeosu.] Journal of the Korean Society of Fisheries and Ocean Technology 53(2): 142–151. [In Korean with English abstract] https://doi.org/10.3796/KSFT.2017.53.2.142

Kim MJ, Hong JB, Han IS, Lee JS, Kim DH (2023) Vulnerability assessment of Korean fisheries to climate change. Marine Policy 155: 105735. https://doi.org/10.1016/j.marpol.2023.105735

Ko JC, Kim BY, Kim MJ, Park SE, Kim JB, Cho HK (2015) [A seasonal characteristic of marine environment and fish assemblage in the coastal waters Jeju Island, Korea from 2012 to 2013.] Susan Haeyang Gyoyuk Yeon-Gu 27(2): 319–344. [In Korean with English abstract] https://doi.org/10.13000/JFMSE.2015.27.2.319

Ko JC, Han SH, Kim BY, Choi JH, Hwang GS (2021) [A seasonal characteristic of fish assemblage in the coastal waters Gapa-do, southern part of Jeju Island.] Journal of the Korean Society of Fisheries and Ocean Technology 57(1): 10–24. [In Korean with English abstract] https://doi.org/10.3796/KSFOT.2021.57.1.010

KODC (2023) Korea Oceanographic Data Center [English version] [Accessed 28 August 2023] https://www.nifs.go.kr/kodc/eng/index.kodc

KOSIS (2023) Korean Statistical Information Service. [English version] [Accessed 28 February 2023] https://kosis.kr/eng/

Lee HE, Yoon WD, Lim DH (2008) Description of feeding apparatus and mechanism in Nemopilema nomurai Kishinouye (Scyphozoa: Rhizostomeae). Ocean Science Journal 43(1): 61–65. https://doi.org/10.1007/BF03022432

Lee SJ, Kim BY, Chang DS (2011) [Long-term variation in catch of Spanish mackerel (Scomberomorus niphonius) related to environmental change in Korean waters.] Journal of the Korean Society of Fisheries and Ocean Technology 47(2): 99–107. [In Korean with English abstract] https://doi.org/10.3796/KSFT.2011.47.2.099

Lee JE, Seong GC, Kim HY, Moon SY (2021a) [Diet composition of Spanish mackerel *Scomberomorus niphonius*, in the south sea of Korea.] Korean Journal of Fisheries and Aquatic Sciences 54(5): 808–813. [In Korean with English abstract] https://doi.org/10.5657/KFAS.2021.0808

Lee K, Go S, Jung S (2021b) Long-term changes in fish assemblage structure in the Korea strait from 1986 to 2010 in relation with climate change. Ocean Science Journal 56(1–2): 182–197. https://doi.org/10.1007/s12601-021-00016-0

Lie HJ, Cho CH (1997) Surface current fields in the eastern East China Sea. Journal of the Korean Society of Oceanography 32(1): 1–7.

Moon SY, Oh HJ, Soh HY (2010) [Seasonal variation of zooplankton communities in the southern coastal waters of Korea.] Ocean Polar Research 32(4): 411–426. [In Korean with English abstract] https://doi.org/10.4217/OPR.2010.32.4.411

Moon SY, Baeck GW, Lee MH, Kim H, Jung KM (2022a) [Spatial and temporal distribution and characteristics of zooplankton communities in the southern coast of Korea from sprint to summer period.] Korean Journal of Fisheries and Aquatic Sciences 55(2): 154–170. [In Korean with English abstract] https://doi.org/10.5657/KFAS.2022.0154

Moon SY, Lee MH, Jung KM, Kim H, Jung JH (2022b) [Spatial and temporal distribution of fish larvae in the southern coast of Korea from spring to summer.] Korean Journal of Fisheries and Aquatic Sciences 55(4): 461–477. [In Korean with English abstract] https://doi.org/10.5657/KFAS.2022.0461

NIFS (2023) [Korean Jellyfish Information System] [Accessed 28 March 2023] [In Korean] https://www.nifs.go.kr/jelly/main.jely

Oh S, Kim KY, Lim WA, Park G, Oh H, Oh W, Lee K (2021) [Vertical distribution of giant jellyfish (Nemolilema nomurai) in the coastal waters of Korea and its correlation analysis by survey method.] Journal of the Korean Society of Fisheries and Ocean Technology 57(4): 351–364. [In Korean with English abstract] https://doi.org/10.3796/KSFOT.2021.57.4.351

Schlitzer R (2021) Ocean Data View. https://odv.awi.de

Shannon CE, Weaver W (1963) The mathematical theory of communication. University of Illinois Press, Urbana, IL, USA, 360 pp.

Shoji J, Tanaka M (2005) Distribution, feeding condition, and growth of Japanese Spanish mackerel (Scomberomorus niphonius) larvae in the Seto Inland Sea. Fish Bulletin 103(2): 371–379.

Song SH, Lee SG, Kim HY (2015) [A study on the management performance of a set-net fishery according to the blooming frequency of jelly fish Nemopliema nomurai in Yeosu.] Journal of the Korean Society of Fisheries and Ocean Technology 51(1): 42–49. [In Korean with English abstract] https://doi.org/10.3796/KSFT.2015.51.1.042

Song H, Song YS, Hwang K, Sohn D (2022) [Characteristics of changes in species composition with water temperature in set-net fishing on the southern coast of the East Sea. Korean Journal of Fisheries and Aquatic Science 55(5): 625–637. [In Korean with English abstract] https://doi.org/10.5657/KFAS.2022.0625

Uye S (2008) Blooms of the giant jellyfish Nemopilema nomurai: A threat to the fisheries sustainability of the East Asian Marginal Seas. Plankton and Benthos Research 3(Suppl.): 125–131. https://doi.org/10.3800/pbr.3.125

Yoo JT, Kim YH, Song SH, Park SW (2016) [Monthly changes in the rate of bycatch fishes and their immature ratio caught by gape net with wings in the coast of Yeosu and Jindo Island, Korea.] Journal of the Korean Society of Fisheries and Ocean Technology 52(1): 72–77. [In Korean with English abstract] https://doi.org/10.3796/KSFT.2016.52.1.072

Yoo JT, Kim YH, Lee SH, Kim JK (2017) Community structure of larval fish assemblage in the coastal waters of southcentral Korea during spring and summer. Korean Journal of Ichthyology 29(1): 80–86.

Yoon WD, Lee HE, Han CH, Chang SJ, Lee KH (2014) Abundance and distribution of Nemopilema nomurai (Scyphozoa, Rhizostomeae) in Korean waters in 2005–2013. Ocean Science Journal 49(3): 183–192. https://doi.org/10.1007/s12601-014-0018-5

Zhang K, Guo J, Xu Y, Jiang Y, Fan J, Xu S, Chen Z (2020) Long-term variations fish community structure under multiple stressors in a semi-closed marine ecosystem in the South China Sea. Science of the Total Environment 745: 140892. https://doi.org/10.1016/j.scitotenv.2020.140892

Zhang W, Ye Z, Tian Y, Yu H, Ma S, Ju P, Watanabe Y (2022) Spawning overlap of Japanese anchovy Engraulis japonicus and Japanese Spanish mackerel Scomberomorus niphonius in the coastal Yellow Sea: A prey–predator interaction. Fisheries Oceanography 31(4): 456–469. https://doi.org/10.1111/fog.12595

Acta Ichthyologica et Piscatoria 54, 2024, 87–94 | DOI 10.3897/aiep.54.108526

PENSOFT.

ACTA ICHTHYOLOGICA ET PISCATORIA

A new species of *Sarcotaces* (Copepoda: Cyclopoida: Philichthyidae) from *Antimora rostrata* (Actinopterygii: Gadiformes: Moridae)

Wojciech PIASECKI[1], Geoffrey A. BOXSHALL[2]

1 *Institute of Marine and Environmental Sciences, University of Szczecin, Szczecin, Poland*
2 *Department of Life Sciences, Natural History Museum, Cromwell Road, London, UK*

https://zoobank.org/3C00B024-0DA1-4226-B07F-E04D0E97652B

Corresponding author: Wojciech Piasecki (wojciech.piasecki@usz.edu.pl)

Academic editor: Jan Kotusz ♦ **Received** 29 February 2024 ♦ **Accepted** 22 March 2024 ♦ **Published** 29 March 2024

Citation: Piasecki W, Boxshall GA (2024) A new species of *Sarcotaces* (Copepoda: Cyclopoida: Philichthyidae) from *Antimora rostrata* (Actinopterygii: Gadiformes: Moridae). Acta Ichthyologica et Piscatoria 54: 87–94. https://doi.org/10.3897/aiep.54.108526

Abstract

Parasitic copepods of the genus *Sarcotaces* occur in galls inside the skeletal musculature of fishes. The gall, hosting a highly metamorphosed drop-shaped female contains also a black fluid capable of staining the fish tissues during filleting. Their marine fish hosts are globally distributed and until recently, eight nominal species have been described from fish hosts representing eight fish families. Females are quite similar in their morphology, therefore the males are used for the species determination. The aim of this study was to provide a detailed morphological characterization of the *Sarcotaces* specimens found in muscles of the blue antimora, *Antimora rostrata* (Günther, 1878) originating from deep open waters of the Atlantic. The present paper describes and illustrates *Sarcotaces antimori* **sp. nov.** The new species differs from its congeners in the shape of the cephalothorax, relative proportions and structure of the caudal rami, and in the setal formula of the antennulae of the male.

Keywords

Antimora rostrata, copepod taxonomy, endoparasite, host–parasite relation, mesoparasite

Introduction

Parasitic copepods (Copepoda: Philichthyidae) of the genus *Sarcotaces* Olsson, 1872 are highly metamorphosed and sexually dimorphic organisms infecting marine fishes. They can be found in galls inside the skeletal muscles of fishes. The gall, hosting a highly metamorphosed drop-shaped female is also filled with a black fluid known to stain the fish tissues during filleting. Despite their spectacular appearance they are rather rarely found (Piasecki et al. 2020, 2022).

There are eight nominal species representing the genus *Sarcotaces* namely, *Sarcotaces arcticus* Collett, 1874; *Sarcotaces verrucosus* Olsson, 1872; *Sarcotaces pacificus* Komai, 1924; *Sarcotaces komaii* Shiino, 1953; *Sarcotaces japonicus* Izawa, 1974; *Sarcotaces shiinoi* Izawa, 1974; *Sarcotaces namibiensis* Reimer, 1991; and *Sarcotaces izawai* Piasecki, Barcikowska, Panicz, Eljasik et Kochmański, 2022. There has been no comprehensive revision of this genus and only one species (*S. izawai*) has also been defined genetically (Piasecki et al. 2022).

Materials and methods

The gall hosting both specimens (male and female) was embedded in the flank of a blue antimora, *Antimora rostrata* (Günther, 1878), caught on the RRS *DISCOVERY* cruise D252 (13–30 April 2001), Stn No. 13951#40 (49°49.9′N, 012°10.8′W), at a depth of 1631–1653 m in the Goban Spur, northwest Atlantic. The parasite gall was collected by R.A. Bray.

The male specimen was examined under a compound light microscope Olympus BX50 using a modified "wooden slide" method of Humes and Gooding (1964) and lactic acid as a clearing medium. The male was stained with lignin pink. The drawings were made using a drawing tube (Olympus). The female was observed under a dissecting microscope and photographed.

Morphological terminology follows, Kabata (1979), and Huys and Boxshall (1991). Thoracic and abdominal somites are numbered using Roman numerals and abbreviated th and abd, respectively.

Two separate attempts were made to extract genetic material from the female. Both attempts were unsuccessful. The types were deposited at the Natural History Museum, London, UK.

Results

The gall dissected from the host fish contained a single female and a single male of a sexually dimorphic copepod parasite. No eggs or nauplius stages were found. It was explicitly identified as representing the genus *Sarcotaces* but it did not resemble any of the hitherto known species. We therefore concluded that these specimens represent a species unknown to science. In the present paper, we provide principal data on all nominal species and illustrated descriptions (Table 1). We also compare principal morphological data of all *Sarcotaces* species (Table 2).

Taxonomy

Phylum Arthropoda
Subphylum Crustacea
Subclass Copepoda
Order Cyclopoida Burmeister, 1835
Family Philichthyidae Vogt, 1877
Genus *Sarcotaces* Olsson, 1872

Sarcotaces antimori sp. nov.

https://zoobank.org/1ACD2032-14ED-42C8-AC32-1E111FD318D8

Figs. 1–3

Locality. Goban Spur, northwestern Atlantic (49°49.9′N, 012°10.8′W)

Host fish. blue antimora, *Antimora rostrata* (Günther, 1878)

Infection site. lateral musculature (flank)

Type material. NHMUK 2022.198 holotype (male) and NHMUK 2022.199 allotype (female)

Description of female. Body highly metamorphosed, semi-pyriform/semi-quadrangular with deep transverse furrows marking apparent segmentation, and without visible appendages. Surface of cephalosome and thoracic somites covered by papilliform protrusions. Deep transverse furrows without papilliform protrusions

Table 1. Available (illustrated) descriptions of nominal species of the genus *Sarcotaces*. [Modified from Piasecki et al 2022].

Species	Sex or stage	Locality	Valid name of host fish	Fish family	Order	Reference
S. verrucosus	**F**	**St. Barthelemy, Caribbean**	***Acanthurus* sp.**	**Acanthuridae**	**Perciformes**	**Olsson 1872**
S. verrucosus	F	Martinique, Caribbean	*Halichoeres radiatus* (Linnaeus, 1758)	Labridae	Perciformes	Dollfus 1928
S. verrucosus	F + M + N	San Matías Gulf, Argentina	*Pseudopercis semifasciata* (Cuvier, 1829)	Pinguipedidae	Perciformes	González and Tanzola 2000
S. arcticus	**F** (no fig.)	**Øksfjord, Finmark, Norway**	***Molva dypterygia* (Pennant, 1784)**	**Lotidae**	**Gadiformes**	**Collett 1874**
S. arcticus	F + N	Collett's material	***Molva dypterygia* (Pennant, 1784)**	Lotidae	Gadiformes	Hjort 1895
S. arcticus	M	Aberdeen, Scotland	***Molva dypterygia* (Pennant, 1784)**	Lotidae	Gadiformes	Aitken 1942
S. arcticus	F + M	Norway	***Molva dypterygia* (Pennant, 1784)**	Lotidae	Gadiformes	Moser et al. 1985
S. arcticus	F + M + N	British Columbia	*Sebastes ruberrimus* (Cramer, 1895)	Sebastidae	Scorpaeniformes	Kuitunen-Ekbaum 1949
S. arcticus	F + M + N	Alaska? California?	*Sebastes* spp.	Sebastidae	Scorpaeniformes	Moser et al. 1985
S. arcticus	F + M	British Columbia	*Sebastes* sp.	Sebastidae	Scorpaeniformes	Kabata 1988
S. pacificus	**F + M + N**	**Tanabe Bay, Japan**	***Antennarius striatus* (Shaw, 1794)**	**Antennariidae**	**Lophiiformes**	**Komai 1924**
S. pacificus	F + M	Sagami, Musaki, Saogiro, Japan	***Antennarius* sp.**	Antennariidae	Lophiiformes	Heegaard 1947
S. pacificus	F + M	Shirama, (near type locality)	***Antennarius striatus* (Shaw, 1794)**	Antennariidae	Lophiiformes	Shiino 1953
S. pacificus	N + C	Tanabe Bay, Japan	***Antennarius striatus* (Shaw, 1794)**	Antennariidae	Lophiiformes	Izawa 1973
S. pacificus	F + M	Tanabe Bay, Japan	***Antennarius striatus* (Shaw, 1794)**	Antennariidae	Lophiiformes	Izawa 1974
S. komaii	**F + M**	**Tosa Bay, Japan**	***Scalicus hians* (Gilbert et Cramer, 1897)**	**Peristediidae**	**Perciformes**	**Shiino 1953**
S. komaii	F + M	Shiino's type material	***Scalicus hians* (Gilbert et Cramer, 1897)**	**Peristediidae**	**Perciformes**	Izawa 1974
S. komaii	F	Cuba	*Sparisoma rubripinne* (Valenciennes, 1840)	Scaridae	Perciformes	Ezpeleta Herce 1974
S. komaii	F + M	Pacific coasts of Japan	*Antimora rostrata* (Günther, 1878)	Moridae	Gadiformes	Avdeev and Avdeev 1975
S. japonicus	**F + M + N**	**Tanabe Bay, Japan**	***Gymnothorax kidako* (Temminck et Schlegel, 1846)**	**Muraenidae**	**Anguilliformes**	**Izawa 1974**
S. shiinoi	**F + M**	**Kumano Sea**	***Acromycter nezumi* (Asano, 1958)**	**Congridae**	**Anguilliformes**	**Izawa 1974**
S. namibiensis	**F + M**	**Namibian coast**	***Selachophidium guentheri* Gilchrist, 1903**	**Ophidiidae**	**Ophidiiformes**	**Reimer 1991**
S. izawai	**F + M + N**	**"Falklands"? Australia?**	***Mora moro* (Risso, 1810)**	**Moridae**	**Gadiformes**	**Piasecki et al. 2022**
***S. antimori* sp. nov.**	**F + M**	**Northwestern Atlantic**	***Antimora rostrata* (Günther, 1878)**	**Moridae**	**Gadiformes**	**This study**

Sarcotaces species in bold represent original descriptions. Fish names in bold are records from the type-host species. Fish names in regular font show records form a fish other than their type-host; F = female, M = male, N = nauplius, C = copepodid. Originally Komai (1924) described only a female and a nauplius. However, Shiino (1953) reported that Komai after reexamination of his material also found a male.

Table 2. Principal morphological data of nominal species of the genus *Sarcotaces*.

Species	FEMALE	MALE							Reference
	Length [mm]	Comments	Body length [mm] (mean)	Caudal ramus length [mm] (mean)	Total length [mm] (mean)	Caudal ramus percentage of total length/body length (mean values) [%]	Antennule	Caudal ramus	
S. verrucosus	15.0	—	—	—	—	—	—	—	Olsson 1872
S. arcticus	39.15	—	—	—	—	—	—	—	Collett 1874
	10.0–90.0	—	—	—	—	—	—	—	Berland 1970
	—	Triangular cephalothorax; posterior somite abruptly narrowing	<3.0	**<1.1**	**<4.1**	**26.6/36.7**	Inadequate description	Single seta, variable in size	Aitken 1942
	—	Triangular (?) cephalothorax	—	—	—	—	3, 2, ?, ?	—	Moser et al. 1985
S. arcticus	5.0–70.0	Host: *Sebastes ruberrimus*; illustrated male with double caudal setae is 3.19/5.07 mm long	1.0–1.28	**?**	**?**	**?**	0, 1, 1, 1, 4	Very high variability (including double setae and no seta et all)	Kuitunen-Ekbaum_1949
S. pacificus	5.0–15.0	—	—	—	—	—	—	—	Komai 1924
	10.0–15.0	Semi-trapezoid cephalothorax; posterior somite abruptly narrowing	**0.94**	**0.35**	**1.29**	**27.1/37.2**	Inadequate description	Strong, 2-segmented seta +2 setules	Heegaard 1947
	1.9–13.0	Semi-triangular/oval cephalothorax; posterior somite abruptly narrowing	1.0–1.4 (1.25) **1.0–1.24 (1.14)**	**0.47–0.55 (0.52)**	**1.53–1.79 (1.67)**	**31.1/45.6**	3, 3, 3, 7	Strong, 2-segmented seta +3 setules; High variability	Izawa 1974
S. komaii	<12.3	Semi-triangular cephalothorax; posterior somite abruptly narrowing	>2.0?	—	—	**41.1/69.8**	Inadequate description	Thin, vermicular	Shiino 1953
	9.5–25.0	Semi-triangular/oval cephalothorax; posterior somite abruptly narrowing	1.3–2.0 (1.62) **1.29–1.98 (1.29)**	**0.94–1.52 (1.16)**	**2.23–2.81 (2.45)**	**54.9/89.9**	4, 4, 3, 9	High variability	Izawa 1974 based on Shiino's type material
S. japonicus	9.0–22.0 (14.7)	Pyriform cephalothorax; posterior somite abruptly narrowing	1.0–1.1 **1.04–1.22 (1.12)**	**0.73–0.79 (0.77)**	**1.82–2.01 (1.88)**	**42.8/68.8**	4, 4, 0, 10	Strong, 2-segmented seta +4 setules	Izawa 1974
S. shiinoi	8.6–21.1	Semi-triangular cephalothorax	1.5–1.8 (1.65) **1.22–1.47 (1.35)**	**0.76–1.05 (0.91)**	**1.98–2.52 (2.25)**	**40.4/67.4**	1, 2, 4, 6	Strong, 2-segmented seta +3 setules	Izawa 1974
S. namibiensis	20.0–32.0	Semi-triangular cephalothorax; posterior somite abruptly narrowing	1.8 **1.74**	**1.04**	**2.78**	**37.4/58.4**	Inadequate description	2-segmented seta	Reimer 1991
S. izawai	25.0–48.0 (35.8)	Semi-triangular/oval cephalothorax; posterior somite not narrowing	2.15–3.52 (2.56)	0.04–0.9 (0.41)	(2.97)	13.8/16.0	4, 4, 2, 7	High variability	Piasecki et al. 2022
S. antimori sp. nov.	15.1	Semi-triangular cephalothorax with very distinct lateral indentations possibly marking traces of thoracic segmentation; posterior somite not narrowing	2.07	0.83	2.90	28.6/40.1	0, 1, 2, 6	Strong seta with small setule	This study

Some data are estimated from the illustrations (**bold** type); the antenna was inadequately described for the majority of species, the mandible (subchelate claw) is uniform in all species; maxillules were only reported for *S. izawai*; the maxillae structure has not been adequately determined in any species; the structure of legs 1 and leg 2 is similar in five species (*S. pacificus*, *S. japonicus*, *S. shiinoi*, *S. izawai*, and *S. antimori* sp. nov.) and in *S. komaii* (where a seta at the base of the exopod of both legs was not reported) and *S. antimori* sp. nov. (where a seta at the base of the exopod of the first leg was not observed).

(Fig. 1A, 1B). Abdominal somites without papilliform protrusions covering surface. Total length reaching 15.1 mm; total width 8.1 mm (Table 2). Body consisting of two parts equal in length. Anterior part semi-cylindrical, blunt, with frontal margin constituting straight line perpendicular to body axis; posterior part slightly wider, semi-conical (tapering posteriorly). Anterior part divided into 5 tightly packed (short) divisions covered with papilliform protrusions and separated by surface furrows. Apparent "segmentation" on dorsal surface not consistently matching furrows on ventral surface. Posterior part of body with two prominent, well-defined somites, diminishing in diameter, and conical abdominal part comprising three somites (abd II–abd IV) tapering stepwise towards conical tip. Surface of posterior part with few papilliform protrusions on dorsal side (Figs. 1B, 2A). Oral lobe located anteriorly on ventral surface, doughnut-shaped, densely covered with papillae around perimeter. Two larger processes present on body surface immediately posterior to oral lobe (Figs. 1A, 2B).

Description of male. Body (Fig. 3A) markedly smaller than that of female, and substantially different in structure; strongly elongate, subcylindrical, unsegmented, with smooth surface. Body consisting of two

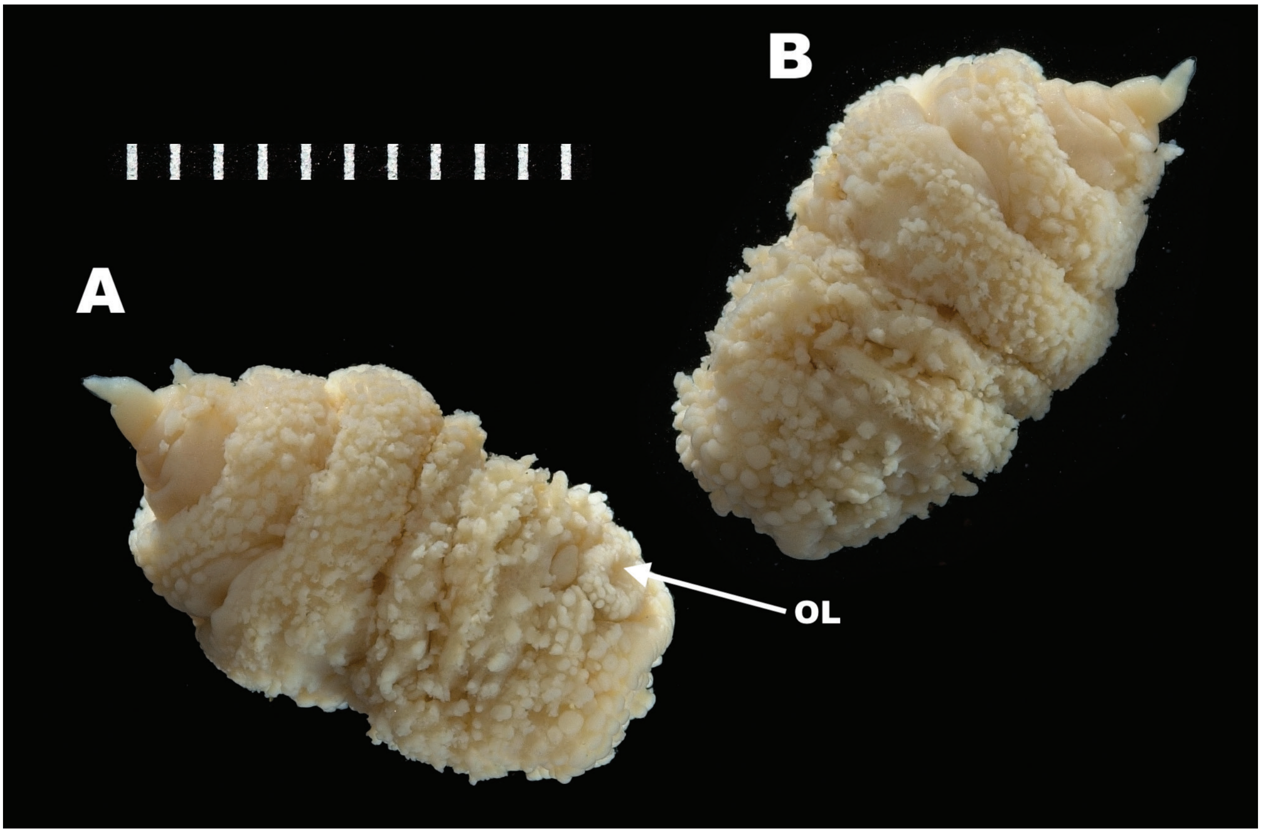

Figure 1. Female of *Sarcotaces antimori* sp. nov. (allotype) from blue antimora, *Antimora rostrata*. (**A**) ventrolateral view; (**B**) dorsolateral view. OL = oral lobe. Scale: 10 mm. Photo: Harry Taylor (NHM Photo Studio, London, UK).

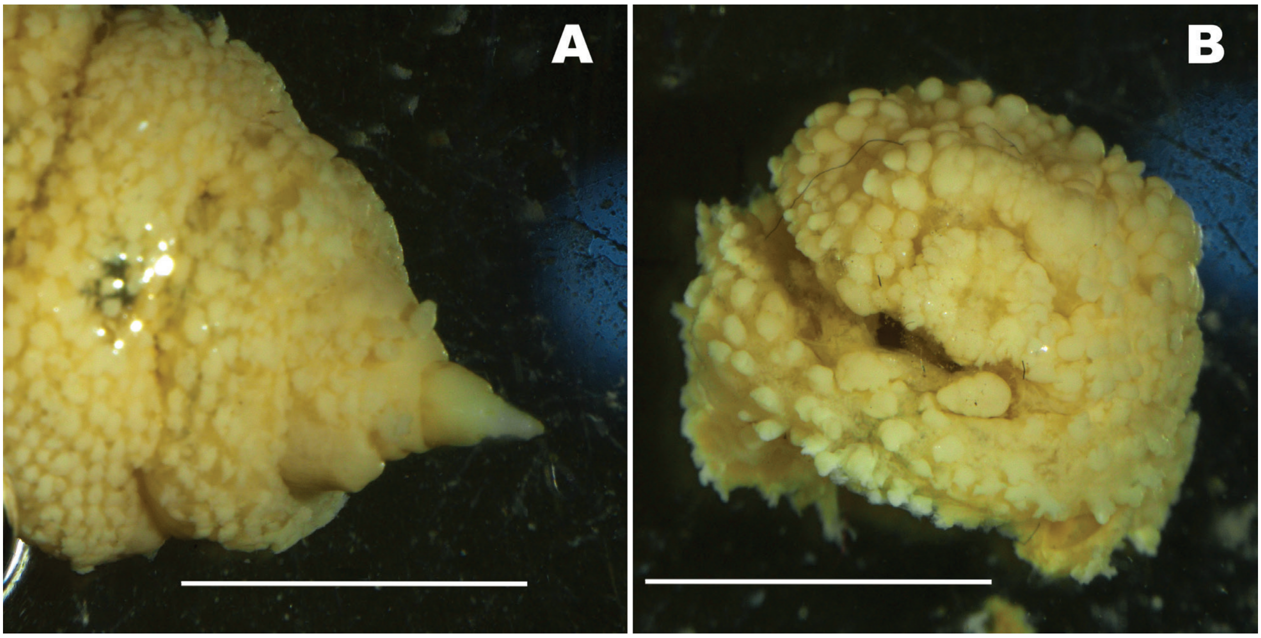

Figure 2. Female of *Sarcotaces antimori* sp. nov. (allotype) from blue antimora, *Antimora rostrata*. (**A**) posterior part; dorsal view; (**B**) Anterior part; vental view. Scale bars: 5 mm. Photo: Dr Brygida Wawrzyniak-Wydrowska (University of Szczecin, Poland).

parts: anterior cephalothorax (20% of body length) and posterior "trunk" (80%). Semi-triangular cephalothorax with three very pronounced lateral indentations marking traces of body segmentation and defining cephalosome from first and second pedigerous somites, the latter bearing prominent posterolateral lobes. Cephalosome with rounded frontal margin produced anteromedially, lateral margins slightly convex; bearing four pairs of appendages. Post-cephalothoracic "trunk" cylindrical and legless, elongate with discrete traces of segmentation; becoming distinctly wider posteriorly and with prominent caudal rami on posterolateral corners. Total body length

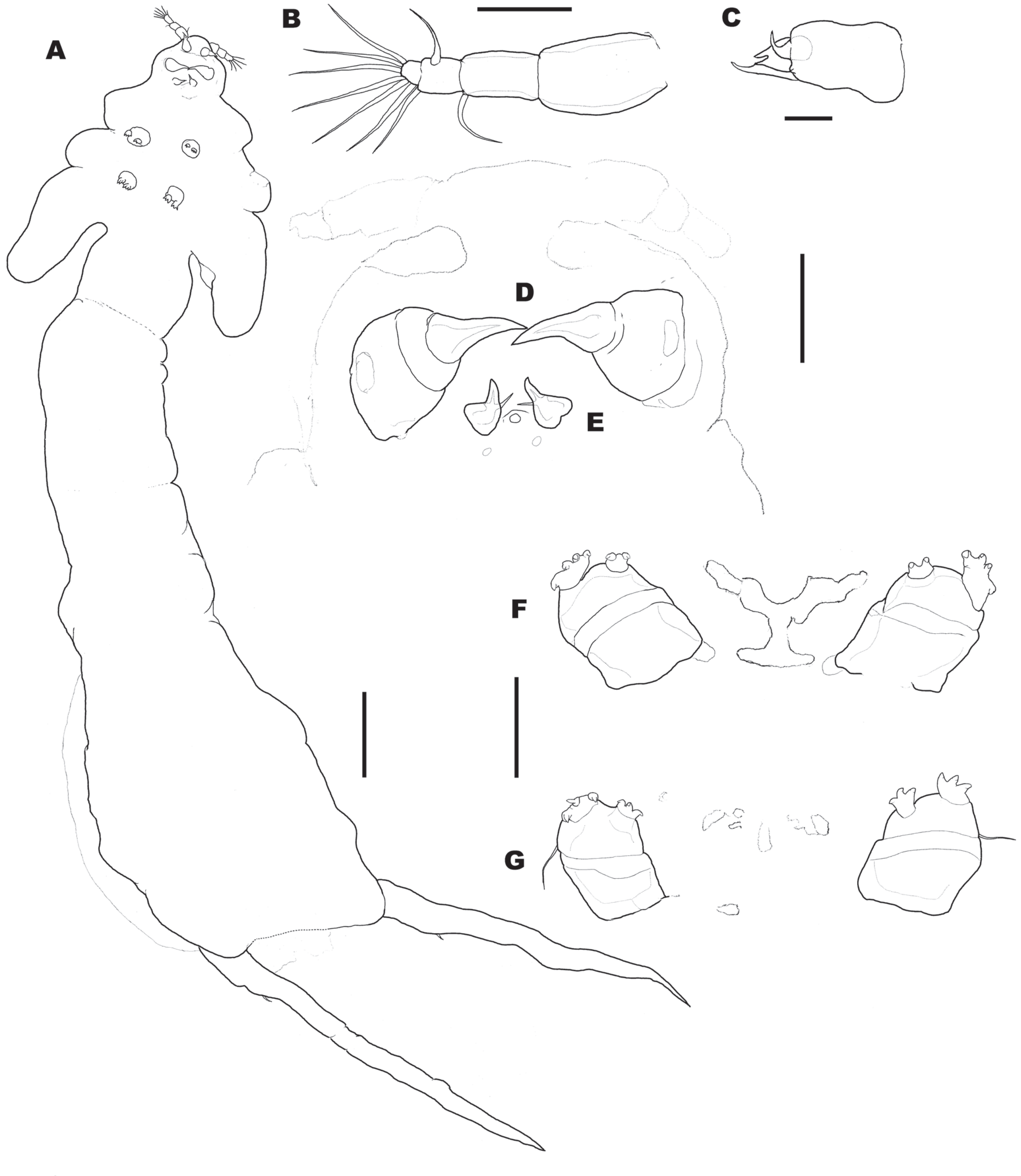

Figure 3. Male of *Sarcotaces antimori* sp. nov. (holotype) from blue antimora, *Antimora rostrata*. Habitus (**A**); antennule (**B**); antenna (**C**); mandibles (**D**); maxillae (**E**); first legs (**F**); second legs (**G**). All images in ventral view. Scale bars: 0.2 mm (A), 0.05 mm (D, E, F, G), 0.02 mm (B), 0.01 mm (C).

of male 2.07 mm, excluding caudal rami, and 2.90 mm with symmetrical caudal rami; caudal ramus length 0.83 mm (Table 2). Maximum cephalothorax width 0.61 mm. Trunk width ranging from 0.21 to 0.54 mm. Caudal rami constituting 28.6% of total length and 40.1% of body length. Cephalothoracic appendages well developed and consisting of antennulae, antennae, mandibles, maxillae, and 2 pairs of legs. Antennule (Fig. 3B) four-segmented with segments diminishing in length and diameter towards tip: first segment longest lacking setation; second segment slightly shorter with single seta posteriorly; third segment slightly longer than wide with one seta anteriorly and one long seta posteriorly; fourth segment short with three long setae posteriorly and three long setae terminally. Antenna (Fig. 3C) indistinctly three-segmented comprising coxobasis plus two-segmented endopod; endopodal segments each bearing single large terminal claw. Mandible (Fig. 3D) large, subchelate, wide at base; tapering towards powerful distal claw. Maxillulae not observed. Maxillae (Fig. 3E) small, uniramous, with triangular base bearing conical terminal segment armed with small seta at base. Maxillipeds absent. First legs

(Fig. 3F) biramous with semi-quadrangular two-segmented protopod: exopod one-segmented and armed with four stout claws; endopod one-segmented with two stout claws. Elaborate, Y-shaped interpodal sclerite present on ventral body surface between first thoracopods. Second legs (Fig. 3G) similar to first: exopod with three stout claws (with single seta at base laterally); endopod with three stout claws. Interpodal sclerite almost completely reduced. Caudal rami very long, thick powerful gently tapering towards distal tip (Fig. 3A), armed with single minute setule near base.

Remarks. The female of *Sarcotaces antimori* sp. nov. differs from that of all known species by possessing very dense coverage over the surface of the cephalosome and thoracic somites with relatively large papilliform protrusions. Another distinct feature of this species is that the surface of the oral lobe is regularly and densely covered with large papilliform protrusions, similar to those covering the rest of the body. This feature distinguishes *Sarcotaces antimori* sp. nov. from its congeners

The male of *Sarcotaces antimori* sp. nov. differs from that of all known species by the deep indentations in the lateral margins of the cephalothorax. Another distinct character is the shape of the trunk which widens substantially posteriorly. In addition, the antennule has a unique setal formula (0, 1, 2, 6) and the first legs lack the outer protopodal seta at the base of the exopod (Table 2).

Etymology. The specific name *antimori* is an adjective derived from the name of the host genus.

Discussion

While comparing the morphological differences between known species of the genus *Sarcotaces* we need to remember about the importance of the host specificity. According to Piasecki et al. (2022), individual *Sarcotaces* species can only infect a specific host fish or closely related species. Those authors broadly discussed the issue of the host specificity in relation to *Sarcotaces*. One of the new arguments supporting the hypothesis of very narrow host specificity are the results of Osman et. al (2014). He studied fishes representing 18 species from the Persian Gulf and *Sarcotaces* was found only in *Epinephelus chlorostigma* (Valenciennes, 1828). McMillan (unpublished[*]) after examining some 284 specimens of six species of the genus *Coelorinchus* (Gadiformes) caught off New Zealand found *Sarcotaces* only in *Coelorinchus aspercephalus* Waite, 1911. There are no other records of this parasitic copepod in any of the 149 valid species (Fricke et al. 2024) of the genus *Coelorinchus*. In European waters, *Sarcotaces arcticus* can only be found in *Molva dypterygia* (Pennant, 1784).

Three of the nine valid species of *Sarcotaces* (*S. arcticus*, *S. izawai*, and *S. antimori* sp. nov.) have been found in fishes representing the order Gadiformes; two (*S. verrucosus* and *S. komaii*) have been reported from fishes representing Perciformes; and another two (*S. japonicus* and *S. shiinoi*) were collected from Anguilliformes fishes. The remaining parasites were recovered from Lophiiformes (*S. pacificus*) and Ophidiiformes (*S. namibiensis*). Despite sharing the same host-fish order, the majority of *Sarcotaces* species have utilized fishes representing different families. There is only one exception: both *S. izawai* and *S. antimori* sp. nov. share the same host-fish family Moridae but they utilize different species and different genera (Table 1). Taking into account the earlier mentioned hypothesis of the narrow host specificity of *Sarcotaces*, we believe that *Sarcotaces* records representing host fishes of higher taxa different from those of the type species should be treated with caution and verified where possible (e.g., Dollfus 1928; Kuitunen-Ekbaum 1949; Ezpeleta Herce 1974; Avdeev and Avdeev 1975; Moser et al. 1985; Kabata 1988; González and Tanzola 2000). Future descriptions of *Sarcotaces* should also be supported by genetic studies. Unfortunately, the only such study has been Piasecki et al (2022). In the presently reported study, however, despite the efforts of two separate teams, we were not able to extract the genetic material.

Despite sharing the same host species (*Antimora rostrata*), *S. komaii* sensu Avdeev and Avdeev (1975) differs from *S. antimori* sp. nov. In the former species, the female is 4.02 cm long, is regularly drop-shaped, body segmentation is regular, the widest somite is just posterior to the oral lobe, and the oral lobe is characteristic, with four peripheral elements, differing in size and armament. The cephalothorax of the male is semi-triangular with distinctly rounded lateral margins lacking indentations that might correspond to inter-segmental boundaries. The trunk is regularly cylindrical and of uniform diameter. In *S. antimori* sp. nov. the female is 15.1 mm long, less drop-shaped and more semi-quadrangular, body segmentation is irregular, the widest somite is located posteriorly, and the oral lobe is doughnut shaped and densely covered by papilliform protrusions. In the male, the cephalothorax has deep lateral indentations separating the cephalosome from the first pedigerous somite and separating the first and second pedigerous somites, the trunk distinctly increases in diameter posteriorly. *Sarcotaces komaii* sensu Avdeev and Avdeev (1975) has been inadequately described and illustrated but its oral lobe is very similar to that of the nominal species (despite the different host fish).

Only a few nominal species have been originally collected in higher numbers. Among them were *Sarcotaces arcticus* with females 10.0–90.0 mm long (Berland 1970) or *S. izawai* representing lengths of 25.0–48.0 mm. Unfortunately, no author has focused their attention on the size of those females at maturity. Consequently, female size does not seem to be a decisive morphological

---

[*] McMillan PJ (1980) New Zealand macrourids of the genus *Coelorinchus* (Pisces: Gadiformes) with detailed descriptions of six common species and notes on aspects of their biology. MSc Thesis; Victoria University of Wellington, New Zealand.

factor. Similarly, we do not know if the size of the protrusions covering the body surface increases with age or not.

In the presently reported study, no nauplius stages were found. Such stages are usually detected when the black fluid surrounding the female in the gall is strained through a fine mesh. Through this procedure also males are detected. The male was found, so it is unlikely that nauplii were overlooked. Nauplius stages are known for *S. arcticus* (see Hjort 1895; Kuitunen-Ekbaum 1949; Moser et al. 1985), *S. pacificus* (see Komai 1924; Izawa 1973), *S. japonicus* (see Izawa 1974), *S. izawai* (see Piasecki et al. 2022), and *S. verrucosus* (see González and Tanzola 2000). The only comprehensive life cycle study was conducted on *S. pacificus* by Izawa (1973) who counted up to 1000 eggs in a gall and reared five nauplius stages followed by a copepodid. The copepodid contains energy reserves in the form of yolk granules, so it is likely that the copepodid represents the infective stage. Nobody has reported egg sacs or their traces. Nauplii were always found freely floating in the black fluid surrounding the female. The hypothetical existence of egg sacs under the particular “safe” conditions of gall seems to be redundant.

Copepods of the genus *Sarcotaces* are mesoparasites sensu Kabata (1976). Even though they are completely hidden inside the host musculature they cannot be referred to as endoparasites because of they maintain constant contact with the external environment via a terminal pore in wall of the gall. The concept of mesoparasitism was widely discussed by Piasecki et al. (2022).

Why do the authors describing *Sarcotaces* females have problems in describing cephalic appendages? We found a possible explanation while watching a video by Jonathan Martin (2009) posted on Flickr. This is the only available footage showing live and moving *Sarcotaces* sp. female. It is evident the oral lobe is hinged anteriorly and can close and open at an angle of 45 degrees. When the lobe is closed, which happens usually in dead females, the cephalic appendages are most likely hidden below it.

Acknowledgments

The authors are indebted to Brygida Wawrzyniak-Wydrowska, Małgorzata Bąk (University of Szczecin), and Harry Taylor (NHM Photo Studio) for their help in the photographic documentation of the study material. Rony Huys (NHM), Remigiusz Panicz, and Piotr Eljasik were involved in genetic studies.

References

Aitken A (1942) An undescribed stage of *Sarcotaces*. Nature 150: 180–181. https://doi.org/10.1038/150180b0

Avdeev GV, Avdeev VV (1975) Parazitičeskie rokoobraznye roda *Sarcotaces* Olsson, 1872 (Copepoda) ot ryb Tihogo Okeana. [Parasitic crustaceans of the genus *Sarcotaces* Olsson, 1872 (Copepoda) from Pacific Ocean Fishes.] Izvestiâ TINRO 96: 227–231. [In Russian]

Berland B (1970) The copepod *Sarcotaces arcticus* Collet, 1874, in the blue ling. Nytt magasin for Zoologi 18(1): 103–104.

Collett D (1874) Om *Sarcotaces arcticus*, en ny Art af en mærkelig Slægt af Fiske-Parasiter. [About *Sarcotaces arcticus*, a new species of a strange genus of fish-parasites.] Forhandlingerne ved de skandinaviske Naturforskeres 11: 387–389. [In Danish and Latin.]

Dollfus RPh (1928) Une hôte nouveau pour *Sarcotaces verrucosus* Olsson 1872 (Copepoda Paras.). Bulletin du Muséum national d’histoire naturelle 34(5): 341–345.

Ezpeleta Herce CR (1974) Nueva localidad y nuevo hospedero para *Sarcotaces komaii* Shiino, 1953 (Copepoda: Sarcotacidae). Poeyana 133: 1–5.

Fricke R, Eschmeyer WN, Van der Laan R (Eds.) (2024) Eschmeyer’s catalog of fishes: genera, species, references. California Academy of Sciences, San Francisco, CA, USA. [Electronic version accessed 20 March 2024] http://researcharchive.calacademy.org/research/ichthyology/catalog/fishcatmain.asp

Gonzalez RA, Tanzola RD (2000) On the presence of *Sarcotaces verrucosus* (Copepoda) in the southwest Atlantic. Acta Parasitologica 45(4): 345–349.

Heegaard PE (1947) Discussion of the genus *Sarcotaces* (Copepoda) with a description of the first known male of the genus. Kunglige Fysiografiska Sällskapets i Lund Förhandlingar 17(12): 122–129.

Hjort J (1895) Zur Anatomie und Entwicklungsgeschichte einer im Fleisch von Fischen schmarotzenden Crustacée (*Sarcotaces arcticus*. Collett). Skrifter udgivne af Videnskabsselskabet i Christiania. I. Mathematisk-naturvidenskabelig Klasse 1895(2): 1–14.

Humes AG, Gooding RU (1964) A method for studying the external anatomy of copepods. Crustaceana 6: 238–240. https://doi.org/10.1163/156854064X00650

Huys R, Boxshall GA (1991) Copepod evolution. Ray Society, Vol. 159, London, UK, 468 pp.

Izawa K (1973) On the development of parasitic Copepoda I. *Sarcotaces pacificus* Komai (Cyclopoida: Phylichthyidae). Publication of the Seto Marine Biological Laboratory 21(2): 77–86. https://doi.org/10.5134/175809

Izawa K (1974) *Sarcotaces*, a genus of parasitic Copepods (Cyclopoida: Philichthyidae), found on Japanese fishes. Publications of the Seto Marine Biological Laboratory 21(3–4): 179–191. https://doi.org/10.5134/175866

Kabata Z (1976) A rational look at parasitic Copepoda and Branchiura. Pp. 175–181. In: Page LA (ed.) Wildlife diseases [Proceedings of the Third International Wildlife Disease Conference held at the University of Munich’s Institute for Zoology and Hydrobiology in Munich, 1975] Plenum Press, New York and London. https://doi.org/10.1007/978-1-4757-1656-6_23

Kabata Z (1979) Parasitic Copepoda of British fishes. Ray Society, Vol. 152, London, UK, 46 pp.

Kabata Z (1988) Copepoda and Branchiura. Pp. 3–127. In: Margolis L, Kabata Z (Eds.) Guide to the parasites of fishes of Canada. Part II—Crustacea. Canadian Special Publication in Fisheries and Aquatic Sciences.

Komai T (1924) Notes on *Sarcotaces pacificus* n. sp., with remarks on its systematic position. Memoirs of the College of Science, Kyoto Imperial University, Series B 1: 265–271.

Kuitunen-Ekbaum E (1949) The occurrence of *Sarcotaces* in Canada. Journal of the Fisheries Research Board of Canada 7c(9): 505–512. https://doi.org/10.1139/f47-040

Martin J (2009) Ewww! Well, mostly Ewww, but also awesome :) Flickr. https://www.flickr.com/photos/dryodora/3608878449

Moser M, Haldorson L, Field LJ (1985) The taxonomic status of *Sarcotaces komaii* and *Sarcotaces verrucosus* (Copepoda: Philichthyidae) and host–parasite relationships between *Sarcotaces arcticus* and *Sebastes* spp. (Pisces). Journal of Parasitology 71(4): 472–480. https://doi.org/10.2307/3281540

Olsson P (1872) Om *Sarcotaces* och *Acrobothrium*, tva nya parasit-slägten fran fiskar. [About *Sarcotaces* and *Acrobothrium*, two new parasite genera from fish.] Öfversigt af Kongliga Vetenskaps-akademiens forhandlingar 1872(9): 39–44. [In Swedish and Latin.]

Osman HAM, Hassan MA, El-Refaey AME (2014) Studies on *Sarcotaces* sp. (Copepoda, Philichthyidae) infestation (black bag disease) among some marine fish species of Arabian Gulf, Saudi Arabia. World Applied Sciences Journal 32(9): 1780–1788.

Piasecki W, Barcikowska D, Keszka S, Panicz R (2020) Parasitic copepods (Crustacea: Copepoda) infecting muscles of a marine fish (Actinopterygii: Moridae)—A spectacular effect on a host fish and a case of seafood identity fraud. Acta Ichthyologica et Piscatoria 50(4): 453–464. https://doi.org/10.3750/AIEP/02932

Piasecki W, Barcikowska D, Panicz R, Eljasik P, Kochmański P (2022) First step towards understanding the specific identity of fish muscle parasites of the genus *Sarcotaces* (Copepoda: Philichthyidae)—New species and first molecular ID in the genus. International Journal for Parasitology: Parasites and Wildlife 18: 33–44. https://doi.org/10.1016/j.ijppaw.2022.03.008

Reimer LW (1991) *Sarcotaces namibiensis* sp. nov., the first evidence of the genus *Sarcotaces* Olsson, 1872, in the South Atlantic (Copepoda). Crustaceana 60(2): 139–144. https://doi.org/10.1163/156854091X00353

Shiino SM (1953) On *Sarcotaces* Olsson, the genus of parasitic copepod, found in Japan. Annual Report of the Prefectural University of Mie, Section 2 (Natural Sciences) 1: 171–183. [In Japanese with English abstract.]

Acta Ichthyologica et Piscatoria 54, 2024, 95–101 | DOI 10.3897/aiep.54.119948

PENSOFT.

ACTA
ICHTHYOLOGICA
ET PISCATORIA

First records of two siluriform fishes: *Bagrichthys micranodus* (Actinopterygii: Siluriformes: Bagridae) and *Pangasianodon hypophthalmus* (Pangasiidae) from Sumatra, Indonesia

Kunto WIBOWO[1], Muslim MUSLIM[2], Muhammad AFRISAL[1,3],
Agus PRIYADI[4], Ruby V. KUSUMAH[5], Lukman LUKMAN[4]

1 *Museum Zoologicum Bogoriense, Research Center for Biosystematics and Evolution, National Research and Innovation Agency, Cibinong, Indonesia*
2 *Program Study of Aquaculture, Department of Fisheries, Faculty of Agriculture, Universitas Sriwijaya, Palembang, Indonesia*
3 *Capture Fisheries Department, Indonesia Defense University, Belu, Indonesia*
4 *Research Center for Conservation of Marine and Inland Water Resources, National Research and Innovation Agency, Cibinong, Indonesia*
5 *Research Center for Fishery, National Research and Innovation Agency, Cibinong, Indonesia*

https://zoobank.org/2AE6F0FB-2A50-4FBB-884A-02C41BF71104

Corresponding authors: Kunto Wibowo (kuntowe@gmail.com); Muslim Muslim (muslim_bda@unsri.ac.id)

Academic editor: Jan Kotusz ♦ **Received** 31 January 2024 ♦ **Accepted** 28 February 2024 ♦ **Published** 4 April 2024

Citation: Wibowo K, Muslim M, Afrisal M, Priyadi A, Kusumah RV, Lukman L (2024) First records of two siluriform fishes: *Bagrichthys micranodus* (Actinopterygii: Siluriformes: Bagridae) and *Pangasianodon hypophthalmus* (Pangasiidae) from Sumatra, Indonesia. Acta Ichthyologica et Piscatoria 54: 95–101. https://doi.org/10.3897/aiep.54.119948

Abstract

A bagrid catfish, *Bagrichthys micranodus* Roberts, 1989, has been reliably reported only from Borneo Island, whereas a pangasiid catfish, *Pangasianodon hypophthalmus* (Sauvage, 1878), originally from the Mekong and Chao Phraya rivers, has been widely introduced for aquaculture throughout southeast Asia. However, an ichthyofaunal survey of Cala Lake, South Sumatra, disclosed significant distribution extensions for both species, that of *B. micranodus* being the first from a land mass other than Borneo Island. Additionally, *P. hypophthalmus* was recorded from a natural freshwater habitat, outside the controlled environments of aquaculture facilities. The specimens are described in detail and comparisons are made with closely related species.

Keywords

distribution, fish fauna, introduced species, morphology, new record

Introduction

Bagrichthys, a bagrid catfish genus, characterized by an elongated and compressed caudal peduncle, dorsally-directed serrae on the posterior margin of the dorsal-fin spine, gill membranes united but not joined to the isthmus, and a long adipose fin without a free posterior margin (Roberts 1989; Ng 2000, 2002), comprises seven valid species, five of which have been recorded from inland Indonesian freshwater bodies, viz. *Bagrichthys hypselopterus* (Bleeker, 1852), *Bagrichthys macropterus* (Bleeker, 1854), *Bagrichthys macracanthus* (Bleeker, 1854), *Bagrichthys micranodus* Roberts, 1989, and *Bagrichthys vaillantii* (Popta, 1906) (see Kottelat et al. 1993; Ng 2000, 2002). Among these, *B. micranodus* and *B. vaillantii* have both been reliably reported only from Borneo Island (Kottelat et al. 1993; Ng 2002; Kottelat 2013).

Pangasianodon, a pangasiid catfish genus, characterized by a terminal mouth, posterior nostril located close behind the anterior nostril, and pelvic fins with 8 or 9 rays, includes the endemic Mekong River and Chao Phraya basin species *Pangasianodon gigas* Chevey, 1931 and *Pangasianodon hypophthalmus* (Sauvage, 1878) (see Rainboth 1996; Kottelat 2001; Gustiano 2009; Gustiano unpublished*). The latter species, originating from Thailand, has been subsequently introduced elsewhere for aquacultural purposes (Froese and Pauly 2023; Secretariat GBIF 2023; Gustiano unpublished).

During an ichthyofaunal survey conducted at Cala Lake, Musi River, South Sumatra, a single specimen of *B. micranodus* and two of *P. hypophthalmus* were successfully collected, being the first documented specimen of *B. micranodus* from other than Borneo Island, and the first record of *P. hypophthalmus* from a natural freshwater habitat, outside the controlled environments of aquaculture facilities.

Materials and methods

The specimens were collected during the dry season (August 2023) from Cala Lake, Musi Banyuasin Regency, South Sumatra, Indonesia. The lake, positioned between 02°56′–02°57′S and 103°58′–104°00′E, is an oxbow lake formed by the meandering central zone of the Musi River. Spanning an area of approximately 120 hectares with a maximum depth reaching 13 meters, the lake undergoes seasonal transformations, including elevated water levels during the rainy season, when a connection with the Musi River facilitates fish migration between the two water bodies, and isolation from the Musi River during the dry season, resulting in distinctly different ecological conditions.

Counts and measurements were made on the left side of the specimens whenever possible, generally following Ng (2000) and Hubbs and Lagler (2004), with the following exception and additional characters: humeral process length follows Roberts (1989); dorsal and pectoral fin and spine lengths were measured from the origins to the tips; and head width and depth were measured at the posterior margin of the eyes. Standard and head lengths are abbreviated as SL and HL, respectively. The morphological descriptions are based only on specimens collected from Cala Lake. Curatorial procedures for the specimens, deposited at the Museum Zoologicum Bogoriense, Indonesia (MZB), followed Motomura and Ishikawa (2013).

Comparative material. *Bagrichthys micranodus*, MZB.3578, holotype, 122.9 mm SL, Kapuas River, Western Kalimantan, Indonesia; *Bagrichthys macropterus*, MZB.3575, non-type, 124.7 mm SL, Kapuas River, Western Kalimantan.

Results

Family Bagridae Bleeker, 1858
Bagrichthys Bleeker, 1857

Bagrichthys micranodus Roberts, 1989

Figs. 1A, 2; Table 1

Material examined. MZB.26910, 179.1 mm SL, Cala Lake, Musi Banyuasin, South Sumatra, Indonesia, 8 August 2023, collected by K. Wibowo, R.V. Kusumah, A. Priyadi, and L. Lukman.

Description. Measurements shown in Table 1. Head small, short and bulbous with short blunt snout (lateral view). Body elongated, compressed, with long caudal peduncle. Head and body covered by smooth skin. Eye oval, with free margin, situated entirely on dorsal half of head. Mouth small, inferior; lips with papillae; jaws without teeth; palate with few teeth covered by soft membrane. Gill openings wide; gill membranes broadly joined, not bound to isthmus. Lateral line complete, midlateral, posterior end slightly curved to upper lobe of caudal fin. Anus and urogenital openings situated midway between pelvic and anal fins. Four pairs of barbels present. Maxillary barbel longest, extending almost to vertical level of posterior edge of opercle. Nasal barbel slender, its length more than twice eye diameter. Inner mandibular barbel shortest, thickened, strongly crenulated. Outer mandibular barbel simple, without crenulations, its length less than that of nasal barbel. Dorsal fin with 2 spines; first very small, hidden under skin; second long, compressed, robust, sharply pointed, shorter than two anterior branched rays, posterior margin with 16 upwardly directed serrae. Adipose fin long, broad, with convex edge, originating from posterior end of dorsal fin to middle of posterior half of caudal peduncle. Pectoral fin with 1 spine and 9 rays; spine larger than second dorsal fin spine, robust, sharply pointed, posterior margin with 23 serrae; spine shorter than two anterior branched rays; origin of pectoral fin about level with posteriormost margin of opercular membrane. Pelvic fin with 6 rays; origin slightly posterior to posterior end of dorsal fin base; tip of adpressed fin not reaching origin of anal fin. Anal fin with 15 rays, positioned below midpoint of adipose fin. Caudal fin with 8 + 9 principal rays, deeply forked; upper and lower lobes pointed, outermost principal fin-rays extended as filaments; dorsal and ventral procurrent rays asymmetric, origins of dorsal lobe rays slightly anterior to that of ventral lobe rays.

Fresh specimen coloration. (Fig. 1A). Head dark brown dorsally, pale whitish ventrally. Body dark brown with two whitish vertical markings; first oblique, extending from origin of adipose fin to anterior part of anal fin base, second behind anal fin. Dorsal fin blackish dorsally, whitish ventrally. Adipose fin grey-greenish, white-edged posteriorly. Pectoral, pelvic, and anal fins black with broad hyaline bases. Caudal fin uniformly whitish.

---

[*] Gustiano R (2003) Taxonomy and phylogeny of Pangasiidae catfishes from Asia (Ostariophysi, Siluriformes). PhD Dissertation, Katholieke Universiteit Leuven, Belgium, 296 pp.

Table 1. Measurements (expressed as percentages of standard and head lengths) of *Bagrichthys micranodus* and *Pangasianodon hypophthalmus* examined in this study.

Character	***Bagrichthys micranodus***		***Pangasianodon hypophthalmus***	
	Non-type MZB.26910	**Holotype MZB.3578**	**Non-type MZB.26911**	**Non type MZB.26912**
Absolute value [mm]				
Standard length (SL)	179.1	122.9	202.9	206.0
Head length (HL)	33.3	25.9	53.3	54.8
Relative value [%SL]				
Head length	18.6	21.1	26.3	26.6
Body depth at dorsal fin origin	21.7	22.2	24.3	24.7
Body depth at anal fin origin	17.4	15.5	22.4	21.9
Body width at widest point of humeral process	15.8	17.0	16.7	17.1
Predorsal fin length	34.1	36.5	40.9	40.6
Preisthmus length	12.2	14.6	11.6	12.1
Prepectoral fin length	18.2	19.4	21.9	22.3
Prepelvic fin length	43.8	45.2	43.7	43.9
Preanal fin length	61.3	61.3	54.9	55.6
Dorsal-fin spine length	18.1	19.6	19.1	19.1
Dorsal-fin length	22.2	24.6	24.0	23.2
Dorsal-fin base length	10.1	11.7	7.8	7.6
Pectoral-fin spine length	19.7	21.4	18.0	17.6
Pectoral fin length	22.7	—	19.8	19.6
Pelvic fin length	14.6	15.6	14.5	13.6
Anal-fin length	18.4	21.5	13.2	—
Anal-fin base length	12.0	11.6	32.5	30.7
Caudal peduncle length	27.6	28.8	15.6	16.2
Caudal peduncle depth	6.5	6.3	8.2	7.9
Relative value [%HL]				
Head width	53.9	51.8	50.3	49.8
Head depth	52.9	51.0	38.5	37.8
Eye diameter	18.7	14.6	15.9	16.4
Snout length	31.4	29.5	34.3	35.5
Distance between anterior nostrils	10.3	11.9	24.9	25.4
Distance between posterior nostrils	—	—	30.7	31.9
Nasal barbel length	46.8	85.2	—	—
Maxillary barbel length	83.2	111.2	52.3	59.2
Outer mandibular barbel length	34.5	65.7	6.2	30.8
Inner mandibular barbel length	16.5	24.3	—	—
Humeral process length	52.9	53.8	31.0	30.9

Family Pangasiidae Bleeker, 1858

Pangasianodon Chevey, 1931

Pangasianodon hypophthalmus (Sauvage, 1878)

Fig. 1B, 1C; Table 1

Material examined. MZB.26911, 202.9 mm SL, MZB.26912, 206.0 mm SL, Cala Lake, Musi Banyuasin, South Sumatra, Indonesia, 10 August 2023, collected by K. Wibowo, R. V. Kusumah, A. Priyadi, and L. Lukman.

Description. Measurements shown in Table 1. Head somewhat depressed, with pointed snout (lateral view). Body elongated, compressed. Head and body covered by smooth skin. Eye oval, situated slightly below horizontal axis of body. Mouth wide, terminal; upper and lower jaws nearly equal, with a band of villiform teeth; upper jaw teeth entirely covered by lower jaw when mouth closed; vomer with narrow, elongated tooth bands. Gill openings wide; gill membranes free, not bound to isthmus or to each other. Lateral line complete, midlateral. Anus and urogenital openings situated closer to anal-fin base than to pelvic fin. Two pairs of barbels present. Maxillary barbel simple, longer than mandibular barbel; maxillary barbel beyond margin of opercle but not reaching pelvic fin base; mandibular barbel simple, its length less than eye diameter in MZB.26911, about twice eye diameter in MZB.26912. Dorsal fin with 2 spines and 7 rays; first very small, hidden under skin; second long, compressed, robust, shorter than two anterior branched rays; posterior margin with several tiny serrae; origin of dorsal fin above level of pectoral fin spine tip. Adipose fin small, positioned closer to caudal fin base than to dorsal fin. Pectoral fin with 1 spine and 10 rays; spine robust, posterior margin with 24 or 25 serrae, spine shorter than two anterior branched rays; tip of adpressed fin not reaching pelvic-fin origin; dorsal edge of pectoral-fin base about level with ventral margin of orbit. Pelvic fin with 8 rays; fin origin level with midpoint of dorsal-fin base; tip of adpressed fin reaching base of fifth or sixth anal-fin ray. Anal fin with 34 rays; fin base long, equal to about one third standard length; branched rays progres-

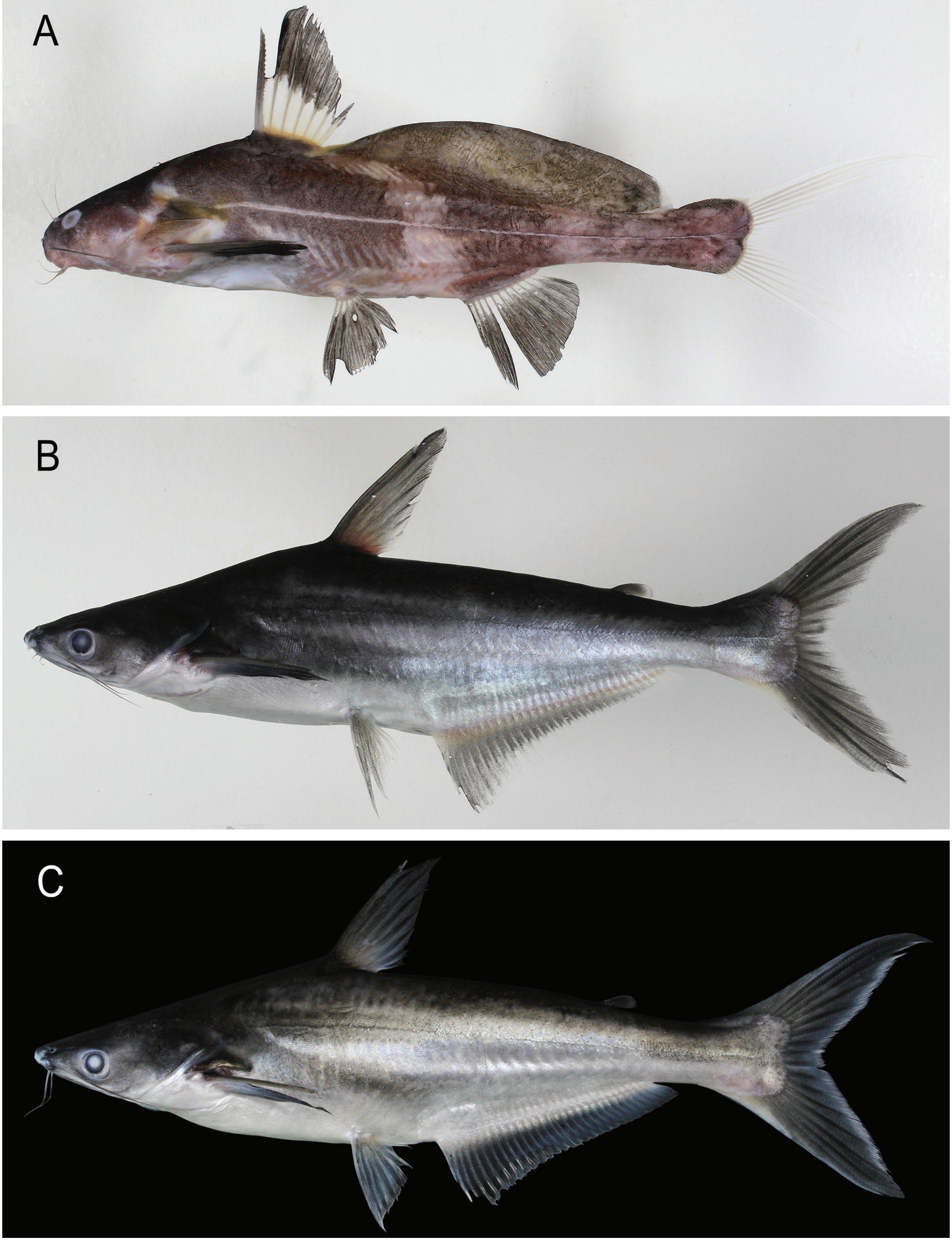

Figure 1. Photographs of fresh specimens of (**A**) *Bagrichthys micranodus*, MZB.26910, 179.1 mm SL, (**B**) *Pangasianodon hypophthalmus*, MZB.26911, 202.9 mm SL, and (**C**) *P. hypophthalmus*, MZB.26912, 206.0 mm SL, collected from Cala Lake, South Sumatra.

sively shorter posteriorly. Caudal fin with 8 + 9 principal rays, deeply forked; upper and lower lobes pointed.

Fresh specimen coloration. (Fig. 1B, 1C). Head and body black dorsally; lateral and ventral surfaces of body pale whitish or silvery; two black lateral stripes joining anteriorly above pectoral fin base. All fins blackish; middle of anal fin with darker stripe; upper and lower caudal fin lobes each with dark grey stripe.

Discussion

The morphology of the bagrid catfish specimen (Fig. 1A) from Cala Lake was very consistent with the morphology of the holotype of *Bagrichthys micranodus* and diagnostic characters of the species given by Roberts (1989) and Kottelat et al. (1993), e.g., mouth small and narrow; oral dentition extremely reduced, only a few scattered teeth covered by soft tissue at palate; posterior margin of second dorsal fin spine with 16 serrae; inner mandibular barbel strongly crenulated; outer mandibular barbel simple; color of fresh specimen dark brown with light whitish areas. The minor difference in the number of serrae on the posterior margin of the second dorsal fin spine in this study (16 serrae; Fig. 2A) compared to previous studies (Roberts 1989; Kottelat et al. 1993; Ng 1999) (15 serrae or fewer) is considered as intraspecific variation.

Bagrichthys micranodus closely resembles the widely distributed Sundaland species *B. macropterus* and Indochinese species *B. obscurus*, particularly in mouth condition, oral dentition, and dorsal fin spine length. However, the former is readily distinguished from both of the latter, having crenulated inner mandibular barbels and simple outer barbels (Fig. 2B), compared with both inner and outer barbels being strongly crenulated in the latter (Roberts 1989; Kottelat et al. 1993; Ng 1999; this study). Additionally, the fresh specimens of *B. micranodus* exhibited dark brown coloration with light whitish areas, contrasting with the pale brown or tan coloration and light creamy areas observed in *B. macropterus*, and uniformly brown coloration (without cream or whitish areas) of *B. obscurus* (see Ng 1999).

Since the Roberts original description in 1989, the known distribution of *B. micranodus* has been restricted to the type locality (Kapuas River, West Kalimantan). Therefore, the Sumatran specimen examined herein represents the first record of *B. micranodus* beyond the confines of Borneo Island (Fig. 3).

Species belonging to the genus *Bagrichthys* are known to reproduce in flooded riparian forests during the rainy season (Rainboth 1996). Kottelat and Widjanarti (2005) reported abundant *B. micranodus* in the Kapuas River during the rainy season, but much reduced numbers during the dry season. However, local fishermen advised that *B. micranodus* was relatively rare in Cala Lake, during both the dry and rainy seasons, the species apparently not entering the lake in large numbers, although relatively abundant in the associated Musi River. This aligns with the report of Kottelat and Widjanarti (2005), which stated that in West Kalimantan, the species was more commonly found in the main river (Kapuas River), compared with lakes.

The pangasiid catfish specimen from Cala Lake closely conformed to the diagnostic characteristics of *Pangasianodon hypophthalmus* provided by Roberts and Vidthayanon (1991), Kottelat (2001), and Gustiano (unpublished*), e.g., head length 26.3%–26.6% of SL, distance between anterior nostrils 24.9%–25.4% of HL, prepectoral length 19.6%–19.8% of SL, anal-fin base length 30.7%–32.5% of SL, preisthmus length 44.3%–45.6% of HL, two blackish strips on the body lateral surface, a dark grey stripe in the middle of the anal fin, and faint dark grey stripes on each caudal fin lobe.

Pangasianodon hypophthalmus has been reported to reach sizes of up to 1300 mm SL (Kottelat 2001), the specimens (202.9–205.96 mm SL) in this study both being considered as juveniles. Such fish (less than 400 mm SL) are characterized by dark well-defined midlateral and abdominal stripes that converge anteriorly above the pectoral fin base (Roberts and Vidthayanon 1991: fig. 9; Rainboth 1996: 153; Kottelat 2001; Fig. 1B, 1C), and the presence of a pair of narrow vomerine tooth bands (Roberts and Vidthayanon 1991: fig. 2e; Kottelat 2001: fig. 55c; Gustiano unpublished: fig. 22c). In larger specimens, the coloration is less distinctive, and the tooth bands are progressively lost.

Native to the Mekong, Chao Phraya, and Maeklong water systems, *P. hypophthalmus* has been introduced to additional river catchments for aquaculture purposes (Froese and Pauly 2023). In fact, the species has been documented as introduced into 11 countries (Secretariat GBIF 2023), following its importation from Thailand to Indonesia in 1972. So far, the fish has been successfully cultivated in several regions of Indonesia, including Sumatera Island (Jambi, Riau, South Sumatra, Lampung), Java Island (Bogor, Sukabumi, Subang), and Borneo Island (South Kalimantan, West Kalimantan) (Solaiman and Sugihartono 2017; Wahyudewantoro and Herawati 2020; Fig. 3). Its discovery in Cala Lake indicates that the species has also been introduced into public waterways, and it is likely that other such occurrences have taken place elsewhere.

The introduction of *P. hypophthalmus* into new environments poses potential risks to native fish populations and the aquatic ecosystem, raising concerns regarding competition for resources, predation on native species, habitat alteration, and the potential spread of diseases. Addressing these potential impacts necessitates the implementation of monitoring programs, ecological assessments, and, if necessary, the application of management strategies. Such strategies may include control measures to limit exotic species' population growth, ecological restoration efforts, and ongoing monitoring programs to assess and adapt management strategies based on evolving ecological dynamics.

The conservation status of *B. micranodus* in The IUCN Red List of Threatened Species is currently listed as Data Deficient (Ng 2019). Although *P. hypophthalmus* has been successfully cultivated in several countries, including Myanmar, Malaysia, and Indonesia, its IUCN status is currently classified as Endangered, due to a significant decline in populations of wild adults in their native habitats due to overfishing (Vidthayanon and Hogan 2011).

---

[*] Gustiano R (2003) Taxonomy and phylogeny of Pangasiidae catfishes from Asia (Ostariophysi, Siluriformes). PhD Dissertation, Katholieke Universiteit Leuven, Belgium, 296 pp.

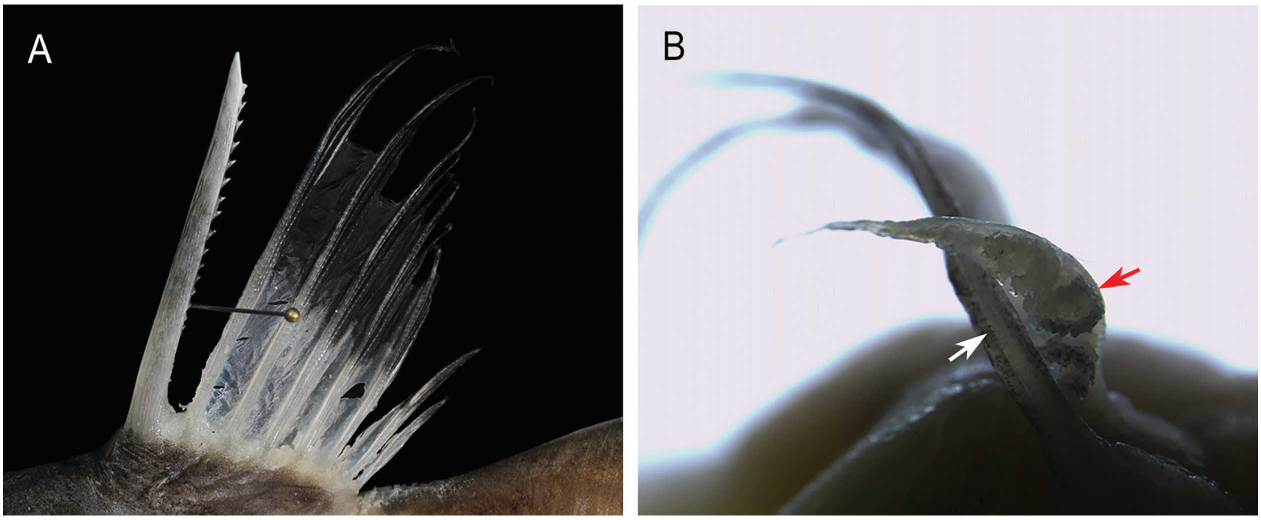

Figure 2. Dorsal fin (**A**) and mandibular barbels (**B**) of *Bagrichthys micranodus*. White and red arrows indicate simple outer and crenulated inner mandibular barbels, respectively.

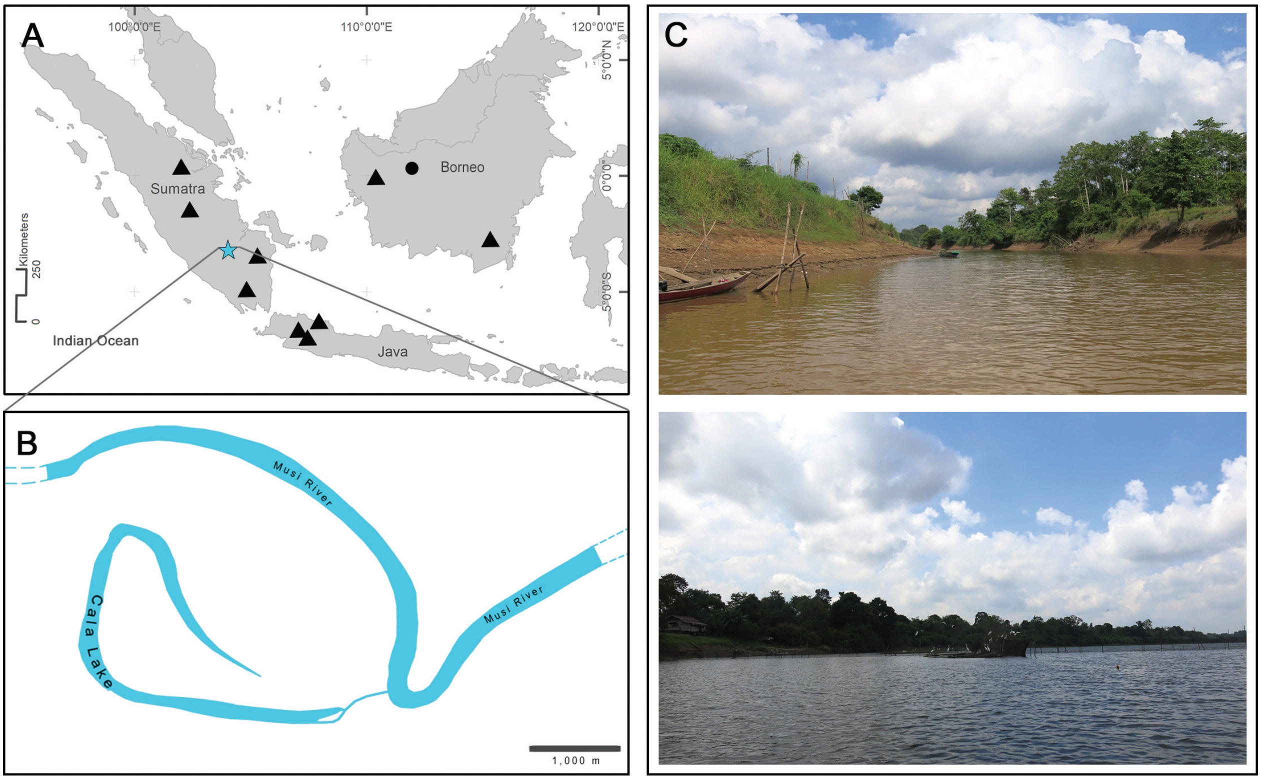

Figure 3. (**A**) Distribution map of *Bagrichthys micranodus* and *Pangasianodon hypophthalmus* in Indonesia; star indicates presently reported specimens of the two species in Cala Lake, South Sumatra; circle and triangles indicate previously reported studies (Roberts 1989; Solaiman and Sugihartono 2017) of *B. micranodus* and *P. hypophthalmus*, respectively. (**B, C**) collection sites of *B. micranodus* and *P. hypophthalmus* from Cala Lake, South Sumatra, examined in this study.

Acknowledgments

We are especially grateful to Mr Kurniawan (Dinas Perikanan Kabupaten Musi Banyuasin) for technical assistance during the survey, to Mr S. Sauri (MZB, Indonesia) for cataloging the specimens, and to Dr G.S. Hardy (Ngunguru, New Zealand) for assisting with the English text and valuable input in reviewing the manuscript. Additionally, we would like to express our sincere thanks to Dr H.H. Tan (National University of Singapore, Singapore), the anonymous reviewer, and the academic editor for their constructive comments. This study was supported by "Program Pendanaan Riset dan Inovasi untuk Indonesia Maju (RIIM) and Lembaga Pengelola Dana Pendidikan (LPDP), Kementerian Keuangan Republik Indonesia" and "Program Pendanaan Riset Rumah Program Organisasi Riset Hayati dan Lingkungan - BRIN".

References

Froese R, Pauly D (Eds) (2023) FishBase. [Version 10/2023] http://www.fishbase.org

Gustiano R (2009) Pangasiid catfishes of Indonesia. Buletin Plasma Nutfah 15(2): 91–100. https://doi.org/10.21082/blpn.v15n2.2009.p91-100

Hubbs CL, Lagler KF (2004) Fishes of the Great Lakes region, revised edition, revised by Gerald R. Smith. MI: University of Michigan Press, Ann Arbor, MI, USA, 276 pp. https://doi.org/10.3998/mpub.17658

Kottelat M (2001) Fishes of Laos. WHT Publications, Colombo, Sri Lanka, 198 pp.

Kottelat M (2013) The fishes of the inland waters of southeast Asia: A catalogue and core bibliography of the fishes known to occur in freshwaters, mangroves and estuaries. Raffles Bulletin of Zoology 27: 1–663.

Kottelat M, Widjanarti E (2005) The fishes of Danau Sentarum National Park and the Kapuas Lakes area, Kalimantan Barat, Indonesia. Raffles Bulletin of Zoology 13: 139–173.

Kottelat M, Whitten AJ, Kartikasari SN, Wirjoatmodjo S (1993) Freshwater fishes of Western Indonesia and Sulawesi. Periplus Editions, Hong Kong, 259 pp [+ 84 pls].

Motomura H, Ishikawa S (Eds) (2013) Fish collection building and procedures manual. English edition. Kagoshima University Museum, Kagoshima and Research Institute for Humanity and Nature, Kyoto, Japan, 70 pp.

Ng HH (1999) *Bagrichthys obscurus*, a new species of bagrid catfish from Indochina (Teleostei: Bagridae). Revista de Biología Tropical 47(3): 545–552.

Ng HH (2000) *Bagrichthys vaillantii* (Popta, 1906), a valid species of bagrid catfish from eastern Borneo (Teleostei: Siluriformes). Zoölogische Mededeelingen 73: 327–332.

Ng HH (2002) *Bagrichthys majusculus*, a new catfish from Indochina (Teleostei, Bagridae). Folia Zoologica 51(1): 49–54.

Ng HH (2019) *Bagrichthys micranodus*. IUCN Red List of Threatened Species 2019: e.T91178545A91178561. [Accessed on 17 January 2024] https://doi.org/10.2305/IUCN.UK.2019-2.RLTS.T91178545A91178561.en

Rainboth WJ (1996) FAO species identification field guide for fishery purposes. Fishes of the Cambodian Mekong. FAO, Rome, 265 pp.

Roberts TR (1989) The freshwater fishes of western Borneo (Kalimantan Barat, Indonesia). Memoirs of the California Academy of Sciences 14: [i–xii +] 1–210.

Roberts TR, Vidthayanon C (1991) Systematic revision of the Asian catfish family Pangasiidae, with biological observations and descriptions of three new species. Proceedings. Academy of Natural Sciences of Philadelphia 143: 97–143.

Secretariat GBIF (2023) *Pangasianodon hypophthalmus* (Sauvage, 1878). GBIF Backbone Taxonomy. Checklist dataset. [Accessed 19 January 2024] https://doi.org/10.15468/39omei

Solaiman S, Sugihartono M (2017) Performance pertumbuhan beberapa populasi Patin Siam (*Pangasianodon hypophthalmus*) di Indonesia. Jurnal Ilmiah Universitas Batanghari Jambi 12(3): 28–34. [In Indonesian]

Vidthayanon C, Hogan Z (2011) *Pangasianodon hypophthalmus*. IUCN Red List of Threatened Species 2011: e.T180689A7649971. [Accessed on 16 January 2024] https://doi.org/10.2305/IUCN.UK.2011-1.RLTS.T180689A7649971.en

Wahyudewantoro G, Herawati T (2020) Aspek biologi: Jenis ikan air tawar Jawa Barat dan wilayah penyebarannya. Unpad Press, Bandung, Indonesia, 214 pp. [In Indonesian]

Acta Ichthyologica et Piscatoria 54, 2024, 103–108 | DOI 10.3897/aiep.54.119085

PENSOFT.

ACTA ICHTHYOLOGICA ET PISCATORIA

First records of two species of snake eels, *Aplatophis chauliodus* and *Ophichthus hyposagmatus* (Actinopterygii: Anguilliformes: Ophichthidae), from Mexico

Luis Fernando DEL MORAL-FLORES[1], Armando T. WAKIDA-KUSUNOKI[2],
Rafael RAMOS-HERNÁNDEZ[3], Arturo GEORGE-ZAMORA[4]

1 *Facultad de Estudios Superiores Iztacala, Universidad Nacional Autónoma de México (UNAM), Tlalnepantla, Estado de México, Mexico*
2 *Centro Regional de Investigación Acuícola y Pesquera de Yucalpetén, Instituto Mexicano de Investigación Pesquera y Acuacultura Sustentables, Yucalpetén, Progreso, Yucatán, Mexico*
3 *Centro Regional de Investigación Acuícola y Pesquera de Veracruz, Instituto Mexicano de Investigación Pesquera y Acuacultura Sustentable, Boca del Rio, Veracruz, Mexico*
4 *Centro Regional de Investigación Acuícola y Pesquera de Puerto Morelos, Instituto Mexicano de Investigación Pesquera y Acuacultura Sustentables, Puerto Morelos, Quintana Roo, Mexico*

https://zoobank.org/4673419C-6522-4F53-B29B-02D8C34CA701

Corresponding author: Luis Fernando Del Moral-Flores (delmoralfer@gmail.com)

Academic editor: Ronald Fricke ♦ **Received** 18 January 2024 ♦ **Accepted** 4 March 2024 ♦ **Published** 20 May 2024

Citation: Del Moral-Flores LF, Wakida-Kusunoki AT, Ramos-Hernández R, George-Zamora A (2024) First records of two species of snake eels, *Aplatophis chauliodus* and *Ophichthus hyposagmatus* (Actinopterygii: Anguilliformes: Ophichthidae), from Mexico. Acta Ichthyologica et Piscatoria 54: 103–108. https://doi.org/10.3897/aiep.54.119085

Abstract

We report herewith the presence of two species of rare snake eels, *Aplatophis chauliodus* Böhlke, 1956 (499 mm in total length [TL]) and *Ophichthus hyposagmatus* McCosker et Böhlke, 1984 (486 mm TL), in Mexican waters of the Gulf of Mexico. Both species were caught using bottom longline at a depth of 50 to 100 m in sandy bottoms in Veracruz, Mexico. Both records are the first for Mexico and the westernmost in the Gulf of Mexico.

Keywords

first country record, Gulf of Mexico, range extension, snake eel, taxonomy, western Atlantic

Introduction

The family Ophichthidae includes fishes commonly known as worm eels, sand eels, shrimp eels, and snake eels (McCosker 2002; Robertson et al. 2023). They prefer coastal habitats in tropical and temperate waters around the world, from the intertidal zone to depths approximating 1300 m. They are mainly marine organisms but some species can also be found in a freshwater environment. They are associated with sandy, muddy bottoms and coral reefs (McCosker 2010; Nelson et al. 2016). The family is characterized by an elongated, cylindrical body, lack of scales, subterminal or lower mouth, pointed or rounded snout, presence of lateral line, separate nostrils, and the anterior nostril in tube shape (McCosker 2002), as well as other diagnostic features: numerous branchiostegal rays and overlapping in the midventral region, united supraorbital canals, presence of supratemporal canals, in adults the frontals fused along their entire length, only the first basibranchial is ossified, first epibranchial connected to the second infrapharyngobranchial by a strip of cartilage, the third hypobranchial is usually cartilaginous, reduction or absence of neural spines, without palatines and pterygoids separated from vomer (McCosker 1977; McCosker et al. 1989).

The ophichthids are one of the most diverse families within the order Anguilliformes and are usually captured for human consumption with some being used as ornamental species (McCosker 2002; Owfi et al. 2014). The family is represented by 62 genera and 364 valid species worldwide (Fricke et al. 2024), and in the Gulf of Mexico, 15 genera with 33 species have been recorded, of which the largest number of species have been recorded in the northern part representing the USA (McEachran and Fechhelm 1998; McEachran 2009). In the western Atlantic, the family was reviewed by McCosker et al. (1989). Several of the recorded species, such as *Aplatophis chauliodus* Böhlke, 1956 and *Ophichthus hyposagmatus* McCosker et Böhlke, 1984 are known from few specimens and much of their biology is unknown.

The fangtooth snake eel, *Aplatophis chauliodus*, was described based on two specimens collected in the Bay of Mayagüez, Puerto Rico, and one specimen from Panama (Böhlke 1956). Subsequently, there were a few records from the Caribbean, to Suriname, including the northern Gulf of Mexico (McCosker et al. 1989; Cervigón 1991; McEachran and Fechhelm 1998). On the other hand, the other species, the faintsaddled snake eel, *Ophichthus hyposagmatus*, has a few records, and is known mainly from the type series; the holotype was collected on the north of the Gulf of México (McCosker and Böhlke 1984). In this paper, we report the presence of these two species in the Mexican area for the first time.

Materials and methods

During the period from January 2021 to October 2023, several catches of anguilliform fish were made in the coastal area of southern Veracruz, near Barra de Sontecomapan. These specimens are used as bait for shark fishing in the region. The fishing gear used is a bottom longline, with a length of 1500 m, and 5 m snood, with 500 number 8 hooks that operate between 50 and 100 m of depth. Two specimens of snake eels were found during this fishing operation and were determined by species with specialized keys (McCosker et al. 1989; McEachran and Fechhelm 1998; McCosker 2002).

Basic morphological measurements were taken from each specimen by calipers based on measurements outlined by Böhlke (1989) and expressed as percentage of total length [% of TL] or head length [% of HL] for comparison with previously published species information (McCosker et al. 1989; Cervigón 1991; Sampaio et al. 2017). The vertebral number was counted on X-ray images. The vertebral formula and cephalic pores were followed by Böhlke (1989) and McCosker et al. (1989). Specimens were fixed with formalin (10%) and preserved in ethyl alcohol (70%) within the Ichthyological Collection of the Facultad de Estudios Superiores Iztacala, Universidad Nacional Autónoma de México under catalog numbers CIFI-1909 and CIFI-2391.

Results

Family Ophichthidae
Subfamily Ophichthinae
Genus *Aplatophis* Böhlke, 1956

Aplatophis chauliodus Böhlke, 1956

English common name: fangtooth snake eel

Spanish common name: Culebra colmilluda

Fig. 1; Table 1

Aplatophis chauliodus Böhlke, 1956.—Böhlke (1956): 3 (Type locality: Mayagüez pier, Puerto Rico).

Material examined. CIFI-2391, 1 specimen (499 mm TL); ca. 8.5 km to the North of Barra de Sontecomapan, Catemaco, Veracruz, Mexico; 18°37′58″N, 094°58′38″W (Fig. 2); 15 Sep. 2023; Armando Campos Pérez leg.

Description. Morphometric data presented in Table 1. Body elongated, cylindrical, without scales. Head length 10.6% of TL, its dorsal margin concave towards snout region; mouth large, with opening angle >90 degrees; tongue black and fleshy; lower jaw length 40.6% of HL; both jaws thin and elongated, bearing large canines; lower jaw with three anterior teeth; upper jaw with four on each side, vomer with one tooth, maxillary teeth in two rows. Snout short and pointed, length 11.7% of HL. Eyes small with diameter 2.9% of HL. Nostrils together, with anterior one tubular, situated in front and below eyes; posterior one elliptical. Trunk large and robust, length 37.5% of TL, with its tail rigid, length 47.8% of TL. Pectoral fin small, length 14.8% of HL, slightly larger than gill slit. Cephalic pores: preoperculomandibular 6 + 2, infraorbital 4 + 2, supraorbital 1 + 2. Total vertebrae 108, predorsal vertebrae 15, preanal vertebrae 54.

Coloration (fresh). Mottled whitish brown, with stronger tonality in dorsal and cephalic region, while more whitish in ventral region. Oral cavity, tongue, and lower jaw dark. In distal portion edges of dorsal and anal fins black.

Genus *Ophichthus* Ahl, 1789

Ophichthus hyposagmatus McCosker et Böhlke, 1984

English common name: faintsaddled snake eel

Spanish common name: Lairón menor

Fig. 3; Table 1

Ophichthus hyposagmatus McCosker et Böhlke, 1984.—McCosker and Böhlke (1984): 24 (Type locality: Gulf of Mexico, South of Destin, Florida.)

Material examined. CIFI-1909, 1 specimen (486 mm TL); ca. 8.1 km to the North of El Carrizal, Catemaco, Veracruz; Mexico; 18°37′15.6″N, 094°55′01.0″W (Fig. 4); 7 Oct. 2021; Armando Campos Pérez leg.

Table 1. Comparative morphometrics data of *Aplatophis chauliodus* and *Ophichthus hyposagmatus* collected in Mexico with previous records.

Character	*Aplatophis chauliodus*				*Ophichthus hyposagmatus*	
	Mexico	**Western Atlantic**	**Venezuela**	**Brazil**	**Mexico**	**Western Atlantic, Type series**
	***n* = 1**	***n* = 10**	***n* = 3**	***n* = 1**	***n* = 1**	***n* = 6**
Absolute values [mm]						
Total length (TL)	499.0	168.0–804.0	566.0–847.0	670.0	486.0	357.0
Predorsal length	130.7	—	—	180.0	64.8	53.0
Head length	72.8	—	—	103.6	51.7	40.0
Trunk length	187	—	—	342.0	168.0	122.0
Tail length	239	—	—	—	268.0	195.0
Preanal length	263	—	—	370.0	218.0	—
Snout length	8.5	—	—	22.5	10.6	9.5
Upper jaw length	30.5	—	—	40.9	22.7	—
Lower jaw length	32.4	—	—	42.3	21.0	—
Orbital diameter	2.1	—	—	4.1	6.2	5.2
Interorbital width	8.5	—	—	—	7.8	4.1
Pectoral fin length	10.8	—	—	16	14.3	11.9
Base of pectoral fin	—	—	—	—	4.6	3.3
Body depth at gill opening	26.2	—	—	32.6	21.3	11.0
Body depth at level of pectoral fins	23.6	—	—	38.6	20.9	—
Body depth at anus	25.2	—	—	38.3	20.3	13.0
Body width at anus	—	—	—	—	16.8	11.2
Gill opening length	—	—	—	—	8.9	6.8
Relative values [% of TL]						
Head length	14.6	14.0–16.0	14.4–16.0	15.5	10.6	11.0–12.0
Trunk length	37.5	34.0–39.0	—	—	34.6	31.0–35.0
Tail length	47.9	46.0–49.0	—	—	55.1	53.0–57.0
Predorsal length	26.2	25.0–28.0	—	—	13.3	14.0–16.0
Body depth (pectoral fins)	4.3	—	5.4–5.6	5.8	4.3	—
Body depth (gill openings)	5.3	—	—	—	4.4	2.9–4.5
Body depth (anus)	5.1	—	4.8–5.1	5.7	4.2	—
Snout length	1.7	—	2.3–2.7	3.3	2.2	—
Orbital diameter	0.4	—	0.3–0.8	0.6	1.3	—
Upper jaw length	6.1	—	8.2	6.1	4.7	—
Lower jaw length	6.5	—	9.4	6.3	4.3	—
Pectoral fin length	2.2	—	2.3–2.6	2.4	2.9	—

Mexico = this study, Western Atlantic (for *Aplatophis chauliodus*) = McCosker et al. (1989), Venezuela = Cervigón (1991), Brazil = Sampaio et al. (2017), Western Atlantic (for *Ophichthus hyposagmatus*) = McCosker and Böhlke (1984); McCosker et al. (1989).

Description. Morphometric data presented in Table 1. Elongated body, without scales and cylindrical body on transverse axis; trunk shorter than tail region (34.6% of TL); tail length 55.1% of TL. Head length moderate, 10.6% of TL; snout conical, length 20.5% of HL, larger than eye diameter; eyes large, length 12.0% of HL; interorbital region flat, its width 15.1% of HL. Two nostrils, with anterior nostril tubular and posterior nostril covered by a flap. Mouth inferior, upper jaw slightly larger than snout, length 43.9% of HL; both jaws with two rows of subequal conical teeth; series of vomerine teeth. Dorsal-fin origin above posterior part of pectoral fins, predorsal distance 13.3% of TL; pectoral fins elongated and larger than eye, length 27.7% of HL. Cephalic pores: preoperculomandibular 6 + 3, infraorbital 4 + 2, supraorbital 1 + 3. Total vertebrae 138, predorsal vertebral 12, preanal vertebral 55.

Coloration (fresh). Body yellowish brown, with whitish shades in ventral region and with greater intensity on dorsum; 16 brown bars that contrast as saddles on dorsum; dorsal region of snout and interorbital space dark brown. Pectoral and dorsal fins translucent, with light brownish shades.

Discussion

The morphology and measurements of both species are consistent with the diagnoses reported for each of them in the western Atlantic (Table 1). Except for the snout length of the *Aplatophis chauliodus* specimen, which was smaller than that in previous reports (1.7 vs. 2.3%–3.3% of TL). This may be a natural variation within the population, due to the extensive modification of the upper jaw (McCosker et al. 1989). This is also one of the possible explanations for the variations observed in the specimen reported from Brazil (Sampaio et al. 2017). The number of total vertebrae observed in this specimen was lower than that reported for

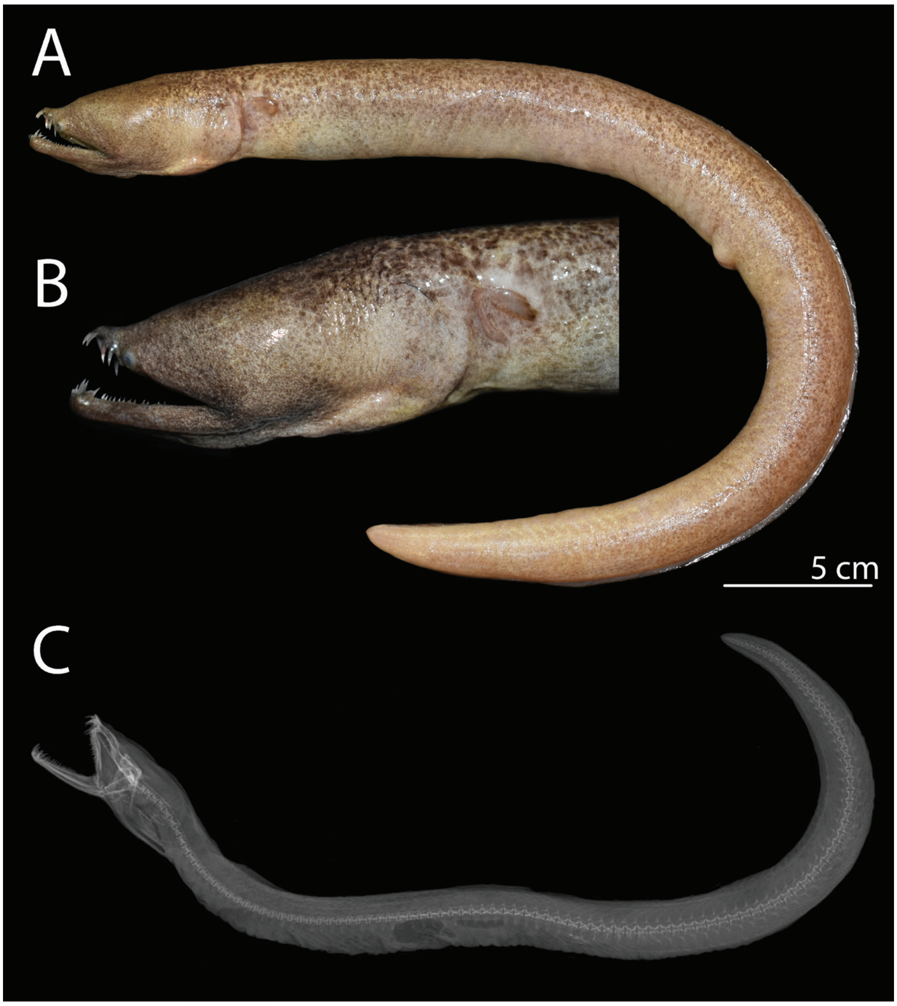

Figure 1. *Aplatophis chauliodus* (CIFI-2391, 499 mm TL) collected off the coasts of Mexico. (**A**) Freshly caught specimen. (**B**) A close-up of the cephalic region. (**C**) X-ray of the entire specimen.

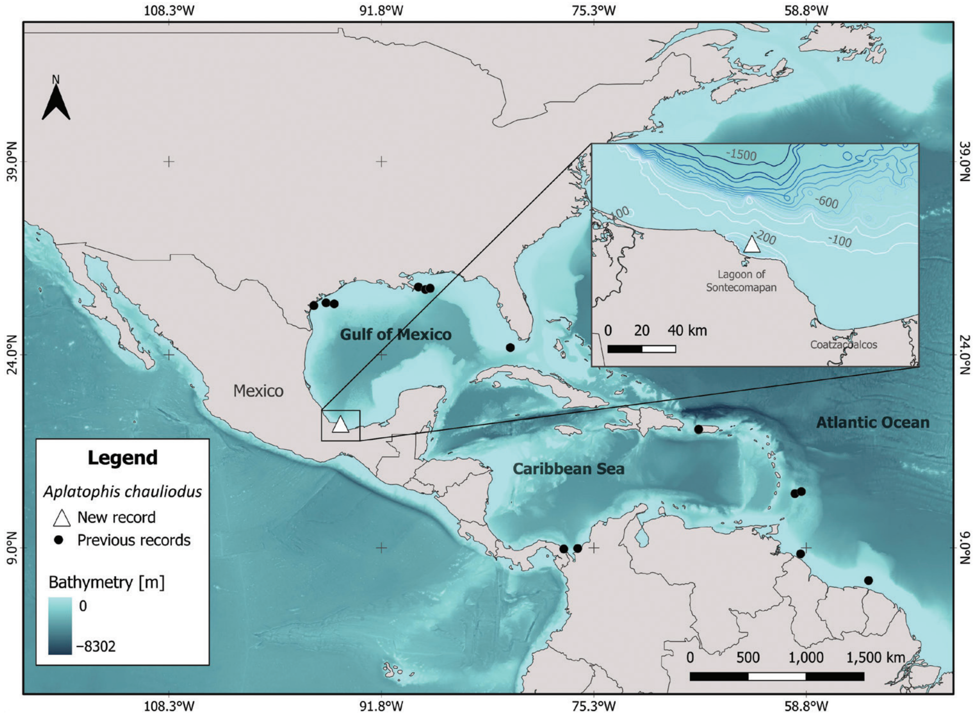

Figure 2. Map showing the distribution in previous records (circles) in the western Atlantic and new record (triangle) of *Aplatophis chauliodus* in Mexico.

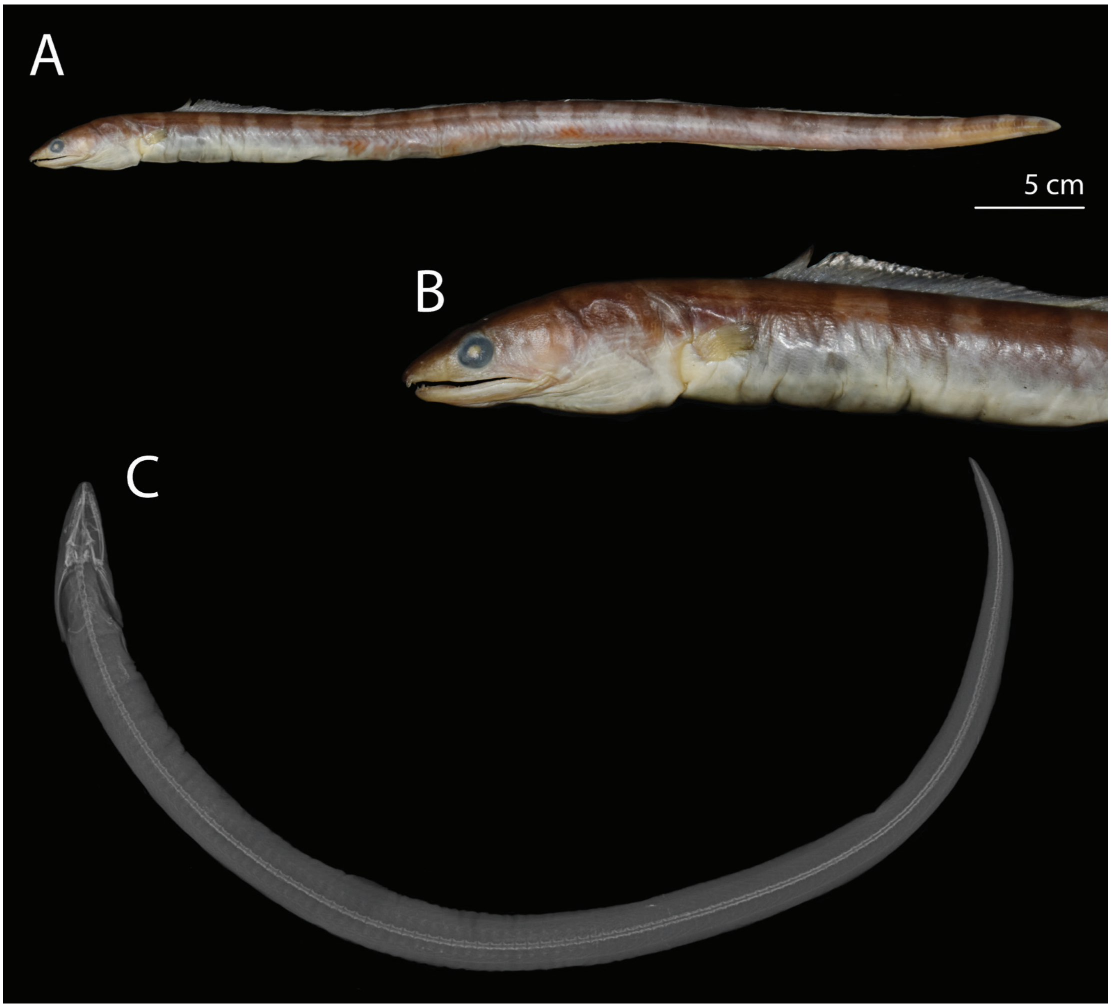

Figure 3. *Ophichthus hyposagmatus* (CIFI-1909, 486 mm TL) collected off the coasts of Mexico. (**A**) Preserved specimen. (**B**) A close-up of the cephalic region. (**C**) X-ray of the entire specimen.

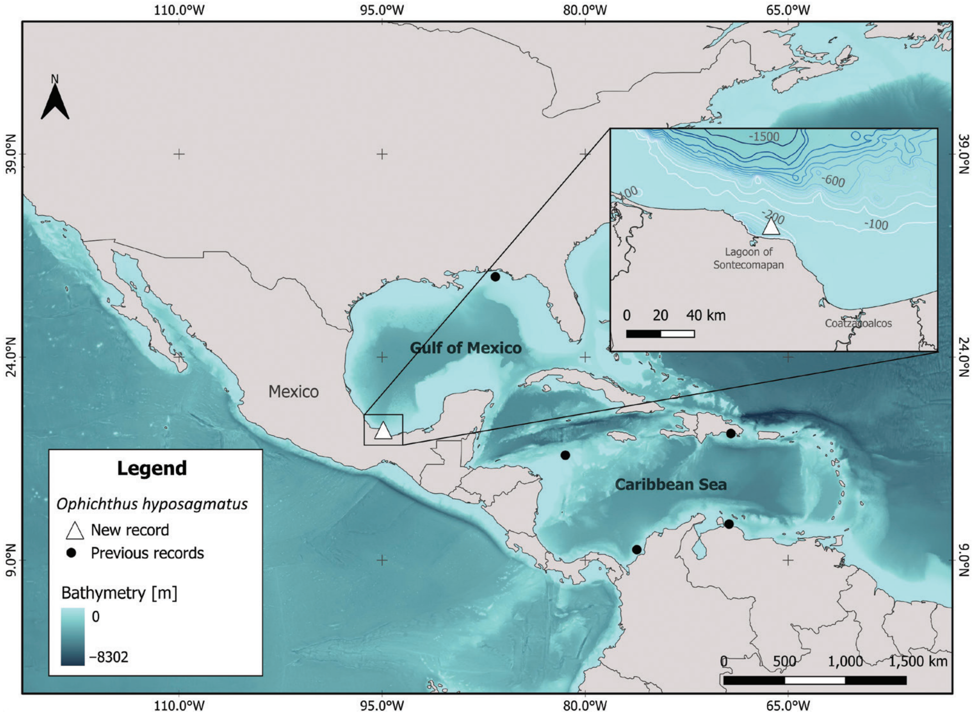

Figure 4. D Map showing the distribution in previous records (circles) in the western Atlantic and new record (triangle) of *Ophichthus hyposagmatus* in Mexico.

the species (108 vs. 110–115) by McCosker et al. (1989), so it is necessary to evaluate possible morphological variation throughout its geographic distribution.

In the case of *Ophichthus hyposagmatus*, so far only six specimens are known to have been captured in the western Atlantic, at depths ranging from 88 to 293 m (McEachran and Fechhelm 1998). According to previous reports of its morphometry, a shorter head length was observed, which may be related to allometric growth, as has been reported in some species of the family Ophichthidae (see Sangun et al. 2007).

The presently reported specimens of *O. hyposagmatus* are smaller than 386 mm TL, indicating that a mature male and female have been found smaller than 400 mm TL (McCosker and Böhlke 1984; McCosker et al. 1989). The Mexican specimen represents a new record in size (486 mm TL) and represents a mature individual. It also represents the second record from the Gulf of Mexico, because the holotype was captured south of Destin, Florida, 29°56′N, 086°38′W (McCosker et al. 1989). Therefore, the Mexican record increases its range by about 1500 km to the Southwestern Gulf of Mexico. In the case of the Mexican record of *A. chauliodus* the range increases by almost 1035 km to the Southeast, from the known records in Texas, USA (McCosker et al. 1989). This shows how little is known about the biology, distribution, and ecology of both species.

Acknowledgments

We would like to thank the community of Salinas Roca Partida, Ver., for the facilities of the fieldwork, A. Campos Pérez for the capture and donation of the specimens contributed, and the SNI-CONAHCyT Program for the support granted. To anonymous reviewers for suggestions that helped improve this paper.

References

Böhlke JE (1956) A small collection of new eels from western Puerto Rico. Notulae Naturae of the Academy of Natural Sciences of Philadelphia (289): 1–13.

Böhlke EB (1989) Methods and terminology. Pp. 1–7. In: Böhlke EB (Ed.) Fishes of the Western North Atlantic. Part Nine. Vol. 1. Orders Anguilliformes and Saccopharyngiformes. Yale University, Sears Foundation for Marine Research. https://doi.org/10.12987/9781933789323-003

Cervigón F (1991) Los peces marinos de Venezuela. Segunda edición. Vol. 1. 2a. Fundación Científica Los Roques, Caracas, Venezuela, 425 pp.

Fricke R, Eschmeyer WN, Fong JD (2024) Eschmeyer's catalog of fishes: Genera/species by family/subfamily. California Academy of Sciences, San Francisco, CA, USA. [Online version, updated 15 Mar 2024.] http://researcharchive.calacademy.org/research/ichthyology/catalog/SpeciesByFamily.asp

McCosker JE (1977) The osteology, classification, and relationships of the eel family Ophichthidae. Proceedings of the California Academy of Sciences (Series 4) 41(1): 1–123.

McCosker JE (2002) Ophichthidae. Snake eels (shrimp eels, worm eels, and sand eels). Pp. 724–733. In: Carpenter KE (Ed.) The living marine resources of the Western Central Atlantic. Vol. 2. Bony fishes Part 1 (Acipenseridae to Grammatidae). FAO Species Identification Guide for Fishery Purposes and American Society of Ichthyologists and Herpetologists Special Publication 5, FAO, Rome.

McCosker JE (2010) Deepwater Indo–Pacific species of the snake-eel genus *Ophichthus* (Anguilliformes: Ophichthidae), with the description of nine new species. Zootaxa 2505(1): 1–39. https://doi.org/10.11646/zootaxa.2505.1.1

McCosker JE, Böhlke EB (1984) Three new species of western Atlantic snake eels (Pisces: Ophichthidae) of the genus *Ophichthus*. Proceedings. Academy of Natural Sciences of Philadelphia 136: 24–31.

McCosker JE, Böhlke EB, Böhlke JE (1989) Family Ophichthidae snake eels and worm eels. Pp. 254–412. In: Böhlke EB (Ed.) Fishes of the Western North Atlantic. Part Nine. Vol. 1. Orders Anguilliformes and Saccopharyngiformes. Yale University, Sears Foundation for Marine Research. https://doi.org/10.12987/9781933789323-012

McEachran JD (2009) Fishes (Vertebrata: Pisces) of the Gulf of Mexico. Pp. 1223–1316. In: Felder DL, Camp DK (Eds.) Gulf of Mexico–Origins, Waters, and Biota. Biodiversity. Texas A&M Press, College Station, TX, USA.

McEachran JD, Fechhelm JD (1998) Fishes of the Gulf of Mexico. Vol. 1: Myxiniformes to Gasterosteiformes. University of Texas Press, Austin, TX, USA, 1112 pp. https://doi.org/10.7560/752061

Nelson JS, Grande TC, Wilson MVH (2016) Fishes of the world. John Wiley and Sons, Inc., Hoboken, NJ, USA, 707 pp. https://doi.org/10.1002/9781119174844

Owfi F, Fatemi MR, Motallebi AA, Coad B (2014) Systematic review of Anguilliformes order in Iranian Museums from the Persian Gulf and Oman Sea. Iranian Journal of Fisheries Science 13(2): 407–426.

Robertson DR, Peña EA, Posada JM, Claro R (2023) Fishes: Greater Caribbean. A guide to the shorefishes of the Caribbean and adjacent areas. Version 3.0 Smithsonian Tropical Research Institute, Balboa, Panamá. https://biogeodb.stri.si.edu/caribbean/es/pages

Sampaio CLS, Duarte Lopes PR, de Oliveira-Silva JT (2017) First record of *Aplatophis chauliodus* (Actinopterygii: Ophichthidae) for the northeastern coast of Brazil, with expansion of its geographic range. Revista Brasileira de Zoociências 18(2): 119–122. https://doi.org/10.34019/2596-3325.2017.v18.24670

Sangun L, Akamca E, Akar M (2007) Weight–length relationships for 39 fish species from the north-eastern Mediterranean coast of Turkey. Turkish Journal of Fisheries and Aquatic Sciences 7(1): 37–40.

Acta Ichthyologica et Piscatoria 54, 2024, 109–114 | DOI 10.3897/aiep.54.117474

PENSOFT.

ACTA
ICHTHYOLOGICA
ET PISCATORIA

New report and range extension of invasive suckermouth armored catfishes of the genus *Pterygoplichthys* (Actinopterygii: Siluriformes: Loricariidae) in the Yucatan Peninsula

Miriam SORIA-BARRETO[1], Demián HINOJOSA-GARRO[1], Jesús Elías GARCÍA-LÓPEZ[1], Ricardo Efraín GÓNGORA CHIN[1]

1 *Laboratorio de Ecología Acuática y Monitoreo Ambiental, Centro de Estudios en Desarrollo Sustentable y Aprovechamiento de la Vida Silvestre (CEDESU), Universidad Autónoma de Campeche, San Francisco de Campeche, Campeche, Mexico*

https://zoobank.org/2B3E5EBF-1BBB-49E4-A7E1-B9C0F489671A

Corresponding author: Demián Hinojosa-Garro (dhinojos@uacam.mx)

Academic editor: Jan Kotusz ♦ **Received** 16 December 2023 ♦ **Accepted** 2 March 2024 ♦ **Published** 20 May 2024

Citation: Soria-Barreto M, Hinojosa-Garro D, García-López JE, Góngora Chin RE (2024) New report and range extension of invasive suckermouth armored catfishes of the genus *Pterygoplichthys* (Actinopterygii: Siluriformes: Loricariidae) in the Yucatan Peninsula. Acta Ichthyologica et Piscatoria 54: 109–114. https://doi.org/10.3897/aiep.54.117474

Abstract

Commonly known as suckermouth armored catfishes or pleco, *Pterygoplichthys* spp. are a group of invasive fishes that are widely distributed in several countries, including Mexico. This paper reports the first records of suckermouth armored catfishes in the Candelaria River, thereby expanding its distribution within the Yucatan Peninsula. Fifteen individuals were collected from three sites in the upper and middle parts of the basin. They represented two phenotypically distinct species of catfishes: (vermiculate) *Pterygoplichthys disjunctivus* (Weber, 1991) and (spotted) *Pterygoplichthys pardalis* (Castelnau, 1855). Adults and juveniles were caught in lotic ecosystems in 2023 during the dry and rainy seasons. Results suggest that the invasive process of the Candelaria River is linked to the San Pedro River upper basin, in El Petén, Guatemala, through floodings enhanced by hurricanes, allowing these species to disperse. These records highlight the importance of connectivity between adjacent watersheds for the dispersal and expansion of these invasive fishes, mainly from rivers neighboring Guatemala. However, further research is necessary to explore the dynamics and connectivity between aquatic ecosystems and the possible mechanisms that promote the invasion of these fishes in this region.

Keywords

alien species, Candelaria River, connectivity, dispersion, Guatemala, Mexico

Introduction

The suckermouth armored catfishes are freshwater fishes native to Costa Rica, Panama, and South America and representing the Loricariidae family, the most diverse of the Siluriformes (see Nelson et al. 2016). Several species of loricariids are commercialized and are of economic interest as aquarium fishes (Courtenay and Stauffer 1990; Hoover et al. 2014). They are commonly known as pleco or loricariids, and including the genus *Pterygoplichthys* Gill, 1858 (see Mendoza et al. 2009). These suckermouth armored catfishes are invasive species that have been introduced into various freshwater ecosystems in different countries. Their establishment and dispersal have been promoted through aquaculture, aquarium practices, and even by biocontrol efforts, causing diverse ecological, economic, and social impacts in aquatic ecosystems (Mendoza et al. 2009; Hoover et al. 2014).

In Mexico, the first record of the suckermouth armored catfish was in 1995 in the Mezcala River in the Balsas basin in Michoacán; subsequently, its presence was recorded in other localities in the Grijalva, Usumacinta, and Balsas River basins (Mendoza et al. 2007). Currently, *Pterygoplichthys* spp. are widely distributed, mainly in the southeastern part of the country. High abundance and wide distribution of these species have been reported in aquatic ecosystems in the Usumacinta River basin (Soria-Barreto et al. 2018) and in the lower part of the Grijalva–Usumacinta basin in the state of Tabasco (Sánchez et al. 2015). In these aquatic ecosystems, the suckermouth armored catfish has successfully established itself, modifying the riverbanks to construct its nests (Lienart unpublished[*]).

The suckermouth armored catfish was absent from the Yucatan Peninsula until 2006 (Wakida-Kusunoki and Amador-del Angel 2008). The first records were in effluents of the Usumacinta River: the San Pedro and San Pablo River, which is the western limit of the Yucatan Peninsula, and in the delta of the Palizada River at Laguna de Términos (Wakida-Kusunoki and Amador-del Angel 2008). Later, its presence was recorded in the Pom–Atasta fluvial lagoon system in Laguna de Términos (Ayala-Pérez et al. 2014). In these aquatic ecosystems, suckermouth armored catfishes are an abundant component of the ichthyofauna (Wakida-Kusunoki and Amador-del Ángel 2011) and have established reproductive populations (Ayala-Pérez et al. 2014). They have exhibited changes in density associated with seasonal changes in the area. For example, during the rainy season, the overflow of the Palizada River allows young suckermouth armored catfishes to colonize nearby pools, in which it interacts with local fish fauna (Escalera-Vázquez et al. 2019).

In recent years, there has been evidence of the eastward dispersion of the armored suckermouth catfishes in the Yucatan Peninsula. For instance, in the Hondo River (Mexico–Belize), the dispersion and establishment of *P. pardalis* was documented over one year. The invasion process was favored by flooding and inter-basin connectivity, mainly from Lake Petén in Guatemala (Schmitter-Soto et al. 2015). Similarly, Álvarez-Pliego et al. (2015) reported that the armored suckermouth catfish is already present in the Chumpan River basin. The invasion source seems to be associated with the Grijalva–Usumacinta basin, a nearby watershed, through an eastward dispersal process across Laguna de Términos. Thus, it is necessary to increase sampling efforts in unexplored aquatic ecosystems to verify the presence of these invasive species, as well as to evaluate their possible effects on environmental variables and the aquatic communities it invades. Therefore, a fish survey was conducted in the Candelaria River basin, the largest basin in the Yucatan Peninsula, to document the presence of suckermouth armored catfishes.

Materials and methods

Study area. The study area was in the Candelaria River in the Yucatan Peninsula, Mexico. The Candelaria River is a basin shared by Guatemala and Mexico. It originates in El Petén in northern Guatemala, flows through the western portion of the state of Campeche in Mexico, and drains into the Natural Protected Area for Flora and Fauna Laguna de Términos, a large brackish lagoon in the Gulf of Mexico. In Guatemala, the river runs for approximately 50 km, and the basin covers 1158 km^2 of its surface area (Gunn et al. 1995). In Mexico, the river is 150 km long, and the basin has a surface area of 10525 km^2 (CONAGUA 2018). The basin is in a semi-karst zone of the Yucatan Peninsula, characterized by the presence of lagoons, rivers, cenotes, and groundwater sources (Gunn et al. 1995). The river flows through rainforest areas and wetlands to the coastal zone, which is characterized by the absence of significant topography (Hudson et al. 2005). This area presents a mean elevation of 200 m AMSL, surrounded by hills up to 380 m AMSL on the eastern side (Gunn et al. 1995). The climate is warm and subhumid with summer rains. The air temperature recorded in the town of Candelaria ranges from 24–28°C, and annual precipitation ranges from 1200–2000 mm (INEGI 2010). The Candelaria River is the most important and largest river in the Yucatan Peninsula. The river flows from the southeast to the north and has important tributaries, such as the Rivers Caribe, La Esperanza, and Las Golondrinas (Gunn et al. 1995). According to data from the CONAGUA hydrometric station 30181 Candelaria, from 2012–2020 the flow of Candelaria River varied from 3.2–395.4 m$^3 \cdot$ s^{-1}, with a mean volume of 40.5 m^3 $\cdot$ s^{-1}, with a mean water temperature of 28.4°C and mean dissolved oxygen concentration of 5.5 mg $\cdot$ L^{-1}. The main channel, the Candelaria River, flows with the Mamantel River into the Panlau Lagoon to the Candelaria–Panlau fluvial lagoon system (Ayala-Pérez et al. 1998; Hudson et al. 2005). In this lagoon system, water temperature ranges between 23.9 to 30.7°C, dissolved oxygen between 3.6 to 6.7 mg $\cdot$ L^{-1}, and surface salinity between 2.4‰ and 18.2‰[**] (Ramos-Miranda et al. 2006). Candelaria River plays a key ecological role based on the amount of water it supplies due to the conservation status of its vegetation, the presence of natural reserves, and the low population density (Kauffer 2010).

Sampling and laboratory methods. Sampling was conducted during the dry and early rainy seasons of 2023. Six sites were selected along the Candelaria River (Fig. 1). At each site, temperature [°C], dissolved oxygen concentration [mg $\cdot$ L^{-1}], conductivity [mS $\cdot$ cm^{-1}], total dissolved

---

[*] Lienart GDH (2010) Biología reproductiva de la especie exótica invasora *Pterygoplichthys pardalis* (Siluriformes: Loricariidae) en los humedales de La Libertad (sitio RAMSAR No. 79), Río Usumacinta, Chiapas, México. MSc Thesis. El Colegio de la Frontera Sur, San Cristóbal de Las Casas, Chiapas, Mexico.

[**] In the wake of the growing criticism of the Practical Salinity Scale concept (and especially "PSU" as a "unit"), Acta Ichthyologica et Piscatoria is in favor of expressing salinity in parts per thousand [‰], regardless if a direct or indirect method was employed to determine the water salinity.

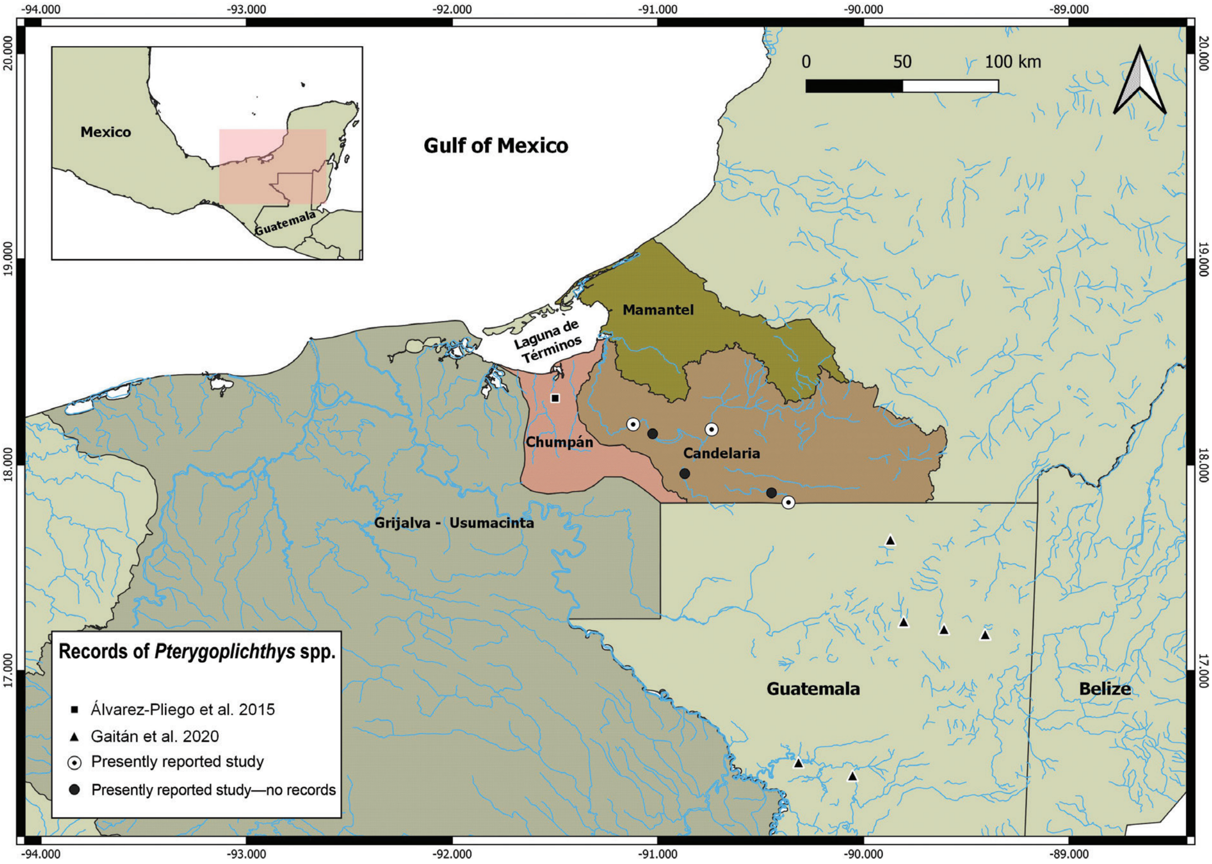

Figure 1. Sampling sites of *Pterygoplichthys* spp. in the Candelaria River basin, Mexico; including *Pterygoplichthys* records in the Chumpan River basin (Álvarez-Pliego et al. 2015) and aquatic ecosystems in Guatemala (Gaitán et al. 2020).

solids (TDS) [$\mathrm{mg \cdot L^{-1}}$], and salinity [‰] were recorded with a YSI model 556 multiparameter instrument. Fish were caught during the day, using cast nets (2 m diameter and 1 cm mesh; five throws at each site) and gill nets (55 m long × 2.5 m high, 2.5–9.0 cm mesh; four hours at each site). Caught fish were preserved in a cooler box until they were placed in freezers at the Laboratorio en Ecología Acuática y Monitoreo Ambiental (LEAMA) at CEDESU. In the laboratory, each fish was weighed with an Acculab VIC-303 precision balance. The standard (SL) was recorded using a 0.1 mm precision Vernier caliper. The ventral coloration pattern of the vermiculate or spotted allowed taxonomic determination of the species as *Pterygoplichthys disjunctivus* (Weber, 1991) and *Pterygoplichthys pardalis* (Castelnau, 1855), respectively (Armbruster and Page 2006). According to the minimum spawning size reported for the Usumacinta River basin, fishes smaller than 195 mm SL were considered juveniles (Lienart unpublished). Subsequently, the specimens were preserved in formalin solution, then washed with running water, and preserved in 70% ethyl alcohol to be deposited in the fish collection of El Colegio de la Frontera Sur (ECOSC) with the following catalog numbers: 14894, 14895, and 14896.

Results

A total of 15 fish specimens were caught. Eleven fish were caught in two tributaries: ten individuals in the La Esperanza River (17.81768557°N, 90.36463064°W) and one individual in the Caribe River (18.172344°N, 90.738351°W). Four individuals were caught in the main channel of the Candelaria River (18.19723276°N, 91.11979406°W). Fish measured 126.2–257 mm in SL and weighed 39–330 g. Based on ventral pattern five fish were identified as *P. disjunctivus* and ten as *P. pardalis* (Table 1, Fig. 2). Adults and juveniles of both species were caught: one adult (reproductive female) and four juveniles of *P. disjunctivus*; and five adults and five juveniles of *P. pardalis*.

Table 1. Principal biometric parameters of suckermouth armored catfishes (*Pterygoplichthys* spp.) from the Candelaria River basin.

Parameters	Ventral pattern					
	Vermiculated (*P. disjunctivus*) *n* = 5			Spotted (*P. pardalis*) *n* = 10		
	Mean	SD	Range	Mean	SD	Range
Standard length [mm]	174.0	39.8	126.2–226.0	193.8	31.4	148.0–257.0
Weight [g]	115.2	77.3	39.3–236.9	149.0	68.3	69.7–300.0

n = number of individuals, SD = standard deviation.

Individuals were caught in environments with rocky and muddy bottoms. The temperatures varied from 28.2 to 30.2°C, salinity from 0.7‰ to 1.3‰, dissolved oxygen concentrations from 2.2 to 6.3 $\mathrm{mg \cdot L^{-1}}$, electrical conductivity from 1.6 to 2.7 $\mathrm{mS \cdot cm^{-1}}$, and TDS from 962 to 1772 $\mathrm{mg \cdot L^{-1}}$ (Table 2).

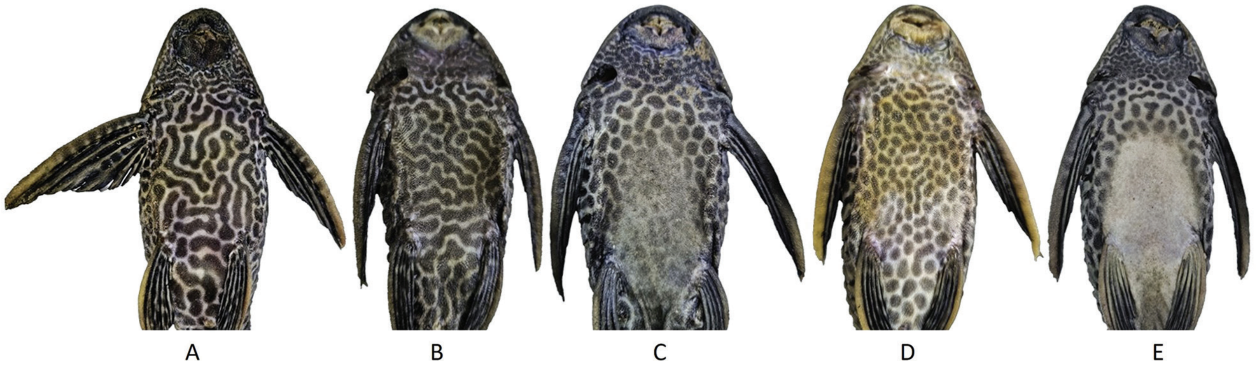

Figure 2. Variation of the ventral pattern of *Pterygoplichthys* spp. in the Candelaria River basin, Campeche. Vermiculate coloration pattern (*P. disjunctivus*) (**A, B**), spotted coloration pattern (*P. pardalis*) (**C–E**).

Table 2. Environmental description and physicochemical properties of sampling sites for the suckermouth armored catfishes (*Pterygoplichthys* spp.) in the Candelaria River, Mexico.

Sampling site	Date	Substrate	Temperature [°C]	DO [mg · L^{-1}]	Salinity [‰]	Conductivity [mS · cm^{-1}]	TDS [mg · L^{-1}]
La Esperanza River, tributary of Candelaria River at San Dimas, Campeche	25 Apr 2023	Rocky	28.7 ± 1.0	3.8 ± 1.1	0.7 ± 0.0	1.6 ± 0.0	968.3 ± 5.7
	30 May 2023		28.2 ± 0.7	2.2 ± 0.7	1.3 ± 0.0	2.7 ± 0.0	1772.0 ± 167.2
Caribe River, tributary of Candelaria River at El Pedregal, Campeche	2 Mar 2023	Soft-muddy	29.9 ± 1.6	6.0 ± 0.5	1.0 ± 0.0	1.8 ± 0.5	1226.7 ± 18.9
Candelaria River at protected area Salto Grande, Campeche	24 Apr 2023	Soft-muddy	30.3 ± 0.0	6.3 ± 0.3	0.7 ± 0.0	1.6 ± 0.0	962.0 ± 1.0
	31 May 2023		31.8 ± 0.6	6.0 ± 0.1	1.3 ± 0.0	2.6 ± 0.3	1620.0 ± 3.0

DO = dissolved oxygen, TDS = total dissolved solids. Values represent the mean ± standard deviation.

Discussion

This work confirms the presence of *Pterygoplichthys* spp. in the Candelaria River. In Mexico, suckermouth armored catfishes are invasive species, especially in the lower part of the Grijalva–Usumacinta basin (Sánchez et al. 2015; Soria-Barreto et al. 2018). Recently, they have been reported in the Chumpan (Álvarez-Pliego et al. 2015) and Hondo rivers in the Yucatan Peninsula (Schmitter-Soto et al. 2015). Their presence in the Candelaria River suggests a range extension within the Yucatan Peninsula. Only 15 individuals were caught, which suggests that the abundance of these species remains low in the basin. However, the presence of adults in the reproductive stage could facilitate its establishment and fast dispersal (Mendoza et al. 2009).

The habitats showed freshwater conditions, with high values of electrical conductivity and total dissolved solids (TDS), which may be a result of the semikarstic nature of the Candelaria River basin (Gunn et al. 1995). Similar values have been reported by CONAGUA at hydrometic station 30181 Candelaria, and in the lower part of the basin (Álvarez-Pliego et al. 2015). Some sites had a low oxygen concentration (~2 mg · L^{-1}). However, this parameter is not a limiting factor for these invasive species due to their anatomical and physiological characteristics, which allow them to obtain oxygen from the air (Mendoza et al. 2009; Hoover et al. 2014).

In the Palizada River, the fish gonad maturation is associated with the flooding pulses (Ayala-Pérez et al. 2014). In other aquatic environments, sexual maturation of suckermouth armored catfishes varies between habitats; however, they are likely to breed at smaller sizes (Hoover et al. 2014). For instance, the size at gonadic maturity for 50% of the population reported in the Las Ilusiones Lagoon in the Grijalva River basin was less than 195 mm SL (Hernández unpublished[*]). Therefore, it is important to evaluate the population structure and dynamics in the Candelaria River basin.

The ventral vermiculate or spotted coloration patterns is a key feature to determine organisms as *P. disjunctivus* or *P. pardalis*, respectively (Armbruster and Page 2006). However, recent mitochondrial DNA studies have indicated that, although suckermouth armored catfishes have highly variable coloration patterns, all the individuals from the Grijalva–Usumacinta basin belong to the same haplotype and correspond to *P. pardalis* or for a hybrid origin (Vargas-Rivas et al. 2023). Therefore, it is important to compare genetically individuals to confirm its taxonomy and possible hybridization in this area.

The distribution of the suckermouth armored catfish in the Candelaria River ranges from the middle to the upper part of the basin (Fig. 1). Dispersal and invasion into the Candelaria River basin seem to occur through connectivity with other nearby aquatic ecosystems. In 2014, there was the first record of the suckermouth armored catfish in

---

[*] Hernández SME (2008) Aspectos reproductivos del loricárido *Pterygoplichthys pardalis* (Castelnau, 1855) en la Laguna de las Ilusiones, Tabasco, Mexico. Undergraduate thesis. Universidad Juárez Autónoma de Tabasco, Villahermosa, Tabasco, Mexico.

the Chumpan River, an adjacent basin to the Candelaria River, which flows into the Laguna de Términos. Authors suggested that these species dispersed from the Grijalva–Usumacinta basin, via Laguna de Términos, enhanced by the seasonal variation in salinity and the tolerance to estuarine conditions of *Pterygoplichthys* (see Álvarez-Pliego et al. 2015). Although, the Panlau Lagoon has low salinity (2.6 ‰) during the nortes season (Ayala-Pérez et al. 1998), which could facilitate its dispersal. Conversely, it seems unlikely that it arrived in the same way as in the Chumpan River. Here salinity in the freshwater–seawater mixing zone has been reported to be higher than 18‰ (Ramos-Miranda et al. 2006), while *Pterygoplichthys* spp. salinity tolerance is down to 10‰ (Capps et al. 2011). In addition, the suckermouth armored catfish is absent in the lower part of the basin (Álvarez-Pliego et al. 2015).

The highest abundance of suckermouth armored catfishes was recorded in La Esperanza River, near the Guatemala border (Fig. 1). Local fishers and inhabitants mentioned that this invasive fish appeared around 13 years ago, after the hurricane Richard through the Yucatan Peninsula in 2010. This suggests that natural invasion occurs through the hydrological connectivity upstream and allows the dispersal of *Pterygoplichthys* spp. through this region. Given the topography of the Guatemalan Petén (Gunn et al. 1995), it is likely to get flooded by extreme rainfall caused by hurricanes and connected adjacent watersheds. This could enhance the dispersal process and invasion of *Pterygoplichthys* spp., through the inter-basin connectivity, as it has been reported for the Hondo River (Schmitter-Soto et al. 2015). If invasion and dispersal are favored by these hydrological events, the presence of suckermouth armored catfishes in the Candelaria River may be a result of the connectivity of aquatic ecosystems, particularly the San Pedro River in Guatemala. Since 2000, the presence of *Pterygoplichthys* spp. has been reported in Guatemala, and its records have increased; it currently has established populations in five sub-basins in northern Guatemala, including the nearby San Pedro basin (Gaitán et al. 2020) (Fig. 1).

The first record and presence of the invasive fish *Pterygoplichthys* spp. is reported in the Candelaria River basin, although its abundance is low, it is distributed in the upper and middle part of the basin. Its invasion and dispersal have occurred naturally, promoted by the presence of hurricanes and connectivity between watersheds in the Petén in Guatemala; the San Pedro River is the most likely source. Considering *Pterygoplichthys* spp. dispersal capacity and its negative effect on aquatic communities and environments, more sampling efforts and studies are required to understand those dispersal mechanisms in this region of Mexico, including spatiotemporal monitoring across the Candelaria basin. Finally, it is important to evaluate its possible effects on aquatic ecosystems and, consequently, on local fisheries.

Acknowledgments

We thank the Ejidos authorities for access and support during sampling activities at the study sites. We are grateful to Sergio E. Padilla Paz and Mauricio González Soria for generating Figure 1 and Figure 2, respectively. Thanks to Alfonso González for an early revision. MSB thanks CONACYT for the postdoctoral grant. We thank an anonymous reviewer for helpful comments on the manuscript.

References

Álvarez-Pliego N, Sánchez AJ, Florido R, Salcedo MÁ (2015) First record of South American suckermouth armored catfishes (Loricariidae, *Pterygoplichthys* spp.) in the Chumpan River system, southeast Mexico. BioInvasions Records 4(4): 309–314. https://doi.org/10.3391/bir.2015.4.4.14

Armbruster JW, Page LM (2006) Redescription of *Pterygoplichthys punctatus* and description of a new species of *Pterygoplichthys* (Siluriformes: Loricariidae). Neotropical Ichthyology 4(4): 401–409. https://doi.org/10.1590/S1679-62252006000400003

Ayala-Pérez LA, Avilés-Alatriste OA, Rojas-Galaviz JL (1998) Estructura de la comunidad de peces en el sistema Candelaria-Panlau, Campeche, México. Revista de Biología Tropical 46(3): 763–774. https://doi.org/10.15517/rbt.v46i3.20452

Ayala-Pérez LA, Peralta-Pineda AD, Álvarez-Guillen H, Amador-del Ángel LE (2014) El pez diablo (*Pterygoplichthys* spp.) en las cabeceras estuarinas de la Laguna de Términos, Campeche. Pp. 313–336. In: Low-Pfeng AM, Quijón PA, Peters-Recagno EM (Eds.) Especies invasoras acuáticas: casos de estudio en ecosistemas de México. SEMARNAT, INECC, UPEI, Ciudad de Mexico, Mexico.

Capps KA, Nico LG, Mendoza-Carranza M, Arévalo-Frías W, Ropicki AJ, Heilpern SA, Rodiles-Hernández R (2011) Salinity tolerance of non-native suckermouth armoured catfish (Loricariidae: *Pterygoplichthys*) in south-eastern Mexico: Implications for invasion and dispersal. Aquatic Conservation 21(6): 528–540. https://doi.org/10.1002/aqc.1210

CONAGUA (2018) Estadísticas del agua en México. Secretaría de Medio Ambiente y Recursos Naturales (SEMARNAT), Ciudad de Mexico, Mexico, 303 pp.

Courtenay WR Jr, Stauffer JR Jr (1990) The introduced fish problem and the aquarium fish industry. Journal of the World Aquaculture Society 21(3): 145–159. https://doi.org/10.1111/j.1749-7345.1990.tb01017.x

Escalera-Vázquez LH, García-López JE, Sosa-López A, Calderón-Cortés N, Hinojosa-Garro D (2019) Impact of the non-native locariid fish *Pterygoplichthys pardalis* in native fish community on a seasonal tropical floodplain in Mexico. Aquatic Ecosystem Health and Management 22(4): 462–472. https://doi.org/10.1080/14634988.2019.1700343

Gaitán CA, Fuentes-Montejo CE, García MJ, Romero-Guevara JC (2020) An update of the invasive *Pterygoplichthys* Gill, 1858 (Actinopterygii, Loricariidae) in Guatemala: New records and notes on its interactions with the local fauna. Neotropical Biology and Conservation 15(3): 285–300. https://doi.org/10.3897/neotropical.15.e53020

Gunn JD, William JF, Hubert RR (1995) A landscape analysis of the Candelaria watershed in Mexico: Insights into paleoclimates affecting upland horticulture in the southern Yucatan Peninsula semi-karst. Geoarchaeology 10(1): 3–42. https://doi.org/10.1002/gea.3340100103

Hoover JJ, Murphy CE, Killgore J (2014) Ecological impacts of suckermouth catfishes (Loricariidae) in North America: A conceptual model. Aquatic Nuisance Species Research Program 14(March): 1–20.

Hudson PF, Hendrickson DA, Benke AC, Varela-Romero A, Rodiles-Hernández R, Minckley WL (2005) Rivers of Mexico. Pp.1030–1084. In: Benke A, Cushing CE (Eds.) Rivers of North America. Academic Press, Elsevier, Burlington, MA, USA. https://doi.org/10.1016/B978-012088253-3/50026-2

INEGI (2010) Compendio de información geográfica municipal 2010 Candelaria Campeche. Instituto Nacional de Estadística y Geografía, Ciudad de Mexico, Mexico, 10 pp.

Kauffer MEF (2010) Hidropolítica del Candelaria: Del análisis de la cuenca al estudio de las interacciones entre el río y la sociedad ribereña. Relaciones 124(31): 187–226. https://doi.org/10.24901/rehs.v31i124.592

Mendoza R, Contreras S, Ramírez C, Koleff P, Álvarez P, Aguilar V (2007) Los peces diablo: Especies invasoras de alto impacto. Biodiversitas 70: 1–5.

Mendoza ARE, Cudmore B, Orr R, Fisher JP, Contreras BS, Courtenay WR, Koleff OP, Mandrak N, Álvarez TP, Arroyo DM, Escalera GC, Güevara SA, Greene G, Lee D, Orge-Mendoza A, Ramírez Martínez C, Stabridis AO (2009) Trinational risk assessment guidelines for aquatic alien invasive species. Test cases for the snakeheads (Channidae) and armored catfishes (Loricariidae) in North American inland waters. CEC Project Report. Commission for Environmental Cooperation. Montreal, Canada, 99 pp.

Nelson JS, Grande TC, Wilson VH (2016) Fishes of the world. 5th edn. John Wiley and Sons, Hoboken NJ, USA, 707 pp. https://doi.org/10.1002/9781119174844

Ramos-Miranda J, Flores-Hernández D, Ayala-Pérez LA, Rendón-von Osten J, Villalobos-Zapata G, Sosa-López A (2006) Atlas hidrológico e ictiológico de la Laguna de Términos. Universidad Autónoma de Campeche, Mexico, 173 pp.

Sánchez AJ, Florido R, Álvarez-Pliego N, Salcedo MÁ (2015) Distribution of *Pterygoplichthys* spp. (Siluriformes: Loricariidae) in the low basin of the Grijalva–Usumacinta. Revista Mexicana de Biodiversidad 86(4): 1099–1102. https://doi.org/10.1016/j.rmb.2015.06.016

Schmitter-Soto JJ, Quintana R, Valdez-Moreno ME, Herrera PRL, Esselman PC (2015) Armoured catfish (*Pterygoplichthys pardalis*) in the Hondo River, Mexico-Belize. Mesoamericana 3: 9–19.

Soria-Barreto M, González-Díaz AA, Castillo-Domínguez A, Álvarez-Pliego N, Rodiles-Hernández R (2018) Diversidad íctica en la cuenca del Usumacinta, México. Revista Mexicana de Biodiversidad 89(Suppl. 2018): S100–S117. https://doi.org/10.22201/ib.20078706e.2018.0.2462

Vargas-Rivas AG, Barba-Macias E, Sánchez AJ, Castellanos-Morales G (2023) Lack of mtDNA genetic diversity despite phenotypic variation and environmental heterogeneity in the exotic suckermouth armored catfish (*Pterygoplichthys pardalis*). Biological Invasions 25(4): 1035–1056. https://doi.org/10.1007/s10530-022-02961-w

Wakida-Kusunoki AT, Amador-del Angel LE (2008) Nuevos registros de los plecos *Pterygoplichthys pardalis* (Castelnau 1855) y *P. disjunctivus* (Weber 1991) (Siluriformes:Loricariidae) en el sureste de México. Hidrobiológica 18(3): 251–256.

Wakida-Kusunoki AT, Amador-del Ángel LE (2011) Aspectos biológicos del pleco invasor *Pterygoplichthys pardalis* (Teleostei: Loricariidae) en el río Palizada, Campeche, México. Revista Mexicana de Biodiversidad 82(2007): 870–878. https://doi.org/10.22201/ib.20078706e.2011.3.739

Acta Ichthyologica et Piscatoria 54, 2024, 115–124 | DOI 10.3897/aiep.54.118586

PENSOFT.

ACTA
ICHTHYOLOGICA
ET PISCATORIA

Taxonomic characterization of five species of emperor fishes (Actinopterygii: Eupercaria: Lethrinidae) based on external morphology, morphometry, and geographic distribution in the northwestern Indian Ocean

Ehsan DAMADI[1], Faezeh YAZDANI MOGHADDAM[2,3], Mehdi GHANBARIFARDI[4]

1 *Department of Biology, Faculty of Science, Shahid Chamran University of Ahvaz, Ahvaz, Iran*
2 *Department of Biology, Faculty of Science, Ferdowsi University of Mashhad, Mashhad, Iran*
3 *Zoological Innovations Research Department, Institute of Applied Zoology, Faculty of Science, Ferdowsi University of Mashhad, Mashhad, Iran*
4 *Department of Biology, Faculty of Science, University of Sistan and Baluchestan, Zahedan, Iran*

https://zoobank.org/F9DB584A-42CC-41BC-8705-DA0F9DD973CB

Corresponding author: Faezeh Yazdani Moghaddam (yazdani@um.ac.ir)

Academic editor: Sanja Matić-Skoko ♦ **Received** 10 January 2024 ♦ **Accepted** 11 March 2024 ♦ **Published** 20 May 2024

Citation: Damadi E, Yazdani Moghaddam F, Ghanbarifardi M (2024) Taxonomic characterization of five species of emperor fishes (Actinopterygii: Eupercaria: Lethrinidae) based on external morphology, morphometry, and geographic distribution in the northwestern Indian Ocean. Acta Ichthyologica et Piscatoria 54: 115–124. https://doi.org/10.3897/aiep.54.118586

Abstract

Species of the genus *Lethrinus*, commonly referred to as emperor fishes, mainly distributed in the Indo–West Pacific, including the Persian Gulf and Gulf of Oman are poorly known. It is difficult to characterize them morphologically, as there are no distinguishing meristic features for the majority of species. We studied the morphological features of 65 specimens representing the genus *Lethrinus* to define and identify the species involved. Among the morphological characters commonly considered in this type of study, we also included new, previously undescribed characters. The results of Tukey's post hoc HSD test for metric and meristic variables, which showed significant differences between species in ANOVA, indicate that most metric traits and the number of scale rows above the lateral line differ significantly among the five morphotypes distinguished. Principal component analysis (PCA) and discriminant function analysis (DFA) effectively showed the morphometric variation between these morphotypes. The characteristics of body depth, head length, pectoral fin length, and caudal fin length are the most distinguishing diagnostic at the species level. We determined that the collected fish specimens represented: *Lethrinus borbonicus* Valenciennes, 1830, *Lethrinus crocineus* Smith, 1959, *Lethrinus lentjan* (Lacepède, 1802), *Lethrinus microdon* Valenciennes, 1830, and *Lethrinus nebulosus* (Forsskål, 1775). We also confirmed their validity as distinct species. Notably, *L. crocineus*, previously known only from the western Indian Ocean (Africa and Socotra), is now reported for the first time from the Persian Gulf and the Gulf of Oman. Lastly, a distribution map for the *Lethrinus* species is included.

Keywords

Gulf of Oman, *Lethrinus*, morphological features, new record, Persian Gulf, taxonomy

Introduction

The Persian Gulf and Gulf of Oman in the northwestern Indian Ocean (NIO) are recognized as two of the largest brackish-water environments of outstanding universal value in the world (Maghsoudlou et al. 2019). The uniqueness of these ecoregions is outstanding due to the description of endemic species and clades with high genetic diversity in recent years (Asgharian et al. 2011; DiBattista et al. 2017; Torquato et al. 2019; Rabaoui et al. 2019; Damadi et al. 2020; Alavi-Yeganeh et al. 2021; Mehraban et al. 2021; Sadeghi et al. 2021; Esmaeili et al. 2022; Damadi et al. 2024). These ecoregions are dynamic coastal environments characterized by a complex system of oceanic processes, and ecological and physiological features (Coles 2003; Feary et al. 2010; Burt et al. 2011; Maghsoudlou et al. 2019). Given the physical complexity, high biodiversity, and endemism of the NIO, it has been considered a model system for the study of processes and patterns that influence the connectivity and fragmentation of marine populations (DiBattista et al. 2017; Torquato et al. 2019; Mehraban et al. 2021). The Lethrinidae Bonaparte, 1831 are a group of large coral reef fishes found mainly in the Indo–West Pacific (IWP) (Carpenter and Allen 1989; Fricke et al. 2024). Members of this family are commonly known as the emperor breams and the family comprises two subfamilies, five genera, and 45 valid species (Fricke et al. 2024). The subfamily Lethrininae comprises only a single genus, *Lethrinus* Cuvier, 1829, and is considered a taxonomically difficult group (Smith 1959; Sato 1971 [cited after Healey et al. 2018]; Carpenter and Allen 1989). As the *Lethrinus* are generally large fish that are exploited by commercial fisheries and sold in fish markets throughout the Indo–Pacific (Carpenter and Allen 1989; Ebisawa and Ozawa 2009), sound fisheries management at the local or regional level is also an issue. In all these cases, the importance of a reliable and effective tool for unambiguous species identification becomes clear, as a lack of, or incorrect, knowledge of taxonomy distorts the conclusions drawn from the comparative results. The emperor fishes of the genus *Lethrinus* differ from fishes of other lethrinid genera by the number of scale rows above the lateral line to the middle spines of the dorsal fin, the scaleless cheek, the smooth edge of the preopercle, and the longer snout (Carpenter 1997). The meristic values of many species overlap considerably and aspects of body shape, proportional measurements, and coloration such as spots, bars, bands, and stripes, are valuable in distinguishing many species (Smith 1959; Sato 1971 [cited after Healey et al. 2018]; Randall 1995; Carpenter 1997; Borsa et al. 2010). The *Lethrinus* species were revised recently, and two new species have been described based on morphological and molecular diagnoses (Carpenter and Randall 2003; Allen et al. 2021), and eight other, potentially new, recently collected species await description (Lo Galbo et al. 2002; Borsa et al. 2013; Mekkawy 2017; Healey et al. 2018). Despite these recent phylogenetic assessments and the taxonomic changes proposed therein, there is still a large gap in basic subtle morphological differences among *Lethrinus* species. Anatomical characteristics of larvae and adults, geographical distribution, and external morphological data are incomplete and scattered in the literature (Smith 1959; Sato 1971 [cited after Healey et al. 2018]; Carpenter and Allen 1989). Members of this genus are particularly difficult to identify in the late larval, juvenile, and adult stages because their body shapes are often similar, and their color patterns vary according to age, behavior, condition, or environment (Wilson 1998; Ponton et al. 2013). Of the 30 species of the genus, four occur in the Persian Gulf and the Gulf of Oman, including *Lethrinus borbonicus* Valenciennes, 1830, *Lethrinus lentjan* (Lacepède, 1802), *Lethrinus microdon* Valenciennes, 1830, and *Lethrinus nebulosus* (Forsskål, 1775) (see Fricke et al. 2024). The first data on *Lethrinus* species in the Persian Gulf and the Gulf of Oman come from Blegvad and Løppenthin (1944), who described *L. nebulosus* and *Lethrinus miniatus* (Forster, 1801). Then, Carpenter et al. (1997) and Grandcourt (2012) added three species, *L. borbonicus*, *L. lentjan*, and *L. microdon* from the southern part of the Persian Gulf. Subsequently, *L. miniatus* was removed from the checklist of fishes in these ecoregions (Carpenter et al. 1997; Grandcourt 2012; Psomadakis et al. 2015). In some cases, molecular phylogenetic studies on the genus *Lethrinus* have suggested that both *L. lentjan* and *L. nebulosus* probably form a hidden diversity in the Persian Gulf and Gulf of Oman (Asgharian et al. 2011; Mekkawy 2017). In addition, some *Lethrinus* species were listed in the general ecological and biology works in the ecoregions (Grandcourt et al. 2006; McIlwain et al. 2006; Taghavi Motlagh et al. 2010). Our specific objectives were to:

- Evaluate the external morphological characters used to diagnose the species for the Persian Gulf and Gulf of Oman representatives.
- Examine the morphometric and meristic variation among *Lethrinus* species based on univariate and multivariate analysis.
- Investigate the distribution and diversity of *Lethrinus* species of the Persian Gulf and Gulf of Oman.
- Report a new record of *L. crocineus* for the first time from these ecoregions.

Material and methods

Specimen collection. A total of 65 specimens were collected between 5 and 50 m depth along the Persian Gulf and the Gulf of Oman at eight stations (Fig. 1). The specimens were collected using gillnets with mesh sizes ranging from 11 to 16 cm, as well as hook-and-line, during the months of May and July in 2022 and 2023. All specimens were photographed on the left side with a Canon Powershot A3300 16-megapixel digital camera positioned on a tripod on a table with a millimeter scale. The collected specimens were preserved in 10% formalin solution and stored in the Zoological Museum of the Ferdowsi University of Mashhad (ZMFUM), Iran (Suppl. material 1). All specimens were identified using the taxonomic keys relevant to the regions (Blegvad and Løppenthin 1944; Randall 1995; Carpenter et al. 1997).

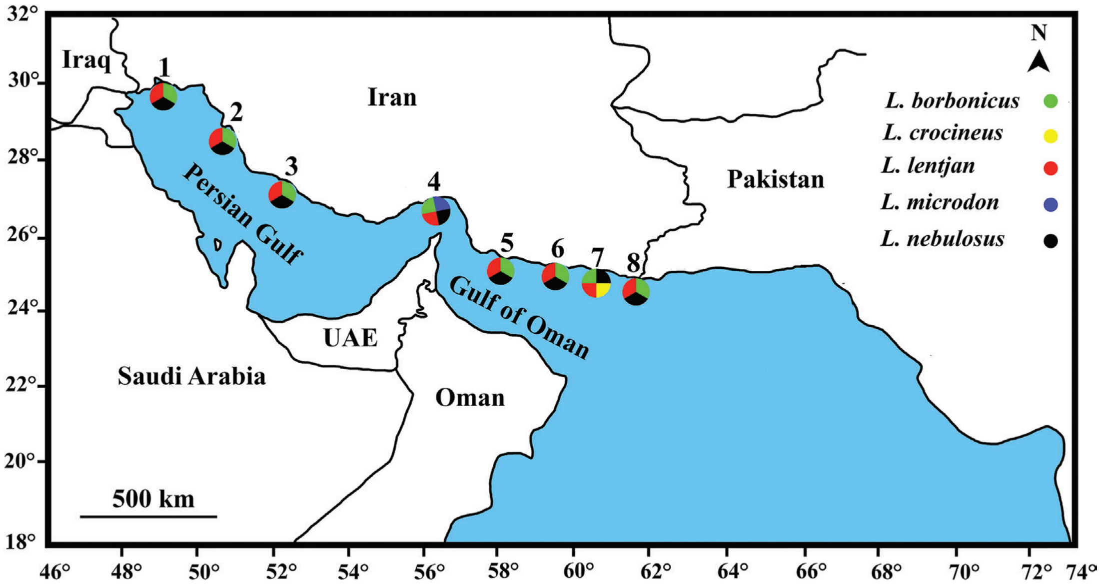

Figure 1. Geographic distribution of *Lethrinus* species in the Persian Gulf and the Gulf of Oman. Abbreviations: 1 = Hendijan, 2 = Bushehr, 3 = Kangan, 4 = Qeshm (Naz Island), 5 = Jask, 6 = Pozm, 7 = Tis, 8 = Beris.

Morphometric analysis. A total of 16 morphometric traits were measured in the laboratory for each specimen. Nine meristic features were counted. Counts and measurements were taken as far as possible on the left side of the fish, following standard methods for *Lethrinus* taxonomy (Allen et al. 2021). The morphometric methods, meristic methods, and the color patterns correspond to those of Allen et al. (2021). For brevity, these characters will be abbreviated as follows: **counts:** DFS = dorsal-fin spines; DFR = dorsal-fin rays; AFS = anal-fin spines; AFR = anal-fin rays; PFR = pectoral-fin rays; LLS = lateral-line scales; SALL = scale rows above lateral line; SBLL = scale rows below lateral line; LSACP = scale around caudal-peduncle; SPS = supratemporal patch of scales. **Measurements:** BD = body depth; HL = head length; OD = orbit diameter; POL = preorbital length; UJL = upper-jaw length; CPD = caudal-peduncle depth; CPL = caudal-peduncle length; PDL = predorsal length; PAL = preanal length; PPL = prepelvic length; LDFB = length dorsal-fin base; LAFB = length anal-fin base; LPF = length pectoral fin; LCF = length caudal fin; OD = orbit diameter [% of HL]. All morphometric variables were divided by the standard length (SL) and head length (HL) before analyses to eliminate the size effect. The data were tested for normality using the Shapiro–Wilk test and for homogeneity using the Levene test. Sex determination was based on the gonads according to Marriott et al. (2010). MANOVA test was used to assess sexual dimorphism between males and females. All statistical analyses were performed in PAST v. 4.03 (Hammer 2020) and SPSS v. 23 (SPSS Inc., Chicago IL). For morphometric traits, one-way analysis of variance (ANOVA) and Tukey's post-hoc test were performed to assess significant differences between species. Subsequently, significant variables were then subjected to PCA and DFA. Given that the use of ratios can result in misleading correlations (Atchley et al. 1976), we utilized the method suggested by Sagnes et al. (1997). Ponton et al. (2013) also outlined a data treatment approach, in line with Sagnes et al. (1997), that was employed to prevent any biases arising from the use of ratios and proportions in measuring fish body characteristics. Prior to being subjected to double-centered PCA, all linear measurements, except SL, were log10 transformed. PCA is an effective method for reducing morphometric data and extracting independent variables. DFA is a predictive model for group membership. The source of discrimination between samples was based on the percentage of correctly and incorrectly classified fish. The holdout leave-one-out cross-validation procedures proposed by Lachenbruch (1967) were also performed to calculate the misclassification rate of DFA.

Ethical statement. Handling and sampling in the Persian Gulf and the Gulf of Oman were approved by the Ethic-Scientific Committee of the Ferdowsi University of Mashhad, Iran, and the Iranian Fisheries Organization (scientific permit IR.UM.REC.1400.183).

Results

Examining *Lethrinus* specimens collected in the Persian Gulf and the Gulf of Oman revealed a total of five *Lethrinus* species. These species are *L. borbonicus*, *L. crocineus*, *L. lentjan*, *L. microdon*, and *L. nebulosus*. The presently reported findings of *Lethrinus crocineus* represent a new record for the marine fauna of the Persian Gulf and the Gulf of Oman. Below are brief descriptions of the morphometric and meristic characteristics of these species as well as univariate and multivariate analyses.

Family Lethrinidae
Genus *Lethrinus* Cuvier, 1829

Lethrinus borbonicus Valenciennes, 1830

English common name: snubnose emperor

Lethrinus borbonicus Valenciennes in Cuvier and Valenciennes, 1830.—Cuvier and Valenciennes (1830): 125; syntypes: MNHN 0000-9092 (1), 0000-9373 (2); Type locality: southwestern Indian Ocean (western Mascarenes: Réunion: Saint Denis).

Material examined. ZMFUM-LE-26-34, 9 specimens (Suppl. material 1), May 2022 to April 2023, depth 20–30 m.

Description. Dorsal-fin rays X, 9; anal-fin rays III, 8; pectoral-fin rays13; tubed lateral-line scales 46–47; 5.5 transverse scale rows above lateral line; 15–16 transverse scale rows below lateral line; 13–15 lower series of scale around caudal-peduncle; high-bodied forms; numerous small scales on inside of pectoral fin base; molariform teeth; cheek without scales; body gray; fins mostly light brown; upper half of body darker than rest of body; posterior margin of opercular membrane gray.

Lethrinus crocineus Smith, 1959

English common name: yellowtail emperor
Fig. 2A

Lethrinus crocineus Smith, 1959. Holotype: SAIAB 22; Paratypes: not studied; Type locality: western Indian Ocean (Mozambique: Pinda).

Material examined. ZMFUM-LE-11-22, 12 specimens (Suppl. material 1), May 2022 to July 2023, depth 40 m.

Description. Dorsal-fin rays X, 9; anal-fin rays III, 8; pectoral-fin rays13; tubed lateral-line scales 46–47; 5.5 transverse scale rows above lateral line; 15–17 transverse scale rows below lateral line; 15–16 lower series of scale around caudal-peduncle; high-bodied forms; numerous small scales on inside of the pectoral fin base; molariform teeth; cheek white and without scales; body gray; fins usually yellowish, except pelvic fin.

Lethrinus nebulosus (Forsskål, 1775)

English common name: spangled emperor
Fig. 2B

Sciaena nebulosa Forsskål in Niebuhr, 1775.—Niebuhr (1775): 52; Holotype: ZMUC P49345; No locality stated (Red Sea).

Material examined. ZMFUM-LE-44-68, 25 specimens (Suppl. material 1), May 2022 to March 2023, depth 5–30 m.

Description. Dorsal-fin rays X, 9; anal-fin rays III, 8; pectoral-fin rays13; tubed lateral-line scales 46–47; 5.5 transverse scale rows above lateral line; 15–17 transverse scale rows below lateral line; 14–15 lower series of scale around caudal-peduncle; high-bodied forms; forked caudal fin; numerous small scales on inner surface of pectoral-fin base; molariform teeth; cheek without scales; body light gray; head with light blue stripes; pale blue stripe dorsally on basal half of pectoral fin; white spots on body.

Lethrinus lentjan (Lacepède, 1802)

English common name: pink ear emperor
Fig. 2C

Bodianus lentjan Lacepède, 1802.—Lacepède (1802): 281, 293; Holotype (unique): MNHN A-7847; No locality stated (probably eastern Indian Ocean, Indonesia Java).

Material examined. ZMFUM-LE-1-10, 10 specimens (Suppl. material 1), August 2022 to July 2023, depth 5–30 m.

Description. Dorsal-fin rays X, 9; anal-fin rays III, 8; pectoral-fin rays13; tubed lateral-line scales 46–47; 5.5 transverse scale rows above lateral line; 15–16 transverse scale rows below lateral line; 14–15 lower series of scale around caudal-peduncle; high-bodied forms; some scales on inside of pectoral fin base; molariform teeth; cheek white and without scales; body gray; pectoral and caudal fins red; inner part of pectoral fin red; posterior edge of opercular membrane red.

Lethrinus microdon Valenciennes, 1830

English common name: smalltooth emperor
Fig. 2D

Lethrinus microdon Valenciennes in Cuvier and Valenciennes, 1830.—Cuvier and Valenciennes (1830): 295, Holotype: MNHN 0000-9073; Type locality: Indonesia: Molucca Islands, northeastern Pulau Buru.

Material examined. ZMFUM-LE-35-43, 9 specimens (Suppl. material 1), May 2022 to March 2023, depth 25–50 m.

Description. Dorsal-fin rays X, 9; anal-fin rays III, 8; pectoral-fin rays13; tubed lateral-line scales 47–48; 4.5 transverse scale rows above lateral line; 16–17 transverse scale rows below lateral line; 15–16 lower series of scale around caudal-peduncle; low-bodied forms; forked caudal fin; no scales on inside of the pectoral fin base; conical teeth; cheek without scales; body gray; fins brown.

Morphometrics. To characterize the morphological variation between *Lethrinus* species, morphometric features were analyzed. The MANOVA results showed no significant difference between males and females, the sexes were pooled in all analyses ($0.0511 < P < 1.0000$) (Suppl. material 2). In the one-way ANOVA analysis, 17 out of 22 traits were found to be significant ($P < 0.0000$) (Suppl. material 2). These traits included 15 morphometric and two meristic traits (Suppl. material 2). The Tukey post hoc test results showed a significant difference between all five species ($P < 0.05$). Specifically, the Tukey post hoc tests for metric traits showed the most significant differences between *L. crocineus* and *L. microdon*, while the differences in meristic variables were most significant between

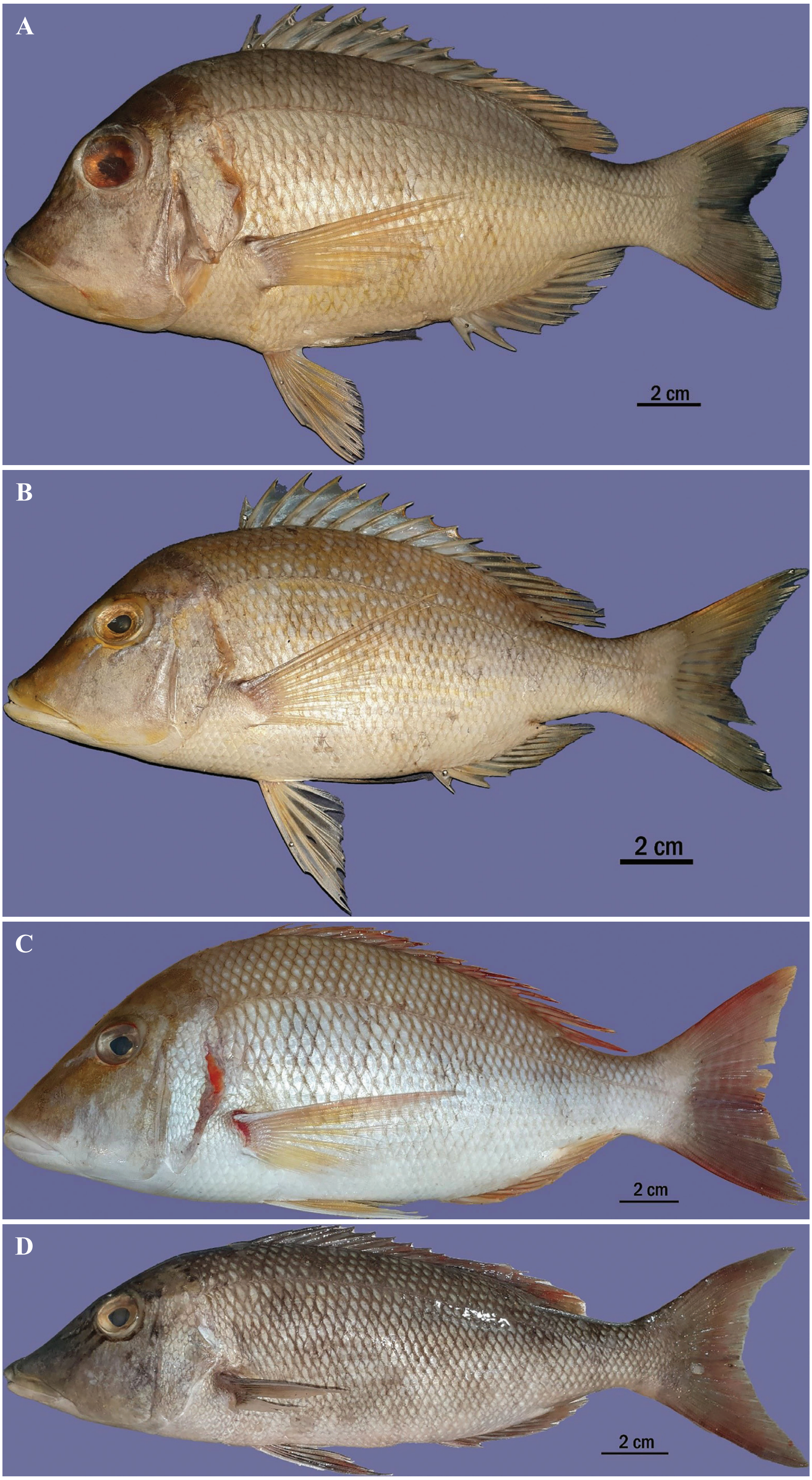

Figure 2. *Lethrinus crocineus* (**A**), ZMFUM-LE-12, (Photo by E. Damadi); *Lethrinus nebulosus* (**B**), ZMFUM-LE-48, (Photo by E. Damadi); *Lethrinus lentjan* (**C**), ZMFUM-LE-8, (Photo by E. Damadi); *Lethrinus microdon* (**D**), ZMFUM-LE-35, (Photo by E. Damadi).

L. microdon and the other species (data not shown). The boxplot of total length shows that *L. nebulosus* is generally larger than the other species; *L. microdon* is medium-sized and the other species are smaller (Fig. 3). As expected, the first principal component (PC1) on metric characters accounted for the highest proportion of variance (99.2%) (Fig. 4A). On the PC1 axis, *L. nebulosus* and *L. microdon* showed a high differentiation from *L. borbonicus*, *L. crocineus*, and *L. lentjan* in the majority of of the measured morphometric traits, including body depth, caudal peduncle depth, pectoral fin length, preorbital length, and caudal fin length. On the PC2 axis, *L. crocineus* showed significant differences from *L. microdon*. PCA on the morphometric traits showed a notable overlapping between *L. borbonicus* and *L. lentjan* on PC1 and PC2. For the majority of meristic traits, *L. microdon* showed a high differentiation from the other species due to its significant scale rows above the lateral line and supratemporal scale patch (Fig. 4B). The PCA results (Fig. 4) were well supported by the DFA analyses (data not shown). The DFA correctly classified 100% of the specimens, which was confirmed by cross-validation of specimens to species based on morphometric and meristic features.

Discussion

This study is the first univariate and multivariate analysis to determine the morphometric and meristic variation and taxonomic validation of *Lethrinus* fishes in the Persian Gulf and Gulf of Oman. The morphological examination of *Lethrinus* specimens collected from the coastal waters of the Persian Gulf and Gulf of Oman confirms the presence of the previously unreported *L. crocineus* in these ecoregions. The discovery of this species in the Persian Gulf and the Gulf of Oman indicates that there is a suitable habitat for *L. crocineus* in these ecoregions and further species of the genus *Lethrinus* could be discovered in the future. This species was previously known from the tropical regions of Africa and Socotra (Heemstra et al. 2004; Fricke et al. 2018; Zajonz et al. 2019). The occurrence of tropical fish in subtropical regions is considered one of the first indicators of climate-induced change in biodiversity (Perry et al. 2005; Munday et al. 2008; Booth et al. 2017; Wabnitz et al. 2018; Bañón et al. 2020). It is assumed that climate change has a major impact on marine biodiversity in the Persian Gulf and the Gulf of Oman (Wabnitz et al. 2018; Khajavi and Alavi-Yeganeh 2020; Damadi et al. 2021; Esmaeili and Eslami Barzoki 2023). In addition, a long-term increase in the temperature of the Persian Gulf and the Gulf of Oman is well documented (Jawad et al. 2011, Piontkovski and Chiffings 2014). Warmer water masses could cause an expansion of the distribution range of *L. crocineus* from its original one in East Africa and Socotra northwards along the northern Gulf of Oman. The presently reported findings add five species of *Lethrinus* to the list of marine fish species in these ecoregions. The low species diversity of *Lethrinus* species in the Persian Gulf and the Gulf of Oman, as compared to neighboring euryhaline environments such as the Arabian Sea (Manilo and Bogorodsky 2003, 12 spp.), the Red Sea (Golani and Fricke 2018, 10 spp.) and Socotra (Zajonz et al. 2019, 10 spp.), is somewhat surprising. This discrepancy could potentially be attributed to various factors, including oceanographic barriers, geological events, and differences in habitat structure (Feary et al. 2010; Burt et al. 2011; Ludt and Rocha 2015; Maghsoudlou et al. 2019; Torquato et al. 2019; Zajonz et al. 2022). One possible hypothesis for the observed low species diversity in the Persian Gulf and Gulf of Oman is that upwelling events along the Omani have restricted stepping-stone connections between these ecoregions and other neighboring euryhaline environments in the Indian Ocean (Glynn 1993; Burt et al. 2011). The lack of suitable habitats due to the last glacial events and environmental factors (i.e., high temperature and salinity) created barriers and altered environmental conditions that likely led to the low biodiversity in the Persian Gulf and Gulf of Oman (Sarnthein 1972; Lokier et al. 2015; Vaughan et al. 2019). Previous authors confirmed the taxonomic validity of *L. lentjan* and *L. nebulosus* (see Asgharian et al. 2011) from the Persian Gulf and Gulf of Oman and

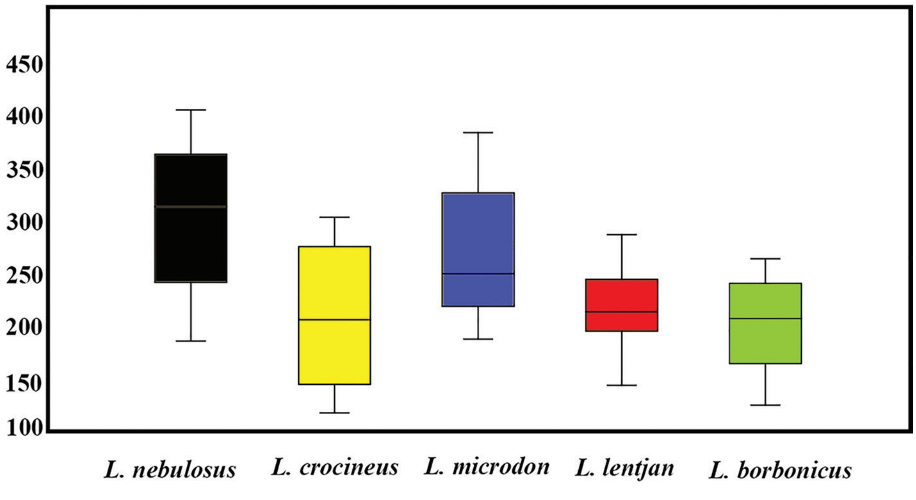

Figure 3. Total length data of the five of *Lethrinus* species samples in the presently reported study in the Persian Gulf and the Gulf of Oman.

showed some cryptic species within these species based on molecular data (Mekkawy 2017). The majority of diagnostic morphological characters at the species level were consistent with previous descriptions by Randall (1995) and Carpenter et al. (1997), except metric characters such as pectoral fin length and caudal fin length and orbit diameter. The univariate and multivariate analyses yielded the same results (Suppl. material 2; Fig. 4). Meristic and metric features showed the greatest differences between *L. microdon* and other species (Fig. 4). *Lethrinus microdon* differs from the other species studied by fewer scale rows above the lateral line (4.5 scales vs. 5.5 scales in congeners); no scales on the inside of the pectoral fin base, a deeper body, 3.2%–3.5% of SL (vs. 2.3%–2.8% in congeners); a longer pectoral fin, 3.8%–4.7% of SL (vs. 3.1%–3.7% in congeners); a deeper caudal-peduncle depth, 10.3%–11.6% of SL (vs. 8.5%–9.6% in congeners). *Lethrinus borbonicus* differs most clearly from *L. lentjan* in the posterior margin of the operculum (gray vs. red in *L. lentjan*) and the base of the pectoral fin (grey vs. red in *L. lentjan*) and a larger orbit diameter, 8.5%–14.1% of HL (vs. 4.2%–5.1% in *L. lentjan*). It differs from *L. nebulosus* in the absence of light blue stripes in front of the eyes (vs. the presence of light blue stripes in front of the eyes in *L. nebulosus*), and the often slightly convex profile of the head near the eyes (vs. profile of the head straight near the eyes in *L. nebulosus*), and a larger orbit diameter, 8.5%–14.1% of HL (vs. 4.4%–5.3% of SL in *L. nebulosus*). *Lethrinus borbonicus* is also different from *L. crocineus* by having median fins gray (vs. yellow in *L. crocineus*), a deeper body, 2.5%–2.8% of SL (vs. 2.3%–2.5% in *L. crocineus*), and a longer pectoral fin, 3.3%–3.5% in SL (vs. 3.1%–3.2% in *L. crocineus*). Based on the meristic features, *L. crocineus* could also be easily confused with *L. nebulosus* and *L. lentjan*, but it differs in having an area on the snout directly in front of the eye with a prominent hump (lacking this prominent hump in *L. lentjan*), a moderately narrow body, 2.4%–2.5% of SL (vs. 2.5%–2.8% in *L. lentjan*), the posterior margin of the operculum gray (vs. red in *L. lentjan*), the base of the pectoral fin grey (vs. red in *L. lentjan*), and the head without light blue stripes and without white spots on the body (vs.

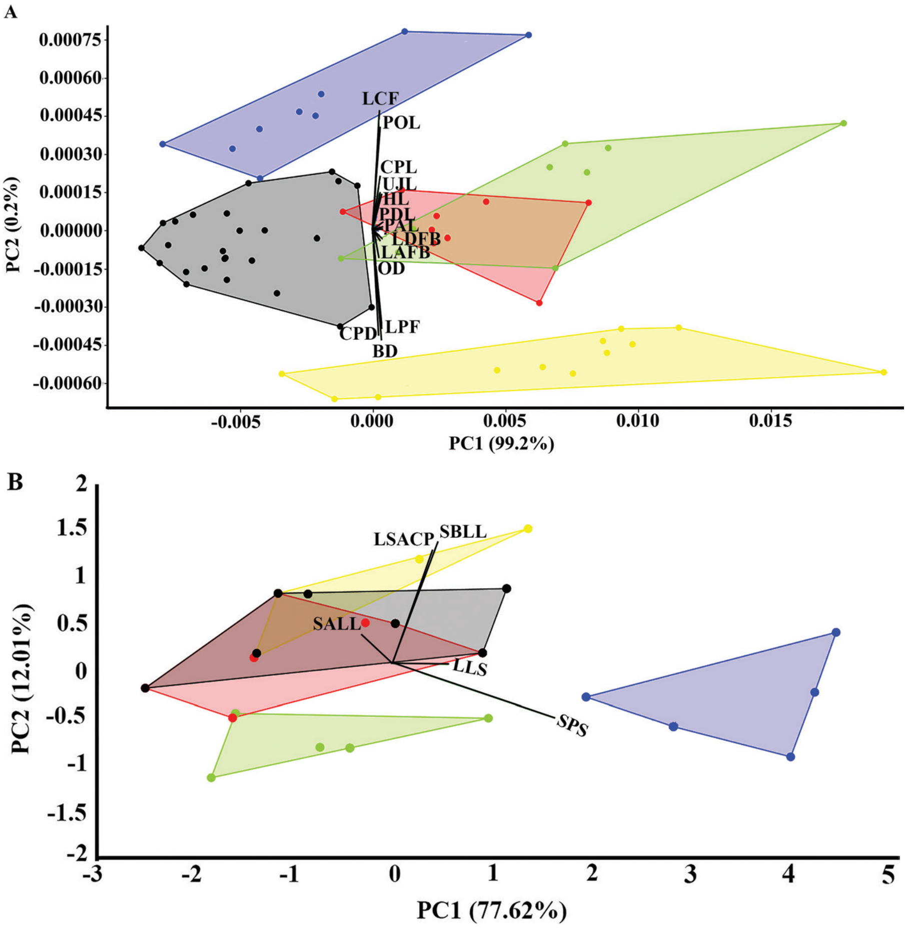

Figure 4. Principal component analysis (PCA) results of the five of *Lethrinus* species samples in the presently reported study in the Persian Gulf and the Gulf of Oman; (**A**) morphospace plotted on 14 morphometric traits; and (**B**) morphospace plotted on 10 meristic traits morphometric traits; *L. borbonicus* (green), *L. crocineus* (yellow), *L. lentjan* (red), *L. microdon* (blue), *L. nebulosus* (black). LLS = lateral-line scales; SALL = scale rows above lateral line; SBLL = scale rows below lateral line; LSACP = scale around caudal-peduncle; SPS = supratemporal patch of scales; BD = body depth; HL = head length; POL = preorbital length; UJL = upper-jaw length; CPD = caudal-peduncle depth; CPL = caudal-peduncle length; PDL = predorsal length; PAL = preanal length; PPL = prepelvic length; LDFB = length dorsal-fin base; LAFB = length anal-fin base; LPF = length pectoral fin; LCF = length caudal fin; OD = orbit diameter [% of HL].

light blue stripes on the head and white spots on the body in *L. nebulosus*). *Lethrinus nebulosus* differs from the closely related *L. lentjan* in morphometric measurements and color patterns. It has the posterior margin of the opercular membrane grey (vs. red in *L. lentjan*), the base of the pectoral fin grey (vs. red in *L. lentjan*), the head with light blue stripes and white spots on the body (vs. lack of light blue stripes on the head and lack of white spots on the body in *L. lentjan*), and a smaller head, 3%–3.2% of SL (vs. 2.6%–2.8% in *L. lentjan*). The morphometric variation of *L. microdon* appears to be associated with trophic ecology (Ali et al. 2016; Thangaraj et al. 2022). Food content analyses revealed that the main dietary components of *L. lentjan* and *L. nebulosus* were slow-moving benthic invertebrates such as mollusks, echinoderms, and crustaceans. In contrast, *L. microdon* predominantly consumed fast-moving prey such as nekton and other groups of invertebrates (Thangaraj et al. 2022). The slender body shape, jaw structure, and feeding behavior of *L. microdon* allow it to consume a far greater proportion of nekton. Given the economic value of emperor fishes in these regions, it is important to note that, besides *L. nebulosus*, the catch of other species has significantly decreased in recent years. This highlights the need to increase attention and conservation efforts to protect these species. In the future, conducting studies with larger sample sizes, if possible, and using additional geometric morphometric and genetic analyses may help clarify specific aspects related to distinguishing the species within this group.

Acknowledgments

We would like to thank the local fishermen for their help in collecting the specimens. Financial support for this research was provided by the Ferdowsi University of Mashhad, Iran.

References

Alavi-Yeganeh MS, Khajavi M, Kimura S (2021) A new ponyfish, *Deveximentum mekranensis* (Teleostei: Leiognathidae), from the Gulf of Oman. Ichthyological Research 68(3): 437–444. https://doi.org/10.1007/s10228-020-00794-y

Ali MKH, Belluscio A, Ventura D, Ardizzone G (2016) Feeding ecology of some fish species occurring in artisanal fishery of Socotra Island (Yemen). Marine Pollution Bulletin 105(2): 613–628. https://doi.org/10.1016/j.marpolbul.2016.01.051

Allen GR, Victor BC, Erdmann MV (2021) *Lethrinus mitchelli*, a new species of emperor fish (Teleostei: Lethrinidae) from Milne Bay Province, Papua New Guinea. Journal of the Ocean Science Foundation 38: 66–77.

Asgharian H, Sahafi HH, Ardalan AA, Shekarriz S, Elahi E (2011) Cytochrome c oxidase subunit 1 barcode data of fish of the Nayband National Park in the Persian Gulf and analysis using meta-data flag several cryptic species. Molecular Ecology Resources 11(3): 461–472. https://doi.org/10.1111/j.1755-0998.2011.02989.x

Atchley WR, Gaskins CT, Anderson D (1976) Statistical properties of ratios: I. Empirical results. Systematic Zoology 25: 137–148. https://doi.org/10.2307/2412740

Bañón R, De Carlos A, Alonso-Fernández A, Ramos F, Baldó F (2020) Apparently contradictory routes in the expansion of two fish species in the eastern Atlantic. Journal of Fish Biology 96(4): 1051–1054. https://doi.org/10.1111/jfb.14290

Blegvad H, Loppenthin B (1944) Fishes of the Iranian Gulf. Danish Scientific Investigations in Iran. Einar Munksgaard, Copenhagen, Denmark, 247 pp.

Booth DJ, Feary D, Kobayashi D, Luiz O, Nakamura Y (2017) 26. Tropical marine fishes and fisheries and climate change. Pp. 875–896. In: Phillips BF, Pérez-Ramírez M (Eds.) Climate change impacts on fisheries and aquaculture: A global analysis. Volume 2. Wiley–Blackwell. https://doi.org/10.1002/9781119154051.ch26

Borsa P, Collet A, Carassou L, Ponton D, Chen WJ (2010) Multiple nuclear and mitochondrial genotyping identifies emperors and large-eye breams (Teleostei: Lethrinidae) from New Caledonia and reveals new large-eye bream species. Biochemical Systematics and Ecology 38(3): 370–389. https://doi.org/10.1016/j.bse.2010.03.007

Borsa P, Bearez P, Paijo S, Chen WJ (2013) *Gymnocranius superciliosus* and *Gymnocranius satoi*, two new large-eye breams (Sparoidea: Lethrinidae) from the Coral Sea and adjacent regions. Comptes Rendus. Biologies 336(4): 233–240. https://doi.org/10.1016/j.crvi.2013.06.003

Burt JA, Feary DA, Bauman AG, Usseglio P, Cavalcante GH, Sale PF (2011) Biogeographic patterns of reef fish community structure in the northeastern Arabian Peninsula CES. ICES Journal of Marine Science 68(9): 1875–1883. https://doi.org/10.1093/icesjms/fsr129

Carpenter KE (1997) Lethrinidae. Emperor snappers. P. 3017. In: FAO identification guide for fishery purposes. FAO, Rome.

Carpenter KE, Allen GR (1989) FAO species catalogue, Volume 9. Emperor fishes and large-eye breams of the World (Family Lethrinidae). An annotated and illustrated catalogue of lethrinid species known to date. FAO Fisheries Synopsis 125: 9.

Carpenter KE, Randall JE (2003) *Lethrinus ravus*, a new species of emperor fish (Perciformes: Lethrinidae) from the western Pacific and eastern Indian oceans. Zootaxa 240(1): 1–8. https://doi.org/10.11646/zootaxa.240.1.1

Carpenter KE, Krupp F, Jones DA, Zajonz U (1997) FAO species identification field guide for fishery purposes: The living marine resources of Kuwait, Eastern Saudi Arabia, Bahrain, Qatar, and the United Arab Emirates. FAO. Rome, 324 pp.

Coles SL (2003) Coral species diversity and environmental factors in the Arabian Gulf and the Gulf of Oman: A comparison to the Indo–Pacific region. Atoll Research Bulletin 507: 1–19. https://doi.org/10.5479/si.00775630.507.1

Cuvier G, Valenciennes A (1830) Histoire naturelle des poissons. Tome Sixième. Livre sixième. Partie I. Des Sparoïdes; Partie II. Des Ménides. Tome sixième. Livre sixième. Partie I. Des Sparoïdes; Partie II. Des Ménides. 1–559, Pls. 141–169.

Damadi E, Moghaddam FY, Ghassemzadeh F, Ghanbarifardi M (2020) *Plectorhinchus makranensis* (Teleostei, Haemulidae), a new species of sweetlips from the Persian Gulf and the Gulf of Oman. ZooKeys 980: 141–154. https://doi.org/10.3897/zookeys.980.50934

Damadi E, Moghaddam FY, Ghassemzadeh F, Ghanbarifardi M (2021) Aspects of morphometry, distribution, and key identification of the genus *Pomadasys* (Perciformes: Haemulidae) from the Persian

Gulf and Gulf of Oman with descriptions of new records. Thalassas 37(2): 671–682. https://doi.org/10.1007/s41208-021-00308-1

Damadi E, Moghaddam FY, Ghanbarifardi M (2024) Taxonomic validation of sweetlips fish (Haemulidae: Plectorhinchinae) from the Persian Gulf and Gulf of Oman based on traditional and geometric morphometrics with notes on their distribution. Thalassas 1–14. https://doi.org/10.1007/s41208-024-00663-9

DiBattista JD, Coker DJ, Sinclair-Taylor TH, Stat M, Berumen ML, Bunce M (2017) Assessing the utility of eDNA as a tool to survey reef-fish communities in the Red Sea. Coral Reefs 36(4): 1245–1252. https://doi.org/10.1007/s00338-017-1618-1

Ebisawa A, Ozawa T (2009) Life-history traits of eight *Lethrinus* species from two local populations in waters off the Ryukyu Islands. Fisheries Science 75(3): 553–566. https://doi.org/10.1007/s12562-009-0061-9

Esmaeili HR, Eslami Barzoki Z (2023) Climate change may impact Nile tilapia, *Oreochromis niloticus* (Linnaeus, 1758) distribution in the southeastern Arabian Peninsula through range contraction under various climate scenarios. Fishes 8(10): e481. https://doi.org/10.3390/fishes8100481

Esmaeili HR, Zarei F, Sholeh V, Sadeghi Y, Sadeghi R, Fricke R (2022) Morphological analysis and DNA barcoding confirm presence of a cryptic fish species, the blotched triplefin, *Enneapterygius ventermaculus* (Teleostei: Blenniiformes: Tripterygiidae), at Qeshm, Persian Gulf. Iranian Journal of Ichthyology 9(1): 1–10.

Feary DA, Burt JA, Bauman AG, Usseglio P, Sale PF, Cavalcante GH (2010) Fish communities on the world's warmest reefs: What can they tell us about impacts of a climate change future? Journal of Fish Biology 77(8): 1931–1947. https://doi.org/10.1111/j.1095-8649.2010.02777.x

Fricke R, Mahafina J, Behivoke F, Jaonalison H, Léopold M, Ponton D (2018) Annotated checklist of the fishes of Madagascar, southwestern Indian Ocean, with 158 new records. FishTaxa 3: 1–432.

Fricke R, Eschmeyer WN, van der Laan R (Eds.) (2024) Eschmeyer's catalog of fishes: genera, species, references. California Academy of Sciences, San Francisco, CA, USA. [Accessed on 5 February 2024] http://researcharchive.calacademy.org/research/ichthyology/catalog/fishcatmain.asp

Glynn PW (1993) Coral reef bleaching: Ecological perspectives. Coral Reefs 12(1): 1–17. https://doi.org/10.1007/BF00303779

Golani D, Fricke R (2018) Checklist of the Red Sea fishes with delineation of the Gulf of Suez, Gulf of Aqaba, endemism and Lessepsian migrants. Zootaxa 4509(1): 1–215. https://doi.org/10.11646/zootaxa.4509.1.1

Grandcourt E (2012) Reef fish and fisheries in the Gulf. Pp. 127–161. In: Riegl BM, Purkis SJ (Eds.) Coral reefs of the Gulf: Adaptation to climatic extremes. Vol. 3 of Coral Reefs of the World. Springer Netherlands, Dordrecht, Netherlands. https://doi.org/10.1007/978-94-007-3008-3_8

Grandcourt EM, Al Abdessalaam TZ, Al Shamsi AT, Francis F (2006) Biology and assessment of the painted sweetlips (*Diagramma pictum* (Thunberg, 1792)) and the spangled emperor (*Lethrinus nebulosus* (Forsskål, 1775)) in the southern Arabian Gulf. Fishery Bulletin 104(1): 75–88.

Hammer O (2020) PAST paleontological statistics v.4.03. Reference manual. University of Oslo, Norway.

Healey AJ, McKeown NJ, Taylor AL, Provan J, Sauer W, Gouws G, Shaw PW (2018) Cryptic species and parallel genetic structuring in lethrinid fish: Implications for conservation and management in the southwest Indian Ocean. Ecology and Evolution 8: 2182–2195. https://doi.org/10.1002/ece3.3775

Heemstra E, Heemstra P, Smale M, Hooper T, Pelicier D (2004) Preliminary checklist of coastal fishes from the Mauritian island of Rodrigues. Journal of Natural History 38(23): 3315–3350. https://doi.org/10.1080/0022293041000l695088

Jawad LA, Hussein SA, Bulbil F (2011) *Ranzania laevis* (Pennant, 1776) (Tetraodontiformes, Molidae): A rare fish in marine waters of Iraq. Journal of Applied Ichthyology 27(4): 1116–1118. https://doi.org/10.1111/j.1439-0426.2010.01609.x

Khajavi M, Alavi-Yeganeh MS (2020) First record of the deep pugnose ponyfish *Secutor ruconius* (Hamilton, 1822) (Perciformes: Leiognathidae) from the Persian Gulf and the Gulf of Oman. Acta Zoologica Bulgarica 72: 495–498.

Lacepède BGE (1802) Histoire naturelle des poissons: IV. chez Plassan: Paris, France. Vol. 4: i–xliv + 1–728, Pl. 1–16.

Lachenbruch PA (1967) An almost unbiased method of obtaining confidence intervals for the probability of misclassification in discriminant analysis. Biometrics 23(4): 639–645. https://doi.org/10.2307/2528418

Lo Galbo AM, Carpenter KE, Reed DL (2002) Evolution of trophic types in emperor fishes (*Lethrinus*, Lethrinidae, Percoidei) based on cytochrome b gene sequence variation. Journal of Molecular Evolution 54(6): 754–762. https://doi.org/10.1007/s00239-001-0076-z

Lokier SW, Bateman MD, Larkin NR, Rye P, Stewarte JR (2015) Late Quaternary sea-level changes of the Persian Gulf. Quaternary Research 84(1): 69–81. https://doi.org/10.1016/j.yqres.2015.04.007

Ludt WB, Rocha LA (2015) Shifting seas: The impacts of Pleistocene sea-level fluctuations on the evolution of tropical marine taxa. Journal of Biogeography 42(1): 25–38. https://doi.org/10.1111/jbi.12416

Maghsoudlou A, Momtazi F, Nasiri K, Pazooki S, Molavi-Arabshahi M, Sepahvand V, Khaledi H (2019) A review on the state of the biodiversity knowledge on Iran's southern seas: Introducing a methodology to evaluate the validity of the reported cases. Marine Biodiversity 49(2): 563–581. https://doi.org/10.1007/s12526-017-0835-8

Manilo LG, Bogorodsky SV (2003) Taxonomic composition, diversity and distribution of coastal fishes of the Arabian Sea. Journal of Ichthyology 43: S75.

Marriott RJ, Jarvis NDC, Adams DJ, Gallash AE, Norriss J, Newman SJ (2010) Maturation and sexual ontogeny in the spangled emperor *Lethrinus nebulosus*. Journal of Fish Biology 76(6): 1396–1414. https://doi.org/10.1111/j.1095-8649.2010.02571.x

McIlwain J, Hermosa GV, Claereboudt M, Al-Oufi HS, Al-Awi M (2006) Spawning and reproductive patterns of six exploited finfish species from the Arabian Sea, Sultanate of Oman. Journal of Applied Ichthyology 22(2): 167–176. https://doi.org/10.1111/j.1439-0426.2006.00723.x

Mehraban H, Zarei F, Esmaeili HR (2021) A prelude to the molecular systematics and diversity of combtooth blennies (Teleostei: Blenniidae) in the Persian Gulf and Oman Sea. Systematics and Biodiversity 19(5): 438–452. https://doi.org/10.1080/14772000.2021.1895900

Mekkawy IAA (2017) Evolutionary lineages in genus *Lethrinus* (family: Lethrinidae) and the corresponding trophic evolution based on DNA barcoding. American Journal of Biochemistry and Molecular Biology 7(1): 1–20. https://doi.org/10.3923/ajbmb.2017.1.20

Munday PL, Jones GP, Pratchett MS, Williams AJ (2008) Climate change and the future for coral reef fishes. Fish and Fisheries 9(3): 261–285. https://doi.org/10.1111/j.1467-2979.2008.00281.x

Niebuhr C (1775) Descriptiones animalium avium, amphibiorum, piscium, insectorum, vermium; quae in itinere orientali observavit Petrus Forskål. Post mortem auctoris edidit Carsten Niebuhr. Hauniae.

Perry AL, Low PJ, Ellis JR, Reynolds JD (2005) Climate change and distribution shifts in marine fishes. Science 308 (5730): 1912–1915. https://doi.org/10.1126/science.1111322

Piontkovski SA, Chiffings T (2014) Long-term changes of temperature in the Sea of Oman and the western Arabian Sea. International Journal of Oceans and Oceanography 8: 53–72.

Ponton D, Carassou L, Raillard S, Borsa P (2013) Geometric morphometrics as a tool for identifying emperor fish (Lethrinidae) larvae and juveniles. Journal of Fish Biology 83(1): 14–27. https://doi.org/10.1111/jfb.12138

Psomadakis PN, Osmany HB, Moazzam M (2015) Field identification guide to the living marine resources of Pakistan. FAO Species Identification Guide for Fishery Purposes, FAO Rome, 386 pp.

Rabaoui L, Yacoubi L, Sanna D, Casu M, Scarpa F, Lin YJ, Qurban MA (2019) DNA barcoding of marine fishes from Saudi Arabian waters of the Gulf. Journal of Fish Biology 95(5): 1286–1297. https://doi.org/10.1111/jfb.14130

Randall JE (1995) Coastal fishes of Oman. University of Hawai'i Press, Honolulu HI, USA, 439 pp.

Sadeghi R, Esmaeili HR, Zarei F, Reichenbacher B (2021) Matrilineal evidence for genetic structure and Late Pleistocene demographic expansion of the ornate goby *Istigobius ornatus* (Teleostei: Gobiidae) in the Persian Gulf and Oman Sea. Marine Ecology (Berlin) 42(1): e12629. https://doi.org/10.1111/maec.12629

Sagnes P, Gaudin P, Statzner B (1997) Shifts in morphometrics and their relation to hydrodynamic potential and habitat use during grayling ontogenesis. Journal of Fish Biology 50(4): 846–858. https://doi.org/10.1111/j.1095-8649.1997.tb01977.x

Sarnthein M (1972) Sediments and history of the Postglacial transgression in the Persian Gulf and northwest Gulf of Oman. Marine Geology 12(4): 245–266. https://doi.org/10.1016/0025-3227(72)90002-3

Smith JLB (1959) Fishes of the family Lethrinidae from the western Indian Ocean. Ichthyological Bulletin Rhodes University 17: 285–295.

Taghavi Motlagh SA, Hashemi SA, Kochanian P (2010) Population biology and assessment of kawakawa (*Euthynnus affinis*) in coastal waters of the Persian Gulf and Sea of Oman (Hormozgan Province). Iranian Journal of Fisheries Science 9: 315–326.

Thangaraj JR, Muthukumarasamy S, Theivasigamani M, Retnamma J (2022) Trophic ecology of four species of emperor fish (*Lethrinus*) in the Gulf of Mannar along the Indian southeast coast. Regional Studies in Marine Science 53: 102442. https://doi.org/10.1016/j.rsma.2022.102442

Torquato F, Range P, Ben-Hamadou R, Sigsgaard EE, Thomsen PF, Riera R, Møller PR (2019) Consequences of marine barriers for genetic diversity of the coral-specialist yellowbar angelfish from the northwestern Indian Ocean. Ecology and Evolution 9(19): 11215–11226. https://doi.org/10.1002/ece3.5622

Vaughan GO, Al-Mansoori N, Burt J (2019) Chapter 1: The Arabian Gulf. Pp. 1–23. In: Sheppard C (Ed.) World Seas: An environmental evaluation. 2nd edn. Elsevier Science, Amsterdam, Netherlands. https://doi.org/10.1016/B978-0-08-100853-9.00001-4

Wabnitz CC, Lam VW, Reygondeau G, Teh L, Al-Abdulrazzak D, Khalfallah M, Cheung WW (2018) Climate change impacts on marine biodiversity, fisheries and society in the Arabian Gulf. PLoS One 13(5): e0194537. https://doi.org/10.1371/journal.pone.0194537

Wilson GG (1998) A description of the early juvenile colour patterns of eleven *Lethrinus* species (Pisces: Lethrinidae) from the Great Barrier Reef, Australia. Records of the Australian Museum 50(1): 55–83. https://doi.org/10.3853/j.0067-1975.50.1998.1274

Zajonz U, Lavergne E, Bogorodsky SV, Saeed FN, Aideed MS, Krupp F (2019) Coastal fish diversity of the Socotra Archipelago Yemen. Zootaxa 4636(1): 1–108. https://doi.org/10.11646/zootaxa.4636.1.1

Zajonz U, Lavergne E, Bogorodsky SV, Krupp F (2022) Biogeography of the coastal fishes of the Socotra Archipelago: Challenging current ecoregional concepts. PLoS One 17(4): e0267086. https://doi.org/10.1371/journal.pone.0267086

Supplementary material 1

List of specimens

Authors: Ehsan Damadi, Faezeh Yazdani Moghaddam, Mehdi Ghanbarifardi

Data type: xlsx

Explanation note: Specimens, localities, accession numbers and coordinates of the five *Lethrinus* species used for the morphometric analysis in the Persian Gulf and Gulf of Oman.

Link: https://doi.org/10.3897/aiep.54.118586.suppl1

Supplementary material 2

Morphological characteristics of *Lethrinus* species

Authors: Ehsan Damadi, Faezeh Yazdani Moghaddam, Mehdi Ghanbarifardi

Data type: xlsx

Explanation note: Statistically significant for each metric and meristic characteristic among the species of *Lethrinus*. Measured characteristics expressed as a percentage of standard length (%SL) and head length (%HL). Asterisks indicate significant P values: *** (< 0.001).

Link: https://doi.org/10.3897/aiep.54.118586.suppl2

Acta Ichthyologica et Piscatoria 54, 2024, 125–129 | DOI 10.3897/aiep.54.118272

PENSOFT.

ACTA
ICHTHYOLOGICA
ET PISCATORIA

Discovery of a ribbon goby, *Oxymetopon compressus* (Actinopterygii: Gobiiformes: Microdesmidae) in Indian waters: A new westernmost record for the genus *Oxymetopon*

Sivakumar RAGUL[1], Gopalan MAHADEVAN[1], Arumugam MURUGAN[2], Ronald FRICKE[3]

1 *Centre of Advanced Study in Marine Biology, Annamalai University, Parangipettai, Tamil Nadu, India*
2 *Crab Meat Processors Association, P &T Colony, Tuticorin, Tamil Nadu, India*
3 *Staatliches Museum für Naturkunde in Stuttgart, Stuttgart, Germany*

https://zoobank.org/E79B865C-14D7-4D00-9070-60F5DAD5CDE9

Corresponding author: Gopalan Mahadevan (marinemahadevan@gmail.com)

Academic editor: Adnan Tokaç ◆ **Received** 4 January 2024 ◆ **Accepted** 1 April 2024 ◆ **Published** 28 May 2024

Citation: Ragul S, Mahadevan G, Murugan A, Fricke R (2024) Discovery of a ribbon goby, *Oxymetopon compressus* (Actinopterygii: Gobiiformes: Microdesmidae) in Indian waters: A new westernmost record for the genus *Oxymetopon*. Acta Ichthyologica et Piscatoria 54: 125–129. https://doi.org/10.3897/aiep.54.118272

Abstract

In October 2023, a single specimen of *Oxymetopon compressus* Chan, 1966 was retrieved from a discarded catch at the Mudasal Odai fish landing center on the southeast coast of India. This study marks the first record of the genus *Oxymetopon* in Indian waters, accompanied by a novel maximum length record. *Oxymetopon compressus*, closely resembles its congener, *Oxymetopon formosum* Fourmanoir, 1967 in having low supraorbital crest and head markings, but differs in having relatively a higher number of anal fin rays, 29 (vs. 27 in *O. formosum*). The anal fin count of *O. compressus* (29) is found higher than the *Oxymetopon curticauda* Prokofiev, 2016 (21–23) and *Oxymetopon filamentosum* Fourmanoir, 1967 (26), whereas it is found lower than the *Oxymetopon cyanoctenosum* Klausewitz et Condé, 1981 and *Oxymetopon typus* Bleeker, 1861 (31). This study describes the distinctive morphological and coloration patterns of the recorded species.

Keywords

Bay of Bengal, distribution, Microdesmidae, new record, ribbon goby

Introduction

The family Microdesmidae, commonly known as wormfish, comprises two subfamilies: Microdesminae and Ptereleotrinae. Within the subfamily Ptereleotrinae, there are eight valid genera and 64 valid species (Fricke et al. 2023). The western Pacific genus *Oxymetopon* Bleeker, 1861 accommodates six valid species (Chan 1966; Fourmanoir 1967; Klausewitz and Condé 1981; Prokofiev 2016): *Oxymetopon compressus* Chan, 1966; *Oxymetopon curticauda* Prokofiev, 2016; *Oxymetopon cyanoctenosum* Klausewitz et Condé, 1981; *Oxymetopon filamentosum* Fourmanoir, 1967; *Oxymetopon formosum* Fourmanoir, 1967; and *Oxymetopon typus* Bleeker, 1861.

Ribbon gobies are predominantly found in silty mud burrows (Klausewitz and Condé 1981; Prokofiev 2016). This study focuses on presenting a novel westernmost distribution record of a ribbon goby species, *Oxymetopon compressus*, in Indian waters, accompanied by a detailed analysis of its morphology, meristic features, and color patterns. One of the newly recorded specimens represents a new maximum length record (94 mm standard length).

Materials and methods

The specimens examined in this study were obtained through monthly trawl bycatch surveys conducted along the southern region of the east coast of India. Mudasal Odai, a prominent fish landing center on India's southeastern coast, was selected for its rich diversity in discarded catches, warranting a comprehensive study (Murugan et al. 2023; Ragul et al. 2024). In October 2023, a single specimen of a gobiid fish representing the genus *Oxymetopon* was identified within the trawl bycatch at the fish landing center in Mudasal Odai (11°29′06″N, 079°46′28″E).

Measurements were conducted using a Mitutoyo CD-6"ASX digital caliper, ensuring a precision of 0.1 mm. Morphometric and meristic characters were documented following Hubbs and Lagler (1964). The collected specimens were preserved in 10% formaldehyde and are housed in the reference museum of the Centre of Advanced Studies in Marine Biology, Annamalai University (CASMBAURM), India.

Identification of the presently reported specimen up to the species level was carried out with reference to Chan (1966), Klausewitz and Condé (1981), and Prokofiev (2016). Family-group classification followed van der Laan et al. (2014), while the genus and species classifications followed Fricke et al. (2023).

Results

Systematic position

Order Gobiiformes
Family Microdesmidae Regan, 1912
Subfamily Ptereleotrinae Bleeker, 1875
Genus *Oxymetopon* Bleeker, 1860

Oxymetopon compressus Chan, 1966

English common name: robust ribbon goby

Fig. 1A–1E; Table 1

Oxymetopon compressus.—Chan (1966): pp. 1–3, fig. 1.—Klausewitz and Condé (1981): pp. 67–76, figs. 5, 5a, 6, 7, 19b, tables I and III.—Koeda and Ho (2019): pp. 85–87.

Oxymetopon compressum.—Prokofiev (2016): pp 175–180, figs. 1c, 2c, table 1 and 2.—Prokofiev (2020): pp. 115, 116, fig. 1f.

Material examined. CASMBAURM/2312819, 1 probably female, 94 mm SL (Fig. 1A–1E), southeast coast of India, off Parangipettai, Mudasal Odai (fish landing center); 11°29′06″N, 079°46′28″E; 9 Oct. 2023, S. Ragul leg.

Description. First dorsal spines VI; second dorsal fin elements I + 29; anal rays I + 29, pelvic rays I + 4; pectoral rays 19; caudal rays 20; predorsal scales 21; gill rakers on 1st arch 26. Meristics and morphometrics in Table 1. Body elongate, laterally compressed, maximum depth (below first dorsal fin) 19.1% of SL, caudal-peduncle depth 9.7% of SL. Straight frontal profile, upward faced lower and upper jaws, 46.0% and 41.5% in HL respectively. A distinct frontal notch present before eye. High dorsal crest (fleshy keel) present. A pair of nasal openings in preorbital region. Mouth oblique, with a single outer row of small, irregular, slightly curved, inward-pointed canine teeth on premaxillary (Fig. 1E). Branchiostegal rays 5/5. Body with small soft ctenoid scales, nape with cycloid scales. Caudal-fin base completely covered with scales. First dorsal fin low (base length 14.5% of SL), second ray 13.5% of SL, connected with second dorsal fin by a low membrane. Second dorsal fin (base length 49.4% of SL) with fourth ray 10.8% of SL; anal fin (base length 42.5% of SL) with third ray 9.2% of SL. Caudal fin lanceolate, pointed, caudal-fin length 30.3% of SL. Pectoral fin rounded, its length 13.6% of SL. Pelvic fin with third ray elongate, pelvic-fin length 14.0% of SL.

Coloration. Freshly dead specimen (Fig. 1A): Head and body pinkish brown; distinct red blotch on upper base of pectoral fin; crest rimmed with bright red; eye with red blotch each on upper and lower margins (Fig. 1D). Three grey-blue iridescent bars traversing eye. Anal fin and lower caudal fin light reddish pink; caudal fin with vertical light orange and pale blue bars. In preserved specimen (Fig. 1B), head and body transitioning to yellowish tint, and belly partially whitish. Anal fin darker compared to fresh state, and caudal fin with prominent dark vertical lines.

Habitat. The robust ribbon goby, *Oxymetopon compressus*, has been reported from a depth range of 10 to 18 m, predominantly on silty-sand bottoms, positioned at the outer edge of coral reefs (Prokofiev 2016). The type specimen, as documented by Chan (1966), was collected on a muddy bottom within the depth range of 14 to 16 m.

In contrast, the presently reported specimen was discovered in a novel habitat, ranging from 20 to 25 m in depth. This new location features muddy-silt washed-out bottom sediments along the Parangipettai coast.

Distribution. *Oxymetopon compressus* has been known only from the western Pacific, from Hong Kong (Chan 1966), Japan: Okinawa, Ryukyu Islands (Ikeda et al. 2000; Akihito et al. 2002), Gulf of Thailand, East Sumatra, Papua New Guinea, Australia: Low Isles, Queensland (Allen and Erdmann 2012) and Vietnam (Prokofiev 2016). The presently reported study expands its distribution to the southeast coast of India in the Indian Ocean.

Discussion

The robust ribbon goby, *Oxymetopon compressus*, differs from its congeners by the number of dorsal-fin rays

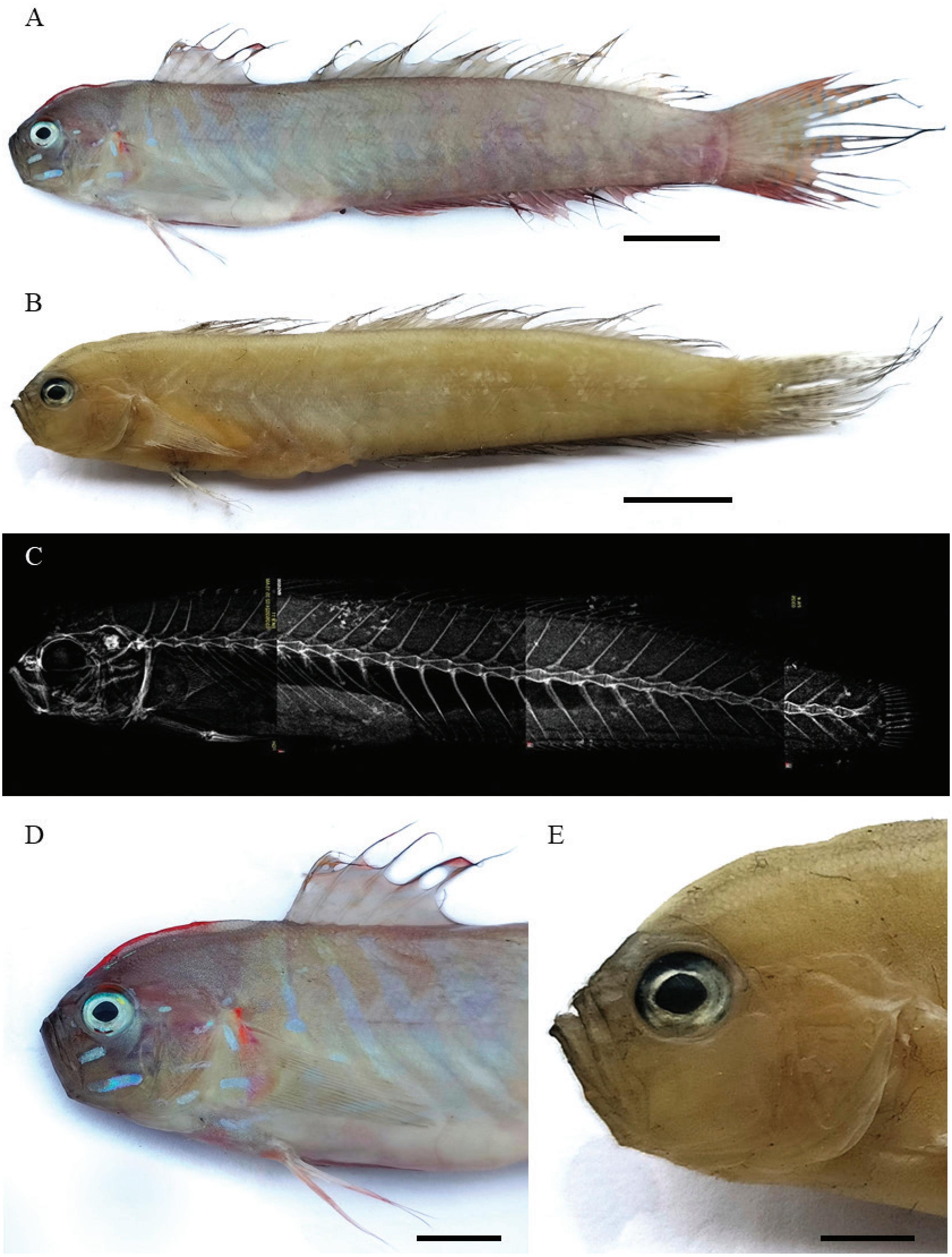

Figure 1. *Oxymetopon compressus* (CASMBAURM 2312819) from southeastern India: (**A–C**) lateral view of (**A**) fresh, (**B**) preserved specimen, and (**C**) radiograph; (**D** and **E**) lateral view of head: (**D**) prominent bright bands and red high crest; (**E**) prominent small scales and canine teeth. Scales: A and B = 10 mm; D and E = 5 mm.

Table 1. Morphometric and meristic data of *Oxymetopon compressus* from Mudasal Odai, India, compared with type specimen.

Character	Chan 1966	Prokofiev 2016	This study
	Holotype Hong Kong	Vietnam	southeastern India
	n = 1	*n* = 12	*n* = 1
Measurements (absolute values) [mm]			
Total length (TL)	—	—	124
Standard length (SL)	66.4	57–82	94
Head length (HL)	12.6	—	14.0
Measurements (relative values) [% of SL]			
Head length	18.9	15.9–20.2 (18.2)	14.9
Greatest body depth at hind base of first dorsal	22.3	17.4–19.3 (18.3)	19.1
Caudal-peduncle depth	11.3	9.1–11.0 (10.2)	9.7
Predorsal (1) length	24.1	—	21.2
Predorsal (2) length	45.2	—	42.2
Preanal length	51.2	—	46.2
Prepectoral length	20.2	—	17.9
Prepelvic length	26.2	—	21.9
Length of first dorsal-fin base	13.6	—	14.5
Length of second ray of first dorsal fin	12.0	—	13.5
Length of second dorsal-fin base	46.7	—	49.4
Length of fourth ray of second dorsal fin	13.6	—	10.8
Length of anal-fin base	41.9	—	42.5
Length of third ray of anal fin	9.0	—	9.22
Pectoral-fin length	18.1	16.3–20.8 (17.9)	13.6
Pelvic-fin length	17.3	14.6–17.5 (16.0)	14.0
Caudal-fin length	37.7	—	30.3
Measurements (relative values) [% of HL]			
Eye diameter	31.8	—	31.2
Upper-jaw length	43.7	—	41.5
Snout length	22.2	—	17.3
Interorbital width	22.2	—	21.1
Counts			
First dorsal-fin elements	VI	VI	VI
Second dorsal-fin elements	I, 30	I, 27–30	I, 29
Anal-fin elements	I, 29	I, 26–29	I, 29
Pectoral-fin rays	20	18–21	19
Pelvic-fin rays	I, 4	I, 4	I, 4
Caudal-fin rays	20	—	20
Predorsal scales	31	—	31
Gill rakers on first arch	32	27–28 (6–7)	32
Vertebral formula	—	10 + 16	10 + 16

and anal-fin rays, especially by the length of the pelvic and pectoral fins and by their color characters. It is distinguished from *O. filamentosum* and *O. typus* by its relatively short first dorsal spines (vs. filamentous in *O. filamentosum* and long in *O. typus*) and by having the anal fin elements of I + 29 (vs. I + 26 in *O. filamentosum* and I + 31 in *O. typus*).

Oxymetopon compressus differs from *O. curticauda* by having a higher number of dorsal and anal fin elements of I + 29 (vs. I + 22–23 and I + 21–23 in *O. curticauda*). *O. compressus* differs from *O. cyanoctenosum* with a more gill rakers count in first gill arch 26 (vs. 21 in *O. cyanoctenosum*) and comparatively length of the pelvic fin is slightly longer than the length pectoral fin but not reaching the anus (vs. elongated pelvic fin which reaches the anus in *O. cyanoctenosum*).

Oxymetopon compressus is most similar to *O. formosum* in sharing low supraorbital crest and head markings (Klausewitz and Condé 1981). However, *O. compressus* differs in the presence of anal fin elements I + 29 (vs. I + 27 in *O. formosum*).

The new record from southern India expands the distribution range of the species by approximately 2200 km to the west (Fig. 2). It indicates that this rare species is apparently much more widespread than previously known and is also expected to occur in the intermediate regions. Additional studies of silty or muddy sediments in the eastern Indian Ocean and western Pacific are needed to assess the full distribution range of *O. compressus*.

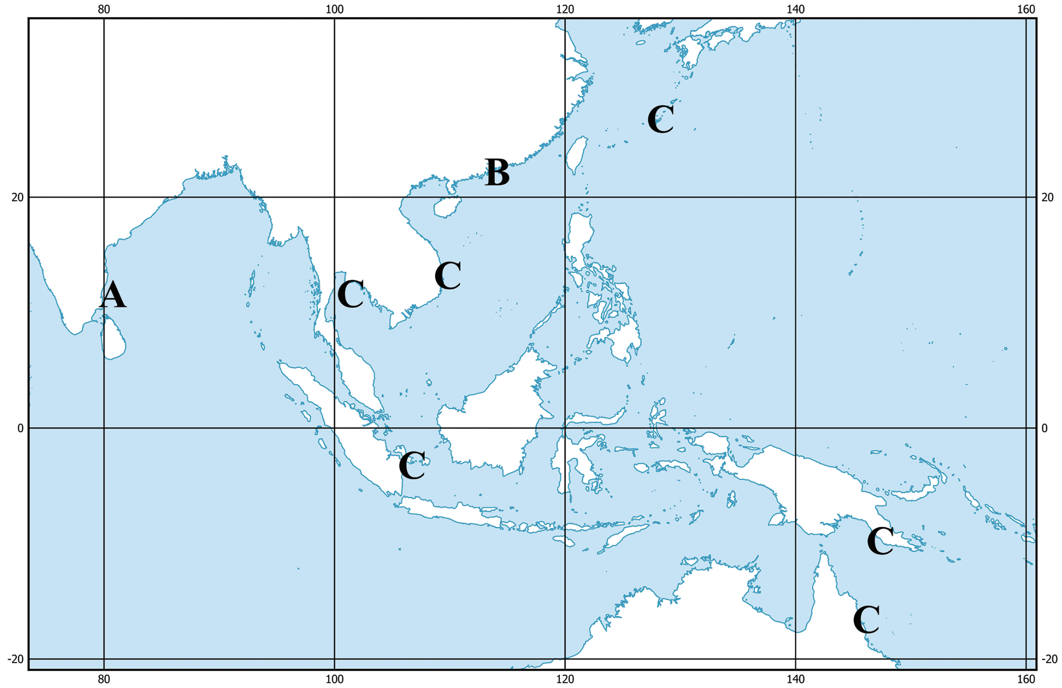

Figure 2. Distribution range of *Oxymetopon compressus*. A = new record; B = type locality; C = other records.

Acknowledgments

The authors are grateful to the Director and Dean of the Faculty of Marine Sciences, Annamalai University, for providing facilities enabling this research. The authors are obliged to Dr Helen K Larson, Museum and Art Gallery of the Northern Territory, Australia for her help in confirming the identification of this species. The authors would also like to thank Mr M. Subramaniyan and Dr M. Divya Sneha for their help in the radiograph of the fish specimen. The authors wish to extend their sincere gratitude to the reviewers for their valuable comments.

References

Akihito SK, Ikeda Y, Sugiyama K (2002) Gobioidei. Pp. 1139–1310. In: Nakabo T (Ed.) Fishes of Japan with pictorial keys to the species (Vol. 2). English edition. Tokai University Press, Tokyo, Japan.

Allen GR, Erdmann MV (2012). Reef fishes of the East Indies. Volumes I–III. Tropical Reef Research, Perth, Australia. https://doi.org/10.1896/054.064.0104

Chan WL (1966) *Oxymetopon compressus*, a new eleotrid fish from Hong Kong. Japanese Journal of Ichthyology 14(1–3). https://doi.org/10.11369/jji1950.14.1

Fourmanoir P (1967) Sur cinq nouvelles especes de poissons du Vietnam. Bulletin du Muséum national d'histoire naturelle 2(2): 267–274.

Fricke R, Eschmeyer WN, van der Laan R (2023) Eschmeyer's catalog of fishes: genera/species by family/subfamily. [Updated 5 December 2023.] California Academy of Sciences, San Francisco, CA, USA. [Electronic version accessed 2 January 2024] http://researcharchive.calacademy.org/research/ichthyology/catalog/SpeciesByFamily.asp

Hubbs CL, Lagler KF (1958) Fishes of the Great Lakes Region. University of Michigan Press, Ann Arbor, MI, USA, 545 pp.

Ikeda Y, Hosoya S, Kozawa T, Kon T, Sakurai Y, Yoshino Y (2000) First record of *Oxymetopon compressus* (Perciformes: Gobioidei: Microdesmidae) from Japan. IOP Diving News 11(12): 2–5. [In Japanese, English abstract]

Klausewitz W, Condé B (1981) *Oxymetopon cyanoctenosum*, n. sp., un nouvel eléotride des Philippines, avec une étude compare du genre (Pisces, Perciformes, Gobioidei, Eleotridae). Revue française d'aquariologie, herpétologie 8(3): 67–76.

Koeda K, Ho H-C (2019) A rare ribbon-goby *Oxymetopon cyanoctenosum* (Actinopterygii: Perciformes: Gobioidei: Microdesmidae): the first and northernmost record from Taiwan. Acta Ichthyologica et Piscatoria 49(1): 85–87. https://doi.org/10.3750/AIEP/02505

Murugan A, Mahadevan G, Subburaman S, Ragul S, Fricke R (2023) First record of the spiny waspfish, *Ablabys macracanthus* (Bleeker, 1852; Scorpaeniformes: Synanceiidae) from Indian coastal waters. Thalassas 1–6. https://doi.org/10.1007/s41208-023-00561-6

Prokofiev AM (2016) Genus *Oxymetopon* (Microdesmidae: Ptereleotrinae) in the coastal areas of Province Khanh Hoa (Vietnam, South China Sea). Journal of Ichthyology 56(2): 175–180. https://doi.org/10.1134/S0032945216020144

Prokofiev AM (2020) Additions to the Gobioidei fauna of Nha Trang and Phan Thiet Bays (South China Sea, Vietnam). Journal of Ichthyology 60(1): 114–117. https://doi.org/10.1134/S0032945220010117

Ragul S, Mahadevan G, Murugan A, Causse R, Kim J-K (2024) New distributional record of the Ward's sleeper goby, *Valenciennea wardii* (Playfair, 1867) (Perciformes: Gobiidae) from Indian waters. Cybium 48(1): 63–65. https://doi.org/10.26028/CYBIUM/2023-038

van der Laan R, Eschmeyer WN, Fricke R (2014) Family-group names of Recent fishes. Zootaxa 3883(2): 1–230. https://doi.org/10.11646/zootaxa.3882.1.1

Acta Ichthyologica et Piscatoria 54, 2024, 131–137 | DOI 10.3897/aiep.54.119501

PENSOFT.

ACTA
ICHTHYOLOGICA
ET PISCATORIA

A new record of an armored searobin, *Paraheminodus kamoharai* (Actinopterygii: Perciformes: Triglidae), from Taiwan, with a checklist of peristediines (Peristediinae) from Taiwan

Yo SU[1], Ching-Feng LIN[2], Tah-Wei CHU[1]

1 *Department and Graduate Institute of Aquaculture, National Kaohsiung University of Science Technology, Kaohsiung, Taiwan*
2 *Department of Theatrical Design and Technology, Taipei National University of the Arts, Taipei, Taiwan*

https://zoobank.org/E31EC4C1-EE33-4415-A072-C5DF31908D4F

Corresponding author: Tah-Wei Chu (twchu@nkust.edu.tw)

Academic editor: Ronald Fricke ♦ **Received** 25 January 2024 ♦ **Accepted** 5 March 2024 ♦ **Published** 14 June 2024

Citation: Su Y, Lin C-F, Chu T-W (2024) A new record of an armored searobin, *Paraheminodus kamoharai* (Actinopterygii: Perciformes: Triglidae), from Taiwan, with a checklist of peristediines (Peristediinae) from Taiwan. Acta Ichthyologica et Piscatoria 54: 131–137. https://doi.org/10.3897/aiep.54.119501

Abstract

A single specimen of a rare species of armored searobin, *Paraheminodus kamoharai* Kawai, Imamura et Nakaya, 2004, is recorded from Taiwan, South China Sea, for the first time. While this particular species has been recorded in the Philippines and Japan, it has never been found in Taiwan. Therefore, our specimen fills the distribution gap of this species in the western Pacific Ocean. A detailed description of the specimen is provided and compared to the data of type specimens. Additionally, a checklist of species recorded from Taiwan is provided. Currently, 20 peristediine species under six genera are recorded from Taiwan's EEZ.

Keywords

biodiversity, biogeography, ichthyology, Scorpaenoidei, Peristediinae, taxonomy

Introduction

The subfamily Peristediinae, otherwise known as armored searobins, currently comprised of six genera and 45 species, is widely distributed from tropical to temperate waters of three major oceans and inhabits depths of 50–1324 m (Richards 1999; Kawai 2008; Fricke et al. 2017, 2024). Among the six genera, the genus *Paraheminodus* Kamohara, 1958 is characterized by having: upper-jaw teeth present; lateral margin of the head smooth, not indented; posterior portions of bony plates on lower lateral rows separated from each other; and all barbels on the lower jaw unbranched, except for posteriormost one (Kawai 2008). Currently, four species are recognized as valid: *Paraheminodus kamoharai* Kawai, Imamura et Nakaya, 2004 from the Philippines; *Paraheminodus laticephalus* (Kamohara, 1952) from Japan; *Paraheminodus longirostralis* Kawai, Nakaya et Séret, 2008 from New Caledonia; and *Paraheminodus murrayi* (Günther, 1880) from the Indo–West Pacific Ocean (Kawai et al. 2008).

The taxonomic study of the Peristediinae in Taiwan has been well studied in recent decades. Kawai and Ho (2019) listed 15 species of peristediines in Taiwan based on literature records (e.g., Shen and Wu 2011; Ho et al. 2013; Kawai 2013, 2019a, 2019b), and included four species from Dong-sha Atoll, South China Sea, of which, *Heminodus philippinus* Smith, 1917 is first recorded from Taiwan' EEZ. After that, Wada et al. (2019) and Kawai and Ho (2020) recorded *Peristedion richardsi* Kawai, 2016 and *Satyrichthys clavilapis* Fowler, 1938 from Taiwan, respectively. As a consequence, 19 peristediine species under six genera have hitherto been known from Taiwan.

Recently, a specimen of an armored searobin of the genus *Paraheminodus* was collected using a bottom trawl from northeastern Taiwan, the northern part of the South China Sea by the second author. A formal description and identification of the specimen is provided and compared to other specimens. Moreover, a checklist of peristediines recorded from Taiwan is provided.

Materials and methods

The specimen was fixed in 4% formaldehyde and transferred to 70% ethanol for preservation. The specimen was deposited in the Pisces Collection of the National Museum of Marine Biology and Aquarium, Pingtung, Taiwan (NMMB-P).

Counts and measurements follow Kawai et al. (2004a, 2004b, 2008). Terminology and methodology of counts of barbels and four rows of bony plates follow Yatou and Okamura (1985). The numbers of paired fins, bony plates, and barbels are presented as left/right whenever available. Gill rakers were counted on the outer face of the first gill arch, with all rudiments included. Terminology of cranial spines follows Miller (1967). All measurements were taken using digital calipers rounding to the nearest 0.1 mm. Morphometric data were expressed as ratios and/or percentages of standard length (SL) and head length (HL), except where otherwise indicated. Data of other specimens were retrieved from Kawai et al. (2004b) and Kawai (2017).

Results

Suborder Scorpaenoidei
Family Triglidae
Subfamily Peristediinae

Paraheminodus kamoharai Kawai, Imamura et Nakaya, 2004

English name: Kamohara's armored searobin
New Chinese name: 蒲原氏副半節魴鮄
Figs. 1–4; Tables 1, 2

Paraheminodus kamoharai Kawai, Imamura et Nakaya, 2004.—Kawai et al. (2004b): 126 (Original description. Type locality: Sulu Sea, the Philippines, 08°11′48″N, 117°58′00″E, depth 285 m).—Kawai 2008: 22 (Listed).—Kawai et al. 2008: 377 (Mentioned, compared to the new species described).—Kawai 2011: 70 (Mentioned).—Kawai 2017: 175 (New record from Japan).

Specimen examined. NMMB-P 39557, 120.1 mm SL, off Daxi fishing port (ca. 24°56′28.16″N, 121°52′12.21″E), Yilan, northwestern Taiwan, 16 September 2023, coll. C.-F. Lin.

Description of NMMB-P 39557. Meristic and morphometric data provided in Tables 1, 2. Dorsal-fin rays VII, 20; pectoral-fin rays 17/17; pelvic-fin rays I, 5/I, 5; anal-fin rays 20; principal caudal-fin rays 12; gill rakers 6 + 1 + 19 = 26; branchiostegal rays 7; bony plates in dorsal row 28/28; bony plates in upper lateral row 34/34 (25th–30th/26th–31st plates with antrorse spine); bony plates in lower lateral row 23/23; bony plates in ventral row 24/24; bony plates before anus 2/2; groups of barbels (lip + chin) 5 + 3/5 + 3. Body fusiform, depth 6.77 in SL, and width 7.22 in SL; its surface covered with bony plates (except for pectoral-fin base, chest, and isthmus). Head large, depressed, and expanded laterally, length 2.87 in SL, and width 3.44 in SL. Rostral projections depressed and elongated, nearly parallel. Interorbital space concave, width 5.07 in HL. Eyes of moderate, width 4.10 in HL. Frontal-1 spine 1, its tip blunt; parietal spine 1, stout, slightly curved backwards. Posttemporal with ridge, and eventually developed as small central spine. Fourth suborbital ridge serrated and bearing 1 (left) or 3 (right) small spines. Nasal, ethmoid, lateral ethmoid, and opercular spines single. Supraorbital spines 3; sphenotic spines 2, both small; and pterotic spine single and small. Rostral, preorbital, frontal-2, supratemporal, third infraorbital spines absent (Figs. 1A, 1B). Mouth large and inferior, upper-jaw length 2.34 in HL, its posterior end before anterior border of orbit; lower-jaw length 2.63 in HL, its anterior tip at about middle of upper jaw, whereas its posterior tip slightly exceeds anterior border of orbit. Single longitudinal ridge starting from base of rostral projection to preopercle. Two preopercular spines: outer one stout, length 2.25 in HL, and inner one rudimentary. Gill rakers on first arch rod-shaped and laterally compressed (except for rudiments), their inner faces covered with minute spinules. Rakers on outer face of first arch longest; rakers on inner face of first arch and both outer and inner faces of second to third arches short. Upper jaw with villiform teeth. Lower jaw, vomer and palatine naked. Lip barbels 5, all simple except for posteriormost one longest and branched, length 1.28 in HL; chin barbels 3, all simple except for posterior one branched at base (Fig. 3). Gill membrane narrowly united anteriorly to base of isthmus. Four rows of bony plates on body, each plate bearing single and recurved spine, except for those in dorsal row on caudal peduncle and two wide plates before anus; 25th–30th /26th–31st bony plates in upper lateral row with single antrorse spine (Fig. 4). Bony plate in anteriormost dorsal row larger than rest. Four anterior bony plates in upper lateral row smaller than rest. Lower lateral row ending at caudal peduncle, near caudal-fin base; other rows ending at caudal-fin base. Dorsal fin originating between first and second bony plates in dorsal row. Anal fin originating just posterior to first bony plate in ventral row. Pectoral-fin length 1.67 in HL, its tip reaching to vertical through base of sixth dorsal-fin soft ray; lower-two rays detached and thickened, with upper one longer than lower. Pelvic-fin length 1.73 in HL, its tip reaching slightly posterior to anus, to second bony plate on ventral row. Caudal fin truncated, slightly rounded.

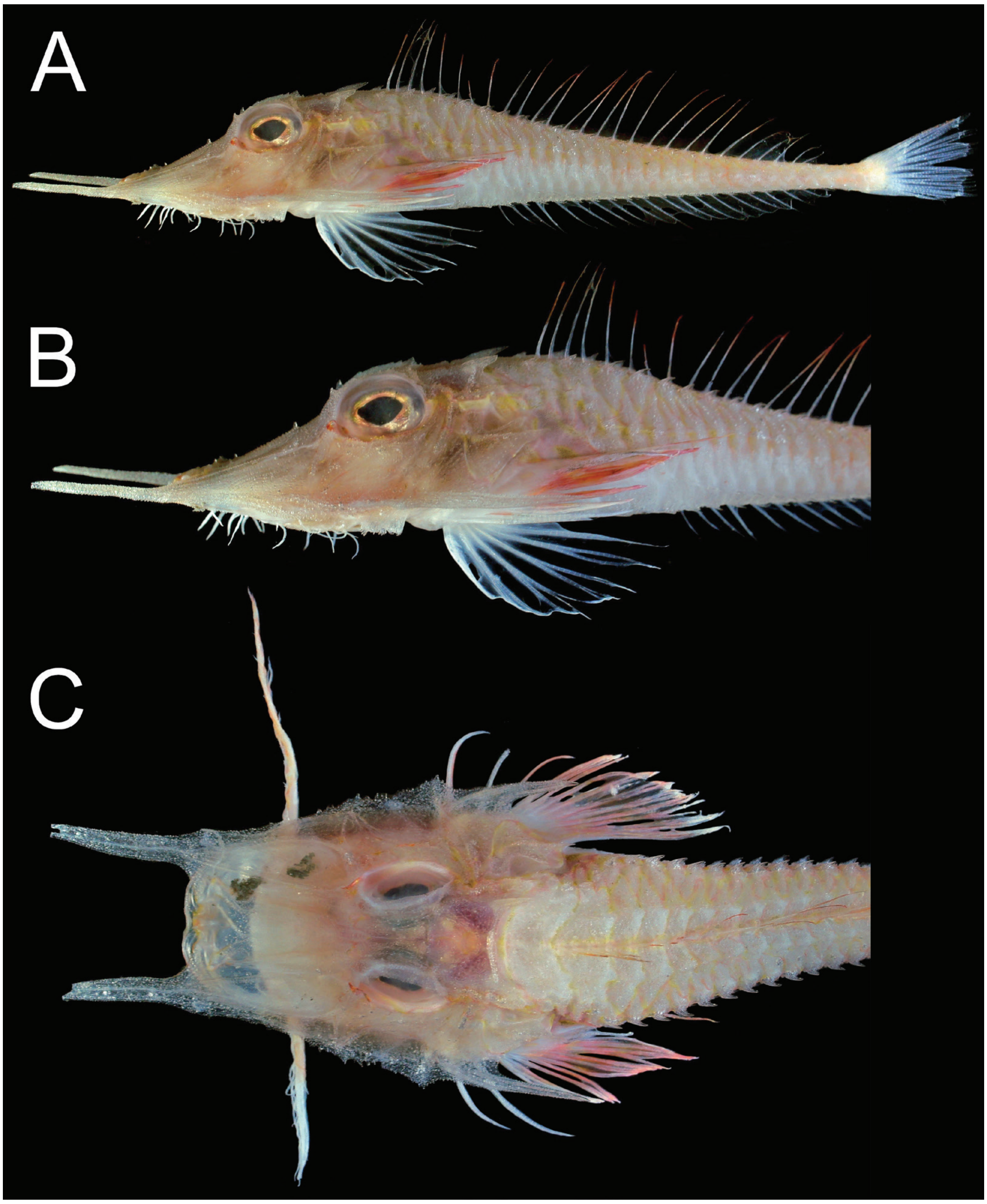

Figure 1. Fresh condition of *Paraheminodus kamoharai*, NMMB-P 39557, 120.1 mm SL. (**A**) Lateral view. (**B**) Close-up image of head in lateral view. (**C**) Close-up image of head in dorsal view. anterior to left. figure not to scale. Photos by C.-F. Lin.

Table 1. Meristic characters of *Paraheminodus kamoharai*. Data were presented as left/right whenever available.

Character	This study	Kawai et al. 2004b		Kawai 2017
	NMMB-P 39557	Holotype	Paratypes (*n* = 2)	FAKU 95640
Dorsal-fin rays	VII, 20	VII, 20	VII, 19–20	VII, 20
Pectoral-fin rays (including two detached rays)	17/17	17	17–18	18
Pelvic-fin rays	I, 5/I, 5	I, 5	I, 5	I, 5
Anal-fin rays	20	20	19	19
Principal caudal-fin rays	12	11	10–12	12
Bony plates in dorsal row	28/28	28	28	29
Bony plates in upper lateral row	34/34	33	33	34
Bony plates in lower lateral row	23/23	22	22–23	23
Bony plates in ventral row	24/24	23	23–24	23
Bony plates before anus	2/2	3	2	2
Bony plates in upper lateral row with antrorse spine	6 (25th–30th)/6 (26th–31st)	6 (25th–30th)	7 (24th–30th)	8 (24th–31st)
Gill rakers	6 + 1 + 19 = 26	5 + 1 + 17 = 23	5 + 1 + 18–19 = 24–25	5 + 1 + 20 = 26
Barbels (lip + chin)	5 + 3/5 + 3	5 + 3	5 + 3	5 + 3
Branchiostegal rays	7	7	7	7

Figure 2. Preserved condition of *Paraheminodus kamoharai*, NMMB-P 39557, 120.1 mm SL. (**A**) Lateral view. (**B**) Dorsal view. (**C**) Ventral view. Photos by Y. Su.

Table 2. Morphometric characters of *Paraheminodus kamoharai*.

Character	This study	Kawai et al. 2004b		Kawai 2017
	NMMB-P 39557	Holotype	Paratypes (*n* = 2)	FAKU 95640
Absolute values [mm]				
Standard length (SL)	120.1	106.9	107.3–114.8	114.2
Relative values [%SL]				
Body depth	14.8	17.8	17.7–19.0	16.9
Body width	13.9	13.4	12.2–14.6	15.0
Head length (HL)	34.9	38.4	37.7–40.4	38.1
Head depth	16.1	16.7	17.6–17.8	17.2
Head width	29.1	30.7	30.6–32.8	30.9
Distance from snout to dorsal fin	36.3	38.5	38.1–39.9	37.0
Distance from snout to anal fin	48.1	49.1	50.8–51.8	51.0
Distance from snout to anus	43.7	44.7	45.0–47.6	46.0
Distance from anus to caudal-fin base	55.1	—	—	46.9
Snout length	18.1	19.8	19.3–19.9	19.7
Rostral-projection length	broken	18.1	16.4	16.2
Longest barbel length	27.3	26.7	25.5–28.5	30.3
Upper-jaw length	14.9	16.3	15.5–16.9	15.4
Lower-jaw length	13.3	14.0	14.0–15.0	14.4
Orbital diameter	8.5	8.5	9.4–9.6	8.8
Interorbital width	6.9	6.4	5.9–6.3	6.2
Preopercular spine length	15.5	—	—	15.5
P length	20.8	25.5	21.8–23.2	22.2
Upper detached P ray	16.9	19.3	15.3–17.7	16.8
Lower detached P ray	13.6	16.0	13.0–14.3	14.4
V length	20.2	21.6	19.3–22.1	21.9
First D spine	10.4	10.1	7.8–9.0	10.5
Caudal-peduncle length	8.5	8.5	9.1–9.4	8.8
Caudal-peduncle depth	3.1	3.3	3.0	2.7

D = dorsal fin, P = pectoral fin, V = pelvic fin.

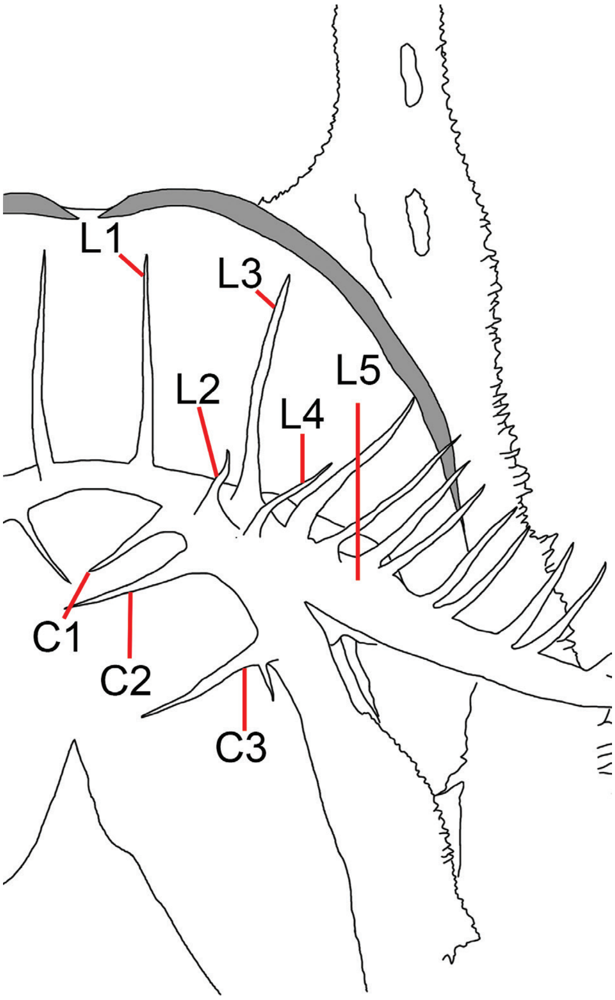

Figure 3. Line drawing of ventral view of *Paraheminodus kamoharai*, NMMB-P 39557, 120.1 mm SL, showing barbels on the lip (L) and chin (C), with villiform tooth patch on upper jaw shaded in grey. Anterior to top. Figure not to scale. Illustrated by Y. Su.

Coloration (fresh). (Fig. 1), head and body reddish yellow. Bony plates on dorsal and upper lateral rows yellow on center and posterior margins. Bony plates on lower lateral and ventral rows pale. Pectoral fin red, slightly tinted with yellow. Pelvic, anal, and caudal fins pale. Dorsal fin pale, with distal half yellow or red. Longest barbel yellow and tinted with red.

Coloration (preserved). (Fig. 2), head, body, all barbels, oral cavity, gill membrane, and arches, and all fins pale. Peritoneum black.

Discussion

Morphological variations. The presently reported specimen is identified as *Paraheminodus kamoharai* in having upper-jaw teeth present (Fig. 3); lateral margin of the head smooth; bony plates on the upper lateral row with an antrorse spine (Fig. 4); rostral-projection length ca. 35% HL (its tip slightly damaged); and pectoral-fin length 59.7% HL (Kawai et al. 2004b, 2008). The meristic characters of our specimen generally agree with the type specimens, with the exception that our specimen possesses one more raker on the upper limb (6, vs. 5; Table 1). On the other hand, several differences in morphometric characters were observed compared to the type specimens. The Taiwanese specimen has a smaller body depth (14.8%SL, vs. 16.9–19.0%SL; Table 2); smaller head length (34.9%SL, vs. 37.7–40.4%SL); slightly smaller distance from the snout to the dorsal fin (36.3%SL, vs. 37.0–39.9%SL); slightly smaller distance from the snout to anal fin (48.1%SL, vs. 49.1–51.8%SL); slightly smaller distance from snout to the anus (43.7%SL, vs. 44.7–47.6%SL); slightly smaller snout length (18.1%SL, vs. 19.3–19.9%SL); slightly smaller upper-jaw length (14.9%SL, vs. 15.4–16.9%SL); slightly smaller lower-jaw length (13.0%SL, vs. 14.0–15.0%SL); slightly smaller pectoral-fin length (20.8%SL, vs. 21.8–25.5%SL); and slightly larger interorbital width (6.9%SL, vs. 5.9–6.4%SL). Since our specimen is by far the largest (120.1 mm SL, vs. 106.9–114.8 mm SL in other specimens), those minor differences are considered ontogenetic variations. However, more specimens are needed to confirm those major differences (e.g., smaller body depth and head length) among different populations or ontogenetic variations.

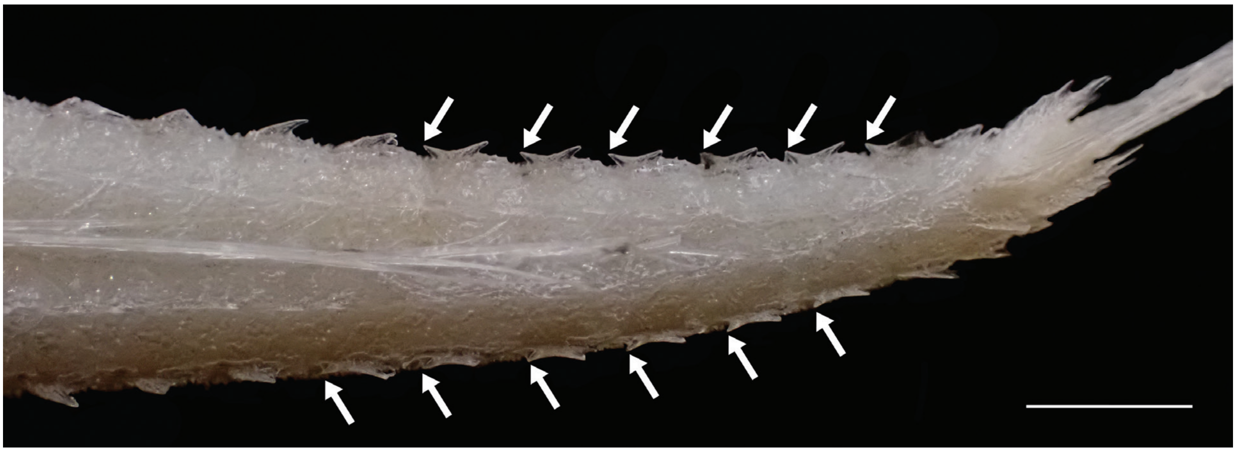

Figure 4. Bony plates on upper lateral row of *Paraheminodus kamoharai*, NMMB-P 39557, 120.1 mm SL, preserved. Arrows point to the antrorse spines. Anterior to left. Scale bar = 5 mm. Photo by Y. Su.

Distribution. This species was previously only known from type specimens collected from the Philippines at a depth of 285 m (Kawai et al. 2004b). Recently, Kawai (2017) reported a specimen collected from Kochi, Japan, representing the northernmost record of this species. Our specimen fills the distribution gap of this species and suggests a wide distribution in the northwest Pacific Ocean.

Checklist of peristediines from Taiwan. Table 3 provides a list of 24 species of Peristediinae recorded from Taiwan, including 20 valid and four invalid species. Among them, four species: *Paraheminodus kamoharai*, *Peristedion longicornutum* Fricke, Kawai, Yato et Motomura, 2017, *Peristedion richardsi*, *Satyrichthys clavilapis* were reported recently (Kawai 2019b; Wada et al. 2019; Kawai and Ho 2020; this study) and represent the northernmost record of each species. On the other hand, four species previously recorded as: "*Peristedion nierstraszi*", "*Satyrichthys isokawae*", "*Satyrichthys piercei*", and "*Scalicus amiscus*" (see Shen 1984a, 1984b; Shao and Chen 1993; Shen and Wu 2011) are now regarded as junior synonyms of *Peristedion riversandersoni* Alcock, 1894, *Satyrichthys moluccensis* (Bleeker, 1850), *Satyrichthys laticeps* (Schlegel, 1852), and *Scalicus hians* (Gilbert et Cramer, 1897), respectively (Kawai 2013, 2016, 2019a).

Table 3. Checklist of peristediine species (Actinopterygii: Perciformes: Triglidae: Peristediinae) recorded from Taiwan.

Species	Chinese name	Reference	Remarks
Gargariscus prionocephalus (Duméril, 1869)	波面黃魴鮄	Shen 1984b; Shao and Chen 1993; Shen and Wu 2011; Yato 2019	
Heminodus philippinus Smith, 1917	菲律賓鬚魴鮄	Kawai and Ho 2019	Only known from Dong-Sha (Pratas) Island
Paraheminodus murrayi (Günther, 1880)	默氏副半節魴鮄	Shen and Wu 2011; Kawai and Ho 2019	
Paraheminodus kamoharai **Kawai, Imamura et Nakaya, 2004**	蒲原氏副半節魴鮄	**This study**	
Peristedion amblygenys Fowler, 1938	鈍頰黃魴鮄	Ho et al. 2013; Yato 2019	
Peristedion liorhynchus (Günther, 1872)	光吻黃魴鮄	Shen and Wu 2011; Ho et al. 2013; Yato 2019	
Peristedion longicornutum Fricke, Kawai, Yato et Motomura, 2017	長角黃魴鮄	Kawai 2019b	
Peristedion orientale Temminck et Schlegel, 1843	東方黃魴鮄	Shen 1984a, 1984b; Chen and Yu 1986; Shao and Chen 1993; Shen and Wu 2011; Ho et al. 2013; Yato 2019	The figure in Shen and Wu 2011 depicts *Satyrichthys rieffeli*
Peristedion richardsi Kawai, 2016	里氏黃魴鮄	Wada et al. 2019; Yato 2019	
Peristedion riversandersoni Alcock, 1894	黑帶黃魴鮄	Shen 1984a, 1984b; Shao and Chen 1993; Shen and Wu 2011; Ho et al. 2013; Kawai and Ho 2019; Yato 2019	Reported as "*Peristedion nierstraszi*" by Shen 1984a, 1984b; Shao and Chen 1993; Shen and Wu 2011; Ho et al. 2013
Satyrichthys clavilapis Fowler, 1938	菲律賓紅魴鮄	Yato 2019; Kawai and Ho 2020	Reported by Yato 2019 as *Satyrichthys* sp.
Satyrichthys laticeps (Schlegel, 1852)	闊頭紅魴鮄	Shen and Wu 2011; Kawai 2013; Yato 2019	Reported by Shen and Wu 2011 as *Satyrichthys piercei*
Satyrichthys milleri Kawai, 2013	米氏紅魴鮄	Kawai 2013; Yato 2019	One paratype (HUMZ 213180) was collected from Taiwan
Satyrichthys moluccensis (Bleeker, 1850)	摩鹿加紅魴鮄	Shen and Wu 2011; Yato 2019	Reported by Shen and Wu 2011 as "*Satyrichthys isokawae*"
Satyrichthys rieffeli (Kaup, 1859)	瑞氏紅魴鮄	Shen 1984a, 1984b; Chen and Yu 1986; Shao and Chen 1993; Shen and Wu 2011; Kawai 2013; Yato 2019	
Satyrichthys welchi (Herre, 1925)	魏氏紅魴鮄	Shen and Wu 2011; Yato 2019	
Scalicus hians (Gilbert et Cramer, 1897)	褐緣叉吻魴鮄	Shen 1984b; Chen and Yu 1986; Shao and Chen 1993; Shen and Wu 2011; Kawai 2019a; Yato 2019	Reported by Shen 1984b; Chen and Yu 1986; Shao and Chen 1993; Shen and Wu 2011 as "*Scalicus amiscus*". The figure in Shen and Wu 2011 depicts *Satyrichthys milleri*
Scalicus orientalis (Fowler, 1938)	東方叉吻魴鮄	Kawai 2019a; Yato 2019	One paratype (USNM 98917) was collected from off Dong-Sha (Pratas) Island
Scalicus paucibarbatus Kawai, 2019	少鬚叉吻魴鮄	Kawai 2019a	One paratype (NMMB-P 12029) was collected from Taiwan
Scalicus quadratorostratus (Fourmanoir et Rivaton, 1979)	方吻叉吻魴鮄	Kawai 2019a	

Acknowledgments

We thank Dr T. Kawai (HUMZ) for assistance in identifying the specimen; Dr H.-C. Ho (NKUST) for reading the early draft, giving critical suggestions, and providing access to facilities; P.-N. Lee (NMMBA) for curatorial assistance; and Y.-C. Hsu (NSYSU) for various assistance in specimen fixation. This study was supported by the National Kaohsiung University of Science Technology (NKUST).

References

Chen JTF, Yu M-J (1986) [A synopsis of the vertebrates of Taiwan. Revised and enlarged edition. Vol. 2.] Commercial Press, Taipei, Taiwan, 548 pp. [In Chinese]

Fricke R, Kawai T, Yato T, Motomura H (2017) *Peristedion longicornutum*, a new species of armored gurnard from the western Pacific Ocean (Teleostei: Peristediidae). Journal of the Ocean Science Foundation 28: 90–102. https://doi.org/10.5281/zenodo.1008818

Fricke R, Eschmeyer WN, Van der Laan R (Eds) (2024) Eschmeyer's catalog of fishes: genera, species, references. California Academy of Sciences, San Francisco, CA, USA. [Accessed 5 April 2024] http://researcharchive.calacademy.org/research/ichthyology/catalog/fishcatmain.asp

Ho H-C, Chee W-L, Chang C-H, Shao K-T (2013) Taxonomic review and DNA barcoding of the fish genus *Peristedion* (Scorpaeniformes: Peristediidae) in Taiwan. Platax 19: 37–55. https://doi.org/10.29926/PLATAX.201312_2013.0003

Kawai T (2008) Phylogenetic systematics of the family Peristediidae (Teleostei: Actinopterygii). Species Diversity 13(1): 1–34. https://doi.org/10.12782/specdiv.13.1

Kawai T (2013) Revision of the peristediid genus *Satyrichthys* (Actinopterygii: Teleostei) with the description of a new species, *S. milleri* sp. nov. Zootaxa 3635(4): 419–438. https://doi.org/10.11646/zootaxa.3635.4.5

Kawai T (2016) *Peristedion richardsi* sp. nov. (Actinopterygii: Teleostei: Peristediidae) from Indonesian waters, with synonymy between *Peristedion riversandersoni* Alcock, 1894 and *Peristedion nierstraszi* Weber, 1913. Zootaxa 4171(2): 335–346. https://doi.org/10.11646/zootaxa.4171.2.6

Kawai T (2017) First Japanese record of *Paraheminodus kamoharai* (Peristediidae) from Kochi, Japan. Japanese Journal of Ichthyology 64: 175–178. [In Japanese with English Abstract] https://doi.org/10.11369/jji.64-175

Kawai T (2019a) Revision of an armored searobin genus *Scalicus* Jordan 1923 (Actinopterygii: Teleostei: Peristediidae) with a single new species. Ichthyological Research 66(4): 437–459. https://doi.org/10.1007/s10228-019-00691-z

Kawai T (2019b) *Peristedion longicornutum* Fricke, Kawai, Yato and Motomura, 2017 (Actinopterygii: Teleostei: Peristediidae) from Philippines and Taiwan. Thailand National History Museum Journal 13: 69–75.

Kawai T, Ho H-C (2019) Records of four species of armored searobins (Teleostei: Peristediidae) from Dongsha Atoll in the South China Sea. Platax 16: 67–75. https://doi.org/10.29926/PLATAX.201912_2019.0005

Kawai T, Ho H-C (2020) First record of an armored searobin, *Satyrichthys clavilapis* Fowler, 1938 (Teleostei: Peristediidae) from Taiwan. Platax 17: 113–117. https://doi.org/10.29926/platax.202012_17.0008

Kawai T, Imamura H, Nakaya K (2004a) *Paraheminodus kochiensis* Kamohara, 1957 (Teleostei: Peristediidae), a junior synonym of *Paraheminodus murrayi* (Günther, 1880), with a comparison of *Paraheminodus murrayi* and *Paraheminodus laticephalus* (Kamohara, 1952). Ichthyological Research 51(1): 73–76. https://doi.org/10.1007/s10228-003-0188-0

Kawai T, Imamura H, Nakaya K (2004b) A new species of armored sea robin, *Paraheminodus kamoharai* (Teleostei: Peristediidae), from the Philippines. Ichthyological Research 51(2): 126–130. https://doi.org/10.1007/s10228-004-0205-y

Kawai T, Nakaya K, Séret B (2008) A new armored searobin *Paraheminodus longirostralis* (Teleostei: Peristediidae) from New Caledonia. Ichthyological Research 55(4): 374–378. https://doi.org/10.1007/s10228-008-0061-2

Miller GC (1967) A new species of western Atlantic armored searobin, *Peristedion greyae* (Pisces: Peristediidae). Bulletin of Marine Science 17: 16–41.

Richards WJ (1999) Family Triglidae. Pp. 2359–2382. In: Carpenter KE, Niem VE (Eds) Species identification guide for fisheries purposes. The living marine resources of the western central Pacific. Volume 4. Bony fishes part 2 (Mugilidae to Carangidae). FAO, Rome.

Shao K-T, Chen J-P (1993) [Subamily Peristediinae.] Pp. 251–252, pls 61-3–62-3. In: Shen S-C (Ed.) [Fishes of Taiwan.] National Taiwan University, Taipei, Taiwan. [In Chinese]

Shen S-C (1984a) [Coastal fishes of Taiwan.] National Taiwan Museum, Taipei, Taiwan, 189 pp. [In Chinese]

Shen S-C (1984b) [Synopsis of fishes of Taiwan.] Southern Materials Center, Taipei, Taiwan, 533 pp. [In Chinese]

Shen S-C, Wu K-Y (2011) [Fishes of Taiwan.] National Museum of Marine Biology and Aquarium, Checheng, Taiwan, 986 pp. [In Chinese]

Wada H, Hata H, Motomura H (2019) First Northern Hemisphere record of a poorly known armored searobin *Peristedion richardsi* (Actinopterygii: Teleostei: Peristediidae) from Taiwan. Species Diversity 24(2): 203–207. https://doi.org/10.12782/specdiv.24.203

Yato T (2019) [Family Peristediidae.] Pp. 557–570. In: Koeda K, Ho H-C (Eds.) [Fishes of southern Taiwan.] National Museum of Marine Biology and Aquarium, Checheng, Taiwan. [In Chinese and English]

Yatou T, Okamura O (1985) *Satyrichthys isokawae* Yatou et Okamura, sp. nov. Pp. 586–589. In: Okamura O (Ed.) Fishes of the Okinawa Trough and the adjacent waters, Vol 2. The intensive research of unexploited fishery resources on continental slopes. Japan Fisheries Resource Conservation Association, Tokyo, Japan. [In English and Japanese]

Acta Ichthyologica et Piscatoria 54, 2024, 139–150 | DOI 10.3897/aiep.54.121813

PENSOFT.

ACTA
ICHTHYOLOGICA
ET PISCATORIA

Additional records of the little sleeper shark, *Somniosus rostratus* (Elasmobranchii: Squaliformes: Somniosidae), in Mediterranean Sea

Gianni INSACCO[1], Bruno ZAVA[1,2], Filippo SPADOLA[3], Danilo SCANNELLA[4], Alan DEIDUN[5], Franco CIGALA-FULGOSI[6], Massimiliano VALASTRO[7], Antonio DI NATALE[7], Corrado PICCINETTI[8], Maria CORSINI-FOKA[9]

1 *Museo Civico di Storia Naturale, Comiso (Ragusa), Italy*
2 *Wilderness Studi Ambientali, Palermo, Italy*
3 *Museo della Fauna, Dipartimento di Scienze Veterinarie, Università degli Studi di Messina, Messina, Italy*
4 *Italian Institute for Environmental Protection and Research (ISPRA), Department for the Monitoring and Protection of the Environment and for the Conservation of Biodiversity, Palermo, Italy*
5 *Oceanography Malta Research Group (OMRG), Department of Geosciences, University of Malta, Msida, Malta*
6 *Strada Martinella 292, 43124 Parma, Italy*
7 *Aquastudio, Messina, Italy*
8 *Laboratorio di Biologia Marina e Pesca dell'Università di Bologna in Fano, Fano (Pescara), Italy*
9 *Hellenic Centre for Marine Research, Institute of Oceanography, Hydrobiological Station of Rhodes, Rhodes, Greece*

https://zoobank.org/D62187AC-2BAF-46E9-92FD-FE68657F23B9

Corresponding author: Danilo Scannella (danilo.scannella@isprambiente.it)

Academic editor: Sanja Matić-Skoko ♦ **Received** 27 February 2024 ♦ **Accepted** 9 April 2024 ♦ **Published** 14 June 2024

Citation: Insacco G, Zava B, Spadola F, Scannella D, Deidun A, Cigala-Fulgosi F, Valastro M, Di Natale A, Piccinetti C, Corsini-Foka M (2024) Additional records of the little sleeper shark, *Somniosus rostratus* (Elasmobranchii: Squaliformes: Somniosidae), in Mediterranean Sea. Acta Ichthyologica et Piscatoria 54: 139–150. https://doi.org/10.3897/aiep.54.121813

Abstract

This study investigates the distribution and morphometrics of the little sleeper shark, *Somniosus rostratus* (Risso, 1827), in the Mediterranean Sea. Ten sharks caught as bycatch between 2009 and 2019 in the northern sectors of the Strait of Sicily, the south Tyrrhenian Sea, the northwestern Ionian Sea, and the south Adriatic Sea using drifting longlines, as well as five retrieved from the Tripoli (Libya) marketplace, were morphologically confirmed to represent *S. rostratus.* The sharks exhibited typical characteristics for this species and were all caught from deep waters, indicating a potential mesopelagic habit. The study also utilized literature reviews and global databases for a comprehensive mapping of *S. rostratus* distribution in the Mediterranean Sea, which revealed sporadic occurrences in the eastern Mediterranean and an absence in the north Adriatic Sea. Morphometric data provided insights into the reproductive characteristics of *S. rostratus*. The study highlights the ecological significance of the Strait of Sicily (Central Mediterranean Sea) for the species, indicating it as a likely spawning area, and underscores the impact of the interactions between sharks and pelagic drifting swordfish fisheries in the Mediterranean, which result in increased mortality rates for threatened shark and ray species. Prioritizing conservation measures for endangered elasmobranch populations is crucial for maintaining marine ecosystem balance and ensuring fishery resource sustainability.

Keywords

biodiversity, distribution, elasmobranch Mediterranean Sea, *Somniosus rostratus*

Introduction

The deep-water little sleeper shark, *Somniosus rostratus* (Risso, 1827), is a rare or apparently rare chondrichthyan (Garibaldi et al. 2012; Guallart et al. 2013), currently assessed at the global level as Least Concern by the IUCN Red List (Finucci et al. 2020).

The little sleeper shark is found at depths from 180 m to 2734 m, reaches a maximum total length of 1314 mm (Weigmann 2016), and apparently feeds mainly on cephalopods, but also benthic invertebrates and fishes (Golani 1986; Garibaldi et al. 2012; Guallart et al. 2013; Barría et al. 2015a; Capapé et al. 2020; Ebert and Dando 2022). The apparent rarity of this shark may be due to several reasons, including a naturally low population density (Garibaldi et al. 2012; Guallart et al. 2013), the inadequacy of the fishing gears deployed in catching this species, and the non-exploitation of deep bottom-dwelling habitats throughout its range.

The general distribution of *S. rostratus* includes the Eastern Atlantic, extending from areas off the United Kingdom and Ireland, to France, Portugal, the Madeira Islands, Canary Islands and Western Sahara, as well as the Western Central Atlantic, possibly from areas located off Cuba, up to the Mediterranean Sea (Compagno 1984; Yano et al. 2004; Ebert and Stehmann 2013; Ebert et al. 2013; Meléndez et al. 2017; Finucci et al. 2020; Ebert and Dando 2022). In the Mediterranean, *S. rostratus* is prevalent in the western sector, albeit not very abundant, and appears sporadically in the eastern sector; to date, it is absent in the north Adriatic and the Black Sea (Goren and Galil 2015; Serena et al. 2020; Damalas et al. 2022; Ebert and Dando 2022).

In this study, the capture of *S. rostratus* from the Strait of Sicily in the central Mediterranean, plus additional records from the Tyrrhenian, Ionian, Adriatic, and Libyan waters is described, and the distribution records of this species in the basin, recently reviewed by Capapé et al. (2020), is updated.

Material and methods

Three specimens of *Somniosus rostratus* were captured in the northern sectors of the Strait of Sicily, by a commercial fishing vessel as swordfish bycatch, two specimens (S1 and S2) on 13 September 2015 off Licata (Fig. 1: map ID 36; Fig. 2A), the third (S3) on 15 September 2015 off Gela (Fig. 1: Map ID 37; Fig. 2A) (Table 1). Mesopelagic drifting longlines (Kirby Sea; fishing hook No. 2) baited with mackerel and squids were used. Catches were carried out during the night. The fishermen declared that they had never landed those sharks before. Between August and September 2016, two additional specimens (S4 and S5) were fished by the same boat and with the same gear reported above, off Scoglitti (Fig. 1: map ID 38; Fig. 2B) (Table 1).

The specimens S1, S3, S4, and S5 were deposited at the Museo Civico di Storia Naturale, Comiso, Italy (MSNC) and S2 was deposited at the Wilderness Studi Ambientali, Palermo, Italy (WSA). At these institutions, selected morphometric measurements were taken to the nearest 1 mm using a digital caliper, following Compagno (1984); weight was determined to the nearest 0.1 g (Table 2). Females were dissected, the uterine contents examined and, in case of pregnancy, eggs and embryos were counted and measured. The following catalog numbers were assigned to the above five sharks: S1, MSNC 4885; S2, WSASr1; S3, MSNC 4886; S4, MSNC 4887; and S5, MSNC 4888.

Other records of *S. rostratus* collected through experimental fishing surveys are furthermore presented (Table 1):

- On 22 July 2009, in the northwestern Ionian Sea, a specimen (S6) (Fig. 1: map ID 27) (Fig. 3) was caught using a drifting longline set with 1100 hooks (soaking time 24 h 30 min), targeting swordfish (six swordfish were captured, with a total weight of 233 kg), along with a specimen of *Pteroplatytrygon violacea* (Bonaparte, 1832) (≈7 kg).
- On 21 and 22 July 2010, two specimens of *S. rostratus* (S7 and S8) were captured in the northwestern Ionian Sea (Fig. 1: map ID 30), using a drifting longline equipped with 1100 hooks (soaking time ≈ 14 h). The longline was targeting swordfish, resulting in the capture of 11 specimens weighing (in total) 395 kg and 8 specimens weighing 411 kg, respectively. Furthermore, on 21 July 2010, a specimen of *Zu cristatus* (Bonelli, 1819) (≈4 kg), along with four specimens of *Ruvettus pretiosus* Cocco, 1833 (total weight ≈ 44 kg), were unintentionally caught and subsequently discarded. On 22 July 2010, only three specimens of *R. pretiosus* (total weight ≈ 44 kg) were caught and discarded.
- On 14 July 2011, a specimen (S9) was captured in the southern Tyrrhenian Sea around the Aeolian Islands (Fig. 1: map ID 31), using a drifting longline (1100 hooks; soaking time 6 h 30 min) targeting swordfish (8 swordfish specimens weighing 167 kg) along with a specimen of *Z. cristatus* (≈4 kg).
- On 4 September 2019, in the southern Adriatic (Fig. 1: map ID 41), a specimen (S10) was caught using a drifting longline. The fishing operation occurred between 03:45 and 09:39 hours.
- In 2006, one of us (ADN) observed the presence of five specimens of *S. rostratus* (S11 to S15) in the Tripoli fish market. After interviewing the fishers, it was ascertained that the five specimens were caught with pelagic longlines, together with other sharks, off the central-western Libyan coast.

For S6–S9 only an approximate weight was obtained, while TL and weight were measured for S10; S6–S10 were discarded. No data were collected for S11–S15.

Table 1. Summary of *Somniosus rostratus* records in the Mediterranean (The majority of records cited after Capapé et al. 2020).

Marine region	Locality	Map ID	Year	Latitude (N), Longitude (E)	Depth [m]	Fishing gear	*N*	*W* [g]	TL [mm]	FL [mm]	Reference
Adriatic Sea	South sector	19									[1]
	Off Apulia	34	2012?		427–788	MEMO					[2] [3]
	South sector	41	2019	41°17′38.92″N, 17°43′31.09″E	1140	MD-LL	1♂	3121	890		**This study** (S10)
	South sector	42	2019	41°45′00.00″N, 17°22′00.12″E	1100	LL	4				Bueloni personal communication
Aegean Sea	North of Crete	10									[4] [5] [6] [7]
	North sector	18	1990–1992		100–500	BT					[8] [7]
Algerian Sea		9									[9]
	100 km off Algiers (Dellys, Cap Djenet, Bou Haroun, Cherchell)	28	2009–2015	36°55′N, 3°53′E			19				[10]
				36°43′N, 3°36′E							
				36°40′N, 4°40′E							
				36°37′N, 2°11′E							
Catalan Sea	Off Barcelona	16	1987	41°02′N, 3°04′E	1975	LL	1♂		680		[11]
	Off Barcelona	22	1994	40°42′N, 1°32′E	180	LL	1♂		650		[11]
	Off Barcelona	23	1999	41°01′N, 2°16′E	534	BT	1♀ pr.		1000		[12]
	Ibiza Channel	35	2013–2014		550–670	BT	20 (8♀ pr.)		874–1042		[13] [14]
Catalan Sea	Gulf of Lions	33	2011–2013		40–2200	BT	5		715–980		[15] [16]
Gulf of Lions	Off Nice	1	1826		Very deep		1♀		310		[17]
	Off Nice	1	1874				1♀ pr.				[18]
	Off Nice	1	1880?								[19]
	Off Nice	1	1880				1♂		705		[20]
	Off Nice	1	1900				1♂		282		[20]
	Off Nice	1	1882?				1♀		490		[20]
Ionian Sea	East of Sicily	4	1892				1				[21]
	East of Sicily, off Simeto River estuary	5	1893		1000		1♀ pr.				[21]
	Northwestern	15	1985–1988?		>200						[22]C
	Eastern sector	21									Questionable in [23]
	Northwestern sector	27	2009	37°48′42.01″N, 16°56′08.99″E		MD-LL	1♀	~5000			**This study** (S6)
	Northwestern sector	30	2010	38°45′15.01″N, 17°51′24.01″E		MD-LL	1	~8000			**This study** (S7)
	Northwestern sector	30	2010	38°53′32.39″N, 17°35′46.79″E		MD-LL	1	~6000			**This study** (S8)
Levantine Sea	Off Haifa	13	1985	32°58′44″N, 34°35′46″E	1330	LL	1♂		775		[24]
	Off Haifa	14	1985–1991	32°31′00″N, 34°02′00″E	1280–1500	LL	8 (2♀ pr.)				[25]
				33°02′00″N, 34°37′00″E							
	Off Israel coasts	17	1988–1999		734–1558	BT					[26]
	Syrian waters	24	2001	35°36′N, 35°39′E	450	LL	76		**1020** (largest)		[27] [28] [29] [30] [31]
	Off Fethiye	25	2008	36°25′00″N, 28°47′00″E	2500	LL	1♀		810		[32]
Libyan Sea	Libyan waters, west	12									[33] [34] [35] [36]
	Tripoli market	NM	2006				5				**This study,** ADN personal observation (S11-S15)
	Off South of Crete	26	2009	34°32′37.68″N, 25°46′30.00″E	1200	OT	1				[37]
Ligurian Sea		2							820		[38 [39]
		2					1♀pr.				[40] [1]
		2									[41] [40] [42] [1]
		2	2010?		>1500	LL	25♂		>655		[43] [44]
		2	2010?		>1500	LL	30♀		Some ♀ > 800		[43] [44]
		2	2015								[45]
	Genova	6	1899				1♀		955		[20]
Ligurian Sea	Sestri Levante	7	1899				1♀		937		[20]
	Sestri Levante	7	1979	44°10′N, 9°25′E			1♀ pr.		822		[20]
	Bonassola	8	1909								[40]
	Ventimiglia	11					1♀		953		[20]

Table continues on next page.

Table 1. Continued.

Marine region	Locality	Map ID	Year	Latitude (N), Longitude (E)	Depth [m]	Fishing gear	*N*	*W* [g]	TL [mm]	FL [mm]	Reference
Strait of Gibraltar and Alboran Sea		39									[46]
Strait of Sicily	Malta Island	32	2011			LL	2♀		935 1036		[47]
	Malta Island	32	2015				1				[48]
	Malta Island	32	2016				1				[48]
	Off Licata	36	2015	36°45′59.93″N, 13°51′36.67″E	~700	MD-LL	2♀ pr.	6850 6650	992 985		**This study** (S1, S2)
	Off Gela	37	2015	36°42′12.00″N, 14°08′09.00″E	~700	MD-LL	1♀ pr.	7480	990		**This study** (S3)
	Off Scoglitti	38	2016	36°45′29.04″N, 14°05′03.40″E		MD-LL	1♀ 1♂	5950 1140	925 618		**This study** (S4, S5)
	Off Ras Jebel, northeastern Tunisian coast	40	2019	37°31′28″N, 10°17′10″E	120	BT			990		[49]
Tyrrhenian Sea	Off Palermo	3	1874				1♀		880		[50]
		20									
	Off Anzio	29	2010			LL	1♀		800		[51]
	Aeolian Islands	31	2011	38°43′31.20″N, 14°59′29.40″E		MD-LL	1	5000			**This study** (S9)
Western Mediterranean		NM	2009–2013	36–44°N, 2–5°E		LL	24			715–980	[52] [16]

LL = longline; BT = bottom trawl; MD-LL = meso-pelagic longlines; NM = not mapped; ? = questionable; pr. = pregnant; TL = total length; FL,= fork length; *W* = weight; OT = otter trawl, MEMO = Marine Environment Monitoring system; S1–S15 = specimens numbered as reported in the text and in Tables 2, 3. [1] Costa (1991); [2] Carluccio et al. (2019); [3] Carluccio et al. (2021); [4] Ananiadis (1961); [5] Economidis (1973); [6] Papaconstantinou (2014); [7] Papaconstantinou and Conides (2021); [8] Labropoulou and Papaconstantinou (2000); [9] Dieuzeide et al. (1953); [10] Kheddam et al. (2016); [11] Barrull and Mate (1995); [12] Barrull and Mate (2001); [13] Guallart et al. (2013); [14] Guallart and García-Salinas (2015); [15] Barría et al. (2015b); [16] Carpentieri et al. (2021); [17] Risso (1826); [18] Moreau (1881); [19] Giglioli (1880); [20] Cigala-Fulgosi and Gandolfi (1983); [21] Sicher (1898); [22] Capezzuto et al. (2010); [23] Papaconstantinou (1990); [24] Golani (1986); [25] Hornung et al. (1993); [26] Galil (2004); [27] Ali and Saad (2003); [28] Saad et al. (2004); [29] Saad et al. (2006); [30] Saad and Alkusairy (2022); [31] Damalas et al. (2022); [32] Irmak and Özden (2021); [33] Compagno (1984); [34] UNEP-MAP RAC/SPA (2005); [35] Séret et al. (2009); [36] Finucci et al. (2020); [37] Tecchio and Ramirez-Llodra (2018); [38] Canestrini (1864); [39] Canestrini (1872); [40] Tortonese (1956); [41] Tortonese (1952); [42] Tortonese (1968); [43] Garibaldi et al. (2012); [44] Garibaldi (2015); [45] Ferrando et al. (2019); [46] Báez et al. (2019); [47] Vella et al. (2013); [48] Vella et al. (2017); [49] Capapé et al. (2020); [50] Doderlein (1881); [51] Psomadakis et al. (2012); [52] De Loyola Fernández et al. (2017). Dr Elia Bueloni is affiliated with the Cooperativa Torpedo, Ravenna.

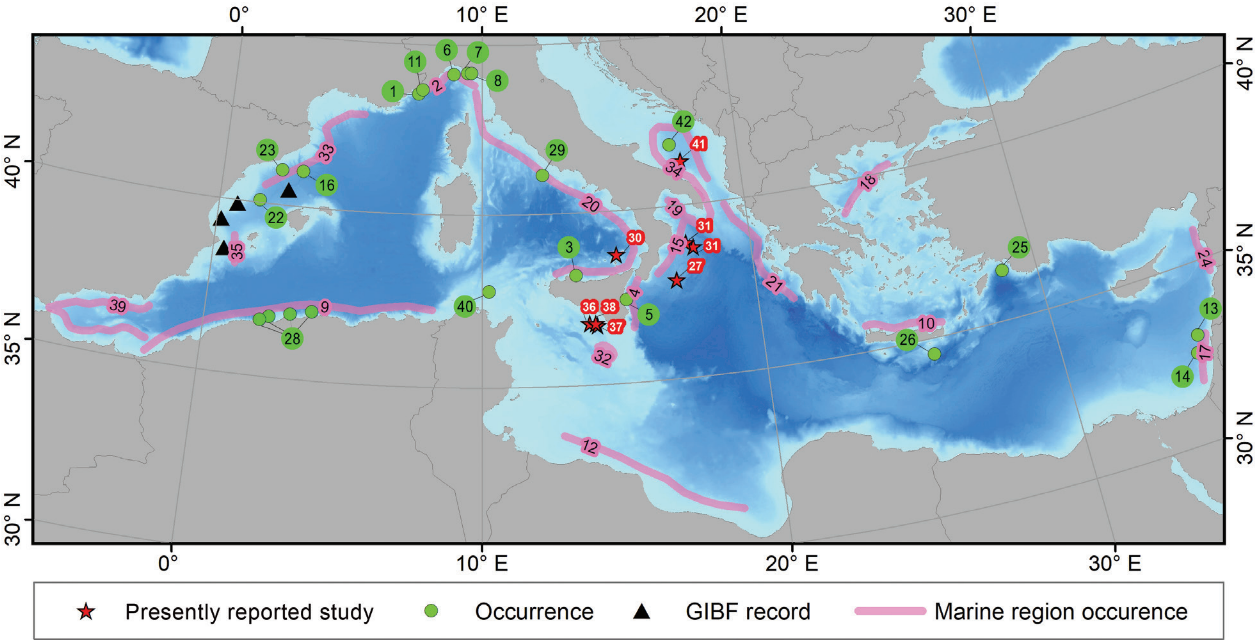

Figure 1. Geographical distribution of *Somniosus rostratus* based on the previous records and presently reported study within the Mediterranean Basin. The red star shows occurrence records for this study; the green circle represents occurrence records with geographic coordinates, from the literature; the pink represents occurrence records without geographic coordinates; and the black triangles are GBIF occurrence records (GIBF 2024). The numbers refer to the "Map ID" in the Table 1 to identify the reference of the record.

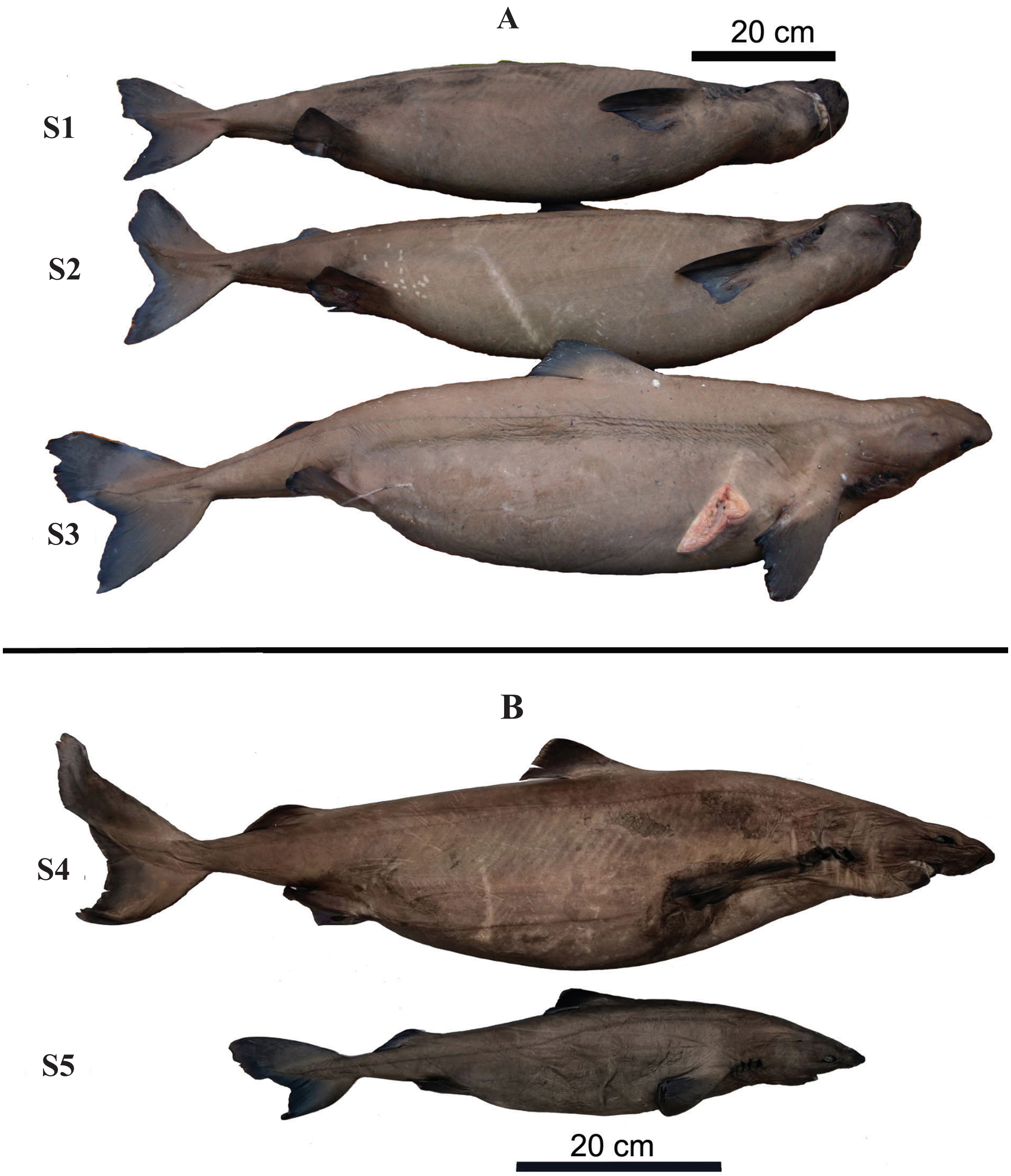

Figure 2. *Somniosus rostratus* from the Strait of Sicily. **A.** females S1 (MSNC 4885), S2 (WSASr1), and S3 (MSNC 4886) captured in 2015 (Fig. 1) Map ID 36 [S1–S2], 37 [S3]. **B**: female S4 (MSNC 4887), and male S5 (MSNC 4888) captured in 2016 (Fig. 1) Map ID 38 [S4–S5].

The geographical distribution of the little sleeper shark was mapped gathering all existing scientific literature concerning previous records of the species in the Mediterranean Sea (Table 1). In addition, any missing data was added using the Global Biodiversity Information Facility (GBIF 2024), excluding all non-georeferenced data. The map was created using Quantum GIS software (QGIS 2020), following the methodology outlined by Sardo et al. (2022).

The records of *S. rostratus* in the Mediterranean Sea provided by Capapé et al. (2020) have been updated, with the addition of information on shark capture and size, when available (Table 1).

Results

All of the fifteen sharks recorded in the presently reported study were identified as *Somniosus rostratus* following the keys and descriptions given by Cigala-Fulgosi and Gandolfi (1983), Compagno (1984), Serena (2005), Ebert et al. (2013), and Capapé et al. (2020) (Table 1).

The four specimens S1–S4 were females with a total length (TL) ranging from 925 mm to 992 mm (973 ± 32 mm) and a weight ranging from 5950 to 7480 g (6732 ± 630 g); the males S5 and S10 were 618 mm and 890 mm TL and 1140 g and 3121 in weight, respectively (Tables 1, 2) (Fig. 2).

Table 2. Selected biometric characters of specimens S1–S5 of *Somniosus rostratus* captured on the Strait of Sicily (specimens defined and illustrated in Fig. 2).

Character	Specimen reference number									
	S1		S2		S3		S4		S5	
Date of capture	13 Sep. 2015		13 Sep.2015		15 Sep. 2015		26 Aug. 2016		14 Sep. 2016	
Sex	♀		♀		♀		♀		♂	
Total weight (g)	6850		6650		7480		5950		1140	
Morphometric characters	mm	[% of TL]	mm	[% of TL]	mm	[% of TL]	mm	[% of TL]	mm	[% of TL]
Total length (TL)	992		985		990		925		618	91.3
Fork length	903	91.0	903	91.7	906	91.5	873	94.4	564	81.6
Precaudal length	812	81.9	806	81.8	805	81.3	772	83.5	504	35.9
Pre-first dorsal length	347	35.0	352	35.7	347	35.1	327	35.4	222	67.0
Pre-second dorsal length	678	68.3	650	66.0	684	69.1	647	69.9	414	20.1
Head length	203	20.5	202	20.5	194	19.6	183	19.8	124	1.6
Eye length	16	1.6	16	1.6	15	1.5	14	1.5	10	1.5
Eye height	13	1.3	13	1.3	12	1.2	11	1.2	9	17.3
Prebranchial length	147	14.8	138	14.0	135	13.6	146	15.8	107	20.7
Prepectoral length	205	20.7	204	20.7	197	19.9	188	20.3	128	61.2
Prepelvic length	609	61.4	612	62.1	626	63.2	594	64.2	378	7.8
Premouth length	63	6.4	65	6.6	65	6.6	55	5.9	48	6.0
Pectoral base	62	6.3	66	6.7	66	6.7	59	6.4	37	12.1
Pectoral anterior margin	123	12.4	122	12.4	113	11.4	118	12.8	75	5.3
Pectoral inner margin	35	3.5	43	4.4	43	4.3	46	5.0	33	9.1
Pectoral posterior margin	75	7.6	80	8.1	94	9.5	98	10.6	56	12.3
Pectoral height	94	9.5	97	9.8	96	9.7	118	12.8	76	8.9
First dorsal base	78	7.9	84	8.5	84	8.5	83	9.0	55	10.5
First dorsal anterior margin	106	10.7	105	10.7	113	11.4	112	12.1	65	6.1
First dorsal inner margin	49	4.9	59	6.0	55	5.6	53	5.7	38	6.6
First dorsal posterior margin	64	6.5	74	7.5	68	6.9	56	6.1	41	18.4
Dorsal margin of caudal	180	18.1	184	18.7	162	16.4	183	19.8	114	7.1
Lower postventral margin of caudal	83	8.4	80	8.1	80	8.1	88	9.5	44	14.4
Preventral margin of caudal	138	13.9	140	14.2	130	13.1	142	15.4	89	91.3

The brief description of the specimens is the following: short snout, pointed in its profile, rounded underside, dorsal fins without spines, equal-sized dorsal fins, anal fin absent, long ventral caudal lobe, first dorsal fin on back closer to pectorals than pelvic fins, short keels on base of caudal fin (Figs. 2, 3, 4A, 4B). Color: body brown, fins darker, snout black. The dental formula obtained from S3 was: 31–31 teeth in the upper jaw and 18–18 teeth in the lower jaw (Fig. 4C).

The selected morphometric measurements of S1–S5, expressed as % of TL (Table 2) as well as the dental formula obtained from S3, were included in the ranges retrieved from the literature (Cigala-Fulgosi and Gandolfi 1983; Golani 1986; Herman et al. 1989; Capapé et al. 2020; Hsu et al. 2020).

Females S1–S3 were pregnant. The number of embryos ranged from 9 to 14 and they were very small, from 2 to 50 mm in length (Table 3) (Fig. 5).

Table 3. Additional biometric characters of three females of *Somniosus rostratus* captured in the Strait of Sicily in 2015 (specimens defined and illustrated in Fig. 2).

Character	Specimen reference number		
	S1	S2	S3
Gonad weight [g]	422 R/788 L	596 R/470 L	416 R/813 L
Liver weight [g]	671	595	429
Intestine weight [g]	281	370	448
Number of embryos in oviducts	4 R/5 L		7 R/7 L
Length of embryos [mm]	2		40–50
Number of ova in oviducts		5 R/4 L	

R = right; L = left.

Discussion

The TL of three of the four females of *Somniosus rostratus* caught from the Strait of Sicily corresponded to the values expected for adult specimens (Barrull and Mate 2001; Guallart et al. 2013) and approached the maximum size observed in Mediterranean waters (Table 1) (Barría et al. 2015b; De Lojola Fernández et al. 2017).

The little sleeper shark is an ovoviviparous species, that gives birth to a litter of 8–17 young whose length ranges between 210 and 280 mm (Compagno 1984; Golani et al. 2006; Froese and Pauly 2022). After evisceration, different developmental stages of gonads in our females of similar size were observed and the low number of ova and embryos counted supported the hypothesis that the species is not very prolific (Capapé et al. 2020).

Somniosus rostratus is generally captured as bycatch by bottom trawlers and mesopelagic longlines at various depths, frequently in deep waters, and it is generally discarded (Séret et al. 2009; FAO 2016; Finucci et al. 2020; Carpentieri et al. 2021). Similarly, specimens in the presently reported study were incidentally caught in the relatively deep waters of the central Mediterranean Sea and of the south Adriatic Sea through drifting mesopelagic longlines used in swordfish fishery. Although generally described as a bathydemersal shark, the wide range of depths at which it has been captured in the Mediterranean (Table 3) and the remains of the mesopelagic cephalopod *Histioteuthis* sp. in its stomach could suggest a mesopelagic

Figure 3. *Somniosus rostratus* (female S6) captured in the northwestern Ionian Sea in 2009 (Fig. 1: map ID 27).

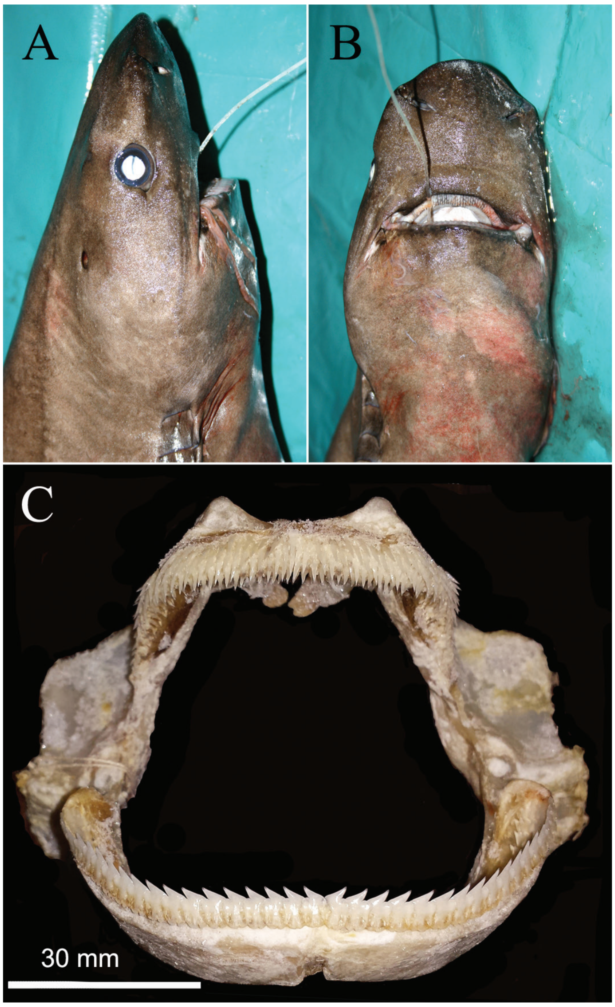

Figure 4. *Somniosus rostratus*. (**A**) Lateral view of head (specimen S2). (**B**) Ventral view of head (specimen S2). (**C**) Anterior view of dissected jaw with full dental armament (specimen S3).

habit for *S. rostratus*, able to actively move in the water column (Guallart et al. 2013; Guallart and García-Salinas 2015; Barría et al. 2015a). Generally, pregnant females are caught near the bottom (Guallart et al. 2013).

Some of the specimens reported in Table 1, as well as embryos, fetuses and/or anatomical parts of this species of shark caught in the basin are deposited in the collections of various Museums of Natural History; for example in Spain (Barrull et al. 1999; Barrull and Mate 2001), France (Yano et al. 2004; Chagnoux 2022), Czech Republic (Šanda and De Maddalena 2003), Italy (Doderlein 1878–1879; Tortonese 1938, 1956; Di Palma 1979; Sarà and Sarà 1990; Vanni 1992; Mizzan 1994; Mancusi et al. 2002; Carnevale et al. 2007), and the United Kingdom (Gray 1851; Ridewood 1921; Yano et al. 2004). Additionally, a number of Mediterranean basin findings are documented in GBIF (2024), covering areas off Valencia and Alicante, Spain, and the southern Adriatic Sea (Fig. 1).

As already observed (Irmak and Özden 2021; Ebert and Dando 2022), the density of records of *S. rostratus* appears highest in the western sector of the Mediterranean Sea, prevalently in the Ligurian and Catalan seas (Fig. 1; Table 3). Abundant bycatches were observed between the Balearic Islands and the Spanish coast (De Loyola Fernández et al. 2017) and off the Ligurian coast (Garibaldi et al. 2012, Garibaldi 2015), while nursery grounds were identified in the eastern and northeastern waters of Spain as well as in the Ligurian Sea (Capapé et al. 2020).

The occurrence of *S. rostratus* is known from the eastern sector of the basin (Goren and Galil 2015; Golani 2021; Damalas et al. 2022), but to date, it appears to be more sporadic in eastern areas than in the western sector (Fig. 1; Table 1). Until recently, the occurrence of *S. rostratus* in the Turkish waters required confirmation (Kabasakal 2019, 2020); the presence of the species was ascertained for the southwestern waters of the country by Irmak and Özden (2021) and *S. rostratus* was therefore added to the shark fauna of the Turkish waters (Kabasakal 2021). In the Aegean waters, the little sleeper shark was rarely observed (Papaconstantinou 2014) and it was not detected during the experimental bottom trawl surveys performed from 2005 to 2014 in the southern sectors of these waters (Peristeraki et al. 2017). In Syrian waters, *S. rostratus* has been reported as frequent by Ali (2018), but it has not been observed in recent surveys (Alkusairy and Saad 2018).

In the central Mediterranean and in the Adriatic Sea, which include the areas of interest of the presently reported note, *S. rostratus* has been found in the Strait of Sicily, the western Ionian, and the South Adriatic Sea (Table 1). Although based on literature (Compagno 1984; Séret et al. 2009; Finucci et al. 2020; Ebert and Dando 2022), the distribution range of *S. rostratus* also comprises the western

Figure 5. *Somniosus rostratus* embryo, approximately 50 mm in length, of the S3 caught in the Strait of Sicily in 2015 (MSNC 4886; Fig. 1: map ID 35; see Table 2).

Libyan waters, the species has not been listed in a recent inventory of the Chondrichthyes of Libyan coasts (Shakman et al. 2023); the occurrence in this region was confirmed by one of us (ADN) in 2006 after the observation of specimens at the fish market of Tripoli. In the Strait of Sicily, the little sleeper shark has been recorded for the first time in Maltese waters, in 2011 (Vella et al. 2013) and, more recently, in 2019, the species was detected for the first time in northeastern Tunisian waters (Capapé et al. 2020).

Additional reasons for the diverse distribution of *S. rostratus* in the various areas of the Mediterranean Sea might be the different degree of coverage of on-board observers on fishing vessels or of landing controls or even the different density or distribution of scientific surveys conducted in the various parts of the basin. Any of these factors is potentially able to bias our perception and knowledge of the geographical distribution of this species.

Although the occurrence of *S. rostratus* is generally known off Sicilian coasts (Tortonese 1956; Ragonese et al. 2013), the species was never reported in various experimental bottom trawl surveys performed in the Sicily Channel during the period 1994–2020 (Scacco et al. 2002; Relini et al. 2010; Ragonese et al. 2013; Geraci et al. 2017; Fernandez-Arcaya et al. 2019; Ragonese 2022; Farrugio and Soldo unpublished*). Consequently, the findings of *S. rostratus* documented here are of huge importance, not only because they determine the presence of this uncommon shark in the northern sectors of the Strait of Sicily, but also because they could indicate the presence of a likely spawning area for the species.

The whole Strait of Sicily is recognized as an Ecologically or Biologically Significant Area (EBSA) (Consoli et al. 2016; UNEP 2016; Di Lorenzo et al. 2018) and the presence of important nurseries and spawning areas for many fishery resources (Consoli et al. 2016), as well as for threatened and endangered species of elasmobranchs, heavily impacted by human pressures such as fishery activities, have been underlined numerous times (Zava et al. 2016, 2020, 2022; Colloca et al. 2019; Geraci et al. 2019; Scannella et al. 2020).

The interaction between sharks and pelagic or mesopelagic drifting swordfish fisheries, which unintentionally catch sharks and other species as bycatch, leading to detrimental impacts on shark populations, is another significant issue raised by this note. These interactions can result in increased mortality rates for sharks and rays, further exacerbating the decline of already threatened and endangered species, many of which are not properly assessed in the Mediterranean Sea, due to the insufficient availability of data. The International Commission for the Conservation of Atlantic Tunas (ICCAT) has the mandate to assess the pelagic species that might be impacted by the fisheries targeting tunas and billfish species and on-board observers have been imposed on a defined percentage of some fleets, but the available data is still insufficient for any reliable assessment of the shark species concerned in the Mediterranean Sea. Understanding the dynamics of this interaction and its ecological consequences is crucial for effective conservation and management efforts concerning this species. Conservation measures that prioritize the protection of endangered elasmobranch populations are crucial for maintaining the balance of marine ecosystems and for ensuring the sustainability of fishery resources.

Conclusions

The presently reported study provides valuable insights into the distribution and morphological characteristics of the deep-water little sleeper shark, S*omniosus rostratus*, in the Mediterranean Sea. It underscores the challenges associated with studying deep-water species, particularly

---

* Farrugio H, Soldo A (2014) Status and conservation of fisheries in the Sicily Channel/Tunisian Plateau. Draft internal report for the purposes of the Mediterranean Regional Workshop to Facilitate the Description of Ecologically or Biologically Significant Marine Areas. 7–11 April 2014, Malaga, Spain.

those with low-population densities or elusive behaviors, and sheds light on the potential reasons for the perceived rarity of *S. rostratus*.

The findings suggest a mesopelagic habit for the little sleeper shark, supported by the range of depths at which it has been captured and the presence of mesopelagic cephalopods in its stomach. Additionally, morphometric data offer insights into the reproductive characteristics of the species, emphasizing the ecological significance of the Strait of Sicily (central Mediterranean Sea) as a potential spawning area. Given the relevance of the Strait of Sicily as an Ecologically or Biologically Significant Area (EBSA), the study underscores the need for effective conservation measures in this region. It encourages further research and monitoring efforts to better understand and protect essential habitats for marine life.

The study reveals that S. *rostratus*, along with other elasmobranchs, is captured as bycatch in pelagic swordfish longline fisheries. The resulting interactions lead to increased mortality rates for vulnerable shark and ray species, highlighting the importance of considering the ecological consequences of bycatch interactions, especially for threatened and endangered elasmobranch populations. The International Commission for the Conservation of Atlantic Tunas (ICCAT) and other relevant bodies are urged to address data gaps and assess the impact of fisheries on the conservation status of deep-water shark species in the Mediterranean.

In conclusion, this research contributes valuable data on the distribution and characteristics of *S. rostratus* and underscores broader conservation challenges related to bycatch interactions. It emphasizes the need for proactive measures to ensure the sustainability of Mediterranean marine ecosystems. The study serves as a call to action for enhanced collaboration between scientific communities, fisheries management organizations, and conservation bodies to address the complexities surrounding the conservation of deep-water shark species in the region.

Acknowledgments

The authors warmly thank Captain Vincenzo Belgiorno of the FV *Santa Barbara* (IPE 956), and its crew, Salvatore Belgiorno, Angelo Cellura, Giuseppe Moncada, and Paolo De Marco for sharing information on the captures of *Somniosus rostratus* and depositing the specimens at the Museo Civico di Storia Naturale di Comiso, Ragusa, Italy. The authors also thank the crews of the MP *Ariete* (04CT01061) and MP *Arcadia* (14ME00571), as well as Dr Elia Bueloni, Centro Sperimentale per la Tutela Degli Habitat (CESTHA), Ravenna; Prof Luca Sineo, Dipartimento Scienze e Tecnologie Biologiche, Chimiche e Farmaceutiche, University of Palermo; and Attia Mohamed, Rhodes, Greece, for technical support; Giovanna Polizzi and Claudia Manno, Wilderness studi ambientali, Palermo, Prof Gianluca Sarà for allowing us to consult the library of the father Dr Raimondo Sarà. Authors are further grateful to anonymous reviewers for helpful and constructive suggestions on the first version of the manuscript.

References

Ali M (2018) An updated checklist of the marine fishes from Syria with emphasis on alien species. Mediterranean Marine Science 19(2): 388–393. https://doi.org/10.12681/mms.15850

Ali M, Saad A (2003) Sharks and rays in Syrian Sea waters. Al-Assad Journal for Engineering Sciences 17: 45–76. [In Arabic, abstract in English]

Alkusairy H, Saad A (2018) Species composition, diversity and length frequency of by-catch sharks from the Syrian coast. International Journal of Research Studies in Zoology 4: 11–21. https://doi.org/10.20431/2454-941X.0401003

Ananiadis KI (1961) Thalassiní enkyklopaídeia. [Marine encyclopedia.] Vol. 3. Argyrou, Athens, Greece, 478 pp. [In Greek]

Báez J, Rodríguez-Cabello C, Bañón R, Brito A, Falcón J, Maño T, Baro J, Macías D, Meléndez M, Camiñas J, Arias-García A, Gil J, Farias C, Artexe I, Sánchez F (2019) Updating the national checklist of marine fishes in Spanish waters: An approach to priority hotspots and lessons for conservation. Mediterranean Marine Science 20(2): 260–270. https://doi.org/10.12681/mms.18626

Barría C, Coll M, Navarro J (2015a) Unravelling the ecological role and trophic relationships of uncommon and threatened elasmobranchs in the western Mediterranean Sea. Marine Ecology Progress Series 539: 225–240. https://doi.org/10.3354/meps11494

Barría C, Navarro J, Coll M, Fernandez-Arcaya U, Sáez-Liante R (2015b) Morphological parameters of abundant and threatened chondrichthyans of the northwestern Mediterranean Sea. Journal of Applied Ichthyology 31(1): 114–119. https://doi.org/10.1111/jai.12499

Barrull J, Mate I (1995) Presencia de tiburón dormilón *Somniosus rostratus* (Risso, 1826) en el mar Catalán (mar Mediterráneo). Miscellània Zoològica 18: 200–202.

Barrull J, Mate I (2001) First record of a pregnant female little sleeper shark *Somniosus rostratus* (Risso, 1826) on the Spanish Mediterranean coast. Boletín Instituto Español de Oceanografía 17(3/4): 323–325.

Barrull J, Mate I, Bueno M (1999) Observaciones de tiburones (Chondrichtyes Euselachii) en aguas de Cataluña (Mediterráneo NO), con algunos aspectos generales de su ecología. Scientia gerundensis 24: 127–151.

Canestrini G (1864) Sopra alcuni pesci poco noti o nuovi del Mediterraneo. Memorie della Reale Accademia delle Scienze di Torino, ser. 2 21: 359–367.

Canestrini G (1872) Fauna d'Italia. Parte terza; Pesci. Vallardi Tipografo-Editore, Milano, 208 pp. https://doi.org/10.5962/bhl.title.11799

Capapé C, Rafrafi-Nouira S, Diatta Y, Reynaud C (2020) First record of little sleeper shark, *Somniosus rostratus* (Elasmobranchii: Squaliformes: Somniosidae), from the Tunisian coast, central Mediterranean Sea. Acta Ichthyologica et Piscatoria 50(4): 475–480. https://doi.org/10.3750/AIEP/02998

Capezzuto F, Carlucci R, Maiorano P, Sion L, Battista D, Giove A, Indennidate A, Tursi A, D'Onghia G (2010) The bathyal benthopelagic fauna in the north-western Ionian Sea: Structure, patterns and interactions. Chemistry and Ecology 26(Suppl. 1): 199–217. https://doi.org/10.1080/02757541003639188

Carluccio A, Maiorano P, Sion L, D'Onghia G (2019) Monitoraggio di pesci cartilaginei in habitat sensibili. Biologia Marina Mediterranea 26(1): 93–94.

Carluccio A, Capezzuto F, Maiorano P, Sion L, D'Onghia G (2021) Deep-water cartilaginous fishes in the central Mediterranean Sea: Comparison between geographic areas with two low impact tools for sampling. Journal of Marine Science and Engineering 9(7): 686. https://doi.org/10.3390/jmse9070686

Carnevale G, Marsili S, Malduca A, Landini W (2007) Catalogue of recent fishes in the Museo di Storia Naturale e del Territorio, Università di Pisa. I. Hyperotreti, Hyperoartia, Chondrichthyes. Atti della Società toscana Scienze naturali. Memorie, Serie B 114: 99–105.

Carpentieri P, Nastasi A, Sessa M, Srour A (Eds.) (2021) Incidental catch of vulnerable species in Mediterranean and Black Sea fisheries—A review. Studies and Reviews No. 101 (General Fisheries Commission for the Mediterranean). FAO, Rome, 317 pp. https://doi.org/10.4060/cb5405en

Chagnoux S (2022) The fishes collection (IC) of the Muséum national d'Histoire naturelle (MNHN-Paris). Version 57.291. MNHN-Museum national d'Histoire naturelle. Occurrence dataset. [Accessed on 31 Dec 2022] https://doi.org/10.15468/tm7whu

Cigala-Fulgosi F, Gandolfi G (1983) Re-description of the external morphology of *Somniosus rostratus* (Risso, 1826), with special reference to its squamation and cutaneous sensory organs, and aspects of their functional morphology (Pisces Selachii Squalidae). Monitore Zoologico Italiano Nuova serie 17: 27–70.

Colloca F, Scannella D, Geraci ML, Falsone F, Batista G, Vitale S, Di Lorenzo M, Bovo G (2019) British sharks in Sicily: Records of long distance migration of tope shark (*Galeorhinus galeus*) from north-eastern Atlantic to Mediterranean Sea. Mediterranean Marine Science 20(2): 309–313. https://doi.org/10.12681/mms.18121

Compagno LJV (1984) FAO Species Catalogue. Sharks of the world. An annotated and illustrated catalogue of shark species known to date. Vol. 4, Part 1. Hexanchiformes to Lamniformes. FAO Fisheries Synopsis 125(4/1): 1–249.

Consoli P, Esposito V, Battaglia P, Altobelli C, Perzia P, Romeo T, Canese S, Andaloro F (2016) Fish distribution and habitat complexity on banks of the Strait of Sicily (Central Mediterranean Sea) from Remotely-Operated Vehicle (ROV) explorations. PLoS One 11(12): e0167809. https://doi.org/10.1371/journal.pone.0167809

Costa F (1991) Atlante dei pesci dei mari italiani. Gruppo Ugo Mursia Editore, Milano, Italy, 438 pp.

Damalas D, Peristeraki P, Gubili C, Lteif M, Otero M, Thasitis I, Ali M, Jemaa S, Mytilineou Ch, Kavadas S, Farrag MMS (2022) Vulnerable megafauna. Deep-sea cartilaginous fish (Chondrichthyes: sharks, rays, skates and chimaeras). Pp. 135–237. In: Otero M, Mytilineou C (Eds.) Deep-sea Atlas of the Eastern Mediterranean Sea. IUCN, Gland, Switzerland, IUCN Centre for Mediterranean Cooperation, Málaga, Spain.

De Loyola Fernández I, Báez JC, García-Barcelona S, Camiñas JA, Macías D (2017) Length–weight relationships of kitefin shark *Dalatias Licha*, and little sleeper shark *Somniosus rostratus* from the Western Mediterranean Sea, and long snouted lancetfish *Alepisaurus ferox* from the eastern North Atlantic Ocean. Turkish Journal of Fisheries and Aquatic Sciences 17(5): 1073–1076. https://doi.org/10.4194/1303-2712-v17_5_24

Di Lorenzo M, Sinerchia M, Colloca F (2018) The North sector of the Strait of Sicily: A priority area for conservation in the Mediterranean Sea. Hydrobiologia 821(1): 235–253. https://doi.org/10.1007/s10750-017-3389-7

Di Palma MG (1979) Il Museo di Zoologia dell'Università di Palermo. Il Naturalista Siciliano. S. IV 3(1–2): 3–16.

Dieuzeide R, Novella M, Roland J (1953) Catalogue des Poissons des côtes algériennes. Squales, raies, chimères. Bulletin de la Station d'Aquiculture et de Pêche de Castiglione, Nouvelle Série 1: 1–274.

Doderlein P (1881) Manuale ittiologico del Mediterraneo, ossia sinossi metodica delle varie specie di pesci riscontrate sin qui nel Mediterraneo ed in particolare nei mari di Sicilia. Parte 2. Sinossi metodica delle specie. Tipografia del Giornale di Sicilia, Palermo, 256 pp.

Doderlein P (1878–1879) Prospetto metodico delle varie specie dio pesci riscontrate sin'ora nelle acque marine e fluviali della Sicilia. Atti dell'Accademia di Scienze, Lettere ed Arti di Palermo (Nuova Serie) 6: 25–63.

Ebert DA, Dando M (2022) Guida a squali, razze e chimere del Mediterraneo e d'Europa. Ricca Editor, Italy, 384 pp.

Ebert DA, Stehmann MFW (2013) Sharks, batoids, and chimaeras of the North Atlantic. FAO Species Catalogue for Fishery Purposes No. 7. FAO, Rome, 523 pp.

Ebert DA, Fowler S, Compagno L (2013) Sharks of the World. Wild Nature Press, Plymouth, UK, 528 pp.

Economidis PS (1973) Katalogos ton ichthyon tis Ellados. [Catalog of the fishes of Greece.] Helleniki Okeanologia kai Limnologia 11: 421–598. [In Greek]

FAO (2016) The state of Mediterranean and Black Sea fisheries. General Fisheries Commission for the Mediterranean. FAO, Rome, 134 pp.

Fernandez-Arcaya U, Bitetto I, Esteban A, Farriols MT, García-Ruiz C, Gil de Sola L, Guijarro B, Jadaud A, Kavadas S, Lembo G, Milisenda G, Maina I, Petovic S, Sion L, Vaz S (2019) Large-scale distribution of a deep-sea megafauna community along Mediterranean trawlable grounds. Scientia Marina 83(S1): 175–187. https://doi.org/10.3989/scimar.04852.14A

Ferrando S, Amaroli A, Gallus L, Aicardi S, Di Blasi D, Christiansen JS, Vacchi M, Ghigliotti L (2019) Secondary folds contribute significantly to the total surface area in the olfactory organ of Chondrichthyes. Frontiers in Physiology 10: 245. https://doi.org/10.3389/fphys.2019.00245

Finucci B, Cheok J, Cotton CF, Kulka DW, Neat FC, Rigby CL, Tanaka S, Walker TI (2020) *Somniosus rostratus*. The IUCN Red List of Threatened Species 2020: e.T161432A124484522. [Accessed on 3 Dec 2022] https://doi.org/10.2305/IUCN.UK.2020-3.RLTS.T161432A124484522.en

Froese R, Pauly D (Eds.) (2022) FishBase. [Version 08/2022] http://www.fishbase.org

Galil BS (2004) The limit of the sea: The bathyal fauna of the Levantine Sea. Scientia Marina 68(S3): 63–72. https://doi.org/10.3989/scimar.2004.68s363

Garibaldi F (2015) By-catch in the mesopelagic swordfish longline fishery in the Ligurian Sea (Western Mediterranean). Collective Volume of Scientific Papers ICCAT 71(3): 1495–1498.

Garibaldi F, Rovellini A, Franco A, Lanteri L, Orsi Relini L (2012) A rare or rarely caught species? The case of little sleeper shark *Somniosus rostratus* in the Ligurian Sea (western Mediterranean). 16th European Elasmobranch Association (EEA) Scientific Conference, Milan (Italy), 22–25 November 2012. Book of Abstracts, 15.

GBIF (2024) GBIF occurrence download. [Accessed on 5 Jan 2024] https://doi.org/10.15468/dl.wxhjca

Geraci ML, Ragonese S, Norrito G, Scannella D, Falsone F, Vitale S (2017) Chondrichthyes in the South of Sicily through 20 years of scientific survey. Pp. 13–37. In: Rodrigues-Filho LF, De Luna Sales JB (Eds.) Chondrichthyes. Multidisciplinary approach. IntechOpen. https://doi.org/10.5772/intechopen.69333

Geraci ML, Di Lorenzo M, Falsone F, Scannella D, Di Maio F, Colloca F, Vitale S, Serena F (2019) The occurrence of Norwegian skate, *Dipturus nidarosiensis* (Elasmobranchii: Rajiformes: Rajidae), in the Strait of Sicily, central Mediterranean. Acta Ichthyologica et Piscatoria 49(2): 203–208. https://doi.org/10.3750/AIEP/02566

Giglioli EH (1880) Elenco dei mammiferi, degli uccelli e dei rettili ittiofagi appartenenti alla Fauna italica e catalogo degli Anfibi e dei Pesci italiani. Pp. 63–117. In: Esposizione internazionale della pesca in Berlino 1880, Sezione italiana: Catalogo degli espositori e delle cose esposte. Stamperia Reale, Firenze.

Golani D (1986) On deep-water sharks caught off the Mediterranean coast of Israel. Israel Journal of Zoology 34(1–2): 23–31.

Golani D (2021) An updated checklist of the Mediterranean fishes of Israel, with illustrations of recently recorded species and delineation of Lessepsian migrants. Zootaxa 4956(1): 1–108. https://doi.org/10.11646/zootaxa.4956.1.1

Golani D, Oztürk B, Başusta N (2006) The fishes of the eastern Mediterranean. Turkish Marine Research Foundation, Istanbul, Turkey, 259 pp.

Goren M, Galil BS (2015) A checklist of the deep sea fishes of the Levant Sea, Mediterranean Sea. Zootaxa 3994(4): 507–530. https://doi.org/10.11646/zootaxa.3994.4.2

Gray JE (1851) List of the specimens of fish in the collection of the British Museum. Part I. Chondropterygii. British Museum (Natural History), London, 160 pp.

Guallart J, García-Salinas P (2015) New insights on the biology and the abundance of the uncommon deep-sea little sleeper shark *Somniosus rostratus* (Somniosidae) from the Balearic Sea (Western Mediterranean): Do mesopelagic habits partially explain rarity of its catches? 19th European Elasmobranch Association (EEA) Scientific Conference, Peniche (Portugal), 9–11 October 2015. Book of Abstracts, 79.

Guallart J, Vicent JJ, Catalan A, Garcia-Salinas P (2013) New data on the uncommon deep-sea shark *Somniosus rostratus* (Squaliformes, Somniosidae) in the Balearic Sea (Western Mediterranean). 17th European Elasmobranch Association (EEA) Scientific Conference, Plymouth (United Kingdom), 1–3 November 2013. Book of Abstracts, 75.

Herman J, Hovestadt-Euler M, Hovestadt DC (1989) Contributions to the study of the comparative morphology of teeth and other relevant ichthyodorulites in living superspecific taxa of Chondrichthyan fishes. Part A: Selachii. No. 3: Order: Squaliformes – Families: Echinorhinidae, Oxynotidae and Squalidae. Bulletin de l'Institut Royal des Sciences Naturelles de Belgique. Biologie 59: 101–158.

Hornung H, Krom MD, Cohen Y, Bernhard M (1993) Trace metal content in deep-water sharks from the eastern Mediterranean Sea. Marine Biology 115(2): 331–338. https://doi.org/10.1007/BF00346351

Hsu H-H, Lin C-Y, Joung S-J (2020) *Somniosus* (*Rhinoscymnus*) *cheni* sp. nov., a new species of sleeper shark (Squaliformes: Somniosidae) from eastern Taiwan, with aspects of embryo biology. Zoological Studies 59: 48. https://doi.org/10.6620/ZS.2020.59-48

Irmak E, Özden U (2021) A rare shark for the Mediterranean: *Somniosus rostratus* (Risso, 1827) (Chondrichthyes: Somniosidae) from the coast of Turkey. Zoology in the Middle East 67(3): 274–276. https://doi.org/10.1080/09397140.2021.1895413

Kabasakal H (2019) A review of shark research in Turkish waters. Annales Series Historia Naturalis 29(1): 1–16. https://doi.org/10.19233/ASHN.2019.01

Kabasakal H (2020) A field guide to the sharks of Turkish waters. Turkish Marine Research Foundation (TUDAV) Publication No: 55, Istanbul, Turkey, 133 pp.

Kabasakal H (2021) Review of shark biodiversity in Turkish waters: Updated inventory, new arrivals, questionable species, and conservation issues. Annales Series Historia Naturalis 31(2): 181–194. https://doi.org/10.19233/ASHN.2021.22

Kheddam H, Justine J-L, Tazerouti F (2016) Hexabothriid monogeneans from the gills of deep sea sharks off Algeria, with the description of *Squalonchocotyle euzeti* n. sp. (Hexabothriidae) from the kitefin shark *Dalatias licha* (Euselachii, Dalatiidae). Helminthologia 53(4): 354–362. https://doi.org/10.1515/helmin-2016-0034

Labropoulou M, Papaconstantinou C (2000) Community structure of deep-sea demersal fish in the North Aegean Sea (Northeastern Mediterranean). Hydrobiologia 440(1/3): 281–296. https://doi.org/10.1023/A:1004199917299

Mancusi C, Nicolosi P, Arculeo M, Barbagli F, Carlini R, Costantini M, Doria G, Fabris G, Maio N, Mattioli G, Mizzan L, Podestà M, Salmaso R, Vanni S, Zuffi M, Serena F, Vacchi M (2002) The presence of elasmobranchs in the collections of the main Italian Natural History Museums. Pp. 97–108. In: Vacchi M, La Mesa G, Serena F, Séret B (Eds.) Proceedings of the 4th European Elasmobranch Association Meeting, Livorno (Italy), 2000. ICRAM, ARPAT and SFI.

Meléndez MJ, Báez JC, Serna-Quintero JM, Camiñas JA, de Loyola Fernàndez I, Real R, Macías D (2017) Historical and ecological drivers of the spatial pattern of Chondrichthyes species richness in the Mediterranean Sea. PLoS One 12(4): e0175699. https://doi.org/10.1371/journal.pone.0175699

Mizzan L (1994) I Leptocardi, Ciclostomi e Selaci delle collezioni del Museo Civico di Storia Naturale di Venezia - 1) Leptocardia, Agnatha, Gnathostomata – Chondrichthyes (esclusi Rajiformes). Bollettino del Museo civico di Storia Naturale di Venezia 45: 123–137.

Moreau E (1881) Histoire naturelle des poissons de la France. Volume1. G. Masson, éditeur, Paris, 498 pp. https://doi.org/10.5962/bhl.title.12541

Papaconstantinou C (1990) Some rare mesopelagic and bathyal fish caught in the Greek seas. Thalassographica 13: 35–39.

Papaconstantinou C (2014) Fauna Graeciae. An updated checklist of the fishes in the Hellenic seas. Monagraphs on Marine Sciences 7. HCMR, Athens, 340 pp.

Papaconstantinou C, Conides A (2021) The fish fauna in the Hellenic seas with emphasis to the Aegean Sea. In: Anagnostou ChL, Kostianoy AG, Mariolakos ID, Panayotidis P, Soilemezidou M, Tsaltas G (Eds.) The Aegean Sea Environment: The Natural System. The Handbook of Environmental Chemistry. Springer, Berlin, Heidelberg, 1–29. https://doi.org/10.1007/698_2020_684

Peristeraki P, Tserpes G, Lampadariou N, Stergiou KI (2017) Comparing demersal megafaunal species diversity along the depth gradient within the South Aegean and Cretan Seas (Eastern Mediterranean). PLoS One 12(9): e0184241. https://doi.org/10.1371/journal.pone.0184241

Psomadakis PN, Giustino S, Vacchi M (2012) Mediterranean fish biodiversity: An updated inventory with focus on the Ligurian and Tyrrhenian seas. Zootaxa 3263(1): 1–46. https://doi.org/10.11646/zootaxa.3263.1.1

QGIS Development Team 2020. QGIS Geographic Information System. Open Source Geospatial Foundation Project. http://qgis.osgeo.org

Ragonese S (2022) Breve storia delle campagne sperimentali con rete a strascico condotte nei mari italiani. Annotazioni karfologiche 6: 1–45. [inclusa l'Appendice]

Ragonese S, Vitale S, Dimech M, Mazzola S (2013) Abundances of demersal charks and chimaera from 1994–2009 scientific surveys in the central Mediterranean Sea. PLoS One 8(9): e74865. https://doi.org/10.1371/journal.pone.0074865

Relini G, Mannini A, De Ranieri S, Bitetto I, Follesa MC, Gancitano V, Manfredi C, Casciaro L, Sion L (2010) Chondrichthyes caught during the MEDITS surveys in Italian waters. Biologia Marina Mediterranea 17(1): 186–204.

Ridewood WG (1921) VIII. – On the calcification of the vertebral centra in sharks and rays. Philosophical Transactions of the Royal Society of London. Series B, Containing Papers of a Biological Character 210(372–381): 311–407. https://doi.org/10.1098/rstb.1921.0008

Risso A (1826) Histoire naturelle des principales productions de l'Europe méridionale et particulièrement celles des environs de Nice et des Alpes maritimes. Vol. 3. Chez F-G Levrault, libraire, Paris et Strasbourg, 544 pp. https://doi.org/10.5962/bhl.title.58984

Saad AA, Alkusairy HH (2022) Atlas of sharks and rays in the Syrian marine waters. Tishreen University and Syrian Society for Aquatic Environment protection (SSAEP), 104 pp.

Saad A, Seret B, Ali M (2004) Liste commentée des Chondrichthyens de Syrie (Méditerranée orientale). Rapport du 37e Congreès de la CIESM: 430.

Saad A, Ali M, Seret B (2006) Shark exploitation and conservation in Syria. Pp. 202–208. In: Başusta N, Keskin Ç, Serena F, Seret B (Eds.) Proceedings of the International workshop on Mediterranean cartilaginous fish with emphasis on southern and eastern Mediterranean. 14th–16th October 2006, Istanbul, Turkey.

Šanda R, De Maddalena A (2003) Collection of the sharks of the National Museum in Prague-Part 1. Complete taxiderms and liquid preservations. Časopis Národního muzea, Řada přírodovědná 172(1–4): 61–70.

Sarà R, Sarà M (1990). La collezione ittiologica Doderlein del Museo di Zoologia di Palermo. Museologia Scientifica 6: 1–23.

Sardo G, Geraci ML, Falsone F, Gancitano S, Gancitano V, Scannella D, Okpala COR, Titone A, Vitale S (2022) First record and otolith morphometric description of an adult lightfish, *Ichthyococcus ovatus* (Actinopterygii: Stomiiformes: Phosichthyidae), caught in the Strait of Sicily (central Mediterranean Sea). Acta Ichthyologica et Piscatoria 52(2): 159–166. https://doi.org/10.3897/aiep.52.84928

Scacco U, Andaloro F, Campagnuolo S, Castriota L, Vacchi M (2002) Cartilaginous fishes as a component of trawl discard in Strait of Sicily. Northwest Atlantic Fisheries Organization-NAFO SCR Doc. 02/87, Serial No. N4708, 13 pp.

Scannella D, Geraci ML, Falsone F, Colloca F, Zava B, Serena F, Di Maio F, Vitale S (2020) A new record of a great white shark, *Carcharodon carcharias* (Chondrichthyes: Lamnidae) in the Strait of Sicily, Central Mediterranean Sea. Acta Adriatica 61(2): 231–238. https://doi.org/10.32582/aa.61.2.13

Serena F (2005) Field identification guide to the sharks and rays of the Mediterranean and Black Sea. FAO Species Identification Guide for Fishery Purposes. FAO, Rome, 97 pp., 11 color plates + egg cases.

Serena F, Abella AJ, Bargnesi F, Barone M, Colloca F, Ferretti F, Fiorentino F, Jenrette J, Moro S (2020) Species diversity, taxonomy and distribution of Chondrichthyes in the Mediterranean and Black Sea. European Zoological Journal 87(1): 497–536. https://doi.org/10.1080/24750263.2020.1805518

Séret B, Guallart J, Vacchi M, Mancusi C, McCormack C (2009) *Somniosus rostratus*. The IUCN Red List of Threatened Species 2009: e.T161432A5422754. https://doi.org/10.2305/IUCN.UK.2009-2.RLTS.T161432A5422754.en

Shakman E, Siafenasar A, Etayeb K, Shefern A, Elmgwashi A, Al Hajaji M, bek Benghazi N, ben Abdalha A, Aissi M, Serena F (2023) National inventory and status of Chondrichthyes in the south Mediterranean Sea (Libyan coast). Biodiversity Journal 14(3): 459–480. https://doi.org/10.31396/Biodiv.Jour.2023.14.3.459.480

Sicher E (1898) I pesci e la pesca nel compartimento di Catania, con due note sui generi *Laemargus* e *Maena*. Atti dell'Accademia Gioenia di Scienze naturali in Catania (Serie IV) 11 (Memoria 5): 1–70.

Tecchio S, Ramirez-Llodra E (2018) Megafaunal data from the 2009 BIOFUN trans-Mediterranean deep-sea cruise. Integrated Marine Information System. https://doi.org/10.14284/311

Tortonese E (1938) Revisione degli squali del Museo Civico di Milano. Atti della Società Italiana di Scienze Naturali e del Museo Civico di Storia Naturale in Milano 77: 283–318.

Tortonese E (1952) Studi sui Plagiostomi. VI. Osservazioni critiche su alcune specie mediterranee. Archivio Zoologico Italiano 37: 383–398.

Tortonese E (1956) Fauna d'Italia. Vol. 2. Leptocardia, Ciclostomata, Selachii. Calderini, Bologna, Italy, 334 pp.

Tortonese E (1968) Il Museo di Storia Naturale di Genova e cento anni di attività ittiologica. Annali del Museo Civico di Storia Naturale di Genova 77: 371–385.

UNEP (2016) Ecologically or Biologically Significant Areas (EBSAs). Sicilian Channel. The Clearing-House Mechanism of the Convention on Biological Diversity (CHM) Information Submission Services, 19 pp. [Accessed on 6 Jan 2023] https://chm.cbd.int/database/record?documentID=204108

UNEP-MAP-RAC/SPA (2005) Chondrichthyan fishes of Libya: Proposal for a research programme. RAC/SPA, Tunis, 31 pp.

Vanni S (1992) Cataloghi del Museo di Storia Naturale dell'Università di Firenze sezione di Zoologia «La Specola». XI. Chondrichthyes. Atti della Società toscana di Scienze naturali. Memorie Serie B 99: 85–114.

Vella A, Vella N, Dent E (2013) First records of the little sleeper shark, *Somniosus rostratus*, in Maltese fisheries landings. Rapports de la Commission internationale pour la mer Méditerranée 40: 495.

Vella A, Vella N, Schembri S (2017) A molecular approach towards taxonomic identification of elasmobranch species from Maltese fisheries landings. Marine Genomics 36: 17–23. https://doi.org/10.1016/j.margen.2017.08.008

Weigmann S (2016) Annotated checklist of the living sharks, batoids and chimaeras (Chondrichthyes) of the world, with a focus on biogeographical diversity. Journal of Fish Biology 88(3): 837–1037. https://doi.org/10.1111/jfb.12874

Yano K, Stevens JD, Compagno LJV (2004) A review of the systematics of the sleeper shark genus *Somniosus* with redescriptions of *Somniosus* (*Somniosus*) *antarcticus* and *Somniosus* (*Rhinoscymnus*) *longus* (Squaliformes: Somniosidae). Ichthyological Research 51(4): 360–373. https://doi.org/10.1007/s10228-004-0244-4

Zava B, Fiorentino F, Serena F (2016) Occurrence of juveniles *Squatina oculata* Bonaparte, 1840 (Elasmobranchii: Squatinidae) in the Strait of Sicily (Central Mediterranean). Cybium 40(4): 341–343. https://doi.org/10.26028/cybium/2016-404-011

Zava B, Insacco G, Corsini-Foka M, Serena F (2020) Updating records of *Squatina aculeata* (Elasmobranchii: Squatiniformes: Squatinidae) in the Mediterranean Sea. Acta Ichthyologica et Piscatoria 50(4): 401–411. https://doi.org/10.3750/AIEP/03033

Zava B, Insacco G, Deidun A, Said A, Ben Suissi J, Nour OM, Kondylatos G, Scannella D, Corsini-Foka M (2022) Records of the critically endangered *Squatina aculeata* and *Squatina oculata* (Elasmobranchii: Squatiniformes: Squatinidae) from the Mediterranean Sea. Acta Ichthyologica et Piscatoria 52(4): 285–297. https://doi.org/10.3897/aiep.52.94694

Acta Ichthyologica et Piscatoria 54, 2024, 151–155 | DOI 10.3897/aiep.54.123825

PENSOFT.

ACTA ICHTHYOLOGICA ET PISCATORIA

Records of *Isistius* sp. (Elasmobranchii: Squaliformes: Dalatiidae), from the Azores archipelago, inferred by fresh bite marks in dolphins

Luís M. D. BARCELOS[1,2*], João B. BARREIROS[1,3*], João P. BARREIROS[1,2]

1 *Centre for Ecology, Evolution and Environmental Changes—Azorean Biodiversity Group, CHANGE, Global Change and Sustainability Institute, Lisbon, Portugal*

2 *Faculty of Agricultural Sciences and Environment, University of the Azores, Angra do Heroísmo, Portugal*

3 *Department of Earth and Environmental Sciences (DISAT), University of Milano-Bicocca, Milan, Italy*

https://zoobank.org/D588742D-6AD9-4870-978E-F6B05A0645CD

Corresponding author: Luís M. D. Barcelos (luis.md.barcelos@uac.pt; ldbarcelos@gmail.com)

Academic editor: Wojciech Piasecki ♦ **Received** 24 March 2024 ♦ **Accepted** 14 May 2024 ♦ **Published** 1 June 2024

Citation: Barcelos LMD, Barreiros JB, Barreiros JP (2024) Records of *Isistius* sp. (Elasmobranchii: Squaliformes: Dalatiidae), from the Azores archipelago, inferred by fresh bite marks in dolphins. Acta Ichthyologica et Piscatoria 54: 151–155. https://doi.org/10.3897/aiep.54.123825

Abstract

The marine waters around the Azores archipelago have been studied for quite a long time. Deeper areas, however, were historically poorly accessible and only now previously unreported species are recorded regularly. Our monitoring efforts of the Azorean ichthyofauna have recently revealed two cases of indirect evidence of the presence of a cookiecutter shark (*Isistius* sp.). The evidence, documented photographically, was in the form of explicit bite marks on two dolphins representing two separate species: the Atlantic spotted dolphin, *Stenella frontalis* (Cuvier, 1829) and the short-beaked common dolphin, *Delphinus delphis* Linnaeus, 1758. The two dolphins swam close to Terceira Island. No specimens have yet been collected. The shape, and size of the wounds observed suggest that they were inflicted by a cookiecutter shark. The fresh state of the injuries suggests they were sustained recently in the proximity of the Azores.

Keywords

bite marks, cookiecutter shark, feeding behavior, new records, North Atlantic, species occurrence

Introduction

The parasitic feeding behavior of fishes is well known and was comprehensively assessed by Zidowitz et al. (2004) and Leung (2014). The review presented by Leung (2014) describes all parasitic feeding including ectoparasitism although this author categorizes sharks involved in this type of feeding as representing a modified form of piscivorism. Carrier et al. (2012) considered cookiecutter sharks (*Isistius* spp.) facultative ectoparasites. Besides their ectoparasitic way of feeding on large fishes and marine mammals, they also prey on smaller fishes, squids, and crustaceans. The most speciose group of ectoparasitic fish are lampreys; others such as remoras are better known for their attachment ability to a vast guild of hosts in a more mutualistic than parasitic relation and which is considered as a commensal relation. Among elasmobranch fishes, cookiecutter sharks and possibly other dalatiid species, such as the kitefin shark, *Dalatias licha* (Bonnaterre, 1788), or the Portuguese dogfish,

---

[*] These authors contributed equally as co-first authors.

Centroscymnus coelolepis Barbosa du Bocage et de Brito Capello, 1864, are the only species showing this distinctive feeding behavior. Carlisle et al. (2021), however, have shown by analysis of biochemical tracers that large epipelagic prey constituted a relatively minor part of their overall diet, and that in turn, small micronektonic and forage species (meso- and epipelagic) are the most important prey group for cookiecutter sharks.

Two species of cookiecutter sharks are recognized as valid: *Isistius brasiliensis* (Quoy et Gaimard, 1824) and *Isistius plutodus* Garrick et Springer, 1964. They are small-sized representatives of the family Dalatiidae with a cosmopolitan distribution mainly in tropical to warm-temperate waters (Feunteun et al. 2018). The maximum reported length for *I. brasiliensis* is 42 cm for males and 56 cm for females (Ebert 2003). The less known and apparently rarer *I. plutodus* has been reported to reach 42 cm TL although similar maximum sizes should be considered (McGrouther 2009). *Isistius plutodus* is only known from fewer than 15 specimens collected mostly in inshore waters from the Pacific and Atlantic Oceans (Wenzel and López Suárez 2012). One was collected in open waters, north of the Azores, expanding the range of the species by 21 degrees of latitude to the North of its known range (Zidowitz et al. 2004). Two females were reported from the southwestern Atlantic by Stehmann and Kukuev (2015) and, more recently, additional records of offshore captures are known (South Atlantic, off Japan, see de Figueiredo Petean and de Carvalho 2018), though, due to its rarity, not nearly as many as *I. brasiliensis*. Even nearer coastal specimens have been caught in deep water or over high depths and still often well offshore or even around the island shelf.

Papastamastiou et al. (2010) characterized cookiecutter sharks as ectoparasitic predators, that leave distinct circular wounds on several types of prey ranging from fish to marine mammals and even underwater structures. These wounds often take on an oval to round shape, varying from superficial tooth punctures for partial bites to deeply incised scoops of flesh for full consumption (Papastamatiou et al. 2010; Grace et al. 2018). In the Azores' EEZ (Exclusive Economic Zone) 63 species of Chondrichthyes are confirmed to occur (Barcelos et al. 2021). Although specimens of *Isistius* spp. from these waters are not known to us, the Azorean Exclusive Economic Zone does fall within the area of distribution for both species (Jahn and Haedrich 1988; Zidowitz et al. 2004).

In this paper, we present evidence of the occurrence of *Isistius* sp. off the Azorean coasts, based on various visual observations made by the authors, who have extensive experience as guides in whale-watching operations and sea-going research, reinforced by photos of two dolphins with unhealed wounds. These kinds of bite marks are very common, in several species of cetaceans from tropical to temperate regions (Dwyer and Visser 2011). The here presented fresh bite marks, prove that *Isistius* species occur in these waters and are probably common (Muñoz-Chápuli et al. 1988; Zidowitz et al. 2004). A characterization of cookiecutter bites was simulated and thoroughly discussed by Grace et al. (2023). This also allows observers to be more confident in observations of potential bites.

Methods

Selected photographs (approximately 100) of the Atlantic spotted dolphin, *Stenella frontalis* (Cuvier, 1829) (Fig. 1) and the short-beaked common dolphin, *Delphinus delphis* Linnaeus, 1758 (Fig. 2), obtained during more than 20 trips, were carefully analyzed, and compared with published data regarding cookiecutter bites (Wenzel and López Suárez 2012; Best and Photopoulou 2016; Grace et al. 2018). The reported sightings of *S. frontalis* on southern inshore waters (38°37.380′N, 027°14.640′W;1500 m from shore) and *D. delphis* on the southwestern inshore waters (38°41.340′N, 027°21.540′W; 500 m from shore), off Terceira Island (Azores archipelago), were on waters more than 200 m deep.

The total lengths of the dolphins mentioned above, and maximum diameters of bite marks were estimated with *Mesurim* 2 software (Cosentino 2020), following a protocol of two steps:

- Defining the scale with the reference object (known size) in the same optical settings of the camera and at approximately the same distance between the camera and the animal.
- Using the scale to measure the bite marks.

Our choice to use this method was made also upon the following issues:

- It is free and can be used directly from a browser, without the need for installation.
- A technician with extensive experience in using the software was present to help with the measurements.
- The software has already been used in other studies related to measurements in the sea (see Ter Halle et al. 2016).

Both cases are considered recent bite marks due to the lacerations with no visible healing processes.

Results

The two wounded dolphins (Figs. 1, 2) show fresh bite marks that fall within the pattern we determined in the Methods section and were photographed during whale-watching tours that took place in August 2022 and June 2023. The *Stenella frontalis* individual had an estimated total length (TL) of 160 cm and the bite mark a maximum diameter of 4 to 5 cm (±1 cm). For the *Delphinus delphis* individual, its estimated TL of 200 cm with a bite mark of approximately 5 or 6 cm (±1 cm) in its maximum diameter.

Figure 1. Atlantic spotted dolphin, *Stenella frontalis*, with a fresh bite mark, observed on 10 August 2022 at 38°37.380′N, 027°14.640′W (photo by João B Barreiros).

Figure 2. Short-beaked common dolphin, *Delphinus delphis*, with fresh bite marks, observed on 25 June 2023 at 38°41.340′N, 027°21.540′W. (photo by João B Barreiros).

Discussion

The Atlantic spotted dolphin is a migratory species associated with warm waters (Shirihai and Jarrett 2006; Carwardine 2019). This species arrives at Azorean waters in early March staying until mid-November (Silva et al. 2014). Since the photos were taken in August, it is unlikely that the animals already had the wounds before arriving in Azorean waters.

The short-beaked common dolphin is a resident species in Azorean waters (Silva et al. 2014), being sighted year-round.

Many reports on their occurrence have been published through studies on bite marks. It is widely accepted that these bite marks, either recent or from healed scars, are proof of their occurrence as an indirect method, given their oceanic habitats and elusive nature (Papastamatiou et al. 2010). For instance, Souto et al. (2007, 2008) cite data of bite marks in cetaceans and sub-Antarctic fur seals from Bahia (northeastern Brazil). One especially interesting report describes cookiecutter bites on a great white shark, *Carcharodon carcharias* (Linnaeus, 1758) (see Hoyos-Padilla et al. 2013).

One case reported by Honebrink et al. (2011) describes the first known cookiecutter bite on a human, in this case, an open water swimmer in Hawaii. The wound had the typical form found in fish and measured 10 cm in diameter for a depth of ca. 4 cm (see also Grace et al. 2023 for the study of simulated cookiecutter bites). Although slightly smaller oval bite marks from 4–5 to 7 cm are given by Jones (1971), this case is within the expected range of measurements taken in fish markets (see Papastamatiou et al. 2010). An anecdotal report by Honebrink et al. (2011) states that cookiecutter sharks may swim in schools and threaten swimmers and other sea-going persons, especially when in pelagic areas during twilight and at nighttime. Estimating the occurrences of these sharks may help to avoid eventual incidents although none have been so far reported. Postmortem scavenging on a human body by *Isistius* was reported by Makino et al. (2004) and Ihama et al. (2009). Again, the shape of the bite marks was unequivocally attributed to cookiecutter sharks.

Given its more temperate distribution, although based on a few records, we think it is more probable that *Isistius plutodus* instead of *I. brasiliensis* occurs in the Azores, also because one specimen was recorded north of the archipelago (Zidowitz et al. 2004).

With the estimation of the distribution, collection efforts can be made to capture some specimens of the sharks, which later, through DNA analysis, would allow the identification of the species.

Conclusion

Given the above results and available data discussed, it is indisputable that cookiecutter sharks are present in Azorean waters. Efforts are being made to collect more data on *Isistius* sp. bites within or close to the Azores' EEZ. We also aim to use eDNA to detect the presence of these species in the areas where the cetaceans were detained.

Acknowledgments

The authors are thankful to Sébastien Lhoumeau for his help in calculating measurements and to the anonymous referees whose comments and suggestions significantly improved earlier versions of the manuscript. Also, thanks to the whale watching companies operating on Terceira Island for their mutual co-operation and sharing of information. Open access was funded by the project FCT-UIDB/00329/2020-2024 (Thematic Line 1 – integrated ecological assessment of environmental change on biodiversity).

References

Barcelos L, Azevedo J, Barreiros J (2021) Updated checklist of Azores Chondrichthyes (Vertebrata: Gnathostomata). Biodiversity Data Journal 9: e62813. https://doi.org/10.3897/BDJ.9.e62813

Best PB, Photopoulou T (2016) Identifying the "demon whale-biter": Patterns of scarring on large whales attributed to a cookie-cutter shark *Isistius* sp. PLoS ONE 11(4): e0152643. https://doi.org/10.1371/journal.pone.0152643

Carlisle AB, Andruszkiewicz Allan E, Kim SL, Meyer L, Port J, Scherrer S, O'Sullivan J (2021) Integrating multiple chemical tracers to elucidate the diet and habitat of cookiecutter sharks. Scientific Reports 11(1): 1–16. https://doi.org/10.1038/s41598-021-89903-z

Carrier JC, Musick JA, Heithaus MR (Eds.) (2012) Biology of sharks and their relatives. CRC Press, 666 pp. https://doi.org/10.1201/b11867

Carwardine M (2019) Handbook of whales, dolphins and porpoises of the World. Bloomsbury Publisher, 528 pp.

Cosentino P (2020) Mesurim2 v 1.63. https://www.pedagogie.ac-nice.fr/svt/productions/mesurim2/ [accessed 22-03-2024]

de Figueiredo Petean FR, de Carvalho M (2018) Comparative morphology and systematics of the cookiecutter sharks, genus *Isistius* Gill (1864) (Chondrichthyes: Squaliformes: Dalatiidae). PLoS ONE 13(8): e0201913. https://doi.org/10.1371/journal.pone.0201913

Dwyer SL, Visser IN (2011) Cookie cutter shark (*Isistius* sp.) bites on cetaceans, with particular reference to killer whales (Orca) (*Orcinus orca*). Aquatic Mammals 37(2): 111–138. https://doi.org/10.1578/AM.37.2.2011.111

Ebert DA (2003) Sharks, rays and chimaeras of California. California Natural History Guides No. 71. University of California Press, 284 pp.

Feunteun A, de Schrevel C, Verhaegen M, Chevallier D, Duchemin M, Ziani N, Montgolfier B (2018) First evaluation of the cookie-cutter sharks (*Isistius* sp.) predation pattern on different cetacean species in Martinique. Environmental Biology of Fishes 101(5): 749–759. https://doi.org/10.1007/s10641-018-0735-1

Grace MA, Dias LA, Maze-Foley K, Sinclair C, Mullin KD, Garrison L, Noble L (2018) Cookiecutter shark bite wounds on cetaceans of the Gulf of Mexico. Aquatic Mammals 43(5): 491–499. https://doi.org/10.1578/AM.44.5.2018.491

Grace MA, Huber D, Travis K, Dooseys MH, Fords J, Deckers S, Manns J (2023) Simulating cookiecutter shark bites with a 3D-printed jaw-dental model. Zoomorphology 142(2): 253–264. https://doi.org/10.1007/s00435-022-00586-0

Honebrink R, Buch R, Galpin P, Burgess GH (2011) First documented attack on a live human by a cookiecutter shark (Squaliformes, Dalatiidae: *Isistius* sp.). Pacific Science 65(3): 365–374. https://doi.org/10.2984/65.3.365

Hoyos-Padilla M, Papastamatiou YP, O'Sullivan J, Lowe CG (2013) Observation of an attack by a cookiecutter shark (*Isistius brasiliensis*) on a white shark (*Carcharodon carcharias*). Pacific Science 67(1): 129–134. https://doi.org/10.2984/67.1.10

Ihama Y, Ninomiya K, Noguchi M, Fuke C, Miyazaki T (2009) Characteristic features of injuries due to shark attacks: A review of 12 cases. Legal Medicine 11(5): 219–225. https://doi.org/10.1016/j.legalmed.2009.06.002

Jahn AE, Haedrich RL (1988) Notes on the pelagic squaloid shark *Isistius brasiliensis*. Biological Oceanography 5(4): 297–309. https://www.tandfonline.com/doi/abs/10.1080/01965581.1987.10749519

Jones EC (1971) *Isistius brasiliensis*, a squaloid shark, the probable cause of crater wounds on fishes and cetaceans. Fish Bulletin 69: 791–798.

Leung TLF (2014) Fish as parasites: An insight into evolutionary convergence in adaptations for parasitism. Journal of Zoology (London, England) 294(1): 1–12. https://doi.org/10.1111/jzo.12148

Makino Y, Tachihara K, Ageda S, Arao T, Fuke C, Miyazaki T (2004) Peculiar circular and C-shaped injuries on a body from the sea. The American Journal of Forensic Medicine and Pathology 25(2): 169–171. https://doi.org/10.1097/01.paf.0000127390.07879.62

McGrouther, M (2009) Largetooth Cookiecutter Shark, *Isistius plutodus* Garrick & Springer, 1964. Australian Museum. [Retrieved on 13 March 2024] https://australian.museum/learn/animals/fishes/largetooth-cookiecutter-shark-isistius-plutodus/

Muñoz-Chápuli R, Salgado JCR, de la Serna JM (1988) Biogeography of *Isistius brasiliensis* in the north-eastern Atlantic, inferred from crater wounds on swordfish (*Xiphias gladius*). Journal of the Marine Biological Association of the United Kingdom 68(2): 315–321. https://doi.org/10.1017/S0025315400052218

Papastamatiou YP, Wetherbee BM, O'Sullivan J, Goodmanlowe GD, Lowe CG (2010) Foraging ecology of cookiecutter sharks (*Isistius brasiliensis*) on pelagic fishes in Hawaii, inferred from prey bite wounds. Environmental Biology of Fishes 88(4): 361–368. https://doi.org/10.1007/s10641-010-9649-2

Shirihai H, Jarrett B (2006) Whales dolphins and seals. A field guide to the Marine Mammals of the world. Bloomsbury Publisher, 384 pp.

Silva MA, Prieto R, Cascão I, Seabra MI, Machete M, Baumgartner MF, Santos RS (2014) Spatial and temporal distribution of cetaceans in the mid-Atlantic waters around the Azores. Marine Biology Research 10(2): 123–137. https://doi.org/10.1080/17451000.2013.793814

Souto LRA, Abrão-Oliveira JG, Nunes JACC, Maia-Nogueira R, Sampaio CLS (2007) Analysis of cookiecutter shark *Isistius* spp. (Squaliformes; Dalatiidae) bites in cetaceans (Mammalia; Cetacea) on the Bahia coast, northeastern Brazil. Biotemas 20(1): 19–25.

Souto LRA, Abrão-Oliveira JG, Maia-Nogueira R, Dórea-Reis LW (2008) Interactions between subantarctic fur seal (*Arctocephalus tropicalis*) and cookiecutter shark (*Isistius plutodus*) on the coast of Bahia, north-eastern Brazil. Marine Biodiversity Records 2: e123. https://doi.org/10.1017/S1755267209000992

Stehmann M, Kukuev EI (2015) Two southeastern Atlantic records of the rare largetooth cookiecutter shark, *Isistius plutodus* (Selachii, Squaliformes, Dalatiidae). Cybium 39(1): 73–77. https://doi.org/10.26028/cybium/2015-391-009

Ter Halle A, Ladirat L, Gendre X, Goudouneche D, Pusineri C, Routaboul C, Tenailleau C, Duployer B, Perez E (2016) Understanding the fragmentation pattern of marine plastic debris. Environmental Science and Technology 50(11): 5668–5675. https://doi.org/10.1021/acs.est.6b00594

Wenzel FW, López-Suárez P (2012) What is known about cookiecutter shark (*Isistius* spp.) interactions with cetaceans in Cape Verde seas? Zoologia Caboverdiana 3(2): 57–66.

Zidowitz H, Fock HO, Pusch C, Von Westernhagen H (2004) A first record of *Isistius plutodus* in the north-eastern Atlantic. Journal of Fish Biology 64(5): 1430–1434. https://doi.org/10.1111/j.0022-1112.2004.00382.x

Acta Ichthyologica et Piscatoria 54, 2024, 157–163 | DOI 10.3897/aiep.54.121303

PENSOFT.

ACTA ICHTHYOLOGICA ET PISCATORIA

Chilomycterus reticulatus (Actinopterygii: Tetraodontiformes: Diodontidae) in the southern Sicilian waters, central Mediterranean Sea

Bruno ZAVA[1,2], Maria CORSINI-FOKA[3], Danilo SCANNELLA[4], Gianni INSACCO[2], Alan DEIDUN[5], Valentina CROBE[6], Fausto TINTI[6]

1 *Wilderness Studi Ambientali, Palermo, Italy*
2 *Museo Civico di Storia Naturale, Comiso (Ragusa), Italy*
3 *Institute of Oceanography, Hellenic Centre for Marine Research. Hydrobiological Station of Rhodes, Rhodes, Greece*
4 *Italian Institute for Environmental Protection and Research (ISPRA), Department for the Monitoring and Protection of the Environment and for the Conservation of Biodiversity, Palermo, Italy*
5 *Oceanography Malta Research Group (OMRG), Department of Geosciences, University of Malta, Msida, Malta*
6 *Department of Biological, Geological and Environmental Sciences, University of Bologna, Ravenna, Italy*

https://zoobank.org/04A58C9F-015E-475E-8FC0-4E7321489406

Corresponding author: Danilo Scannella (danilo.scannella@isprambiente.it)

Academic editor: Paraskevi Karachle ♦ **Received** 20 February 2024 ♦ **Accepted** 28 May 2024 ♦ **Published** 19 July 2024

Citation: Zava B, Corsini-Foka M, Scannella D, Insacco G, Deidun A, Crobe V, Tinti F (2024) *Chilomycterus reticulatus* (Actinopterygii: Tetraodontiformes: Diodontidae) in the southern Sicilian waters, central Mediterranean Sea. Acta Ichthyologica et Piscatoria 54: 157–163. https://doi.org/10.3897/aiep.54.121303

Abstract

A recently discovered fish specimen representing the family Diodontidae has been documented in the waters off Mazara del Vallo in southwest Sicily, Italy. A detailed description of the morphological and meristic characteristics of the specimen is reported. Molecular identification was performed through sequence analysis of the Cytochrome Oxidase subunit I (COI). The specimen was identified as *Chilomycterus reticulatus* (Linnaeus, 1758) both morphologically and genetically. The finding marks the third confirmed record of *Chilomycterus reticulatus* in the Mediterranean Sea and Italian waters. The significance of the presence of this uncommon fish in the basin is briefly discussed, shedding light on its occurrence and potential implications.

Keywords

Citizen scientists, cryptogenic species, DNA barcoding, Mediterranean Sea, non-indigenous species, range expanding species, rare species, spotfin burrfish

Introduction

In the Mediterranean Sea, four distinct species, representing the family Diodontidae have been identified: the spotfin porcupinefish, *Diodon hystrix* Linnaeus, 1758; the spotbase burrfish, *Cyclichthys spilostylus* (Leis et Randall, 1982); the spotfin burrfish, *Chilomycterus reticulatus* (Linnaeus, 1758) (see Kovačić et al. 2021); and the Guinean burrfish, *Chilomycterus mauretanicus* (Le Danois, 1954) (see Evans et al. 2020). The species *Diodon hystrix* and *Chilomycterus reticulatus* are both distributed globally in warm waters areas of the Pacific, Indian, and Atlantic oceans (Froese and Pauly 2023). In the Mediterranean, the first valid record for *Diodon hystrix* dates back to 1953 from the waters of the Gulf of Taranto, Ionian Sea, Italy, central Mediterranean (Anonymous 1954; Torchio 1963). Subsequently, in 2016, the species was reported in the Balearic Islands, Spain, the western Mediterranean (Ordines et al. 2018) and additionally, in the eastern Mediterranean, notably in 2017 off the coast of Cyprus (Kleitou et al. 2020) and in 2019 in the waters off Lebanon (Bariche et al. 2020).

To date, two records of *Chilomycterus reticulatus* have been reported in the basin. These records are based on two specimens found dried on the shoreline: one in 2008 in the south Sardinian Sea, specifically on S. Antioco's Island in the western Mediterranean (Follesa et al. 2009), and the second in March 2023 in Santa Marinella near Civitavecchia harbor in the Central Tyrrhenian Sea. The latter was reported solely in an official press release by the Italian Institute for Environmental Protection and Research (ISPRA 2023). Notably, the species was also sighted in 2012 during scuba diving in the Mediterranean waters off France, according to Casassovici and Brosens (2022). Furthermore, an additional specimen of *Chilomycterus reticulatus*, originating from Trieste in the north Adriatic Sea, Italy, and dating back to either July 27, 1858, or July 27, 1868, is listed in the collection of the Swedish Museum of Natural History (Catalogue number NMR 8907) (https://artedi.nrm.se/nrmfish/index.php).

The spotbase burrfish, *Cyclichthys spilostylus*, is distributed in the Indo–Pacific Ocean, including the Red Sea (Golani and Fricke 2018); to date, it has been recorded in the Mediterranean waters off Israel in 1992 and 2009 (Golani 2010; Golani et al. 2010), and in Turkey in 2011 (Erguden et al. 2012). Finally, the Guinean burrfish, *Chilomycterus mauretanicus*, with a tropical west African natural range, has been recorded once in the Alboran Sea, western Mediterranean, in 2008 (Garrido et al. 2014). Among the four diodontids mentioned above, only *Cyclichthys spilostylus* is considered a non-indigenous species introduced in the Mediterranean via the Suez Canal from the Red Sea (Lessepsian immigrant) (Golani 2021), while the possible pathway of arrival in the basin of the other three species is under discussion.

In the present study, the occurrence of the spotfin burrfish, *Chilomycterus reticulatus*, is documented for the third time in the whole Mediterranean Sea and in Italian waters, based on a morphological and molecular study carried out on a specimen collected during summer 2023 in the shallow waters of southwest Sicily, central Mediterranean. The possible provenance of this uncommon species in the Mediterranean is briefly discussed.

Material and methods

A strange spiny balloon-like fish was caught alive on 31 August 2023, with a fishing rod from the shore by a young amateur angler near the port of Mazara del Vallo, southwestern Sicily, Italy (37.645677°W, 012.578223°E) at about 5 m of depth on a rocky substrate, sea surface temperature approximately 27°C. Photos of the fish were shared on Facebook. One of the authors (BZ) soon contacted the angler and alerted him about possible danger if the fish was consumed. The specimen was immediately shipped (frozen) to the facilities of the Wilderness Studi Ambientali in Palermo. The sample was photographed and weighed, morphometric measurements were taken with a caliper (accuracy 0.1 mm), and the meristic data were determined. For the taxonomic identification of the sample, Leis (1986, 2001, 2002, 2006, 2016), Fischer and Bianchi (1984), and Fahay (2007) were consulted.

Samples of muscle and fins preserved in 99% ethanol were sent to the Department of Biological, Geological, and Environmental Sciences of the University of Bologna for genetic analysis. DNA was extracted using the Wizard® SV Genomic DNA Purification System by Promega, according to the manufacturer's protocol. The quality of the extracted gDNA was assessed on a 1% agarose gel electrophoresis. The mitochondrial gene Cytochrome oxidase subunit 1 (COI) was amplified and sequenced with the M13-tailed primer cocktail (COI-3; C_FishF1t1–C_FishR1t1) described by Ivanova et al. (2007). The PCR reaction was performed in a 25 µL total volume containing 3 µL of gDNA template, 1 × PCR buffer, 25 µM of $MgCl_2$, 0.5 mM dNTPs, 0.1 µM of each primer cocktail, and 0.25 U GoTaq G2 Flexi DNA polymerase (Promega). Amplification was performed in a T-gradient thermocycler (Biometra) with an initial denaturation of 2 min at 94°C, followed by 35 cycles of 30 s at 94°C, 30 s at 52°C, 60 s at 72°C, and a final extension of 10 min at 72°C. The PCR product was evaluated on a 2% agarose gel.

From the NCBI database (https://www.ncbi.nlm.nih.gov), 66 available COI sequences belonging to 12 species of the family Diodontidae were retrieved. The molecular identification was performed with a neighbor-joining (NJ) method (Saitou and Nei 1987) using MEGA 11 (Tamura et al. 2021) with p-distance (Collins and Cruickshank 2013) and pairwise deletion. To estimate support for the nodes, 1000 bootstrap replicates (Felsenstein 1985) were performed.

The specimen is currently deposited at the Museo Civico di Storia Naturale di Comiso, Italy (inventory number MSNC 4918).

Results

The thawed specimen, with a total length of 310 mm and a weight of 1160 g, presented the following main characteristics: body moderately robust, head width 2.4 in standard length; almost rounded anal and caudal fins; a single (unsutured) tooth in each jaw; body covered with immovable spines (Fig. 1A, 1A-inset, 1B, 1C, 1D), with three roots under the skin (Fig. 1B-inset); one spine on the dorsal surface of caudal peduncle (Fig. 1D); 9 spines from snout to dorsal fin base; nostrils positioned in front of eyes; nostrils not closed at the top, but each having the appearance of two lips (Fig. 1C). Dorsal-fin rays 12, pectoral-fin rays 21–21, anal-fin rays 11, and caudal-fin rays 10; approximately 14 spines from lower jaw to anus (Fig. 1A-inset, B); 61 spines sparse on the whole belly. Color: greyish background with numerous small

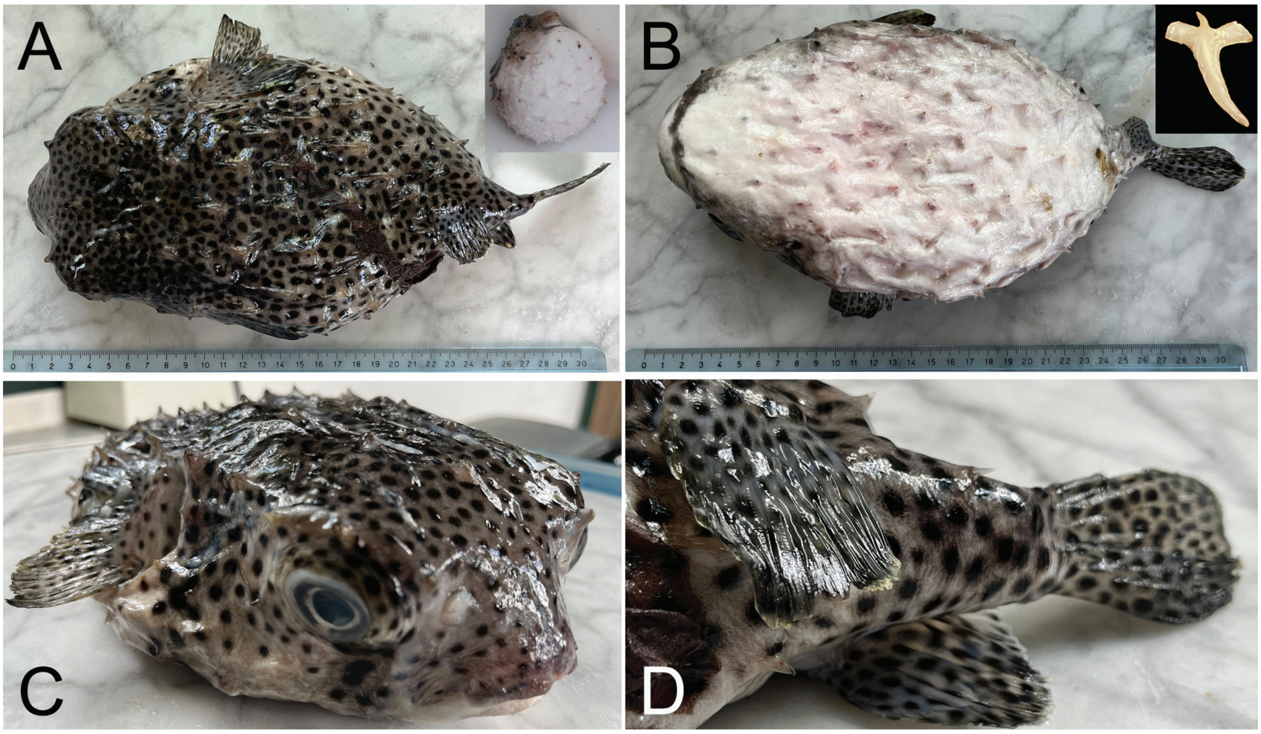

Figure 1. *Chilomycterus reticulatus* from Mazara del Vallo, Sicily, Italy. **A**: dorsal view (inset A: freshly caught specimen, inflated), **B**: ventral view (inset B: a three-rooted body spine), **C**: head profile, **D**: tail with a single spine on its upper side. (Photos A, B, C, D by G. Polizzi, inset in A by R. Figuccia).

Table 1. Morphometric characters of a specimen of *Chilomycterus reticulatus* caught in Mazara del Vallo, Sicily, Italy, August 2023.

Character	Value	
	Absolute [mm]	Relative [% SL]
Total length	310	
Standard length (SL)	255	
Head length	86	33.7
Head width (HW)	107	42.0
Head depth	95	37.3
Eye diameter	20	7.8
Snout length	22	8.6
Gill opening length	37	14.5
Body depth	77	30.2
Interorbital length	91	35.7
Postorbital length	50	19.6
Pectoral fin height	41	16.1
Prepectoral length	105	41.2
Pectoral fin base length	40	15.7
Predorsal length	197	77.3
Dorsal fin base length	27	10.6
Dorsal fin height	40	15.7
Preanal length	210	82.4
Anal fin base length	18	7.1
Anal fin height	36	14.1
Precaudal length	243	95.3
Caudal peduncle length	31	12.2
Caudal peduncle depth	25	9.8
Caudal fin length	46	18.0

dark spots that characteristically extend to cover the majority of the fins (Fig. 1A, 1C, 1D), whitish ventrally (Fig. 1B), a dark band on the chin, under the lower jaw (Fig. 1A-inset, D). The values of the main measurements of our specimen and their percentage of standard length are presented in Table 1.

The results of genetic analysis validated the morphological identification of the specimen as *Chilomycterus reticulatus*. In the reconstruction of the NJ tree (Fig. 2), the 652 bp COI sequence (Accession Number: PP267988) clustered within the *Chilomycterus reticulatus* clade, exhibiting robust support with a bootstrap value of 99%.

Discussion

The morphological and morphometric characters, as well as the coloration observed in the Diodontidae specimen from Sicily, as described above, agreed with the description of *Chilomycterus reticulatus* by Leis (1986, 2001, 2002, 2006, 2016). The accuracy of this identification was unequivocally confirmed by genetic analysis. The shape of the nostrils of our sample is characteristic of the genus *Chilomycterus* Brisout de Barneville, 1846. In particular, when comparing the main measurements of our specimen, as a percentage of the standard length, they partially differed from those reported by Follesa et al. (2009). This discrepancy is likely due to the inherent challenges of accurately comparing measurements from a dried specimen with those from a flaccid, defrosted specimen, as noted in the study. The spotfin burrfish, *Chilomycterus reticulatus*, reaches a maximum standard length of 75 cm. In its life stages, from eggs and larvae to juveniles of about 20 cm, it tends to be pelagic, often associated with floating weeds. Larger fish are benthic, inhabiting mostly rocky reefs,

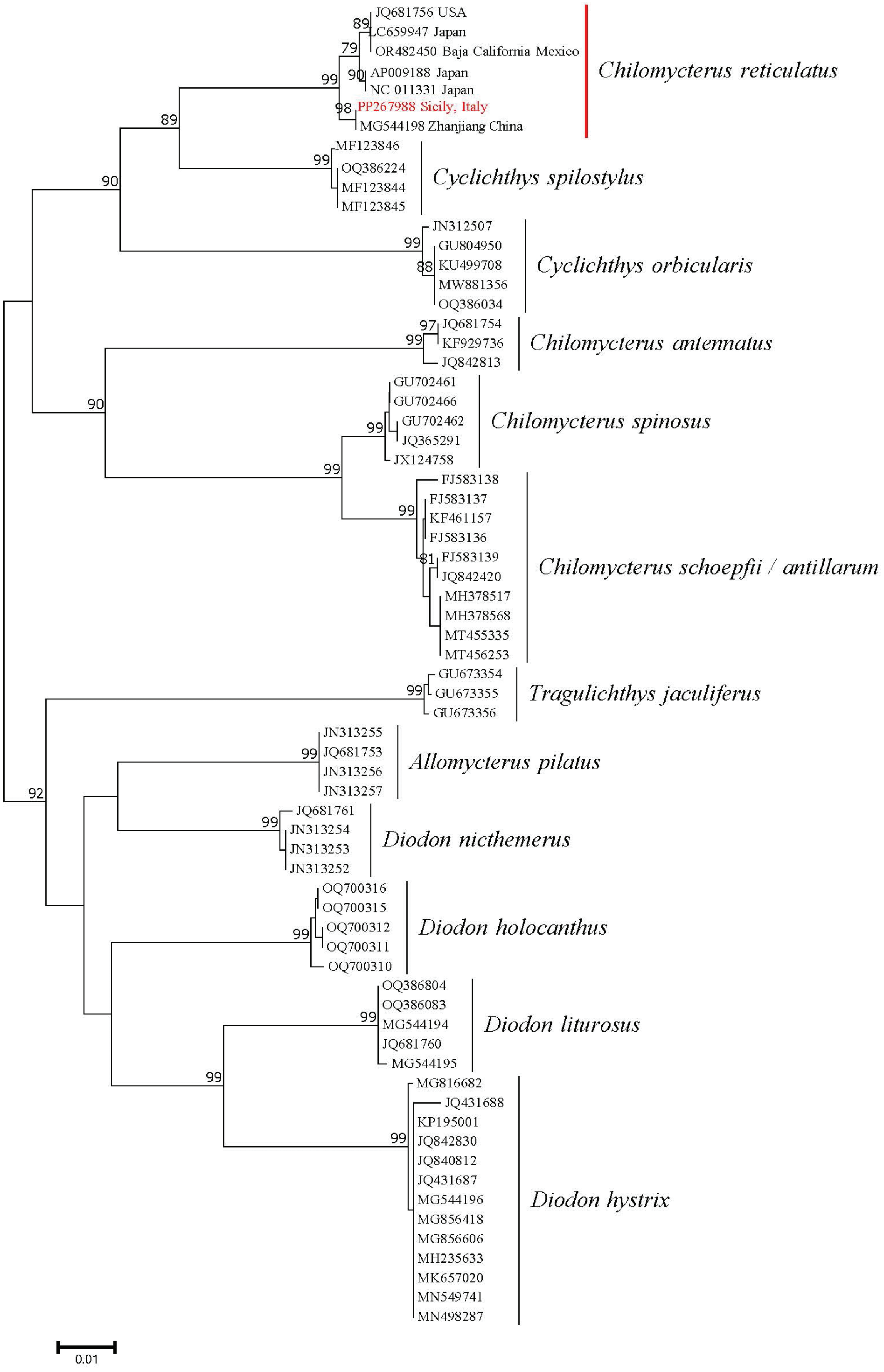

Figure 2. Neighbor-Joining tree based on COI genetic p-distances of 12 Diodontidae taxa. Numbers near nodes indicate bootstrap values (≥70%). A distance scale bar is given.

coral reefs, and sandy bottoms down to 100 m of depth or more (Leis 2016; Castro et al. 2021; Froese and Pauly 2023). Usually solitary, spotfin burrfish adopt a bracing posture against the substrate to sleep at night, while they appear to be more active during the day, feeding predominantly on hard-shelled invertebrates (Espino et al. 2019; Arndt and Evans 2022; Froese and Pauly 2023).

Spotfin burrfish are preyed upon by large carnivorous fish such as dorados, sharks, and wahoo (Snow 2024). Toxicity for *Chilomycterus* spp. has been reported (Halstead 1965) and *Chilomycterus reticulatus* is listed as a poisonous fish in Australia (Froese and Pauly 2023), posing a potential risk to human health if consumed. It is listed as edible in Japan (Noguchi and Arakawa 2008). Generally considered of no commercial value in fishery, the species has only limited interest in the ornamental fish trade, since it is suitable only for large display tanks (public aquaria or zoo) (Meerwasser-Lexikon Team 2022).

According to Leis (1986), the pelagic stage of *Chilomycterus reticulatus* is blue dorsally with dark spots also on the back and belly, while the benthic adults are grey to brown with small black spots on the upper surface and fins and a black gill band. The capture method, the color, and the size of the specimen of *Chilomycterus reticulatus* from Sicily allowed us to consider it as a benthic adult, smaller than the specimen of 470 mm total length washed up on the Sardinian beach (Follesa et al. 2009).

The presently reported finding constitutes the third confirmed record of *Chilomycterus reticulatus* in the Mediterranean and in Italian waters, after that of Follesa et al. (2009) and ISPRA (2023). These findings, with the addition of an underwater sighting from France (Casassovici and Brosens 2022), could indicate that the occurrence of the species, although rare, is no longer casual. Details on the 19th-century specimen of *Chilomycterus reticulatus* collected in the northeastern Adriatic and preserved at the Swedish Museum of Natural History were not available.

Relini and Orsi Relini (1995) emphasized that the presence of fishes representing the order Tetraodontiformes in the basin could have historical roots, possibly extending back to remote times. This suggests the plausible existence of a small native population of this diodontid in the western basin. The pelagic early life and juvenile stages of *Chilomycterus reticulatus* could facilitate its dispersion in the Mediterranean regions, aided by currents, but the cryptic habits of the adults and the probable rarity of individuals could render its observation or capture difficult. In fact, the first individual of *Chilomycterus reticulatus* was found stranded on a beach (Follesa et al. 2009), while in our case it was caught by fishing rod from the shore, demonstrating a lack of catchability by commercial fleets in the Mediterranean so far, as highlighted by Ordines et al. (2018) for the cofamilial *Diodon hystrix*.

The development of marine research, combined with the intensification of fishermen and citizen scientists' input in marine biodiversity observations, the diffused use of social media platforms, and in general the increasing speed of information exchange and dissemination due to innovative technological instruments could probably explain the recent density of records of *Diodon hystrix* in 2016, 2017, 2019 (Bariche et al. 2020) and the present one of *Chilomycterus reticulatus* in 2023 in the Mediterranean. On the other hand, the warming of Mediterranean waters linked to global climate change (Galil 2023) may favor the enhancement and development of the population of this warm-water species. The increase in sightings and spread of *Chilomycterus reticulatus* in the Canary Islands and Madeira Archipelago observed in recent decades could be associated with the ongoing seawater warming observed in both regions (Espino et al. 2019; Castro et al. 2021).

The casual finding of this species in 2008 (Follesa et al. 2009) and in 2023 (ISPRA 2023) led to the suggestion that this fish, exhibiting tropical affinities, might be a vagrant visitor or a range-expanding newcomer (or neonative), naturally expanding its distribution from the Atlantic through the Strait of Gibraltar (Psomadakis et al. 2012; Zenetos et al. 2022).The locations of first finding off southern Sardinia (Follesa et al. 2009), followed by subsequent sightings in the central Tyrrhenian Sea (ISPRA 2023), and the presently reported one in south Sicily, as well as the underwater observation in south France (Casassovici and Brosens 2022), could corroborate a possible arrival from the Atlantic and potential establishment of a small population. It is to be noted that our *Chilomycterus reticulatus* was captured from the shallow waters of southwest Sicily, located along the Sicily Strait, a hydrological, geological, biogeographical transitional zone between the western and eastern sub-basins of the Mediterranean, where range expanding species from the Atlantic and non-indigenous species from the Red Sea are detected (Azzurro et al. 2014; Deidun et al. 2021).

The Mediterranean Sea is the hot-spot region in the world for biological invasions due to the introduction of non-indigenous species (NIS), mainly through the man-made Suez Canal (Galil 2023). Although widely distributed in the Indo–Pacific oceans, *Chilomycterus reticulatus* is unreported in the Red Sea (Golani and Fricke 2018), consequently an introduction via the Suez Canal corridor appears unlikely at present.

Prudently, Evans et al. (2020) included *Chilomycterus reticulatus* among the cryptogenic fish species of the Mediterranean, denoting species that cannot be definitively classified as native or introduced (sensu Carlton 1996). The circumtropical nature of this fish, coupled with minimal genetic differentiation between populations in different regions of the world, as confirmed by the genetic analysis described in the present work, adds to the challenge of determining the potential origin of Mediterranean specimens. A similar complexity has recently been recognized for *Diodon hystrix* (see Kleitou et al. 2020).

Scientific research aimed at monitoring any increase in the Mediterranean population of this toxic warm-water fish, possibly with the support of citizen-scientist observations, is important, not only to minimize the risk to human health (Malloggi et al. 2023), but also to evaluate its role in biological assemblages and the food web, and to assess potential impacts on Mediterranean biodiversity.

Acknowledgments

The authors warmly thank the young angler Kevin Bibiche Nour, who captured the *Chilomycterus reticulatus* reported in this paper, and Roberto Figuccia for sharing the first photos of the fish and providing the authors with the specimen and information on its collection. They also acknowledge the support of Marcello Bascone (Mazara del Vallo) and Giovanna Polizzi (Wilderness Studi Ambientali, Palermo). They are grateful to anonymous reviewers for useful and constructive comments and suggestions on the first version of the manuscript.

References

Anonymous (1954) Un pesce istrice nel Golfo di Taranto (« Il Bolletino di Pesca ». 1954, n. 1). Pp. 519–521. In: Fioravanzo G. (Ed.) Marine da pesca e sport subacqueo. Rivista Marittima 86(2): 519–523.

Arndt E, Evans J (2022) Diel activity of littoral and epipelagic teleost fishes in the Mediterranean Sea. Reviews in Fish Biology and Fisheries 32(2): 497–519. https://doi.org/10.1007/s11160-022-09697-9

Azzurro E, Ben Souissi J, Boughedir W, Castriota L, Deidun A, Falautano M, Ghanem R, Zammit-Mangion M, Andaloro F (2014) The Sicily Strait: A transnational observatory for monitoring the advance of non-indigenous species. Biologia Marina Mediterranea 21(1): 105–106.

Bariche M, Al-Mabruk SA, Ateş MA, Büyük A, Crocetta F, Dritsas M, Edde D, Fortič A, Gavriil E, Gerovasileiou V, Gökoğlu M, Huseyinoglu FM, Karachle PK, Kleitou P, Terbiyik Kurt T, Langeneck J, Lardicci C, Lipej L, Pavloudi C, Pinna M, Rizgalla J, Rüştü Özen M, Sedano F, Taşkin E, Yildiz G, Zangaro F (2020) New alien Mediterranean biodiversity records (March 2020). Mediterranean Marine Science 21(1): 129–145. https://doi.org/10.12681/mms.21987

Carlton JT (1996) Biological invasions and cryptogenic species. Ecology 77(6): 1653–1655. https://doi.org/10.2307/2265767

Casassovici A, Brosens D (2022) Diveboard–Scuba diving citizen science observations. Version 54.51. Diveboard. Occurrence dataset. https://doi.org/10.15468/tnjrgy

Castro N, Schäfer S, Parretti P, Monteiro JG, Gizzi F, Chebaane S, Almada E, Henriques F, Freitas M, Vasco-Rodrigues N, Silva R, Radeta M, Freitas R, Canning-Clode J (2021) A new signal of tropicalization in the northeast Atlantic: The spread of the spotfin burrfish *Chilomycterus reticulatus* in Madeira Archipelago and its invasion risk. Diversity 13(12): 639. https://doi.org/10.3390/d13120639

Collins RA, Cruickshank RH (2013) The seven deadly sins of DNA barcoding. Molecular Ecology Resources 13(6): 969–975. https://doi.org/10.1111/1755-0998.12046

Deidun A, Insacco G, Galdies J, Balistreri P, Zava B (2021) Tapping into hard-to-get information: The contribution of citizen science campaigns for updating knowledge on range-expanding, introduced and rare native marine species in the Malta–Sicily Channel. BioInvasions Records 10(2): 257–269. https://doi.org/10.3391/bir.2021.10.2.03

Erguden D, Bayhan YK, Turan C (2012) First record of spotbase burrfish, *Cyclichthys spilostylus* (Actinopterygii: Tetraodontiformes: Diodontidae), from the marine waters of Turkey. Acta Ichthyologica et Piscatoria 42(2): 137–140. https://doi.org/10.3750/AIP2011.42.2.07

Espino F, Tuya F, del Rosario A, Bosch NE, Coca J, González-Ramos AJ, del Rosario F, Otero-Ferrer FJ, Moreno ÁC, Haroun R (2019) Geographical range extension of the spotfin burrfish, *Chilomycterus reticulatus* (L. 1758), in the Canary Islands: A response to ocean warming? Diversity 11(12): 230. https://doi.org/10.3390/d11120230

Evans J, Arndt E, Schembri PJ (2020) Atlantic fishes in the Mediterranean: Using biological traits to assess the origin of newcomer fishes. Marine Ecology Progress Series 643: 133–143. https://doi.org/10.3354/meps13353

Fahay MP (2007) Early stages of fishes in the western North Atlantic Ocean. Vol. 2, Scorpaeniformes through Tetraodontiformes. Northwest Atlantic Fisheries Organization-NAFO, 932–1696.

Felsenstein J (1985) Confidence limits on phylogenies: An approach using the bootstrap. Evolution 39(4): 783–791. https://doi.org/10.2307/2408678

Fischer W, Bianchi G (Eds.) (1984) FAO species identification sheets for fishery purposes. Western Indian Ocean; (Fishing Area 51). FAO, Rome.

Follesa MC, Mulas A, Porcu C, Cau A (2009) First record of *Chilomycterus reticulatus* (Osteichthyes: Diodontidae) in the Mediterranean Sea. Journal of Fish Biology 74(7): 1677–1681. https://doi.org/10.1111/j.1095-8649.2009.02229.x

Froese R, Pauly D (Eds.) (2023) FishBase. [Version 02/2023] http://www.fishbase.org

Galil BS (2023) A sea, a canal, a disaster: The Suez Canal and the transformation of the Mediterranean biota. Pp. 199–215. In: Lutmar C, Rubinovitz Z (Eds.) The Suez Canal: Past lessons and future challenges. Palgrave Studies in Maritime Politics and Security. Palgrave Macmillan, Cham. https://doi.org/10.1007/978-3-031-15670-0_10

Garrido A, Ibanez-Yuste AJ, Norman C, Terron-Sigler A (2014) First record of *Chilomycterus spinosus mauretanicus* (Osteichthyes: Diodontidae) in the Mediterranean Sea. Marine Biodiversity Records 7: e79. https://doi.org/10.1017/S1755267214000530

Golani D (2010) Colonization of the Mediterranean by Red Sea fishes via the Suez Canal. Pp. 145–188. In: Golani D, Appelbaum-Golani B (Eds.) Fish invasions of the Mediterranean Sea: Change and renewal. Pensoft Publishers, Sofia–Moscow.

Golani D (2021) An updated checklist of the Mediterranean fishes of Israel, with illustrations of recently recorded species and delineation of Lessepsian migrants. Zootaxa 4956(1): 1–108. https://doi.org/10.11646/zootaxa.4956.1.1

Golani D, Fricke R (2018) Checklist of the Red Sea fishes with delineation of the Gulf of Suez, Gulf of Aqaba, endemism and Lessepsian migrants. Zootaxa 4509(1): 1–215. https://doi.org/10.11646/zootaxa.4509.1.1

Golani D, Salameh P, Sonin O (2010) First record of the emperor angelfish, *Pomacanthus imperator* (Teleostei: Pomacanthidae) and the second record of the spotbase burrfish *Cyclichthys spilostylus* (Teleostei: Diodontidae) in the Mediterranean. Aquatic Invasions 5(2, Suppl. 1): S41–S43. https://doi.org/10.3391/ai.2010.5.S1.010

Halstead BW (1965) Poisonous and venomous marine animals of the world: Vertebrates. U.S. Government Printing Office, 1070 pp.

ISPRA (2023) Comunicato stampa. Ritrovato sulla costa laziale un pesce istrice tropicale:è il secondo esemplare segnalato nel mediterraneo dal 2008. Istituto Superiore per la Protezione e la Ricerca Ambientale (ISPRA).

Ivanova NV, Zemlak TS, Hanner RH, Hebert PD (2007) Universal primer cocktails for fish DNA barcoding. Molecular Ecology Notes 7(4): 544–548. https://doi.org/10.1111/j.1471-8286.2007.01748.x

Kleitou P, Giovos I, Antoniou C, Ioannou G, Bernardi G (2020) The third record of black-spotted porcupinefish *Diodon hystrix* Linnaeus, 1758 in the Mediterranean Sea. Journal of Applied Ichthyology 36(2): 227–230. https://doi.org/10.1111/jai.13999

Kovačić M, Lipej L, Dulčić J, Iglesias SP, Goren M (2021) Evidence-based checklist of the Mediterranean Sea fishes. Zootaxa 4998(1): 1–115. https://doi.org/10.11646/zootaxa.4998.1.1

Leis JM (1986) Diodontidae. Pp. 903–907. In: Smith MM, Heemstra PC (Eds.) Smiths' sea fishes. Springer-Verlag, Berlin–Heidelberg–New York–London–Paris–Tokyo.

Leis JM (2001) Diodontidae Porcupinefishes (burrfishes). Pp. 3958–3965. In: Carpenter KE, Niem VH (Eds.) FAO species identification guide for fishery purposes. The living marine resources of the Western Central Pacific. Volume 6. Bony fishes part 4 (Labridae to Latimeriidae), estuarine crocodiles, sea turtles, sea snakes and marine mammals. FAO, Rome.

Leis JM (2002) Diodontidae. Pp. 2007–2013. In: Carpenter KE (Ed.) FAO species identification guide for fishery purposes. The living marine resources of the Western Central Atlantic. Volume 3: Bony fishes part 2 (Opistognathidae to Molidae), sea turtles and marine mammals. FAO, Rome.

Leis JM (2006) Nomenclature and distribution of the species of the porcupinefish family Diodontidae (Pisces, Teleostei). Memoirs of the Museum of Victoria 63(1): 77–90. https://doi.org/10.24199/j.mmv.2006.63.10

Leis JM (2016) Diodontidae Porcupine fishes (burrfishes, spiny puffers). Pp. 3074–3079. In: Carpenter KE, De Angelis N (Eds.) FAO Species Identification Guide for Fishery Purposes. The living marine resources of the Eastern Central Atlantic. Volume 4: Bony fishes part 2 (Perciformes to Tetradontiformes) and Sea turtles. FAO, Rome.

Malloggi C, Rizzo B, Giusti A, Guardone L, Gasperetti L, Dall'Ara S, Armani A (2023) First toxicological analysis of the pufferfish *Sphoeroides pachygaster* collected in Italian Waters (Strait of Sicily): Role of citizens science in monitoring toxic marine species. Animals 13(11): 1873. https://doi.org/10.3390/ani13111873

Meerwasser-Lexikon Team (2022) *Chilomycterus reticulatus* spotfin burrfish. Meerwasser-Lexikon; Reeflex.net.

Noguchi T, Arakawa O (2008) Tetrodotoxin – Distribution and Accumulation in aquatic organisms, and cases of human intoxication. Marine Drugs 6(2): 220–242. https://doi.org/10.3390/md20080011

Ordines F, Deudero S, Sintes-Vila J, Sbragaglia V, Fricke R, Azzurro E (2018) A new record of *Diodon hystrix* (Actinopterygii: Tetraodontiformes: Diodontidae) in the Mediterranean Sea. Acta Ichthyologica et Piscatoria 48(4): 403–407. https://doi.org/10.3750/AIEP/02440

Psomadakis PN, Giustino S, Vacchi M (2012) Mediterranean fish biodiversity: An updated inventory with focus on the Ligurian and Tyrrhenian seas. Zootaxa 3263(1): 1–46. https://doi.org/10.11646/zootaxa.3263.1.1

Relini M, Orsi Relini O (1995) Pesci palla in Mediterraneo, presenze antiche e recenti. Biologia Marina Mediterranea 2(2): 509–511.

Saitou N, Nei M (1987) The neighbor-joining method: A new method for reconstructing phylogenetic trees. Molecular Biology and Evolution 4(4): 406–425. https://doi.org/10.1093/oxfordjournals.molbev.a040454

Snow J (2024) Spotfin burrfish, *Chilomycterus reticulatus*. Mexican Fish.com.

Tamura K, Stecher G, Kumar S (2021) MEGA11: Molecular Evolutionary Genetics Analysis version 11. Molecular Biology and Evolution 38(7): 3022–3027. https://doi.org/10.1093/molbev/msab120

Torchio M (1963) Accertata presenza di un rappresentante della famiglia Diodontidae in Mediterraneo. Atti della Società Italiana di Scienze Naturali e del Museo Civico di Storia Naturale di Milano 102(3): 277–281.

Zenetos A, Albano PG, López Garcia E, Stern N, Tsiamis K, Galanidi M (2022) Established non-indigenous species increased by 40% in 11 years in the Mediterranean Sea. Mediterranean Marine Science 23(1): 196–212. https://doi.org/10.12681/mms.29106

Acta Ichthyologica et Piscatoria 54, 2024, 165–176 | DOI 10.3897/aiep.54.124289

PENSOFT.

ACTA
ICHTHYOLOGICA
ET PISCATORIA

Can stocking with advanced European grayling fry strengthen its populations in the wild?

Mladen AVRAMOVIĆ[1], Jan TUREK[1], Pavel LEPIČ[1], Mariusz SZMYT[2], Jan PASTEJŘÍK[1], Tomáš RANDÁK[1]

1 *University of South Bohemia in České Budějovice, Faculty of Fisheries and Protection of Waters, South Bohemian Research Center of Aquaculture and Biodiversity of Hydrocenoses, Vodňany, Czech Republic*

2 *Department of Ichthyology and Aquaculture, Faculty of Animal Bioengineering, University of Warmia and Mazury in Olsztyn, Olsztyn, Poland*

https://zoobank.org/0F5CB4E7-2D3C-43A0-B333-9F60054317F5

Corresponding author: Mladen Avramović (mavramovic@frov.jcu.cz)

Academic editor: Predrag Simonović ♦ **Received** 30 March 2024 ♦ **Accepted** 19 June 2024 ♦ **Published** 2 August 2024

Citation: Avramović M, Turek J, Lepič P, Szmyt M, Pastejřík J, Randák T (2024) Can stocking with advanced European grayling fry strengthen its populations in the wild? Acta Ichthyologica et Piscatoria 54: 165–176. https://doi.org/10.3897/aiep.54.124289

Abstract

European grayling, *Thymallus thymallus* (Linnaeus, 1758) (Actinopterygii: Salmoniformes: Salmonidae), represents one of the highly attractive riverine fishing species in Europe. Its populations have declined in the Czech Republic due to various adverse factors. Current approaches for strengthening these populations based on restocking with artificially reared 1+ or 2+ old individuals have proven to be ineffective. This study focuses on the possibilities of supporting or restoring these populations by reintroducing two-month-old, fast-growing fry reared in ponds. In June 2021, 5400 advanced fry marked with Alizarin Red (ARS) were introduced into three free-flowing South Bohemian streams. The recapture rates and biometric data (length and weight) of stocked grayling were assessed at the release sites as well as further downstream. The first electrofishing monitoring was conducted at the end of the growing season (October) and after their first winter (March). Water temperature and flow rate at the stocking sites were monitored throughout the growing season. The substantial number of recaptured individuals across all monitored sites suggests that the fry successfully adapted to their new habitat and significantly contributed to the composition of local fish communities. Downstream movement of stocked fry correlated with lower water temperatures and higher flows. Our findings demonstrate that some introduced individuals successfully overwintered at all three reintroduction sites. Marking with ARS has proven to be a very effective non-invasive method of group marking juvenile fish and is suitable for monitoring stocking programs. The production and stocking of fast-growing advanced fry of European grayling is thus a promising strategy for revitalizing and strengthening the populations of this threatened fish in running waters.

Keywords

adaptability of stocked fish, ARS marking, grayling stocks production, natural discharge, restocking grayling

Introduction

The European grayling, *Thymallus thymallus* (Linnaeus, 1758) (Actinopterygii: Salmoniformes: Salmonidae) (thereafter referred in the text as EG), represents an attractive recreational fishing species that fell under fisheries management programs in the mid-20th century (Janković 1964; Northcote 1995). Nowadays, the wild population has declined dramatically through its natural range due to flow regulation and water quality degradation (Northcote 1995; Thorfve and Carlstein 1998; Thorfve 2002; Turek et al. 2012), hydropeaking (Hayes et al. 2021), and severe bird predation (Jepsen et al. 2018). Despite efforts to counter this decline, restocking projects, usually based on restocking with farmed 1+ and 2+-year-old fish, have proven ineffective, resulting in notably low recapture rates in natural habitats (Turek et al. 2012, 2018; Avramović et al. 2024). Consequently, exploring different release sizes of stocked fish is recommended for more effective restocking (Lorenzen 2005). Specifically, the release of early stages (0+) could improve stocking success (Carlstein 1997; Czerniawski et al. 2015) and mitigate the development of rearing-related traits in salmonids, which often hinders their survival in natural environments (Fraser et al. 2011).

Rearing techniques influence post-stocking recaptures of EG (Carlstein 1997). During the early stages, grayling can be fed with zooplankton (Luczynski et al. 1986) to aid their successful adaptation in the wild (Czerniawski et al. 2015). Supplementing or fully transitioning to dry pellets in the first summer can enhance survivability in ponds (Carlstein 1993) and lead to satisfactory post-stocking biometrics for grayling in lotic water bodies (Carlstein 1997). However, the stocking programs with pond-reared EG fry fed on the zooplankton remain unassessed in natural riverine habitats.

Along with the tendency of stocked grayling to drift downstream (Thorfve and Carlstein 1998; Horká et al. 2015), the extent of fish disappearance from stocking sites is supposed to correspond to the habitat capacity. Thus, mass stocking events can lead to density-dependent mortality due to increased competition (Hühn et al. 2014; Lorenzen and Camp 2019). Furthermore, the viability of stocking 0+ stages is uncertain due to potential mortality caused by environmental factors (Lorenzen and Camp 2019), which play a crucial role in determining outcomes of stocking salmonids (Brignone et al. 2022). Rapid increases in water flow in small streams increase the risk of young salmonids being swept away (Jowett and Richardson 1989; Hayes et al. 2010; Warren et al. 2015). In cold water, these challenges further hinder fish as they impair their swimming abilities (Enders et al. 2008) and increase the risk of stranding (Poff et al. 1997; Auer et al. 2017, 2023).

In general, the growth of EG 0+ has to be optimized during the main growing season by low discharge and warm temperatures (Marsh et al. 2022). The optimal growth temperature for EG has been identified as 17.3°C (Mallet et al. 1999) and higher temperatures are supposed to reduce growth (Persat and Pattee 1981) and recruitment of 0+ stages (Charles et al. 2006). Additionally, stocking in summer may encounter high diel amplitudes in water temperature (T_a) that significantly affect fish performance (Malcolm et al. 2008). These amplitudes tend to affect juveniles more than adults (Auer et al. 2023) and lead to increased metabolic costs (Beauregard et al. 2013) that have a negative impact on salmonid growth (Meeuwig et al. 2004). In winter, predation by cormorants can severely affect grayling populations (Jepsen et al. 2018), while in shallower streams herons also pose a threat and cause significant losses amongst stocked fish (Miyamoto et al. 2017). Submerged wooden structures can help reduce predation rates (Miyamoto et al. 2017) and boost fish site fidelity during this period (Watz 2017).

Any assessment of the success of a stocking program must include the monitoring of post-stocking recapture rates and fish performance (Waples et al. 2007), with the precondition that appropriate fish marking for subsequent stocked fish detection such as Alizarin Red (ARS) has been employed (Hühn et al. 2014; Halačka et al. 2018). In the South Bohemian streams in the Czech Republic, the abundance of EG was found to be concerningly low, indicating the urgent demand for restocking. Therefore, the aims of this study were:

- To establish a rearing and monitoring program of advanced grayling fry to aid natural population recovery.
- To evaluate if stocked fish would adapt successfully and result in acceptable recapture rate, and lengths and weights that would mirror those of natural streams.
- To assess displacement of grayling fry from the release site.
- To describe stocking outcomes in relation to the water temperature and discharge throughout the growing season.
- To provide valuable recommendations for future EG reintroductions.

We assumed that the stocked fish would adapt successfully. Due to their previous experiences of living in a pond with natural prey and the fact that the stocking took place in the middle of the growing season, we predicted acceptable recapture rates and body growth rates in natural streams. Also, our study discusses stocking outcomes in relation to the water temperature and discharge throughout the growing season.

Material and methods

Rearing of European grayling advanced fry. A total of 20 000 grayling fry were purchased from the hatchery Kachní farma Holýšov and transported on 18 May 2021 to a small pond (0.1 ha) with maximum depths of 100–120 cm situated in the experimental pond area of the Faculty of Fisheries and Protection of Waters, University of South Bohemia in České Budějovice (FFPW USB) in Vodňany. The water chemistry parameters (pH, O_2 [mg · L^{-1}]) were monitored using the WTW pH 3310 and WTW oxi 3205 equipment, respectively (Table 1). The water temperature was monitored in the rearing pond with dataloggers (Minikin Tie, Ø = 20 mm, www.emsbrno.cz) (Table 1). The grayling fry initially consumed just natural food in the pond until zooplankton were continuously added. The pond's water temperature exhibited an exponential increase from 18 May to 28 June 2021 during the rearing period, with a mean temperature of 18.7°C (SD ± 3.3). The pond rearing program finished at the time when the final ten days of pond water temperatures had a mean of 22.8°C.

Table 1. Basic water parameters measured on the day of harvesting in the pond and in the three stocking stretches (28 June) the day before release. The fish (European grayling, *Thymallus thymallus*) gradually acclimatized over 24 h to the water temperature of ~17°C.

Site	Dissolved O_2 [$mg \cdot L^{-1}$]	pH	Temperature [°C]
Pond	9.51	8.03	24.3
Chvalšinský	8.60	8.05	17.7
Blanice	9.40	7.72	17.2
Zlatý	9.02	7.65	16.2

After approximately six weeks of rearing, 5400 grayling fry had survived in the pond out of the initial 20 000 stocked fry, with a survival rate of 27%. The mean standard length of the fry was 5.43 ± 0.34 cm (n = 100, mean ± SD), with a mean weight of 2.2 ± 0.39 g, and the mean Fulton's condition factor ($K = 100 \times (W \cdot L^{-3})$) of 0.82 ± 0.07. We translocated the fry into a tank where mass-marking was performed using ARS. The chosen methodology for marking the 0+ fish (Halačka et al. 2018) was a one-hour free-swimming session in an aerated dilution of ARS 150 $mg \cdot L^{-1}$. The next day (29 June), fish were divided into three equal groups (3 × 1800 fry) and driven (~30 min) in aerated tanks filled with water at temperatures that matched the selected natural streams. No fish mortality was observed after either the mass-marking or transportation. The fish were released at the upstream-most location of the selected stretches of river.

Stocking sites. All three chosen stocking sites are natural, free-flowing water bodies with no artificial flow regulation upstream from the release sites (Fig. 1). Their discharge regimes are largely determined by rainfall dynamics and subsequent runoffs. Besides the typical cold-water species, a considerable number of thermophilic species in the Chvalšinský and Zlatý streams originated from the upstream inflow of nearby ponds or, in the case of Blanice, had migrated upstream from the Husinec Reservoir.

The river Blanice is the most important right-hand tributary of the Otava, which it joins at the village of Putimi at river km 32.28. The total length of the Blanice River is 94.73 km and it has a catchment area of 861.91 km^2. The stretch in which the graylings were stocked is located approximately 1 km upstream from the reservoir inflow point at river km 60 (37 ha; 2.5×10^6 m^3). The stocking stretch has a steeper gradient and higher velocity than the other localities used in this study. It is 170 m long, with a mean width of 10.5 m (9–12 m) and depths in the range of 20–80 cm. The study site lies at an altitude of 570 m above sea level (GPS: 49.0334836°N, 13.9645994°E) and has a mean annual flow of 1.8 $m^3 \cdot s^{-1}$. The Blanice River runs through a mountain range surrounded by tall coniferous forests, while the deciduous trees and bushes form a riparian buffer along the stream. The riverbed is rich with large rocks that help form numerous pockets or pools—hence the local name of this stretch of the Blanice as "pocket water"—and the remaining bottom materials are pebbles and gravel, which also form the banks.

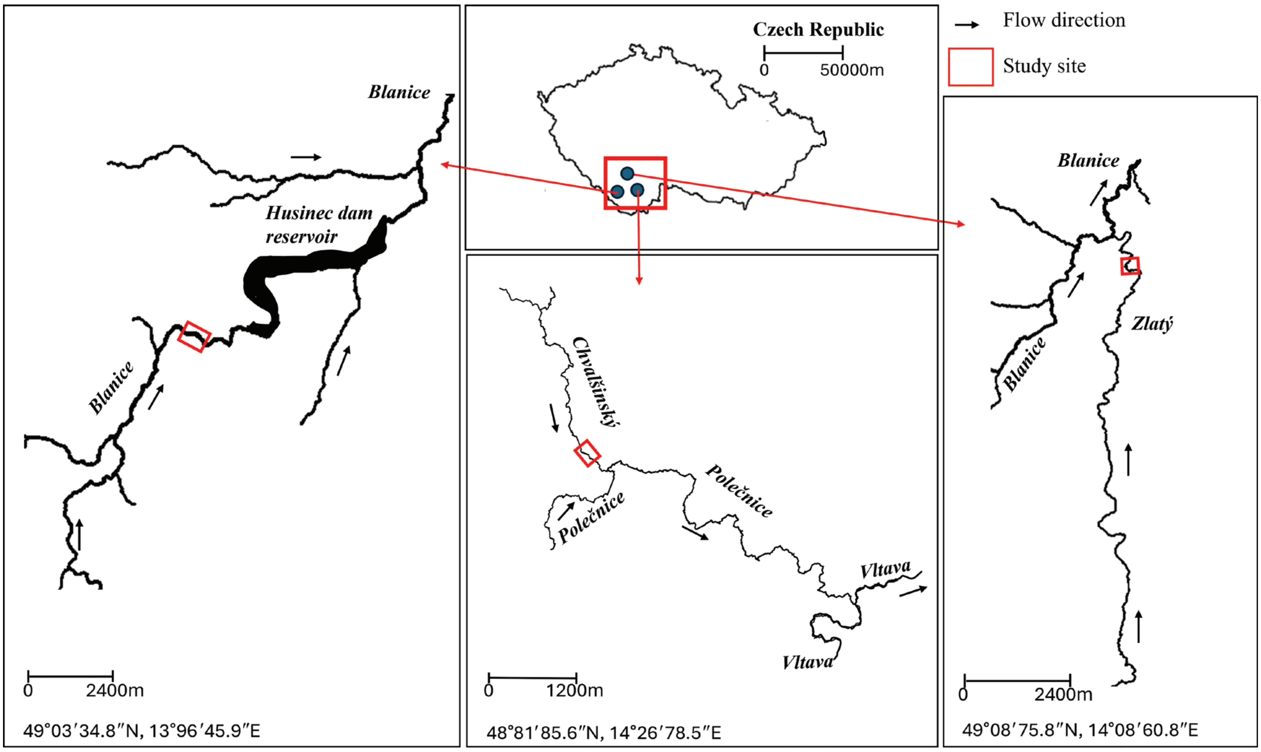

Figure 1. Release sites of European grayling, *Thymallus thymallus*, in three streams: Blanice, Chvalšinský, and Zlatý in the Czech Republic.

Chvalšinský potok (Polečnice) is a river in the Český Krumlov district, a left-bank tributary of the Vltava River. Its total length is 32.8 km and has a catchment area of 197.9 km^2. Grayling were released into a section of the river located below Kájov village, approximately 5.5 km upstream from where it joins the Vltava (GPS: 48.8185678°N, 14.2678514°E). This stocking stretch is a typical riffle-and-pool type stream, with a mean annual flow of 1.1 m^3 · s^{-1}. This sequence is repeated along the stream and there are fast rapids along narrow stretches with larger stones, followed by sections of long, deep, and calm pools with a sand and gravel streambed. The stretch length is 180 m, with a mean width of 3.5 m (2–5 m) and depths in the range of 10–100 cm. The site is at an altitude of 519 m above sea level. Generally, the banks are moderately steep, although some stretches have one steep eroded bank with a flat opposite bank formed from gravel and sand deposition (sand bar). Upstream from the study site, there is a small village whose wastewater probably increases the risk of eutrophication. The study site is surrounded by deciduous forest and cultivated meadows, and along the stream, the riparian vegetation has formed well-developed canopy cover.

The Zlatý stream is the longest tributary of the river Blanice in South Bohemia, into which it flows at river km 41. The total length of this stream is 36.7 km and it has a catchment area of 92.3 km^2. The section where the grayling were stocked is located near the village of Šipoun, 3 km upstream from the confluence with the river Blanice (GPS: 49.0875896°N, 14.0860800°E). Relatively deep pools, weak rapids, and shallow gradients characterize the chosen stretch of this stream. The length of the chosen stretch is 200 m, with a mean width of 2.25 m (1.5–3 m) and depths in the range of 10–160 cm. The streambed is sandy to gravelly, with a layer of clay deposits in places, and a slow current. The mean annual flow here is 0.51 m^3 · s^{-1}. It flows through a plain with meadows forming meanders and has a well-developed riparian vegetation dominated by willows of various ages. The low dense canopy is tunnel-like in some parts since the root systems extend into the stream and provide shelter for fish. The site is at an altitude of 445 m above sea level. It is distinguished from the previous two streams by its steeper banks, as well as by its considerable clay deposits and higher turbidity. The high discharge does not seem to have any significant impact on the width of this stream.

The fish communities vary between stretches (Fig. 2) but have in common brown trout, *Salmo trutta* Linnaeus, 1758, as the dominant salmonid species. Beside EG and brown trout, other fish species present at the release sites were: brook trout, *Salvelinus fontinalis* (Mitchill, 1814); perch, *Perca fluviatilis* Linnaeus, 1758; chub, *Squalius cephalus* (Linnaeus, 1758); dace, *Leuciscus leuciscus* (Linnaeus, 1758); roach, *Rutilus rutilus* (Linnaeus, 1758); bullhead, *Cottus gobio* Linnaeus, 1758; common carp, *Cyprinus carpio* Linnaeus, 1758; stone loach, *Barbatula barbatula* (Linnaeus, 1758); stone moroko, *Pseudorasbora parva* (Temminck et Schlegel, 1846); gudgeon, *Gobio gobio* (Linnaeus, 1758); burbot, *Lota lota* (Linnaeus, 1758); Eurasian minnow, *Phoxinus phoxinus* (Linnaeus, 1758); pikeperch, *Sander lucioperca* (Linnaeus, 1758); and river lamprey, *Lampetra fluviatilis* (Linnaeus, 1758). Lastly, it is important to note that otters and herons prey heavily on fish stocks in these stretches, and predation pressure from larger fish, especially brown trout, can be assumed to occur also.

Sampling. On 28 June 2021, the fish populations along chosen stretches (150 m) of selected natural streams were monitored via an electrofishing survey to provide data about the composition of fish communities. We performed single-pass electrofishing by using two back-pack generators with pulsed-DC (FEG 1500, EFKO-Germany) and other standard equipment for electrofishing. Also, two additional back-pack pulsed-DC electrofishing units (FEG 3000, EFKO-Germany) were placed at the upper border of each site to prevent fish from escaping upstream. The depth of the studied stretches varied, and we used corresponding cathode lengths of 100–150 cm, while the anode hope diameter was 30 cm. The streams' conductivities were within the range of 140–260 µS · cm^{-1}. The setting parameters of generators entirely corresponded to the character and conductivity of the monitored streams.

The post-stocking electrofishing survey was performed in the stocking stretches approximately 3.5 months (105 days) after stocking (11 October 2021). We used the same electrofishing method and equipment as we used for pre-stocking monitoring. The composition of the fish communities was monitored in the same stretches as before stocking took place. Additionally, we monitored 300 m of the river downstream from the stocking site to detect the displacement of stocked fish. The detection of ARS fluorescent marks on the fins of all caught grayling juveniles was checked by using laser pointers (green, ʎ = 532 nm, 50 mW, www.eclipsera.cz) and laser protection glasses (ʎ = 190–540 nm, www.eclipsera.cz). For continuous measuring of the stream temperature at 30-min intervals, we used dataloggers (Minikin Tie, Ø = 20 mm, www.emsbrno.cz) installed close to the banks from 29 June to 11 October 2021. During this period, we collected data relating to the daily discharge levels of stocked streams from the Czech Hydrometeorological Institute (CHMI). The weight and length of all collected fish were measured; temperature data loggers were removed from the water and their data extracted.

Data analysis. For the purposed of this study, we designed the site-specific discharge severity index (D_s) to reflect the discharge severity observed in particular streams during the monitoring period (Suppl. material 1: fig. S1). This index was calculated based on discharge components, the number of peak occurrences, the peak magnitude, and stream slope (Suppl. material 1: tables S1–S4). The equation below represents the final step of D_s calculation by summing site-specific weighted conditions (WC_i)

$$D_s = \sum \mathrm{WC}_i$$

A higher D_s number reveals the existence of a more severe discharge; regime; the resulting D_s values were used

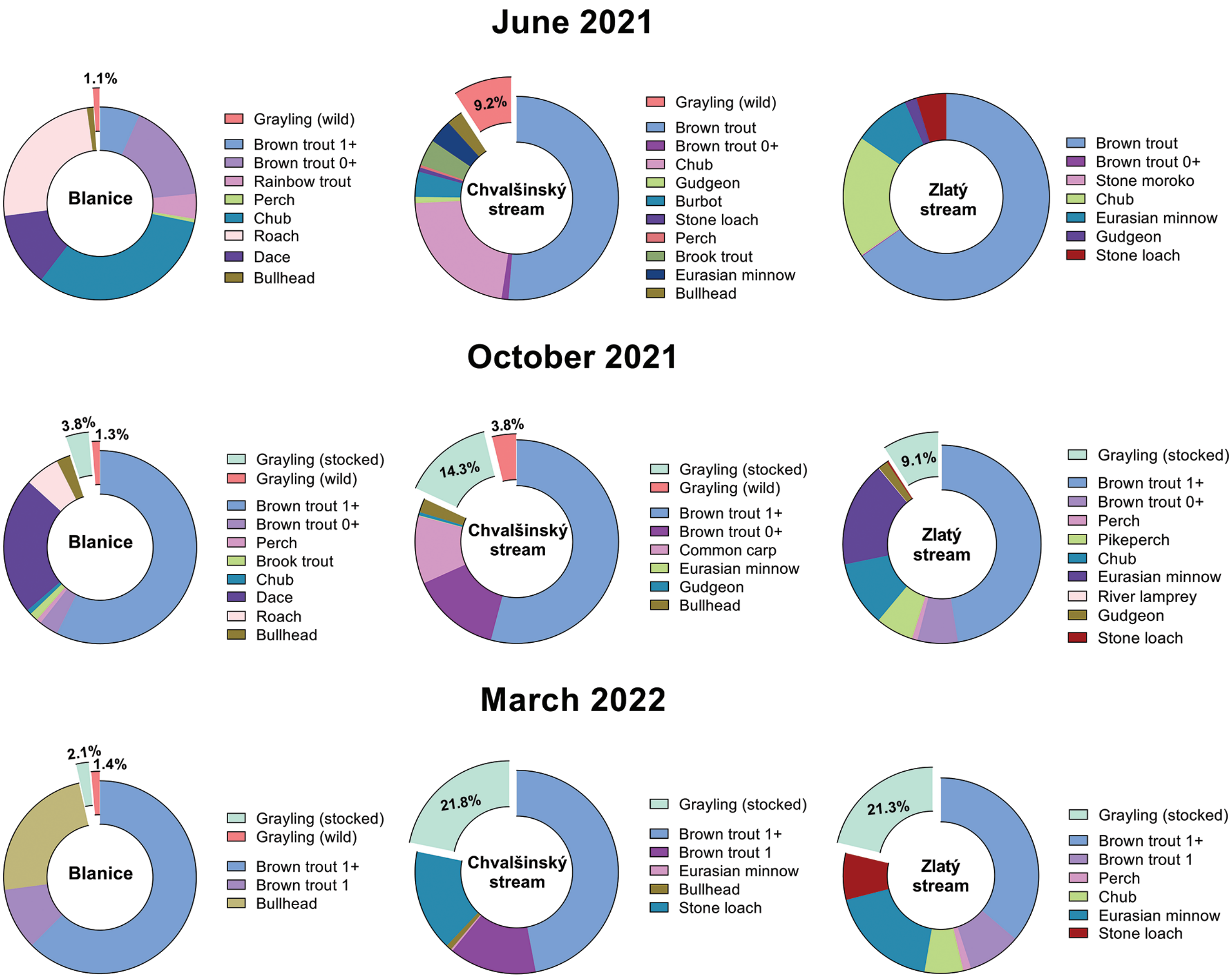

Figure 2. The changes in fish communities at the stocking sites after the three electrofishing monitoring sessions in three streams in the Czech Republic. Values represent biomass [$g \cdot m^{-2}$] expressed in percentages. The pie graphs depict the fish communities recorded in June prior to stocking (top), in October at the end of the growing season (middle), and as overwintering communities in March (bottom).

subsequently in the principal component analysis (PCA). By summing all the measured points extracted from temperature dataloggers, we calculated the time exposure (in hours) of stocked fry to temperatures (range 4–21°C) during the whole of the experiment (Suppl. material 1: fig. S2). We calculated the diel temperature amplitude (T_a) of every stream to compare differences between the maximum and minimum diel temperature values throughout the monitoring period. We recorded the total recapture rates which includes fish recaptured 3.5 months after stocking, both at the release site and within 300 m downstream in the river, relative to the total number stocked. Then, site fidelity of stocked fish, which relates to the fish being recaptured at the initial release site at the end of the growing seasons (October) and in the period from October to spring (March). We also calculated displacement by comparing the number of fish recaptured at a site versus fish recaptured in a 300-m downstream section. Lastly, we calculated overwinter recapture rate refers to fish recaptured at the release site after the winter (March), compared to those detected in same place in a previous electrofishing event (October).

The statistical analysis was performed with the software GraphPad Prism (version 9.5.0). A chi-squared test was used to assess differences in total recapture rates, site fidelity, displacement, and overwintering between the three stocked stretches by looking at stocked grayling recapture rates. A one-way ANOVA followed by a post-hoc Tukey's test was used to assess the differences between the three stocking groups taking into account measured biometric parameters (length, weight, and condition factor) and also for differences in temperature amplitude levels. The three datasets of measured stream temperatures did not pass the D'Agostino-Pearson (omnibus K2) normality test so we used the Kruskal–Wallis non-parametric test with Dunn's multiple comparisons test to assess the differences in temperature between the three sites. Accepted significant differences for values were $P < 0.05$. A cluster analysis (PCA) was conducted using the seven variables to demonstrate the relation between the stocking sites. The variables originating from the monitoring conducted in October used in the PCA were recapture (RC), standard length (SL), condition factor (K), displacement (DP), mean temperature (T_m), discharge severity index (D_s), and diel temperature amplitude (T_a).

Ethical statement. This study was conducted following the ethical guidelines of the Czech Republic and received approval from the relevant ethics committee. The treatment and welfare of fish fully adhered to the legal requirements in the Czech Republic (§ 7 Law No. 114/1992 on The Protection of Nature and Landscape and § 6, 7, 9, and 10 Regulation No. 419/2012 on the Care, Breeding, and Use of Experimental Animals).

Results

The electrofishing survey conducted in October revealed differences in site fidelity and displacement between streams when looking at recapture rates of stocked grayling (Table 2). In March, recapture rates decreased from October at every site and varied between streams.

The tested standard lengths and weights increased significantly from the initial state up to October, with both parameters for the Chvalšinský stream group being significantly higher than the groups from the other two streams (Table 3). The significant standard length and weight increase is presented in Fig. 3. The comparisons of condition factors in the recaptured autumn group, showed increased values for Chvalšinský ($P < 0.001$) and Zlatý stream ($P < 0,032$), while the K value significantly decreased in the Blanice fish group ($P < 0.001$). The recaptured group of Chvalšinský exhibited higher K values compared to both Blanice ($P < 0.001$) and Zlatý ($P < 0.001$) groups.

High discharge events mainly occurred in the first month after stocking (Suppl. material 1: fig. S1). The mean discharge was 0.74 $m^3 \cdot s^{-1}$ (SD ± 0.59) for Chvalšinský, 1.35 $m^3 \cdot s^{-1}$ (SD ± 1.02) for Blanice and 0.28 $m^3 \cdot s^{-1}$ (SD ± 0.25) for Zlatý stream, with calculated discharge severity indices (D_s) of 36.4, 47.0 and 17.5, respectively (Suppl. material 1: tables S–S4). Low discharge levels did not last for long during the monitoring period. Comparing the timing of discharge peaks and corresponding stream temperature, we found no signs of thermal discharge peaking or any connection between discharge peak events and alterations in water temperature.

The analyzed stream temperatures (Kruskal–Wallis, Dunn's post-test) revealed that the Blanice stream was the coldest (mean ± SD, 13.9 ± 2.6°C, $P < 0.001$), followed by Chvalšinský (14.1 ± 2.4°C) and Zlatý (14.5 ± 2.5°C). We found that Blanice had a significantly greater diel temperature amplitude (± 2.8°C) than the other two sites. The same comparisons revealed no significant differences between Chvalšinský (± 2.0°C) and Zlatý (± 1.9°C); additionally, Chvalšinský had a narrower temperature range than the other two (Suppl. material 1: fig. S2).

The PCA depicts the cluster separation of recaptured grayling 3.5 months after stocking. We selected the first two principal components (PCs) based on Kaiser's rule (<1 eigenvalue), which described 82.81% of the variance. PC1 described 54.28% and PC2 28.53%. Loadings for principal components show the correlation between the variables and PCs (Table 4). The variables located on the same side of the plot are positively correlated with each other but negatively correlated with variables on the opposite side of the plot. The variables DP, T_a, and D_s with negative loadings are all strongly associated with PC1, but are only very weakly-to-moderately correlated with PC2. Their high negative loadings are significant contributors to PC1 and place them close to the Blanice cluster, which underlines the high values of these variables in the Blanice recapture group. T_m is positioned close to the Zlatý stream cluster and strongly negatively correlates with DP. Conversely, variables SL and RC have high negative loadings and contribute strongly to PC2. They are positioned close to the Chvalšinský stream group, revealing the high values for this cluster. Lastly, the variable T_a shows a strong negative correlation with K, while D_s exhibits a negative correlation with K, albeit to a slightly lesser extent.

Table 2. Total recapture rates, site fidelity, displacement rates, and overwinter recapture rates of stocked advanced fry of the European grayling, *Thymallus thymallus*, in three streams in the Czech Republic.

Stream	Total number of fish stocked	Total recapture rate [%]	Site fidelity [%]	Displacement rate [%]	Overwinter recapture rate [%]
Chvalšinský	1800	4.2^a	3.7^a	13.2^a	13.6^a
Blanice	1800	2.5^b	1.7^b	33.3^b	6.7^b
Zlatý	1800	1.5^c	1.3^b	14.8^c	78.0^b

Superscript letters following the values represent statistical differences between recaptured groups (Chi-square test, $P < 0.05$).

Table 3. Complete biometric data of recaptured stocked fry of the European grayling, *Thymallus thymallus*, in three streams in the Czech Republic, obtained in October 2021 at stocking sites 3.5 months after stocking (autumn recapture) and, in 300 m of the river downstream from the stocking site (displacement), and at the stocking sites in March for overwintering monitoring (March recapture).

Stocking site	Site recapture				Displacement				Overwintering			
	n	SL [cm]	*W* [g]	*K*	*n*	SL [cm]	*W* [g]	*K*	*n*	SL [cm]	*W* [g]	*K*
Chvalšinský	66	13.7 ± 1.0^a	34.5 ± 0.8^a	0.89 ± 0.09^a	10	11.95 ± 0.67	24.6 ± 3.5	1.39 ± 0.03	9	15.18 ± 0.35	48.6 ± 3.3	0.93 ± 0.07
Blanice	30	11.5 ± 0.6^b	19.1 ± 0.6^b	0.78 ± 0.07^b	15	10.58 ± 0.17	14.9 ± 0.7	1.25 ± 0.02	2	12.23 ± 0.64	22.4 ± 3.1	0.78 ± 0.07
Zlatý	23	11.4 ± 0.7^b	20.5 ± 0.8^b	0.82 ± 0.05^b	4	11.30 ± 0.25	17.5 ± 1.4	1.21 ± 0.07	18	13.58 ± 0.29	33.3 ± 2.1	0.86 ± 0.07

n = number of fish, SL = standard length, *W* = weight, *K* = condition factor. The values are mean ± standard deviation); superscript letters following the values represent statistical differences between recaptured groups (Tukey post-hoc test, $P < 0.05$).

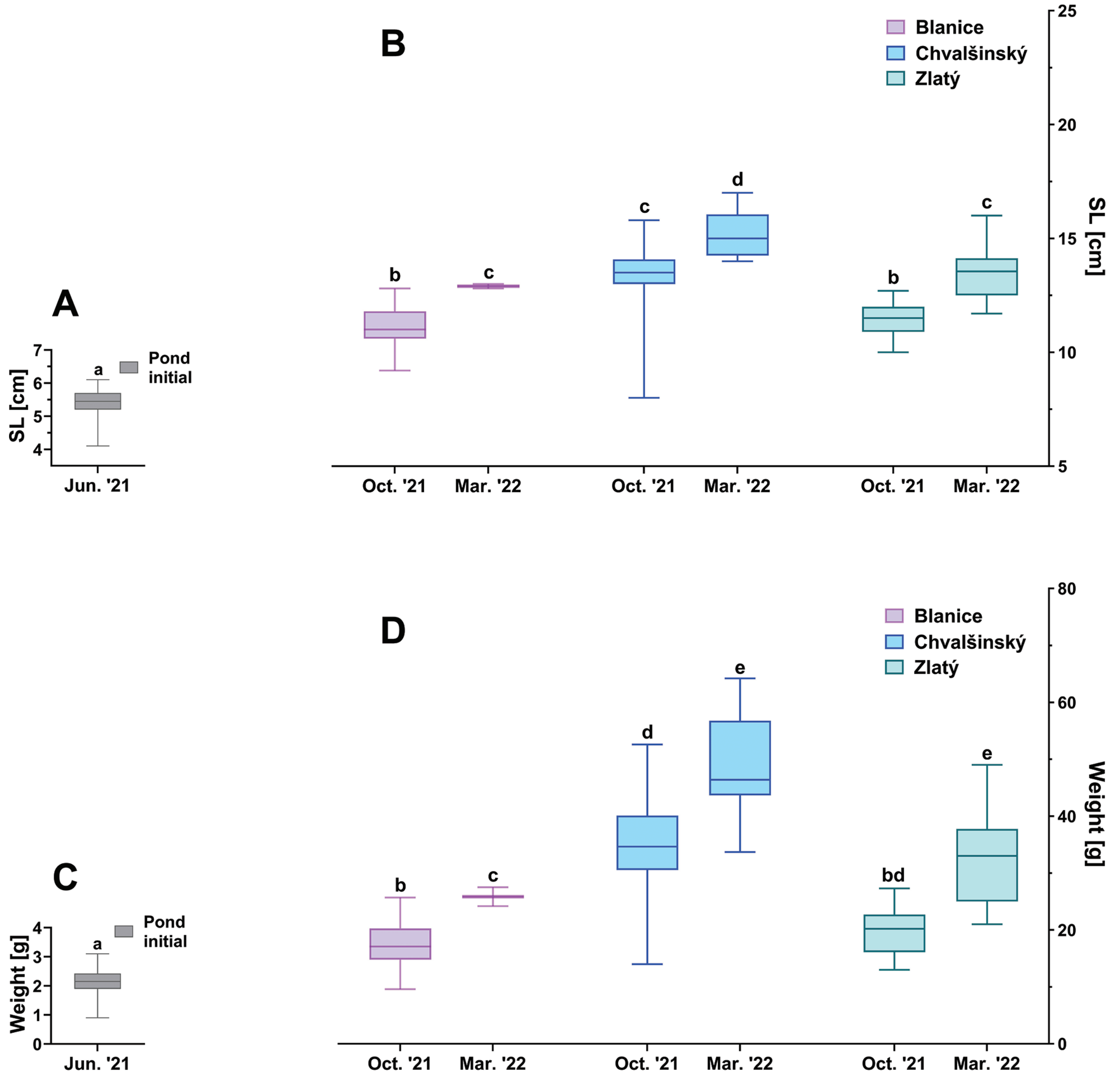

Figure 3. Significant standard length and weight growth in stocked European grayling, *Thymallus thymallus*, from their pre-stocking state (**A**, **C**) in June (2021) and after recapture events (**B**, **D**) in three streams in the Czech Republic in October (2021) and March (2022).

Discussion

The summer mass-stocking performed with advanced fry European grayling notably strengthened the wild grayling population at all three stocked sites. Recorded post-release biomasses 3.5 months after release and after the first winter (Fig. 2) demonstrated an increased presence of EG in each stream. Advanced fry exhibited a substantial increase in weight and length, which varied between the stocked streams, thus reflecting the differences in their habitats. In this study, ARS was justified as a reliable medium for successfully marking young fish stages (Hühn et al. 2014) and a non-invasive detection method (Turek et al. 2024). It was successfully applied for the first time on 0+ EG and fulfilled the needs of the monitoring restocking program for quick ARS trace identification on tail-fin rays, thereby ensuring continuous workflow in the field.

Table 4. The obtained loadings of the variables used in the cluster analysis.

Variable	PC1	PC2
T_a	–0.89	0.42
T_m	0.97	0.24
DP	–1.00	–0.07
RC	–0.13	–0.94
SL	0.22	–0.84
K	0.24	–0.35
D_s	–0.98	–0.21

T_a = diel amplitude in water temperature, T_m = mean temperature, DP = displacement, RC = recapture, SL = standard length, K = condition factor, D_s = discharge severity index.

The increase in pond water temperature (~23°C) signaled the end of the rearing program because, in salmonids at this temperature, growth is halted (Crisp 1996;

Hartman and Jensen 2017) and approaches to the sublethal temperatures which depresses feeding rates (Meeuwig et al. 2004). In pond conditions, temperature-induced mortality along with disease in EG can occur at 17.2°C (Carlstein 1993). However, in the warmer pond water, we detected a good final survivability (27%) followed by the high condition factor of fry fed on zooplankton (Table 1). It confirms that EG fry are tolerant to a steady temperature increase in rearing conditions (Szmyt et al. 2013). The additional advantage of high temperatures in the pond is that they are thought to contribute to the uprising of a critical thermal maximum in grayling (Lohr et al. 1996), thus preventing temperature-induced mortality in the wild.

Post-stocking biometric parameters recorded after 3.5 months suggest satisfactory adaptation by stocked fry (Table 2), with the only drop in K compared to the initial state occurring in the Blanice group. This confirms the adaptive potential of the 0+ age category after being fed on natural food (Carlstein 1997; Czerniawski 2015). Recaptured fish exhibited rapid growth after stocking in all three stretches, with more than a twofold increase in standard length during the growing season in their natural habitat. This growth pattern closely resembles the developmental dynamics observed in young, wild conspecifics (Persat and Pattee 1981). Therefore, we conclude that recaptured survivors were able to utilize the favorable stream conditions during the growing season, as shown by their mean length that exceeded even that of intensively tank-reared 0+ EG harvested during the same period (Carlstein 1993).

Our results show that extended exposure to colder water leads to reduced biometrics (Blanice fish group), while warmer streams provide longer growth-favorable temperatures and better biometrics. We conceived the timing of the stocking to coincide with the growth-favorable conditions in summer including high prey abundance for grayling (Thorfve and Carlstein 1998) and higher water temperatures (Deegan et al. 1999; Mallet et al. 1999; Marsh et al. 2022). Accordingly, in July at the beginning of the adaptation to the riverine environment 0+ grayling faced little dietary overlap with 0+ brown trout (Degerman et al. 2000). Therefore, the timing was probably suitable for preventing poor nutrition and starvation, which could cause exhaustion and subsequent mortality amongst the stocked fish (Bachman 1984). Cold water can be a stronger growth-limiting factor in juvenile salmonids than limitations on feeding (Nicieza and Metcalfe 1997). However, colder water can significantly decrease feeding efficiency in reared grayling at 5°C (Watz et al. 2014). Additionally, this stretch of Blanice is further from sources of fertilizers—which could lead to smaller prey organisms (Deegan et al. 1999)—than the two other streams that are near upstream towns (Chvalšinský) or agricultural fields (Zlatý). Conversely, there were also no growth-limiting temperature ranges in the Chvalšinský stream during the growing season, as reflected in the higher biometrics at this site (Table 3).

Recorded displacement in downstream stretches also varied and was strongly associated with the severity of natural discharge regimes, cold water, and the high diel temperature amplitude (Fig. 4). Stocked fry recaptured at Blanice experienced the highest D_s index, with one flood-like event during the growing season (Fig. 4) that led to the highest level of displacement. This confirmed the inability of 0+ grayling to withstand this kind of impact and resulted in increased drift (Auer et al. 2023) as occurs in other young salmonids (Jowett and Richardson 1989; Hayes et al. 2010; Warren et al. 2015). Accordingly, the domestication of salmonids can induce pronounced morphological changes in body shape as a response to the environment (Pulcini et al. 2013; Bajić et al. 2018) and reduce swimming abilities (Reinbold et al. 2009). Therefore, it is not reasonable to expect high post-release site fidelity of 0+ stocked grayling in steep streams with demanding natural discharge. These conditions also imply higher energy demands (Heggenes and Traaen 1988) and reduce the growth in 0+ EG (Marsh et al. 2022), which might explain the low biometry in the Blanice stocked group compared to the two other groups.

We did not find any clear natural discharge thermal peaking patterns at the study sites. However, we showed that the most pronounced disappearance of 0+ grayling up to March occurred in the coldest stocking stream (Blanice), which had the highest diel T_a and $D_{s.}$ In addition, the Blanice site was the shallowest and the disappearance could have been prompted by a lack of thermally stratified deep pools, whose presence is important for juvenile salmonids (Nielsen et al. 1994). Coupled with the high diel T_a, this lack of pools may have forced fish to seek appropriate thermal habitats (Fausch and Bramblett 1991; Hartman and Jensen 2017), resulting in higher displacement. The same deeper pools could provide refuge for the fry, creating microhabitats with lower water velocity (Fausch and Bramblett 1991).

The lowest total recapture rate during the growing season was at Zlatý, which was characterized by the highest mean temperatures. Even so, based on the literature these temperature ranges cannot be regarded as either sublethal or lethal. However, they may have caused a steep decrease in juvenile European grayling recruitment (Charles et al. 2006), which could explain our results. This site had the lowest D_s, and stranding was supposed not to be pronounced in streams with steeper banks (Tuhtan et al. 2012). The disappearance from the release site on the Zlatý was more likely driven by strong density-dependent displacement due to the small habitat capacity that would have reduced competition. It is known that intraspecific density affects 0+ EG recruitment (Bašić et al. 2018), while habitat spatial limitation is thought to lead to displacement caused by population self-thinning (Hayes et al. 2010). An additional aspect could be the presence of the well-developed riparian canopy along this stretch, which might negatively affect the survival of small grayling during the growing season (Marsh et al. 2021).

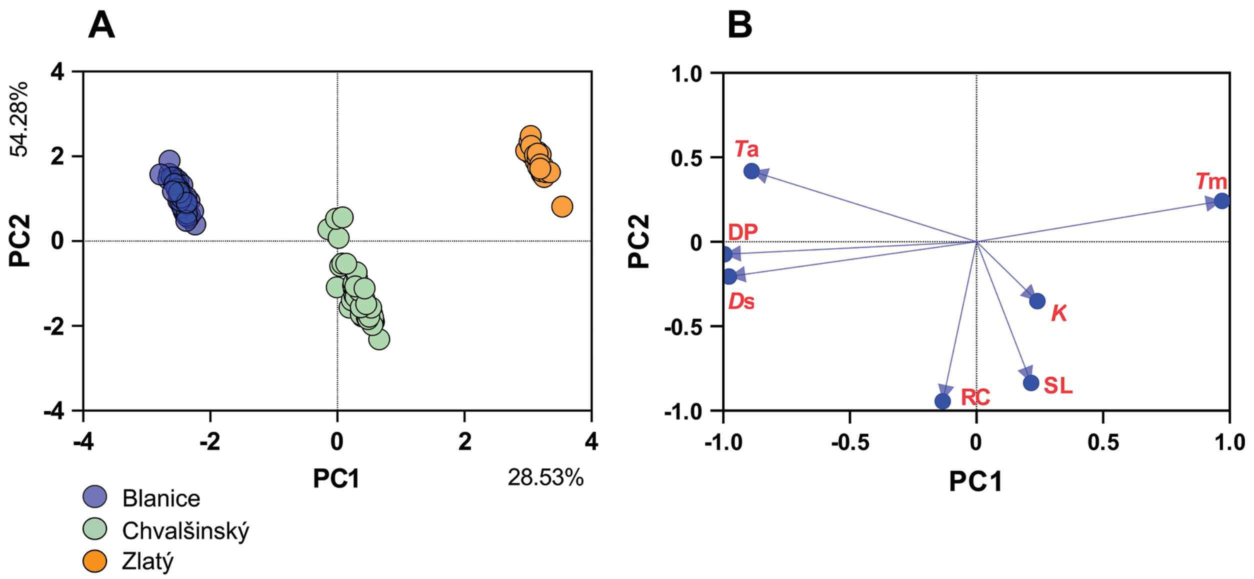

Figure 4. PCA score (**A**) and loading (**B**) plots of European grayling, *Thymallus thymallus*, in three streams in the Czech Republic. On the scores plot, individual fish are represented by a single dot. Explanation of variables: RC = number of recaptured fish 3.5 months after stocking at the stocking site; SL = standard length; K = condition factor; D_s = discharge severity index; DP = number of fish recaptured in the downstream stretch; T_m = mean temperature for the monitored period; T_a = the level of diel variation between maximal and minimal temperature values.

Our study provides evidence that the first winter creates strong selective pressure on fish communities and can significantly reduce fish biomasses (Suppl. material 1: tables S5–S7). In our study it increased the disappearance of 0+ stocked grayling, especially at Blanice (autumn/spring = 30/2), thereby confirming the high magnitude of overwintering loss in young stocked salmonids (Biro et al. 2021). Despite this, the proportion of stocked grayling fry at the release sites did substantially increase in comparison with autumn in two of the streams, Chvalšinský and Zlatý. Furthermore, recaptured fish in October to March significantly grew (SL) at every site (Table 3), confirming that autumn and winter still can provide growth-supportive conditions for grayling 0+, although not nearly as much as reported for 1+ and 2+ grayling (Marsh et al. 2022). The highest biometrics in the Chvalšinský group did not correspond with high overwinter recapture (winter loss 86%), which implies that local habitat characteristics can dictate the extent of overwinter mortality (Hurst 2007). It seems that the thick canopy of riparian vegetation at Zlatý and its submerged parts favored both overwinter survival and site fidelity in this site (78%). This implies that such streams could serve as valuable refuges for the desirable long-term adaptation of stocked grayling fry over the first winter and, potentially, at the start of the growing season these individuals can be longitudinally translocated within the water body.

In this stocking region, where fish predators are abundant and winter freezing affects ponds, predation is crucial in determining mortality in small streams. Accordingly, herons can be attracted by increased densities after stocking and become the main fish predators in shallow water habitats (Miyamoto et al. 2017). Given that reared salmonids suffer from heron predation (Petersson and Järvi 2006), the availability of appropriate shelters such as riparian canopy trees and submerged vegetation may have mitigated the impact of this type of predation.

In this stocking experiment, advanced grayling fry (5–6 cm) were released in the middle of the growing season to ensure appropriate stocking size and timing, reducing post-stocking losses. It was shown that this length of grayling fry has already demonstrated enhanced swimming abilities that allows better habitat use than the smaller conspecifics (Bardonnet et al. 1991). Conversely, using younger grayling fry, such as sac fry (2–2.5 cm), for stocking could make them vulnerable to unfavorable discharges (Poff et al. 1997; Auer et al. 2017) and lead to massive post-stocking displacement (Valentin et al. 1994).

Release sites with heterogeneous habitats, rich in-stream shelters, and thermal and flood refuge zones were considered to ensure the viability of stocked grayling. Evidently, stretches with steep gradients with frequent flood-like discharges should be avoided as stocking sites for 0+ grayling, with careful consideration of stocking size being crucial, given their significant impact on population abundances (Jowett and Richardson 1989; Hayes et al. 2010) and even lead to subsequent local extinctions (Warren et al. 2015). In the hydropeaking rivers that negatively impact 0+ grayling (Auer et al. 2017), our results imply that effective stocking actions should be performed farther from hydropower plants due to hydropeaking events whose effects tend to decrease downstream (Greimel et al. 2018). Finally, the stocking outcomes for grayling fry depend on stochastic natural events, which implies the need for stocking actions to be repeated to match the most favorable seasonal conditions and support their recruitment.

Besides serving as an example of how stocking practices can be evaluated, this study could be a starting point in enlightening the reasons behind the stocking failures with EG. We suggest further research to focus on the seasonal comparison between post-stocked grayling and wild conspecifics, e.g. their growth and survival rates, age of maturation, and reproduction potential (Rulifson and Laney 1999), to direct future management actions.

Conclusion

This stocking program study describes a perspective approach for the long-term enhancement of wild European grayling populations. The rearing technique was suitable for rearing large numbers of grayling fry with good adaptability to the wild environment. For identifying young EG, we recommend using ARS as a non-invasive detection procedure, particularly when assessing restocking programs aimed at conserving endangered species.

Acknowledgments

The research was supported by the Ministry of Education, Youth and Sports of the Czech Republic under the project PROFISH (CZ.02.1.01/0.0/0.0/16_019/0000869) and by the Ministry of Agriculture of the Czech Republic – project of National Agency for Agricultural Research (NAZV) No. QK23020064.

References

Auer S, Zeiringer B, Führer S, Tonolla D, Schmutz S (2017) Effects of river bank heterogeneity and time of day on drift and stranding of juvenile European grayling (*Thymallus thymallus* L.) caused by hydropeaking. Science of the Total Environment 575: 1515–1521. https://doi.org/10.1016/j.scitotenv.2016.10.029

Auer S, Hayes DS, Führer S, Zeiringer B, Schmutz S (2023) Effects of cold and warm thermopeaking on drift and stranding of juvenile European grayling (*Thymallus thymallus*). River Research and Applications 39(3): 401–411. https://doi.org/10.1002/rra.4077

Avramović M, Turek J, Tomčala A, Mráz J, Bláha M, Let M, Szmyt M, Randák T (2024) Assessing the acclimatisation to the wild of stocked European graylings *Thymallus thymallus* by monitoring lipid dynamics and food consumption. Knowledge and Management of Aquatic Ecosystems 2024(425): e10. https://doi.org/10.1051/kmae/2024008

Bachman RA (1984) Foraging behavior of free-ranging wild and hatchery brown trout in a stream. Transactions of the American Fisheries Society 113(1): 1–32. https://doi.org/10.1577/1548-8659(1984)113<1:FBOFWA>2.0.CO;2

Bajić A, Jojić V, Snoj A, Miljanović B, Askeyev O, Askeyev I, Marić S (2018) Comparative body shape variation of the European grayling *Thymallus thymallus* (Actinopterygii, Salmonidae) from wild populations and hatcheries. Zoologischer Anzeiger 272: 73–80. https://doi.org/10.1016/j.jcz.2017.12.005

Bardonnet A, Gaudin P, Persat H (1991) Microhabitats and diel downstream migration of young grayling (*Thymallus thymallus* L.). Freshwater Biology 26: 365–376. https://doi.org/10.1111/j.1365-2427.1991.tb01404.x

Bašić T, Britton JR, Cove RJ, Ibbotson AT, Gregory SD (2018) Roles of discharge and temperature in recruitment of a cold-water fish, the European grayling *Thymallus thymallus*, near its southern range limit. Ecology Freshwater Fish 27(4): 940–951. https://doi.org/10.1111/eff.12405

Beauregard D, Enders E, Boisclair D (2013) Consequences of circadian fluctuations in water temperature on the standard metabolic rate of Atlantic salmon parr (*Salmo salar*). Canadian Journal of Fisheries and Aquatic Sciences 70(7): 1072–1081. https://doi.org/10.1139/cjfas-2012-0342

Biro PA, Post JR, Beckmann C (2021) Autumn lipid reserves, overwinter lipid depletion, and high winter mortality of rainbow trout in experimental lakes. Canadian Journal of Fisheries and Aquatic Sciences 78(6): 738–743. https://doi.org/10.1139/cjfas-2020-0276

Brignone S, De Santis V, Putelli T, Molina C, Piccinini A, Carmichael RA, Volta P (2022) What's the effectiveness of stocking actions in small creeks? The role of water discharge behind hatchery trout downstream movement. PeerJ 10: e14069. https://doi.org/10.7717/peerj.14069

Carlstein M (1993) Natural food and artificial, dry starter diets: Effects on growth and survival in intensively reared European grayling. Aquaculture International 1(2): 112–123. https://doi.org/10.1007/BF00692615

Carlstein M (1997) Effects of rearing technique and fish size on post-stocking feeding, growth and survival of European grayling, *Thymallus thymallus* (L.). Fisheries Management and Ecology 4(5): 391–404. https://doi.org/10.1046/j.1365-2400.1997.00068.x

Charles S, Mallet J-P, Persat H (2006) Population dynamics of grayling: Modelling temperature and discharge effects. Mathematical Modelling of Natural Phenomena 1(1): 31–48. https://doi.org/10.1051/mmnp:2006002

Crisp DT (1996) Environmental requirements of common riverine European salmonid fish species in fresh water with particular reference to physical and chemical aspects. Hydrobiologia 323(3): 201–221. https://doi.org/10.1007/BF00007847

Czerniawski R, Domagala J, Krepski T, Pilecka-Rapacz M (2015) The effect of the live diet given to hatchery-reared fry of the European grayling (*Thymallus thymallus*) on their survival and growth in the wild. Turkish Journal of Fisheries and Aquatic Sciences 15(3): 633–638. https://doi.org/10.4194/1303-2712-v15_3_07

Deegan LA, Golden HE, Harvey CJ, Peterson BJ (1999) Influence of environmental variability on the growth of age-0 and adult Arctic grayling. Transactions of the American Fisheries Society 128(6): 1163–1175. https://doi.org/10.1577/1548-8659(1999)128<1163:IOEVOT>2.0.CO;2

Degerman E, Näslund I, Sers B (2000) Stream habitat use and diet of juvenile (0+) brown trout and grayling in sympatry. Ecology Freshwater Fish 9(4): 191–201. https://doi.org/10.1111/j.1600-0633.2000.eff090401.x

Enders EC, Stickler M, Pennell CJ, Cote D, Alfredsen K, Scruton DA (2008) Variations in distribution and mobility of Atlantic salmon parr during winter in a small, steep river. Hydrobiologia 609(1): 37–44. https://doi.org/10.1007/s10750-008-9401-5

Fausch KD, Bramblett RG (1991) Disturbance and fish communities in intermittent tributaries of a western great plains river. Copeia 1991(3): 659–674. https://doi.org/10.2307/1446392

Fraser D, Weir L, Bernatchez L, Hansen MM, Taylor EB (2011) Extent and scale of local adaptation in salmonid fishes: review and meta-analysis. Heredity 106: 404–420. https://doi.org/10.1038/hdy.2010.167

Greimel F, Schülting L, Graf W, Bondar-Kunze E, Auer S, Zeiringer B, Hauer C (2018) Hydropeaking impacts and mitigation. Pp. 91–110. In: Schmutz S, Sendzimir J (Eds.) Riverine ecosystem management: Science for governing towards a sustainable future. Springer International Publishing, Cham, Switzerland. https://doi.org/10.1007/978-3-319-73250-3_5

Halačka K, Poštulková E, Kopp R, Mareš J, Vetešník L (2018) Možnosti značení vysazovaných ryb pomocí ARS – aplikace a detekce. Pp. 37–43. In: Kopp R, Mareš J, Grmela J (Eds.) Účelové rybí obsádky na vodárenských nádržích. Brno, Czech Republic, 11 October 2018.

Hartman KJ, Jensen OP (2017) Anticipating climate change impacts on Mongolian salmonids: Bioenergetics models for lenok and Baikal grayling. Ecology Freshwater Fish 26(3): 383–396. https://doi.org/10.1111/eff.12282

Hayes JW, Olsen DA, Hay J (2010) The influence of natural variation in discharge on juvenile brown trout population dynamics in a nursery tributary of the Motueka River, New Zealand. New Zealand Journal of Marine and Freshwater Research 44(4): 247–269. https://doi.org/10.1080/00288330.2010.509905

Hayes HDS, Lautsch E, Unfer G, Greimel F, Zeiringer B, Höller N, Schmutz S (2021) Response of European grayling, *Thymallus thymallus*, to multiple stressors in hydropeaking rivers. Journal of Environmental Management 292: 112737. https://doi.org/10.1016/j.jenvman.2021.112737

Heggenes J, Traaen T (1988) Downstream migration and critical water velocities in stream channels for fry of four salmonid species. Journal of Fish Biology 32(5): 717–727. https://doi.org/10.1111/j.1095-8649.1988.tb05412.x

Horká P, Horký P, Randák T, Turek J, Rylková K, Slavík O (2015) Radio-telemetry shows differences in the behaviour of wild and hatchery-reared European grayling *Thymallus thymallus* in response to environmental variables. Journal of Fish Biology 86(2): 544–557. https://doi.org/10.1111/jfb.12575

Hühn D, Lübke K, Skov C, Arlinghaus R (2014) Natural recruitment, density-dependent juvenile survival, and the potential for additive effects of stock enhancement: An experimental evaluation of stocking northern pike (*Esox lucius*) fry. Canadian Journal of Fisheries and Aquatic Sciences 71(10): 1508–1519. https://doi.org/10.1139/cjfas-2013-0636

Hurst TP (2007) Causes and consequences of winter mortality in fishes. Journal of Fish Biology 71(2): 315–345. https://doi.org/10.1111/j.1095-8649.2007.01596.x

Janković D (1964) Synopsis of biological data on European grayling (*Thymallus thymallus* (Linnaeus) 1758). FAO Fisheries Synopsis, No. 24, F1. FAO, Rome, 50 pp.

Jepsen N, Ravn HD, Pedersen S (2018) Change of foraging behavior of cormorants and the effect on river fish. Hydrobiologia 820(1): 189–199. https://doi.org/10.1007/s10750-018-3656-2

Jowett IG, Richardson J (1989) Effects of a severe flood on instream habitat and trout populations in seven New Zealand rivers. New Zealand Journal of Marine and Freshwater Research 23(1): 11–17. https://doi.org/10.1080/00288330.1989.9516335

Lohr SC, Byorth PA, Kaya CM, Dwyer WP (1996) High-temperature tolerances of fluvial Arctic grayling and comparisons with summer river temperatures of the big Hole River, Montana. Transactions of the American Fisheries Society 125(6): 933–939. https://doi.org/10.1577/1548-8659(1996)125<0933:HTTOFA>2.3.CO;2

Lorenzen K (2005) Population dynamics and potential of fisheries stock enhancement: Practical theory for assessment and policy analysis. Philosophical Transactions of the Royal Society of London, Series B, Biological Sciences 360(1453): 171–189. https://doi.org/10.1098/rstb.2004.1570

Lorenzen K, Camp EV (2019) Density-dependence in the life history of fishes: When is a fish recruited? Fisheries Research 217: 5–10. https://doi.org/10.1016/j.fishres.2018.09.024

Luczynski M, Zaporowski RR, Golonka JS (1986) Rearing of European grayling, *Thymallus thymallus* L., larvae using dry and live food. Aquaculture Research 17(4): 275–280. https://doi.org/10.1111/j.1365-2109.1986.tb00114.x

Malcolm IA, Soulsby C, Hannah DM, Bacon PJ, Youngson AF, Tetzlaff D (2008) The influence of riparian woodland on stream temperatures: Implications for the performance of juvenile salmonids. Hydrological Processes 22(7): 968–979. https://doi.org/10.1002/hyp.6996

Mallet JP, Charles S, Persat H, Auger P (1999) Growth modelling in accordance with daily water temperature in European grayling (*Thymallus thymallus* L.). Canadian Journal of Fisheries and Aquatic Sciences 56(6): 994–1000. https://doi.org/10.1139/f99-031

Marsh JE, Cove RJ, Britton JR, Wellard RG, House A, Gregory SD (2021) Medium-term environmental changes influence age-specific survival estimates in a salmonid population. Freshwater Biology 66(8): 1530–1545. https://doi.org/10.1111/fwb.13736

Marsh JE, Cove RJ, Britton JR, Wellard RG, Bašić T, Gregory SD (2022) Density-dependence and environmental variability have stage-specific influences on European grayling growth. Oecologia 199(1): 103–117. https://doi.org/10.1007/s00442-022-05163-2

Meeuwig MH, Dunham JB, Hayes JP, Vinyard GL (2004) Effects of constant and cyclical thermal regimes on growth and feeding of juvenile cutthroat trout of variable sizes. Ecology Freshwater Fish 13(3): 208–216. https://doi.org/10.1111/j.1600-0633.2004.00052.x

Miyamoto K, Squires TE, Araki H (2017) Predation of stocked masu salmon (*Oncorhynchus masou*) by riparian wildlife. Canadian Journal of Fisheries and Aquatic Sciences 14: 127472. https://doi.org/10.1101/127472

Nicieza AG, Metcalfe NB (1997) Growth compensation in juvenile Atlantic salmon: Responses to depressed temperature and food availability. Ecology 78(8): 2385–2400. https://doi.org/10.1890/0012-9658(1997)078[2385:GCIJAS]2.0.CO;2

Nielsen JL, Lisle TE, Ozaki V (1994) Thermally stratified pools and their use by steelhead in northern California streams. Transactions of the American Fisheries Society 123(4): 613–626. https://doi.org/10.1577/1548-8659(1994)123<0613:TSPATU>2.3.CO;2

Northcote TG (1995) Comparative biology and management of Arctic and European grayling (Salmonidae, *Thymallus*). Reviews in Fish Biology and Fisheries 5(2): 141–194. https://doi.org/10.1007/BF00179755

Persat H, Pattee E (1981) The growth rate of young grayling in some French rivers. SIL Proceedings, 1922–2010 21: 1270–1275. https://doi.org/10.1080/03680770.1980.11897171

Petersson E, Järvi T (2006) Anti-predator response in wild and sea-ranched brown trout and their crosses. Aquaculture 253(1–4): 218–228. https://doi.org/10.1016/j.aquaculture.2005.08.012

Poff N, Allan JD, Bain M, Karr J, Prestegaard K, Richter B, Sparks R, Stromberg J (1997) The Natural Flow Regime. Bioscience 47(11): 769–784. https://doi.org/10.2307/1313099

Pulcini D, Wheeler PA, Cataudella S, Russo T, Thorgaard GH (2013) Domestication shapes morphology in rainbow trout *Oncorhynchus mykiss*. Journal of Fish Biology 82(2): 390–407. https://doi.org/10.1111/jfb.12002

Reinbold D, Thorgaard GH, Carter PA (2009) Reduced swimming performance and increased growth in domesticated rainbow trout, *Oncorhynchus mykiss*. Canadian Journal of Fisheries and Aquatic Sciences 66(7): 1025–1032. https://doi.org/10.1139/F09-064

Rulifson R, Laney W (1999) Striped bass stocking programs in the United States: Ecological and resource management issues. Canadian Stock Assessment Secretariat, Research Document 99/007. Fisheries and Oceans Canada, Ottawa.

Szmyt M, Goryczko K, Grudniewska J, Lejk A, Wisniewska A, Woźniak M (2013) Preliminary results of European grayling (*Thymallus thymallus* L.) fry rearing to the autumn fingerlings stage. Polish Journal of Natural Sciences 28: 471–483.

Thorfve S (2002) Impacts of in-stream acclimatization in post-stocking behaviour of European grayling in a Swedish stream. Fisheries Management and Ecology 9(5): 253–260. https://doi.org/10.1046/j.1365-2400.2002.00305.x

Thorfve S, Carlstein M (1998) Post-stocking behaviour of hatchery-reared European grayling, *Thymallus thymallus* (L.), and brown trout, *Salmo trutta* L., in a semi-natural stream. Fisheries Management and Ecology 5(2): 147–159. https://doi.org/10.1046/j.1365-2400.1998.00087.x

Tuhtan JA, Noack M, Wieprecht S (2012) Estimating stranding risk due to hydropeaking for juvenile European grayling considering river morphology. KSCE Journal of Civil Engineering 16(2): 197–206. https://doi.org/10.1007/s12205-012-0002-5

Turek J, Horký P, Zlábek V, Velisek J, Slavik O, Randák T (2012) Recapture and condition of pond-reared, and hatchery-reared 1+ European grayling stocked in addition to wild conspecifics in a small river. Knowledge and Management of Aquatic Ecosystems 405(405): 10. https://doi.org/10.1051/kmae/2012016

Turek J, Zlábek V, Velíšek J, Lepič P, Červený D, Randák T (2018) Influence of geographic origin on post-stocking survival and condition of European grayling (*Thymallus thymallus*) in a small river. Aquatic Living Resources 31: 29. https://doi.org/10.1051/alr/2018019

Turek J, Lepic P, Bořík A, Galicová P, Nováková P, Avramović M, Randák T (2024) Evaluation of large-scale marking with alizarin red S in different age rainbow trout fry for nonlethal field identification. Acta Ichthyologica et Piscatoria 54: 43–48. https://doi.org/10.3897/aiep.54.117547

Valentin S, Sempeski P, Souchon Y, Gaudin P (1994) Short-term habitat use by young grayling (*Thymallus thymallus* L.) under variable flow conditions in an experimental stream. Fisheries Management and Ecology 1: 57–65. https://doi.org/10.1111/j.1365-2400.1970.tb00006.x

Waples RS, Ford MJ, Schmitt D (2007) Chapter 21; Empirical results of salmon supplementation in the northeast Pacific: A preliminary assessment. Pp. 383–403 In: Bert TM (Ed.) Ecological and genetic implications of aquaculture activities. Vol 6. Methods and Technologies in Fish Biology and Fisheries, Springer, Dordrecht, Netherlands. https://doi.org/10.1007/978-1-4020-6148-6_21

Warren M, Dunbar MJ, Smith C (2015) River flow as a determinant of salmonid distribution and abundance: A review. Environmental Biology of Fishes 98(6): 1695–1717. https://doi.org/10.1007/s10641-015-0376-6

Watz J (2017) Overwintering behaviour of stocked brown trout: effects of the rearing environment and river habitat complexity. In: 50th Anniversary Symposium of the Fisheries Society of the British Isles, 3–7 July 2017, University of Exeter, UK. http://urn.kb.se/resolve?urn=urn:nbn:se:kau:diva-65010

Watz J, Bergman E, Piccolo J, Greenberg L (2014) Prey capture rates of two species of salmonids (*Salmo trutta* and *Thymallus thymallus*) in an artificial stream: Effects of temperature on their functional response. Marine and Freshwater Behaviour and Physiology 47(2): 93–99. https://doi.org/10.1080/10236244.2014.900210

Supplementary material 1

Calculation of the discharge data in order to descrbie the hydrological conditions of three analyzed streams

Authors: Mladen Avramović, Jan Turek, Pavel Lepič, Mariusz Szmyt, Jan Pastejřík, Tomáš Randák

Data type: docx

Explanation note: **table S1.** The overview of discharge levels of monitored stretches with the frequency of detected discharge peaks placed according to their discharge magnitude. The discharge peaks classification starts with two-fold and finishes on the six-fold increase from mean discharge. **table S2.** Discharge conditions of monitored stocking stretches. **table S3.** Slope coefficients of monitored stretches. **tables S4.** The final calculation of the discharge severity indices (D_s) represented by total values for every stream. **table S5.** Fish community data recorded during three recapture events on the Blanice river. **table S6.** Fish community data recorded during three recapture events on the Chvalšinský stream. **table S7.** Fish community data recorded during three recapture events on the Zlatý stream. **fig. S1.** Recorded discharge dynamics of the three stocking stretches after the fish release on 29 June 2021 until recapture on 11 October 2021. Measurements obtained from the nearest CHMI monitoring stations. **fig. S2.** Duration of exposure of stocked European grayling fry in the three studied streams to the observed temperature ranges from 29 June to 11 October 2021.

Link: https://doi.org/10.3897/aiep.54.124289.suppl1

Acta Ichthyologica et Piscatoria 54, 2024, 177–187 | DOI 10.3897/aiep.54.121328

PENSOFT.

ACTA
ICHTHYOLOGICA
ET PISCATORIA

A new loach species of the genus *Vanmanenia* (Actinopterygii: Cypriniformes: Gastromyzontidae) from hill streams of Vietnam

Huong Thi Thanh DANG[1], Huyen Thi DUONG[1], Fan LI[2], Huy Quang NGUYEN[1], Hau Duc TRAN[1,3]

1 *Faculty of Biology, Hanoi National University of Education, Hanoi, Vietnam*
2 *Shanghai Natural History Museum, Branch of Shanghai Science and Technology Museum, Shanghai, China*
3 *Institute of Natural Science (INS), Hanoi National University of Education, Hanoi, Vietnam*

https://zoobank.org/2E462FD3-3959-4CB1-AF59-A61389442EC3

Corresponding authors: Hau Duc Tran (hautd@hnue.edu.vn); Huy Quang Nguyen (huynqbio.hnue@gmail.com)

Academic editor: Jan Kotusz ♦ **Received** 14 March 2024 ♦ **Accepted** 28 May 2024 ♦ **Published** 9 August 2024

Citation: Dang HTT, Duong HT, Li F, Nguyen HQ, Tran HD (2024) A new loach species of the genus *Vanmanenia* (Actinopterygii: Cypriniformes: Gastromyzontidae) from hill streams of Vietnam. Acta Ichthyologica et Piscatoria 54: 177–187. https://doi.org/10.3897/aiep.54.121328

Abstract

Recent ichthyofauna surveys in Phia Oac-Phia Den National Park, Vietnam, yielded 16 specimens of loach representing the genus *Vanmanenia*. These specimens were uniform in morphology and distinct from known species, leading to the designation of a new species, *Vanmanenia duci* **sp. nov.** This species is distinguished from congeners by the following combination of characters: pectoral fin: I, 15; pelvic fin: I, 8; lateral line scales 77–83; the distance from the anus to the posterior insertion of the pelvic fin being greater than from the anus to the anal fin origin; a lateral black stripe from the gill opening to the caudal fin base; a black spot at the caudal fin origin equal to the eye diameter; and a lower lip with three large papillae, with the middle one being larger. The new species differs from *Vanmanenia caldwelli* (Nichols, 1925) by its mouth soft-tissue structures and lower morphometric values and from *Vanmanenia ventrosquamata* (Mai, 1978) and *Vanmanenia caobangensis* Nguyen, 2005 by having more lateral line scales and lower body depth. Additionally, *Vanmanenia duci* **sp. nov.** has a larger eye and wider interorbital space compared to other species in Vietnam. This species is found in the Red River basin in Vietnam and the Bang Giang River flowing into China, indicating high potential for freshwater fish diversity in these river systems.

Keywords

Bang Giang River, Gam River, new species, northern Vietnam, taxonomy, *Vanmanenia*

Introduction

The genus *Vanmanenia* Hora, 1932, commonly known as hillstream loaches represents the family Gastromyzontidae, currently accommodates 24 species (Fricke et al. 2023). Some of its species were formerly assigned to *Homalosoma* Boulenger, 1901 (see Silas 1953). A total of 22 species can be found in southern China and Vietnam, i.e., *Vanmanenia caldwelli* (Nichols, 1925); *Vanmanenia caobangensis* Nguyen, 2005; *Vanmanenia gymnetrus* Chen, 1980; *Vanmanenia hainanensis* Chen et Zheng, 1980; *Vanmanenia homalocephala* Zhang et Zhao, 2000; *Vanmanenia lineata* (Fang, 1935); *Vanmanenia maculata* Yi, Zhang & Shen, 2014; *Vanmanenia microcephala* Li, Zhou et Che, 2019; *Vanmanenia microlepis* Nguyen, 2005; *Vanmanenia monofasciodorsala* Nguyen, 2005; *Vanmanenia multiloba* (Mai, 1978); *Vanmanenia nahangensis* Nguyen, 2005; *Vanmanenia pingchowensis*

(Fang, 1935); *Vanmanenia polylepis* Pan, Liu et Zhang, 1983; *Vanmanenia pseudostriata* Zhu, Zhao, Liu et Niu, 2019; *Vanmanenia serrilineata* Kottelat, 2000; *Vanmanenia stenosoma* (Boulenger, 1901); *Vanmanenia striata* Chen, 1980; *Vanmanenia tetraloba* (Mai, 1978); *Vanmanenia trifasciodorsala* Nguyen, 2005; *Vanmanenia ventrosquamata* (Mai, 1978); and *Vanmanenia xinyiensis* Zheng et Chen, 1980 (see Li et al. 2019; Deng and Zhang 2020, 2021; Cai et al. 2021), and eight species in Vietnam (Nguyen 2005). Species in this genus prefer living in the fast-flowing waters of mountain brooks of China, Laos, and Vietnam (Yue et al. 2000; Yi et al. 2014). Thus, they could be diverse in the upper reaches of large rivers in northern Vietnam, such as the Red River and the Bang Giang River. In fact, of eight species recorded in northern Vietnam, seven are distributed in the Red River, i.e., *V. microlepis* , *V. monofasciodorsala*; *V. multiloba*, *V. nahangensis*, *V. tetraloba*, *V. trifasciodorsala*, and *V. ventrosquamata* (see Nguyen et al. 2019) and two species from the Bang Giang River in Cao Bang Province, i.e., *V. ventrosquamata* and *V. caobangensis* (see Nguyen 2005; Deng and Zhang 2020) (Fig. 1).

During the first surveys of the ichthyofauna in in Phia Oac-Phia Den National Park, Cao Bang Province, northern Vietnam (Fig. 2) in 2020 and 2021, 16 specimens of *Vanmanenia* were collected. Details of their external morphology indicated that all of them were one species, and they did not conform to any of the hitherto known species of the genus *Vanmanenia*. Therefore, we decided to describe these specimens as a new species, *Vanmanenia duci* sp. nov. and provide a differential diagnosis to distinguish it from all its congeners.

Materials and methods

Two fieldwork surveys were carried out in May 2020 and May 2021 in Phia Oac-Phia Den National Park, Nguyen Binh District, Cao Bang Province, northern Vietnam. In this area, there are two different river basin systems, including the Gam River, one of the largest tributaries of the Red River, and the Bang Giang River, known as the Zuo River in China, an upper tributary of the Yu River in southern China (Pearl River basin) (Figs. 1, 2). Fish samples were collected by a hand net and by electro-fishing within 30 min per sampling site under the permission of local authorities. From these surveys, a total of 16 specimens of loach representing the genus *Vanmanenia* was collected at stations DO.02 in the Gam River, DO.05, and DO.07 in the Bang Giang River (Fig. 2). Fish were fixed in 10% formalin solution, and subsequently preserved in 70% ethanol in the Museum of Biology, Hanoi National University of Education. Measurements and counts followed by Yi et al. (2014) and were taken from the left side of each specimen. Measurements were made point-to-point, to the nearest 0.1 mm using calipers, and expressed as a percentage.

Comparative material. *Vanmanenia caldwelli*: SOU 201807801, 5 specimens, 30.15–62.13 mm SL; China: Fujian Province: Fuqing City; Min River; 7 July 2018.

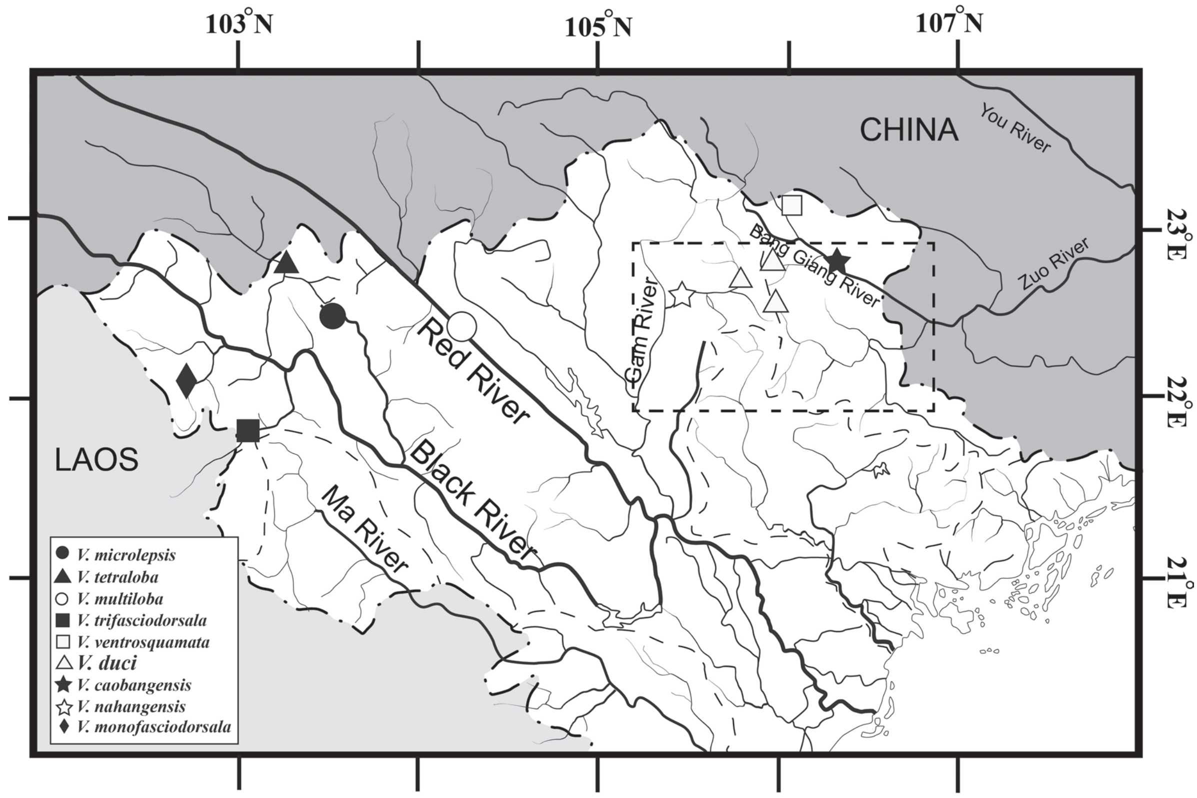

Figure 1. Distribution of species of the genus *Vanmanenia* in northern Vietnam.

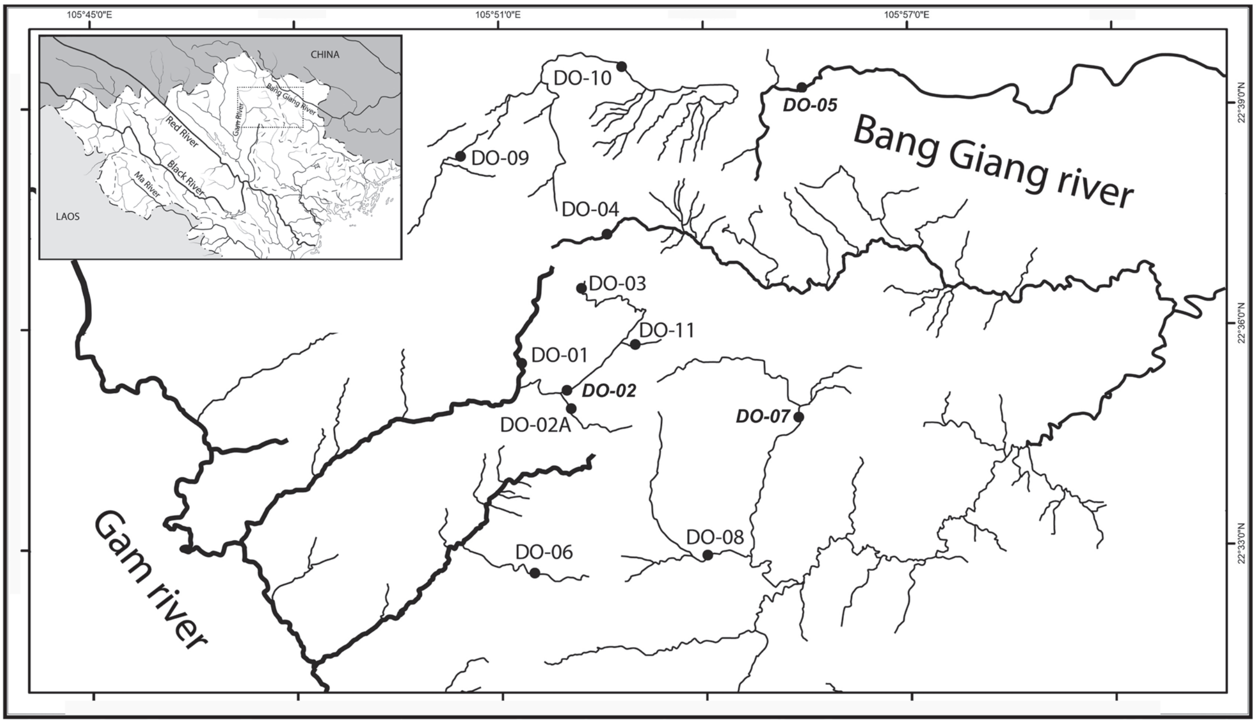

Figure 2. Sampling sites of *Vanmanenia duci* sp. nov. in Phia Oac-Phia Den National Park, Cao Bang Province, northern Vietnam.

Results

Taxonomy

Family Gastromyzontidae
Genus *Vanmanenia* Hora, 1932

Vanmanenia duci sp. nov.

https://zoobank.org/D50DDA23-9C06-4915-88D7-F5258F4F017E
Figs. 3, 4, Table 1

Type locality. Vietnam, Cao Bang Province, Nguyen Binh District, Bang Giang River basin, 20°34′731″N, 105°55′407″E.

Holotype. HNUE-F00293, 47.6 mm SL, Vietnam, Cao Bang Province, Nguyen Binh District, Bang Giang River basin, 20°34′731″N, 105°55′407″E, ca. 760 m above sea level, 24 May 2020, coll. H.D. Tran, V.S. Ngo, and H.V. Pham; electro-fishing, medium speed current stream with stone and gravel bottom, both the sides fringed by plants.

Paratypes (*n* = 15). HNUE-F00294-296, 3 ex., 33.0–50.1 mm SL, data same as for holotype. HNUE-F00297-298, 2 ex., 35.8–39.4 mm SL, same locality as for holotype, 8 May 2021, coll. H.D. Tran, V.S. Ngo, H.Q. Nguyen, N.T. Nguyen, and A.N.T. Do. HNUE-F00299-303, 5 ex., 32.4–52.1 mm SL, Vietnam, Cao Bang Province, Nguyen Binh District, Gam River, 22°35′197″N, 105°51′903″E, 1005 m above sea, 21 May 2020, coll. H.D. Tran, V.S. Ngo, and H.V. Pham; electro-fishing and hand net, fast speed current stream with large stone and sandy bottom, both the sides fringed by plants. HNUE-F00304-305, 2 ex., 48.3–54.0 mm SL, same locality as for HNUE-F00299, 7 May 2021, coll. H.D. Tran, V.S. Ngo, H.Q. Nguyen, N.T. Nguyen, and A.N.T. Do. HNUE-F00306, 1 ex., 41.3 mm SL, 8 May 2021, other data same as for HNUE-F00303. HNUE-F00307-308, 2 ex., 39.1–40.3 mm SL, Vietnam: Cao Bang Province, Nguyen Binh District, Bang Giang River basin, 22°39′289″N, 105°55′339″E, 500 m above sea, 22 May 2020, coll. H.D. Tran, V.S. Ngo, and H.V. Pham; electro-fishing and hand net, fast speed current stream with gravel bottom.

Diagnosis. *Vanmanenia duci* sp. nov. can be distinguished from congeners by following combination of characters: pectoral fin rays: I, 15; pelvic fin rays: I, 8; lateral line scales: 77–83; anus farther posterior insertion of pelvic fin than to anal fin origin, caudal peduncle depth approximately as caudal peduncle length (8.2%–8.5%), distance from pelvic fin to pectoral fin (39.1%) larger than distance from pelvic fin to anal fin (29.8%). It has a broad midlateral black stripe running from behind head to caudal-peduncle base. Black dotted stripe stretching from base of pectoral fin to posterior end of anal fin. Lower lip with three large papillae; median wider than two lateral ones. Rostral fold divided into three triangular lobules of same size. Distinct black dot at base of pelvic and pectoral fins, and fleshy black protrusion in pelvic fin base.

Description. Meristic and morphometric data for type specimens are presented in Table 1. View of body and its mouth structures are shown in Figs. 3, 4, 5A. Body elongate, anteriorly depressed before dorsal-fin origin and posteriorly compressed laterally. Body width almost as wide as body depth. Dorsal profile of head and predorsal body slightly curved, and flat ventral profile. Moderate gill opening extending to ventral surface for short distance in front of pectoral fin base (Fig. 3).

Figure 3. *Vanmanenia duci* sp. nov., HNUE-F00293, SL = 47.6 mm in Phia Oac-Phia Den National Park, Cao Bang Province, northern Vietnam.

Head depressed, slightly longer than wide, and wider than deep. Snout broadly rounded in dorsal view and bluntly pointed in lateral view. Small eyes situated dorsolaterally in posterior half of head, with interorbital space bigger than eye diameter. Nostrils large, closer to eyes than to snout. Small fleshy papillae above top of head and edges of the eyes. Mouth inferior, medium-sized and curved, with muzzle grooves and muzzle folds in front. Snout groove wide and shallow, extending to corner of mouth (Fig. 3). Lips fleshy; upper lip covered with conspicuous papillae, and shallow groove present with rostral fold and, disconnected from lower lip at corners of mouth; lower lip with three large papillae, slightly tips curved, one median bigger than lateral two ones. Rostral fold divided into three triangular lobules same size, and two pairs of lobulated papillae between the folds, with inner side mastoid. Two pairs of rostral barbels, outer pair larger than inner pair, and about 1/2 of eye diameter (Fig. 5A). Body covered by small scales, present except on anterior pectoral fin to pelvic fin base, and on ventral surface in front of and between bases of pectoral fins. Lateral line complete and straight. No spine on dorsal fin, with 3 simple and 7 branched rays. Its origin anterior to pelvic fin origin, closer to caudal fin base than to tip of snout, and distal margin slightly straight. Two simple and 5 branched rays on anal fin, and its origin nearer to anus than to caudal fin base. One simple and 15 branched rays on pectoral fin, much longer than head length. Its base

Figure 4. Aquarium photograph of *Vanmanenia duci* sp. nov. (HNUE-F00293, 47.6 mm SL) from northern Vietnam.

Table 1. Morphometric and meristic data for examined materials of *Vanmanenia duci* sp. nov. from Phia Oac-Phia Den National Park, Vietnam.

Character	***Vanmanenia duci* sp. nov.**			
	Holotype	**Paratypes (*n* = 15)**		
		Mean	**SD**	**Range**
Absolute morphometric values [mm]				
Standard length (SL)	47.6	42.5	7.03	32.4–54.0
Relative morphometric values [% in SL]				
Body depth	16.4	15.6	0.02	12.2–18.7
Predorsal length	53.0	51.2	0.01	48.6–53.7
Prepelvic length	55.5	54.4	0.01	51.7–56.8
Preanal length	84.7	84.4	0.01	82.9–86.1
Pectoral-to pelvic-fin insertion	40.1	39.1	0.02	34.3–41.9
Pelvic-fin insertion to anal-fin origin (PFAF)	29.6	29.8	0.01	27.6–31.1
Pectoral-fin base length	10.1	9.5	0.01	7.1–10.7
Pelvic-fin base length	4.4	4.2	0.01	3.6–5.0
Dorsal-fin base length	13.5	11.6	0.01	9.9–13.6
Anal-fin base length	5.3	4.6	0.01	3.7–6.0
Anus to anal-fin origin	8.8	9.5	0.02	7.1–14.7
Caudal-peduncle length (CPL)	7.9	8.2	0.01	7.5–9.8
Caudal-peduncle depth	8.4	8.5	0.01	7.9–9.1
Pectoral-fin length	29.4	29.2	0.01	27.8–30.0
Pelvic-fin length	20.2	19.7	0.01	18.8–20.9
Anal-fin length	16.4	16.1	0.01	14.2–19.3
Dorsal-fin length	23.5	22.5	0.01	20.5–24.1
Head length (HL)	16.2	16.0	0.01	15.4–16.7
Relative morphometric values [% in CPL]				
Caudal-peduncle depth	106.7	102.8	0.04	92.5–111.1
Relative morphometric values [% in PFAF]				
Anus to anal-fin origin	12.7	13.8	0.03	10.4–21.0
Relative morphometric values [% in HL]				
Head depth	66.2	64.6	0.06	52.8–79.5
Snout length	58.4	65.6	0.04	59.2–72.5
Head width	83.8	82.6	0.04	75.5–88.5
Eye diameter	24.0	25.7	0.03	21.0–30.4
Interorbital width	54.6	56.0	0.02	52.8–61.5
Mouth width	20.1	21.9	0.02	18.9–26.5
Meristic data				
Dorsal-fin rays	III, 7	III, 7		
Pectoral-fin rays	I, 15	I, 15		
Pelvic-fin rays	I, 8	I, 8		
Anal-fin rays	II, 5	II, 5		
Lateral-line scales	83	77–83		

Values of Mean, SD, and Range do not include the holotype.

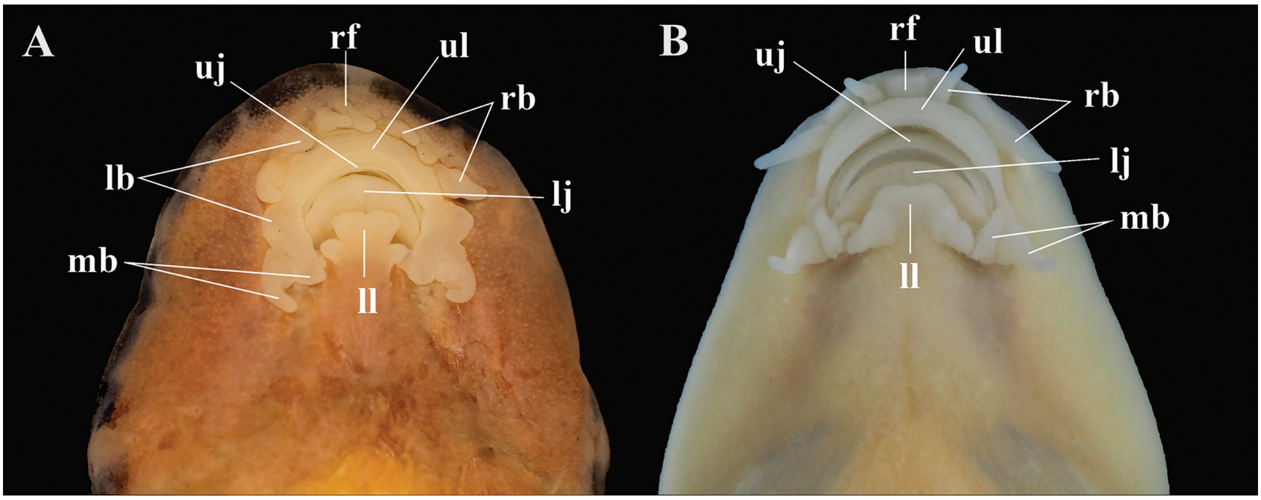

Figure 5. Mouth soft-tissue structures of two very similar species of *Vanmanenia* in Vietnam and China: (**A**) *Vanmanenia duci* sp. nov., HNUE-F00293, 47.6 mm SL, (**B**) *Vanmanenia caldwelli*, 62.1 mm SL (photo by Fan Li). Abbreviations: lj = lower jaw, mb = maxillary barbel, rb = rostral barbel, rf = rostral fold, uj = upper jaw, ul = upper lip, ll = lower lip, lb = lobulated papillae.

slightly behind lower extremity of eye, tip of adpressed fin not reaching pelvic-fin insertion. One simple and 8 branched rays on pelvic fin. Its origin closer to caudal fin base than to snout tip and tip of adpressed fin touching or exceeding anus, but far from anal fin origin. Anus positioned closer to anal fin origin than to base of pelvic fin. Caudal fin slightly concave, with lower lobe slightly longer than upper lobe.

Coloration (freshly collected). Body yellowish-brown; belly a pale ivory color (Figs. 3, 4). Head with small, irregular, black bars and blotches on cheeks and snout. Dorsum with eight or nine black blotches and irregular small blotches. Round black protrusions on pectoral and pelvic fin bases. One brown-black band across rays on dorsal fin, and two in caudal fin. Pectoral and pelvic fins pale yellow. Midlateral black stripe from behind head to caudal fin base. A brown-black dotted stripe along from pectoral-fin base to posterior insertion of the anal fin; caudal fin base with a black spot of eye size (Fig. 4).

Coloration (preserved). Specimens fixed in formalin solution with yellowish body and head; belly yellow. Black bars present on behind of head to caudal fin base. Black dotted stripes from posterior end of pectoral fin to anal fin. These fins pale whitish, with black bands across rays of dorsal and caudal fins (Fig. 3).

Distribution. *Vanmanenia duci* sp. nov. is known only from three localities in the Phia Oac-Phia Den National Park, Cao Bang Province, northern Vietnam (Fig. 2). Other species of *Vanmanenia* are distributed in different localities of the Red River and Bang Giang River.

Habitat and ecology. Figure 6 shows the three known localities of *Vanmanenia duci* sp. nov. The holotype was found in a narrow forests stream with medium speed current and gravel bottom (Fig. 6A). Co-occurring fish species included *Parazacco* sp. (Duong et al. 2022); *Liniparhomaloptera* cf. *qiongzhongensis* Zheng et Chen, 1980;

Figure 6. Habitat of *Vanmanenia duci* sp. nov., in the Gam River (DO.02) and Bang Giang River (DO.05, DO.07) in Phia Oac-Phia Den National Park, northern Vietnam.

Schistura sp.; *Carassius auratus* (Linnaeus, 1758); *Discogobio* sp., *Rhinogobius duospilus* (Herre, 1935) (see Nguyen et al. 2024). Several paratypes were found in a fast speed current forest stream with large stones and sand as bottom (Fig. 6B). This sampling site is next to the road, where a new bridge is under construction. There were several other fish species, including *Schistura* sp. (see Nguyen et al. 2024) and *Chimarrichthys nami* (Tran, Nguyen, Dang, Nguyen et Nguyen, 2023). At the third sampling site (Fig. 6C), accompanying fish species included *Beaufortia pingi* (Fang, 1930); *Schistura* spp.; *Barbodes semifasciolatus* (Günther, 1868); *Discogobio microstoma* (Mai, 1978); *Onychostoma gerlachi* (Peters, 1881); *Discogobio* spp.; *Hemibarbus* cf. *umbrifer* (Lin, 1931); and *Gambusia affinis* (Baird et Girard, 1853) (see Nguyen et al. 2024).

Etymology. The specific name is in honor of Vietnamese ichthyologist, Prof. Nguyen Huu Duc, who had spent his whole life studying freshwater fishes in Vietnam.

Discussion

Species group with black mid-lateral stripe. *Vanmanenia duci* sp. nov. differs from all other species of *Vanmanenia* except *V. caldwelli*, *V. lineata*, and *V. homalocephala* by having a broad black midlateral stripe on the body (vs. having bars or irregular blotches) (Figs. 3, 4, 7 in the presently reported study; fig. 278 in Yue et al. 2000; fig. 1 in Zhang and Zhao 2000). *Vanmanenia homalocephala* and *V. lineata* are distributed in Xi-Jiang of the Pearl River basin (Yue et al. 2000; Zhang and Zhao 2000; Deng and Zhang 2020). The new species could be distinguished from *V. lineata* by maxillary barbel and lower lip in the mouth (fig. 1 in Li et al. 2019; Fig. 5A in the presently reported study). *Vanmanenia homalocephala* and *Vanmanenia duci* sp. nov. could be distinguished by scales in lateral line (95–100 vs. 77–83) and color pattern on the back (5–6 vs. 19 dark saddle-backed stripes) (fig. 1 in Zhang and Zhao 2000; Fig. 3 in the presently reported study).

The last species having a black midlateral stripe on the body is *V. caldwelli*, which is distributed in Min-Jiang River (Deng and Zhang 2021), far from the study site. Both *V. caldwelli* and *Vanmanenia duci* sp. nov. share the same gross morphology (Table 2). However, values of the majority of the measurements of *Vanmanenia duci* sp. nov. are lower than the range of measurements of *V. caldwelli*, such as body depth (12.2%–18.7%), caudal-peduncle depth (7.9%–9.1%), or head length (15.4%–16.7%), although snout length and eye diameter of *Vanmanenia duci* sp. nov. are larger than those of *V. caldwelli* (59.2%–72.5%, 21.0%–30.4%; respectively) (Table 2). In addition, the distance from the anus to posterior end of pelvic fin is farther than the distance from the anus to anterior insertion of the anal fin (vs. closer). Both species have a longitudinal black stripe on the body (Figs. 3, 7), but the starting position of this stripe in the two species is different. It starts from the tip of the snout in *V. caldwelli* and just behind the head in *Vanmanenia duci* sp. nov. The mouth structure is

Table 2. Morphometric and meristic data for examined materials of *Vanmanenia duci* sp. nov. in Vietnam and its very similar species, *Vanmanenia caldwelli* in China.

Character	Species, locality, reference, and number of specimens						
	***Vanmanenia duci* sp. nov.**	***Vanmanenia caldwelli***					
	Gam and Bang Giang Rivers, Vietnam	**Min River, Fuqing City, China**	**Yenping, Chungan, Fukein, China**	**Min-Jiang basin, China**	**Yenping, Fukien, China**	**Min-Jiang basin at Chong'an, south China**	**Min-Jiang basin, China**
	This study	**This study**	**Silas 1953**	**Deng and Zhang 2020**	**Nichols 1925**	**Yi et al. 2014**	**Yue et al. 2000**
	***n* = 16**	***n* = 5**	***n* = 4**	***n* = 10**	***n* = 1**	***n* = 8**	***n* = 16**
Absolute morphometric values [mm]							
Standard length (SL)	32.4–54.0	30.2–62.1	—	40.7–56.4	48	49.3–70.5	41–72
Relative morphometric values [% in SL]							
Body depth	12.2–18.7	18.1–20.4	14.3–14.8	17.1–20.1	20	14.3–17.7	21.7–28.6
Predorsal length	48.6–53.7	51.9–55.3	—	50.9–53.3	—	50.1–52.2	50.0–52.6
Prepelvic length	51.7–56.8	55.2–59.5	—	55.0–60.7	—	52.2–57.1	52.6–55.6
Preanal length	82.9–86.1	80.6–84.2	—	80.9–87.8	—	80.8–85.5	—
Pectoral-to pelvic-fin insertion	34.3–41.9	33.9–39.2	—	37.1–42.8	—	36.6–41.2	—
Pelvic-fin insertion to anal-fin origin	27.6–31.1	24.4–27.6	—	24.6–28.4	—	24.8–27.9	—
Caudal-peduncle depth	7.9–9.1	10.3–13.4	—	9.1–11.2	—	9.2–10.2	10.0–11.0
Pectoral-fin length	27.8–30.0	19.8–22.9	—	22.4–26.7	—	22.9–26.2	—
Pelvic-fin length	18.8–20.9	15.2–20.0	—	19.1–23.4	—	18.9–20.9	—
Anal-fin length	14.2–19.3	16.0–18.1	—	16.6–19.7	—	15.9–19.4	—
Dorsal-fin length	20.5–24.1	21.2–22.8	—	19.8–24.9	—	22.4–25.0	—
Head length (HL)	15.4–16.7	18.6–20.7	20.0–21.1	20.5–22.6	21.7	18.4–20.6	16.7–18.9
Relative morphometric values [% in HL]							
Snout length	59.2–72.5	43.2–48.1	33.3–44.4	40.0–49.2	50.0	45.5–56.1	41.7–55.6
Eye diameter	21.0–30.4	20.5–27.8	19.1–23.5	24.9–30.7	20.0	19.3–24.7	16.7–22.2
Meristic data							
Dorsal-fin rays	III, 7	III, 8	III, 8	III, 7	10	III, 7	III, 7
Pectoral-fin rays	I, 15	I, 13	I, 13–14	I, 13	—	I, 13–15	I, 13–15
Pelvic-fin rays	I, 8	I, 8	I, 6–7	I, 8	—	I, 8	I, 8
Anal-fin rays	II, 5	II, 5 ; II, 6	III, 5	II, 5	7	II, 5	II, 5
Lateral-line scales	77–83	—	150	70–81	150	76–92	76–92

somewhat similar between the two species since they have a lower lip with three triangular lobes, the middle lobe larger than two lateral lobes, two pairs of maxillary barbel at the corner of the mouth, and the outer pair is larger than the lateral lobes (Fig. 5A, 5B). Nevertheless, the upper lip of *Vanmanenia duci* sp. nov. is thin, with four conspicuous lobulated papillae, rostral barbels alternate with lobulated papillae and rostral folds clear (vs. a thick upper lip, lobulated papillae are absent and rostral folds are unclear in *V. caldwelli*). The lower jaw of *V. duci* sp. nov. is larger and deeper (vs. small and shallow) (Figs. 5A, 5B). Besides, both species have a slightly black spot in the middle caudal fin base, but *Vanmanenia duci* sp. nov. has a black spot equal to the eye diameter (vs. smaller than the eye diameter). Moreover, the number of black bands across rays of dorsal and caudal fins of species *Vanmanenia duci* sp. nov. are fewer than those in *V. caldwelli* (1, 2 vs. 2, 3, respectively). The caudal fin shape is also clearly different between the two species (slightly truncate in *Vanmanenia duci* sp. nov. vs. forked in *V. caldwelli*) (Figs. 3, 7). There is a larger black dot at the base of the pelvic and pectoral fins and a fleshy larger black protrusion of pelvic fin base in the new species than those in *V. caldwelli*. The new species has a black dotted stripe along from the posterior end of the pectoral fin to the posterior insertion of the anal fin (vs. absent in *V. caldwelli*) (Figs. 3, 7).

Species group without black mid-lateral stripe. The new species was collected in the Red River and the Bang Giang River (a tributary of the Pearl River in China) (Fig. 1). Thus, the presently reported study attempted to compare the morphology of the new species with known

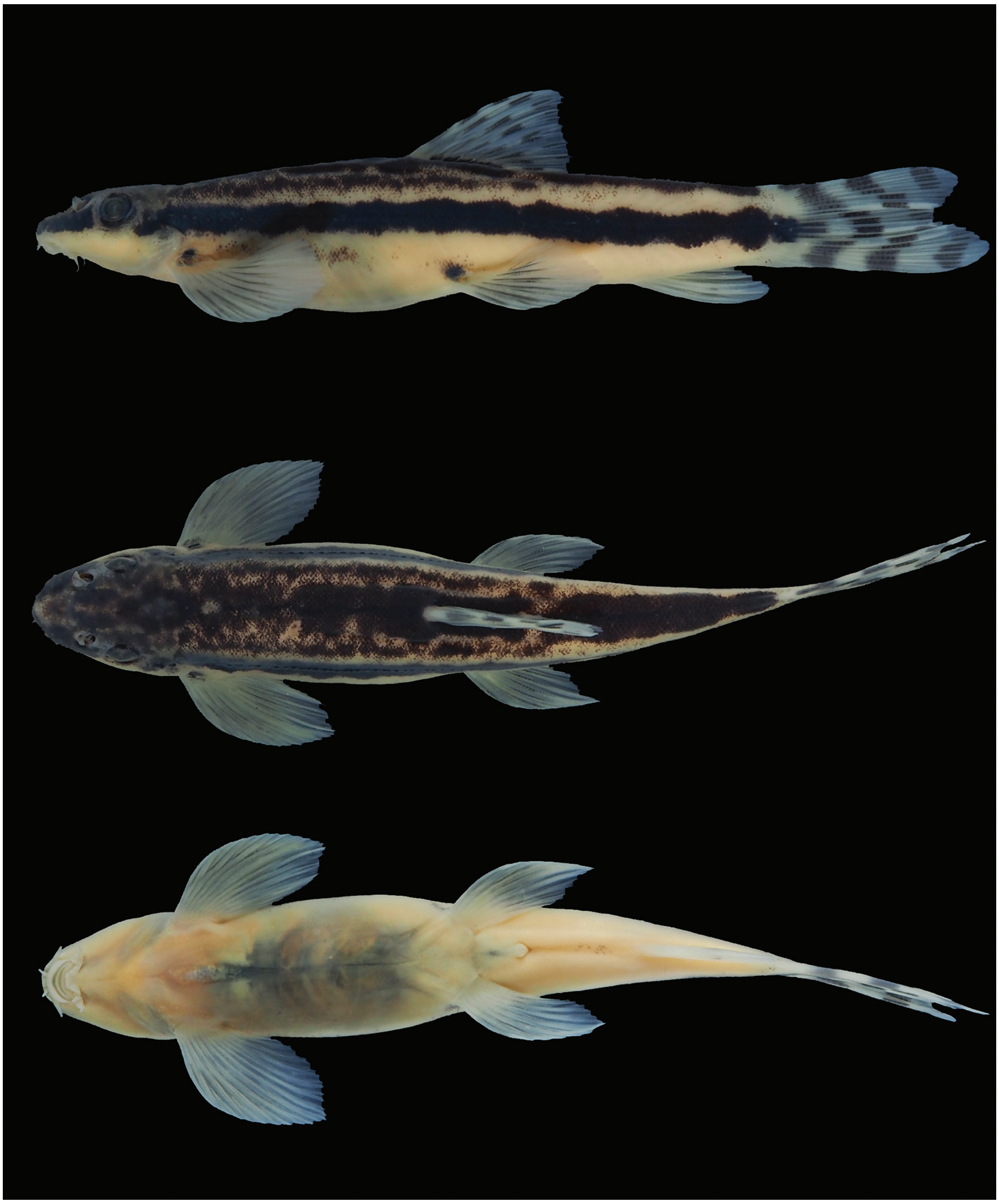

Figure 7. *Vanmanenia caldwelli* (62.1 mm SL) collected from the Min River, in Fuqing City, Fujian Province, China (Photos by Fan Li).

species of *Vanmanenia* in this group from the Red River and the Pearl River basins.

In the Red River, two species *V. tetraloba*, *V. striata* are present in this group from China (Li et al. 2019). These two species are different from the new species by body color patterns (flank with 11–21 vermiculations presence vs. absence) and mouth soft-tissue structures (figs. 7, 8 in Li et al. 2019; fig. 3 in Yi et al. 2014; Figs. 3, 5A, 5B, 8A, 8B, 8C in the presently reported study). As we can see from Fig. 1, this genus is diverse in the Red River basin located in Vietnam. Differences between *Vanmanenia duci* sp. nov. and the six species of *Vanmanenia* occurring in the Red River basin from Vietnam are listed in Tables 3, 4. The new species could be distinguished from its congeners in the Red River basin by the number of scales in the lateral line (Table 3). For example, the new species has fewer lateral-line scales (77–83) than *V. tetraloba* (104–112), *V. trifasciodorsala* (169), *V. monofasciodorsala* (164), and *V. microlepis* (124–135). Furthermore, *Vanmanenia duci* sp. nov. has a shorter head than *V. nahangensis* (15.4%–16.7% vs. 20.70%) (Table 3), which is distributed in the Gam River, a different tributary of the Red River opposite to the Black River, where other four species of *Vanmanenia* present (Fig. 1). The records of this new species and others, such as *Pareuchiloglanis* sp. (Tran et al. 2021), *Parazacco* sp. (Duong et al. 2022), and *Chimarrichthys nami* (see Tran et al. 2023) further indicate that the Red River basin is a home of many freshwater fish species (Nguyen et al. 2019). In the Pearl River, in addition to *V. lineata* and *V. homalocephala* as mentioned above, there are four species of this genus, i.e., *V. gymnetrus*, *V. intermidia*, *V. pingchowensis*, and *V. polylepis* in China. The new species differs from *V. gymnetrus*, *V. intermidia*, and *V. pingchowensis* in body color patterns (a broad black midlateral stripe on the body vs. absence) and mouth soft-tissue structures (fig. 1 in Li et al. 2019; figs. 2, 3, 7 in Deng and Zhang 2020; Figs. 3, 5A, 5B in the presently reported study). *Vanmanenia duci* sp. nov. can be distinguished from *V. polylepis* by the patch type on the caudal-fin base (complete vs. dissociated) (Li et al. 2019; Fig. 3 in the presently reported study). This character is also available to indicate the new species differing from

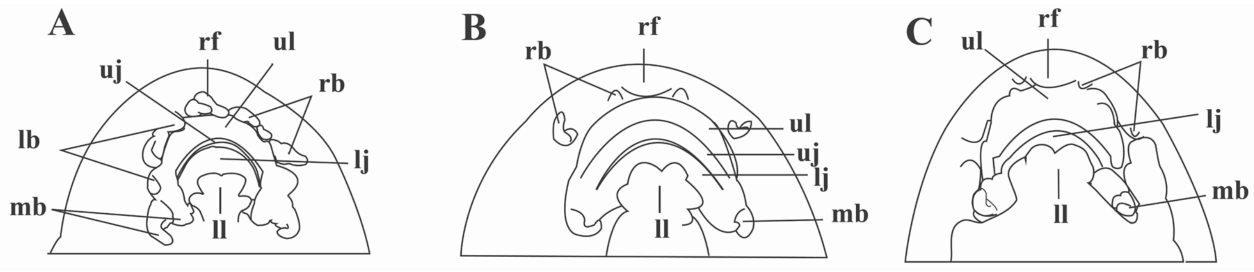

Figure 8. Mouth soft-tissue structures of three species of *Vanmanenia* distributed in the same river basin, the Red River in Vietnam and China: (**A**) *Vanmanenia duci* sp. nov., HNUE-F00304, 47.60 mm SL; (**B**) *Vanmanenia striata*, IHB 646482, 53.20 mm SL (Yi et al. 2014); (**C**) *Vanmanenia tetraloba*, SWFC 0512252, 75.30 mm SL (Li et al. 2019. Abbreviations: lj = lower jaw, mb = maxillary barbel, rb = rostral barbel, rf = rostral fold, uj = upper jaw, ul = upper lip, ll = lower lip, lb = lobulated papillae.

Table 3. Comparison meristic and morphometric data of *Vanmanenia duci* sp. nov. with other species of *Vanmanenia* occurring in northern Vietnam.

Character	**Species, locality, reference, and number of specimens**								
	***Vanmanenia duci* sp. nov.**	***Vanmanenia ventrosquamata***	***Vanmanenia tetraloba***	***Vanmanenia trifasciodorsala***	***Vanmanenia caobangensis***	***Vanmanenia nahangensis***	***Vanmanenia monofasciodo-rsala***	***Vanmanenia microlepis***	***Vanmanenia multiloba***
	Red River, Pearl River	**Pearl River**	**Red River**	**Red River**	**Pearl River**	**Red River**	**Red River**	**Red River**	**Red River**
		This study		**Nguyen 2005**			**Mai 1978**		
	***n* = 16**	***n* = 1**	***n* = 7**	***n* = 9**	***n* = 5**	***n* = 1**	***n* = 5**	***n* = 3**	**—**
Absolute morphometric values [mm]									
Standard length (SL)	32.4–54.0	73.2	52.0–80.0	64.5–77.3	45.0–61.0	59.0	72.0–92.5	63.0–84.0	48.0–71.0
Relative morphometric values [% in SL]									
Body depth	12.2–18.7	16.4	15.4–19.6	16.0–19.7	18.0–22.3	18.7	19.6–20.8	21.1–22.8	17.0
Caudal-peduncle length (CPL)	7.5–9.8	12.6	10.2–13.7	10.1–14.1	10.8–12.4	9.2	11.3–12.6	11.2–12.8	—
Caudal-peduncle depth	7.9–9.1	8.4	7.8–9.0	7.8–8.8	9.1–9.6	10.2	8.9–10.7	9.3–9.5	—
Head length (HL)	15.4–16.7	16.4	18.9–21.1	20.3–22.5	20.0–21.2	20.7	22.7–23.9	20.5–24.5	19.7
Relative morphometric values [% in CPL]									
Caudal-peduncle depth	92.5–111.1	87.0	65.8–82.7	56.2–87.7	77.5–86.2	109.9	70.4–87.7	75.2–84.8	—
Relative morphometric values [% in HL]									
Eye diameter	21.0–30.4	18.2	14.5–18.6	16.4–17.3	17.1–20.7	18.9	13.0–16.4	12.1–16.9	19.1
Interorbital width	52.4–61.5	46.3	35.0–5	32.4–39.5	39.1–47.0	43.5	36.0–40.7	43.7–46.1	—
Meristic data									
Dorsal-fin rays	III, 7	III, 7	III, 7	II, 7	III, 7	III, 7	II, 7	II, 7	I, 7
Pectoral-fin rays	I, 15	I, 15	I, 14–15	I, 15	I, 15–16	I, 17	I, 14–16	I, 15	—
Pelvic-fin rays	I, 8	I, 8	I, 8	I, 8	I, 8	I, 7	I, 8	I, 9	—
Anal-fin rays	II, 5	I, 5	II, 5	II, 5	II, 5	I, 5	II, 5	II, 5	I, 5
Lateral-line scales	77–83	69–70	104–112	169	64–67	60	164	124–135	90–100

Table 4. Morphological comparison among nine species of *Vanmanenia* in northern Vietnam.

Parameter	Species and reference								
	***Vanmanenia duci* sp. nov.**	***Vanmanenia ventrosquamata***	***Vanmanenia tetraloba***	***Vanmanenia trifasciodorsala***	***Vanmanenia caobangensis***	***Vanmanenia nahangensis***	***Vanmanenia monofasciodorsala***	***Vanmanenia microlepis***	***Vanmanenia multiloba***
	This study	**Nguyen 2005**	**Nguyen 2005**	**Nguyen 2005**	**Nguyen 2005**	**Nguyen 2005**	**Nguyen 2005**	**Nguyen 2005**	**Mai 1978**
Lobes on lower lip structures	3 triangular lobules; median one wider than two lateral ones	3 lobules; median one wider than two lateral ones	3 lobules nearly equal in width	3 lobules nearly equal in width	3 lobules; median one wider than two lateral ones	3 lobules; median one wider than two lateral ones	3 lobules; median one wider than two lateral ones	3 lobules nearly equal in width	—
Barbels at mouth corner	2 pairs	2 pairs	1 pair	1 pair	1 pair	2 pairs	1 pair	1 pair	1 pair
Position of dorsal fin base	Farther to snout tip than to caudal-fin origin	Between snout tip and caudal-fin origin	Between snout tip and caudal-fin origin	Between snout tip and caudal-fin origin	Farther to snout tip than to caudal-fin origin	Between snout tip and caudal-fin origin	Closer to snout-tip than to caudal-fin origin	Farther to snout tip than to caudal-fin origin	Between snout tip and caudal-fin origin
Position of anal fin base	Closer to anus than to caudal-fin origin	Between anus and caudal-fin origin	Closer to anus than to caudal-fin origin	—	Closer to anus than to caudal-fin origin	Between anus and caudal-fin origin	Between anus and caudal-fin origin	Closer to anus than to caudal-fin origin	—
Anus position	Farther to pelvic-fin posterior insertion than to anal-fin origin	Closer to pelvic-fin posterior insertion than to anal-fin	Between pelvic-fin posterior insertion and anal-fin origin	Between pelvic-fin posterior insertion and anal-fin origin	Between pelvic-fin posterior insertion and anal-fin origin	Between pelvic-fin posterior insertion and anal- fin origin	Closer to pelvic-fin posterior insertion than to anal-fin origin	Between pelvic-fin posterior insertion and anal-fin origin	Closer to pelvic-fin posterior insertion than to anal-fin origin
Shape of caudal fin	Slightly concave	Slightly concave	Slightly concave	Deeply concave	Obliquely concave	Slightly concave	Slightly concave	Slightly concave	Truncate
Scales distribution	Absent from prepectoral-fin to pelvic-fin origin; small scales present on postpelvic fin	Absent on prepectoral-fin; small scales present from postpectoral fin to caudal fin	Absent on chest and abdomen; small scales present on origin of prepelvic fin	Absent on chest and abdomen to pelvic-fin insertion	Absent on prepectoral fin; small scales present on postpectoral fin	Absent on prepectoral fin; small scales present on postpectoral fin to anal fin	Absent from chest to pelvic-fin origin; few areas with scales present on anterior part of both sides of pelvic-fin origin	Absent on chest and abdomen anterior to pelvic fins	Absent on chest
Coloration	Longitudinal black stripe from back of head to caudal fin origin base along lateral line on side of body; 8–9 brown-black saddles across back of head to caudal fin base; black spot slightly smaller than eye diameter at caudal fin origin	Many large and small irregular black blotches on dorsal profile, darker on lateral line; black blotch on belly border; large patch at caudal fin base	8–10 brown-black saddles across dorsal midline to caudal fin base; horizontal black bars thick and thin in front, and short and dark at back of body; longitudinal dark black stripe along lateral line	5 black saddles on dorsal profile: two spots in front of dorsal fin, and 3 dark spots behind dorsal fin; 28–30 irregular, evenly spaced black saddles	7 large round black blotches on dorsal profile; many black saddles on lateral line; black blotch bar on near belly border; many dark black spots in middle of caudal fin rays	6–8 round black spots across dorsal midline to caudal-fin base; irregular black notches on lateral line	4 wide, evenly spaced black saddles on dorsal profile and body: 1 on predorsal fin, 1 near end of dorsal-fin origin, and 2 on caudal fin bas; 19–21 irregular black horizontal bars on both sides of body; being shorter in anterior and posterior parts and longer in the mone; no bar on belly and lower part of caudal fin	20–22 horizontal black bars, being thicker and narrower in anterior part, and larger, heavier, and sparser in posterior one, mostly connected between both sides of body; no longitudinal black stripe along lateral line; black dot on upper caudal fin	Many irregularly arranged black blotches on body; large black dot on caudal fin base

V. lineata, *V. homalocephala*, *V. caldwelli*, *V. striata*, and *V. pingchowensis* (see Li et al. 2019). There are two species of *Vanmanenia* in the Pearl River from Vietnam, i.e., *V. caobangensis* and *V. ventrosquamata* (Fig. 1). *Vanmanenia duci* sp. nov. has a slightly similar number of fin rays as *V. ventrosquamata* and *V. caobangensis* (Table 3), but the new species has a shorter head than *V. caobangensis* (7.54%–9.81% vs. 20.04%–21.23%) and shorter caudal-peduncle than *V. ventrosquamata* (7.54%–9.81% vs. 12.56%). In addition, *Vanmanenia duci* sp. nov. is further distinct from the species from the Red River and Pearl River basins in Vietnam in having a bigger eye, and a wider interorbital (Table 3).

Remarkably, *Vanmanenia duci* sp. nov. differs from other species of the genus in the Red River and Pearl River systems in Vietnam by presenting a longitudinal black stripe from the back of the head to the caudal fin origin along the lateral line on the side of the body and mouth soft-tissue structures (Figs. 3, 5A; Table 4).

Acknowledgments

This research was funded by The NEF Bio-ecological Nature Conservation Project in the Mountainous Region of North Vietnam (Nagao Natural Environment Foundation, Japan/Central Institute for Natural Resources and Environmental Studies). Thanks to V.S. Ngo, T.T. Tran, H.V. Pham, N.T. Nguyen, A.N.T. Do, who assisted in collecting specimens. We thank anonymous reviewers for their comments that helped improve the manuscript.

References

Cai X, Deng S, Shen Z (2021) Complete mitochondrial genome of *Vanmanenia hainanensis* (Cypriniformes: Gastromyzontidae). Mitochondrial DNA. Part B, Resources 6(5): 1636–1637. https://doi.org/10.1080/23802359.2021.1927215

Deng SQ, Zhang E (2020) *Vanmanenia intermedia* Fang, 1935, a valid hillstream species of loach (Teleostei: Gastromyzontidae) from the middle Yangtze River basin, southwest China. Zootaxa 4819(1): 109–127. https://doi.org/10.11646/zootaxa.4819.1.5

Deng SQ, Zhang E (2021) *Vanmanenia marmorata*, a new species of loach (Teleostei: Gastromyzontidae) from the middle Chang-Jiang Basin in Guizhou Province, south China. Biodiversity Data Journal 9: e72432. https://doi.org/10.3897/BDJ.9.e72432

Duong TH, Tran DH, Dang TTH, Nguyen QH (2022) Mô tả các mẫu vật thuộc giống cá chuôn *Parazacco* (Cypriniformes: Cyprinidae) thu ở Bắc Việt Nam [Description of specimens of genus *Parazacco* (Cypriniformes: Cyprinidae) collected in Northern Vietnam.] Tap chi Khoa hoc và Cong Nghe – Dai hoc Thai Nguyen— TNU Journal of Science and Technology 227(14): 388–396. [In Vietnamese with English abstract] https://doi.org/10.34238/tnu-jst.6510

Fricke R, Eschmeyer WN, Van der Laan R (Eds.) (2023) Eschmeyer's catalog of fishes: genera, species, references. California Academy of Sciences, San Francisco, CA, USA. [Electronic version accessed 8 August 2023] http://researcharchive.calacademy.org/research/ichthyology/catalog/fishcatmain.asp

Li X, Zhou W, Che X (2019) Loaches of *Vanmanenia* (Cypriniformes: Gastromyzontidae) from Yunnan, China with description of a new species. Zootaxa 4603(1): 125–144. https://doi.org/10.11646/zootaxa.4603.1.6

Mai DY (1978) Định loại cá nước ngọt các tỉnh phía Bắc Việt Nam. [Identification of freshwater fish in the northern provinces of Vietnam.] Nha xuat ban Khoa hoc va Ki thuat—Science and Technics Publishing House, Hanoi, Vietnam, 340 pp. [In Vietnamese]

Nguyen VH (2005) Cá nước ngọt Việt Nam, Tập 2 [Freshwater Fish of Vietnam, Volume II.] Nha xuat ban Nong nghiep—Agricultural Publishing House, Hanoi, Vietnam, 760 pp. [In Vietnamese]

Nguyen HD, Ngo TMH, Tran DH (2019) List of fish in the Hong River, Viet Nam. Proceedings of the First National Conference on Ichthyology in Vietnam. Nha xuat ban Khoa hoc Tu nhien và Cong nghe—Publishing House for Science and Technology, Hanoi, Vietnam, 22–39.

Nguyen QH, Dang TTH, Ta TT, Duong TH, Tran DH (2024) Bước đầu ghi nhận về khu hệ cá tại Vườn Quốc gia Phia Oắc-Phia Đén, tỉnh Cao Bằng, Bắc Việt Nam. [Preliminary data on the ichthyofauna in Phia Oac-Phia Den National Park, Cao Bang Province, northern Vietnam.] Tap chi Khoa hoc và Cong Nghe – Dai hoc Thai Nguyen— TNU Journal of Science and Technology 229(13): 52–60. [In Vietnamese with English abstract] https://doi.org/10.34238/tnu-jst.10286

Nichols JT (1925) *Homaloptera caldwelli*, a new Chinese loach. American Museum Novitates 1925(172): [Unknown page number].

Silas EG (1953) Classification, zoogeography and evolution of the fishes of the cyprinoid families Homalopteridae and Gastromyzonidae. Records of the Indian Museum 50(2): 173–264. https://doi.org/10.26515/rzsi/v50/i2/1953/162072

Tran DH, Dang TTH, Ta TT, Ngo TX (2021) Mô tả loài cá chiên bẹt *Pareuchiloglanis* sp. (Siluriformes: Sisoridae) ở lưu vực sông Đà, địa phận huyện Phong Thổ, tỉnh Lai Châu. [Description of *Pareuchiloglanis* sp. (Siluriformes: Sisoridae) in the Da River basin belonging to Phong Tho district, Lai Chau province.] Tap Chi Khoa Hoc Tu Nhien—HNUE Journal of Science 66(4F): 103–115. [In Vietnamese with English abstract] https://doi.org/10.18173/2354-1059.2021-0073

Tran DH, Nguyen HD, Dang TTH, Nguyen QH, Nguyen TN (2023) A new species of *Euchiloglanis* Regan, 1907 (Actinopterygii: Sisoridae) from Vietnam. Acta Zoologica Bulgaria 75(1): 3–11.

Yi WJ, Zhang E, Shen JZ (2014) *Vanmanenia maculata*, a new species of hillstream loach from the Chang-Jiang Basin, south China (Teleostei: Gastromyzontidae). Zootaxa 3802(1): 085–097. https://doi.org/10.11646/zootaxa.3801.2.7

Yue P, Shan X, Zhang E, Chen J, Luo Y, Chen Y, Lin R, Chu X, Cao W, Tang W, Cai M (2000) Fauna Sinica, Osteichthyes, Cypriniformes III. Science Press, Beijing, China, 661 pp.

Zhang CG, Zhao YH (2000) [A new species of the genus *Vanmanenia* from Guangxi, China.] Dong Wu Fen Lei Xue Bao—Acta Zootaxonomica Sinica 25(4): 458–461. [In Chinese with English abstract]

Acta Ichthyologica et Piscatoria 54, 2024, 189–201 | DOI 10.3897/aiep.54.123026

PENSOFT.

ACTA
ICHTHYOLOGICA
ET PISCATORIA

Mitochondrial markers revealed genetic panmixia in the data-deficient yellowfin snapper, *Lutjanus xanthopinnis* (Actinopterygii: Eupercaria: Lutjanidae), from a hotspot of the southern region of the South China Sea

Md Moshiur RAHMAN[1,2], Nur Asma ARIFFIN[1], Ying Giat SEAH[1,3], Siti Azizah Mohd NOR[4], Tun Nurul Aimi MAT JAAFAR[1], Nuralif Fakhrullah Mohd NUR[1], Ahasan HABIB[1]

1 *Faculty of Fisheries and Food Science, Universiti Malaysia Terengganu, Terengganu, Malaysia*

2 *Faculty of Fisheries, Sylhet Agricultural University, Sylhet, Bangladesh*

3 *Fish Division, South China Sea Repository and Reference Centre, Institute of Oceanography and Environment, University Malaysia Terengganu, Terengganu, Malaysia*

4 *Institute of Climate Adaptation and Marine Biotechnology (ICAMB), Universiti Malaysia Terengganu, Terengganu, Malaysia*

https://zoobank.org/58A0F92E-016E-4007-A9A0-119BD3DBC8AF

Corresponding authors: Ahasan Habib (a.habib@umt.edu.my); Nur Asma Ariffin (nurasma@umt.edu.my)

Academic editor: Jolanta Kiełpińska ♦ **Received** 14 March 2024 ♦ **Accepted** 3 July 2024 ♦ **Published** 17 September 2024

Citation: Rahman MM, Ariffin NA, Seah YG, Nor SAM, Mat Jaafar TNA, Nur NFM, Habib A (2024) Mitochondrial markers revealed genetic panmixia in the data-deficient yellowfin snapper, *Lutjanus xanthopinnis* (Actinopterygii: Eupercaria: Lutjanidae), from a hotspot of the southern region of the South China Sea. Acta Ichthyologica et Piscatoria 54: 189–201. https://doi.org/10.3897/aiep.54.123026

Abstract

Understanding the genetic structure and diversity of marine fish is crucial for a sustainable management program. We examined the genetic diversity and historical demographics of the yellowfin snapper, *Lutjanus xanthopinnis* Iwatsuki, Tanaka et Allen, 2015, in the coastal waters of east Peninsular Malaysia which is bordered by the southern part of the South China Sea using the mitochondrial genes (mtDNA) D-loop and Cytochrome b (*Cyt-b*). A total of 99 (D-loop) and 78 (*Cyt-b*) specimens of *L. xanthopinnis* were successfully sequenced from six locations within the range of species distribution along the Malaysian South China Sea. In the presently reported study, the lack of genetic differentiation among populations can be attributed to historical demographic events, eggs and planktonic larvae' ability to disperse, spawning patterns, and the absence of physical barriers in the geographical landscape. Maximum likelihood gene trees demonstrated that the populations under study had limited structuring and formed a panmictic population that lacks support for internal clades. The AMOVA (Analysis of Molecular Variance) and population pairwise Φ_{ST} values indicated high genetic exchange between the study areas. A high level of haplotype diversity (D-loop: 0.948–1.000; *Cyt-b*: 0.542–0.928), low nucleotide diversity (D-loop: 0.0095–0.0159; *Cyt-b*: 0.0022–0.0049) and starlike haplotype network indicates a recent expansion of *L. xanthopinnis* populations in Malaysian South China Sea. However, neutrality and goodness of fit tests revealed non-significant values. Furthermore, the BSP (Bayesian skyline plot) analysis estimated population expansion events during the late Pleistocene. During this epoch, the fluctuation in sea level may have led to an increase in the abundance of resources and favorable habitats for the yellowfin snapper. The presently reported findings could initiate efficient management strategies for *L. xanthopinnis* along the coastal areas of the Malaysian South China Sea and other nearby nations that share the same waterways.

Keywords

control region, *Cyt-b*, genetic diversity, Malaysia, panmictic population, population expansion

Introduction

Snappers, members of the family Lutjanidae, constitute an abundant and diverse fishery resource. They comprise 17 genera, with 113 documented species in the Atlantic and Indo–Pacific regions of tropical and subtropical waters (Froese and Pauly 2023). Amongst the Lutjanidae family, the genus *Lutjanus* contains the highest number of species, amounting to 73 (Allen 1985). This genus is regarded as a valuable fisheries resource that is both ecologically and commercially significant across its range of distribution (Messias et al. 2019), including Malaysia (Adibah et al. 2018).

The yellowfin snapper, *Lutjanus xanthopinnis* Iwatsuki, Tanaka et Allen, 2015, is a small lutjanid species that was previously mistaken for *Lutjanus madras* (Valenciennes, 1831) widely distributed throughout the western Pacific and Indian Oceans, spanning from Sri Lanka to the Andaman Sea and the Malay Peninsula, towards the southeast to Indonesia, Malaysia, and Brunei, to the Philippines, north to China and Taiwan, and south to Japan (Iwatsuki et al. 2015). Due to its initial taxonomic conundrum with *L. madras*, basic information about the biogeography, ecology, biology, and population stock status of *L. xanthopinnis* is highly limited (Arai et al. 2023). As a result, the present conservation status of *L. xanthopinnis* is classified as Data Deficient (Carpenter et al. 2019). This "*L. xanthopinnis* + *L. madras*" mixed species group is caught using gillnets and trawl nets (Rahman et al. 2023). It is subjected to commercial exploitation and contributes to Malaysia's annual fish landing statistics. Landings of *Lutjanus* species have steadily risen over the last decade (2013–2022) in Malaysia, reaching 15 391 tonnes annually (DOF 2023).

Understanding the genetic population structure of marine fish is crucial, and fisheries management should be based on this knowledge (Gonzalez et al. 2023). Its implementation could mitigate the risk of genetic resource depletion (Laikre et al. 2005). Habib and Sulaiman (2016) reported that identifying stock structure is one of the cornerstones of assessing fisheries stock, particularly for marine fish. Therefore, basic population parameters such as the number and distribution of fish stocks, dispersal pattern, and genetic diversity are needed for a sustainable management and conservation program (Tan et al. 2019; Kasim et al. 2020; Mohd Yusoff et al. 2021). Genetic studies can provide valuable insights into these factors, aiding in determining the optimal management scale for the target species (Ovenden et al. 2015; Alam et al. 2017). Despite its significant contribution to the economy, only a few studies have been conducted on the genetic diversity, population structure, and demographic history of snappers from the biodiverse South China Sea (Guo et al. 2007; Li and Chu-Wu 2007), including Malaysian waters (Halim et al. 2022).

Genetic markers, such as mitochondrial DNA (mtDNA), are highly effective in assessing genetic variation including at species-level population genetics. Furthermore, it is extensively employed in evolutionary genetics and allows the estimation of population history parameters such as divergence time among different groups (Habib and Sulaiman 2017; Tan et al. 2019). Mitochondrial DNA markers are preferred and reliable because they are present in vast quantities in cells and have a mutation rate greater (10–17 times) than nuclear DNA (Allio et al. 2017). The mtDNA D-loop and *Cyt-b* markers were used in the population genetics and demography of the data-deficient *L. xanthopinnis* natural populations in the East Peninsular Malaysian waters of the South China Sea. The non protein-coding D-loop and protein-coding *Cyt-b* regions have been extensively used as population genetic markers in numerous marine fish, including snappers (Silva et al. 2018; Hernández-Álvarez et al. 2020; Veneza et al. 2023).

Currently, there is only one population genetic study of *L. xanthopinnis* based on the *COI* (Cytochrome c oxidase subunit I) gene (Arai et al. 2023), restricting our understanding of this biological resource. Hence, the key objective of the presently reported study was to assess the population genetics and demographic history of this species, *L. xanthopinnis*, in the South China Sea off East Peninsular Malaysia through the analysis of the two mitochondrial regions (D-loop and *Cyt-b*). The findings of this study would be crucial and serve as a point of reference for the management and conservation strategies of this species.

Materials and methods

Sampling and preservation. A total of 120 samples of yellowfin snapper were obtained from fish landing ports at six distinct geographical areas within the range of species distribution along the East Peninsular Malaysian waters of the South China Sea in 2022 (Table 1, Fig. 1). Subsequently, all specimens were identified using several systematic morphological traits described by Iwatsuki et al. (2015) and specimens were randomly validated using a molecular technique based on *COI* genes. This species can be distinguished from other *Lutjanus* species by its yellow stripes, predominantly yellow fins, preopercular flange with several embedded scales, and a pair of small rounded to elliptical nostrils on each side of the snout. A fin clip from each specimen was excised and stored in 95% ethanol. Samples were kept in 1.5 mL centrifuge tubes at 4°C until further analysis.

Table 1. Sampling sites, coordinates, and collection dates of *Lutjanus xanthopinnis* from Malaysian South China Sea.

Sampling site (population)	Coordinates	Date
Kota Bharu, Kelantan	6°08′03.5″N, 102°14′00.8″E	4 May 2022
Tok Bali, Kelantan	5°54′29.5″N, 102°28′08.0″E	7 Oct 2022
Pulau Kambing, Terengganu	5°19′19.4″N, 103°07′44.2″E	13 Aug 2022
Dungun, Terengganu	5°19′19.4″N, 103°07′44.2″E	10 Jul 2022
Kuantan, Pahang	3°47′10.7″N, 103°19′25.4″E	26 Aug 2022
Mersing, Johor	2°26′48.8″N, 103°49′38.5″E	14 Oct 2022

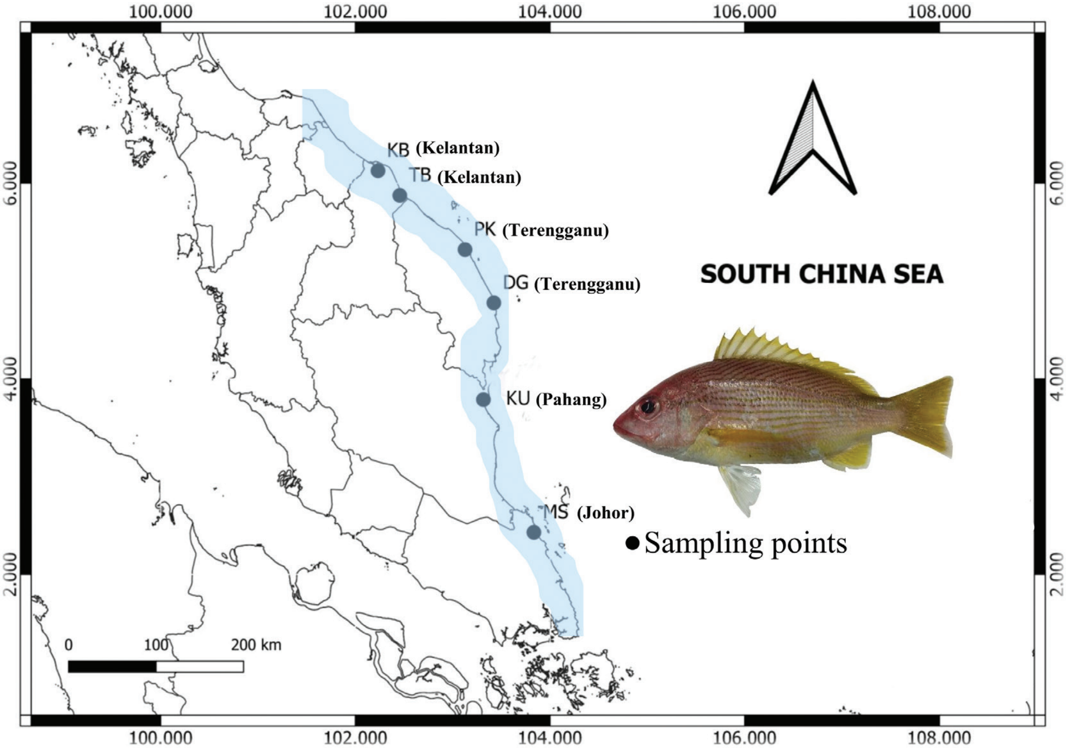

Figure 1. Sampling sites of *Lutjanus xanthopinnis* in the Malaysian waters of the South China Sea. Abbreviations: KB = Kota Bharu, TB = Tok Bali, PK = Pulau Kambing, DG = Dungun, KU = Kuantan, MS = Mersing. The blue-shaded area denotes the natural range of the yellowfin snapper in the area of study.

DNA extraction and quantification. Total genomic DNA was extracted from fin tissue using salt extraction (Aljanabi and Martinez 1997). The extracted DNA samples were assessed for their purities and concentrations using the BioDropand and then kept in 1.5 mL centrifuge tubes at –20°C before amplification.

Polymerase chain reaction (PCR) amplification and sequencing. The preserved DNA samples were PCR amplified using the partial mitochondrial DNA control region (D-loop) and Cytochrome b (*Cyt-b*). The primers used were as follows: (a) D-loop control region A (5′–ATTCCACCTCTAACTCCCAAAGCTAG–3′, forward) and G (5′–CGTCGGATCCCATCT TCAGTGTTATGCTT–3′, reverse) (Lee et al. 1995) (b) *Cyt-b* (forward 5′-GTG ACT TGA AAA ACC ACC GTT G-3′) and (reverse 5′-CTC CAT CTC CGG TTT ACA AGA C-3′) (Song et al. 1998). The final volume of 25 µL PCR reaction solution contained 3 µL of genomic DNA, 0.5 µL of 10 µmol forward primer, 0.5 µL of 10 µmol reverse primer, 12.5 µL of Taq polymerase Bioline red mix, and 8.5 µL of double distilled water (ddH$_2$O). The thermal protocol for D-loop was: initial denaturation (94°C for 5 min), followed by 35 cycles of reaction, denaturation (95°C for 60 s), annealing (56°C for 90 s), extension at (72°C for 60 s), final extension (72°C for 10 min), and last hold at 4°C. The *Cyt-b* gene was amplified under the following conditions: initial denaturation (94°C for 80 s), 30 cycles of reaction, denaturation at (94°C for 42 s), annealing (47°C for 45 s), extension (72°C for 60 s), final extension (72°C for 5 min), and last hold at 4°C. The PCR results were observed on 1.5% agarose gel stain with SYBR Safe to verify their existence and determine the size of the amplified DNA fragment. All satisfactorily PCR amplified products were later sent to Apical Scientific Sdn Bhd in Selangor, Malaysia, for sequencing. An Applied Biosystem ABI3730×1 capillary-based DNA sequencer was used to perform the sequencing.

Sequence alignment and editing. The ClustalW program incorporated in MEGA 11 software (Tamura et al. 2021) was utilized to verify and align the multiple sequences. Identification of DNA sequences was verified with the Basic Local Alignment Search Tool (BLAST) method available in the National Centre for Biotechnology Information database (NCBI) (http://blast.ncbi.nlm.nih.gov/Blast.cgi) before subsequent processing. The aligned sequence was transformed into a haplotype file in DnaSP 6.0 (Rozas et al. 2017). All haplotypes have been submitted to GenBank and have been assigned accession numbers OR756024–OR756105 (D-loop) and OR764550–OR764577 (*Cyt-b*).

Genetic diversity, phylogenetic, and population structure analyses. The number of haplotypes, polymorphic sites, and genetic diversity indices of haplotype and nucleotide diversity were performed using Arlequin v3.5 (Excoffier and Lischer 2010). The phylogenetic relations of haplotypes were estimated using the Maximum Likelihood (ML) approach employed in MEGA 11. Tamura 3-parameter (Tamura 1992) with Gamma distribution and invariant sites (T92 + G + I) and Hasegawa–Kishino–Yano (Hasegawa et al. 1985) with Gamma distribution (HKY + G) were identified to have the lowest BIC score (Bayesian Information Criterion) for the D-loop and *Cyt-b* sequences, respectively in MEGA 11. The statistical support for the Maximum Likelihood (ML) tree was assessed by 1000 bootstrap replicates (Felsenstein 1985). The brownstripe snapper *Lutjanus vitta* was employed as an outgroup taxon (D-loop sequence, FJ887832) and (*Cyt-b* sequence, DQ900677). A median-joining network (MJN) was accomplished through the utilization of the median-joining approach outlined in the PopART (Population analysis with reticulate trees) software (Leigh and Bryant 2015) for an overview of mutational differences between haplotypes.

The Φ_{ST} (Population pairwise comparisons) for both data sets were calculated by Arlequin v3.5 software, and the statistical significance of the pairwise comparisons was assessed using 10 000 permutations. In addition, AMOVA (Analysis of Molecular Variance) was performed using the Arlequin 3.5 software to evaluate the population partitioning of *L. xanthopinnis* across the South China Sea off East Peninsular Malaysia based on the fixation index F_{ST} values.

Demographic history and population expansion. The historical demographic expansions of the *Lutjanus xanthopinnis* populations were examined. To analyze the deviation from neutrality, Tajima's D (Tajima 1989) and Fu's F_s (Fu 1997) were performed. The population Θ_0 (before expansion), Θ_1 (after expansion), and τ (relative time since population expansion) were calculated as historical demographic variables in Arlequin 3.5. The values of τ were transformed to estimate the T (actual time since population expansion) using the equation

$$T = \tau \cdot 2\mu k^{-1}$$

where μ is the sequence mutation rate per site per generation and k is the length of sequence (Yildirim 2016). In the presently reported study, one mutation rate was used for D-loop (i.e., 3.6% per million years) (Donaldson and Wilson 1999), while a mutation rate of 1% per million years was used for *Cyt-b* (Bowen et al. 2001; Lessios 2008). The Bayesian skyline analysis was conducted using the software BEAST version 2.2.0 (Bouckaert et al. 2019), where the effective population size (N_E) changes were examined over time. Since no population structuring was detected (refer to the "Results" of this study), the analysis was based on a single population model. The data was prepared using the BEAUti, and the subsequent analysis consisted of 108 iterations. A burn-in period of 10^7 iterations was implemented, with sampling occurring every 10^4 iterations. All analyses underwent automatic optimization, and the outcomes were obtained with Tracer version 1.7.1 (Rambaut et al. 2018).

In addition, the goodness of fit test parameters, namely Harpending's raggedness index (H_{RI}) and the sum of squared deviations (SSD), were calculated in Arlequin 3.5 to determine whether the sequence data deviated significantly from the expected outcomes of a population expansion model. Moreover, mismatch distribution analyses were conducted using Arlequin 3.5 software with the graph created using the R tool (R Core Team 2023). The mismatch distribution reveals whether the population of *L. xanthopinnis* was demographically expanding, stable, or declining over time. A population at equilibrium displays a multimodal distribution pattern, whereas a recently expanded population displays a unimodal distribution pattern (Slatkin and Hudson 1991; Rogers and Harpending 1992).

Results

Genetic diversity. A total of 99 and 78 distinct specimens of *Lutjanus xanthopinnis* were successfully sequenced for the mtDNA D-loop and *Cyt-b* fragments, respectively from 120 specimens. The final dataset of D-loop sequences (844 base pairs) revealed 96 polymorphic sites (65 parsimony informative and 31 singletons variable sites), generating 82 haplotypes, of which only four (4.88%) were found in two to six localities. In contrast, the remaining 78 (95.12%) were either singleton haplotypes or exclusive to a single locality. The *Cyt-b* aligned sequences (751 base pairs) revealed 35 polymorphic sites (25 singleton variables and 10 parsimony informative sites), defining 28 haplotypes where 8 (28.58%) were found in two to six localities, and 20 (71.42%) were exclusive to one locality or singleton haplotypes. The D-loop fragment was AT-dominant (62.3%). However, *Cyt-b* gene sequences showed almost similar percentages of AT (50.11%) and CG (49.89%). In all sampled locations, *L. xanthopinnis* revealed a high level of haplotype diversity (D-loop: 0.948–1.000; *Cyt-b*: 0.542–0.928), but the diversity of nucleotide was low (D-loop: 0.0095–0.0159; *Cyt-b*: 0.0022–0.0049) (Table 2).

Phylogenetic and population genetic structure. Based on the phylogenetic analysis derived from the D-loop and *Cyt-b* markers, an ML tree with internal weakly supported clades was revealed (<70%). No geographic partitioning of the haplotype was observed within its haplotypes (Fig. 2A, Suppl. material 1, Fig. 2B). Furthermore, the median-joining network inferred from both genes supported this lack of partitioning among the studied populations (Figs. 3, 4). A complex reticulated network was generated by the 82 D-loop haplotypes (Fig. 3), while 28 *Cyt-b* haplotypes provided a well-defined network pattern (Fig. 4). A single dominant haplotype (Hap_01) was identified in the D-loop sequence followed by Hap_06 and

Table 2. Genetic polymorphisms, neutrality test, mismatch distribution and goodness of fit tests for *Lutjanus xanthopinnis* populations inferred from the mitochondrial DNA D-loop (844 base pairs) and *Cyt-b* (751 base pairs) sequences.

Population	Genetic diversity					Neutrality test				Mismatch distribution			Goodness of fit tests			
	N	N_H	N_{PS}	H	D_N	Tajimas'*D*		Fu's F_S		Θ_0	Θ_1	τ	SSD		H_{RI}	
						Value	*P*	Value	*P*				Value	*P*	Value	*P*
D-loop																
TB	18	16	49	0.986	0.013	–0.72	0.24	**–4.69**	0.02	10.07	183.282	3.90	0.0123	0.37	0.0174	0.49
KB	15	14	51	0.990	0.014	–0.94	0.16	**–4.10**	0.03	7.32	58.911	6.65	0.0157	0.38	0.0155	0.81
PK	13	13	49	1.000	0.015	–0.67	0.25	**–4.55**	0.01	8.10	3614.991	7.00	0.0138	0.39	0.0256	0.54
KU	20	19	53	0.994	0.012	–1.26	0.09	**–9.29**	0.001	14.40	6837.57	0.00	0.0127	0.38	0.0159	0.50
MS	18	13	47	0.947	0.010	–1.35	0.07	–1.93	0.18	0.002	15.449	11.00	0.0124	0.74	0.0198	0.79
DG	15	15	41	1.000	0.009	–1.51	0.05	**–8.71**	0.008	5.50	6854.957	2.00	0.0193	0.41	0.0248	0.56
Overall	99	82	96	—	—	—	—	—		—	—	6.639	—		—	
Mean	17			0.986	0.012	–1.08	0.14	**–5.54**	0.04	7.566	2927.527	5.092	0.0144	0.44	0.0198	0.61
Cyt-b																
TB	14	8	13	0.769	0.003	–1.30	0.09	–2.20	0.08	0.00	4.934	4.756	0.0151	0.70	0.0440	0.79
KB	11	8	13	0.927	0.004	–0.71	0.25	–2.31	0.07	0.005	27.363	4.496	0.0061	0.71	0.0290	0.82
PK	10	7	12	0.911	0.004	–1.25	0.11	–1.98	0.07	0.079	16.653	3.461	0.0112	0.61	0.0562	0.49
KU	16	6	10	0.541	0.002	**–1.59**	0.04	–1.09	0.21	0.004	1.743	4.736	0.0801	0.29	0.2888	0.17
MS	15	8	14	0.895	0.003	–1.21	0.11	–1.70	0.16	0.018	8.441	3.844	0.0070	0.77	0.0287	0.83
DG	12	8	12	0.848	0.003	–1.57	0.05	**–3.20**	0.01	0.00	4.221	4.977	0.0307	0.47	0.0835	0.58
Overall	78	28	35	—	—	—	—	—		—	—	4.176	—		—	
Mean	13			0.815	0.003	–1.27	0.11	–2.08	0.1	0.017	10.559	4.378	0.0250	0.59	0.0884	0.61

Bold type denotes significant difference at a level of 5%; N = number of samples, N_H = number of haplotypes, N_{PS} = number of polymorphic sites, H = haplotype diversity, D_N = nucleotide diversity, Θ_0/Θ_1 = Mismatch distribution before/after expansion, τ = relative time since population expansion, SSD = sum of squared deviations, H_{RI} = Harpending's raggedness index; TB = Tok Bali, KB = Kota Bharu, PK = Pulau Kambing, KU = Kuantan, MS = Mersing, DG = Dungun.

Hap_24. Among the *Cyt-b* haplotypes, Hap_03 exhibited the highest level of dominance, followed by Hap_01 and Hap_04. The Hap_03 was observed in all sampling areas and is regarded as the ancestral haplotype based on its dominance and central position where all haplotypes radiate (Clement et al. 2000). A network including an ancestral haplotype often exhibits a star-burst pattern or star-like, with the ancestral haplotype positioned at its center (Ferreri et al. 2011).

The Φ_{ST} (pairwise comparisons) analysis revealed limited and non-significant structuring of *L. xanthopinnis* populations from the Malaysian waters of the South China Sea for both D-loop: −0.0212 to 0.0780) (Table 3) and *Cyt-b*: −0.0359 to 0.1899 (Table 4). Negative Φ_{ST} values indicate higher differences within the sample compared to the variation across different samples. Subsequently, the absence of population partition among the investigated groups was supported by AMOVA. The AMOVA

Table 3. Pairwise Φ_{ST} (below the diagonal) and associated *P* values (above the diagonal) between sampling sites of *Lutjanus xanthopinnis* inferred by mtDNA D-loop region.

Population	Tok Bali	Pulau Kambing	Kuantan	Kota Bahru	Mersing	Dungun
Tok Bali		0.1335	0.2364	0.0292	0.4735	0.4503
Pulau Kambing	0.0297		0.0345	0.3180	0.0088	0.3150
Kuantan	0.0101	0.0645		0.2594	0.5715	0.0204
Kota Bahru	–0.0061	–0.0045	0.0471		0.7408	0.3000
Mersing	0.0071	0.0780	0.0043	0.0152		0.8005
Dungun	–0.0114	0.0734	–0.0128	0.0132	–0.0212	

Table 4. Pairwise Φ_{ST} (below the diagonal) and associated *P* values (above the diagonal) between sampling sites of *Lutjanus xanthopinnis* inferred by mtDNA *Cyt-b* region.

Population	Tok Bali	Kota Bahru	Pulau Kambing	Kuantan	Mersing	Dungun
Tok Bali		0.17206	0.74161	0.68112	0.20453	0.00515
Kota Bahru	0.0384		0.06465	0.74111	0.12434	0.24493
Pulau Kambing	–0.03352	–0.03597		0.23978	0.36917	0.02307
Kuantan	0.01387	0.18997	0.08439		0.18642	0.86496
Mersing	–0.02673	0.05859	0.01717	0.01024		0.51678
Dungun	–0.00615	0.13248	0.04497	–0.03304	–0.0113	

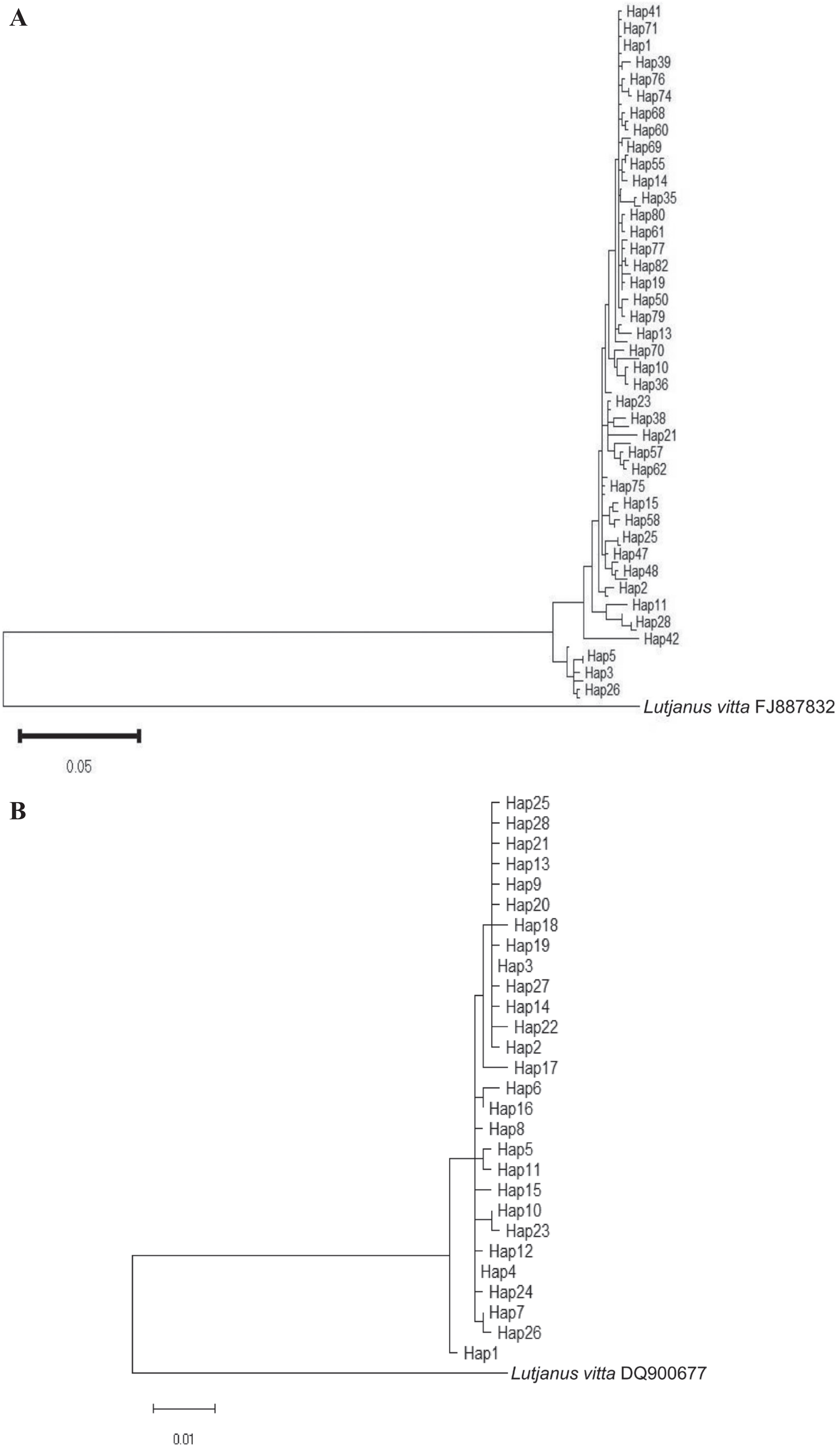

Figure 2. Maximum likelihood (ML) gene trees of *Lutjanus xanthopinnis* haplotypes from the Malaysian waters of the South China Sea inferred from (**A**) D-loop (tree was compressed for a better illustration) (**B**) *Cyt-b* marker. Branches are drawn to scale and bootstrap values <70% are not shown. (The original D-loop ML tree is presented in Suppl. material 1).

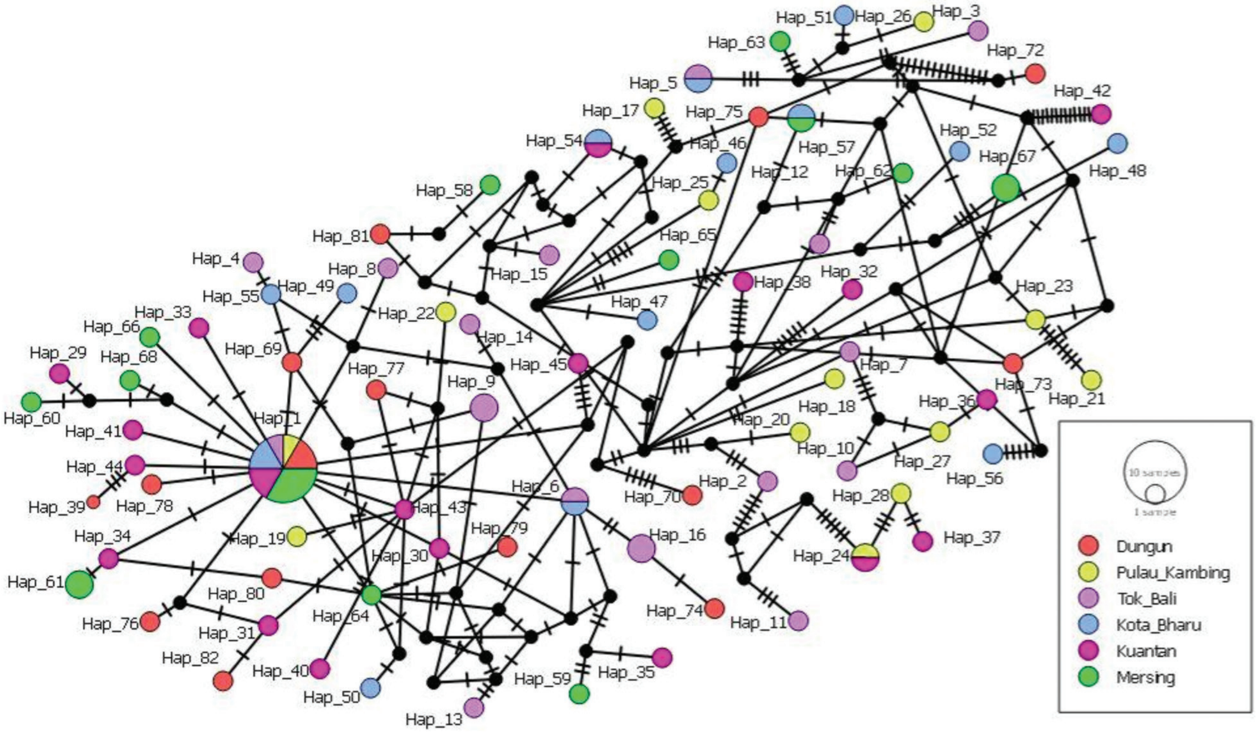

Figure 3. Median-joining haplotypes network diagram of *Lutjanus xanthopinnis* from the Malaysian waters of the South China Sea inferred from D-loop gene. Node size corresponds to the haplotype frequencies; minimum node size is one individual. Black dots indicate median vector. Dashed line is nucleotide mutation.

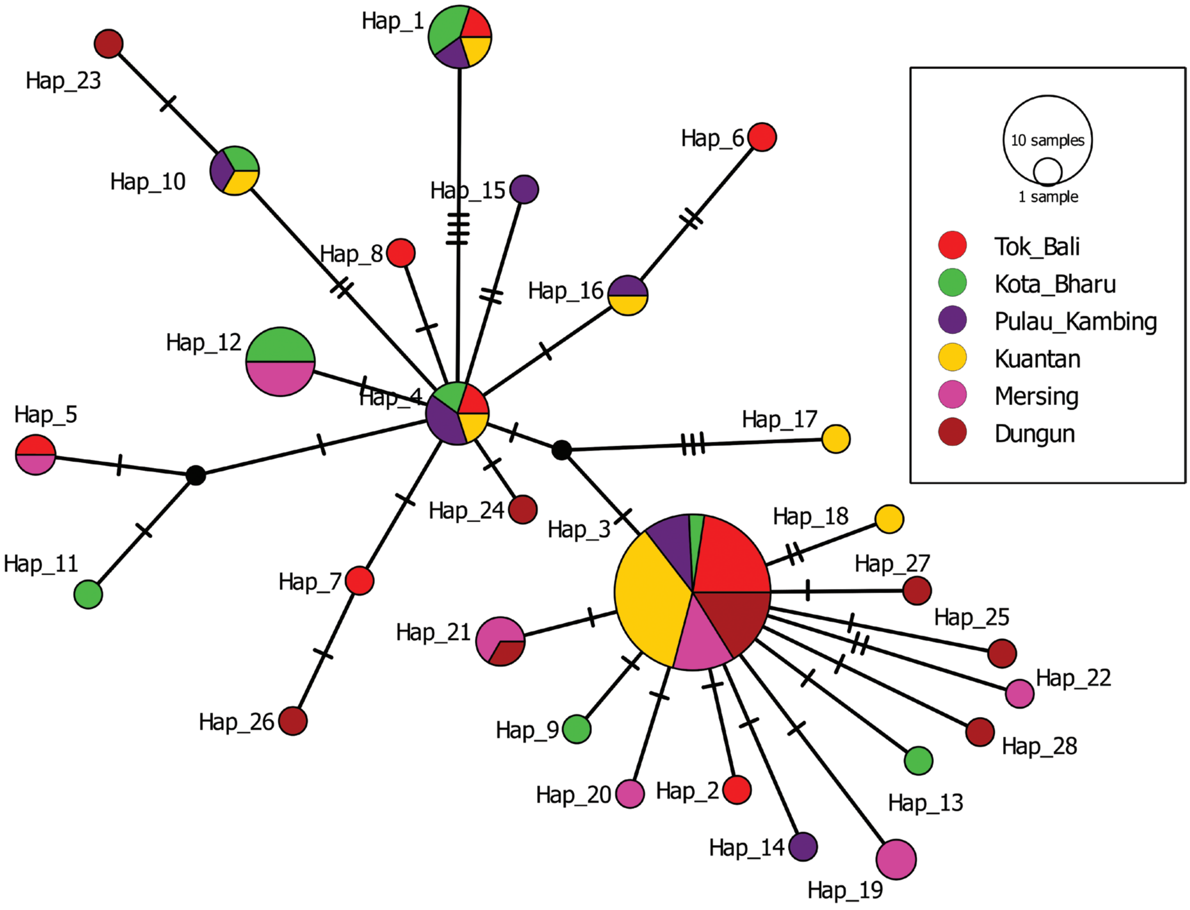

Figure 4. Median-joining haplotypes network diagram of *Lutjanus xanthopinnis* from the Malaysian waters of the South China Sea inferred from *Cyt-b* gene. Node size corresponds to the haplotype frequencies; minimum node size is one individual. Black dots indicate median vector. Dashed line is nucleotide mutation.

results revealed that the intra-population genetic variance was more significant than the inter-population genetic variation for both fragments (Tables 5, 6).

Table 5. Results of AMOVA for *Lutjanus xanthopinnis* inferred by mtDNA D-loop region.

Source of variation	df	Sum of squares	Variance components	Percentage of variation	*P* value
Among populations	5	35.167	0.10395 Va	1.91	0.067
Within populations	93	495.257	5.32534 Vb	98.09	
Total	98	530.424	5.42929		
Fixation Index (F_{ST}) = 0.019					

Table 6. Results of AMOVA for *Lutjanus xanthopinnis* inferred by mtDNA *Cyt-b* region.

Source of variation	df	Sum of squares	Variance components	Percentage of variation	*P* value
Among populations	5	9.688	0.04480 Va	3.19	0.08
Within populations	72	97.812	1.35849 Vb	96.81	
Total	77	107.5	5.42929		
Fixation Index (F_{ST}) = 0.031					

Demographic history. Both neutrality tests (Tajima's *D* and Fu's F_S) showed negative values, and non-significant *P* values at $P > 0.05$ in all studied populations as deduced by the *Cyt-b* and D-loop genes of mtDNA, respectively (Table 2). The disparities in population sizes after (θ_1) and before expansion (θ_0) for the D-loop marker were 7.566 and 2927.52, while 0.017 and 10.559 were estimated from the *Cyt-b* gene (Table 2). The τ value of D-loop was 5.092, while *Cyt-b* was 4.378 (Table 2). The estimated expansion period for *L. xanthopinnis* was 109 246 and 280 254 years ago, inferred by D-loop and *Cyt-b* genes. The Bayesian skyline plot (BSP) analysis indicated that increases in effective population size (N_E) were approximately 87 746 years ago, as inferred from the D-loop (Fig. 5A). In comparison, expansion started 75 244 years ago based on the *Cyt-b* marker (Fig. 5B). For both the total data sets and all sample stations, the Harpending's raggedness index (H_{RI}) and the sum of squared deviations (SSD) showed values that were low and not statistically significant (Table 2). The mismatch distribution (Fig. 6) conformed to the sudden expansion model despite distinct bimodality based on the low and non-significant values in the goodness of fit tests (H_{RI} and SSD).

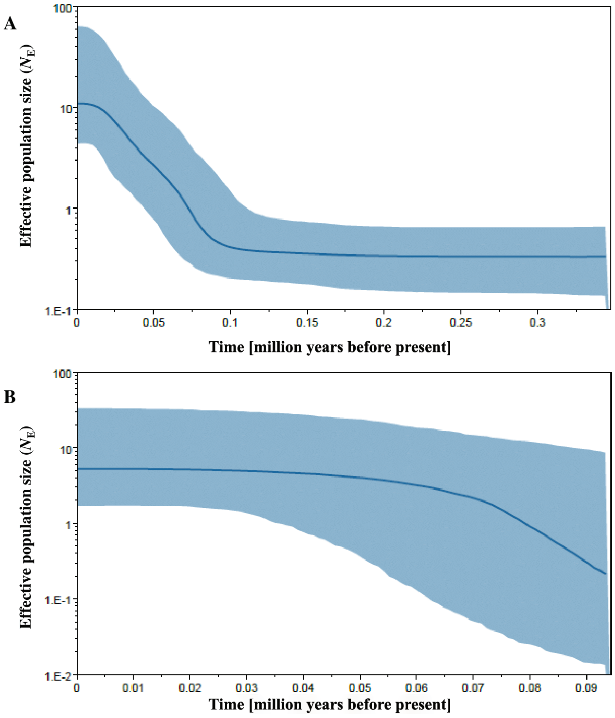

Figure 5. Bayesian Skyline Plots of the mtDNA (**A**) D-loop marker and (**B**) *Cyt-b* gene of *Lutjanus xanthopinnis* populations from Malaysian waters of the South China Sea. The dark blue line represents the mean and the shaded blue band indicates the standard error.

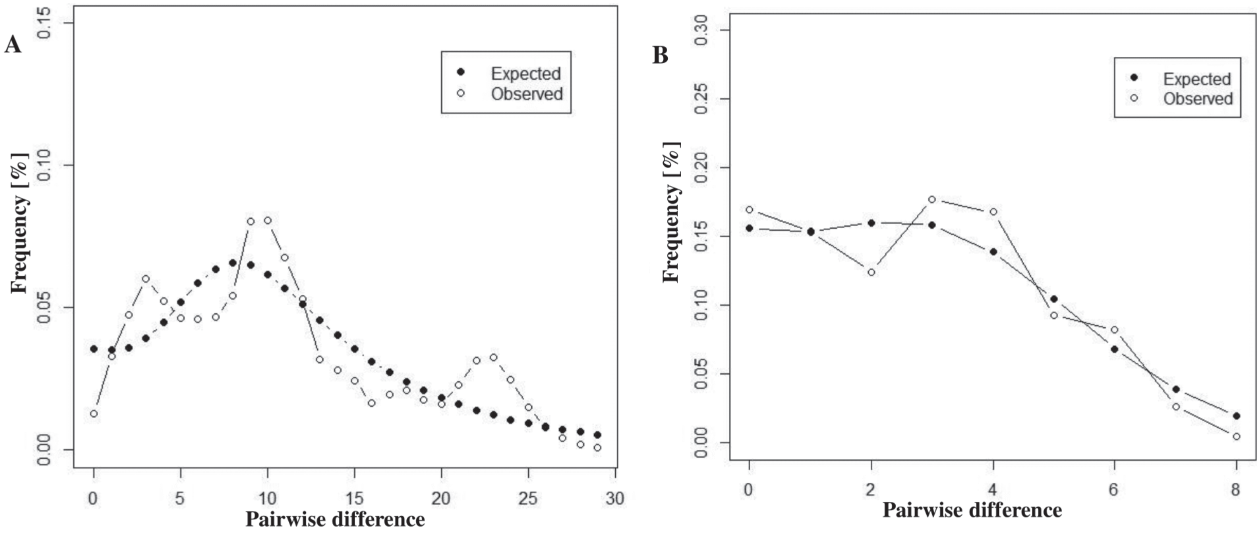

Figure 6. Mismatch distributions (pairwise number of differences) for the mtDNA (**A**) D-loop (**B**) *Cyt-b* genes of *Lutjanus xanthopinnis* from Malaysian waters of the South China Sea.

Discussion

The yellowfin snapper, *Lutjanus xanthopinnis* has only been recognized as a valid species since 2015 (Iwatsuki et al. 2015), although it had been subject to commercial exploitation in a mixed group with *L. madras* with which it had been erroneously synonymized. Thus, it is crucial to investigate the population genetics of this species to implement an efficient management strategy. The presently reported study is the first to investigate the population genetics of *L. xanthopinnis* from the waters of the South China Sea, bordering East Peninsula Malaysia using a combination of two mitochondrial markers.

Genetic diversity. The present levels of nucleotide and haplotype diversity can shed light on the demographic trends of communities in the past (Grant and Bowen 1998). Estimating a population's genetic diversity is based on these two basic metrics (Nei and Li 1979). The presently reported study reveals a high level of haplotype diversity (D-loop: 0.948–1.000; *Cyt-b*: 0.542–0.928) and low nucleotide diversity (D-loop: 0.0095–0.0159; *Cyt-b*: 0.0022–0.0049) observed in all locations where *L. xanthopinnis* was sampled (Table 2). A combination of high haplotype diversity (H) and low nucleotide diversity (D_N) suggests the presence of a large population that has undergone recent expansion, allowing for the persistence of recently generated alleles in the population without sufficient time to gather more nucleotide alternatives within the haplotypes (Grant and Bowen 1998; Delrieu-Trottin et al. 2017; Kasim et al. 2020; Tovar Verba et al. 2023). These findings coincide with earlier studies on several *Lutjanus* species, including the red snapper *Lutjanus campechanus* ($H = 0.946$, $D_N = 0.021$) (Garber et al. 2004), crimson snapper, *Lutjanus erythropterus* ($H = 0.946$, $D_N = 0.03$) (Zhang et al. 2006), southern red snapper, *Lutjanus purpureus* ($H = 0.99$, $D_N = 0.026$) (Gomes et al. 2012), mangrove red snapper *Lutjanus argentimaculatus* ($H = 0.929$, π- 0.003) (Gopalakrishnan et al. 2018), and dog snapper *Lutjanus jocu* ($H = 0.996$, $D_N = 0.036$) (Souza et al. 2019). In addition, the trend in genetic diversity estimates between the two markers in all aligns with the results reported by Silva et al. 2018, with the D-loop region having a greater level of genetic diversity than the *Cyt-b* because of the higher polymorphic sites and mutation rate in the former.

Population genetics structure. The populations of *L. xanthopinnis* from this part of the South China Sea of Malaysian waters showed no geographical structuring based on two mtDNA fragments. All statistical analyses corroborated this: gene trees consisting of a single clade (Fig. 2; Suppl. material 1) and undetermined genetic partition of haplotype networks (Figs. 3, 4), the statistically non-significant value of pairwise Φ_{ST} (Tables 3, 4) as well as lack of genetic differentiation in AMOVA (Tables 5, 6). These findings indicate a significant amount of genetic exchanges between the populations of *L. xanthopinnis* attributed to substantial gene flow. This trend is consistent with earlier research conducted on similar species in different regions of the world (Gomes et al. 2012; Gopalakrishnan et al. 2018; Souza et al. 2019; Veneza et al. 2023), which reflects a common evolutionary pattern among species in this group. A number of factors influence the genetic differentiation and flow of genes among marine organisms, such as planktonic larval stage, extended lifespan, distances and directions of dispersal and spawning pattern (Froukh and Kochzius 2007; Palumbi 2003; Pineda et al. 2007; Haye et al. 2014). The planktonic larval stage is believed to be a crucial determinant of the population genetic patterns of snapper (Tovar Verba et al. 2023). Facilitated by marine currents, the larvae could travel in a long-distance movement, thereby ensuring the continued existence of genetic connectivity. Furthermore, snappers form extensive spawning aggregations across their entire habitat (Claro and Lindeman 2003; Malafaia et al. 2021; Motta et al. 2022). Rahman et al. (2024) reported that *L. xanthopinnis* has a higher tendency to create spawning aggregations in the waters of Malaysia. The vast migration of adult individuals to breeding aggregations also contributes to genetic homogeneity. Typically, marine fishes exhibit minimal genetic differentiation because they can theoretically disperse throughout their life stages as there are no physical barriers preventing passage between basins of the ocean (Mandal et al. 2012).

Demographic history. Our study found that the populations of *L. xanthopinnis* throughout the East Peninsular Malaysian waters had recently undergone a population expansion history. However, the multimodal distribution curve in the mismatch analysis (Fig. 6) suggests population stability. But other lines of evidence such as the median-joining network displayed a star-like pattern, Tajima's D and Fu's F_S show negative values, while H_{RI} and SSD have non-significant values. These findings collectively suggest the presence of a recent demographic expansion. Previous studies on *Lutjanus* have exhibited the same historical demographic pattern. These have been reported in *Lutjanus synagris* (Linnaeus, 1758) (see Silva et al. 2018), *Lutjanus purpureus* (Poey, 1866) (see Gomes et al. 2012), and *Lutjanus argentimaculatus* (Forsskål, 1775) (see Gopalakrishnan et al. 2018). The tau value estimated a population expansion between 109 246 and 280 254 years ago for the mtDNA gene markers, D-loop and *Cyt-b*, respectively.

Additionally, the BSP analysis indicated that the population expansion occurred around 87 746 and 75 244 years ago. These events overlapped with the late Pleistocene, as shown in Fig. 5. The late Pleistocene Epoch is characterized by alternating glaciation and deglaciation periods at approximately 100 000-year intervals (Imbrie et al. 1992). The climatic shifts during the late Pleistocene resulted in alterations in temperature and salinity, consequently affecting the worldwide circulation of the ocean patterns (Bond et al. 1997; Petit et al. 1999). During glaciations, sea levels receded by 120–140 m below the current level, exposing most shallow water habitats. This significantly impacted marine life demographics, including eradication, displacement, recolonization, and population expansion (Hewitt 2000; Lambeck et al. 2002; Liu et al. 2006). Population expansions during the late Pleistocene period have also been previously reported in several other snappers for example in *Lutjanus erythropterus* (see Zhang et al. 2006), *L. purpureus* (see Gomes et al. 2012), *Lutjanus synagris* (Linnaeus, 1758) (see Silva et al. 2018), and *Lutjanus alexandrei* Moura et Lindeman, 2007 (see Veneza et al. 2023).

Based on this preliminary data, the *L. xanthopinnis* populations in the Malaysian waters bordered by the South China Sea could be considered a single stock unit as no population structuring was observed. However, this was based on two maternally inherited mtDNA markers. Furthermore, our work is constrained in its ability to examine other regions of the South China Sea due to the scarcity of specimens from other regions of Malaysian waters and the absence of haplotype sequences in any accessible database. Additional analysis should be conducted with autonomous, genomic nuclear markers, such as a microsatellite marker for a holistic approach to understanding the population genetic pattern in this region. This would also entail examining a broader geographical coverage and increasing the number of samples, particularly from other regions within the South China Sea.

Conclusions

The population structure of *Lutjanus xanthopinnis* still needs to be better understood, particularly in Malaysia. This is a significant challenge from a management perspective. The initial baseline population genetic data on *L. xanthopinnis* populations in the Malaysian South China Sea is crucial for authorities' planning and management strategies. Based on preliminary data, the *L. xanthopinnis* populations in the South China Sea of Malaysia could be considered a single stock unit because the two mtDNA markers revealed no population structure was present. According to their estimated demographic history, populations of *L. xanthopinnis* significantly expanded in the Late Pleistocene. When combined with other relevant data, this genetic information may help create efficient management strategies for Malaysia and other nearby nations that share the same waterways.

Acknowledgments

The study was funded by the Fundamental Research Grant Scheme (FRGS) with project reference FRGS/1/2021/WAB05/UMT/02/4, and the authors gratefully acknowledge the Malaysian Ministry of Higher Education (MoHE) for their support. We also appreciated the logistical assistance provided by the Faculty of Fisheries and Food Science at Universiti Malaysia Terengganu.

References

Adibah AB, Adamson EA, Juliana LH, Nor Mohd SA, Wei-Jen C, Man A, Darlina MN (2018) DNA barcoding of Malaysian commercial snapper reveals an unrecognized species of the yellow-lined *Lutjanus* (Pisces: Lutjanidae). PLoS ONE 13(9): e0202945. https://doi.org/10.1371/journal.pone.0202945

Alam MM, Westfall KM, Pálsson S (2017) Historical demography and genetic differentiation of the giant freshwater prawn *Macrobrachium rosenbergii* in Bangladesh based on mitochondrial and dd RAD sequence variation. Ecology and Evolution 7(12): 4326–4335. https://doi.org/10.1002/ece3.3023

Aljanabi SM, Martinez I (1997) Universal and rapid salt-extraction of high quality genomic DNA for PCR-based techniques. Nucleic Acids Research 25(22): 4692–4693. https://doi.org/10.1093/nar/25.22.4692

Allen GR (1985) FAO species catalogue: Vol. 6. Snappers of the world: An annotated and illustrated catalogue of lutjanid species known to date (No. 6). FAO, Rome.

Allio R, Donega S, Galtier N, Nabholz B (2017) Large variation in the ratio of mitochondrial to nuclear mutation rate across animals: Implications for genetic diversity and the use of mitochondrial DNA as a molecular marker. Molecular Biology and Evolution 34(11): 2762–2772. https://doi.org/10.1093/molbev/msx197

Arai T, Taha H, Alidon N, Jumat J, Azmey S, Zan ND, Jaafar TNAM, Habib A (2023) Mitochondrial cytochrome c oxidase subunit I gene analysis of the yellowfin snapper, *Lutjanus xanthopinnis* in the Indo–Pacific region and a note on *Lutjanus lutjanus* population structure. Heliyon 9(9): e19348. https://doi.org/10.1016/j.heliyon.2023.e19348

Bond G, Showers W, Cheseby M, Lotti R, Almasi P, DeMenocal P, Paul P, Heidi C, Irka H, Bonani G (1997) A pervasive millennial-scale cycle in North Atlantic Holocene and glacial climates. Science 278(5341): 1257–1266. https://doi.org/10.1126/science.278.5341.1257

Bouckaert R, Vaughan TG, Barido-Sottani J, Duchêne S, Fourment M, Gavryushkina A, Heled J, Jones G, Kühnert D, De Maio N, Matschiner M, Mendes FK, Müller NF, Ogilvie HA, du Plessis L, Popinga A, Rambaut A, Rasmussen D, Siveroni I, Suchard MA, Wu C-H, Xie D, Zhang C, Stadler T, Drummond AJ (2019) BEAST 2.5: An advanced software platform for Bayesian evolutionary analysis. PLoS Computational Biology 15(4): e1006650. https://doi.org/10.1371/journal.pcbi.1006650

Bowen BW, Bass AL, Rocha LA, Grant WS, Robertson DR (2001) Phylogeography of the trumpetfishes (*Aulostomus*): Ring species complex on a global scale. Evolution 55(5): 1029–1039. https://doi.org/10.1554/0014-3820(2001)055[1029:POTTAR]2.0.CO;2

Carpenter KE, Al Abdali FSH, Al Buwaiqi B, Al Kindi ASM, Ambuali A, Borsa P, Govender A, Russell B (2019) *Lutjanus xanthopinnis*. IUCN Red List of Threatened Species 2019: e.T137566591A137566868. [Accessed on 02 August 2024.] https://doi.org/10.2305/IUCN.UK.2019-2.RLTS.T137566591A137566868.en

Claro R, Lindeman KC (2003) Spawning aggregation sites of snapper and grouper species (Lutjanidae and Serranidae) on the insular shelf of Cuba. Gulf and Caribbean Research 14(2): 91–106. https://doi.org/10.18785/gcr.1402.07

Clement M, Posada DCKA, Crandall KA (2000) TCS: A computer program to estimate gene genealogies. Molecular Ecology 9(10): 1657–1659. https://doi.org/10.1046/j.1365-294x.2000.01020.x

Delrieu-Trottin E, Mona S, Maynard J, Neglia V, Veuille M, Planes S (2017) Population expansions dominate demographic histories of endemic and widespread Pacific reef fishes. Scientific Reports 7(1): 40519. https://doi.org/10.1038/srep40519

DOF (2023) Annual fisheries statistics 2022. Department of Fisheries Malaysia. http://www.dof.gov.my/en/fishery-statistics

Donaldson KA, Wilson Jr RR (1999) Amphi-panamic geminates of snook (Percoidei: Centropomidae) provide a calibration of the divergence rate in the mitochondrial DNA control region of fishes. Molecular Phylogenetics and Evolution 13(1): 208–213. https://doi.org/10.1006/mpev.1999.0625

Excoffier L, Lischer HE (2010) Arlequin suite ver 3.5: A new series of programs to perform population genetics analyses under Linux and Windows. Molecular Ecology Resources 10(3): 564–567. https://doi.org/10.1111/j.1755-0998.2010.02847.x

Felsenstein J (1985) Confidence limits on phylogenies: An approach using the bootstrap. Evolution; International Journal of Organic Evolution 39(4): 783–791. https://doi.org/10.2307/2408678

Ferreri M, Qu W, Han BO (2011) Phylogenetic networks: A tool to display character conflict and demographic history. African Journal of Biotechnology 10(60): 12799–12803. https://doi.org/10.5897/AJB11.010

Froese R, Pauly D (Eds) (2023) FishBase. [Version 10/2023] http://www.fishbase.org

Froukh T, Kochzius M (2007) Genetic population structure of the endemic fourline wrasse (*Larabicus quadrilineatus*) suggests limited larval dispersal distances in the Red Sea. Molecular Ecology 16(7): 1359–1367. https://doi.org/10.1111/j.1365-294X.2007.03236.x

Fu YX (1997) Statistical tests of neutrality of mutations against population growth, hitch hiking and background selection. Genetics 147(2): 915–925. https://doi.org/10.1093/genetics/147.2.915

Garber AF, Tringali MD, Stuck KC (2004) Population structure and variation in red snapper (*Lutjanus campechanus*) from the Gulf of Mexico and Atlantic coast of Florida as determined from mitochondrial DNA control region sequence. Marine Biotechnology 6(2): 175–185. https://doi.org/10.1007/s10126-003-0023-7

Gomes G, Sampaio I, Schneider H (2012) Population Structure of *Lutjanus purpureus* (Lutjanidae-Perciformes) on the Brazilian coast: Further existence evidence of a single species of red snapper in the western Atlantic. Anais da Academia Brasileira de Ciências 84(4): 979–999. https://doi.org/10.1590/S0001-37652012000400013

Gonzalez F, Barria P, Ponce F, Mora S (2023) Population Genetic Structure of Marine Fishes. https://doi.org/10.5772/intechopen.112694

Gopalakrishnan A, Vineesh N, Ismail S, Menon M, Akhilesh KV, Jeena NS, Paulton MP, Vijayagopal P (2018) Mitochondrial signatures revealed panmixia in *Lutjanus argentimaculatus* (Forsskål 1775). Journal of Genetics 97(1): 179–187. https://doi.org/10.1007/s12041-018-0899-7

Grant WAS, Bowen BW (1998) Shallow population histories in deep evolutionary lineages of marine fishes: Insights from sardines and anchovies and lessons for conservation. Journal of Heredity 89(5): 415–426. https://doi.org/10.1093/jhered/89.5.415

Guo Y, Wang Z, Liu C, Liu L, Liu Y (2007) Phylogenetic relationships of South China Sea snappers (genus *Lutjanus*; family Lutjanidae) based on mitochondrial DNA sequences. Marine Biotechnology 9(6): 682–688. https://doi.org/10.1007/s10126-007-9012-6

Habib A, Sulaiman Z (2016) High genetic connectivity of narrow-barred Spanish mackerel (*Scomberomorus commerson*) from the South China, Bali and Java Seas. Zoology and Ecology 26(2): 93–99. https://doi.org/10.1080/21658005.2016.1161121

Habib A, Sulaiman Z (2017) Mitochondrial DNA analyses of narrow-barred Spanish mackerel (*Scomberomorus commerson*) sampled from the Arabian Sea, the Bay of Bengal, and the Indo–Malay archipelago. Zoology and Ecology 27(3–4): 245–250. https://doi.org/10.1080/21658005.2017.1385990

Halim LJ, Rahim I, Mahboob S, Al-Ghanim KA, Asmiaty AMAT, Naim DM (2022) Phylogenetic relationships of the commercial red snapper (Lutjanidae sp.) from three marine regions. Journal of King Saud University - Science 34(2): 101756. https://doi.org/10.1016/j.jksus.2021.101756

Hasegawa M, Kishino H, Yano TA (1985) Dating of the human-ape splitting by a molecular clock of mitochondrial DNA. Journal of Molecular Evolution 22(2): 160–174. https://doi.org/10.1007/BF02101694

Haye PA, Segovia NI, Muñoz-Herrera NC, Gálvez FE, Martínez A, Meynard María C (2014) Phylogeographic structure in benthic marine invertebrates of the southeast Pacific coast of Chile with differing dispersal potential. PLoS ONE 9(2): e88613. https://doi.org/10.1371/journal.pone.0088613

Hernández-Álvarez C, Bayona-Vásquez NJ, Domínguez-Domínguez O, Uribe-Alcocer M, Díaz-Jaimes P (2020) Phylogeography of the pacific red snapper (*Lutjanus peru*) and spotted rose snapper (*Lutjanus guttatus*) in the inshore Tropical Eastern Pacific. Copeia 108(1): 61–71. https://doi.org/10.1643/CG-18-157

Hewitt G (2000) The genetic legacy of the Quaternary ice ages. Nature 405(6789): 907–913. https://doi.org/10.1038/35016000

Imbrie J, Boyle EA, Clemens SC, Duffy A, Howard WR, Kukla G, Kutzbach J, Martinson DG, McIntyre A, Mix AC, Molfino B, Morley JJ, Peterson LC, Pisias NG, Prell WL, Raymo ME, Shackleton NJ, Toggweiler JR (1992) On the structure and origin of major glaciation cycles 1. Linear responses to Milankovitch forcing. Paleoceanography 7(6): 701–738. https://doi.org/10.1029/92PA02253

Iwatsuki Y, Tanaka F, Allen GR (2015) *Lutjanus xanthopinnis*, a new species of snapper (Pisces: Lutjanidae) from the Indo–west Pacific, with a redescription of *Lutjanus madras* (Valenciennes 1831). Journal of the Ocean Science Foundation 17: 22–42.

Kasim NS, Jaafar TNAM, Piah RM, Arshaad WM, Nor SAM, Habib A, Ghaffar MA, Sung YY, Danish-Daniel M, Tan MP (2020) Recent population expansion of longtail tuna *Thunnus tonggol* (Bleeker, 1851) inferred from the mitochondrial DNA markers. PeerJ 8: e9679. https://doi.org/10.7717/peerj.9679

Laikre L, Palm S, Ryman N (2005) Genetic population structure of fishes: Implications for coastal zone management. Ambio 34(2): 111–119. https://doi.org/10.1579/0044-7447-34.2.111

Lambeck K, Esat TM, Potter EK (2002) Links between climate and sea levels for the past three million years. Nature 419(6903): 199–206. https://doi.org/10.1038/nature01089

Lee WJ, Conroy J, Howell WH, Kocher TD (1995) Structure and evolution of teleost mitochondrial control regions. Journal of Molecular Evolution 41(1): 54–66. https://doi.org/10.1007/BF00174041

Leigh JW, Bryant D (2015) POPART: Full-feature software for haplotype network construction. Methods in Ecology and Evolution 6(9): 1110–1116. https://doi.org/10.1111/2041-210X.12410

Lessios HA (2008) The great American schism: Divergence of marine organisms after the rise of the Central American Isthmus. Annual Review of Ecology, Evolution, and Systematics 39(1): 63–91. https://doi.org/10.1146/annurev.ecolsys.38.091206.095815

Li L, Chu-Wu L (2007) Genetic diversity and molecular markers of five snapper species. Chinese Journal of Agricultural Biotechnology 4(1): 39–46. https://doi.org/10.1017/S1479236207001210

Liu JX, Gao TX, Yokogawa K, Zhang YP (2006) Differential population structuring and demographic history of two closely related fish species, Japanese sea bass (*Lateolabrax japonicus*) and spotted sea bass (*Lateolabrax maculatus*) in northwestern Pacific. Molecular Phylogenetics and Evolution 39(3): 799–811. https://doi.org/10.1016/j.ympev.2006.01.009

Malafaia PN, França AR, Olavo G (2021) Spawning aggregation sites of the cubera snapper, *Lutjanus cyanopterus*, on the continental shelf of Bahia state, northeastern Brazil. Fisheries Research 242: 106037. https://doi.org/10.1016/j.fishres.2021.106037

Mandal A, Rao D, Karuppaiah D, Gopalakrishnan A, Pozhoth J, Samraj YCT, Doyle RW (2012) Population genetic structure of *Penaeus monodon*, in relation to monsoon current patterns in southwest, east and Andaman coastal waters of India. Gene 491(2): 149–157. https://doi.org/10.1016/j.gene.2011.10.002

Messias MA, Alves TI, Melo CM, Lima M, Rivera-Rebella C, Rodrigues DF, Madi RR (2019) Ethnoecology of Lutjanidae (snappers) in communities of artisanal fisheries in northeast Brazil. Ocean and Coastal Management 181: 104866. https://doi.org/10.1016/j.ocecoaman.2019.104866

Mohd Yusoff NIS, Mat Jaafar TNA, Vilasri V, Mohd Nor SA, Seah YG, Habib A, Wong LL, Danish-Daniel M, Sung YY, Mazlan AG, Mat Piah R, Tan MP (2021) Genetic diversity, population structure and historical demography of the two-spined yellowtail stargazer (*Uranoscopus cognatus*). Scientific Reports 11(1): 13357. https://doi.org/10.1038/s41598-021-92905-6

Motta FS, Freitas MO, Rolim FA, Abilhoa V, Pereira Filho GH (2022) Direct evidence of a spawning aggregation of cubera snapper (*Lutjanus cyanopterus*) in southeastern Brazil and its management implications. Fisheries Research 252: 106339. https://doi.org/10.1016/j.fishres.2022.106339

Nei M, Li WH (1979) Mathematical model for studying genetic variation in terms of restriction endonucleases. Proceedings of the National Academy of Sciences of the United States of America 76(10): 5269–5273. https://doi.org/10.1073/pnas.76.10.5269

Ovenden JR, Berry O, Welch DJ, Buckworth RC, Dichmont CM (2015) Ocean's eleven: A critical evaluation of the role of population, evolutionary and molecular genetics in the management of wild fisheries. Fish and Fisheries 16(1): 125–159. https://doi.org/10.1111/faf.12052

Palumbi SR (2003) Population genetics, demographic connectivity, and the design of marine reserves. Ecological Applications 13(sp1): 146–158. https://doi.org/10.1890/1051-0761(2003)013[0146:PGDCAT]2.0.CO;2

Petit JR, Jouzel J, Raynaud D, Barkov NI, Barnola JM, Basile I, Bender M, Chappellaz J, Davis M, Delaygue G, Stievenard M (1999) Climate and atmospheric history of the past 420,000 years from the Vostok ice core, Antarctica. Nature 399(6735): 429–436. https://doi.org/10.1038/20859

Pineda J, Hare JA, Sponaugle S (2007) Larval transport and dispersal in the coastal ocean and consequences for population connectivity. Oceanography (Washington, D.C.) 20(3): 22–39. https://doi.org/10.5670/oceanog.2007.27

R Core Team (2023) R: A language and environment for statistical computing. R Foundation for Statistical Computing, Vienna, Austria. http://www.R-project.org

Rahman MM, Ariffin NA, Seah YG, Jaafar TNAM, Habib A (2023) Length–weight relationships and relative condition factors of three coral-associated *Lutjanus* species from Terengganu waters of the South China Sea, Malaysia. Turkish Journal of Zoology 47(4): 216–221. https://doi.org/10.55730/1300-0179.3134

Rahman MM, Ariffin NA, Seah YG, Jaafar TNAM, Fadzli MH, Habib A (2024) Reproductive features of data-deficient yellowfin snapper, *Lutjanus xanthopinnis* (Actinopterygii: Eupercaria: Lutjanidae), from east-coast of Peninsular Malaysia: Implications for sustainable fisheries management. Acta Ichthyologica et Piscatoria 54: 63–74. https://doi.org/10.3897/aiep.54.112995

Rambaut A, Drummond AJ, Xie D, Baele G, Suchard MA (2018) Posterior summarization in Bayesian phylogenetics using Tracer 1.7. Systematic Biology 67(5): 901–904. https://doi.org/10.1093/sysbio/syy032

Rogers AR, Harpending H (1992) Population growth makes waves in the distribution of pairwise genetic differences. Molecular Biology and Evolution 9(3): 552–569.

Rozas J, Ferrer-Mata A, Sánchez-DelBarrio JC, Guirao-Rico S, Librado P, Ramos-Onsins SE, Sánchez-Gracia A (2017) DnaSP 6: DNA sequence polymorphism analysis of large data sets. Molecular Biology and Evolution 34(12): 3299–3302. https://doi.org/10.1093/molbev/msx248

Silva D, Martins K, Oliveira J, da Silva R, Sampaio I, Schneider H, Gomes G (2018) Genetic differentiation in populations of lane snapper (*Lutjanus synagris*–Lutjanidae) from Western Atlantic as revealed by multilocus analysis. Fisheries Research 198: 138–149. https://doi.org/10.1016/j.fishres.2017.10.005

Slatkin M, Hudson RR (1991) Pairwise comparisons of mitochondrial DNA sequences in stable and exponentially growing populations. Genetics 129(2): 555–562. https://doi.org/10.1093/genetics/129.2.555

Song CB, Near TJ, Page LM (1998) Phylogenetic relations among percid fishes as inferred from mitochondrial cytochrome b DNA sequence data. Molecular Phylogenetics and Evolution 10(3): 343–353. https://doi.org/10.1006/mpev.1998.0542

Souza ASD, Dias Júnior EA, Perez MF, Cioffi MDB, Bertollo LAC, Garcia-Machado E, Marcelo NSV, Galetti PMJ, Molina WF (2019) Phylogeography and historical demography of two sympatric Atlantic snappers: *Lutjanus analis* and *L. jocu*. Frontiers in Marine Science 6: 545. https://doi.org/10.3389/fmars.2019.00545

Tajima F (1989) Statistical method for testing the neutral mutation hypothesis by DNA polymorphism. Genetics 123(3): 585–595. https://doi.org/10.1093/genetics/123.3.585

Tamura K (1992) Estimation of the number of nucleotide substitutions when there are strong transition-transversion and G+ C-content biases. Molecular Biology and Evolution 9(4): 678–687.

Tamura K, Stecher G, Kumar S (2021) MEGA 11: Molecular evolutionary genetics analysis version 11. Molecular Biology and Evolution 38(7): 3022–3027. https://doi.org/10.1093/molbev/msab120

Tan MP, Amornsakun T, Siti Azizah MN, Habib A, Sung YY, Danish-Daniel M (2019) Hidden genetic diversity in snakeskin gourami, *Trichopodus pectoralis* (Perciformes, Osphronemidae), inferred from the mitochondrial DNA CO1 gene. Mitochondrial DNA, Part B, Resources 4(2): 2966–2969. https://doi.org/10.1080/23802359.2019.1662741

Tovar Verba J, Stow A, Bein B, Pennino MG, Lopes PF, Ferreira BP, Meghana M, Sergio MQL, Pereira RJ (2023) Low population genetic structure is consistent with high habitat connectivity in a commercially important fish species (*Lutjanus jocu*). Marine Biology 170(1): 5. https://doi.org/10.1007/s00227-022-04149-1

Veneza I, da Silva R, Ferreira C, Mendonça P, Sampaio I, Evangelista-Gomes G (2023) Genetic connectivity and population expansion inferred from multilocus analysis in *Lutjanus alexandrei* (Lutjanidae–Perciformes), an endemic snapper from northeastern Brazilian coast. PeerJ 11: e15973. https://doi.org/10.7717/peerj.15973

Yildirim Y (2016) Genetic structure of *Pleurobranchaea maculata* in New Zealand. PhD thesis in Genetics, New Zealand Institute for Advanced Study, Massey University, Auckland, New Zealand.

Zhang J, Cai Z, Huang L (2006) Population genetic structure of crimson snapper *Lutjanus erythropterus* in East Asia, revealed by analysis of the mitochondrial control region. ICES Journal of Marine Science 63(4): 693–704. https://doi.org/10.1016/j.icesjms.2006.01.004

Supplementary material 1

Phylogenetic tree

Authors: Md Moshiur Rahman, Nur Asma Ariffin, Ying Giat Seah, Siti Azizah Mohd Nor, Tun Nurul Aimi Mat Jaafar, Nuralif Fakhrullah Mohd Nur, Ahasan Habib

Data type: png

Link: https://doi.org/10.3897/aiep.54.123026.suppl1

Acta Ichthyologica et Piscatoria 54, 2024, 203–208 | DOI 10.3897/aiep.54.127385

PENSOFT.

ACTA ICHTHYOLOGICA ET PISCATORIA

Length–weight relations of underutilized nine fish species (Actinopterygii) from set-net fishery, Mie, Japan

Mio KATO[1], Yutaro KAWANO[1], Minoru KANAIWA[1]

1 *Faculty of Bioresources, Mie University, Tsu, Japan*

https://zoobank.org/E7535C55-C464-460E-B6E2-57FEC5889A33

Corresponding author: Minoru Kanaiwa (kanaiwa@bio.mie-u.ac.jp)

Academic editor: Rodolfo Reyes ♦ **Received** 13 May 2024 ♦ **Accepted** 6 June 2024 ♦ **Published** 24 September 2024

Citation: Kato M, Kawano Y, Kanaiwa M (2024) Length–weight relations of underutilized nine fish species (Actinopterygii) from set-net fishery, Mie, Japan. Acta Ichthyologica et Piscatoria 54: 203–208. https://doi.org/10.3897/aiep.54.127385

Abstract

Bycatch, the unintentional capture of non-target species, poses a significant challenge in fisheries management worldwide. Underutilized bycatch species often lack biological information, hindering the assessment of their stock status and the implementation of appropriate management strategies. This study investigated the length–weight relations (LWRs) of 9 of 14 underutilized bycatch fish species collected from set-net fisheries in Nishiki, Mie Prefecture, Japan, during the 2018–2020 fishing seasons. The following fish species were studied: *Hyperoglyphe japonica* (Döderlein, 1884); *Labracoglossa argenteiventris* Peters, 1866; *Macroramphosus sagifue* Jordan et Starks, 1902; *Microcanthus strigatus* (Cuvier, 1831); *Ostorhinchus semilineatus* (Temminck et Schlegel, 1843); *Parapriacanthus ransonneti* Steindachner, 1870; *Rexea prometheoides* (Bleeker, 1856); *Siganus fuscescens* (Houttuyn, 1782); *Upeneus japonicus* (Houttuyn, 1782). A total of 251 fishing operations were conducted, and the collected fish specimens were measured for length (fork length) and wet weight. Simple regression analysis was performed on the logarithm of length and weight data to estimate the LWR parameters (a, b, and R^2) for each species. The estimated values of the relative growth coefficient (b) ranged from 2.862 to 3.311, and the coefficients of determination (R^2) were above 0.8 for all species, indicating robust LWR estimations. Notably, five species were not previously listed or credibly described in FishBase, and four were new records for the Japanese coast. This study provides new biological information on LWRs for underutilized bycatch fish species, contributing to our understanding of their population dynamics and supporting future management efforts for sustainable fisheries and biodiversity conservation.

Keywords

biodiversity conservation, bycatch, fisheries management, length–weight relation, population dynamics, set-net fishery, stock assessment, underutilized fish species

Introduction

The waters surrounding Japan boast exceptionally high species diversity, even on a global scale (Fujikura et al. 2010). Various fishing methods have been employed along Japan's coast since ancient times. These methods, including set nets, seine nets, trawl nets, and gillnets, capture a diverse array of fish species. In coastal fisheries, the primary target species for catch are those with high commercial value and large landings. However, due to the wide variety of species targeted for catch, unintentional bycatch of other species is common.

Bycatch refers to catches that are not specifically targeted, utilized, or managed catches. It is reported to constitute 40.4% of the global ocean catch (Hall 1996; Davies et al. 2009). This unintentional bycatch threatens the stock status of the affected fish species. The lack of information for stock assessment poses a significant challenge (Hall 1996). Accumulating detailed information on biological characteristics, in addition to species, size, and weight, is essential to consider appropriate bycatch management.

However, studies on bycatch of non-target fish species (i.e., often underutilized), excluding sea turtles, marine mammals, and seabirds, usually provide broad, country-specific, or fishery-specific examples (Alverson et al. 1994; Kelleher 2005; Finkbeiner et al. 2011; Oliver et al. 2015). These studies lack biological data (Kindong et al. 2020; Armelloni et al. 2021; Heimann et al. 2023). Information on underutilized fish is seldom recorded during fish surveys (Stohs and Harmon 2022), hindering assessments of their distribution, abundance, and population structure. Fish surveys often record bycatch of non-fish vertebrates and large crustaceans, which can result in undesirable mortality of both target and non-target species.

Length–weight relations (LWR) are crucial ecological data for understanding underutilized fish species. LWR provides valuable insights into fish population dynamics, aiding in stock assessments, size limit determinations, and fishing quota settings (Rodríguez-García et al. 2023). Understanding the LWR of each fish species enables tracking changes in body mass index and length composition, estimating growth patterns, and body condition of sampled fish specimens (Shubhadeep et al. 2022). Establishing LWRs for newly recorded fish species is vital for estimating biological weights and observing changes over time (Kodeeswaran et al. 2020). Thus, summarizing LWRs of bycatch species is crucial for enhancing our comprehension of fish populations and providing valuable insights for future research and management endeavors.

The set-net fishery is one of Japan's primary fisheries, contributing approximately 40% of the total production in Japan's coastal fisheries (Akiyama 2007; Anonymous 2024). It represents a passive fishing method, leading to the capture of various species due to low selectivity yet raising concerns about bycatch (Cheng and Chen 1997; Akiyama 2007). This study aimed to estimate the length–weight relations (LWR) of underutilized bycatch fish species collected from set nets in Nishiki, Oki-cho, Mie Prefecture, facing the Pacific Ocean.

Materials and methods

The study was conducted on large set nets operating in the northern coastal area of the Kumano-nada Sea. This set net was positioned off the coast of Nishiki, Taiki-cho, Watarai-gun, Mie Prefecture (34°11′38″N, 136°24′31″E) (Fig. 1) and comprised a total length of 230 m with an installed depth of 50 m. The set net consisted of two final chambers with the top covered. Surveys were conducted 26 times during the 2018 fishing season (28 Nov. 2018–17 Jun. 2019), 94 times during the 2019 fishing season (2 Dec. 2019–21 Jul. 2020), and 131 times during the 2020 fishing season (2 Dec. 2020–18 Jun. 2021), totaling 251 operations.

During the study, researchers boarded a set-net fishing boat to collect underutilized bycatch species that the fishermen sorted after the catch was hauled on board. The remainder of the catch was landed at Nishiki Port (34°12′54″N, 136°23′40″E). The landed catch was further sorted on a sorting table, and underutilized fish species that were discarded in the process were also collected. The collected

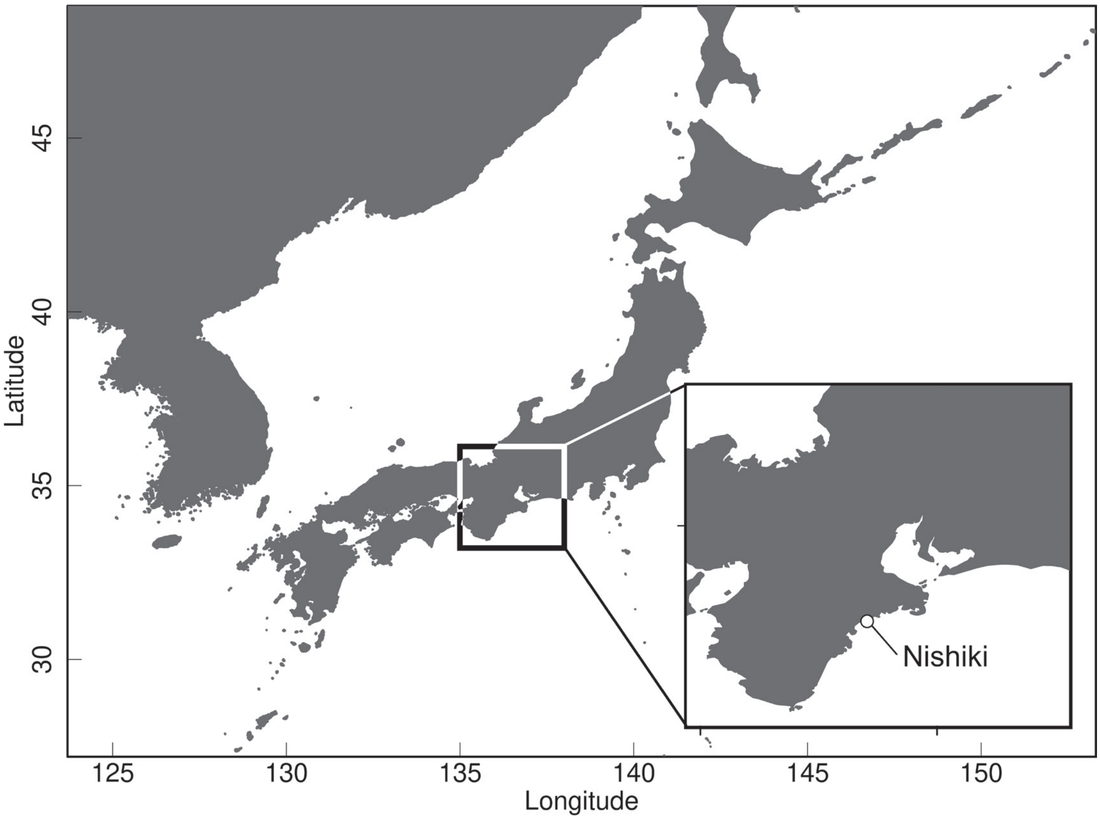

Figure 1. Location of the Nishiki in Mie Prefecture, Japan.

unutilized bycatch species were measured for length (fork length) and wet weight. Fork length was measured in 1 cm increments, weight less than 1 kg in 1 g increments, and weight greater than 1 kg in 10 g increments. Species identification was based on standard literature (Nakabo 2013).

In the analysis, simple regression analysis was performed on the logarithm of fork length (L) and weight (W) (log L, log W) for the bony fish species that could be discriminated to species. The calculated Cook's distance was rounded to the second decimal place, and values greater than 1 were excluded as outliers (Cook and Weisberg 1982). After outliers were excluded, species with ten or more observations were considered for analysis. For each analyzed fish species, the relation between L and W was applied to the allometric equation

$$W = aL^b$$

to calculate the initial growth coefficient a, relative growth coefficient b, and determination coefficient R^2. The statistical analyses were performed with R 4.2.2 (R Core Team 2022).

A large-scale language models, Claude 3 (https://www.anthropic.com/claude), were used for the English review of this manuscript.

Results

The survey revealed that a total of 679.4 tonnes of total catch weight was landed during 251 operations during the 2018–2020 fishing season. A total of 208 species with a total weight of 5.9 tonnes of underutilized bycatch species were recovered, representing 1% of the total catch weight landed. Bony fish species comprised 152 species and 1227 kg, or 31% of the total. The analyzed bony fishes encompassed 14 species from 13 orders and 14 families. Five of these species were removed from the final results because three species of them had either significantly low R^2 values such as *Abudefduf vaigiensis* (Quoy et Gaimard, 1825); *Lagocephalus sceleratus* (Gmelin, 1789); and *Pempheris schwenkii* Bleeker, 1855 or were deviated significantly from the a or b values of existing reports in FishBase (Froese and Pauly 2024), such as *Pterocaesio trilineata* Carpenter, 1987, and *Spratelloides gracilis* (Temminck et Schlegel, 1846). Commonly exploited species like *Engraulis japonicus* Temminck et Schlegel, 1846 and *Sardinops melanosticta* (Temminck et Schlegel, 1846) were also caught as bycatch at the study site but were excluded from the analysis in this study. The presently reported study focused on a total of 909 fish individuals representing the following nine fish species: *Hyperoglyphe japonica* (Döderlein, 1884); *Labracoglossa argenteiventris* Peters, 1866; *Macroramphosus sagifue* Jordan et Starks, 1902; *Microcanthus strigatus* (Cuvier, 1831); *Ostorhinchus semilineatus* (Temminck et Schlegel, 1843); *Parapriacanthus ransonneti* Steindachner, 1870; *Rexea prometheoides* (Bleeker, 1856); *Siganus fuscescens* (Houttuyn, 1782); *Upeneus japonicus* (Houttuyn, 1782). Those fishes belonged to eight orders and nine families (Table 1).

The relation between weight (W) and fork length (L) was plotted for 9 species (Fig. 2), revealing distinct patterns for each fish species. The number of samples, along with length, weight, and estimated values of a, b, and R^2 for each fish species, are presented in Table 1. The a values ranged from 0.003 (*Rexea prometheoides*) to 0.019 (*Parapriacanthus ransonneti*; *Upeneus japonicus*), while the b values ranged from 2.862 (*Macroramphosus sagifue*) to 3.311 (*Hyperoglyphe japonica*). High coefficients of determination (R^2 values) ranging from 0.806 (*Parapriacanthus ransonneti*) to 0.994 (*Hyperoglyphe japonica*) were obtained for all species.

Table 1. Length–weight relation (LWR) parameters of 9 underutilized fish species sampled in Nishiki, Japan.

Species	***n***	**Fork length [cm]**		**Weight [g]**		**Regression parameters**				
[FAMILY]		**Range**	**Mean ± SD**	**Range**	**Mean ± SD**	***a***	**95% CI of *a***	***b***	**95 CI of *b***	**R^2**
Hyperoglyphe japonica [CENTROLOPHIDAE]	13	11.2–24.9	20.15 ± 3.91	25–400	162.46 ± 104.20	0.012	0.010–0.015	3.311	3.225–3.397	0.994
Labracoglossa argenteiventris [KYPHOSIDAE]	155	4.6–16.7	8.35 ± 2.27	1–72	9.89 ± 13.64	0.007	0.006–0.009	3.272	3.170–3.373	0.963
Macroramphosus sagifue [CENTRISCIDAE]	53	4.4–9.6	7.31 ± 1.23	1–7	2.70 ± 1.37	0.008	0.005–0.015	2.862	2.569–3.154	0.881
Microcanthus strigatus [KYPHOSIDAE]	37	3.7–16.2	10.33 ± 5.02	1–135	50.24 ± 45.29	0.012	0.002–0.064	3.125	2.559–3.691	0.924
Ostorhinchus semilineatus [APOGONIDAE]	397	4.7–11.5	7.33 ± 1.43	1–25	6.69 ± 4.51	0.014	0.012–0.017	3.034	2.945–3.124	0.919
Parapriacanthus ransonneti [PEMPHERIDAE]	97	4.9–7.8	6.20 ± 0.62	2–9	4.35 ± 1.38	0.019	0.011–0.032	2.971	2.676–3.265	0.806
Rexea prometheoides [GEMPYLIDAE]	19	18.3–22.2	20.30 ± 0.96	43–90	62.26 ± 10.50	0.003	0.0004–0.020	3.307	2.662–3.952	0.866
Siganus fuscescens [SIGANIDAE]	119	13.3–38.6	29.99 ± 5.28	33–1160	531.24 ± 232.70	0.008	0.005–0.012	3.239	3.114–3.363	0.957
Upeneus japonicus [MULLIDAE]	22	8.8–17.0	13.84 ± 2.08	9–77	41.05 ± 16.63)	0.011	0.005–0.025	3.091	2.794–3.388	0.957

a is the intercept and b is the slope of the linear LWR regression; CI is the confidence interval.

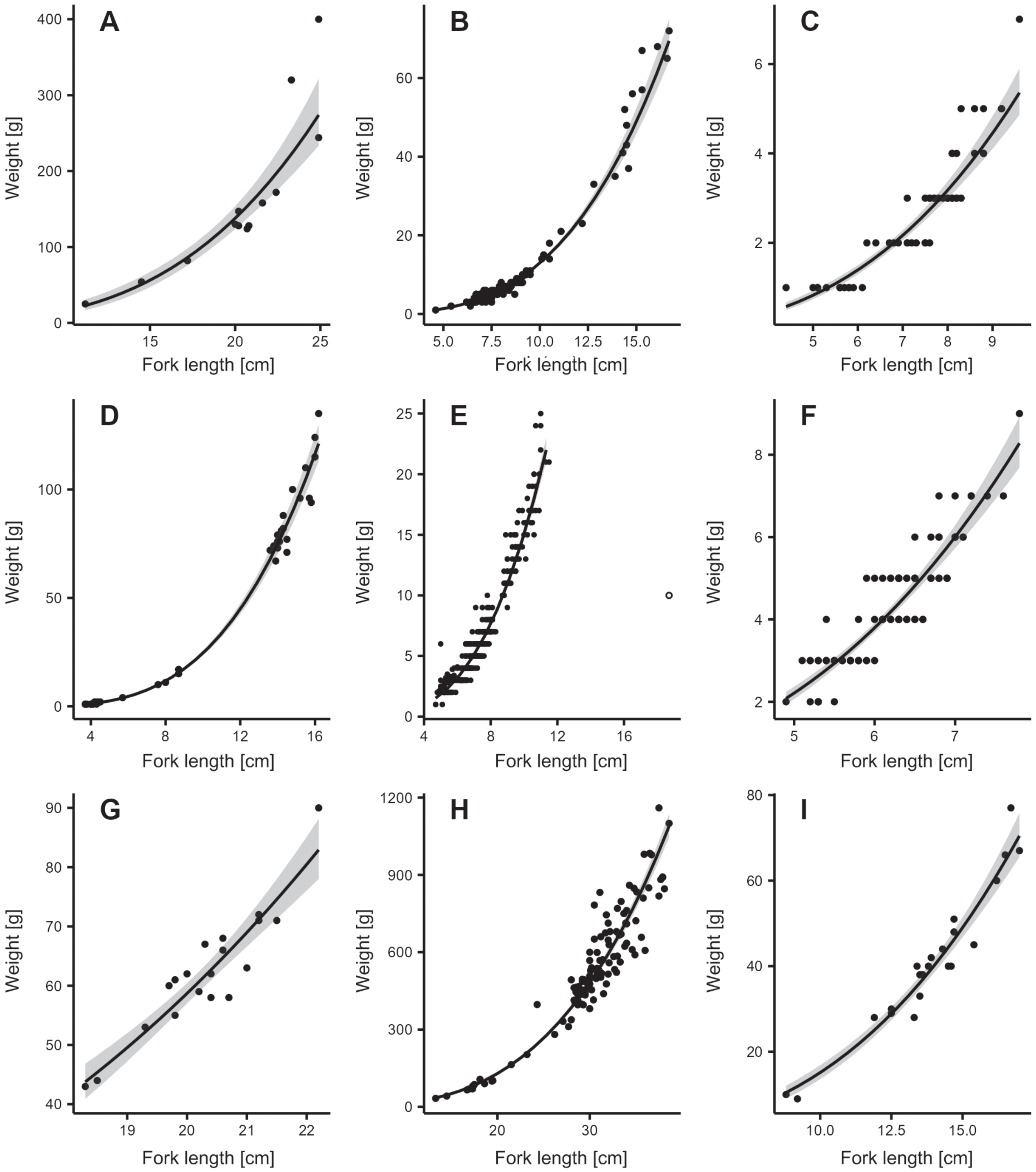

Figure 2. Length–weight relations (LWR) of 9 underutilized fish species. Black dots indicate observations used in the analysis, white dots indicate observations excluded from the analysis, and solid black lines indicate estimated curves and shaded areas indicate confidence intervals. (**A**) *Hyperoglyphe japonica*; (**B**) *Labracoglossa argenteiventris*; (**C**) *Macroramphosus sagifue*; (**D**) *Microcanthus strigatus*; (**E**) *Ostorhinchus semilineatus*; (**F**) *Parapriacanthus ransonneti*; (**G**) *Rexea prometheoides*; (**H**) *Siganus fuscescens*; (**I**) *Upeneus japonicus*.

Discussion

The survey results indicated that underutilized fish accounted for only 1% of the total catch weight, a significantly low value compared to other regions (Akiyama 2007). Among the estimated length–weight relations (LWR) of fish species reported in this study, five species (*Hyperoglyphe japonica*, *Labracoglossa argenteiventris*, *Microcanthus strigatus*, *Parapriacanthus ransonneti*, and *Rexea prometheoides*) were not listed or credibly described in FishBase (Froese and Pauly 2024). Additionally, four novel species (*Macroramphosus sagifue*, *Ostorhinchus semilineatus*, *Siganus fuscescens*, and *Upeneus japonicus*) for which no credible LWRs had been reported for the Japanese coast were newly reported. Therefore, this study's major significance lies in providing new biological information on these fish species.

Nine of the estimated LWR equations demonstrated high accuracy, with coefficient of determination (R^2) greater than 0.8 and b values within a realistic range of 2.8623.311 (Froese 2006). On the other hand, all specimens used for *Hyperoglyphe japonica* considered to be juveniles (Kawano and Shigenaga 2011) and further information is required. Therefore, improving the accuracy of these parameters requires ensuring sufficient populations over a broader size range (Froese et al. 2011).

Alverson et al. (1994) classified discard problems in the northwest Atlantic were classified into four groups:

- Marketable species too small or otherwise prohibited from landings.
- Species for which no current market exists but are caught along with commercial or recreational species.
- Species-specific fleet sectors discarding another fisheries target species.
- Non-fishery bycatch species, including marine mammals, turtles, and birds.

Regulatory approaches and management actions to address these problems are also discussed. In Japanese coastal fisheries, juvenile individuals of the target fish, belonging to category 1 in the Alverson et al. (1994) classification, are often caught as bycatch, but biological information is limited if the species themselves are not commercially utilized. None of the 9 species discussed in this study were utilized along the Mie Prefecture coast, and no biological information was available for any of them. Therefore, identifying LWR in this study provides fundamental and important information for assessing these fish species' stock status and future stock management. However, for many underutilized fish species in coastal waters, the actual bycatch and even the existence of biological data are unknown (Alverson et al. 1994). Considering that enhancing such primary data is essential for proper resource management and biodiversity conservation (Pauly et al. 2013), bycatch assessments in various fishing modes in different regions should be pursued, along with the comprehensive collection and accumulation of biological information on underutilized fish species in the future (Zeller et al. 2017).

Acknowledgments

We would like to express our sincere gratitude to several individuals and organizations for their invaluable contributions to this study. First, we thank Mr. Kei Taniguchi of the Nishiki Branch of MieGaiwan fisheries cooperative association for facilitating access to the study site in Nishiki port. His assistance was crucial for conducting field research. We are also deeply grateful to the staff of Nishiki Ohshiki Co., Ltd. for their cooperation during fishing operations, which enabled us to collect essential data for this study. Furthermore, we extend our appreciation to the members of the Fish population dynamics Laboratory at Mie University for their dedicated help with various aspects of data collection. This research would not have been possible without the generous support of these individuals and organizations. We sincerely thank them for their time and efforts.

References

Akiyama S (2007) [Discards in large-scale set net in Tateyama Bay.] Nippon Suisan Gakkaishi 73(6): 1103–1108. [In Japanese with English abstract] https://doi.org/10.2331/suisan.73.1103

Alverson DL, Freeberg MH, Pope JG, Murawski SA (1994) A global assessment of fisheries bycatch and discards. FAO Fisheries Technical Paper. No. 339. Rome, FAO, 233 pp.

Anonymous (2024) [2022 Fishery and Aquaculture Production Statistics.] Ministry of Agriculture, Forestry and Fisheries. [In Japanese] https://www.maff.go.jp/j/tokei/kouhyou/kaimen_gyosei/index.html

Armelloni EN, Scanu M, Masnadi F, Coro G, Angelini S, Scarcella G (2021) Data poor approach for the assessment of the main target species of rapido trawl fishery in Adriatic Sea. Frontiers in Marine Science 8: e552076. https://doi.org/10.3389/fmars.2021.552076

Cheng IJ, Chen TH (1997) The incidental capture of five species of sea turtles by coastal setnet fisheries in the eastern waters of Taiwan. Biological Conservation 82(2): 235–239. https://doi.org/10.1016/S0006-3207(97)00027-X

Cook RD, Weisberg S (1982) Residuals and Influence in Regression. Chapman and Hall, New York.

Davies RWD, Cripps SJ, Nickson A, Porter G (2009) Defining and estimating global marine fisheries bycatch. Marine Policy 33(4): 661–672. https://doi.org/10.1016/j.marpol.2009.01.003

Finkbeiner EM, Wallace BP, Moore JE, Lewison RL, Crowder LB, Read AJ (2011) Cumulative estimates of sea turtle bycatch and mortality in USA fisheries between 1990 and 2007. Biological Conservation 144(11): 2719–2727. https://doi.org/10.1016/j.biocon.2011.07.033

Froese R (2006) Cube law, condition factor and weight–length relationships: History, meta-analysis and recommendations. Journal of Applied Ichthyology 22(4): 241–253. https://doi.org/10.1111/j.1439-0426.2006.00805.x

Froese R, Pauly D (Eds.) (2024) FishBase. [version 02/2024] https://www.fishbase.org

Froese R, Tsikliras AC, Stergiou KI (2011) Editorial note on weight–length relations of fishes. Acta Ichthyologica et Piscatoria 41(4): 261–263. https://doi.org/10.3750/AIP2011.41.4.01

Fujikura K, Lindsay D, Kitazato H, Nishida S, Shirayama Y (2010) Marine biodiversity in Japanese waters. PLoS ONE 5(8): e11836. https://doi.org/10.1371/journal.pone.0011836

Hall MA (1996) On bycatches. Reviews in Fish Biology and Fisheries 6(3): 319–352. https://doi.org/10.1007/BF00122585

Heimann T, Verkamp H, McNamee J, Bethoney ND (2023) Mobilizing the fishing industry to address data gaps created by shifting species distribution. Frontiers in Marine Science 10: e1043676. https://doi.org/10.3389/fmars.2023.1043676

Kawano M, Shigenaga Y (2011) [Maturation and spawning of *Hyperoglyphe japonica* in the southwestern Japan Sea off Yamaguchi Prefecture.] Bulletin of Yamaguchi Prefectural Fisheries Research Center No 9: 99–103. [In Japanese with English abstract]

Kelleher K (2005) Discards in the World's marine fisheries. An update. FAO Fisheries Technical Paper 470. FAO, Rome, 134 pp.

Kindong R, Gao C, Pandong NA, Ma Q, Tian S, Wu F, Sarr O (2020) Stock status assessments of five small pelagic species in the Atlantic and Pacific oceans using the length-based Bayesian estimation (LBB) method. Frontiers in Marine Science 7: e592082. https://doi.org/10.3389/fmars.2020.592082

Kodeeswaran P, Jayakumar N, SriHari M, Durairaja R, Praveenraj J, Abarna KM, Moulitharan N (2020) Length–weight relationship of seven bycatch fish species caught along the Chennai coast, Bay of Bengal, Eastern Indian Ocean. Journal of Applied Ichthyology 36(2): 246–248. https://doi.org/10.1111/jai.14008

Nakabo T (Ed.) (2013) [Fishes of Japan with pictorial keys to the species Third edition.] Tokai University Press, Hadano, Japan, 2428 pp. [In Japanese]

Oliver S, Braccini M, Newman SJ, Harvey ES (2015) Global patterns in the bycatch of sharks and rays. Marine Policy 54: 86–97. https://doi.org/10.1016/j.marpol.2014.12.017

Pauly D, Hilborn R, Branch TA (2013) Fisheries: Does catch reflect abundance? Nature 494(7437): 303–306. https://doi.org/10.1038/494303a

R Core Team (2022) R: A language and environment for statistical computing. R Foundation for Statistical Computing, Vienna, Austria. https://www.R-project.org/

Rodríguez-García C, Castro-Gutiérrez J, Domínguez-Bustos ÁR, García-González A, Cabrera-Castro R (2023) Every fish counts: Challenging length–weight relationship bias in discards. Fishes 8(5): e222. https://doi.org/10.3390/fishes8050222

Shubhadeep G, Loveson E, Muktha M, Indira D, Behera PR, Jasmin F, Manas HM, Phalguni P, Madhumita D, Gourisankar R, Satishkumar M, Dineshbabu AP, Gopalakrishnan A (2022) Length–weight relations for finfish species landed as trawl by-catch from north-western Bay of Bengal. Journal of Applied Ichthyology 38(6): 621–623. https://doi.org/10.1111/jai.14357

Stohs SM, Harmon KM (2022) Bayesian prediction of fishery biological impacts from limited data: A deep-set buoy gear case study. Fisheries Research 249: e106228. https://doi.org/10.1016/j.fishres.2022.106228

Zeller D, Cashion T, Palomares M, Pauly D (2017) Global marine fisheries discards: A synthesis of reconstructed data. Fish and Fisheries 19(1): 30–39. https://doi.org/10.1111/faf.12233

Acta Ichthyologica et Piscatoria 54, 2024, 209–212 | DOI 10.3897/aiep.54.122733

ACTA
ICHTHYOLOGICA
ET PISCATORIA

New record of the cutthroat eel, *Meadia roseni* (Actinopterygii: Anguilliformes: Synaphobranchidae), from Vietnam

Hsuan-Ching HO[1,2], Quang Van VO[3,4]

1 *Department and Graduate Institute of Aquaculture, National Kaohsiung University of Science and Technology, Kaohsiung, Taiwan*
2 *Australian Museum, Sydney, Australia*
3 *Institute of Oceanography, Vietnam Academy of Science and Technology (VAST), Nha Trang, Vietnam*
4 *Graduate University of Science and Technology (GUST), VAST, Ha Noi, Vietnam*

https://zoobank.org/B00AE4BA-4A15-430D-85BD-E9780191C692

Corresponding author: Quang Van VO (quangvanvo@gmail.com)

Academic editor: Ronald Fricke ♦ **Received** 11 March 2024 ♦ **Accepted** 19 June 2024 ♦ **Published** 27 September 2024

Citation: Ho H-C, Vo QV (2024) New record of the cutthroat eel, *Meadia roseni* (Actinopterygii: Anguilliformes: Synaphobranchidae), from Vietnam. Acta Ichthyologica et Piscatoria 54: 209–212. https://doi.org/10.3897/aiep.54.122733

Abstract

A large individual of *Meadia roseni* Mok, Lee et Chang, 1991 is reported from central Vietnam for the first time, which also represents the first record outside the type locality, Taiwan. Herein we document the expansion of the distribution of this species, along with a detailed description and fresh color photos. The new finding may suggest that *M. roseni* has a broader distribution but somewhat restricted in the northern South China Sea.

Keywords

biodiversity, fish fauna, ichthyology, new record, taxonomy

Introduction

The genus *Meadia*, commonly referred to as arrowtooth eels, is a small group of moderately slender fishes that comprises three nominal species. Böhlke (1951) described the genus to accommodate the abyssal cutthroat eel, *Dysomma abyssale* Kamohara, 1938, originally described from Japan. A second species, *Meadia roseni* Mok, Lee et Chang, 1991 from southern Taiwan was described subsequently. Recently, Vo et al. (2021) described the third species, *Meadia minor* Vo et Ho, 2021 from Vietnam, and discussed the identification of some closely related genera.

Meadia roseni was originally described based on a single specimen and later recorded by several authors (Ho et al. 2015a, 2015b). However, none of these records were from outside Taiwanese waters, even after many intensive collecting activities in the past 20 years in nearby areas (Ho, personal observation). Recently, a large individual of *M. roseni* was collected by the first author from a local fishing port (Lương Sơn, Nha Trang) which represents the first record of the species outside Taiwan, as well as the first record of Vietnam. Herein, we provide a detailed description of the species based on the newly recorded specimen collected from Vietnam.

Methods and materials

Total length (TL) and head length (HL) are used throughout. Methods for making measurements, counts, and terminology follow Böhlke (1989) and Vo et al. (2021). Specimens examined were deposited at the fish collection of the National Museum of Marine Biology and

Aquarium, Taiwan (NMMB-P). Comparative materials were listed in Vo et al. (2021), with additional specimens collected from Taiwan and examined by the first authors. The format for species description and data for comparison followed Vo et al. (2021).

Results

Family Synaphobranchidae
Genus *Meadia* Böhlke, 1951

Meadia roseni Mok, Lee et Chan, 1991

Fig. 1

Meadia roseni Mok, Lee et Chan, 1991.—Mok et al. (1991): 39, figs. 1–3 (type locality: off Tongkang [Dong-gang], southwestern Taiwan, 22°21′05″N, 120°12′46″E, depth 1020 m).—Shen et al. (1993): 109 (Taiwan; short description). Smith (1999): 1661 (western central Pacific; list).—Randall and Lim (2000): 585 (South China Sea; list).—Ho and Shao (2011): 22 (Taiwan; type catalog).—Ho et al. (2015a): 8 (Taiwan; checklist).—Ho et al. (2015b): 179 (Taiwan; annotated checklist).—Vo et al. (2021): 187 (Taiwan; description).

Specimen examined. NMMB-P39330, 845 mm TL, Lương Sơn fishing port, ca. 12°20′6.7″N, 109°12′14.6″E, Nha Trang city, Vietnam, South China Sea, 13 January 2024, coll. H.-C. Ho.

Description of NMMB-P39330. Body rather robust, moderately slender, body depth at gill opening 13.1 times in TL; head and trunk slightly compressed, becoming more compressed on tail posteriorly. Body depth relatively uniform, narrowing gradually to caudal fin. Anal fin much higher than dorsal fin, about twice of depth; height of anal fin about 1/4 of body depth without fins, continuous with small caudal fin. Pectoral fin well developed, lower end of fin base at around upper end of gill opening; pectoral-fin length 25.0% (4.0 times in) HL. Head moderately long, rather robust, its length 15.5% (6.5 times in) TL; origin of dorsal fin slightly behind gill opening, above vertical through anterior 1/3 of pectoral fin, predorsal length 17.2% (5.8) TL; trunk short, 8.3% (12.1) TL; anus well anterior, about 1/2 head length behind pectoral-fin base; preanal length 23.8% (4.2) TL; tail very long, tail length 76.2% (1.3) TL. Head moderately slender, with bump in dorsal profile; snout blunt anteriorly and broad dorsally, densely covered with numerous papillae and flashy bumps; snout length 27.4% (3.6) HL; tip of snout projecting beyond lower jaw; eye moderately small, covered by thick and semitransparent membrane, its anterior margin above middle of upper jaw; eye diameter 7.7% (13.0) HL or 3.6 times in snout length; interorbital space very broad, flat or slightly concave, width 18.8% (5.3) HL; postorbital space broad. Anterior nostrils tubular, directed anteriorly; posterior nostril a small rounded pore with low rim and anterior flap, situated in front of eye, slightly higher than lower margin of eye. Lower jaw shorter than upper, its tip reaching first pore of supraorbital series. End of mouth gape well behind eye, upper-jaw length 31.7% (3.2) HL. Gill opening large, semi-circular, its upper end right below lower end of pectoral-fin base. Head pores small. Head pores: SO 4 (including ethmoid), anterior 3 all restricted to anterior portion of snout, opening of first pore directed forward; AD 1; IO 6;5, 2 pores between nostrils, 2 below eye, 2 (1 on left side) behind eye; POM 10 (11 on left side), anterior 8 pores along lower jaw, two pores behind rictus, last pore (penultimate pore on left side) and 1 eye diameter behind rictus; ST 0; F 0. Lateral line almost complete, canal extending to about 1 eye diameter before caudal fin base; pores rather small along entire lateral line, rather small and indistinct on posterior end. Lateral-line pores: PPLL 9, PDLL 14, PALL 31, and total ca. 195. Tooth on jaw blunt to conical, somewhat granular, interspaces densely covered with numerous cirri making teeth not easily recognized; oval patch of moderately large teeth with about 13 small teeth along anterior and lateral margins on intermaxillary; followed by long patch of about 12 enlarged and stout teeth arranged in about 3 rows at middle, followed by small stout teeth posteriorly. Maxilla with long band of about 4–5 rows of slightly pointed teeth, those on outer row smallest, those on inner rows gradually larger innerly. Lower jaw with about 5–6 rows of stout teeth anteriorly, gradually becoming 4 rows posteriorly, those on outer row smallest, those on inner row gradually becoming larger innerly. Vertebrae: PDV 13, PAV 30, PCV 63, TV 197. Fin rays: 41 dorsal-fin rays before anal-fin origin; 430 total dorsal-fin rays; 394 total anal-fin rays.

Coloration. Body uniformly grayish brown to dark brown (Fig. 1A). Anterior 2/3 of dorsal fin grayish brown with broad pale margin, gradually becoming darker and the margins becoming narrower, darkened at about one head length from posterior end; anterior half of anal fin with narrow pale margin, becoming darker and the margins becoming narrower, darkened at about one head length from posterior end; caudal fin black. Peritoneum pale with fine black pepper dots, stomach and intestines pale.

Discussion

The present reported specimen represents the first record of Vietnam, as well as the only record outside Taiwan. It may suggest that *Meadia roseni* has a broader distribution range. However, compared to other synaphobranchids, *M. roseni* may have a more or less restricted range, mostly found in the northern part of the South China Sea. Although intensive samplings were made in the past decades, there are still many eel species new to the ichthyofauna of Vietnam (Vo et al. 2019, 2021, 2024; Vo and Ho 2020, 2021), which suggests a high eel diversity in Vietnam.

Compared to Vo et al. (2021), the Vietnamese specimen has a slightly longer head (15.5%, vs. 13.6%–14.3% TL), predorsal length (17.2%, vs. 15.4%–15.9% TL) and preanal length (23.8%, vs. 22.0%–23.5% TL). It also has

Figure 1. *Meadia roseni* Mok, Lee et Chang, 1991, off Nha Trang, Vietnam, fresh. (**A**) Lateral view. (**B**) Lateral view of head. A pin is inserted at origin of dorsal fin.

a slightly shorter snout (27.4%, vs. 28.0%–31.2% HL), smaller eye (7.7%, vs. 8.5%–9.8% HL) and broader interorbital space (18.8%, vs. 16.0%–17.0% HL). The arrangement of teeth is also slightly different. In general, there are more teeth compared to those from Taiwan. We examined a number of specimens from Taiwan and found that the number of teeth is lower in smaller specimens (<500 mm TL) and gradually becoming more in larger specimens, suggesting a growth change in the species reported in this study.

There are 2 infraorbital pores behind the eye on the right side of the Vietnamese specimen. We also found that there are 2 pores on the left side of one specimen (NMMB-P17799, 443 mm TL) and 2 on both sides of another specimen (NMMB-P17799, 520 mm TL) collected from Taiwan, which suggest some variation of head pores present in this species. In addition, we also counted 10–12 preopercular-mandibular pores in Taiwanese specimens, but mostly 10 or 11 in general.

Comparative materials. *Meadia roseni*: NMMB-P17799 (2 specimens, 443–520 mm TL), Dong-gang, Pingtung, southern Taiwan, 7 Sep. 2012. NMMB-P18092 (1, 495), Dong-gang, 7 Sep. 2012. NMMB-P24461 (1, 696), Dong-gang, 27 Jun. 2016. NMMB-P25976 (1, 435), Dong-gang, 21 Feb. 2017. NMMB-P26690 (1, 500), Dong-gang, 10 Jul. 2017. NMMB-P31634 (1, 475), Dong-gang, 29 Mar. 2017. Other specimens listed in Vo et al. (2021).

Acknowledgments

This study is supported by the National Kaohsiung University of Science and Technology, Kaohsiung, Taiwan, the National Science and Technology Council, Taiwan, and the Vietnam Academy of Science and Technology (VAST) for QVV (grant VAST06.05/23–24). We thank C.T. Tran for his help in preparing the specimens and Y. Su for preparing the figures.

References

Böhlke JE (1951) *Meadia*, a new genus for the West Pacific dysommid eel, *Dysomma abyssale* Kamohara. Stanford Ichthyological Bulletin 4(1): 6.

Böhlke EB (1989) Methods and terminology. Pp. 1–7. In: Böhlke EB (Ed.) Fishes of the Western North Atlantic. Memoirs of the Sears Foundation for Marine Research, Volume 1, part 9. Sears Foundation of Marine Research, New Haven, CT, USA.

Ho HC, Shao KT (2011) Annotated checklist and type catalog of fish genera and species described from Taiwan. Zootaxa 2957(1): 1–74. https://doi.org/10.11646/zootaxa.2957.1.1

Ho HC, McCosker JE, Smith DG, Shao KT (2015a) Introduction to the systematics and biodiversity of eels (orders Anguilliformes and Saccopharyngiformes) of Taiwan. Zootaxa 4060(1): 5–18. https://doi.org/10.11646/zootaxa.4060.1.3

Ho HC, Smith DG, McCosker JE, Hibino Y, Loh KH, Tighe KA, Shao KT (2015b) Annotated checklist of eels (orders Anguilliformes and Saccopharyngiformes) from Taiwan. Zootaxa 4060(1): 140–189. https://doi.org/10.11646/zootaxa.4060.1.16

Kamohara T (1938) [On the offshore bottom-fishes of Province Tosa, Shikoku, Japan.] Maruzen Kobushiki Kaisha, Tokyo, Japan, 86 pp. [In Japanese]

Mok HK, Lee CY, Chan HJ (1991) *Meadia roseni*, a new synaphobranchid eel from the coast of Taiwan (Anguilloidea: Synaphobranchidae). Bulletin of Marine Science 48(1): 39–45.

Randall JE, Lim KKP (2000) A checklist of the fishes of the South China Sea. Raffles Bulletin of Zoology (Suppl. 8): 569–667.

Shen SC, Lee SC, Shao KT, Mok HK, Chen CC, Chen CH, Tseng CS (1993) [Fishes of Taiwan.] National Taiwan University, Taipei, Taiwan, 956 pp. [In Chinese]

Smith DG (1999) Synaphobranchidae, cutthroat eels. Pp. 1658–1661. In: Carpenter KE, Niem VH (Eds.) Species Identification Guide for Fisheries Purposes. The Living Marine Resources of the Western Central Pacific. Volume 3. Batoid Fishes, Chimeras and Bony Fishes Part 1 (Elopidae to Linophrynidae). FAO, Rome.

Vo QV, Ho HC (2020) A new species of *Atractodenchelys* (Synaphobranchidae, Anguilliformes) from Vietnam. Zootaxa 474(3): 588–594. https://doi.org/10.11646/zootaxa.4742.3.12

Vo QV, Ho HC (2021) A new species of the snake eel genus *Ophichthus* from Vietnam, with a new record of *Echelus polyspondylus* McCosker & Ho, 2015. Raffles Bulletin of Zoology 69: 71–79. https://doi.org/10.26107/RBZ-2021-0006

Vo QV, Hibino Y, Ho HC (2019) A new species of the snake eel genus *Ophichthus*, with additional records from Viet Nam (Anguilliformes: Ophichthidae). Zoological Studies 58(43): 1–14. https://doi.org/10.6620/ZS.2019.58-43

Vo QV, Ho HC, Dao HC, Tran HHT (2021) A new arrowtooth eel of genus *Meadia* (Synaphobranchidae: Ilyophinae) from Vietnam, South China Sea. Zootaxa 4952(1): 181–191. https://doi.org/10.11646/zootaxa.4952.1.11

Vo QV, Ho HC, Dao HC, Tran, TC (2024) New species of the eel genera *Dysomma* and *Dysommina* from Vietnam, South China Sea (Anguilliformes: Synaphobranchidae). Journal of Fish Biology 104(4): 1067–1078. https://doi.org/10.1111/jfb.15638

Acta Ichthyologica et Piscatoria 54, 2024, 213–220 | DOI 10.3897/aiep.54.126623

PENSOFT

ACTA
ICHTHYOLOGICA
ET PISCATORIA

Length–weight relationships for 14 cypriniform freshwater fish species (Actinopterygii) from the Upper Mississippi River Basin

Justin C. BAGLEY[1,2,3], Maria Florencia BREITMAN[2]

1 *Department of Biology and Environmental Science, Auburn University at Montgomery, Montgomery, AL, USA*
2 *Department of Biology, Virginia Commonwealth University, Richmond, VA, USA*
3 *Present address: Field Operations Division, Alabama Department of Environmental Management, Montgomery, AL, USA*

https://zoobank.org/AEE1D39C-0C54-4210-B947-6A43CB24DE61

Corresponding author: Justin C. Bagley (justin.bagley@adem.alabama.gov)

Academic editor: Rodolfo Reyes ♦ **Received** 28 May 2024 ♦ **Accepted** 18 July 2024 ♦ **Published** 7 October 2024

Citation: Bagley JC, Breitman MF (2024) Length–weight relationships for 14 cypriniform freshwater fish species (Actinopterygii) from the Upper Mississippi River Basin. Acta Ichthyologica et Piscatoria 54: 213–220. https://doi.org/10.3897/aiep.54.126623

Abstract

Here, we use long-term monitoring data from fisheries surveys across six Mississippi River reaches spanning > 750 river miles (>1200 km) to estimate length–weight relationships (LWRs) for 14 cypriniform fishes native to the Upper Mississippi River system. Relationships between $\log_{10}$-transformed values of fish total weights [g] and total lengths [cm] were analyzed using standard linear modeling and hypothesis-testing approaches. Focal species included four North American minnows in family Leuciscidae [*Cyprinella lutrensis* (Baird et Girard, 1853), *Notropis atherinoides* Rafinesque, 1818, *Notropis hudsonius* (Clinton, 1824), and *Paranotropis volucellus* (Cope, 1865)] and 10 suckers in the family Catostomidae [*Carpiodes carpio* (Rafinesque, 1820), *Carpiodes cyprinus* (Lesueur, 1817), *Carpiodes velifer* (Rafinesque, 1820), *Cycleptus elongatus* (Lesueur, 1817), *Ictiobus bubalus* (Rafinesque, 1818), *Ictiobus niger* (Rafinesque, 1819), *Moxostoma anisurum* (Rafinesque, 1820), *Moxostoma carinatum* (Cope, 1870), *Moxostoma erythrurum* (Rafinesque, 1818), and *Moxostoma macrolepidotum* (Lesueur, 1817)]. Congruent with previous studies, estimates of parameter *b* were consistent with isometric or weakly allometric growth and ranged from 2.834 (*P. volucellus*) to 3.351 (*C. elongatus*), while estimates of parameter *a* ranged from 0.002 (*C. elongatus*) to 0.014 (*C. velifer*).

Keywords

fisheries, freshwater fishes, length–weight relationships, Midwestern USA, Mississippi River

Introduction

The Upper Mississippi River (UMR) is a large (>490 000 km^2) and complex floodplain river drainage and represents amongst the most culturally, economically, and biologically significant rivers in North America (Carlson et al. 1995; Black et al. 1999; Weitzell et al. 2003; Gaffigan et al. 2021). The UMR system includes Mississippi River reaches with navigable channels north of Cairo, IL (37°00′18.6″N, 89°10′34.9″W; i.e., confluence with the Ohio River), the Illinois River and Waterway, as well as the St. Croix, Minnesota, Black, and Kaskaskia rivers (Fig. 1; Gaffigan et al. 2021). With ~190 fish species, including several species of Threatened, Endangered or Special Concern status [e.g., *Miniellus topeka* (Gilbert, 1884), federal status: Endangered], the freshwater fish assemblage of the UMR is diverse and ecologically unique and makes up around ~17% of the continental freshwater fish fauna (Burr and Page 1986; Pitlo et al. 1995; Page and Burr 2011; JCB, unpublished results). The UMR also boasts a diverse collection of mussel, amphibian, bird, and mammal assemblages that are prioritized for conservation (Weitzell et al. 2003). Not surprisingly, given its biodiversity and abundance of natural resources, the UMR has provided for a multitude of human uses historically and today, leading to great benefits, but also to widespread anthropogenic impacts and environmental degradation. For example, while the UMR adds ~US$1 billion in annual benefits to the national economy through boating, fishing, and other commercial and recreational activities (Gaffigan et al. 2021), the river has also been heavily altered. Navigational infrastructure is extensive, including ~1200 miles (~1900 km) of navigation channels and 37 locks and dams, many of which present at least partial barriers to fish movement (Fremling et al. 1989; but see Tripp et al. 2014). Biotic communities have also become altered by introductions of non-indigenous aquatic species that represent a major threat to native taxa, including zebra mussel, *Dreissena polymorpha* (Pallas, 1771) (Dreissenidae), as well as Asian major carps, such as Bighead Carp, *Hypophthalmichthys nobilis* (Richardson, 1845), and Silver Carp, *Hypophthalmichthys molitrix* (Valenciennes, 1844) (Xenocyprididae).

Many aspects of the UMR freshwater fish fauna have been well studied, including patterns of fish ecology, evolution, distribution, community composition, and fisheries management (e.g., Smith et al. 1971; Pitlo et al. 1995; Mundahl and Simon 1999; Dettmers et al. 2001; Piller et al. 2005; Chick et al. 2006; Bessert and Ortí 2008; Bart et al. 2010; Ardren et al. 2022). Indeed, the need for fisheries research in the UMR was realized by Smith (1949) and has since had a longstanding history, including recent studies of relevance to natural resource management and ecosystem restoration (e.g., Crimmins et al. 2015). Nevertheless, the basic ecology of UMR fishes remains incompletely characterized in many areas that have received only sporadic research attention, including length–weight relationships (LWRs; Froese 2006), body condition, and functional ecology of species in local ecosystems (e.g., Garvey et al. 2010). In the case of LWRs, understanding how fish weight changes as a function of body size provides critical information for comparing the condition of individuals and populations, calculating growth rates, imputing missing weight or length values, estimating length at first maturity and building food-web models of ecosystems (e.g., Froese 2006; Jellyman et al. 2013; Heymans et al. 2016; Hashiguti et al. 2019; Bagley et al. 2022).

In this study, we describe LWRs for 14 minnow and sucker species from the ray-finned fish order Cypriniformes that are native to the UMR. We use data from the Upper Mississippi River Restoration–Environmental Management Program (hereafter, the "Long Term Resource Monitoring Program"—LTRMP), a federally supported partnership established through the Environmental Management Program of the 1986 US Water Resources Development Act (WRDA; Garvey et al. 2010). Fishes have been sampled in LTRMP areas since 1989 using variable gear and multi-species approaches for sampling non-game species and species of economic value (Ickes et al. 2005). Data were from six navigation reaches, five on the Mississippi River and one on the Illinois River (Fig. 1), with thousands of local sampling sites nested within these areas. A previous population ecology study by Kirby and Ickes (2006) examined length-frequency distributions and LWRs for five commercially and recreationally important UMR fish species using LTRMP data collected from 1993 to 2002. They found that LWR model slopes were significantly different by the area over 10 years, overall, and that model slopes were significantly different year to year in *Pomoxis nigromaculatus* (Lesueur, 1829), *Ictalurus punctatus* (Rafinesque, 1818), *Cyprinus carpio* Linnaeus, 1758, and *Sander vitreus* (Mitchill, 1818). However, slope parameters were not significantly different by year in *Sander canadensis* (Griffith et Smith, 1834). Importantly, LWR slope parameters were above 3.0 for all species and years, indicating positive allometric growth, except for slopes between 2.0 and 3.0 during four years for *C. carpio* and the authors hypothesized that the timing of Mississippi River flood events had an important effect on fish productivity and growth (Kirby and Ickes 2006). Whereas previous authors limited their work on UMR fish LWRs to species meeting restrictive sampling criteria, we selected closely related species from order Cypriniformes (Actinopterygii) that have overlapping geographical ranges (Page and Burr 2011), limited LWR data in FishBase (Froese and Pauly 2024) usually from only one or two studies (Table 1), and sufficient sample sizes for LWR parameter estimation.

Materials and methods

The study area included all six LTRMP study reaches, also known as "field stations," within the UMR (Fig. 1), as follows [given as field station name (associated city, located at or near reach), navigational pool designation, and river mile range]: (1) Field Station 1 (Lake City, MN), Pool 4, river mile 752–797, excluding Lake Pepin; (2) Field Station 2 (Onalaska, WI), Pool 8, river mile 679–703; (3) Field Station 3 (Bellevue, IA), Pool 13, river mile 523–557; (4) Field Station 4 (Brighton, IL), Pool 26, river mile 202–242; (5) Field Station 5 (Jackson, MO), Open River, river mile 1–81; and (6) Field Station 6 (Havana, IL), La Grange Pool, river mile 80–158. Here, all river miles are on the Mississippi River, except for those of the Field Station 6 reach, which are located on the Illinois River (Fig. 1). The LTRMP field stations span a wide range of variation in floodplain characteristics, geomorphology, navigational infrastructure, and land-use change and cover (Kirby and Ickes 2006).

Data were compiled from online servers using the "Query Fisheries Data" function available through the Upper Midwest Environmental Sciences Center website (https://www.umesc.usgs.gov/data_library/fisheries/fish1_query.shtml; accessed 29 March 2024). We downloaded gear-specific data for day electrofishing (code "D"), as available for all sample areas, stratum

Table 1. List of 14 cypriniform fish species examined in the presently reported study. Information summarized for our focal species in this Table includes their valid species names (Fricke et al. 2024), standard names, geographical distribution in the Upper Mississippi River system (field stations 1–6), and the prior state of knowledge of their length–weight relationships (LWRs).

Family	Species	AFS standard name (LTRMP fish code)	Geographical distribution (UMR)	Prior LWR number
Leuciscidae	*Cyprinella lutrensis* (Baird et Girard, 1853)	Red Shiner (RDSN)	4, 5	1
Leuciscidae	*Notropis atherinoides* Rafinesque, 1818	Emerald Shiner (ERSN)	1–5	1
Leuciscidae	*Notropis hudsonius* (Clinton, 1824)	Spottail Shiner (STSN)	1, 2, 3, 6	1
Leuciscidae	*Paranotropis volucellus* (Cope, 1865)	Mimic Shiner (MMSN)	1, 2	1
Catostomidae	*Carpiodes carpio* (Rafinesque, 1820)	River Carpsucker (RVCS)	1–6	9
Catostomidae	*Carpiodes cyprinus* (Lesueur, 1817)	Quillback (QLBK)	1–6	2
Catostomidae	*Carpiodes velifer* (Rafinesque, 1820)	Highfin Carpsucker (HFCS)	1–4, 6	2
Catostomidae	*Cycleptus elongatus* (Lesueur, 1817)	Blue Sucker (BUSK)	2–6	1
Catostomidae	*Ictiobus bubalus* (Rafinesque, 1818)	Smallmouth Buffalo (SMBF)	1–6	7
Catostomidae	*Ictiobus niger* (Rafinesque, 1819)	Black Buffalo (BKBF)	2–6	1
Catostomidae	*Moxostoma anisurum* (Rafinesque, 1820)	Silver Redhorse (SVRH)	1, 2	2
Catostomidae	*Moxostoma carinatum* (Cope, 1870)	River Redhorse (RVRH)	1, 2, 5	2
Catostomidae	*Moxostoma erythrurum* (Rafinesque, 1818)	Golden Redhorse (GDRH)	1–4, 6	3
Catostomidae	*Moxostoma macrolepidotum* (Lesueur, 1817)	Shorthead Redhorse (SHRH)	1–6	2

AFS = American Fisheries Society (Page et al. 2013, 2023); LTRMP = Long Term Resource Monitoring Program, a federally supported partnership established through the Environmental Management Program of the 1986 US Water Resources Development Act (WRDA; Garvey et al. 2010); "Geographical distribution (UMR)" indicates each species range within the study area, based on our final edited dataset, given by field station numbers 1–6 shown in Fig. 1 (see details in the Materials and methods). Prior LWR number = the number of LWR records available for the species prior to this study, based on FishBase data (Froese and Pauly 2024); and UMR = Upper Mississippi River.

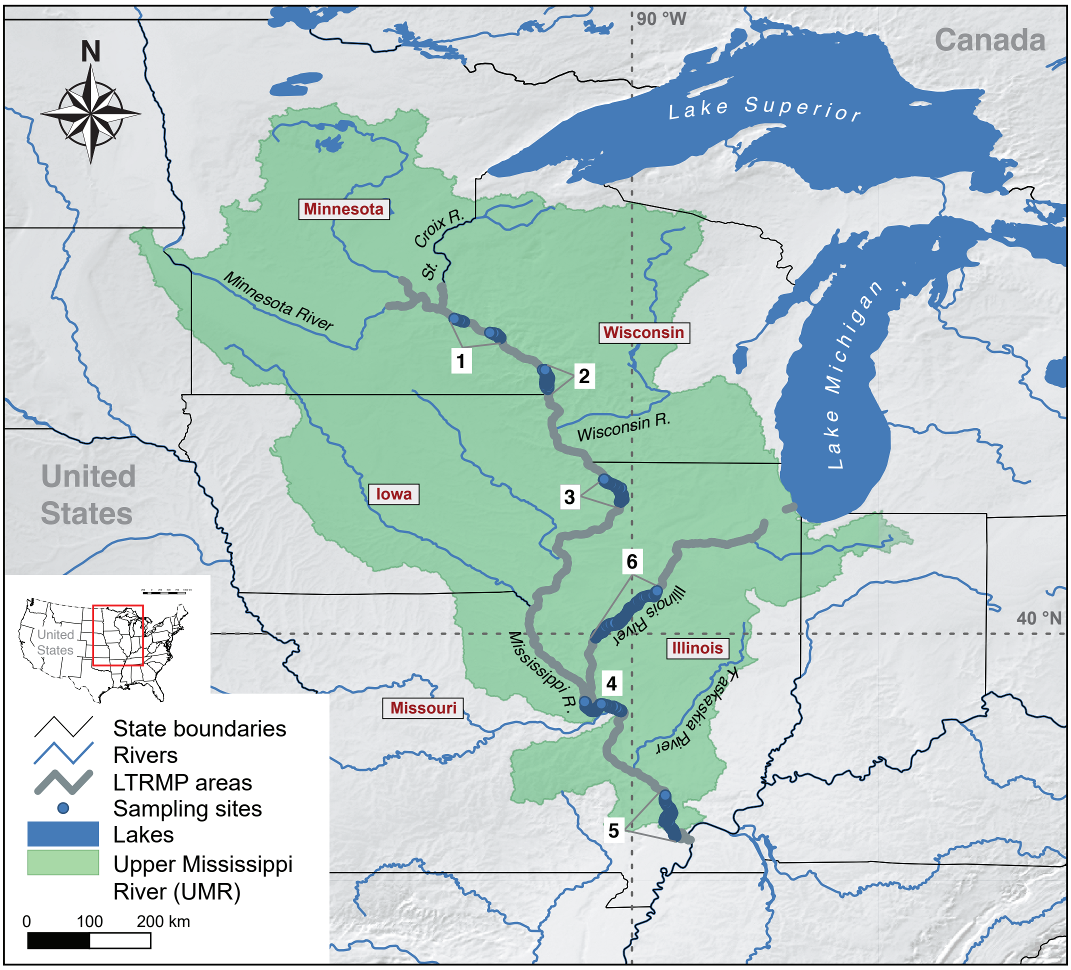

Figure 1. Map of the study area and sampling localities. The Upper Mississippi River (UMR) study area (light green shading) and fish survey localities (blue points) are mapped over major administrative and physiographic features, including States (thin black lines; also labels for those through which the UMR flows), major rivers and lakes (blue lines and shading) and Long Term Resource Monitoring Program (LTRMP) study areas (thick grey lines). The LTRMP study reaches or "field stations" are defined by the sampled areas and labelled 1–6 (for additional details, see text and accompanying Mendeley Data accession, with archived version: http://dx.doi.org/10.17632/8s7vmk4jct.1). Several river systems named in the text are labelled in italics.

classes (habitats), and time periods (01/01/1989 to 31/10/2022). The daytime boat electrofishing results included 682 982 collection records from all six study reaches over the 34-year period from 1989 to 2022. Data were edited "by eye," parsed, and summarized in Microsoft Excel. After the removal of unidentified specimens and young-of-the-year fish, records summed to a total catch of ~1.9 million individual fish/groups, representing 159 different species. We filtered these records to length and weight measures for individuals, where group width ("grp_wdth" parameter) was set blank (USGS 2024). From these data, 14 cypriniform fish species were selected for study for reasons outlined above, including sufficient sampling ($n > 30$) for linear modeling analyses. Focal taxa included four North American minnows from family Leuciscidae—*Cyprinella lutrensis* (Baird et Girard, 1853), *Notropis atherinoides* Rafinesque, 1818, *Notropis hudsonius* (Clinton, 1824), and *Paranotropis volucellus* (Cope, 1865)—and 10 suckers in the family Catostomidae—*Carpiodes carpio* (Rafinesque, 1820), *Carpiodes cyprinus* (Lesueur, 1817), *Carpiodes velifer* (Rafinesque, 1820), *Cycleptus elongatus* (Lesueur, 1817), *Ictiobus bubalus* (Rafinesque, 1818), *Ictiobus niger* (Rafinesque, 1819), *Moxostoma anisurum* (Rafinesque, 1820), *Moxostoma carinatum* (Cope, 1870), *Moxostoma erythrurum* (Rafinesque, 1818), and *Moxostoma macrolepidotum* (Lesueur, 1817). Table 1 summarizes the taxonomy, standard names, and prior LWR data for these species. By parsing the data using fish codes in the metadata (USGS 2024; Table 1), we obtained a species-level dataset with length (L) measured as total length (TL) to the nearest millimeter [mm], converted to centimeters [cm] and weight (W; wet body mass) measured to the nearest 0.01 to 1 gram [g] for each specimen. Standard fish names used in this paper are formally accepted common names, adopted by the American Fisheries Society (Page et al. 2013, 2023).

The LWR was estimated for each species using best practices (e.g., Froese 2006; Froese et al. 2011). First, we performed $\log_{10}$-transformation of the L and W variables, then we used bivariate scatterplots to identify potential outlier points, which were removed prior to further analyses. Next, regression parameters were estimated by linear modeling analyses using the ordinary least squares (OLS) method, because the expected relationships between the x and y variables are asymmetric for LWRs (Smith 2009) and OLS on $\log_{10}$-transformed data is the most used model, allowing for comparisons with previous studies. Here, OLS is performed using a linearized form of the LWR model, which is given as:

$$\log(W) = \log(a) + b\log(L)$$

where W is weight, L is length in cm, a is a constant at the y-intercept and b represents the slope, which is also a constant (Clark 1928; Le Cren 1951; Froese 2006). Parameters $\log(a)$, b, and their 95 confidence intervals (CIs; based on 1999 permutations of the data) were estimated using the PAST (PAleontological STatistics) v.4.0.3 (Hammer et al. 2001). Final a values were derived from model parameters as $a = 10^{\log(a)}$. We tested the null hypothesis of $b = 3$, consistent with "isometric" growth, against the alternative hypothesis $b \neq 3$, indicating allometric growth, using two-tailed t-tests implemented with the *pt* function in R v.4.3.2 (R Core Team 2023). Statistical significance was assessed using an alpha value of 0.05 for all analyses. Edited (log-transformed) and raw length–weight data and associated collections data used in this study are made available in a Mendeley Data accession (archived version: http://dx.doi.org/10.17632/8s7vmk4jct.1).

Results

After data cleaning including removal of $n = 935$ outliers (~12%), the final, edited dataset contained L and W values for $n = 7731$ specimens from the 14 focal cypriniform fish species (Table 1). Intraspecific sample sizes ranged from $n = 21$ to $n = 2813$, with a mean ± standard error (SE) of 552.2 ± 782.2 individuals (Table 2). Maximum L values ranged from 6.5 cm TL in the Mimic Shiner, *Paranotropis volucellus*, which was the smallest species, to 89.0 cm TL in Black Buffalo, *Ictiobus niger*, the largest species. Similarly, the maximum W values ranged from 2.1 g (0.0021 kg) in *P. volucellus* to 10566.0 g (10.566 kg) in *I. niger* (Table 2).

In all cases, the inferred length–weight relationships were highly statistically significant in OLS regressions ($P < 0.001$), with generally high goodness-of-fit indicated by R^2 statistics for each model (Table 2). The R^2 statistics were above 0.950 for 93% (13) of taxa, indicating that outliers were sufficiently removed prior to analysis such that more than 95% of the variance in fish W values was explained by the independent variable, fish L (Froese 2006). The only species with an R^2 less than 0.950 after outlier removal was *Cyprinella lutrensis*, possibly due to its relatively small sample size or undetected measurement error. Parameter a estimates ranged from 0.00220 in *Cycleptus elongatus* to 0.014 in *Carpiodes velifer*, while parameter b estimates were generally above 3.0 (10/14 or ~71% of cases) and ranged from $b = 2.834$ in *P. volucellus* to $b = 3.351$ in *C. elongatus*. Consistent with allometric growth, the b parameter was significantly different ($P < 0.05$) from $b = 3$ during t-tests for nine species, including *Notropis atherinoides*, *P. volucellus*, *Cyprinus carpio*, *C. elongatus*, *Ictiobus bubalus*, *I. niger*, *Moxostoma anisurum*, *Moxostoma erythrurum*, and *Moxostoma macrolepidotum* (Table 3). Consistent with isometric growth, t-tests of the null hypothesis of $b = 3$ were not significant ($P > 0.05$) in the remaining five species—*C. lutrensis*, *Notropis hudsonius*, *Carpiodes cyprinus*, *C. velifer*, and *Moxostoma carinatum* (Table 3), four of which also had b 95% CIs that included 3.0 (Table 2).

Table 2. Length–weight relationships for 14 cypriniform freshwater fishes from the Upper Mississippi River.

Family	Species	*n*	Total length (TL) [cm]	Weight [g]	*a* [95% CIs]	*b* [95% CIs]	R^2
Leuciscidae	*Cyprinella lutrensis*	54	4.1–7.2	0.7–3.8	0.009 [0.006, 0.017]	*3.112* *[2.688, 3.413]*	0.854
Leuciscidae	*Notropis atherinoides*	518	2.0–9.2	0.1–5.3	0.009 [0.008, 0.009]	2.894 [2.851, 2.938]	0.974
Leuciscidae	*Notropis hudsonius*	66	4.4–10.3	0.7–10.4	0.008 [0.007, 0.009]	3.058 [3.002, 3.117]	0.994
Leuciscidae	*Paranotropis volucellus*	21	2.2–6.5	0.1–2.1	0.010 [0.008, 0.012]	2.834 [2.697, 2.933]	0.992
Catostomidae	*Carpiodes carpio*	1094	2.9–61.0	0.3–3676.0	0.012 [0.012, 0.013]	3.025 [3.010, 3.041]	0.996
Catostomidae	*Carpiodes cyprinus*	100	8.5–59.6	8.2–2940.0	0.014 [0.012, 0.018]	*2.966* *[2.902, 3.026]*	0.991
Catostomidae	***Carpiodes velifer***	**53**	**12.0–51.4**	**25.0–2072.0**	**0.014** **[0.012, 0.019]**	***2.970*** *[2.889, 3.031]*	**0.993**
Catostomidae	*Cycleptus elongatus*	54	19.5–78.6	44.0–5710.0	0.002 [0.001, 0.005]	3.351 [3.139, 3.450]	0.984
Catostomidae	*Ictiobus bubalus*	2813	11.3–78.2	26.0–7800.0	0.012 [0.011, 0.012]	3.063 [3.052, 3.073]	0.994
Catostomidae	*Ictiobus niger*	522	18.1–89.0	85.0–10566.0	0.010 [0.009, 0.011]	3.106 [3.071, 3.138]	0.980
Catostomidae	*Moxostoma anisurum*	396	7.3–59.9	4.0–2650.0	0.009 [0.009, 0.010]	3.033 [3.006, 3.057]	0.992
Catostomidae	*Moxostoma carinatum*	81	22.0–71.4	129.8–4205.0	0.008 [0.005, 0.014]	*3.098* *[2.938, 3.191]*	0.989
Catostomidae	*Moxostoma erythrurum*	245	5.0–52.5	1.0–1805.0	0.008 [0.007, 0.010]	3.082 [3.029, 3.145]	0.990
Catostomidae	*Moxostoma macrolepidotum*	1714	5.7–55.5	2.0–1800.0	0.010 [0.009, 0.010]	3.027 [3.012, 3.043]	0.994

a is the intercept and *b* is the slope of the linear LWR regression; CIs values are 95% confidence intervals of the respective regression parameters; n is sample size R^2 is the coefficient of determination (adjusted values from regressions). Cases where the 95% CIs for *b* estimates overlapped $b = 3$, consistent with the null hypothesis of isometric growth, are set in *italic* font. Species in bold denote new maximum length.

Table 3. Results of *t*-tests applied to evaluate the null hypothesis of $b = 3$. Tests were conducted in R (R Core Team 2023), based on species *b* estimates and sample size data presented in Table 2.

Family	Species	df	*t*	*P*
Leuciscidae	*Cyprinella lutrensis*	52	0.627	0.533
Leuciscidae	*Notropis atherinoides*	516	−5.107	**<0.001**$^{\text{HS}}$
Leuciscidae	*Notropis hudsonius*	64	1.941	0.0567
Leuciscidae	*Paranotropis volucellus*	19	−2.790	**0.0117**
Catostomidae	*Carpiodes carpio*	1092	4.169	**<0.001**$^{\text{HS}}$
Catostomidae	*Carpiodes cyprinus*	98	−1.219	0.226
Catostomidae	*Carpiodes velifer*	51	−0.851	0.399
Catostomidae	*Cycleptus elongatus*	52	6.003	**<0.001**$^{\text{HS}}$
Catostomidae	*Ictiobus bubalus*	2811	14.043	**<0.001**$^{\text{HS}}$
Catostomidae	*Ictiobus niger*	520	5.423	**<0.001**$^{\text{HS}}$
Catostomidae	*Moxostoma anisurum*	394	2.387	**0.0174**
Catostomidae	*Moxostoma carinatum*	79	1.882	0.0635
Catostomidae	*Moxostoma erythrurum*	243	4.166	**<0.001**$^{\text{HS}}$
Catostomidae	*Moxostoma macrolepidotum*	1712	4.545	**<0.001**$^{\text{HS}}$

df = degrees of freedom, *P* = *P*-value, *t* = Student's *t* statistic and cases of significant *p*-values are set in bold font. $^{\text{HS}}$ = highly significant *P*-value less than 0.1% of the alpha level of 0.05.

Discussion

The standard allometric equation, $W = aL^b$, is widely employed in fisheries science to estimate length–weight relationships by using log-transformation of the data to linearize the relationship between these variables (Le Cren 1951). When the slope of the LWR meets the condition $b = 3$, then growth is said to be isometric, with individuals attaining similar body proportions at all sizes. Otherwise, when $b > 3$, then growth is positively allometric with larger specimens increasing more in height (i.e., body depth) or width (i.e., plumpness) than in length and when $b < 3$ obtains, then growth is negatively allometric with larger specimens becoming more elongate and less plump than smaller specimens (Blackwell et al. 2000; Froese 2006). Strong trends of allometric growth are considered rare amongst fishes, such that $b > 3.5$ and $b < 2.5$ are more likely explained by sampling artifacts, such as limited coverage of the full size-class range of the species (Carlander 1977) or extreme body shapes (e.g., disc-like or keeled body forms), while isometric and weakly allometric LWR patterns with $b = 2.5$–3.5 are common across fish diversity (reviewed by Froese 2006).

Our results for cypriniform fishes of the Upper Mississippi River are largely in line with these general expectations, with *b* estimates for all 14 study taxa falling between 2.5 and 3.5 (Table 2). However, the null hypothesis of $b = 3$ was only supported by evidence from 95% CIs for *b* in four species (~29%; Table 2) and by *t*-test results in five species (~36%; Table 3). Only one of these taxa, *Carpiodes velifer*, met sampling requirements for interpretation (cf. Froese 2006; Froese et al. 2011) and is concluded to exhibit isometric growth. Interestingly, results for *C. velifer* revealed a new maximum TL of 51.4 cm for the species and the related specimen was caught in Pool 8 (07/03/2018, Mississippi River 1.72 mi (2.77 km) S of Wildcat Park and Landing; 43°40′2.1″N, 91°16′30.8″W) and weighed 2.1 kg, which is also a new maximum improving the LWR. The remaining four taxa for which *t*-tests supported $b = 3$—*C. lutrensis*, *N. hudsonius*, *C. cyprinus*, and *M. carinatum*—had relatively small sample sizes that were statistically valid, but still less than 100 individuals. While isometric or weakly allometric growth seems likely for these taxa, we consider their LWRs provisional, and we recommend additional studies based on larger sample sizes in the future. If imputing missing weight values for these taxa, we suggest doing so only for the sampled length classes.

In contrast to the above findings, *t*-tests rejected the null hypothesis of $b = 3$ in nine species, indicating support for at least weak allometric growth (Table 3). Seven of these had sufficient numerical, geographical, and size-class sampling, as well as R^2 goodness-of-fit statistics, to meet the LWR requirements for confidence interpretation of growth patterns, as follows. *Notropis atherinoides*, the only leuciscid in this category, had a *b* estimate less than 3.0, consistent with negative allometric growth (Table 2). This matches the body shape of this species, which is an elongated minnow with a small head (Mettee et al. 1996; Page and Burr 2011) and it strongly supports faster growth in length than plumpness during the course of development. The remaining six taxa were catostomids with *b* estimates greater than 3.0, consistent with positive allometric growth, supporting faster growth in plumpness and or body depth than length throughout life (Table 2). Three of these were redhorse suckers from genus *Moxostoma*, including *M. carinatum*, *M. erythrurum*, and *M. macrolepidotum*. These species have terete (rounded) bodies and relatively long heads, for example, with head length and body depth proportions around ~21% to ~37% of standard length (e.g., Mettee et al. 1996; JCB, unpublished results). The remaining three species were deeper-bodied suckers from the genera *Carpiodes* and *Ictiobus* with more fusiform (torpedo-shaped) body shape—*C. carpio*, *I. bubalus*, and *I. niger*. These suckers have smaller snouts than their *Moxostoma* counterparts, but relatively large head proportions. They also have much deeper bodies than *Moxostoma* because their backs arch higher, rounding up behind the head to the dorsal fin origin (e.g., Mettee et al. 1996; Page and Burr 2011). Perhaps unsurprisingly, these three species had the highest *b* point estimates in our study (Table 2), with the greatest *b* estimate of 3.106 belonging to *I. niger*, the largest species and this suggest these species add girth both medially and into body depth during development.

Overall, while we consider our LWR estimations valid, three minnow species and three sucker species were relatively rare ($n \leq 100$) in the LTRMP dataset and one of these taxa, *P. volucellus*, had a very small sample size ($n = 21$; Table 2). This could reflect gear artefacts, since we only used data from boat electrofishing, which is generally biased towards smaller individuals (Miranda 2009) and species common to shallower habitats and riverbanks, for example, *C. carpio* (cf. Mettee et al. 1996). Alternatively, this may reflect the greater rarity of these species in main river channel habitats as compared with lower-order tributaries and lakes. Therefore, we recommend additional sampling targeting tributary populations of UMR minnow species and also the use of data from additional gear types, which would be fruitful for comparative purposes and to improve species-level LWR calculations of these taxa in the future.

The focal species had previous LWR estimates available from FishBase (Froese and Pauly 2024) (Table 1) and our parameter estimates generally agreed with previous models within ~2%–5%. Yet, the previous LWRs were from different areas or populations within the focal species ranges. Thus, additional LWRs, based on samples from new areas such as the UMR, remain useful, because they allow nuanced applications of the LWR to the newly sampled areas. Additionally, when the goal is to apply the LWR at the species level (e.g., data imputation) or to a non-analog season or geographical area, then taking the geometric mean of *a* and *b* across all available studies is suggested (Froese 2006), which is less influenced by extreme values and is suitable for logarithmic data. Each additional LWR study provides a new data point for geometric mean calculation. Our results substantially improve available estimates for six species for which only a single LWR estimate was available, including all four minnows and the suckers *C. elongatus* and *I. niger* (Table 1). For example, the FishBase LWR (Froese and Pauly 2024) for *C. elongatus* was based on Swingle's (1965) study of only six specimens, as reported in Carlander (1969) and the FishBase LWR for *I. niger* was calculated from a single International Game Fish Association world record (Crawford 1993). Prior LWRs for other species were, at times, based on very large sample sizes, for example, where Swingle (1965) evaluated $n = 13\,623$ fish when estimating LWR parameters for *N. atherinoides* in Alabama. Nonetheless, we more confidently estimated *a* and *b* for *C. elongatus* and *I. niger* based on a range of size classes represented by much larger samples of $n = 54$ and $n = 522$ specimens, respectively (Table 2). Overall, these results provide new insights into LWRs for Upper Mississippi cypriniform fishes and will be useful for calculating fish biomass or imputing missing data in future studies of the species-rich and economically important fish fauna of the UMR.

Acknowledgments

This work was supported by the Department of Biology and Environmental Sciences at Auburn University at Montgomery. We thank the Upper Midwest Environmental Science Center (UMESC) and staff for their collection efforts and for providing access to the Long Term Resource Monitoring Program (LTRMP) fisheries data analyzed in this study. Additionally, we thank the Editor and one anonymous external reviewer for providing helpful comments and suggestions on an earlier draft of this manuscript.

References

Ardren WR, Jordan GR, DeHaan PW, Waples RS (2022) Demographic and evolutionary history of pallid and shovelnose sturgeon in the upper Missouri River. Journal of Fish and Wildlife Management 13(1): 124–143. https://doi.org/10.3996/JFWM-21-035

Bagley JC, Breitman MF, Johnson JB (2022) Length–weight relation for seven Neotropical freshwater fish species (Actinopterygii) endemic to Central America. Acta Ichthyologica et Piscatoria 52(3): 183–187. https://doi.org/10.3897/aiep.52.86467

Bart Jr HL, Clements MD, Blanton RE, Piller KR, Hurley DL (2010) Discordant molecular and morphological evolution in buffalofishes (Actinopterygii: Catostomidae). Molecular Phylogenetics and Evolution 56(2): 808–820. https://doi.org/10.1016/j.ympev.2010.04.029

Bessert ML, Ortí G (2008) Genetic effects of habitat fragmentation on blue sucker populations in the upper Missouri River (*Cycleptus elongatus* Lesueur, 1918). Conservation Genetics 9(4): 821–832. https://doi.org/10.1007/s10592-007-9401-4

Black R, McKenney B, O'Connor A, Gray E, Unsworth R (1999) Economic profile of the upper Mississippi River region. Industrial Economics, Incorporated, Cambridge, MA, USA, 84 pp.

Blackwell BG, Brown ML, Willis DW (2000) Relative weight (W_r) status and current use in fisheries assessment and management. Reviews in Fisheries Science 8(1): 1–44. https://doi.org/10.1080/10641260091129161

Burr BM, Page LM (1986) Zoogeography of fishes of the lower Ohio–upper Mississippi basin. Pp. 287–324. In: Hocutt CH, Wiley EO (Eds.) The zoogeography of North American freshwater fishes. John Wiley and Sons, New York, NY, USA.

Carlander KD (1969) Handbook of freshwater fishery biology, Vol. 1. Iowa State University Press, Ames, IA, USA, 752 pp.

Carlander KD (1977) Handbook of freshwater fishery biology, Vol. 1. Iowa State University Press, Ames, IA, USA, 431 pp.

Carlson BD, Propst DB, Stynes DJ, Jackson RS (1995) Economic impact of recreation on the upper Mississippi River system. Technical Report EL-95-16, US Army Corps of Engineers, Waterways Experiment Station, 45 pp. https://doi.org/10.21236/ADA294201

Chick JH, Pegg MA, Koel TM (2006) Spatial patterns of fish communities in the upper Mississippi River system: Assessing fragmentation by low-head dams. River Research and Applications 22(4): 413–427. https://doi.org/10.1002/rra.912

Clark FN (1928) The weight–length relationship of the California sardine (*Sardina caerulea*) at San Pedro. Division of Fish and Game, Fish Bulletin No. 12, 59 pp.

Crawford R (1993) World record game fishes 1993. The International Game Fish Association, Pompano Beach, FL, USA.

Crimmins SM, Boma P, Thogmartin WE (2015) Projected risk of population declines for native fish species in the upper Mississippi River. River Research and Applications 31(2): 135–142. https://doi.org/10.1002/rra.2741

Dettmers JM, Gutreuter S, Wahl DH, Soluk DA (2001) Patterns in abundance of fishes in main channels of the upper Mississippi River system. Canadian Journal of Fisheries and Aquatic Sciences 58(5): 933–942. https://doi.org/10.1139/f01-046

Fremling CR, Rasmussen JL, Sparks RE, Cobb SP, Bryan CF, Claflin TO (1989) Mississippi River fisheries: A case history. Canadian Special Publication of Fisheries and Aquatic Sciences 106: 309–351. https://openriver.winona.edu/calfremlingpapers/34

Fricke R, Eschmeyer WN, van der Laan R [Eds.] (2024) Eschmeyer's catalog of fishes: Genera, species, references. California Academy of Sciences, San Francisco, CA, USA. [Accessed on 5 April 2024] http://researcharchive.calacademy.org/research/ichthyology/catalog/fishcatmain.asp

Froese R (2006) Cube law, condition factor and weight–length relationships: History, meta-analysis and recommendations. Journal of Applied Ichthyology 22(4): 241–253. https://doi.org/10.1111/j.1439-0426.2006.00805.x

Froese R, Pauly D [Eds.] (2024) FishBase. [Version 02/2024] http://www.fishbase.org

Froese R, Tsikliras AC, Stergiou KI (2011) Editorial note on weight–length relations of fishes. Acta Ichthyologica et Piscatoria 41(4): 261–263. https://doi.org/10.3750/AIP2011.41.4.01

Gaffigan M, Fennell AM, Hunt VR, Hocker JW, Gilbert C, Kirby G, Moye T, Royer D (2021) US Army Corps of Engineers: Information on the Navigation and Ecosystem Sustainability Program. Technical Report GAO-21-240R, US Army Corps of Engineers, Government Accountability Office, Washington, DC, USA, 15 pp.

Garvey J, Ickes B, Zigler S (2010) Challenges in merging fisheries research and management: The upper Mississippi River experience. Hydrobiologia 640(1): 125–144. https://doi.org/10.1007/s10750-009-0061-x

Hammer Ø, Harper DAT, Ryan PD (2001) PAST: Paleontological statistics software package for education and data analysis. Palaeontologia Electronica 4(1): 1–9.

Hashiguti DT, Soares BE, Wilson KL, Oliveira-Raiol RD, Montag LFDA (2019) Comparing three methods to estimate the average size at first maturity: A case study on a curimatid exhibiting polyphasic growth. Ecology Freshwater Fish 28(2): 266–273. https://doi.org/10.1111/eff.12451

Heymans JJ, Coll M, Link JS, Mackinson S, Steenbeek J, Walters C, Christensen V (2016) Best practice in Ecopath with Ecosim food-web models for ecosystem-based management. Ecological Modelling 331: 173–184. https://doi.org/10.1016/j.ecolmodel.2015.12.007

Ickes BS, Bowler MC, Bartels AD, Kirby DJ, DeLain S, Chick JH, Barko VA, Irons KS, Pegg MA (2005) Multiyear synthesis of the fish component from 1993 to 2002 for the long term resource monitoring program. Technical Report 2005-T005, US Geological Survey, Upper Midwest Environmental Sciences Center, La Crosse, WI, USA, 60 pp.

Jellyman PG, Booker DJ, Crow SK, Jellyman DJ (2013) Does one size fit all? An evaluation of length–weight relationships for New Zealand's freshwater fish species. New Zealand Journal of Marine and Freshwater Research 47(4): 450–468. https://doi.org/10.1080/00288330.2013.781510

Kirby DJ, Ickes BS (2006) Temporal and spatial trends in the frequency of occurrence, length-frequency distributions, length–weight relationships, and relative abundance of upper Mississippi River fish. Technical Report 2006-T002, US Geological Survey, Upper Midwest Environmental Sciences Center, La Crosse, WI, USA, 68 pp.

Le Cren ED (1951) The length–weight relationship and seasonal cycle in gonad weight and condition in the perch (*Perca flavescens*). Journal of Animal Ecology 20(2): 201–219. https://doi.org/10.2307/1540

Mettee MF, O'Neil PE, Pierson JM (1996) Fishes of Alabama and the Mobile Basin. Oxmoor House, Birmingham, AL, USA, 820 pp.

Miranda LE (2009) Standardizing electrofishing power for boat electrofishing. Pp. 223–230. In: Bonar SA, Hubert WA, Willis DW (Eds.) Standard methods for sampling North American freshwater fishes. American Fisheries Society, Bethesda, MD, USA. https://doi.org/10.47886/9781934874103.ch14

Mundahl ND, Simon TP (1999) Development and application of an index of biotic integrity for coldwater streams of the upper Midwestern United States. Pp. 383–415. In: Simon TP (Ed.) Assessing the sustainability and biological integrity of water resources using fish communities. CRC Press, Boca Raton, FL, USA. https://doi.org/10.1201/9781003068013-19

Page LM, Burr BM (2011) A field guide to freshwater fishes of North America north of Mexico. Houghton Mifflin Harcourt, Boston, MA, USA, 663 pp.

Page LM, Espinosa-Pérez H, Findley LT, Gilbert CR, Lea RN, Mandrak NE, Mayden RL, Nelson JS (2013) Common and Scientific Names of Fishes from the United States, Canada, and Mexico, 7th Edn. American Fisheries Society, Special Publication 34, Bethesda, MD, USA, 384 pp.

Page LM, Bemis KE, Dowling TE, Espinosa-Pérez HS, Findley LT, Gilbert CR, Hartel KE, Lea RN, Mandrak NE, Neighbors MA, Schmitter-Soto JJ (2023) Common and Scientific Names of Fishes from the United States, Canada, and Mexico, 8th Edn. American Fisheries Society, Bethesda, MD, USA, 435 pp.

Piller KR, Wilson CC, Lee CE, Lyons J (2005) Conservation genetics of inland lake trout in the upper Mississippi River basin: Stocked or native ancestry? Transactions of the American Fisheries Society 134(4): 789–802. https://doi.org/10.1577/T04-040.1

Pitlo Jr J, Van Vooren A, Rasmussen J (1995) Distribution and relative abundance of upper Mississippi River fishes. Upper Mississippi River Conservation Committee, Rock Island, IL, USA.

R Core Team (2023) R: A language and environment for statistical computing. R Foundation for Statistical Computing, Vienna, Austria. https://www.R-project.org/

Smith Jr LL (1949) Cooperative fishery survey of the upper Mississippi River. Transactions of the American Fisheries Society 76(1): 279–282. https://doi.org/10.1577/1548-8659(1946)76[279:CFSOTU]2.0.CO;2

Smith RJ (2009) Use and misuse of the reduced major axis for line-fitting. American Journal of Physical Anthropology 140(3): 476–486. https://doi.org/10.1002/ajpa.21090

Smith PW, Lopinot AC, Pflieger WL (1971) A distributional atlas of upper Mississippi River fishes. Biological Notes 073. https://doi.org/10.5962/bhl.title.15867

Swingle WE (1965) Length–weight relationships of Alabama fishes. Agricultural Experiment Station, Auburn University, Auburn, AL, USA, 87 pp.

Tripp S, Brooks R, Herzog D, Garvey J (2014) Patterns of fish passage in the upper Mississippi River. River Research and Applications 30(8): 1056–1064. https://doi.org/10.1002/rra.2696

USGS [US Geological Survey] (2024) Fisheries liability disclosure and format description—Disclaimer. Upper Midwest Environmental Sciences Center. [04/05/2024] https://www.umesc.usgs.gov/cgi-bin/ltrmp/fish/fish_meta.pl

Weitzell RE, Khoury ML, Gagnon P, Schreurs B, Grossman D, Higgins J (2003) Conservation priorities for freshwater biodiversity in the upper Mississippi River basin. Nature Serve and The Nature Conservancy.

Acta Ichthyologica et Piscatoria 54, 2024, 221–233 | DOI 10.3897/aiep.54.130966

ACTA
ICHTHYOLOGICA
ET PISCATORIA

Evaluation of ecological health of Hainan Island inshore waters in the South China Sea based on preliminary fish biotic integrity index (Actinopterygii and Elasmobranchii)

Peimin YU[1*], Zhengli LUO[2,3*], Liangming WANG[2,4,5], Yan LIU[2,5], Yingbang HUANG[2], Binbin SHAN[2,5], Changping YANG[2,5], Dianrong SUN[2,5]

1 *Fisheries and Fisheries Administration, Ministry of Agriculture and Rural Affairs, Beijing, China*
2 *South China Sea Fisheries Research Institute, Chinese Academy of Fisheries Sciences, Guangzhou, China*
3 *School of Fisheries, Zhejiang Ocean University, Zhoushan, China*
4 *Sanya Tropical Fisheries Research Institute, Sanya, China*
5 *Key Laboratory of Marine Ranching, Ministry of Agriculture and Rural Affairs, Guangzhou, China*

https://zoobank.org/6A90954E-DFD3-4670-980F-D4245C9FCA2D

Corresponding author: Dianrong Sun (drsun73@scsfri.ac.cn)

Academic editor: Sanja Matić-Skoko ♦ **Received** 1 July 2024 ♦ **Accepted** 6 September 2024 ♦ **Published** 14 October 2024

Citation: Yu P, Luo Z, Wang L, Liu Y, Huang Y, Shan B, Yang C, Sun D (2024) Evaluation of ecological health of Hainan Island inshore waters in the South China Sea based on preliminary fish biotic integrity index (Actinopterygii and Elasmobranchii). Acta Ichthyologica et Piscatoria 54: 221–233. https://doi.org/10.3897/aiep.54.130966

Abstract

The well-being of marine ecosystems significantly influences biodiversity and ecological equilibrium amidst pressing challenges such as overfishing, water pollution, and climate change. Drawing upon data from two fishery stock surveys conducted in the inshore waters of Hainan Island in 2022, this study undertook a comprehensive evaluation of the marine ecosystem's health status in the region. Employing the Fish Index of Biological Integrity (F-IBI) analysis method, coupled with an examination of the structural and functional aspects of the fish community, our research sheds light on the prevailing conditions. Our study revealed a spatial dichotomy within the fish communities of the study area and delineated them into two distinct groups: the northwestern and southeastern ones, with evident disparities in community structure between the two. By employing indicator screening and calculation, we segmented the fish health index in the inshore waters of Hainan Island into five tiers. Despite discernible anthropogenic influences, the ecological health of these waters remained generally robust. Notably, the mean F-IBI of fall (56.30) significantly exceeded that of spring (48.16) ($P < 0.01$). Furthermore, regarding spatial distribution, the ecological well-being of the southeastern waters surpassed that of the northwestern and Qionghzhou Strait waters. This study represents a pioneer endeavor to apply ecological health assessment methodologies towards informing resource management and conservation strategies for the inshore fisheries of Hainan Island. By furnishing a scientific foundation, our research contributes to the pursuit of sustainable marine ecological development within this locale.

Keywords

ecological health assessment, environmental factors, fish community structure, F-IBI, Hainan Island

---

[*] These authors contributed equally to this work.

Introduction

Amid escalating pressures on the global marine environment, the conservation of marine biodiversity and ecosystem health has captured international focus (Palumbi et al. 2009). Marine ecosystems, harboring a significant portion of the planet's biodiversity, are essential for providing irreplaceable resources, including food, medicinal products, ecological services, and cultural values (Parsons et al. 2014; Canonico et al. 2019). Situated as the second largest island of China, Hainan Island features a unique and intricate marine ecosystem. The island's biodiversity and ecological conditions are critical to maintaining regional and global ecological balance and promoting sustainable development (He et al. 2014; Hu et al. 2018).

Hainan Island's strategic geographic location, abundant marine biological resources, and dynamic marine environment have made the inshore waters a pivotal site for marine scientific research and resource management. Recent challenges such as global climate change (Poloczanska et al. 2013), overfishing (Pauly and Zeller 2016), marine pollution (Jambeck et al. 2015), and habitat degradation (Halpern et al. 2015) have posed significant threats to the biodiversity in these waters, thereby garnering substantial attention from the scientific and regulatory communities. It has been observed that the coastal economic activities of Hainan Island increasingly threaten marine life and their habitats, with biodiversity and living marine resources experiencing various disturbances (Wang et al. 2008; Fu et al. 2018). Addressing the challenge of accurately assessing ecological health remains a critical research priority (Borja et al. 2008).

In response to these challenges, the Index of Biological Integrity (IBI) and the Fish-based Index of Biotic Integrity (F-IBI) have emerged as prominent tools for assessing the health of freshwater and marine ecosystems (Karr 1981; Liao and Huang 2013; Li et al. 2018), and the approach was initially proposed by Karr (1981) and has evolved into one of the most extensively utilized indicators in research on aquatic ecosystem health (Kerans and Karr 1994). The handling and identification of fish are comparatively easier compared to other organisms, as they exhibit higher sensitivity towards environmental stresses. Additionally, being positioned at the top of the food chain enhances the potential application of indicators based on fish communities (Karr 1991). The F-IBI, in particular, offers a comprehensive measure of ecosystem health by amalgamating data on fish community structure, species diversity, and functional groups (Huang et al. 2022). For instance, Abhijna and Kumar (2017) used F-IBI to examine the biological integrity of two Indian lakes, and Veli-Akkulam and Vellayani found that the biological integrity of the lakes far away from the source of pollution was preserved. Conversely, Li et al. (2013) applied the F-IBI to highlight the detrimental effects of dam construction on the fish communities of the Lancang/Mekong River. Hence, the F-IBI provides a robust framework for quantifying ecosystem health and guiding conservation and resource management strategies.

As an integral component of the South China Sea ecosystem, the marine ecological health of inshore Hainan Island waters influences not only local biodiversity and fisheries but also broader stability and sustainability of the regional marine ecosystem. Although extensive research has been conducted on the biodiversity in Hainan's inshore waters, studies focusing on their ecological health are scant (Sun et al. 2012). This study leverages bottom trawl fishery survey data collected in May and September 2022, while the F-IBI construction method was introduced, and the research objectives are to:

- Delineate the structure and distribution patterns of the fish community.
- Develop an ecological health assessment index tailored for the inshore waters of Hainan Island.
- Evaluate the health status of this study area.

Materials and methods

Study area. The inshore waters of Hainan Island (Fig. 1) are renowned for their rich biodiversity and distinctive marine ecosystems. This unique geographic setting (17°47′00″–20°12′00″N and 108°21′00″–111°33′00″E) hosts a diverse array of ecologically significant environments including coral reefs, seagrass meadows, and shoals. Notably, these waters are also abundant in mangrove ecosystems, particularly around Haikou and Wenchang, providing crucial habitats for a variety of fishes, crustaceans, and birds. Several national nature reserves have been established within this region to conserve the marine biodiversity. These include the Coral Reef National Reserve, Tongguling National Reserve, the Dongzhaigang National Nature Reserve in Sanya, and the Boundary Island National Marine Park in Lingshui. These reserves play a pivotal role in conserving coral reef ecosystems and serve as invaluable natural laboratories for scientific research. Furthermore, the unique currents and rich plankton communities present in the waters around Hainan Island are central to the studies on geographic distribution of marine organisms, marine ecological dynamics, and primary productivity (Liu 2013; Li et al. 2014).

Data sources. In the spring (May) and fall (September) of 2022, we conducted two surveys on marine ecology and fishery resources in the inshore waters of Hainan Island. In this study, our surveys employed an otter trawler *Guibeiyu 69068* with main engine power of 436 kW. The headrope length of the trawl net measured 37.7 m and the codend mesh was 20 cm. Considering the variations in the surrounding environment of Hainan Island, we established a total of 50 survey stations encompassing the shallow region with a depth of 200 meters (Liu 2013; Li et al. 2014). This area is characterized by high fishing activity around Hainan Island, thus enabling a more comprehensive survey and analysis to reasonably evaluate the ecological health status of this region. For each survey, at

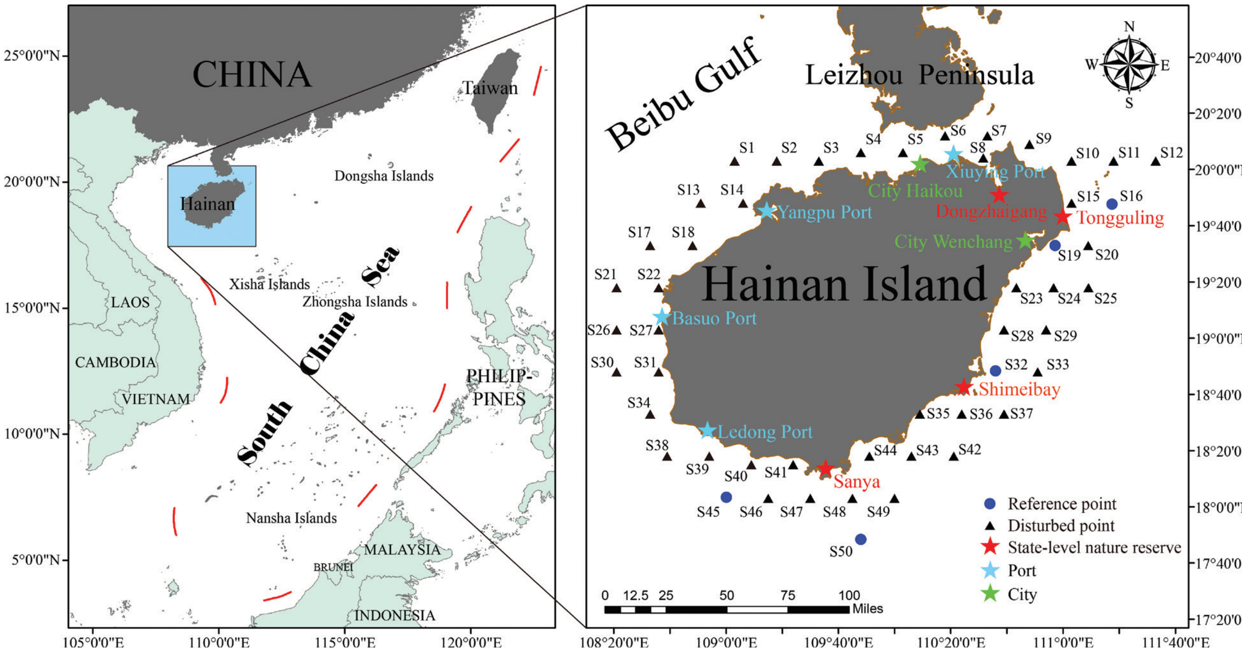

Figure 1. Stations for fishery resources survey in the inshore waters of Hainan Island.

each station one trawl was conducted lasting one hour at a steady speed of around 3 knots. All the trawl samplings were conducted during daytime.

For the sorting of the captured fishes, we referred to the most recent ichthyological literature (Shen and Wu 2011; Chen 2014; Chen and Zhang 2015; Wu and Zhong 2021) while the taxonomic status of species was verified using Fricke et al (2024) and WoRMS Editorial Board (2024). Fish samples from each station were sorted, weighed, counted, and biologically measured on-site, with weight measurements recorded to the nearest 0.1 g. Samples that could not be identified to species level onboard were cryopreserved for further identification in the laboratory.

F-IBI reference point selection. Currently, there is no uniform international standard for selecting reference points in marine studies, which are generally categorized into two types: those that utilize historical data as the baseline (Li et al. 2018), and those that choose areas either untouched or minimally impacted by human activities (Das et al. 2013) as the baseline. However, the inshore waters of Hainan Island present challenges in this regard due to the absence of comprehensive historical data and the lack of areas completely free from human disturbance (Stoddard et al. 2006). Consequently, for this study, five survey stations (S16, S19, S32, S45, and S50) were selected as reference sites for this study. These stations represent well-preserved marine habitats that are minimally disturbed by human activities. They are primarily situated in the sea area adjacent to the national nature reserve or in natural sea areas distanced from human influences.

Screening of F-IBI candidate indicators. In this study, we selected a total of 25 candidate indicators sensitive to ecological disturbances, such as species composition and abundance, trophic guild, thermal tolerance, reproductive guild, and habitat preference (Li et al. 2013; Li et al. 2018; Karr 1981) (Table 1). The selection process involved several screening steps: (1) Distribution range screening (Barbour et al. 1996): indicators were excluded if the number of species was fewer than 10 across all survey stations, if the variation in proportions across all stations was less than 10%, or if more than 90% of the indicator values at all stations were zero. (2) Discriminative ability screening (Zhu et al. 2021): indicators were removed if the medians for reference and observation sites fell within the 25th to 75th percentile range of each other. (3) Calculation of correlation coefficients (Zhang et al. 2020): the remaining indicators underwent correlation analysis, and any with a correlation coefficient ($|R|$) less than 0.9 were retained ($|R| < 0.9$); otherwise, the more informative of the correlated indicators was selected. (In Suppl. material 1, we have added specific data and detailed calculations and results for the ten indicators retained.)

F-IBI calculations. Among the standardization methods for IBI system evaluation, the ratio method is the most accurate and effective method (Wang et al. 2005), so the ratio method was used in this study. The standardization of each indicator was divided into two methods (Zhao et al. 2019):

The index of decreasing value as interference increases and its standardized index mode are as follows

$$P_{ij} = O_{ij} \times S_{i95}^{-1} \times 100$$

where: P_{ij} and O_{ij} are the standardized index and raw value of the i^{th} indicator at the j^{th} survey site, respectively, and S_{i95} is the standardized threshold for the i^{th} indicator, taking the raw value of the i^{th} indicator at the 95th percentile of all survey sites.

Table 1. Candidate indicators for the F-IBI and their expected directions of response to disturbance.

Indicator	Candidate Indicators	Response to Disturbance	Condition
Species composition and abundance	Number of individuals (M1)	Decrease	Exclusion
	Species of fish (M2)	Decrease	Remain
	(H') Shannon–Wiener index (M3)	Decrease	Remain
	Percentage of Gobiidae (M4)	Increase	Exclusion
	Maean catch per unit net trip/kg·h^{-1} (M5)	Decrease	Exclusion
	(D) Margalef index (M6)	Decrease	Remain
	Percentage of Perciformes (M7)	Increase	Remain
Trophic guild	Percentage of piscivorous fish (M8)	Decrease	Remain
	Percentage of carnivorous fish (M9)	Decrease	Exclusion
	Percentage of omnivorous fish (M10)	Increase	Exclusion
	Percentage of zooplanktivorous fish (M11)	Increase	Exclusion
	Percentage of benthivorous fish (M12)	Decrease	Remain
Thermal tolerance	Percentage of warm-water fish (M13)	Increase	Exclusion
	Percentage of warm-temperate fish (M14)	Decrease	Exclusion
	Percentage of cold-temperate fish (M15)	Decrease	Exclusion
Reproductive guild	Percentage of pelagic-spawning fish (M16)	Increase	Exclusion
	Percentage of demersal-spawning fish (M17)	Increase	Exclusion
	Percentage of adhesive-sinking egg fish (M18)	Decrease	Exclusion
	Percentage of adhesive-floating egg fish (M19)	Decrease	Exclusion
	Percentage of ovoviviparous fish (M20)	Increase	Exclusion
Habitat preference	Percentage of demersal fish in the continental shelf sandy-muddy bottom (M21)	Decrease	Remain
	Percentage of near-bottom fish in the continental shelf (M22)	Decrease	Remain
	Percentage of mid-upper water column fish in the continental shelf (M23)	Increase	Remain
	Percentage of reef-associated fish (M24)	Decrease	Remain
	Percentage of oceanic fish (M25)	Increase	Exclusion

The index of increasing value as interference increases and its standardized index mode are as follows

$$P_{ij} = (\max O_{ij} - O_{ij}) \times (\max O_{ij} - S_{i5})^{-1}$$

where: $\max O_{ij}$ is the maximum value of the i^{th} indicator across all survey sites, and S_{i5} is the standardized threshold for the i^{th} indicator, taken as the raw value of the 5th percentile of the i^{th} indicator across all survey sites.

The F-IBI value for each survey site is the mean of the standardized indices of each parameter at that site

$$\mathrm{IBI}_j = \frac{1}{m}\sum_{i}^{m} = 1P_{ij}$$

Where: IBI_j is the F-IBI value of the j^{th} survey site and m is the number of indicators after screening.

The 25% quartile of the F-IBI score at the reference points was classified as a health criterion, and F-IBI values above this criterion were evaluated as healthy. F-IBI values below this criterion were categorized into four intervals from high to low, representing good, fair, poor and bad ecosystem health, respectively.

Data analysis—Index of Relative Importance (IRI). The ecological dominance of fish communities during different seasons was evaluated using the index of relative importance (IRI), calculated using three components (Pinkas et al. 1971; Martin et al. 1996).

$$\mathrm{IRI} = (N\% + W\%) \times F\%$$

where $N\%$ is the percentage of individuals of a specific fish species in relation to the total catch, $W\%$ is the percentage of the total weight that a particular fish species contributes to the overall catch weight, and $F\%$ is the frequency of occurrences of that species across all sampling stations. Based on the IRI, species classifications are as follows: species with an IRI value of 1000 or more are deemed dominant; those with IRI values ranging from 100 to 1000 are considered important; species with IRI values between 10 and 100 are categorized as common; and species with IRI values less than 10 are classified as rare.

Data analysis—calculation of diversity indices. The Shannon–Wiener diversity index (H') was used in this study to calculate community species diversity based on biomass density (Li and Chen 2008). The improved formula proposed by Wilhm (1970) was employed for the calculation, which is defined as follows

$$H' = -\textstyle\sum_{i=1}^{S}(P_i \in P_i)$$

Margalef species richness index (D)

$$D = (S - 1) \cdot (\ln N)^{-1}$$

where S represents the total number of fish species captured in the study area, P_i denotes the weight percentage of the i^{th} fish species, and N represents the total number of individuals of captured fishes.

Similarity analysis of community structure. We determined potential spatial clustering of fish community structure using cluster rank clustering, which is based on the group-averaged connectivity of the Bray–Curtis similarity matrix. Prior to calculation, fish abundance data were square root transformed (Clarke 1993). To evaluate the significance of changes in community structure between groups, we utilized an Analysis of Similarity (ANOSIM) method, focusing on fish species composition and relative abundance (Clarke 1993). Non-metric Multidimensional Scaling (NMDS) was subsequently applied to validate the clustering accuracy and characterize the fish composition in the inshore waters of Hainan Island. The effectiveness of NMDS was gauged using a stress coefficient, with values under 0.05 indicating a well-represented two-dimensional dot plot, values between 0.05 and 0.10 suggesting generally credible results, and values between 0.10 and 0.20 offering some interpretative significance (Clarke and Ainsworth 1993).

Results

Fish species composition. In the spring and fall surveys, we captured a total of 363 fish species from 24 orders, 114 families, and 226 genera (Suppl. material 2), of which 347 were ray-finned fishes (Actinopterygii) spanning 18 orders, 105 families, and 217 genera, representing 95.59% of the total number of species. The most prevalent order was Perciformes, represented by 181 species from 56 families and 107 genera, comprising 49.86% of the total number of species, and including nine Gobiidae species (2.48%). The next most common order was Scorpaeniformes (10.74%), with 39 species across 8 families and 31 genera, followed by Pleuronectiformes (9.37%), with 34 species in 7 families and 19 genera, and Anguilliformes (6.06%), with 22 species in 8 families and 13 genera. Species from other orders constituted < 5% of the total. Additionally, we recorded 15 species of elasmobranchs (Elasmobranchii) (4.13%) from 5 orders, 8 families, and 8 genera. Notably, Myliobatiformes had the highest species count (5 species), while Orectolobiformes only 1 species. In addition to numerous ray-finned fished and elasmobranchs, we collected also a single species representing Cyclostomata (Fig. 2). The most frequently occurring species were: *Acropoma japonicum* Günther, 1859, *Decapterus maruadsi* (Temminck et Schlegel, 1843), *Saurida tumbil* (Bloch, 1795), *Saurida undosquamis* (Richardson, 1848), *Champsodon atridorsalis* Ochiai et Nakamura, 1964, and *Photopectoralis bindus* (Valenciennes 1835), appearing in > 60% of the survey sites (Table 2).

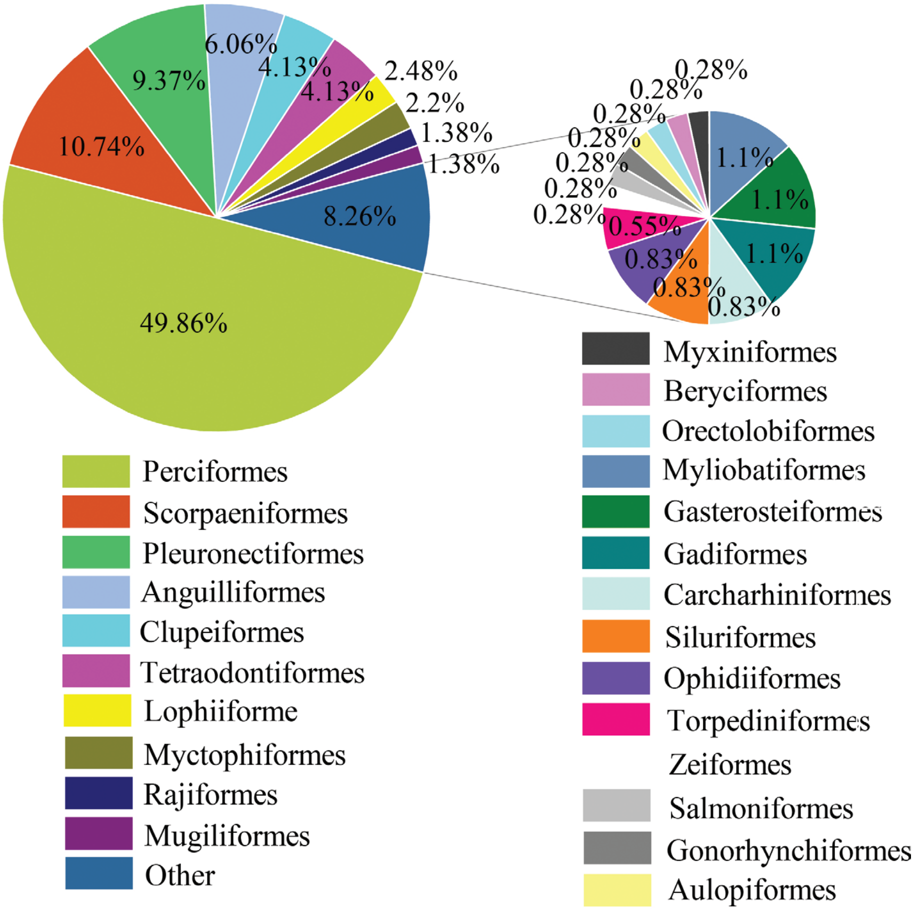

Figure 2. Composition of fish species in the inshore waters of Hainan Island.

Table 2. Dominant species (IRI > 100) in the inshore waters of Hainan Island.

Season	Species	*F* [%]	*W* [%]	*N* [%]	IRI
Spring	*Acropoma japonicum* Günther, 1859	36	22.39	61.32	3013.82
	Decapterus maruadsi (Temminck et Schlegel, 1843)	62	12.94	10.86	1475.74
	Thamnaconus hypargyreus (Cope, 1871)	44	7.96	4.50	548.26
	Trachurus japonicus (Temminck et Schlegel, 1844)	58	4.21	2.46	386.92
	Upeneus japonicus (Houttuyn, 1782)	52	4.25	3.15	385.01
	Psenopsis anomala (Temminck et Schlegel, 1844)	50	5.89	0.53	321.09
	Saurida tumbil (Bloch, 1795)	72	2.59	0.44	217.72
	Champsodon atridorsalis Ochiai et Nakamura, 1964	64	1.11	1.92	194.26
	Saurida undosquamis (Richardson, 1848)	70	1.79	0.32	147.97
Fall	*Photopectoralis bindus* (Valenciennes 1835)	64	2.13	9.29	730.84
	Saurida tumbil (Bloch, 1795)	52	5.34	2.94	646.08
	Champsodon atridorsalis Ochiai et Nakamura, 1964	36	0.59	7.94	528.74
	Leiognathus berbis (Valenciennes, 1835)	34	2.23	6.45	451.21
	*Johnius belangeri*i (Cuvier, 1830)	54	6.09	4.80	392.12
	Saurida undosquamis (Richardson, 1848)	42	2.97	2.17	380.45
	*Pennahia macrocephalu*s (Tang, 1937)	46	7.66	3.29	372.31
	Acropoma japonicum Günther, 1859	32	1.83	8.56	332.49
	Upeneus japonicus (Houttuyn, 1782)	50	3.64	3.90	331.61
	Brachypleura novaezeelandiae Günther, 1862	30	1.75	2.99	256.09
	Pennahia aneus (Bloch, 1793)	38	3.04	2.68	240.42
	Decapterus maruadsi (Temminck et Schlegel, 1843)	32	1.94	0.77	200.44
	Terapon theraps Cuvier, 1829	74	2.61	1.27	178.53
	Rogadius asper (Cuvier, 1829)	44	2.66	1.90	145.78
	Upeneus sulphureus Cuvier, 1829	78	1.31	1.05	118.03
	Ilisha melastoma (Bloch et Schneider, 1801)	62	2.01	1.76	113.01
	*Parargyrops edit*a Tanaka, 1916	74	2.04	0.82	108.69

Based on dietary preferences, the survey identified 48 piscivorous species (13.22% of the total), 2 generalist species (0.55%), 142 omnivorous species (39.12%), 33 zooplanktivorous species (9.09%), and 138 benthic-animal-feeding species (38.02%). Thermally, 335 species (92.29%) are warm-temperate, 25 species (6.89%) are warm-water, and 3 species (0.83%) are cold-temperate species. Regarding reproductive types, 323 species (88.98%) lay floating eggs, 13 species (3.58%) lay attached eggs, 7 species (1.93%) lay adhesive sinking eggs, 5 species (1.38%) lay adhesive floating eggs, and 15 species (4.13%) are ovoviviparous. Ecologically, 244 species (67.22%) are demersal or near-demersal, 61 species (16.80%) are pelagics, and 58 species (15.98%) are reef-associated (Suppl. material 2).

Spatial patterns of fish communities. Hierarchical cluster analysis (CA), using group-averaged connectivity and based on the Bray–Curtis similarity matrix, spatially classifies all survey sites into two groups in both seasons (Fig. 3). In the spring season, group I is primarily located in the northwestern waters in the Beibu Gulf and Qiongzhou Strait. This region features dense human population, heavy marine traffic, and significant anthropogenic interferences. Conversely, group II is distributed in the southeastern waters and characterized by open-sea environment, several protected areas, an intact natural landscape, and less anthropogenic interferences. Dominant fish species in the spring season include *Acropoma japonicum*, *Decapterus maruadsi*, and *Trachurus japonicus* (Temminck et Schlegel, 1844) (Table 2). NMDS plots indicate significant differences between the two groups with only partial overlap. The NMDS plots are consistent with CA, confirming the meaningfulness of the classifications. ANOSIM confirms highly significant differences in fish community structure between the two clusters ($R = 0.527$, $P < 0.01$). In the fall season, the clustering remains unchanged in spatial distribution as compared to that of the spring season. Featuring dominant species include *Photopectoralis bindus*, *Saurida tumbil*, and *Johnius belangerii* (Cuvier, 1830) (Table 2). NMDS plots indicate that the stress was < 0.2, suggesting some explanatory significance. ANOSIM also shows a highly significant difference ($R = 0.72$, $P < 0.01$) in the structure of fish community between the two groups.

Selection of core indicators and establishment of F-IBI. The 25 candidate indicators presented in Table 1 underwent an initial distributional range test, resulting in the exclusion of candidates M4, M9, M11, M15, M17–M20, and M25 due to nonapplicability. The remaining 16 indicators were assessed for discriminating ability using the box-and-line plot method. It was determined that the medians of six indicators—M1, M5, M10, M13, M14, and M16—fell within the 25th to 75th percentile range of the opposing side (Fig. 4). Subsequently, Pearson analysis was conducted to refine the selection, identifying M2, M3, M6, M7, M8, M12, and M21–M24 as core indicators for constructing the Fish-based Index of Biotic Integrity (F-IBI), as detailed in Fig. 5. These core indicators were standardized as shown in Table 1, and F-IBI

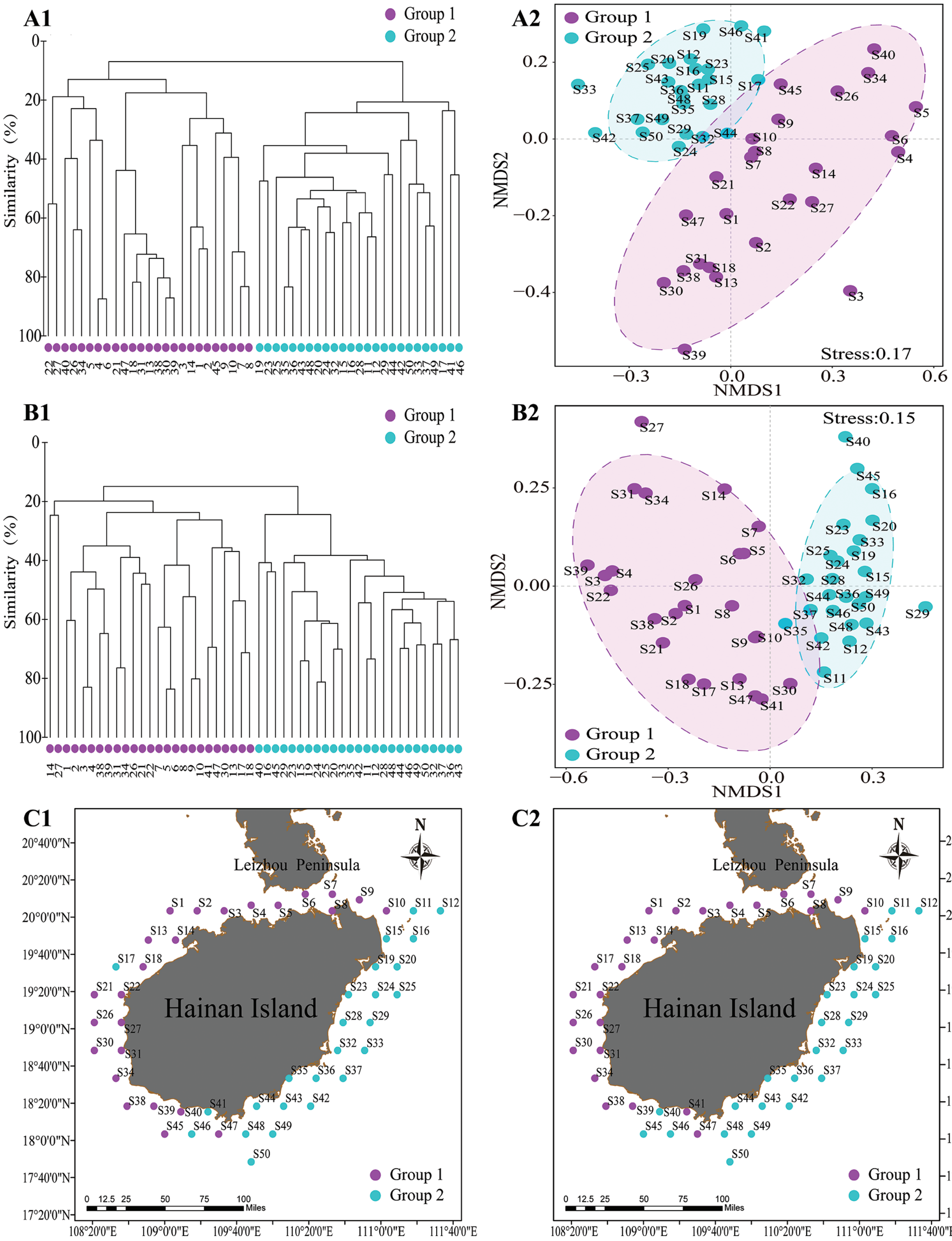

Figure 3. Clustering and NMDS plots fish trawl samples in the inshore waters of Hainan Island in spring (**A1** and **A2**) and fall (**B1** and **B2**). Spring and fall (**C1** and **C2**) Group 1 Group 2 site distribution map.

values were calculated for each station in each season (Fig. 6). The health assessment system's grading criteria for the inshore waters of Hainan Island, as outlined in Table 3, categorizes the ecological status as follows: F-IBI ≥ 68.58 indicates "healthy"; 51.44 ≤ F-IBI < 68.58 signifies "good"; 34.29 ≤ F-IBI < 51.44 denotes "fair"; 17.15 ≤ F-IBI < 34.29 reflects "poor"; and F-IBI < 17.15 represents "bad".

Table 3. Grading criteria for the health assessment system in the inshore waters of Hainan Island.

F-IBI value	Health status
>68.58	Healthy
51.44–68.58	Good
34.29–51.44	Fair
17.15–34.29	Poor
<17.15	Bad

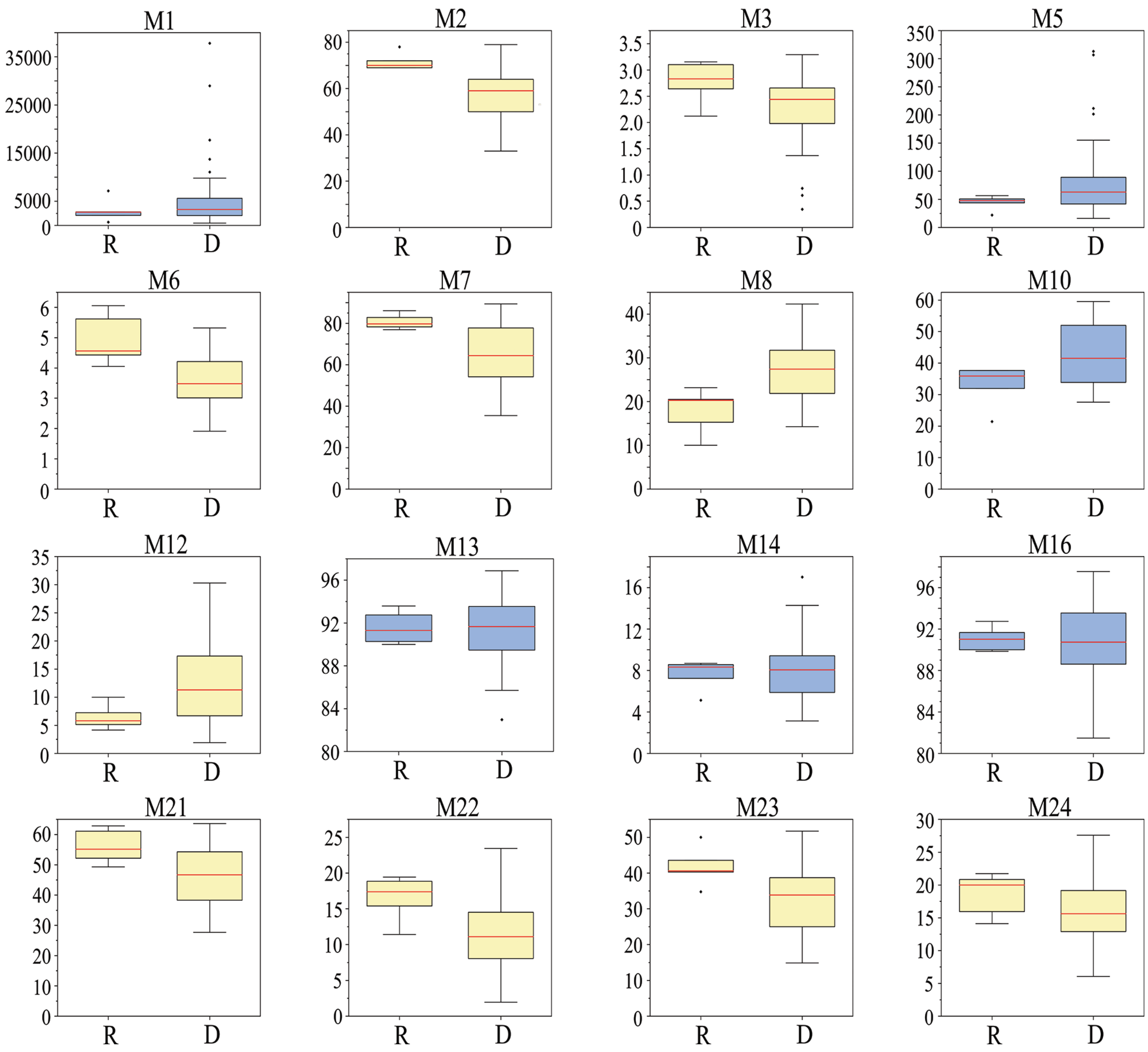

Figure 4. Box plots of the differences of the 16 candidate indicators between the reference points (R) and the disturbed points (D). Yellow represents indicators that did not meet the discriminant filter criteria, while blue signifies indicators that successfully passed the discriminant filter and proceeded to undergo Person correlation analysis.

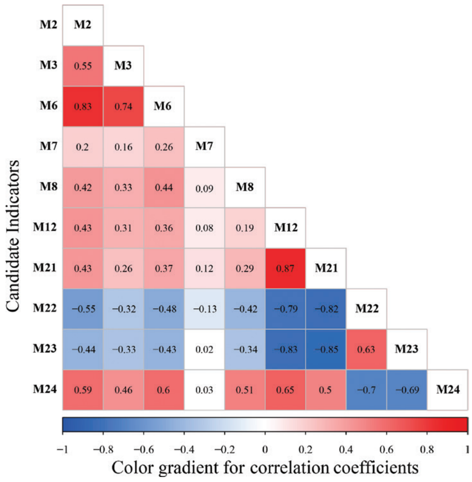

M2	M2									
M3	0.55	M3								
M6	0.83	0.74	M6							
M7	0.2	0.16	0.26	M7						
M8	0.42	0.33	0.44	0.09	M8					
M12	0.43	0.31	0.36	0.08	0.19	M12				
M21	0.43	0.26	0.37	0.12	0.29	0.87	M21			
M22	−0.55	−0.32	−0.48	−0.13	−0.42	−0.79	−0.82	M22		
M23	−0.44	−0.33	−0.43	0.02	−0.34	−0.83	−0.85	0.63	M23	
M24	0.59	0.46	0.6	0.03	0.51	0.65	0.5	−0.7	−0.69	M24

Figure 5. Coefficients of Pearson correlation between the 10 candidate indicators.

Patterns of ecological health. The F-IBI assessments indicated that the majority of sampled sites were in "good" or "fair" health in both seasons (Suppl. material 3, Fig. 6). Seasonal variations were also observed, with F-IBI values ranging from 25.50 to 62.89 in spring and from 41.01 to 70.06 in fall, and the corresponding mean values were 48.16 ± 8.99 and 56.30 ± 7.77, respectively. The ecological health of Hainan Island's inshore waters showed improvement in fall as compared to spring. A one-way analysis of variance (ANOVA) confirmed a highly significant difference between the two seasons ($F = 23.498$, $P < 0.01$). Spatially, no site exhibited extremely poor health in either season, with the highest F-IBI scores recorded at station S45 in spring and at station S16 in fall. Overall, sites in the southeastern waters showed better ecological health than those in the northwestern and Qiongzhou Strait waters.

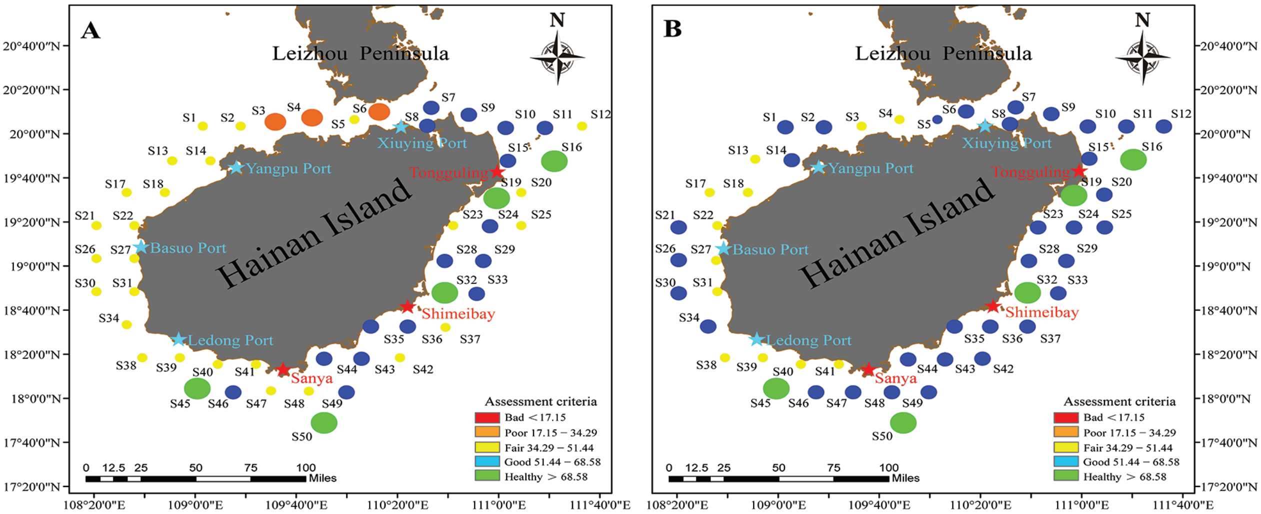

Figure 6. Results of health assessment for the inshore waters of Hainan Island using fish-based index of biological integrity (F-IBI) separately for (**A**) spring and (**B**) fall season.

Discussion

Analysis of fish community structure. Fish community structure is a critical aspect in marine ecological study, indicating biodiversity, ecosystem health, and the impact of environmental changes (Bellwood et al. 2004). The diversity of fish species is one of the important indicators of ecosystem health (Loreau et al. 2001; Cardinale et al. 2012). In China, where Hainan Island serves as a significant fishery base, analyzing the fish community structure in its inshore waters is vital for guiding management and conservation efforts. This study highlights a high proportion of bony fishes and the dominance of Perciformes, indicating robust species diversity and good ecosystem health (Figs 3, 6, Table 2), aligning with findings by Magurran (2013) and Worm et al. (2006) on the relationship between biodiversity and ecosystem stability. Moreover, the spatial distribution patterns of fish communities are shaped by various environmental factors, including water temperature, salinity, pollution, and habitat destruction (Jackson et al. 2001; Heino et al. 2009), with human activities such as overfishing, marine pollution, and habitat degradation posing direct threats to fish diversity and distribution (Pauly et al. 1998; Worm et al. 2006).

Hierarchical clustering and NMDS suggest that differences in spatial distribution of fishes are related to variations in circulation patterns, fishing intensity, and habitat types. Fish communities in spring and fall primarily clustered into two regions—northwest and southeast waters—reflecting significant ecological differences. The northwest waters in the Beibu Gulf and Qiongzhou Strait experience substantial anthropogenic impact from fishing activities and marine traffic, creating a complex and disturbed environment. Conversely, the southeast waters are characterized by more protected zones and lesser human disturbance and maintain a more natural and intact ecological state. Differences in seafloor topography also influence community clustering, with shallow shoals and deep troughs in the northwest and marginal ditches and canyons in the southeast featuring complex terrain and varying slopes (Lin 1995; Zhao et al. 2007). Additionally, both regions support high plankton biomass and distribution of the food resources plays a crucial role in attracting fish aggregations (Xie et al. 2019). In summary, differences in fish community composition are influenced by a multitude of factors, however, the underlying mechanisms through which each factor exerts its influence necessitate comprehensive exploration using more extensive biological and environmental data.

F-IBI system construction. This study introduces the F-IBI system and modifies it to assess the ecological health of the specific marine environment inshore waters around the Hainan Island. Unlike its applications in rivers and lakes (Angermeier and Schlosser 1987; Aparicio et al. 2011), our study has shown that indices based on fish thermotolerance and habitat preference are useful for classifying biological integrity of the regions fish community.

The study aims to develop an F-IBI index system tailored to the specific conditions off Hainan Island, with a particular focus on commercial demersal fish species, which are crucial due to the increased fishing pressure and the significance to local fisheries. Fish belonging to different taxa exhibit distinct responses to fishing pressure and environmental changes, thereby rendering these indicators dynamic throughout various epochs. The vastness and ecological complexity of Hainan's maritime area necessitate a flexible and adaptive approach to indicator selection and modification. For instance, certain indicators, such as trophic guild, thermal tolerance, are influenced by interannual variability or extreme climate conditions (Brandl et al. 2020; Ilarri et al. 2022), impacting the reliability of the indicators. Additionally, biogeographic variations may cause divergent life histories and strategies among the same fish species across different marine areas (Cowman et al. 2017), necessitating careful consideration and adjustment of indicators based on empirical data. Therefore, constructing an F-IBI index system is an iterative process, requiring ongoing revisions based on real-world conditions and scientific advances. This continuous improvement ensures the scientific accuracy and reliability of the system, thereby providing a more effective approach for evaluating and managing the marine ecosystem health surrounding Hainan Island.

Evaluation of local ecosystem health. The F-IBI system primarily assesses ecosystem health based on the structure and function of fish communities. However, to evaluate ecosystem health more comprehensively, it is also necessary to integrate indicators of human impacts on the marine environment. In this study, seasonal variations were evident, with mean F-IBI scores of 48.16 in spring and 56.30 in fall, indicating an improvement in ecological health during the latter season compared with previous studies (Su et al. 2022). Research has demonstrated a correlation between F-IBI scores and the intensity of anthropogenic impacts; higher human interference generally results in lower F-IBI scores (Liu et al. 2016). The waters surrounding Hainan Island are closed to fishing activities from May to August, and the survey for the fall expedition was conducted in early September. Following a few months of fishing moratorium, the offshore waters experience reduced fishing pressure, leading to resource recovery. Consequently, both the resource status and ecological environment are expected to reach an improved state during this season. Therefore, it is anticipated that the index in fall may surpass that observed in spring. Other factors influencing F-IBI scores include physical and chemical conditions of the marine environment, such as water temperature, salinity, and oxygen levels (Lou et al. 2015). For instance, affected by industrial waste discharges, the waters surrounding the western portion of Hainan Island and the Qiongzhou Strait exhibit adverse physical and chemical environments. These conditions have the potential to detrimentally impact marine ecosystems, consequently resulting in lower F-IBI scores (Li et al. 2017), negatively impacting the marine ecosystem and thus reducing F-IBI scores. In the northwest waters of Hainan Island, where F-IBI scores were adversely affected by nearby coastal development activities such as tourism and port construction, which restrict the available space and resources for marine life (Cen et al. 2012; Sun et al. 2014). Furthermore, severe coral bleaching, especially in the western waters, has drastically affected fish habitats and breeding grounds, diminishing species diversity and lowering F-IBI scores (Lang 2023). In contrast, sites near national nature reserves (e.g., S16, S36, S47) exhibited higher F-IBI scores due to less human disturbance and more intact and diverse habitats.

Conclusions

This study found that bony fishes constituted the majority of the catch, with Perciformes being the predominant order. The analysis categorized the fishes according to their dietary preferences, thermal tolerances, reproductive strategies, and ecological behaviors, which illustrated the varied distribution of fish across the surveyed area. Hierarchical cluster analysis and NMDS further segregated the survey sites into two distinct groups, underscoring spatial variations. The F-IBI assessments indicated that most sites exhibited good or fair ecological health in both seasons, with noticeable improvements in fall. Notably, the ecological health of the fish community was superior in the southeastern part of the study area to the northwestern sectors. This study presents a comprehensive scientific evaluation of the fishery resources and ecological well-being in the nearshore waters surrounding Hainan Island, offering essential insights for future fishery development planning and ecosystem management strategies within the region.

Acknowledgments

This study was supported by the Science and Technology Fundamental Resources Investigation Program (Grant No. 2023FY100803), the Central Public-interest Scientific Institution Basal Research Fund, CAFS (NO.2023TD93), Biodiversity, Germplasm Resources Bank and Information Database Construction of the South China Sea Project (NO. HNDW2020-112), the Hainan Provincial Natural Science Foundation of China under contract No. 324QN367, and Guangzhou Basic and Applied Basic Research Project (2023A04J1511).

References

Abhijna UG, Kumar AB (2017) Development and evaluation of fish index of biotic integrity (F-IBI) to assess biological integrity of a tropical lake Veli-Akkulam, south India. International Journal of Fisheries and Aquatic Studies 5(3): 153–164.

Angermeier PL, Schlosser IJ (1987) Assessing biotic integrity of the fish community in a small Illinois stream. North American Journal of Fisheries Management 7(3): 331–338. https://doi.org/10.1577/1548-8659(1987)7<331:ABIOTF>2.0.CO;2

Aparicio E, Carmona-Catot G, Moyle PB, García-Berthou E (2011) Development and evaluation of a fish-based index to assess biological integrity of Mediterranean streams. Aquatic Conservation 21(4): 324–337. https://doi.org/10.1002/aqc.1197

Barbour MT, Gerritsen J, Griffith GE, Frydenborg R, McCarron E, White JS, Bastian ML (1996) A framework for biological criteria for Florida streams using benthic macroinvertebrates. Journal of the North American Benthological Society 15(2): 185–211. https://doi.org/10.2307/1467948

Bellwood DR, Hughes TP, Folke C, Nyström M (2004) Confronting the coral reef crisis. Nature 429(6994): 827–833. https://doi.org/10.1038/nature02691

Borja A, Dauer DM, Diaz R, Llansó RJ, Muxika I, Rodríguez JG, Schaffner L (2008) Assessing estuarine benthic quality conditions in Chesapeake Bay: A comparison of three indices. Ecological Indicators 8(4): 395–403. https://doi.org/10.1016/j.ecolind.2007.05.003

Brandl SJ, Johansen JL, Casey JM, Tornabene L, Morais RA, Burt JA (2020) Extreme environmental conditions reduce coral reef fish biodiversity and productivity. Nature Communications 11(1): 3832. https://doi.org/10.1038/s41467-020-17731-2

Canonico G, Buttigieg PL, Montes E, Muller-Karger FE, Stepien C, Wright D, Benson A, Helmuth B, Costello M, Sousa-Pinto I, Saeedi H, Newton J, Appeltans W, Bednaršek N, Bodrossy L, Best BD, Brandt A, Goodwin KD, Iken K, Marques AC, Miloslavich P, Ostrowski M, Turner W, Achterberg EP, Barry T, Defeo O, Bigatti G, Henry LA, Ramiro-Sánchz B, Durán P, Morato T, Roberts JM, García-Alegre A, Cuadrado MS, Murton B (2019) Global observational needs and resources for marine biodiversity. Frontiers in Marine Science 6: 367. https://doi.org/10.3389/fmars.2019.00367

Cardinale BJ, Duffy JE, Gonzalez A, Hooper DU, Perrings C, Venail P, Narwani A, Mace GM, Tilman D, Wardle DA, Kinzig AP, Daily GC, Loreau M, Grace JB, Larigauderie A, Srivastava DS, Naeem S (2012) Biodiversity loss and its impact on humanity. Nature 486(7401): 59–67. https://doi.org/10.1038/nature11148

Cen J-Y, Ou L-J, Lü SG, Zhang Y, Li X, Jiang T, Lü S-H (2012) [Studies on ecological characteristics of plankton during jellyfish bloom in Qinglan Port.] Haiyang yu huzhao = Oceanologia et Limnologia Sinica 43(3): 595–601. [In Chinese]

Chen YJ (2014) [Studies of fish species diversity and ecological fauna in Taiwan Strait.] Third institute of Oceanography, State Oceanic Administration, Xiamen, China, 80 pp. [In Chinese]

Chen DG, Zhang MZ (2015) [Marine fishes of China.] China Ocean University Press, Qingdao, China, 4435 pp. [In Chinese]

Clarke KR (1993) Non-parametric multivariate analyses of changes in community structure. Australian Journal of Ecology 18(1): 117–143. https://doi.org/10.1111/j.1442-9993.1993.tb00438.x

Clarke KR, Ainsworth M (1993) A method of linking multivariate community structure to environmental variables. Marine Ecology Progress Series 92: 205–219. https://doi.org/10.3354/meps092205

Cowman PF, Parravicini V, Kulbicki M, Floeter SR (2017) The biogeography of tropical reef fishes: Endemism and provinciality through time. Biological Reviews of the Cambridge Philosophical Society 92(4): 2112–2130. https://doi.org/10.1111/brv.12323

Das MK, Sharma AP, Vass KK, Tyagi RK, Suresh VR, Naskar M, Akolkar AB (2013) Fish diversity, community structure and ecological integrity of the tropical River Ganges, India. Aquatic Ecosystem Health and Management 16(4): 395–407. https://doi.org/10.1080/14634988.2013.851592

Fricke R, Eschmeyer WN, van der Laan R (Eds.) 2024. Eschmeyer's catalog of fishes: Genera, species, references. California Academy of Sciences, San Francisco, CA, USA. [Accessed on 23 September 2024] http://researcharchive.calacademy.org/research/ichthyology/catalog/fishcatmain.asp

Fu XM, Zhang MQ, Liu Y, Wang LH, Shao CL, Hu Y, Wang XY, Su LR, Wang N, Wang CY (2018) Protective exploitation of marine bioresources in China. Ocean and Coastal Management 163: 192–204. https://doi.org/10.1016/j.ocecoaman.2018.06.018

Halpern BS, Frazier M, Potapenko J, Casey KS, Koenig K, Longo C, Lowndes JS, Rockwood RC, Selig ER, Selkoe KA, Walbridge S (2015) Spatial and temporal changes in cumulative human impacts on the world's ocean. Nature Communications 6(1): 7615. https://doi.org/10.1038/ncomms8615

He LJ, Zhou SB, Li XM, Lin W (2014) [Coastal marine pollution situation and the impacts on biodiversity in Hainan Island.] Qiongzhou Daxue xuebao = Journal of Qiongzhou University 21(5): 99–103. [In Chinese]

Heino J, Virkkala R, Toivonen H (2009) Climate change and freshwater biodiversity: Detected patterns, future trends and adaptations in northern regions. Biological Reviews of the Cambridge Philosophical Society 84(1): 39–54. https://doi.org/10.1111/j.1469-185X.2008.00060.x

Hu ZM, Kantachumpoo A, Liu RY, Sun ZM, Yao JT, Komatsu T, Uwai S, Duan DL (2018) A late Pleistocene marine glacial refugium in the south-west of Hainan Island, China: Phylogeographical insights from the brown alga *Sargassum polycystum*. Journal of Biogeography 45(2): 355–366. https://doi.org/10.1111/jbi.13130

Huang X, Xu J, Liu B, Guan X, Li J (2022) Assessment of aquatic ecosystem health with Indices of Biotic Integrity (IBIs) in the Ganjiang River system, China. Water 14(3): 278. https://doi.org/10.3390/w14030278

Ilarri M, Souza AT, Dias E, Antunes C (2022) Influence of climate change and extreme weather events on an estuarine fish community. Science of the Total Environment 827: 154190. https://doi.org/10.1016/j.scitotenv.2022.154190

Jackson JBC, Kirby MX, Berger WH, Bjorndal KA, Botsford LW, Bourque BJ, Bradbury RH, Cooke R, Erlandson J, Estes JA, Hughes TP, Kidwell S, Lange CB, Lenihan HS, Pandolfi JM, Peterson CH, Steneck RS, Tegner MJ, Warner RR (2001) Historical overfishing and the recent collapse of coastal ecosystems. Science 293(5530): 629–637. https://doi.org/10.1126/science.1059199

Jambeck JR, Geyer R, Wilcox C, Siegler TR, Perryman M, Andrady A, Narayan R, Law KL (2015) Plastic waste inputs from land into the ocean. Science 347(6223): 768–771. https://doi.org/10.1126/science.1260352

Karr JR (1981) Assessment of biotic integrity using fish communities. Fisheries 6(6): 21–27. https://doi.org/10.1577/1548-8446(1981)006<0021:AOBIUF>2.0.CO;2

Karr JR (1991) Biological integrity: A long-neglected aspect of water resource management. Ecological Applications 1(1): 66–84. https://doi.org/10.2307/1941848

Kerans BL, Karr JR (1994) A benthic index of biotic integrity (B-IBI) for rivers of the Tennessee Valley. Ecological Applications 4(4): 768–785. https://doi.org/10.2307/1942007

Lang SK (2023) [The status and cause analysis of coral bleaching in Hainan Island and Xisha Island.] Hainan Tropical Ocean University, Sanya, China, 79 pp. [In Chinese]

Li YQ, Chen GB (2008) [Research status of marine fish communities in Chinese sea area.] Yuye xinxi yu zhanlue = Fishery Information and Strategy 23: 16–21. [In Chinese]

Li J, Dong S, Peng M, Yang Z, Liu S, Li X, Zhao C (2013) Effects of damming on the biological integrity of fish assemblages in the middle Lancang–Mekong River basin. Ecological Indicators 34: 94–102. https://doi.org/10.1016/j.ecolind.2013.04.016

Li RH, Liu SM, Li YW, Zhang GL, Ren JL, Zhang J (2014) Nutrient dynamics in tropical rivers, lagoons, and coastal ecosystems of eastern Hainan Island, South China Sea. Biogeosciences 11(2): 481–506. https://doi.org/10.5194/bg-11-481-2014

Li F, Lin ZF, Wen JS, Wei YS, Gan HY, He HJ, Lin JQ, Xia Z, Chen BS, Guo WJ, Tan CS, Cai HY (2017) Risk assessment of trace metal-polluted coastal sediments on Hainan Island: A full-scale set of 474 geographical locations covering the entire island. Marine Pollution Bulletin 125(1–2): 541–555. https://doi.org/10.1016/j.marpolbul.2017.09.057

Li T, Huang X, Jiang X, Wang X (2018) Assessment of ecosystem health of the Yellow River with fish index of biotic integrity. Hydrobiologia 814(1): 31–43. https://doi.org/10.1007/s10750-015-2541-5

Liao JQ, Huang Y (2013) [Research progress on using index of biological integrity to assess aquatic ecosystem health.] Yingyong shengtai xuebao = Chinese Journal of Applied Ecology 24: 295–302. [In Chinese]

Lin MH (1995) [Submarine geomorphology of the eastern continental shelf of the Hainan Island.] Haiyang dizhi yu disiji dizhi = Marine Geology and Quaternary Geology 15(4): 37–46. [In Chinese]

Liu JY (2013) Status of marine biodiversity of the China Seas. PLoS One 8(1): e50719. https://doi.org/10.1371/journal.pone.0050719

Liu M, Qu XD, Peng WQ, Li DY, Zhang HB, Yang CG (2016) [Development and application of a fish-based index of biological integrity for the Hun-Tai River basin.] Huanjing kexue yanjiu = Research of Environmental Sciences 29(3): 343–352. [In Chinese]

Loreau M, Naeem S, Inchausti P, Bengtsson J, Grime JP, Hector A, Hooper DU, Huston MA, Raffaelli D, Schmid B, Tilman D, Wardle DA (2001) Biodiversity and ecosystem functioning: Current knowledge and future challenges. Science 294(5543): 804–808. https://doi.org/10.1126/science.1064088

Lou FR, Cheng GP, Chen BJ, Li WH, Lan JH, Zheng HF, Qin ZB, Zhang YF (2015) [The ecosystem health assessment of Hongshui River cascade reservoirs, China, based on fish-index of biotic integrity.] Danshui yuye = Freshwater Fisheries 45(4): 36–40. [In Chinese]

Magurran AE (2013) Ecological diversity and its measurement. Princeton University Press, Princeton, NJ, USA, 178 pp.

Martin GR, Twigg LE, Robinson DJ (1996) Comparison of the diet of feral cats from rural and pastoral Western Australia. Wildlife Research 23(4): 475–484. https://doi.org/10.1071/WR9960475

Palumbi SR, Sandifer PA, Allan JD, Beck MW, Fautin DG, Fogarty MJ, Halpern BS, Incze LS, Leong JA, Norse E, Stachowicz JJ, Wall DH (2009) Managing for ocean biodiversity to sustain marine ecosystem services. Frontiers in Ecology and the Environment 7(4): 204–211. https://doi.org/10.1890/070135

Parsons ECM, Favaro B, Aguirre AA, Bauer AL, Blight LK, Cigliano JA, Coleman MA, Cot IM, Draheim M, Fletcher S, Foley MM, Jefferson R, Jones MC, Kelaher BP, Lundquist C, Mccarthy JB, Nelson A, Patterson K, Walsh L, Wright AJ, Sutherland WJ (2014) Seventy-one important questions for the conservation of marine biodiversity. Conservation Biology 28(5): 1206–1214. https://doi.org/10.1111/cobi.12303

Pauly D, Zeller D (2016) Catch reconstructions reveal that global marine fisheries catches are higher than reported and declining. Nature Communications 7(1): 10244. https://doi.org/10.1038/ncomms10244

Pauly D, Christensen V, Dalsgaard J, Froese R, Torres Jr JF (1998) Fishing down marine food webs. Science 279(5352): 860–863. https://doi.org/10.1126/science.279.5352.860

Pinkas L, Oliphant MS, Iverson ILK (1971) Food habits of albacore, bluefin tuna, and bonito in California waters. Fish Bulletin 152(1): 11–46.

Poloczanska ES, Brown CJ, Sydeman WJ, Kiessling W, Schoeman DS, Moore PJ, Brander K, Bruno JF, Buckley LB, Burrows MT, Duarte CM, Halpern BS, Holding J, Kappel CV, O'Connor MI, Pandolfi JM, Parmesan C, Schwing F, Thompson SA, Richardson AJ (2013) Global imprint of climate change on marine life. Nature Climate Change 3(10): 919–925. https://doi.org/10.1038/nclimate1958

Shen SJ, Wu GY (2011) Fishes of Taiwan. National Museum of Marine Biology and Aquarium, Pingtung, Taiwan, China, 896 pp. [In Chinese]

Stoddard JL, Larsen DP, Hawkins CP, Johnson RK, Norris RH (2006) Setting expectations for the ecological condition of streams: The concept of reference condition. Ecological Applications 16(4): 1267–1276. https://doi.org/10.1890/1051-0761(2006)016[1267:SEFTEC]2.0.CO;2

Su L, Xu Y, Qiu Y, Sun M, Zhang K, Chen Z (2022) Long-term change of a fish-based index of biotic integrity for a semi-enclosed bay in the Beibu Gulf. Fishes 7(3): 124. https://doi.org/10.3390/fishes7030124

Sun DR, Li Y, Wang XH (2012) [Seasonal changes of species composition and diversity of fishes in coastal waters of Hainan Island, China.] Nanfang shuichan kexue = South China Fisheries Science 8(1): 1–7. [In Chinese]

Sun RX, Wang YG, Lian GS, Lin M (2014) [Distribution and community characteristics of planktonic copepods in the northwest coastal waters off Hainan Island.] Shengwu duoyangxing = Biodiversity Science 22(3): 320–328. https://doi.org/10.3724/SP.J.1003.2014.13137 [In Chinese]

Wang BX, Yang LF, Hu BJ, Shan LN (2005) [A preliminary study on the assessment of stream ecosystem health in south of Anhui Province using Benthic-Index of Biotic Integrity.] Shengtai xuebao = Acta Ecologica Sinica 6: 1481–1490. [In Chinese]

Wang Q, Yu D, Li ZQ, Wang LG (2008) The effect of typhoons on the diversity and distribution pattern of aquatic plants on Hainan Island, South China. Biotropica 40(6): 692–699. https://doi.org/10.1111/j.1744-7429.2008.00430.x

Wilhm JL (1970) Range of diversity index in benthic macroinvertebrate populations. Research Journal of the Water Pollution Control Federation 42(5): 221–224.

Worm B, Barbier EB, Beaumont N, Duffy JE, Folke C, Halpern BS, Jackson JBC, Lotze HK, Micheli F, Palumbi SR, Sala E, Selkoe KA, Stachowicz JJ, Watson R (2006) Impacts of biodiversity loss on ocean ecosystem services. Science 314(5800): 787–790. https://doi.org/10.1126/science.1132294

WoRMS Editorial Board (2024). World Register of Marine Species. Maintained at the Flanders Marine Institute (VLIZ). https://www.marinespecies.org [Accessed 2024-09-23.] https://doi.org/10.14284/170

Wu HL, Zhong JS (2021) [Key to marine and estuarial fishes of China.] China Agriculture, Beijing, China, 1437 pp. [In Chinese]

Xie FW, Liang JL, Xing KM (2019) [Distribution characteristics of zooplankton in summer and fall in the coastal waters of Hainan Island.] Haian gongcheng = Coastal Engineering 38(4): 280–293. [In Chinese]

Zhang Y, Ban X, Li E, Wang Z, Xiao F (2020) Evaluating ecological health in the middle-lower reaches of the Hanjiang River with cascade reservoirs using the planktonic index of biotic integrity (P-IBI). Ecological Indicators 114: 106282. https://doi.org/10.1016/j.ecolind.2020.106282

Zhao HT, Wang LR, Yuan JY (2007) [Origin and time of Qiongzhou Strait.] Haiyang dizhi yu disiji dizhi = Marine Geology and Quaternary Geology 27: 33–40. [In Chinese]

Zhao C, Shao N, Yang S, Ren H, Ge Y, Zhang Z, Zhao Y, Yin X (2019) Integrated assessment of ecosystem health using multiple indicator species. Ecological Engineering 130: 157–168. https://doi.org/10.1016/j.ecoleng.2019.02.016

Zhu H, Hu XD, Wu PP, Chen WM, Wu SS, Li ZQ, Zhu L, Xi YL, Huang R (2021) Development and testing of the phytoplankton biological integrity index (P-IBI) in dry and wet seasons for Lake Gehu. Ecological Indicators 129: 107882. https://doi.org/10.1016/j.ecolind.2021.107882

Supplementary material 1

Fish species ecological habits catalog in the nearshore waters of Hainan Island

Authors: Peimin Yu, Zhengli Luo, Liangming Wang, Yan Liu, Yingbang Huang, Binbin Shan, Changping Yang, Dianrong Sun

Data type: docx

Link: https://doi.org/10.3897/aiep.54.130966.suppl1

Supplementary material 2

Health assessment results of the coastal waters of Hainan Island based on Fish Biological Integrity Index

Authors: Peimin Yu, Zhengli Luo, Liangming Wang, Yan Liu, Yingbang Huang, Binbin Shan, Changping Yang, Dianrong Sun

Data type: docx

Link: https://doi.org/10.3897/aiep.54.130966.suppl2

Supplementary material 3

Seasonal variations

Authors: Peimin Yu, Zhengli Luo, Liangming Wang, Yan Liu, Yingbang Huang, Binbin Shan, Changping Yang, Dianrong Sun

Data type: xlsx

Link: https://doi.org/10.3897/aiep.54.130966.suppl3

Acta Ichthyologica et Piscatoria 54, 2024, 235–241 | DOI 10.3897/aiep.54.122366

PENSOFT.

ACTA
ICHTHYOLOGICA
ET PISCATORIA

Mitochondrial evidence on the phylogenetic position of the Southeast Asian catfish genus *Encheloclarias* Myers, 1937 (Actinopterygii: Siluriformes: Clariidae): Evolutionary and conservation implications

Sébastien LAVOUÉ[1], Jamsari Amirul Firdaus JAMALUDDIN[1],
Abdullah Halim MUHAMMAD-RASUL[2], Mohd Lokman ILHAM-NORHAKIM[3,4],
Khaironizam Md ZAIN[1]

1 *School of Biological Sciences, Universiti Sains Malaysia, Pulau Pinang, Malaysia*
2 *Tropical Infectious Diseases Research and Education Centre (TIDREC), Universiti Malaya, Kuala Lumpur, Malaysia*
3 *Environmental Management and Conservation Research Unit (eNCORe), Faculty of Applied Sciences and Technology, Universiti Tun Hussein Onn Malaysia (Pagoh Campus), Johor, Malaysia*
4 *Kim Ichthyologist Centre, Kg Parit Samsu, Jalan Temenggong Ahmad, Johor, Malaysia*

https://zoobank.org/BB3C8740-5E20-41F2-8C72-E36CEA690CF9

Corresponding author: Sébastien Lavoué (microceb@hotmail.com)

Academic editor: Eva Decru ♦ **Received** 13 March 2024 ♦ **Accepted** 15 August 2024 ♦ **Published** 14 October 2024

Citation: Lavoué S, Jamaluddin JAF, Muhammad-Rasul AH, Ilham-Norhakim ML, Zain KM (2024) Mitochondrial evidence on the phylogenetic position of the Southeast Asian catfish genus *Encheloclarias* Myers, 1937 (Actinopterygii: Siluriformes: Clariidae): Evolutionary and conservation implications. Acta Ichthyologica et Piscatoria 54: 235–241. https://doi.org/10.3897/aiep.54.122366

Abstract

The phylogenetic position of the Southeast Asian catfish genus *Encheloclarias* Myers, 1937 within the family Clariidae is inferred herein using three mitochondrial nucleotide markers: *cytochrome b*, *cytochrome oxidase subunit I*, and *16S* rRNA genes. We found that *Encheloclarias* is neither exclusively related to the African taxa having extended neural spines posterior to the dorsal fin (*Encheloclarias* shares with some of these taxa the presence of an adipose fin, as opposed to absent in all other clariid taxa) nor to the Asian species of the genus *Clarias* Scopoli, 1777. *Encheloclarias* is hypothesized to be the sister group of all other clariids, except *Horaglanis* Menon, 1951. The inferred position of *Encheloclarias* confirms that the adipose fin in this genus has an evolutionary origin independent to that of the adipose fin found in some African clariids. *Encheloclarias* is not only ecologically remarkable, being adapted to acidic peat swamps in Southeast Asia, but it is also an ancient lineage sheltering in these habitats. However, the precise timing of the colonization of peat swamps by *Encheloclarias* remains to be investigated. The phylogenetic position of *Encheloclarias* further underscores the importance of studying and protecting the remaining peat swamp habitats in Southeast Asia and their distinctive aquatic fauna.

Keywords

adaptation, adipose fin, convergence, molecular phylogenetics, peat swamp forests, Teleostei

Introduction

The Southeast Asian genus *Encheloclarias* was established by Myers in Herre and Myers (1937) to reclassify a clariid species originally described as *Heterobranchus tapeinopterus* Bleeker, 1853. *Encheloclarias* is one of three genera in the family Clariidae (walking catfishes) occurring in Asia, alongside *Clarias* Scopoli, 1777 and *Horaglanis* Menon, 1951. The Clariidae is otherwise distributed in Africa, where it exhibits the greatest generic diversity with 14 genera (including *Clarias*, which is found in both Asia and Africa). There are currently six valid species of *Encheloclarias* (see Fricke et al. 2024), most of which are known from only a few specimens, indicating their possible rarity (Ng and Lim 1993; Tan et al. 2023). *Encheloclarias* species inhabit acidic peat swamp habitats of Southeast Asia (Malaysia, Singapore, Indonesia, and Brunei), where they burrow into the peat soil layer (Ng and Lim 1993; Ng and Tan 2000). The smallest species is *Encheloclarias baculum* Ng et Lim, 1993 (5.7 cm reported maximum SL), while the largest is *Encheloclarias velatus* Ng et Tan, 2000 (16.9 cm reported maximum SL). There is still limited information on the biology, morphology (especially osteology), and evolution of this genus (Ng and Lim 1993; Teugels and Adriaens 2003; Tan et al. 2023). The phylogenetic position of this genus is virtually unknown.

Within the Clariidae, *Encheloclarias* possesses an adipose fin (Fig. 1), a feature it shares with only few African taxa such as *Heterobranchus* Geoffroy St. Hilaire, 1809, *Dinotopterus* Boulenger, 1906, and *Clarias ngamensis* Castelnau, 1861. Although the adipose fin is externally similar between these African taxa and *Encheloclarias*, its structure differs between them (Teugels and Adriaens 2003). The adipose fin in African taxa is supported by elongated neural spines while there is no osteological support in that of *Encheloclarias*. Therefore, the presence of an adipose fin in African taxa and *Encheloclarias* is not considered an evidence of their close relationship. Teugels and Adriaens (2003) wrote "Based on zoogeographical evidence, *Horaglanis* and *Encheloclarias* probably descended independently from Asian *Clarias*." Subsequent phylogenetic works on clariids, including those by Devaere et al. (2007) and Pouyaud et al. (2009), did not include *Encheloclarias*.

The absence of phylogenetic information on *Encheloclarias* limits discussion on the evolution of the Clariidae. For example, the independent origins of the adipose fin in the Clariidae have not yet been confirmed and it is also unclear whether the presence of an adipose fin in *Encheloclarias* represents the ancestral or derived condition in this family (Stewart et al. 2014).

In this work, we infer the phylogenetic position of *Encheloclarias* by reconstructing the phylogeny of 13 (out of 16) clariid genera using three mitochondrial markers: the *cytochrome b* (*cytb*), *cytochrome oxidase subunit I* (*COI*), and *16S rRNA* (*16S*) genes.

Materials and methods

Specimen collection and molecular sampling. Fragments of the *cytb* (~600 bp), *COI* (~655 bp), and *16S* (~700 bp) nucleotide sequences from three specimens of *Encheloclarias curtisoma* Ng et Lim, 1993 were newly determined for this study. Specimens were collected using dipnets from three peat swamp forests (Pondok Tanjung, North Selangor, and Ayer Hitam) in West Peninsular Malaysia. A tissue sample from each specimen was excised after euthanasia by rapid cooling in ice-water after capture, a procedure recommended by Blessing et al. (2010), then preserved in 95% ethanol, and finally stored at room temperature. Specimens were formalin-fixed in a 10% formalin solution for two weeks, then rinsed with tap water before being transferred into 70% ethanol. All three specimens are deposited in the Makmal Rujukan Zoologi (Zoological Reference Laboratory), Universiti Sains Malaysia (USMFC), under the following catalogue numbers USMFC (19) 00031 (locality: Pondok Tanjung; specimen code: APT57), USMFC (19) 00032 (North Selangor; BNS79), and USMFC (19) 00033 (Ayer Hitam; JAH37).

The molecular dataset was completed by selecting additional *cytb*, *COI*, and *16S* sequences available in GenBank representing a total of (alongside *Encheloclarias curtisoma*) 12 genera and 28 species of the Clariidae (Table 1). The three missing clariid genera are the African *Uegitglanis* Gianferrari, 1923, *Platyclarias* Poll, 1977, and *Xenoclarias* Greenwood, 1958. *Heteropneustes fossilis* (Bloch, 1794) (family Heteropneustidae) which is closely related to the Clariidae (see Diogo et al. 2003; Sullivan et al. 2006), was included in the dataset along with a more distantly catfish outgroup, *Occidentarius platypogon* (Günther, 1864) (family Ariidae).

Figure 1. Photo of a live specimen of *Encheloclarias curtisoma* (Clariidae) from the locality Ayer Hitam (Johor, Peninsular Malaysia) showing the dorsal fin and the adipose fin.

DNA extraction, PCR amplification, and sequencing. Total genomic DNA was extracted from the fin clip using a modified CTAB (Cetyl Trimethyl Ammonium Bromide) method (Grewe et al. 1993). Each gene was separately amplified by PCR amplification carried out with a T100™ Thermal Cycler (BIO-RAD, Hercules, California, USA). A 655 base pairs (bp) long fragment *COI* gene was amplified using the primer set FishF1 (5′–TCA ACC AAC CAC AAA GAC ATT GGC AC–3′) and FishR1 (5′–TAG ACT TCT GGG TGG CCA AAG AAT CA–3′) (Ward et al. 2005). The partial *cytb* gene (~600 bp) was amplified using the following primer set: L15267 (5′–AAT GAC TTG AAG AAC CAC CGT–3′) and H15891 (5′–GTT TGA TCC CGT TTC GTG TA–3′) (Briolay et al. 1998). A ~700 bp long fragment of the *16S* gene was amplified using the primer set 16S_F (5′–CTC GTA CCT TTT GCA TCA TG–3′) and 16S_R (5′–AAG TGA TTG CGC TAC CTT TG–3′) (Pouyaud et al. 2009). Each PCR mixture was carried out in a total volume of 25 µL, which contained 10.5 µL of ddH2O, 12.5 µL of 2X MyTaq™ Red Mix buffer (Meridian Bioscience, Ohio, USA), 0.5 µL of each 10 µM primer, and 1.0 µL of genomic DNA.

The PCR for *COI* gene was carried out under following thermal cycling conditions: initial denaturation at 95°C for 4 min, followed by 30 cycles of denaturation at 94°C for 30 s, primer annealing at 47.9°C for 50 s, primer extension at 72°C for 1 min and final extension for 7 min at 72°C. The PCR for *cytb* and *16S* genes was carried out following the protocol of Pouyaud et al. (2009). Successful PCR samples were sent to Apical Scientific Sdn. Bhd. (Selangor, Malaysia) for purification and bidirectional sequencing using Sanger technology using the same PCR primers.

Sequence editing alignment procedure and phylogenetic reconstruction. Chromatograms were edited and the consensus sequence for each gene and specimen of *Encheloclarias curtisoma* was built by assembling the forward and reverse sequences using MEGA v11.0 (Tamura et al. 2021). Sequences were deposited in GenBank under accession numbers PP273447-PP273449 (*cytb*), and PP274029 and PP274030 (*16S*) and in BOLD under accession numbers NCTF1312-24, NCTF757-24, and NCTF799-24 (*COI*), (Table 1). Nucleotide sequences of *cytb* and *COI* were separately aligned by hand, and

Table 1. List of species of the Clariidae examined in this study along with information on specimens and molecular markers used. Bold GenBank and BOLD accession numbers indicate sequences determined in presently reported study.

Species	Specimen code	GenBank and BOLD accession numbers		
		cytb	*COI*	*16S*
Asian species				
Encheloclarias curtisoma Ng et Lim, 1993	APT57	**PP273447**	**NCTF1312-24**	**PP274029**
	BNS79	**PP273448**	**NCTF757-24**	**PP274030**
	JAH37	**PP273449**	**NCTF799-24**	—
Clarias fuscus (Lacepède, 1803)	—	KM029965	KM029965	KM029965
Clarias macrocephalus Günther, 1864	—	MT109097	MT109097	MT109097
Clarias batrachus (Linnaeus, 1758)	—	KC572134	KC572134	KC572134
Clarias dussumieri Valenciennes, 1840	—	MG644387	MG644387	MG644387
Clarias punctatus (Linnaeus, 1758)	IRD 1986	MW012844	—	MW012795
Clarias kapuasensis Sudarto, Teugels et Pouyaud, 2003	IRD 4678	MW012799	—	MW012775
Clarias leiacanthus Bleeker, 1851	IRD 4464	MW012805	—	MW012776
Clarias nieuhofii Valenciennes, 1840	MNHN 2003-0295(615)	MW012829	—	MW012788
Clarias olivaceus Fowler, 1904	IRD 4901	MW012833	—	MW012789
Clarias planiceps Ng, 1999	IRD 2127	MW012837	—	MW012791
Clarias pseudoleiacanthus Sudarto, Teugels et Pouyaud, 2003	ZRC 47145(4548)	MW012838	—	MW012792
Clarias pseudonieuhofii Sudarto, Teugels et Pouyaud, 2004	IRD 4664	MW012840	—	MW012793
Horaglanis krishnai Menon, 1951	—	OP832214	OP825111	OP824400
Horaglanis abdulkalami Babu, 2012	—	OP832203	OP825094	OP824386
African species				
Clarias camerunensis Lönnberg, 1895	—	OP936082	OP936082	OP936082
Clarias gariepinus (Burchell, 1822)	—	KT001082	KT001082	KT001082
Clarias gabonensis Günther, 1867	—	AY995129	—	—
Bathyclarias gigas Jackson, 1959	—	AF235928	—	—
Channallabes apus (Günther, 1873)	—	AF126820	—	—
Clariallabes longicauda (Boulenger, 1902)	—	AY995124	—	—
Dinotopterus cunningtoni Boulenger, 1906	—	AY995126	—	—
Gymnallabes typus Günther, 1867	—	AY995132	—	—
Heterobranchus longifilis Valenciennes, 1840	—	AF126828	—	—
Heterobranchus bidorsalis Geoffroy St. Hilaire, 1809	—	AF126825	—	—
Dolichallabes microphthalmus Poll, 1942	—	JF262202	—	—
Platyallabes tihoni (Poll, 1944)	—	JF297961	—	—
Tanganikallabes mortiauxi Poll, 1943	—	JF297962	—	—
Pseudotanganikallabes prognatha Wright, 2017	SAIAB 80226	KF650734	—	—
Outgroups				
Heteropneustes fossilis (Bloch, 1794)	—	AP012013	AP012013	AP012013
Occidentarius platypogon (Günther, 1864)	—	KY930717	KY930717	KY930717

cytb = *cytochrome b*, *COI* = *cytochrome oxidase I*, *16S* = *16S rRNA*.

no alignment required any indels. Sequences of *16S* gene were automatically aligned using MAFFT with all parameter selection left as "default" (Katoh et al. 2019).

Separate phylogenetic analyses were first conducted on each individual marker dataset which allow to compare their respective quantity and quality of phylogenetic signal and detect possible topological incongruence. In the absence of supported incongruence, we then combined all three mitochondrial genes together. The total alignment comprises 3107 nucleotide positions. Phylogenetic analyses employed Maximum Likelihood (ML) and Bayesian inference.

The ML tree was built using the software RAxML-NG (Kozlov et al. 2019) as implemented in the graphical interface raxmlGUI 2.0 (Edler et al. 2021). Mitochondrial data were first divided into four partitions: the non-coding *16S* gene and the first, second, and third codon positions of the combined *cytb* and *COI* protein-coding genes. The best models of nucleotide substitution for each of these partitions was selected with ModelTest-NG (Darriba et al. 2020) (as implemented in RAxML-NG) as K80 + Γ, HKY, TN93 + Γ, and GTR + Γ, respectively. Bootstrap proportions were calculated (1000 replicates) to assess the robustness of each node. The trees were visualized with FigTree v1.4.4 (Rambaut 2018).

A time-calibrated Bayesian phylogenetic tree was inferred under a relaxed molecular clock in the BEAST2 version 2.6.4 suite (Bouckaert et al. 2019). For this analysis, *Horaglanis* and the outgroup *Occidentarius platypogon* were excluded. We used the same four partitions and the same models of sequence evolution as for the ML analysis, except for the first codon positions partition's model which was changed from K80 + Γ to the most similar one, JC69 + Γ (this is because K80 is not implemented in BEAST2). A Relaxed Clock Log Normal model and a Birth and Death tree model were selected. The age of the most recent common ancestor of the Heteropneustidae and the Clariidae was constrained to 50 million years old which corresponds to the maximum age of the oldest clariid fossil excavated (Gayet 1987). Two independent MCMC runs were carried out, each for 100 million generations, and parameter values and trees were sampled every 50 thousand generations. The log files generated by BEAST2 from each run were visualized with Tracer v1.7.1 (Rambaut et al. 2018) to confirm that analyses reached convergence. Twenty-five percent of the resulting trees of each run were discarded as burn-in before combining the remaining trees into a single file and calculating the maximum credibility consensus tree and mean node ages. The resulting time-calibrated tree was visualized and exported with FigTree v1.4.4.

Results

Our mitochondrial dataset includes three molecular markers for 29 species of the Clariidae, currently classified into 13 genera. The total amount of missing data reaches approximately 48% but it neither affected the tree topology, which was stable across the different analyses, nor the robustness of the nodes of interest, relative to the phylogenetic position of *Encheloclarias*, that are all supported by high statistical values.

The Maximum Likelihood (ML) phylogenetic tree of the family Clariidae, including *Horaglanis*, is visualized in Suppl. material 1. This tree is fully resolved with several relationships supported by Bootstrap Proportion (BP) values greater than 80%. Branch length heterogeneity is detected in this reconstruction, with the genus *Horaglanis* having a much longer branch than any other taxa. In this tree, the Clariidae is not recovered as monophyletic because *Horaglanis* is found to be the sister group to the clade comprising the Heteropneustidae and the rest of the Clariidae (Suppl. material 1). Although the phylogenetic hypothesis of the *Horaglanis* outside the Clariidae has already been proposed based on morphology (e.g., Diogo et al. 2003), its long branch (due to a fast mitochondrial rate of substitutions) could mislead the inference in our tree (Bergsten 2005). Because of that, and because *Horaglanis* is not the main object of this study, we removed *Horaglanis* from the dataset for the subsequent analyses. The exclusion of *Horaglanis* does not affect the other phylogenetic relationships, especially the position of *Encheloclarias* as shown in the ML tree and in the time-calibrated Bayesian tree (Fig. 2A and Fig. 2B, respectively).

In both ML and Bayesian trees (Fig. 2A, 2B), the species-rich genus *Clarias* is paraphyletic, with all African genera nested within it. African clariids form a monophyletic group (BP = 80%, Posterior probability [PP] = 1) that is the sister group to *Clarias dussumieri* Valenciennes, 1840, a south Asian (Indian subcontinental region) species. Other species of Asian *Clarias* form a monophyletic group (BP = 79%, PP = 1) that is the sister group to the clade comprising the African clariids and *Clarias dussumieri* (BP = 85%, PP = 1). The African species having elongated neural spines form also a monophyletic group (BP < 80%, PP = 1). In all reconstructions, *Encheloclarias* is consistently inferred as the sister group to all other clariid genera (except *Horaglanis* when it is included in the analysis; see Suppl. material 1 and explanations above).

In the time-calibrated Bayesian tree (Fig. 2B), the time divergence between the *Encheloclarias* and the rest of the clariids is estimated to 46.8 million years [95% Credibility Interval [CI] = 50.0–41.4 million years] whereas the mean age of the crown group *Encheloclarias curtisoma* is estimated to 5.1 million years old [95% CI = 7.8–2.8 million years old].

Discussion

The phylogenetic position of *Encheloclarias*. Although some progress has been made in resolving the phylogeny of the Clariidae (see Teugels and Adriaens 2003; Devaere et al. 2007; Pouyaud et al. 2009; De Alwis et al. 2023), the phylogeny remains only partially resolved, partly because some genera are still understudied (i.e., *Uegitglanis*, *Platyclarias*, *Horaglanis*, and *Encheloclarias*) and their affinities remain elusive (Diogo et al. 2003; Teugels and Adriaens 2003; Devaere et al. 2007; Pouyaud et al. 2009).

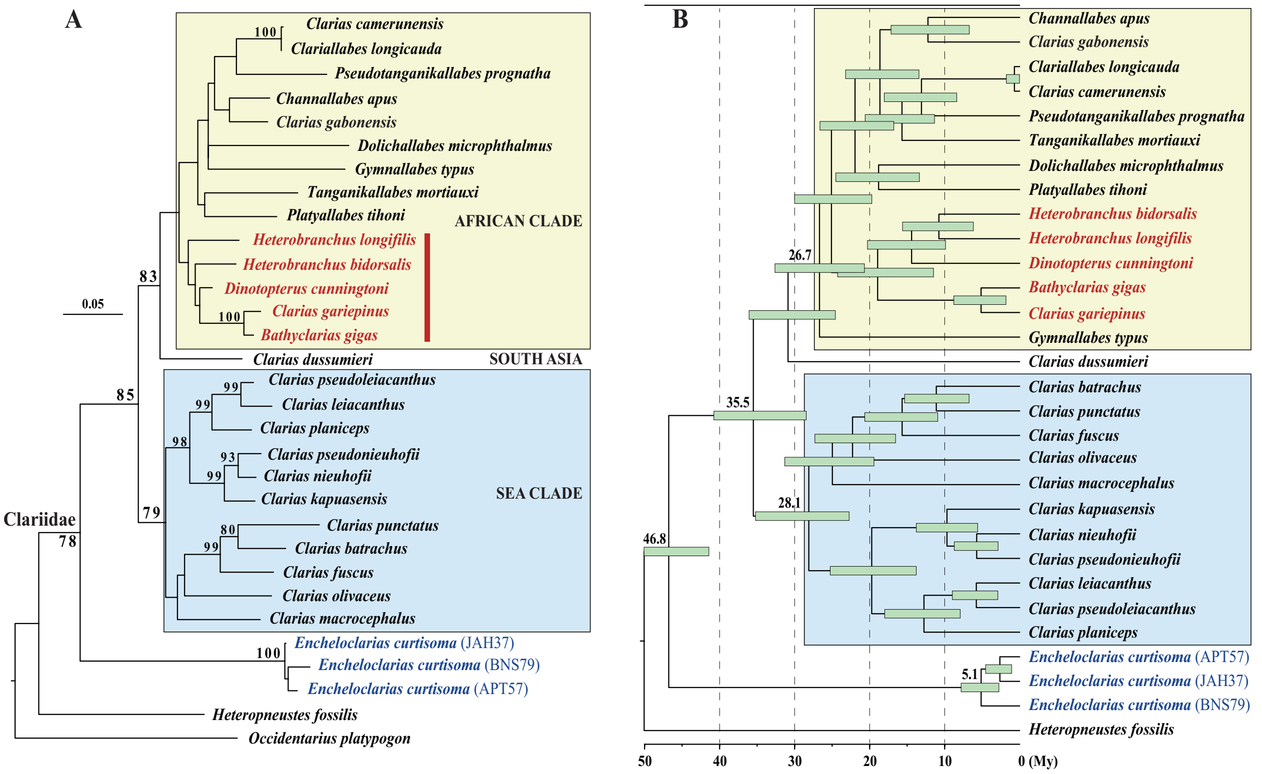

Figure 2. Phylogenetic trees of the family Clariidae showing the position of *Encheloclarias*. (**A**) ML Phylogenetic tree inferred using RAxML-NG. Branch lengths proportional to number of substitutions. Bootstrap Proportions shown at corresponding nodes if >75%. Names of the African species of Clariidae having extended neural spines posterior to dorsal fin (with or without an adipose fin) are highlighted in red. African and Southeast Asian (SEA) clades, comprising *Clarias* species, are highlighted in cream and blue, respectively. (**B**) Time-calibrated Bayesian phylogenetic tree inferred using BEAST2 v.2.6.4. Time scale in millions of years (My). Green bars at nodes indicate 95% Credibility Intervals for the ages of the corresponding nodes. Ages and posterior probability values for selected nodes indicated above and below, respectively. Dataset excludes *Horaglanis* because of its faster rate of molecular evolution relative to other taxa examined (see text for explanations).

This situation limits the understanding of the evolution of this group (e.g., Devaere et al. 2007, Stewart et al. 2014). Teugels and Adriaens (2003) summarized the phylogenetic information known at that time by presenting a morphology-based cladogram in which the African clariids (except *Uegitglanis*) and the Asian clariids (i.e., Asian *Clarias*, *Horaglanis*, and *Encheloclarias*) are reciprocally monophyletic. The position of *Uegitglanis* was left unresolved.

Using genetic data, we confirm herein the monophyly of the African clariids (Pouyaud et al. 2009), along with the monophyly of African taxa having elongated neural spines (indicated in red in Fig. 2A, 2B) within the African clariids (Devaere et al. 2007). Recently, De Alwis et al. (2023) inferred the non-monophyly of the Asian *Clarias* because South Asian *Clarias dussumieri* was found to be more closely related to African clariids than to Southeast Asian *Clarias*. A result replicated in our study. None of the previous genetic studies included *Encheloclarias*.

Herein, we infer that *Encheloclarias* is the sister group of the remaining clariids, not considering *Horaglanis* that we excluded from our analysis because the inference of the phylogenetic position of *Horaglanis* using only mitochondrial data may be unreliable due to its faster rate of molecular evolution. This hypothesis seems to not have been proposed before. Two previous hypotheses suggesting that *Encheloclarias* is closely related either to some African taxa such as *Heterobranchus*, *Dinotopterus*, and *Clarias ngamensis* (based on the shared presence of an adipose fin in these taxa) or to the Asian *Clarias* (as suggested by Teugels and Adriaens 2003) are therefore rejected. The inferred phylogenetic position of *Encheloclarias* has evolutionary and conservation implications that are briefly discussed below.

Evolution of the adipose fin in the Clariidae. Stewart et al. (2014) examined the evolution of the adipose fin in fish (Teleostei), highlighting the case of the Clariidae, in which most taxa possess only one long dorsal fin, apart from few taxa that have one dorsal fin and an adipose fin. Stewart et al. (2014) expressed uncertainty regarding the evolution of the adipose fin in the Clariidae, specifically whether the presence of an adipose fin represents the ancestral condition in this family. They lamented the lack of phylogenetic information on *Encheloclarias*.

Our phylogenetic results imply that the adipose fin in *Encheloclarias* and African taxa (such as *Heterobranchus*, and *Dinotopterus*) is not homologous, having evolved independently twice. This conclusion is also supported by the observation that the structure of the adipose fins in these two lineages differs. In African taxa, the adipose fin is supported by elongated neural spines, whereas in

Encheloclarias, it is not (Teugels and Adriaens 2003). Moreover, the early divergence of *Encheloclarias* does not allow us to dismiss the possibility that the adipose fin condition in *Encheloclarias* might represent the ancestral state for the Clariidae, as discussed by Stewart et al. (2014). However, the sole phylogenetic criterion is not sufficient to determine the ancestral condition of the dorsal and adipose fins at the origin of the Clariidae, given that three possibilities appear equally parsimonious: that of *Heteropneustes* with one short dorsal fin, that of *Encheloclarias* with one dorsal fin and one adipose fin, and that of the other clariids (excluding derived *Heterobranchus*, *Dinotopterus*, and *Clarias ngamensis*) with one long dorsal fin.

Conservation of *Encheloclarias* and their peat swamp habitats. Peat swamps in Southeast Asia are spatially dynamic environments known to harbor unique aquatic fauna, including many endemic fish species remarkably adapted to the highly acidic black waters (Ng et al. 1994; Fahmi-Ahmad et al. 2024). The evolution of these species remains poorly investigated. Genetic evidence suggests that some lineages adapted to peat swamp conditions millions of years ago, and subsequent allopatric diversification accounts for the observed diversity within these lineages (Fam et al. 2024). Nonetheless, additional data are required to assess the generality of this hypothesis and to determine whether the adaptation and diversification timeline is consistent across peat swamp lineages.

Encheloclarias represents one such lineage of fish adapted to the acidic peat swamps of Southeast Asia (Ng and Lim 1993). We estimated the mean age of divergence between *Encheloclarias* and the rest of the Clariidae to be 46.8 million years. This age is consistent with the timeline of the early diversification of the Clariidae proposed by Lundberg et al. (2007) based on a different set of calibrations and a different method of reconstruction. Thus, *Encheloclarias* is notable not only for its adaptation to acidic waters but also as an ancient and species-poor lineage. The genetic examination of other *Encheloclarias* species is needed to estimate the age of the crown group of the genus, and therefore to determine the minimum date of its colonization of peat swamps (herein, estimated to be only about 5 million years based on only one species, *Encheloclarias curtisoma*).

The possibility that the ancestors of *Encheloclarias* adapted to peat swamp environmental conditions millions of years ago further underscores the uniqueness of the fauna adapted to Southeast Asia's peat swamp forests. Yet, these remaining peat swamps continue to face severe threats.

Acknowledgments

This work was funded by the Ministry of Natural Resources, Environment and Climate Change, Malaysia (NRECC), through the National Conservation Trust Fund for Natural Resources (NCTF) [KeTSA(S)600-2/1/48/5(30)], titled "Revisiting the diversity and biogeography of freshwater fishes of Peninsular Malaysia through large-scale species identification approach." A permit for sampling activities was obtained through the Malaysia Access and Benefit-Sharing (MyABS) system, administered by the Ministry of Natural Resources, Environment, and Climate Change (NRECC) (permit application: Ref/888058). We thank the director of the Johor State Forestry Department Dato' Haji Salim Bin Aman for granting permission to join the Scientific Expedition on Biological Diversity in Ayer Hitam State Park on 15 and 16 April 2019. Finally, we thank two anonymous reviewers for their comments and suggestions that improved our manuscript.

References

Bergsten J (2005) A review of long-branch attraction. Cladistics 21(2): 163–193. https://doi.org/10.1111/j.1096-0031.2005.00059.x

Blessing JJ, Marshall JC, Balcombe SR (2010) Humane killing of fishes for scientific research: A comparison of two methods. Journal of Fish Biology 76(10): 2571–2577. https://doi.org/10.1111/j.1095-8649.2010.02633.x

Bouckaert R, Vaughan TG, Barido-Sottani J, Duchene S, Fourment M, Gavryushkina A, Heled J, Jones G, Kuhnert D, De Mario N, Matschiner M, Mendes FK, Muller NF, Ogilvie HA, du Plessis L, Popinga A, Rambaut A, Rasmussen D, Siveroni IA, Suchard MA, Wu CH, Xie D, Zhang C, Stadler T, Drummond AJ (2019) BEAST 2.5: An Advanced Software Platform for Bayesian Evolutionary Analysis. PLoS Computational Biology 15(4): e1006650. https://doi.org/10.1371/journal.pcbi.1006650

Briolay J, Galtier N, Brito RM, Bouvet Y (1998) Molecular phylogeny of Cyprinidae inferred from cytochrome *b* DNA sequences. Molecular Phylogenetics and Evolution 9(1): 100–108. https://doi.org/10.1006/mpev.1997.0441

Darriba D, Posada D, Kozlov AM, Stamatakis A, More B, Flouri T (2020) ModelTest-NG: A new and scalable tool for the selection of DNA and protein evolutionary models. Molecular Biology and Evolution 37(1): 291–294. https://doi.org/10.1093/molbev/msz189

De Alwis PS, Kundu S, Gietbong FZ, Amin MHF, Lee S-R, Kim H-W, Kim AR (2023) Mitochondriomics of *Clarias* fishes (Siluriformes: Clariidae) with a new assembly of *Clarias camerunensis*: Insights into the genetic characterization and diversification. Life 13(2): e482. https://doi.org/10.3390/life13020482

Devaere S, Jansen G, Adriaens D, Weekers P (2007) Phylogeny of the African representatives of the catfish family Clariidae (Teleostei, Siluriformes) based on a combined analysis: Independent evolution towards anguilliformity. Journal of Zoological Systematics and Evolutionary Research 45(3): 214–229. https://doi.org/10.1111/j.1439-0469.2006.00399.x

Diogo R, Chardon M, Vandewalle P (2003) On the osteology and myology of the cephalic region and pectoral girdle of *Heteropneustes fossilis* (Teleostei: Siluriformes), with comments on the phylogenetic relationships between *Heteropneustes* and the clariid catfishes. Animal Biology 53: 379–396. https://doi.org/10.1163/157075603322556283

Edler D, Klein J, Antonelli A, Silvestro D (2021) raxmlGUI 2.0: A graphical interface and toolkit for phylogenetic analyses using RAxML. Methods in Ecology and Evolution 12(2): 373–377. https://doi.org/10.1111/2041-210X.13512

Fahmi-Ahmad M, Halim MRA, Ilham-Norhakim ML, Arshad MNA, Zakaria ZA, Ghani IFA, Aqmal-Naser M, Mustafa SN, Abdul-Latiff MAB, Amal MNA, Ahmad AB, Zain KM (2024) A preliminary checklist of fish species in the peat swamp forest of Ayer Hitam Utara State Park Forest, Johor, Malaysia. Pertanika Journal of Tropical Agricultural Science 47(1): 251–270. https://doi.org/10.47836/pjtas.47.1.18

Fam YQ, Jamaluddin JAF, Muhammad-Rasul AH, Ilham-Norhakim ML, Rosely NFN, Lavoué S (2024) Contrasting genetic and morphological differentiation among allopatric lineages of a stenotopic miniature rasborin, *Boraras maculatus*, in Peninsular Malaysia. Journal of Fish Biology 104(1): 171–183. https://doi.org/10.1111/jfb.15572

Fricke R, Eschmeyer WN, Van der Laan R (2024) Eschmeyer's catalog of fishes: Genera, species, references. California Academy of Sciences, San Francisco, CA, USA. [Electronic version accessed in January 2024] http://researcharchive.calacademy.org/research/ichthyology/catalog/fishcatmain.asp

Gayet M (1987) Lower vertebrates from the Early-Middle Eocene Kuldana Formation of Kohat (Pakistan): Holostei and Teleostei. Contributions from the Museum of Paleontology. University Michigan 27: 151–193.

Grewe PM, Krueger CC, Aquadro CF, Bermingharn E, Kinsaid HL, Bernie M (1993) Mitochondrial DNA variation among lake trout (*Salvelinus namaycush*) strains stocked into Lake Ontario. Canadian Journal of Fisheries and Aquatic Sciences 50(11): 2397–2403. https://doi.org/10.1139/f93-264

Herre AWCT, Myers GS (1937) A contribution to the ichthyology of the Malay Peninsula. Bulletin of the Raffles Museum 13: 5–75.

Katoh K, Rozewicki J, Yamada KD (2019) MAFFT online service: Multiple sequence alignment, interactive sequence choice and visualization. Briefings in Bioinformatics 20(4): 1160–1166. https://doi.org/10.1093/bib/bbx108

Kozlov AM, Darriba D, Flouri T, Morel B, Stamatakis A (2019) RAxML-NG: A fast, scalable and user-friendly tool for maximum likelihood phylogenetic inference. Bioinformatics (Oxford, England) 35(21): 4453–4455. https://doi.org/10.1093/bioinformatics/btz305

Lundberg JG, Sullivan JP, Rodiles-Hernandez R, Hendrickson DA (2007) Discovery of African roots for the Mesoamerican Chiapas catfish, *Lacantunia enigmatica*, requires an ancient intercontinental passage. Proceedings. Academy of Natural Sciences of Philadelphia 156(1): 39–53. https://doi.org/10.1635/0097-3157(2007)156[39:DOARFT]2.0.CO;2

Ng PKL, Lim KKP (1993) The Southeast Asian catfish genus *Encheloclarias* (Teleostei: Clariidae), with descriptions of four new species. Ichthyological Exploration of Freshwaters 4(1): 21–37.

Ng HH, Tan HH (2000) A new species of *Encheloclarias* from Sumatra. Journal of Fish Biology 57(2): 536–539. https://doi.org/10.1111/j.1095-8649.2000.tb02193.x

Ng PKL, Tay JB, Lim KKP (1994) Diversity and conservation of blackwater fishes in Peninsular Malaysia, particularly in the North Selangor peat swamp forest. Hydrobiologia 285(1–3): 203–218. https://doi.org/10.1007/BF00005667

Pouyaud L, Sudarto, Paradis E (2009) The phylogenetic structure of habitat shift and morphological convergence in Asian *Clarias* (Teleostei, Siluriformes: Clariidae). Journal of Zoological Systematics and Evolutionary Research 47(4): 344–356. https://doi.org/10.1111/j.1439-0469.2008.00507.x

Rambaut A (2018) FigTree v1.4.4. https://github.com/rambaut/figtree/releases

Rambaut A, Drummond AJ, Xie D, Baele G, Suchard MA (2018) Posterior summarization in Bayesian phylogenetics using Tracer 1.7. Systematic Biology 67(5): 901–904. https://doi.org/10.1093/sysbio/syy032

Stewart TA, Smith WL, Coates MI (2014) The origins of adipose fins: An analysis of homoplasy and the serial homology of vertebrate appendages. Proceedings of the Royal Society, Biological Sciences 281(1781): 20133120. https://doi.org/10.1098/rspb.2013.3120

Sullivan JP, Lundberg JG, Hardman M (2006) A phylogenetic analysis of the major groups of catfishes (Teleostei: Siluriformes) using rag1 and rag2 nuclear gene sequences. Molecular Phylogenetics and Evolution 41(3): 636–662. https://doi.org/10.1016/j.ympev.2006.05.044

Tamura K, Stecher G, Kumar S (2021) MEGA11: Molecular Evolutionary Genetics Analysis Version 11. Molecular Biology and Evolution 38(7): 3022–3027. https://doi.org/10.1093/molbev/msab120

Tan ZW, Toh EXP, Cai Y, Tan HH, Yeo DCJ (2023) Discovery of *Encheloclarias* (Teleostei: Clariidae) from Singapore, with notes on morphology and distribution. Raffles Bulletin of Zoology 71: 196–206. https://doi.org/10.26107/RBZ-2023-0015

Teugels GG, Adriaens D (2003) Taxonomy and phylogeny of Clariidae: An overview. Pp. 465–487. In: Arratia G, Kapoor G, Chardon BGM, Diogo R (Eds.) Catfishes. Science Publishers, Enfield, NH, USA.

Ward RD, Zemlak TS, Innes BH, Last PR, Hebert PDN (2005) DNA barcoding Australia's fish species. Philosophical Transactions of the Royal Society of London. Series B, Biological Sciences 360(1462): 1847–1857. https://doi.org/10.1098/rstb.2005.1716

Supplementary material 1

Bayesian 50% consensus phylogenetic trees of the family Clariidae showing the position of *Encheloclarias*

Authors: Sébastien Lavoué, Jamsari Amirul Firdaus Jamaluddin, Abdullah Halim Muhammad-Rasul, Mohd Lokman Ilham-Norhakim, Khaironizam Md Zain

Data type: pdf

Explanation note: **A**) dataset including the genus *Horaglanis*; **B**) dataset excluding *Horaglanis* because of its higher rate of molecular evolution relative to other taxa examined (see text for details). Branch lengths proportional to number of substitutions. Posterior probabilities shown at corresponding nodes if < 1. Names of the species of Clariidae having two dorsal fins are highlighted in red. African and Southeast Asian (SEA) clades are highlighted in cream and blue, respectively.

Link: https://doi.org/10.3897/aiep.54.122366.suppl1

Acta Ichthyologica et Piscatoria 54, 2024, 243–247 | DOI 10.3897/aiep.54.134405

PENSOFT.

ACTA
ICHTHYOLOGICA
ET PISCATORIA

First record of *Priacanthus blochii* (Actinopterygii: Eupercaria: Priacanthidae) from Malaysia

Shintaro HASHIMOTO[1], Reo KOREEDA[1], Md Repin IZARENAH[2], Ying Giat SEAH[3,4], Hiroyuki MOTOMURA[5]

1 *Graduate School of Agriculture, Forestry and Fisheries, Kagoshima University Kagoshima, Kagoshima, Japan*
2 *Department of Fisheries Malaysia, Ministry of Agriculture and Food Security, Putrajaya, Malaysia*
3 *Faculty of Fisheries and Food Science, Universiti Malaysia Terengganu, Terengganu, Malaysia*
4 *South China Sea Repository and Reference Centre, Institute of Oceanography and Environment, Universiti Malaysia Terengganu, Terengganu, Malaysia*
5 *Kagoshima University Museum, Kagoshima, Japan*

https://zoobank.org/4707DDDA-E4A6-4A7B-85B4-B938D75C28A3

Corresponding author: Shintaro Hashimoto (k1028515@kadai.jp)

Academic editor: Ronald Fricke ♦ **Received** 10 August 2024 ♦ **Accepted** 13 September 2024 ♦ **Published** 25 October 2024

Citation: Hashimoto S, Koreeda R, Izarenah MR, Seah YG, Motomura H (2024) First record of *Priacanthus blochii* (Actinopterygii: Eupercaria: Priacanthidae) from Malaysia. Acta Ichthyologica et Piscatoria 54: 243–247. https://doi.org/10.3897/aiep.54.134405

Abstract

A single specimen collected off Perak, Malaysia was identified as *Priacanthus blochii* Bleeker, 1853, being characterized by 13 dorsal-fin soft rays, 14 anal-fin soft rays, the dorsal and anal fins relatively low and rounded distally, 21 total gill rakers on the first arch, 77 scales in lateral series, the 10th dorsal-fin spine 1.59 times the length of the second dorsal-fin spine, the pectoral-fin length 48.0% of the head length, the posterior margin of the caudal fin convex, a black blotch absent anteriorly on the dorsal-fin membrane, and a single large black blotch on the pelvic-fin base. In Southeast Asian waters, *P. blochii* has been recorded to date, from Thailand (Andaman Sea), the Philippines, and Indonesia. A previous Malaysian record, based on a photograph purported to be of *P. blochii*, was identified here as *Priacanthus sagittarius* Starnes, 1988, the specimen reported here being the first record of *P. blochii* from Malaysia.

Keywords

Andaman Sea, distribution, morphology, paeony bulleye, specimen-based records, Strait of Malacca

Introduction

The bigeye genus *Priacanthus* Oken, 1817 includes 13 species (Starnes 1988; Hashimoto and Motomura 2024). Of these, *Priacanthus blochii* Bleeker, 1853, *Priacanthus fitchi* Starnes, 1988, *Priacanthus hamrur* (Forsskål, 1775), *Priacanthus macracanthus* Cuvier, 1829, *Priacanthus sagittarius* Starnes, 1988, *Priacanthus tayenus* Richardson, 1846, and *Priacanthus zaiserae* Starnes et Moyer, 1988 have been recorded from Southeast Asia (Starnes 1988, 1999; Vidthayanon 1999; Kuiter and Tonozuka 2004; Satapoomin 2011; Allen and Erdmann 2012). *Priacanthus blochii* has been collected from depths of 15 to 30 m and is considered to prefer reef areas (Starnes 1988). This species has been recorded from various parts of Indonesia (Starnes 1988; Iwatsuki et al. 1997; Kimura et al. 2003; Kuiter and Tonozuka 2004; Randall 2005; Allen and Erdmann 2012; White et al. 2013; Gloerfelt-Tarp and Kailola 2022), but not from neighboring Malaysian waters.

A single specimen of *P. blochii* was collected in January 2024 from the Strait of Malacca, off Perak, Malaysia. Although Ambak et al. (2010) had previously recorded *P. blochii* from Malaysia based on a photograph, the latter was re-identified here as representing *P. sagittarius*.

In fact, Southeast Asian records of confirmed *P. blochii* exist to date only for Thailand (Andaman Sea), the Philippines, and Indonesia (Starnes 1988; Kuiter and Tonozuka 2004; Randall 2005; Iwatsuki 2009; Satapoomin 2011; Allen and Erdmann 2012), the specimen from Perak therefore being the first verified, specimen-based record of *P. blochii* from Malaysia.

Material and methods

The collection of metric and meristic data followed Hubbs and Lagler (1958) and Starnes (1988). Measurements were made with calipers to the nearest 0.1 mm. Standard length is abbreviated as SL. The last two soft rays of the dorsal and anal fins were counted as single rays. Curatorial procedures for KAUM specimens followed Motomura and Ishikawa (2013); institutional codes follow Sabaj (2020).

Results and discussion

Family Priacanthidae Günther, 1859
Genus *Priacanthus* Oken, 1817

Priacanthus blochii Bleeker, 1853

English common name: paeony bulleye

Fig. 1, Table 1

Material examined. KAUM–I. 193393, 107.1 mm SL, off Perak, Malaysia, bottom trawl, 17 January 2024, coll. by Reo Koreeda et al.

Description. Counts and measurements given in Table 1. Body oval, laterally compressed. Dorsal profile from snout to base of fifth dorsal-fin spine gently elevated, thereafter gradually lowering to caudal-fin base. Ventral profile of body lowering from lower-jaw tip to pelvic-fin insertion, subsequently parallel to body axis, and elevating from origin of anal fin to caudal-fin base. Lateral line complete, originating above anterodorsal tip of opercle and rapidly rising to just below third dorsal-fin spine base, subsequently lowering to caudal peduncle, thereafter straight to caudal-fin base. Scales very small, ctenoid, non-deciduous, present on entire body, except lips and posterior margin of opercle. Posterior edge of preopercle serrated. Long spine on angle of preopercle, its posterior tip barely reaching opercular margin. Snout short, smaller than eye. Eye large, rounded. Anterior and posterior nostrils located anterior to orbit, close to each other; anterior nostril oval, with short broad flap posteriorly; posterior nostril slit-like, with convex flap on lower half of anterior margin. Gill rakers well developed, rod-shaped, with small dense spines.

Mouth large, terminal, posterior tip of maxilla beyond anterior margin of eye. Mandible protruding considerably beyond maxilla. Lower-jaw tip pointed, slightly above level of eye center. Upper jaw with 2 rows of conical teeth, curving backwards. Lower-jaw teeth slightly larger than upper-jaw teeth, conical, curving backwards, 2 rows anteriorly, a single row posteriorly. Vomerine teeth patch V-shaped, each end extending outwardly, teeth small, conical, dense, curving slightly backwards. Elongate palatine teeth similar to upper jaw teeth, 2 rows anteriorly, a single row posteriorly.

Dorsal-fin origin just above uppermost point of posterior tip of opercle, 10th spine longest, third soft ray longest. Anal-fin origin just below eighth dorsal-fin spine base. Posterior end of dorsal-fin base slightly anterior to posterior end of anal-fin base. Anus just anterior to anal-fin origin. Uppermost point of pectoral-fin base slightly anterior to posterior tip of opercle, below level of lower eye margin. Lowermost point of pectoral-fin base just below third dorsal-fin spine base. Posterior margin of pectoral fin round, reaching below sixth dorsal-fin spine base. Pelvic-fin insertion below and slightly behind posterior margin of eye. Base of last ray of pelvic fin slightly posterior to uppermost point of pectoral-fin base. Second pelvic-fin ray longest, last ray connected to abdomen by membrane. Posterior tip of depressed pelvic fin slightly beyond base of second anal-fin spine. Caudal fin truncate, posterior margin convex.

Color when fresh (Fig. 1). Body uniformly reddish silver. Dorsal surface of head red. Dorsal-, anal-, and pelvic-fin spines and rays slightly pale red, membrane reddish black. Base of anal- and pelvic-fin membrane yellowish. Fin membrane connecting last pelvic-fin ray and body whitish. Pectoral fin transparent, rays reddish. Caudal fin red, posterior margin blackish. Pupil black, iris pale red.

Distribution. *Priacanthus blochii* is widely distributed in the Indo–West Pacific region (Starnes 1988; Heemestra 2022). In Southeast Asia, the species has been recorded from Andaman Sea (southwestern coast of Thailand), the Philippines (Luzon, Panay, and Pamilikan), and Indonesia [Sumatra, Java, Bali, North Sulawesi, Maumere (Flores), Ambon, and West Papua] (Starnes 1988; Iwatsuki et al. 1997; Kimura et al. 2003; Kuiter and Tonozuka 2004; Randall 2005; Iwatsuki 2009; Satapoomin 2011; Allen and Erdmann 2012; White et al. 2013; Kawama 2017; Gloerfelt-Tarp and Kailola 2022). The presently reported specimen from Perak represents the first Malaysian record of the species (Fig. 2).

Remarks. Identification of the Perak specimen was based on the following combination of characters, which closely matched the diagnostic features of *Priacanthus blochii* given by Starnes (1988): 13 dorsal-fin soft rays; 14 anal-fin soft rays; dorsal and anal fins relatively low and rounded distally; 21 total gill rakers on first arch; 77 scales in lateral series; 10th dorsal-fin spine 1.59 times length of second dorsal-fin spine; pectoral-fin length 48.0% of head length; posterior margin of caudal fin convex; lacking a black blotch on first two spinous dorsal membranes; single large black blotch on pelvic-fin base. Moreover, the counts and measurements of the Perak specimen matched with specimens of *P. blochii* from the Seychelles reported by Starnes (1988).

Although Ambak et al. (2010) reported *P. blochii* from Malaysia, based on a photograph, the figured individual had the 10th dorsal-fin spine strongly elongated, together with the dorsal- and anal-fin rays, and the anterior portion of the dorsal fin black, all characteristics of *P. sagittarius* shown by Starnes (1988, 1999). Furthermore, the distribution of *P. blochii* given by Starnes (1999) includes Malaysia. However, the distribution map in Starnes

Figure 1. Fresh specimen of *Priacanthus blochii* from Perak, Malaysia (KAUM–I. 193393, 107.1 mm SL).

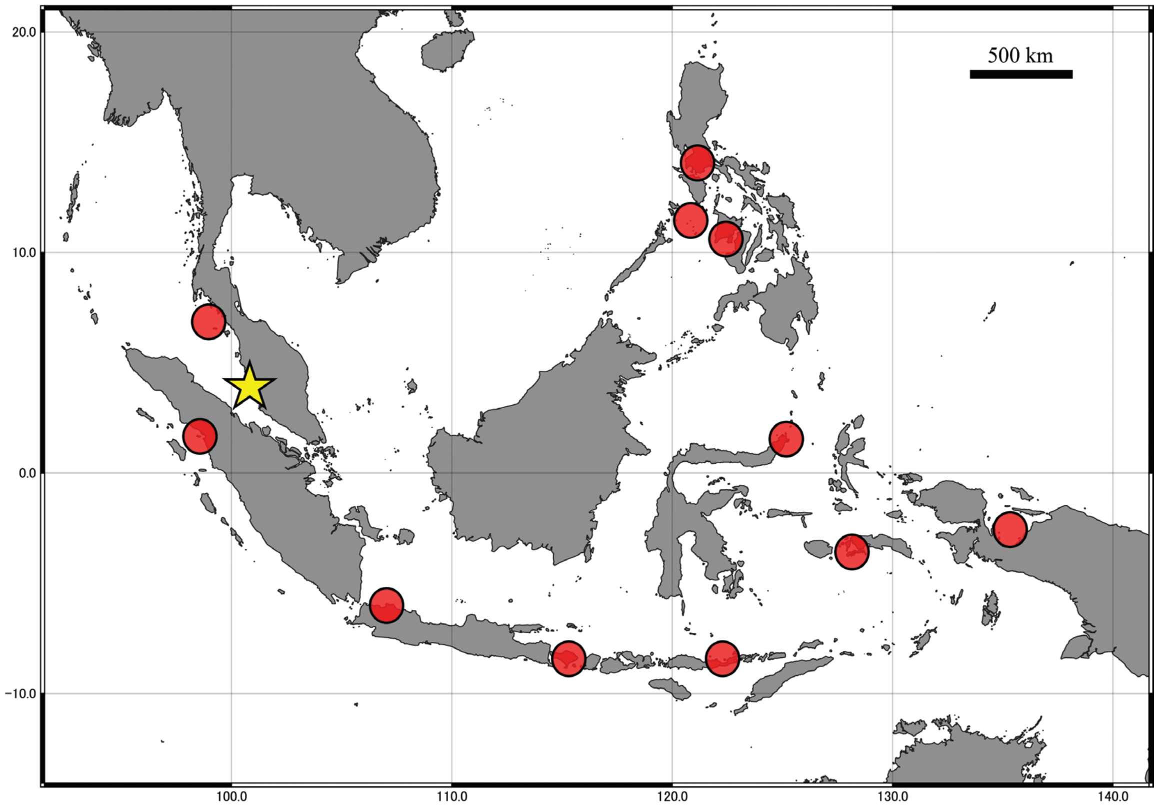

Figure 2. Distributional records of *Priacanthus blochii* in Southeast Asia. Star: based on specimen examined in this study; circles: literature records.

Table 1. Counts and measurements of specimens of *Priacanthus blochii*.

Character	Perak, Malaysia	Seychelles (*n* = 8)	
	KAUM–I. 193393	Range	Mode or mean
Morphometric data; absolute values [mm]			
Standard length (SL)	107.1	103.1–228.5	
Head length (HL)	38.1	37.1–73.7	56.8
2nd dorsal-fin spine length (2DFSL)	10.3	13.8–19.1	15.9
Morphometric data; relative values [%SL]			
Body depth at 6th dorsal-fin spine	37.7	34.1–39.8	36.8
Body width at pectoral-fin base	14.2	14.3–16.0	15.0
Head length	35.6	32.3–37.7	34.8
Head depth	35.7	32.0–36.5	33.9
Snout length	9.7	9.3–10.7	10.0
Orbit diameter	15.4	14.0–16.5	15.2
Eyelid inside diameter	13.2	10.8–14.6	12.9
Interorbital width	7.8	6.6–8.4	7.8
Upper-jaw length	18.6	17.4–19.4	18.6
Predorsal-fin length	32.2	31.2–37.2	33.7
Preanal-fin length	58.9	55.7–60.6	58.0
Prepelvic-fin length	35.9	33.7–39.3	35.5
Dorsal-fin base length	57.3	54.8–59.4	57.6
1st dorsal-fin spine length	6.0	6.6–8.4	7.3
2nd dorsal-fin spine length	9.6	8.4–10.2	9.4
3rd dorsal-fin spine length	11.7	10.3–13.1	11.7
10th dorsal-fin spine length	15.3	11.7–15.6	14.6
Longest dorsal-fin ray length	19.1	18.3–22.0	20.0
Anal-fin base length	35.6	34.4–37.6	36.0
1st anal-fin spine length	7.3	7.4–9.5	8.6
2nd anal-fin spine length	10.7	10.1–13.0	11.9
3rd anal-fin spine length	14.5	12.7–15.6	14.7
Longest anal-fin ray length	20.4	19.0–22.7	21.1
Longest pectoral-fin ray length	17.1	16.6–17.4	17.0
Pelvic-fin spine length	20.5	20.3–23.3	21.7
1st pelvic-fin ray length	28.4	27.1–30.4	29.0
Caudal-fin length	24.6	22.5–25.6	24.3
Caudal-peduncle length	14.3	13.4–15.9	14.6
Caudal-peduncle depth	8.8	8.7–9.7	9.1
Morphometric data; relative values [%HL]			
Longest pectoral-fin ray length	48.0	45.4–51.6	48.9
Morphometric data; relative values [%2DFSL]			
10th dorsal-fin spine length	1.59	1.43–1.70	1.59
Meristic data			
Dorsal-fin rays	X, 13	X, 13–14	13
Anal-fin rays	III, 13	III, 13–15	14
Pectoral-fin rays	18	17–18	17
Pelvic-fin rays	I, 5	I, 5	
Gill rakers on upper limb	5	5–6	5
Gill rakers on lower limb	16	16–17	17
Lateral-line scales	69	68–74	
Scales in lateral series	76	76–83	
Vertical scale rows	48	48–51	
Scale rows above lateral line	10	10–12	
Scale rows bellow lateral line	37	36–40	

(1999) probably connects the points shown in Starnes (1988), and no specimens from Malaysia are shown in Starnes (1988, 1999). Therefore, the presently reported specimen, from Perak, Malaysia, represents the first record of *P. blochii* from Malaysia.

Comparative material examined. *Priacanthus blochii*: 8 specimens (103.1–228.5 mm SL) from Seychelles: ANSP 108322, 2 specimens, 171.7–228.5 mm SL, North Island, Mahé; ANSP 108323, 2 specimens, 156.0–181.6 mm SL, between Rouge Point and St. Pierre Islet, Curieuse Island; ANSP 108335, 173.6 mm SL, St. Anns Bay between Praslin and Round islands; ANSP 108340, 140.7 mm SL, Ressource Island, Amirante Islands; ANSP 108425, 103.1 mm SL, D'Arros Island, Amirante Islands; ANSP 159098, 157.5 mm SL, Beau Vallon Bay, Mahé.

Acknowledgments

We are especially grateful to M. Sabaj and M. H. Arce (ANSP) for opportunities to examine specimens and providing specimen photographs, and Y. Hibino (KMNH) and volunteers and students at the Kagoshima University Museum, Kagoshima (KAUM) for curatorial assistance; We extend our gratitude to S.A. Mat Piah, N.A. Abd Latiff, J.N. Lee, and M.S. Ali (UMT) for their support during the field survey. Graham S. Hardy (Ngunguru, New Zealand) read the manuscript and provided help with English. This study was supported in part by the Universiti Malaysia Terengganu (UMT) through Strategic Research Grant (UMT/SRG-2023/55435); Department of Fisheries Malaysia (PRK.ML.630-1 Jld 5(7)), JSPS KAKENHI Grant Numbers 20H03311, 21H03651, 23K20304 and 24K02087; the JSPS Core-to-Core CREPSUM JPJSCCB20200009; and the "Establishment of Glocal Research and Education Network in the Amami Islands" project of Kagoshima University adopted by the Ministry of Education, Culture, Sports, Science and Technology, Japan. The specimens will be deposited at the Kagoshima University Museum as a collaborative research gift and used for scientific research purposes. We acknowledge the support and facilities provided by the Fisheries Development Authority of Malaysia (LKIM), Malaysia Fish Industries General Association, and the South China Sea Repository and Reference Centre, UMT. Special thanks go to the Japan Society for the Promotion of Science (JSPS): Core-to-Core project Collaborative Research and Education Project in Southeast Asia for Sustainable Use of Marine Ecosystems (CREPSUM) for endless support in marine fish diversity studies. This research is a part of the dissertation of the first author. All authors agree with the article publication and dissertation submission.

References

Allen GR, Erdmann MV (2012) Reef fishes of the East Indies. Vol. 1. Tropical Reef Research, Perth, WA, Australia, xiv + 424 pp.

Ambak MZ, Isa MM, Zakaria MZ, Ghaffar MA (2010) Fishes of Malaysia. Universiti Malaysia Terengganu, Kuala Terengganu, Malaysia, xii + 334 pp.

Gloerfelt-Tarp T, Kailola PJ (2022) Trawled fishes of southern Indonesia and northwestern Australia. Australian Society for Fish Biology, x + 422 pp. [Electronic version accessed 9 August 2024] https://www.asfb.org.au/trawled-fishes-of-southern-indonesia-and-northwestern-australia

Hashimoto S, Motomura H (2024) A new species of bigeye, *Priacanthus gracilis* (Perciformes: Priacanthidae), from eastern Australia. Ichthyological Research. https://doi.org/10.1007/s10228-024-00969-x

Heemstra PC (2022) Family Priacanthidae. Pp. 155–159. In: Heemstra PC, Heemstra E, Ebert DA, Holleman W, Randall JE (Eds.) Coastal fishes of the western Indian Ocean. Vol. 3. South African Institute for Aquatic Biodiversity, Makhanda, South Africa.

Hubbs CL, Lagler KF (1958) Fishes of the Great Lakes region. Bulletin of Cranbrook Institute of Science 26: 1–213.

Iwatsuki Y (2009) Priacanthidae. Pp. 100–102. In: Kimura S, Satapoomin U, Matsuura K (Eds.) Fishes of Andaman Sea, west coast of southern Thailand. National Museum of Nature and Science, Tokyo, Japan.

Iwatsuki Y, Sakuragi O, Yamashita T, Kimura S (1997) Records of *Priacanthus blochii* and *P. fitchi* from southern Japan (Perciformes: Priacanthidae). Japanese Journal of Ichthyology 44(2): 101–106.

Kawama K (2017) Priacanthidae. Pp. 94–96. In: Motomura H, Alama UB, Muto N, Babaran RP, Ishikawa S (Eds.) Commercial and bycatch market fishes of Panay Island, Republic of the Philippines. Kagoshima University Museum, Kagoshima, University of the Philippines Visayas, Iloilo, and Research Institute for Humanity and Nature, Kyoto.

Kimura S, Peristiwady T, Suharti SR (2003) Priacanthidae. Pp. 59–60. In: Kimura S, Matsuura K (Eds.) Fishes of Bitung, northern tip of Sulawesi, Indonesia. National Museum of Nature and Science, Tokyo, Japan.

Kuiter RH, Tonozuka T (2004) Pictorial guide to Indonesian reef fishes. Part 1. PT Dive and Dive's, Bali. vi + 302 pp.

Motomura H, Ishikawa S (2013) Fish collection building and procedures manual. English edition. The Kagoshima University Museum, Kagoshima and the Research Institute for Humanity and Nature, Kyoto, Japan, 70 pp.

Randall JE (2005) Reef and shore fishes of the South Pacific. New Caledonia to Tahiti and Pitcairn Islands. University of Hawai'i Press, Honolulu HI, USA, xii + 707 pp.

Sabaj MH (2020) Codes for natural history collections in ichthyology and herpetology. Copeia 108(3): 593–669. https://doi.org/10.1643/ASIHCODONS2020

Satapoomin U (2011) The fishes of southwestern Thailand, the Andaman Sea—A review of research and a provisional checklist of species. Research Bulletin – Phuket Marine Biological Center 70: 29–77.

Starnes WC (1988) Revision, phylogeny and biogeographic comments on the circumtropical marine percoid fish family Priacanthidae. Bulletin of Marine Science 43: 117–203.

Starnes WC (1999) Priacanthidae. Pp. 2291–2352. In: Carpenter KE, Niem VH (Eds.) FAO species identification guide for fishery purposes. The living marine resources of the western central Pacific. Vol. 4. Bony fishes part 2 (Mugilidae to Carangidae). FAO, Rome.

Vidthayanon C (1999) Species composition and diversity of fishes in the South China Sea, area II: Sarawak, Sabah and Brunei Darussalam waters. Pp. 224–242. In: Southeast Asian Fisheries Development Center (Eds.) Proceedings of the Second Technical Seminar on Marine Fishery Resources Survey in the South China Sea, Area II: Sarawak, Sabah and Brunei Darussalam Waters. Southeast Asian Fisheries Development Center, Kuala Lumpur, Malaysia.

White WT, Last PR, Dharmadi, Faizah R, Chodrijah U, Prisantoso BI, Pogonoski JJ, Puckridge M, Blaber SJM (2013) Market fishes of Indonesia. Australian Centre for International Agricultural Research, Canberra, ACT, Australia, 438 pp.

Acta Ichthyologica et Piscatoria 54, 2024, 249–260 | DOI 10.3897/aiep.54.134294

PENSOFT.

ACTA
ICHTHYOLOGICA
ET PISCATORIA

Diversity of fish otoliths from the Gulf of Mexico and the Caribbean Sea: Report on the first digital collection of fish otoliths (Actinopterygii) from the Atlantic region of Mexico

Maribel BADILLO ALEMÁN[1], Ariana SOLÍS GÓMEZ[2], Alfredo GALLARDO TORRES[1], Eduardo PACHECO GONGORA[1], Xavier CHIAPPA-CARRARA[1,3]

1 *Laboratorio de Biología de la Conservación, Facultad de Ciencias, Universidad Nacional Autónoma de México, Mérida, Mexico*
2 *Posgrado en Ciencias del Mar y Limnología, Universidad Nacional Autónoma de México, Mérida, Mexico*
3 *Laboratorio Nacional de Biología del Cambio Climático, Consejo Nacional de Humanidades, Ciencias y Tecnología, Mexico City, Mexico*

https://zoobank.org/511FB7B7-0F70-49A8-9E17-81DE31E950F9

Corresponding author: Xavier Chiappa-Carrara (xcc@ciencias.unam.mx)

Academic editor: Ken Longenecker ♦ **Received** 9 August 2024 ♦ **Accepted** 20 September 2024 ♦ **Published** 28 October 2024

Citation: Badillo Alemán M, Solís Gómez A, Gallardo Torres A, Pacheco Gongora E, Chiappa-Carrara X (2024) Diversity of fish otoliths from the Gulf of Mexico and the Caribbean Sea: Report on the first digital collection of fish otoliths (Actinopterygii) from the Atlantic region of Mexico. Acta Ichthyologica et Piscatoria 54: 249–260. https://doi.org/10.3897/aiep.54.134294

Abstract

The Otolith Collection of Fishes from the Gulf of Mexico and Caribbean Sea was created with the objective to conserve and illustrate the diversity of these structures from species living in the Gulf of Mexico, the Caribbean Sea, and the freshwater and brackish systems of the Yucatan Peninsula, incorporating morphological descriptions and morphometric data. Otoliths, non-skeletal calcareous structures that develop in the inner ear of fish, are essential for balance and hearing. They have become pivotal tools for age and growth determination, population analysis, and ecological, trophic, and archaeological studies due to their resistance to degradation and the extensive information they provide about the environment and physiology of fish. The collection now includes otoliths from 214 species, representing 67 families, obtained through sampling campaigns and collaborations with local fishermen. The otoliths are extracted using techniques that ensure the integrity of the structures for later preservation. High-resolution images were obtained using optical and scanning electron microscopy, and these images are stored in an online database. This database facilitates research and teaching by providing public access to digital specimens and associated data. In addition to fostering academic development, this collection represents a significant step towards the creation of a national platform for otolith data analysis, aligned with international efforts to digitize biological collections. Despite the financial and logistical challenges involved in building and maintaining biological collections, this collection demonstrates its value as an essential resource for taxonomic, systematic, and ecological studies, as well as for biodiversity education and awareness. The online availability of the collection not only facilitates access to data but also promotes innovation and international collaboration in the study of fishes and their habitats.

Keywords

biological collection, digitization, fish, image analysis, online collection

Introduction

Throughout history, biological collections have played a fundamental role in documenting the biodiversity of our planet. They provide essential information for the knowledge, exploitation, and sustainable use of our biological capital, and they assist in the analysis of trends derived from environmental changes. Additionally, they contribute necessary information for studies on environmental health, epidemiology, and national security, proving to be irreplaceable tools for investigating cases of biological terrorism (Suarez and Tsutsui 2004) and determining the effects of anthropogenic activities (Izzo et al. 2018). The information generated from the analysis of specimens kept in biological collections has motivated changes in public policies on the sustainable use of natural resources, significantly impacting social welfare (Anonymous 2020).

Biological collections are not only essential repositories for taxonomic and systematic work on the biota but also contribute to the development of other scientific disciplines. They play a crucial role in education by raising awareness of the need to document and conserve biodiversity and by enabling the development of new skills in research and data analysis. Therefore, the role of biological collections transcends purely scientific objectives and should be considered necessary tools that benefit society (Kellner 2024).

At different regional levels, collections maintain and catalog specimens of local ecosystems, creating, preserving, and increasing information on species distribution, identifying endemic or invasive species, and evaluating changes in biodiversity over time (Oré-Villalba 2017; Meineke et al. 2018). Thus, biological collections are essential references in conservation efforts, including those focused on endangered species and their habitats.

As fishes have been a group of interest for centuries, they are part of several biological collections, notable for their diversity of forms and adaptations. Approximately 36 893 valid fish species are recognized (Fricke et al. 2024), equivalent to more than half of all living vertebrates. Mexico, with its high diversity of fishes, boasts at least 2763 species (Espinosa-Pérez 2014), of which 1816 are found in the Gulf of Mexico and the Caribbean Sea (Robertson and Van Tassel 2023). In this region, fishing activities by industrial and artisanal fleets, along with recreational activities such as diving and sport fishing, are depleting natural populations (De la Cruz et al. 2016). Given that many fish species present on the Atlantic coast of Mexico have economic, nutritional, cultural, ecological, or evolutionary importance, it is necessary to know the specific identity of organisms and study aspects of their biology, ecology, and biogeography, underscoring the relevance of scientific collections.

Although specimens deposited in ichthyological collections are useful for various research purposes, their importance in paleontological, archaeological, and trophic studies is particularly noteworthy. In trophic studies, for example, prey of piscivorous organisms are often identified by examining stomach contents, vomit, or feces (Baker et al. 2024). This methodology is limiting when the prey's degree of digestion is advanced. However, other structures such as otoliths (Baker et al. 2014), which may be present in the digestive tract of ichthyophagous organisms due to their resistance to degradation and retention of original characteristics in many situations (Rivaton and Bourret 1999; Tuset et al. 2008), can be recognized. In paleontology and archaeology, zooarchaeological remains, including otoliths, are valuable for reconstructing environmental conditions, such as the distribution and extent of water bodies, and recognizing the species used by ancient cultures (Lin et al. 2022).

Otoliths are non-skeletal calcareous concretions (Nolf 1985; Maisey 1987) that grow within the vestibular system of vertebrates, particularly in the membranous labyrinth of the inner ear. In bony fishes, the inner ear consists of three semicircular canals and three otic chambers, each housing an otolith. Depending on the chamber in which they are located, otoliths are called sagitta (in the sacculum), lapillus (in the utricle), and asteriscus (in the lagena). These structures play a crucial role in balance, orientation, and sound detection (Platt and Popper 1981; Gauldie and Nelson 1988; Campana and Thorrold 2001). Otoliths are composed of calcium carbonate ($CaCO_3$) in the form of aragonite and other inorganic salts, with crystals embedded in an organic matrix composed of a fibrous protein called otolin, deposited concentrically around a nucleus (Martínez Pérez et al. 2018). The presence of several elements is related to metabolically regulated processes and is influenced by both endogenous and exogenous factors. Therefore, otoliths can provide information on the physiological aspects of organisms and the environments in which they developed (Volpedo and Echeverría 2003). These characteristics have made otoliths key tools in research on age and growth (Francis and Campana 2004), population dynamics, trophic studies, archaeological analyses, and present and past environmental conditions.

Sagittae have a particular morphology that varies among species, making them useful as auxiliary structures in organism identification and for distinguishing between phylogenetically close species (Volpedo and Echeverría 2003). Analyzing the shape, size, and structural characteristics of otoliths not only allows for species identification but also helps investigate evolutionary relationships and reconstruct phylogenetic histories.

Rojo (2015) emphasized the importance of incorporating otoliths into fish collections, as they enable the extraction of biological information about species that is otherwise unattainable through the analysis of other structures such as spines, scales, or bones. Otoliths store unique data on the life history of organisms and the environmental conditions of their habitats. It is in this context that the Otolith Collection of Fishes from the Gulf of Mexico and Caribbean Sea was created and registered with the Mexican Ministry of Environment and Natural Resources (SEMARNAT, registration code DGVS-CC-305-18).

The main objective of this collection is to preserve otoliths of a wide variety of species, including those of economic and ecological importance, as well as endangered and endemic species from the Gulf of Mexico and the Caribbean Sea, and freshwater and brackish systems of the Yucatan Peninsula. The addition of the Mexican

Atlantic Fish Otolith Collection (Martínez Pérez et al. 2011; Del Moral-Flores et al. 2016) and proper curation and maintenance have turned this collection into a national reference, contributing to research in disciplines such as biology, ecology, biogeography, archaeology, and fisheries, among others. To enhance this purpose and facilitate access to specimens and other resources such as databases or software for shape analysis, this collection is available online. Public access to information is thus guaranteed, scientific collaboration is encouraged, and educational and training opportunities are improved (Monfils et al. 2017), extending these benefits to a wide geographical extent.

Methods

Specimen collection. Since 2011, multiple campaigns have been conducted in various localities of the Gulf of Mexico and the Caribbean Sea to obtain bony fish specimens, which serve as the primary input of biological material. Specific sampling methods have been employed, involving different fishing gears operated under catch permits obtained from the competent authorities. Additionally, visits have been made to markets, fish markets, and ports, and agreements have been established with fishermen from different areas to direct sampling efforts towards certain species of interest. The Otolith Collection of Fishes from the Gulf of Mexico and the Caribbean Sea has been enriched by the addition of the Mexican Atlantic Fish Otolith Collection (Martínez Pérez et al. 2011; Del Moral-Flores et al. 2016).

It is important to note that otolith extraction requires that the specimens be fresh or frozen, as otoliths preserved in unneutralized formalin or alcohol degrade, reducing the chances of correct identification (Hecht 1990) and limiting their usefulness as collection specimens.

After collection, each fish is identified to the species level using taxonomic keys and guides. Biometric data, such as total length (TL), standard length (SL), cephalic length (CL), body height, weight, and, when possible, sex, are recorded for each specimen. Capture data, including locality, date, and geographic coordinates, are also documented.

Otolith extraction. Two techniques are employed for otolith extraction. One method involves lifting the operculum, removing the gills, and breaking the bony capsules to expose and extract the otoliths with forceps. The other method involves separating the head from the body and removing the gill arches and surrounding tissue to locate the bony capsules. The blades of a pair of scissors are inserted into the center of the first vertebra, using them as a lever to lift the ventral bone of the capsule and expose the otoliths. These procedures are performed under a stereoscopic microscope.

Once extracted, the otoliths are cleaned of residual tissue, and detailed morphometric measurements, including perimeter, area, height, width, and acoustic sulcus dimensions, are obtained using Zen Pro software (Zeiss). These data allow for the calculation of different morphometric indices useful in species comparison.

The terminology used for the morphological descriptions of sagittae is derived from the works of Mascareñas Osorio et al. (2003), Tuset et al. (2008), Volpedo et al. (2017), and Martínez Pérez et al. (2018).

Otoliths are stored in vials labeled with biometric and capture data, including a unique identification code for each specimen. The vials are placed in boxes, which are labeled and stored in the collection under controlled temperature and humidity conditions to ensure long-term preservation.

Digitization of the collection. The digitization of the Otolith Collection of Fishes from the Gulf of Mexico and the Caribbean Sea is a key component in improving the accessibility and usefulness of the stored specimens. This collection includes a photographic archive of approximately 2600 otolith images obtained using optical and scanning electron microscopy techniques. These images are used not only for documentation and preservation but also to facilitate research and comparative analysis.

High-resolution images of the otoliths are obtained using an advanced Zeiss AxioZoom stereo microscope, which provides continuous magnification and excellent depth of field, crucial for capturing the morphological details of the structures. These images are used for both taxonomic identification and morphometric studies. Additionally, a scanning electron microscope (Jeol 7600F FESEM) is used to obtain high-resolution images with a large depth of field, allowing for the visualization of ultrastructural details of otoliths not perceptible with optical microscopy. This equipment is essential for studies requiring detailed analysis of the otolith surface and its microstructures.

Images are selected to highlight the distinctive characteristics of each otolith, with angles and focus optimized for this purpose. Each image is edited to standardize the black background, enhancing contrast and facilitating the visualization of morphological details. A watermark with the collection logo is added to each image to ensure provenance and maintain the collection’s identity.

The digitized images are stored in a database management system that allows easy access and retrieval. Each image is associated with the biometric and capture data of the corresponding specimen, including the unique identification code.

Results

Physical specimens. The Otolith Collection of the Gulf of Mexico and Caribbean Sea comprises 3001 lots, representing 214 species from 67 families (Table 1). Sciaenidae is the most represented with 17 species, followed by Carangidae and Haemulidae, with 15 and 11 species, respectively.

Table 1. List of species of the Otolith Collection of the Gulf of Mexico and the Caribbean Sea. Taxonomic classification according to Fricke et al. (2024) and Van der Laan (2024).

Family	Species	*N*	Size range [mm]	
			Total length	Standard length
Lepisosteidae	*Atractosteus tropicus* Gill, 1863	2	540–593	—
Elopidae	*Elops saurus* Linnaeus, 1766	38	87–613	
Megalopidae	*Megalops atlanticus* Valenciennes, 1847	2	—	385–426
Albulidae	*Albula vulpes* (Linnaeus, 1758)	6	351–292	—
Ophichthidae	*Ahlia egmontis* (Jordan, 1884)	1	365	—
Engraulidae	*Anchoa cayorum* (Fowler, 1906)	7	90	—
	Anchoa cubana (Poey, 1868)	2	—	55
	Anchoa lamprotaenia Hildebrand, 1943	34	89–130	—
	Cetengraulis edentulus (Cuvier, 1829)	9	—	94–140
Dorosomatidae	*Dorosoma petenense* (Günther, 1867)	6	—	104–140
	Harengula clupeola (Cuvier, 1829)	10	51.47–130	—
	Harengula jaguana Poey, 1865	15	110–160	—
	Opisthonema oglinum (Lesuer, 1818)	24	33–250	—
	Sardinella aurita Valenciennes, 1847	3	—	156–163
Cyprinidae	*Ctenopharyngodon idella* (Valenciennes, 1844)	1	261	—
Characidae	*Astyanax altior* Hubbs, 1936	23	55.7–79.1	—
Heptapteridae	*Rhamdia guatemalensis* (Günther, 1864)	4	91.5–1293	—
Ariidae	*Ariopsis felis* (Linnaeus, 1766)	108	56–402	—
	Bagre marinus (Mitchill, 1815)	106	267–540	—
Synodontidae	*Saurida brasiliensis* Norman, 1935	2	—	184–203
	Synodus foetens (Linnaeus, 1766)	22	52.4–376	—
Phycidae	*Urophycis floridana* (Bean et Dresel, 1884)	5	256–327	—
Holocentridae	*Holocentrus adscensionis* (Osbeck, 1765)	5	92–280	—
	Holocentrus rufus (Walbaum, 1792)	2	110–115	—
	Myripristis jacobus Cuvier,1829	2	166–180	—
Ophidiidae	*Brotula barbata* (Bloch et Schneider, 1801)	3	372–550.8	—
	Ophidion holbrookii Putnam, 1874	3	77–141	—
Batrachoididae	*Opsanus beta* (Goode et Bean, 1880)	6	—	98–205
	Opsanus dichrostomus Collette, 2001	2	105–130	—
	Sanopus reticulatus Collette, 1983	12	280–590	—
Pomatomidae	*Pomatomus saltatrix* (Linnaeus, 1766)	8	420–524	—
Scombridae	*Euthynnus alletteratus* (Rafinesque, 1810)	1	450	—
	Scomberomorus brasiliensis Collette, Russo et Zavala-Camin, 1978	5	—	290–360
	Scomberomorus cavalla (Cuvier, 1829)	4	695–750	—
	Scomberomorus maculatus (Mitchill, 1815)	4	480–590	—
Trichiuridae	*Trichiurus lepturus* Linnaeus, 1758	8	—	268–884
Dactylopteridae	*Dactylopterus volitans* (Linnaeus, 1758)	3	86–92	—
Mullidae	*Mulloidichthys martinicus* (Cuvier,1829)	2	250–268	—
	Pseudopeneus maculatus (Bloch, 1793)	1	223	—
	Upeneus parvus Poey, 1852	3	—	115–145
Callionymidae	*Chalinops pauciradiatus* (Gill, 1865)	6	27.2–36.9	—
Eleotridae	*Dormitator maculatus* (Bloch, 1792)	6	45–90	—
	Gobiomorus dormitor Lacepède, 1800	6	—	147–186
Gobiidae	*Awaous banana* (Valenciennes, 1837)	2	—	51–62
	Gobionellus oceanicus (Pallas, 1770)	5	—	93–159
	Gobiosoma robustum (Ginsburg, 1933)	6	28.2–36.3	—
Centropomidae	*Centropomus parallelus* Poey, 1860	3	—	158–181
	Centropomus undecimalis (Bloch, 1792)	25	370–473	—
Sphyraenidae	*Sphyraena barracuda* (Edwards, 1771)	22	247–1015	—
	Sphyraena guachancho Cuvier, 1829	9	—	148–583
Polynemidae	*Polydactylus octonemus* (Girard, 1858)	3	—	78–195
Cyclopsettidae	*Cyclopsetta chittendeni* Bean, 1895	117	218–315	—
	Cyclopsetta fimbriata (Goode et Bean, 1885)	51	77–390	—
	Syacium papillosum (Linnaeus, 1758)	34	231–275	—
Paralichthyidae	*Citharichthys macrops* Dressel, 1885	1	153	—
	Citharichthys spilopterus Günther, 1862	5	—	56–138
	Paralichthys albigutta Jordan et Gilbert, 1882	2	139–530	—
Achiridae	*Achirus lineatus* (Linnaeus, 1758)	10	60–93.3	—
	Trinectes maculatus (Bloch et Schneider, 1801)	1	94.4	—
Carangidae	*Alectis ciliaris* (Bloch, 1787)	1	302	—
	Caranx crysos (Mitchill, 1815)	27	271–405	—

Table continues on next page.

Table 1. Continued.

Family	Species	*N*	Size range [mm]	
			Total length	Standard length
Carangidae	*Caranx hippos* (Linnaeus, 1766)	17	233–370	—
	Caranx latus Agassiz, 1831	8	121–259	—
	Caranx ruber (Bloch, 1793)	4	246–305	—
	Chloroscombrus chrysurus (Linnaeus, 1766)	6	—	17–182
	Hemicaranx amblyrhynchus (Cuvier, 1833)	1	—	240
	Oligoplites saurus (Bloch et Schneider, 1801)	16	106–278	—
	Selar crumenophthalmus (Bloch, 1793)	6	—	185–207
	Selene setapinnis (Mitchill, 1815)	5	—	149–185
	Selene vomer (Linnaeus, 1758)	7	305–315	—
	Trachinotus carolinus (Linnaeus, 1766)	3	300–305	—
	Trachinotus falcatus (Linnaeus, 1758)	21	96–520	—
	Trachinotus goodei Jordan et Evermann, 1896	5	218–295	—
	Trachinotus meeki Brind, 1918	1	116.1	—
Echeneidae	*Echeneis neucratoides* Zuiew, 1786	10	320–523	—
Rachycentridae	*Rachycentron canadum* (Linnaeus, 1766)	3	219–690	—
Cichlidae	*Mayaheros urophthalmus* (Günther, 1862)	11	123.9–235	—
	Oreochromis niloticus (Linnaeus, 1758)	1	245	—
	Parachromis friedrichsthalii (Heckel, 1840)	3	103–113	—
	Parachromis motaguensis (Günter, 1867)	4	230–269	—
	Petenia splendida (Günther, 1862)	5	238–265	—
	Rocio octofasciata (Regan, 1903)	10	48–74.5	—
	Thorichthys meeki Brind, 1918	3	54.1–96.7	—
Pomacentridae	*Abudefduf saxatilis* (Linnaeus, 1758)	5	75.4–156	—
	Neopomacentrus cyanomos (Bleeker, 1856)	10	32.1–85.8	—
	Stegastes leucostictus (Müller et Troschel, 1848)	2	106.5–109.5	—
	Stegastes xanthurus (Poey, 1860)	2	94.6–97.7	—
Atherinopsidae	*Atherinomorus stipes* (Müller et Troschel, 1848)	21	38.4–56.63	—
	Menidia colei Hubbs, 1936	9	11.5–33	—
	Menidia sp.	12	19.6–24.38	—
Rivulidae	*Cynodonichthys tenuis* Meek, 1904	1	41	—
	Kryptolebias marmoratus (Poey, 1880)	1	30	—
Fundulidae	*Fundulus grandissimus* Hubbs, 1936	41	90.6–160	—
	Fundulus persimilis Miller, 1955	19	78.6–122.2	—
	Lucania parva (Baird et Girard, 1855)	9	24–35.3	—
Cyprinodontidae	*Cyprinodon artifrons* Hubbs, 1936	57	16.4–45	—
	Floridichthys polyommus Hubbs, 1936	43	62–120	—
	Jordanella pulchra (Hubbs, 1936)	14	28–35.4	—
Poeciliidae	*Belonesox belizanus* Kner, 1860	12	55.9–91.5	—
	Gambusia yucatana Regan, 1914	14	19.8–36.5	—
	Poecilia mexicana Steindachner, 1863	3	74.1–88.8	—
	Poecilia velifera (Regan, 1914)	18	38–79	—
	Pseudoxiphophorus bimaculatus (Heckel 1848)	2	55–59.8	—
Belonidae	*Strongylura marina* (Walbaum, 1792)	10	260–332	—
	Strongylura notata (Poey, 1860)	42	195–433	—
	Strongylura timucu (Walbaum, 1792)	9	230	—
	Tylosurus crocodilus (Perón et Lesueur, 1821)	11	65–1020	—
Hemiramphidae	*Chriodorus atherinoides* Goode et Bean, 1882	28	109–190	—
	Hemiramphus brasiliensis (Linnaeus, 1758)	6	300	—
	Hyporhamphus unifasciatus (Ranzani, 1841)	43	140–326	—
Mugilidae	*Mugil cephalus* Linnaeus, 1758	14	127–232	—
	Mugil curema Valenciennes,1836	17	120–434	—
	Mugil trichodon Poey,1875	8	39.7–183	—
Serranidae	*Diplectrum formosum* (Linnaeus, 1766)	26	125–248	—
	Hypoplectrus ecosur Victor, 2012	7	58.1–115	—
	Serranus subligarius (Cope, 1870)	7	64.2–92	—
Epinephelidae	*Cephalopholis cruentata* (Lacepède, 1802)	6	270–305	—
	Cephalopholis fulva (Linnaeus, 1758)	1	235	—
	Epinephelus adscensionis (Osbeck, 1765)	12	—	31–256
	Epinephelus morio (Valenciennes, 1828)	14	270–480	—
	Hyporthodus niveatus (Valenciennes, 1828)	3	350–367	—
	Mycteroperca bonaci (Poey, 1860)	3	345–625	—
Grammistidae	*Rypticus maculatus* Holbrook, 1855	3	140–142	—
Labridae	*Halichoeres radiatus* (Linnaeus, 1758)	1	—	264

Table continues on next page.

Table 1. Continued.

Family	Species	*N*	Size range [mm]	
			Total length	Standard length
Labridae	*Lachnolaimus maximus* (Walbaum, 1792)	23	140–325	—
	Nicholsina usta (Valenciennes, 1840)	4	95–165	—
	Scarus coeruleus (Edwards, 1771)	1	130	—
	Sparisoma rubripinne (Valenciennes, 1840)	2	385	—
Triglidae	*Prionotus punctatus* (Bloch, 1793)	2	280–	—
	Prionotus scitulus Jordan et Gilbert, 1882	2	214–215	—
	Prionotus tribulus Cuvier, 1829	4	175–300	—
Scorpaenidae	*Pterois volitans* (Linnaeus, 1758)	1	—	95.2
	Scorpaena brasiliensis Cuvier, 1829	5	155–215	—
	Scorpaena plumieri Bloch, 1789	14	105–240	—
Kyphosidae	*Kyphosus sectatrix* (Linnaeus, 1758)	4	140–427	—
Priacanthidae	*Priacanthus arenatus* Cuvier, 1829	3	310–325	—
	Pristigenys alta (Gill, 1862)	1	45	—
Malacanthidae	*Caulolatilus cyanops* Poey, 1866	1	—	290
Lutjanidae	*Lutjanus analis* (Cuvier, 1828)	2	398	—
	Lutjanus apodus (Walbaum,1792)	1	206	—
	Lutjanus buccanella (Cuvier, 1828)	2	—	180–191
	Lutjanus campechanus (Poey, 1860)	3	455–470	—
	Lutjanus cyanopterus (Cuvier,1828)	1	206	—
	Lutjanus griseus (Linnaeus, 1758)	20	69.2	—
	Lutjanus jocu (Bloch et Schneider, 1801)	1	348	—
	Lutjanus synagris (Linnaeus, 1758)	38	185–405	—
	Ocyurus chrysurus (Bloch, 1791)	24	68.9–321	—
	Rhomboplites aurorubens (Cuvier, 1829)	15	260–277	—
Gerreidae	*Diapterus auratus* Ranzani, 1842	6	—	134–173
	Diapterus rhombeus (Cuvier, 1829)	5	—	116–139
	Eucinostomus argenteus (Baird et Girard, 1855)	4	96.4–117.5	—
	Eucinostomus gula (Quoy et Gaimard, 1824)	42	66–113	—
	Eucinostomus harengulus Goode et Bean, 1879	5	—	61–95
	Eucinostomus melanopterus (Bleeker, 1863)	2	—	61–56
	Eugerres brasilianus (Cuvier, 1830)	7	180–280	—
	Eugerres plumieri (Cuvier, 1830)	45	96–317	—
	Gerres cinereus (Walbaum, 1792)	26	107.4–265	—
Haemulidae	*Anisotremus virginicus* (Linnaeus, 1758)	25	181–367	—
	Conodon nobilis (Linnaeus, 1758)	6	—	57–185
	Haemulon aurolineatum Cuvier, 1830	24	162–249	—
	Haemulon bonariense Cuvier, 1830	8	150–342	—
	Haemulon carbonarium Poey, 1860	6	—	147–265
	Haemulon flavolineatum (Desmarest, 1823)	6	—	155–185
	Haemulon parra (Desmarest, 1823)	3	—	215–259
	Haemulon plumierii (Lacepède, 1801)	102	160–315	—
	Haemulon sciurus (Shaw,1803)	4	186–253	—
	Orthopristis chrysoptera (Linnaeus, 1766)	26	127.1–244	—
	Rhonciscus crocro (Cuvier, 1830)	2	—	192–211
Sparidae	*Archosargus probatocephalus* (Walbaum, 1792)	24	176–610	—
	Archosargus rhomboidalis (Linnaeus, 1758)	67	85.1–280	—
	Calamus bajonado (Bloch et Schneider, 1801)	15	215–540	—
	Calamus calamus (Valenciennes, 1830)	11	191–300	—
	Calamus campechanus Randall et Caldwell, 1966	18	185–249	—
	Calamus nodosus Randall et Caldwell, 1966	6	229–310	—
	Calamus pennatula Guichenot, 1868	3	282	—
	Calamus proridens Jordan et Gilbert, 1884	5	210–275	—
	Lagodon rhomboides (Linnaeus, 1766)	31	44.5–207	—
	Stenotomus chrysops (Linnaeus, 1766)	1	—	210–521
Sciaenidae	*Bairdiella chrysoura* (Lacepède, 1802)	5	82.2–165	—
	Bairdiella ronchus (Cuvier, 1830)	19	139–270	—
	Corvula batabana (Poey, 1860)	2	156.6–160	—
	Cynoscion arenarius Ginsburg, 1930	92	160–423	—
	Cynoscion jamaicensis (Vaillant et Bocourt, 1883)	2	—	256–268
	Cynoscion nebulosus (Cuvier, 1830)	92	110–490	—
	Cynoscion nothus (Holbrook, 1848)	6	130–245	—
	Eques lanceolatus (Linnaeus, 1758)	32	80–335	—

Table continues on next page.

Table 1. Continued.

Family	Species	*N*	Size range [mm]	
			Total length	Standard length
Sciaenidae	*Menticirrhus americanus* (Linnaeus, 1758)	191	204–400	—
	Menticirrhus littoralis (Holbrook, 1847)	11	91–365	—
	Menticirrhus saxatilis (Bloch et Schneider, 1801)	3	—	226–236
	Micropogonias furnieri (Desmarest,1823)	59	74–412	—
	Micropogonias undulatus (Linnaeus, 1766)	39	86–425	—
	Pareques umbrosus (Jordan et Eigenmann, 1889)	7	55–210	—
	Pogonias cromis (Linnaeus, 1766)	1	84	—
	Stellifer lanceolatus (Holbrook, 1855)	6	—	75–96
	Umbrina coroides Cuvier, 1830	7	—	80–214
Lobotidae	*Lobotes surinamensis* (Bloch, 1790)	6	320–570	—
Pomacanthidae	*Holacanthus bermudensis* Goode, 1876	8	65–337	—
	Pomacanthus arcuatus (Linnaeus, 1758)	5	87–498	—
Chaetodontidae	*Chaetodon ocellatus* Bloch, 1787	34	40–124	—
Ephippidae	*Chaetodipterus faber* (Broussonet, 1782)	16	63.8–354	—
Acanthuridae	*Acanthurus chirurgus* (Bloch, 1787)	4	316	—
	Acanthurus coeruleus Bloch et Schneider, 1801	5	201–255	—
	Acanthurus tractus Poey, 1860	5	244–325	—
Ogcocephalidae	*Ogcocephalus cubifrons* (Richardson, 1836)	2	125–215	—
Diodontidae	*Chilomycterus schoepfii* (Walbaum, 1792)	13	96–285	—
	Diodon hystrix Linnaeus, 1758	1	490	—
Tetraodontidae	*Lagocephalus laevigatus* (Linnaeus, 1766)	5	330–554	—
	Sphoeroides nephelus (Goode et Bean, 1882)	6	124.6–280	—
	Sphoeroides spengleri (Bloch, 1785)	8	54–111.2	—
	Sphoeroides testudineus (Linnaeus, 1758)	7	157–235	—
Ostraciidae	*Acanthostracion quadricornis* (Linnaeus, 1758)	11	90–270	—
Monacanthidae	*Monacanthus ciliatus* (Mitchill, 1818)	4	81–136	—
	Stephanolepis hispida (Linnaeus, 1766)	2	160	—
Balistidae	*Balistes capriscus* Gmelin, 1789	10	240–495	—

N = number of specimens.

The species with the highest number of specimens in the collection are *Menticirrhus americanus* (Linnaeus, 1758) with 191 lots, *Ariopsis felis* (Linnaeus, 1766) with 108 lots, *Bagre marinus* (Mitchill, 1815) with 106 lots, and *Haemulon plumierii* (Lacepède, 1801) with 102 lots. Each lot typically contains all three pairs of otoliths: sagitta, asteriscus, and lapillus.

The collection includes otoliths from specimens collected along the coasts of the states of Tamaulipas, Veracruz, Campeche, and Yucatan, which is the best-represented state with 1700 lots, followed by Campeche with 894 lots and Veracruz with 368 lots. Additionally, the collection contains 23 lots of otoliths from Cuba.

Figures 1, 2 illustrate the sagittal otoliths of the majority of the families included in the collection. These images on the collection's web page are accompanied by morphological descriptions and morphometric characteristics such as length, height, perimeter, and area of both the sagitta and the acoustic sulcus. These variables allow for the calculation of shape indices, including circularity, rectangularity, aspect ratio, and the proportion of the area occupied by the acoustic sulcus. The diversity of the shape of the saccular otoliths is notable, ranging from simple ellipsoids to complex patterns with species-specific projections and invaginations. The dorsal and ventral margins can be smooth, scalloped, lobed, serrated, or serrate. The anterior and posterior regions exhibit significant variability, being pointed, angulated, rounded, truncate, oblique, lanceolate, bilobed, double-pointed, or irregular. Many species have an indentation in the anterior region, the ostial fissure, which delineates the rostral and antirostral regions. The characteristics of the fissure, whether deep or shallow, angulated or rounded, affect the shape and size of these sections. The acoustic sulcus, a longitudinal depression along the medial face of the sagitta, consists of the ostium anteriorly and the cauda posteriorly. In some instances, thickening of the edges, known as cristae, and dorsal or ventral depressions are present along the acoustic sulcus.

The Website. The online catalog of the Fish Otolith Collection of the Gulf of Mexico and Caribbean Sea (https://otolitos.unam.mx) aims to organize and present the information in a user-friendly yet comprehensive manner, available to academics, students, and anyone interested in fish biology and ecology.

The website features a detailed database with information on each otolith, including species, location, size, and weight of the specimen, collector, and morphological parameters of the otolith. It also includes a gallery of images or scientific illustrations of the species and photographs of the otoliths obtained through optical and electron microscopy. Detailed morphological descriptions of the left sagitta of each species are accessible.

Before publication on the website, the quality of the digital data is verified to ensure high-value information that can positively impact research and education.

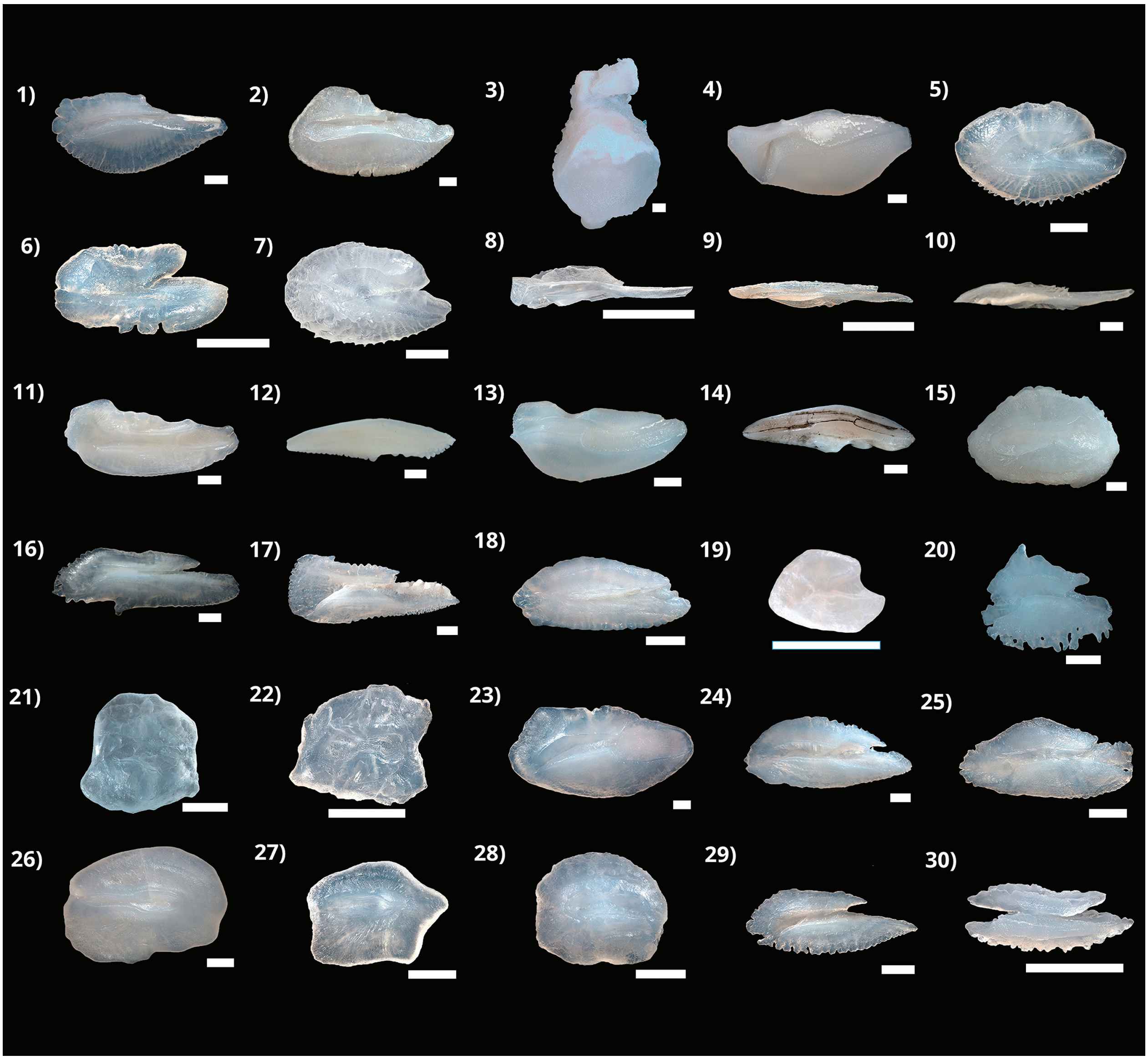

Figure 1. Diversity of sagittae otoliths from the Collection of Otoliths of Fishes from the Gulf of Mexico and the Caribbean Sea; **Part 1**: 1) *Elops saurus*, 2) *Megalops atlanticus* 3) *Atractosteus tropicus*, 4) *Albula vulpes*, 5) *Anchoa cayorum*, 6) *Dorosoma petenense*, 7) *Cetengraulis edentulus*, 8) *Astyanax altior*, 9) *Rhamdia guatemalensis*, 10) *Bagre marinus*, 11) *Saurida brasiliensis*, 12) *Urophycis floridana*, 13) *Holocentrus adscensionis*, 14), *Brotula barbata*, 15) *Sanopus reticulatus*, 16) *Pomatomus saltatrix*, 17) *Scomberomorus maculatus*, 22) *Awaous banana*, 23) *Centropomus parallelus*, 24) *Sphyraena barracuda*, 25) *Polydactylus octonemus*, 26) *Cyclopsetta chittendeni*, 27) *Citharichthys spilopterus*, 28) *Achirus lineatus*, 29) *Hemicaranx amblyrhynchus*, 30) *Echeneis neucratoides*. Scale bar = 1 mm.

To facilitate consultation, the webpage offers search functions by taxon (family, genus, or species) and keywords related to otolith characteristics. Additionally, didactic resources such as videos on otolith extraction and description techniques, and the use of relevant equipment for their study are available. The otolith collection webpage can be accessed at https://otolitos.unam.mx.

Publications and analytical tools. Derived from the curatorial work of the collection and the information on each specimen, a catalog with descriptive cards of the sagittal otoliths of 155 fish species from the Gulf of Mexico was published (Martínez Pérez et al. 2018). This catalog includes standardized descriptions of the shape, as well as some morphometric data of the structure, acoustic sulcus, and shape indices. Currently, a second edition of the catalog is being prepared, which will include information on species added in recent years.

Additionally, a software, Invariant Otolith Shape Analysis (IOSA), which can be downloaded here, https://sites.google.com/view/jorge-perez/community#h.hh1lv19s6hlj, has been developed to automatically obtain morphometric descriptors and shape invariants of otoliths from their images, based on the methodology proposed by Hevia-Montiel et al. (2021).

Recently, the collection has been used to corroborate the presence of fish remains in the Mayan archaeological record. This information will deepen our understanding of pre-Hispanic fishing practices and infer possible changes in some fish populations in the region.

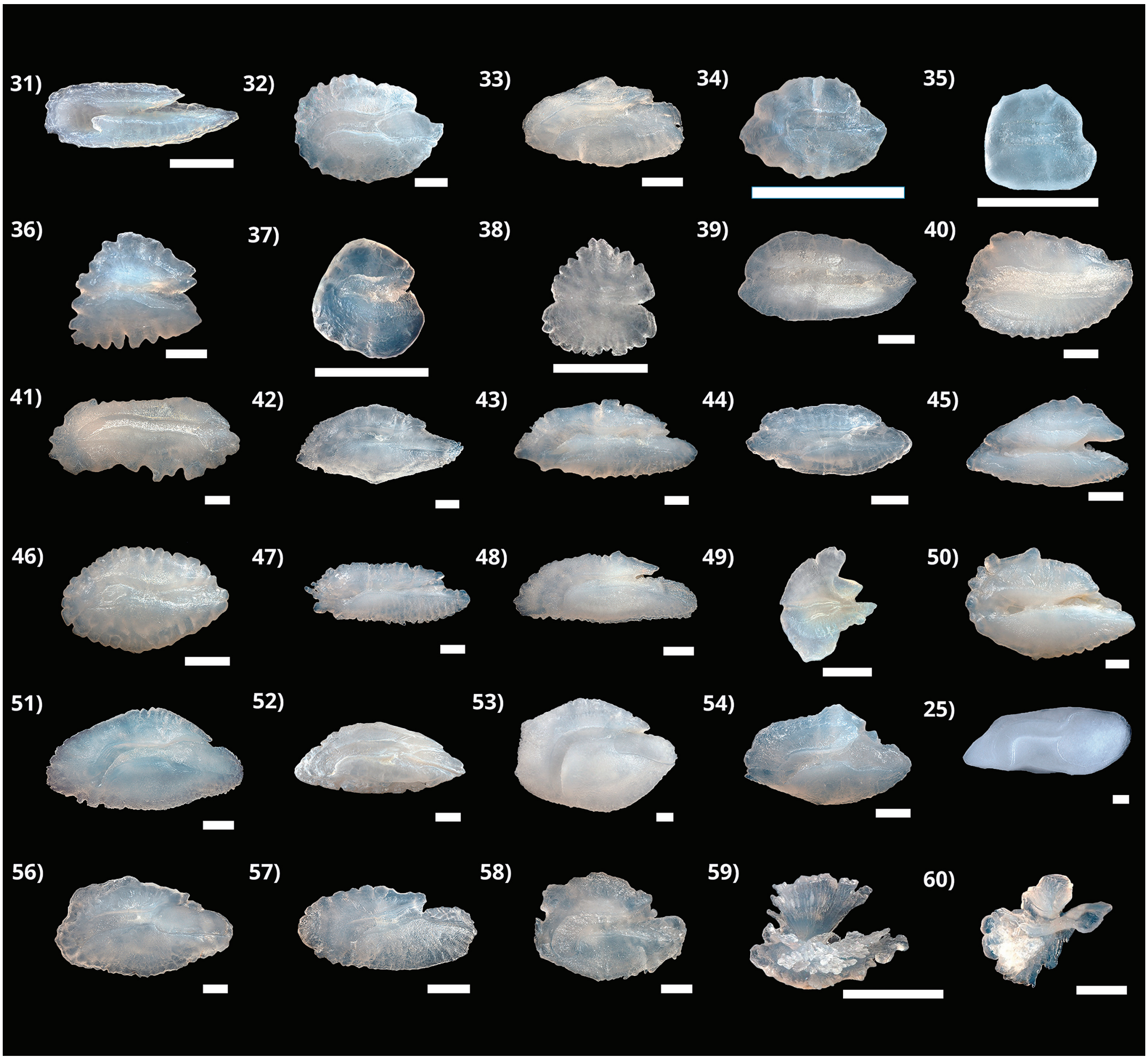

Figure 2. Diversity of sagittae otoliths from the Collection of Otoliths of Fishes from the Gulf of Mexico and the Caribbean Sea; **Part 2**: 31) *Rachycentron canadum*, 32) *Mayaheros urophthalmus*, 33) *Abudefduf saxatilis*, 34) *Menidia colei*, 35) *Cynodonichthys tenuis*, 36) *Fundulus grandissimus*, 37) *Cyprinodon artifrons*, 38) *Belonesox belizanus*, 39) *Strongylura timucu*, 40) *Hemiramphus brasiliensis*, 41) *Mugil cephalus*, 42) *Diplectrum formosum*, 43) *Epinephelus adscensionis*, 44) *Rypticus maculatus*, 45), *Lachnolaimus maximus*, 46) *Prionotus punctatus*, 47) *Scorpaena plumieri*, 48) *Kyphosus sectatrix*, 49) *Priacanthus arenatus*, 50) *Caulolatilus cyanops*, 51) *Lutjanus griseus*, 52) *Gerres cinereus*, 53) *Haemulon plumierii*, 54) *Lagodon rhomboides*, 55) *Cynoscion nebulosus*, 56) *Pomacanthus arcuatus*, 57) *Chaetodon ocellatus*, 58) *Achirus lineatus*, *Acanthurus coeruleus*, 59) *Sphoeroides testudineus*, 60) *Balistes capriscus*. Scale bar = 1 mm.

Discussion

The Otolith Collection of the Gulf of Mexico and the Caribbean Sea is a sample of the richness and ichthyological diversity of the region. It has a collection of 214 species belonging to 67 families, which represent a significant percentage (just over 11%) of the total number of species recorded for the Gulf of Mexico and the Caribbean Sea (Robertson and Van Tassel 2023). The families and species better represented in the collection reflect the specific composition of the local ichthyofauna, its ecological importance, and its relevance to the regional economy. This extensive taxonomic representation provides an invaluable database for biodiversity, taxonomy, and systematic studies of fishes in the region.

The otoliths in this collection come from specimens obtained in various geographic regions, enabling the study of species distribution and population variability in different localities of the Gulf of Mexico and the Caribbean. With 3001 lots in total, the collection provides a robust data set for statistical analyses, intraspecific variability studies, and temporal trend evaluations.

Otoliths are invaluable in paleontological, archaeological, and biological explorations, such as analyzing the stomach contents of piscivorous species. Reference collections have been established to assist in species identification from remains found in archaeological contexts, as documented by Disspain et al. (2016) and Lambrides et al. (2024). The catalogs by Mascareñas Osorio et al. (2003) and Martínez Pérez et al. (2018), along with the website www.otolitos.unam.mx, support research efforts in Mexico.

The digitization of biological collections, including the Otolith Collection of the Gulf of Mexico and the Caribbean Sea, is crucial for making scientific information universally accessible. Digitization transforms specimen information into digital formats, allowing for easy access and analysis by anyone with an internet connection. This approach modernizes the use of biological collections, eliminating the need for physical travel or loan requests, which risk loss or damage to the specimens.

Digitization also fosters new research topics and addresses global challenges related to climate change, food security, and conservation (Soltis 2017). The online presence of the Otolith Collection makes it the first digital otolith collection in Mexico, facilitating international collaboration and knowledge dissemination. This effort aligns with global initiatives like the "Integrated Digitized Biocollections" (iDigBio), the "European Distributed System of Scientific Collections" (DiSSCo), and the "Innovation and Consolidation for Large Scale Digitization of Natural Heritage" (ICEDIG). These programs promote the networking of collections worldwide, contributing to the "global museum" concept (Bakker et al. 2020).

Despite the benefits of digitization, physical specimens remain the primary source of verifiable data. Digital information complements but does not replace physical specimens. Increased online accessibility often leads to more visits to collections and loan requests for physical specimens (Vollmar et al. 2010). Therefore, preserving physical specimens in optimal conditions is a primary task for the curatorial staff of the Otolith Collection.

Additionally, the webpage offers accessible image processing software that employs invariant descriptors, as detailed by Hevia-Montiel et al. (2021). These descriptors are independent of rotation, scale, or translation, thereby ensuring consistent results. This software provides additional information beyond traditional descriptors, such as otolith area or perimeter (Hevia-Montiel et al. 2021), which is particularly beneficial in taxonomic studies that rely on limited structures for species identification. By offering a user-friendly interface that allows the application of image processing through a webpage, the tool significantly broadens its user base. Enhancing collaboration is crucial, especially in studies involving these structures, where there is an increasing demand for web-based tools that enable researchers to browse and search images and data in conjunction with biological analyses.

The contributions of biological collections to knowledge, education, and innovation are immense but often unrecognized (Anonymous 2020; Kellner 2024). Many scientific communities have highlighted the risks of inadequate funding for maintaining the infrastructure necessary for the proper functioning of these collections (Finkel 2024; Kellner 2024). Thus, the online presence of the Otolith Collection is a vital step toward creating a national platform that supports the analysis of bony fish otoliths in various contexts, including paleontological, archaeological, biological, and ecological studies (Begg et al. 2005; Disspain et al. 2016).

Conclusion

Otoliths serve multiple research purposes, including paleontological, archaeological, and biological explorations, and support species identification in archaeological contexts. The Otolith Collection of the Gulf of Mexico and Caribbean Sea represents the ichthyological diversity of the region, encompassing 214 species of 67 families, reflecting over 11% of the total species richness in the region. The collection's species composition mirrors the local ichthyofauna's ecological importance and its significance to the regional economy, making it a crucial resource for biodiversity studies.

With specimens collected from various regions, the collection provides valuable data for studying species distribution, population variability, and temporal trends in the Gulf of Mexico and the Caribbean. Furthermore, digitizing the Otolith Collection enhances global accessibility, facilitates international collaboration, and supports research on critical global challenges, such as climate change and conservation. The collection's website offers innovative image-processing software that improves species identification and taxonomic studies, making these tools widely accessible to researchers. It is important to note that while digitization expands access to the collection, physical specimens remain the primary source of verifiable data, highlighting the need for their preservation. Therefore, we emphasize the importance of adequate funding for maintaining this and other biological collections, as they contribute significantly to knowledge, education, and innovation.

Acknowledgments

Authors wish to express their gratitude to the many students (especially Kylie López Castillejos, Atl Gerardo Palacios Díaz, Diego Muñoz Pérez, José Emilio García Pérez, Jonathan de la Cruz), fishermen (especially Fernando Mex and Enrique Mex), and colleagues (especially Daniel Arceo Carranza, Claudia Durruty Lagunes, Manuel Valenzuela Jiménez) who participated in the collection of scientific material, laboratory work, analysis, and curatorship of the Otolith Collection from the Gulf of Mexico and Caribbean Sea. We appreciate the generous donation of the Mexican Atlantic Fish Otolith Collection by José Antonio Martínez Pérez from the Facultad de Estudios Superiores Iztacala, Universidad Nacional Autónoma de México. This project was funded by PAPIIT-DGAPA-UNAM (IG201121).

References

Anonymous (2020) Biological Collections: Ensuring Critical Research and Education for the 21st Century. National Academies Press, Washington, DC, USA, 229 pp. https://doi.org/10.17226/25592

Baker R, Buckland A, Sheaves M (2014) Fish gut content analysis: Robust measures of diet composition. Fish and Fisheries 15(1): 170–177. https://doi.org/10.1111/faf.12026

Baker R, Crawford HM, Sheaves M (2024) Stomach contents analysis. Pp. 31–50. In: Calver MC, Loneragan NR (Eds.) Quantifying diets of wildlife and fish. Practical and applied methods. CSIRO Publishing, Australia. https://doi.org/10.1071/9781486315017

Bakker FT, Antonelli A, Clarke JA, Cook JA, Edwards SV, Ericson PGP, Faurby S, Ferrand N, Gelang M, Gillespie RG, Irestedt M, Lundin K, Larsson E, Matos-Maraví P, Müller J, von Proschwitz T, Roderick GK, Schliep A, Wahlberg N, Wiedenhoeft J, Källersjö M (2020) The global museum: Natural history collections and the future of evolutionary science and public education. PeerJ 8: e8225. https://doi.org/10.7717/peerj.8225

Begg GA, Campana SE, Bowler AJ, Suthers IM (2005) Otolith research and application: Current directions in innovation and implementation. Marine and Freshwater Research 56(5): 477–483. https://doi.org/10.1071/MF05111

Campana SE, Thorrold SR (2001) Otoliths, increments, and elements: Keys to a comprehensive understanding of fish populations? Canadian Journal of Fisheries and Aquatic Sciences 58(1): 30–38. https://doi.org/10.1139/f00-177

De la Cruz Torres J, Martínez Pérez JA, Badillo Alemán M, Del Moral Flores LF, Franco López J, Chiappa-Carrara X (2016) Familias de peces óseos del golfo de México: Clave ilustrada y descripción. Universidad Nacional Autónoma de México; SIIES, Mérida, Mexico, 187 pp.

Del Moral-Flores LF, Martínez-Pérez JA, Ramírez-Villalobos AJ, De la Cruz-Torres J, Farías-Tafolla B (2016) Colección de Peces del Laboratorio de Zoología de la FES Iztacala, UNAM. Pp. 370–377. In: Del Moral-Flores LF, Ramírez-Villalobos AJ, Martínez-Pérez JA, González-Acosta AF, Franco-López J (Eds.) Colecciones ictiológicas de Latinoamérica, Facultad de Estudios Superiores Iztacala, UNAM/Sociedad Ictiológica Mexicana AC, México.

Disspain MC, Ulm S, Gillanders BM (2016) Otoliths in archaeology: Methods, applications and future prospects. Journal of Archaeological Science, Reports 6: 623–632. https://doi.org/10.1016/j.jasrep.2015.05.012

Espinosa-Pérez H (2014) Biodiversidad de peces en México. Revista Mexicana de Biodiversidad 85: 450–459. https://doi.org/10.7550/rmb.32264

Finkel E (2024) Australian museum's plan to cut research draws fire from scientists. Science. https://doi.org/10.1126/science.z5zinzd

Francis RICC, Campana SE (2004) Inferring age from otolith measurements: A review and a new approach. Canadian Journal of Fisheries and Aquatic Sciences 61(7): 1269–1284. https://doi.org/10.1139/f04-063

Fricke R, Eschmeyer WN, van der Laan R (Eds.) 2024. Eschmeyer's catalog of fishes: Genera, species, references. California Academy of Sciences, San Francisco, CA, USA. [Accessed on 15 July 2024] http://researcharchive.calacademy.org/research/ichthyology/catalog/fishcatmain.asp

Gauldie RW, Nelson DGA (1988) Aragonite twinning and neuroprotein secretion are the cause of daily growth rings in fish otoliths. Comparative Biochemistry and Physiology. A. Comparative Physiology 90(3): 501–509. https://doi.org/10.1016/0300-9629(88)90227-7

Hecht T (1990) Otoliths: An introduction to their morphology and use in the identification of Southern Ocean fishes. Pp. 64–69. In: Gon O, Heemstra PC (Eds.) Fishes of the Southern Ocean, JLB Smith Institute of Ichthyology, Grahamstown, South Africa.

Hevia-Montiel N, Pérez-González J, Gallardo-Torres A, Badillo-Alemán M, Chiappa-Carrara X (2021) Invariant morphological descriptors from otolith shape in environment automatic classification. Journal of Applied Ichthyology 37(4): 534–544. https://doi.org/10.1111/jai.14207

Izzo C, Reis-Santos P, Gillanders BM (2018) Otolith chemistry does not just reflect environmental conditions: A meta-analytic evaluation. Fish and Fisheries 19(3): 441–454. https://doi.org/10.1111/faf.12264

Kellner AWA (2024) Biological collections in danger? Anais da Academia Brasileira de Ciências 96(1): e2024961. https://doi.org/10.1590/0001-376520242024961

Lambrides ABJ, Ristevski J, Mein E, van Zoelen JD, McNiven IJ, Leavesley M, David B, Ulm S, Weisbecker V (2024) Fishboneviz: Enhancing the availability of zooarchaeological fish reference collections through an open access 3D database. Australian Archaeology 90(2): 1–13. https://doi.org/10.1080/03122417.2024.2350098

Lin C-H, Wang Y-C, Ribas-Delulofeu L, Chang C-W, Li K-T (2022) Changes in marine resource consumption over the past 5000 years in southwestern Taiwan revealed by fish otoliths. Journal of Archaeological Science, Reports 42: 103400. https://doi.org/10.1016/j.jasrep.2022.103400

Maisey JG (1987) Notes on the structure and phylogeny of vertebrate otoliths. Copeia 1987(2): 495–499. https://doi.org/10.2307/1445791

Martínez Pérez JA, Del Moral Flores LF, Volpedo AV, Tello Musi JL, Chávez Arteaga M (2011) Creación de la colección de otolitos sagita de la Facultad de Estudios Superiores Iztacala. Revista de Zoología 22: 63–66.

Martínez Pérez JA, Morquecho León MRK, Farías Tafolla B, Badillo Alemán M, Gallardo-Torres A, Chiappa-Carrara X (2018) Catálogo de otolitos sagitta de peces del golfo de México. Universidad Nacional Autónoma de México, Mexico, 199 pp.

Mascareñas Osorio I, Aburto Oropeza MO, Balart Pérez EF (2003) Otolitos de peces de arrecife del Golfo de California. Universidad Autónoma de Baja California Sur/Centro de Investigaciones Biológicas del Noroeste SC, Mexico, 120 pp.

Maslenikov KP (2021) Specimens by the millions: Managing large, specialized collections at the University of Washington Burke Museum Fish Collection. Ichthyology and Herpetology 109(2): 397–406. https://doi.org/10.1643/t2019314

Meineke EK, Davies TJ, Daru BH, Davis CC (2018) Biological collections for understanding biodiversity in the Anthropocene. Philosophical Transactions of the Royal Society B: Biological Sciences 374(1763): 20170386. https://doi.org/10.1098/rstb.2017.0386

Monfils AK, Powers KE, Marshall CJ, Martine CT, Smith JF, Prather LA (2017) Natural history collections: Teaching about biodiversity across time, space, and digital platforms. Southeastern Naturalist 16(sp10): 47–57. https://doi.org/10.1656/058.016.0sp1008

Nolf D (1985) *Otolithi piscium*. Volume 10 of book series: Schultze H (Ed.) Handbook of palaeoichthyology, Gustav Fisher Verlag, New York, NY, USA, 145 pp.

Oré-Villalba DO (2017) Catálogo fotográfico de otolitos de peces marinos y dulceacuícolas del Perú. Boletín – Instituto del Mar del Perú 32(2): 136–213.

Platt C, Popper AN (1981) Fine structure and function of the ear. Pp. 3–38. [Page range of this article, please.] In: Tavolga WN, Popper AN, Fay RR (Eds.) Hearing and sound communication in fishes. Proceedings in Life Sciences. Springer, New York, NY, USA. https://doi.org/10.1007/978-1-4615-7186-5_1

Rivaton J, Bourret P (1999) Les otolithes des poisons de l'Indo-Pacifique. Documents Scientifiques et Techniques II 2. Institut de recherche pour le développement, Nouvelle-Caledonie, France, 378 pp.

Robertson DR, Van Tassell J (2023) Shorefishes of the Greater Caribbean: Online information system. Version 3.0 Smithsonian Tropical Research Institute, Balboa, Panamá. https://biogeodb.stri.si.edu/caribbean/en/pages

Rojo AL (2015) Report in the fish otolith collection at the Nova Scotia Museum. Curatorial Report Number 105, Nova Scotia Museum, Halifax, NS, Canada, 176 pp. https://ojs.library.dal.ca/NSM/article/view/6440/5676 [Electronic version accessed 21/07/2024]

Soltis PS (2017) Digitization of herbaria enables novel research. American Journal of Botany 104(9): 1281–1284. https://doi.org/10.3732/ajb.1700281

Suarez AV, Tsutsui ND (2004) The value of museum collections for research and society. Bioscience 54(1): 66–74. https://doi.org/10.1641/0006-3568(2004)054[0066:TVOMCF]2.0.CO;2

Tuset VM, Lombarte A, Assis CA (2008) Otolith atlas for the western Mediterranean, north and central eastern Atlantic. Scientia Marina 72(S1): 7–198. https://doi.org/10.3989/scimar.2008.72s1199

Van der Laan R, Fricke R, Eschmeyer WN (Eds.) (2024) Eschmeyer's catalog of fishes: Classification. California Academy of Sciences, San Francisco, CA, USA. [Accessed on 21 July 2024] http://www.calacademy.org/scientists/catalog-of-fishes-classification

Vollmar A, Macklin JA, Ford L (2010) Natural history specimen digitization: Challenges and concerns. Biodiversity Informatics 7(2): 93–112. https://doi.org/10.17161/bi.v7i2.3992

Volpedo AV, Echeverría D (2003) Ecomorphological patterns of the sagitta in fish on the continental shelf off Argentine. Fisheries Research 60(2–3): 551–560. https://doi.org/10.1016/S0165-7836(02)00170-4

Volpedo AV, Thompson GA, Avigliano E (2017) Atlas de otolitos de peces de Argentina. CAFP-BACAPES, Buenos Aires, 321 pp.

Acta Ichthyologica et Piscatoria 54, 2024, 261–268 | DOI 10.3897/aiep.54.135448

PENSOFT.
ACTA ICHTHYOLOGICA ET PISCATORIA

First records of two triplefins, *Enneapterygius rhothion* and *Enneapterygius olivaceus* (Actinopterygii: Blenniiformes: Tripterygiidae), from Australia and Vanuatu

Yuna DEWA[1], Hiroyuki MOTOMURA[2]

1 *United Graduate School of Agricultural Sciences, Kagoshima University, Kagoshima, Japan*
2 *Kagoshima University Museum, Kagoshima, Japan*

https://zoobank.org/1F507CB1-0C06-4381-9CBF-CB0A9FFC8263

Corresponding author: Yuna Dewa (k2533560@kadai.jp)

Academic editor: Ronald Fricke ♦ **Received** 24 August 2024 ♦ **Accepted** 7 October 2024 ♦ **Published** 31 October 2024

Citation: Dewa Y, Motomura H (2024) First records of two triplefins, *Enneapterygius rhothion* and *Enneapterygius olivaceus* (Actinopterygii: Blenniiformes: Tripterygiidae), from Australia and Vanuatu. Acta Ichthyologica et Piscatoria 54: 261–268. https://doi.org/10.3897/aiep.54.135448

Abstract

Presently reported single specimen of *Enneapterygius rhothion* Fricke, 1997, previously considered endemic to waters off New Caledonia and Vanuatu, represents the first record from Australia and the northernmost record of the species. In addition, *Enneapterygius olivaceus* Dewa, Tashiro, et Motomura, 2023, originally described from Japan and the Philippines, is also newly recorded from Australia and Vanuatu, being the first record of the species from the Southern Hemisphere.

Keywords

distribution, *Enneapterygius minutus*, morphology, South Pacific

Introduction

Fish species representing the tripterygiid genus *Enneapterygius* Rüppell, 1835 inhabit intertidal rock pools and subtidal rocky or coral reefs in tropical to temperate Indo–Pacific waters. They are characterized by a discontinuous lateral line, the first dorsal fin with three spines, anal fin with one spine, pelvic fin with one spine and two soft rays, and head, opercle, pectoral-fin base, and abdomen (in the majority of species) scaleless (Fricke 1997; Holleman 2005; Motomura et al. 2005, 2015; Chiang and Chen 2008).

To date, 19 species of *Enneapterygius* have been recorded from Australia (Fricke 1994, 1997; Hoese 2006; Tashiro and Motomura 2018; Dewa et al. 2023). *Enneapterygius rhothion* Fricke, 1997, previously known only from New Caledonia and Vanuatu (Fricke 1997, 2002), is newly recorded from Green Island, Queensland, Australia. In addition, 18 specimens of *Enneapterygius olivaceus* Dewa, Tashiro, et Motomura, 2023, were collected from Lizard Island, Queensland, and represent the first record of that species from Australia. Together with two specimens previously identified as *Enneapterygius minutus* (Günther, 1877) from Vanuatu, but here identified as *E. olivaceus*, they also constitute the first records of the species from the southwest Pacific Ocean. Detailed descriptions of the Australian specimens of both *E. rhothion* and *E. olivaceus* are provided herein.

Material and methods

Counts and measurements followed Fricke (1997) and Dewa et al. (2023), with the mandibular-pore formula following Hansen (1986). The pectoral-fin ray formula, beginning with the dorsalmost ray (left side), are designated unbranched + branched + unbranched rays = total pectoral-fin rays. Small dorsal and ventral scales on the body were counted as ½ scales. Measurements were made to the nearest 0.1 mm with needle-point calipers under a dissecting microscope. Standard length, pored lateral-line scales, and notched lateral-line scales are abbreviated as SL, PLL, and NLL, respectively. Institutional codes follow Sabaj (2020).

Type specimens examined. *Enneapterygius rhothion*: SMNS 18322, holotype, male, 28.9 mm SL, Touaourou, Grand Terre, New Caledonia, 22°10′36″S, 166°57′51″E, 0.6 m depth, 26 July 1996, R. Fricke leg.; SMNS 18698, paratype, male, 23.4 mm SL, Dillons Bay, Erromango Island, Vanuatu, 0–1 m depth, 25–26 May 1996, J.T. Williams leg.; SMNS 18773, paratypes, 7 males, 23.4–27.8 mm SL, Seche Croissant Reef, Grand Terre, New Caledonia, 22°02′00″S, 166°02′12″E, 2 m, 1 Aug. 1996, M. Kulbicki leg.

Results

Family Tripterygiidae
Enneapterygius Rüppell, 1835

Enneapterygius rhothion Fricke, 1997

English name: New Caledonian blackhead surf triplefin
Figs. 1, 2, 3; Table 1

Material examined. AMS I. 5088, male, 32.5 mm SL, Green Island, Queensland, Australia, 17°13′48″S, 145°58′11″E, 1901, C. Hedley leg.

Description. Counts and measurements given in Table 1. Body moderately elongate, slightly compressed anteriorly, progressively more compressed posteriorly (Fig. 1A). Dorsal profile of snout straight, steep. Mouth slightly oblique; posterior margin of maxilla extending beyond anterior margin of pupil; anterior tip of upper jaw slightly above level of lower margin of orbit (lateral view). Medial supratemporal canal with two branches (Fig. 2A). Anterior nostril a membranous tube, at mid-eye level, slightly closer to eye than to upper lip; nasal tentacle slender, unbranched, with pointed tip; posterior nostril opening circular, without membranous tube (Fig. 2A). Eye oriented dorsolaterally, with small, pointed tentacle, slightly longer than nasal tentacle, on posterodorsal margin. Interorbital space narrow, its width less than pupil diameter. Opercular margin slightly pointed, reaching below base of 3rd spine of first dorsal fin.

Lateral line discontinuous, with anterior series of pored scales ending below base of 11th spine of 2nd dorsal fin; second scale of posterior series of notched scales below third scale from last pored scale, ending at caudal-fin base; body scales ctenoid; scales absent on head (including maxilla, interorbital space, preopercle, and opercle), pectoral-fin base, pre- and inter-pelvic-fin region, abdomen, pre-dorsal-fin region, and all fin membranes, except basal part of caudal fin.

First dorsal fin triangular, origin over and slightly forward of midpoint between pre-opercular and opercular margins; 1st spine of first dorsal fin damaged, 2nd spine longer than 3rd spine. Origin of second dorsal fin just above 4th pored lateral-line scale, 3rd spine longest, spines thereafter becoming gradually shorter posteriorly, forming rounded margin. Third dorsal fin damaged, its origin just above 20th scale row of longitudinal series. Anal-fin membranous margin deeply incised between rays; anal fin origin just below 7th spine base of second dorsal fin, its posteriormost tip close to caudal-fin base. Pectoral fin damaged (posterior tip lost); upper and lowermost pectoral-fin base level with bases of 3rd and 2nd spines, respectively, of first dorsal fin. Pelvic fin origin

Figure 1. Photographs of preserved specimen of *Enneapterygius rhothion* (**A**: AMS I. 5088, male, 32.5 mm SL, Australia; **B**: SMNS 18322, holotype, male, 28.9 mm SL, New Caledonia, Photo by M. Meguro).

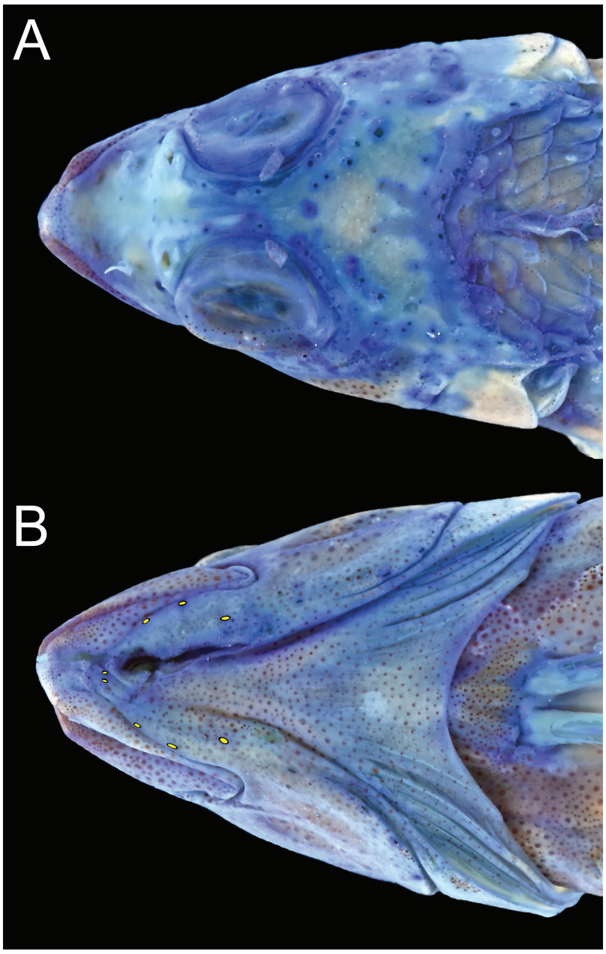

Figure 2. Photographs of **A**: dorsal and **B**: ventral views of head of *Enneapterygius rhothion* (AMS I. 5088, male, 32.5 mm SL, Australia), showing cephalic sensory system.

vertically below base of 1st spine of first dorsal fin. Caudal fin rounded, its length less than head length.

Nuptial male coloration (in preservative). Based on Fig. 1A. Body generally yellowish white; brownish pigmentation forming faint A- and X-shaped bars on lateral surface of body. Head, including snout, lips, cheek, and opercle, and pectoral-fin base brown with numerous melanophores. Pre-pelvic region brown (extending to just behind pelvic-fin base). Orbital tentacle pale brown. First and second dorsal fins dark brown. Third dorsal fin damaged, but brownish basally. Pectoral, pelvic, anal and caudal fins whitish.

Distribution. Currently known from New Caledonia (Chesterfield Islands, Grande Terre, Ile des Pins, and Loyalty Islands), Vanuatu (Erromango Island), and Australia (Fricke 1997, 2002; this study) (Fig. 3).

Remarks. The morphometric and meristic characters of the single specimen collected from Australia (AMS I. 5088, male, 32.5 mm SL) agreed closely with the type series of *E. rhothion* re-examined in this study (Table 1), and much of the original description of the species provided by Fricke (1997). However, although Fricke (1997) described the species as having a short orbital tentacle of length 0.6%–0.9% of SL, both the presently reported specimen and holotype of *E. rhothion* had relatively long orbital tentacles (1.6%–2.1% of SL). In addition, the mandibular pore formula of the species should be revised, the examined specimens having 3–4 + 2 + 3–4 (total 8–10 pores) [vs. 4–5 + 2 + 4–5 (total 10–12) in the original description]. Individual mandibular pore counts were as follows: 4 + 2 + 4 (holotype and 3 paratypes); 3 + 2 + 3 (4 paratypes and non-type Australian specimen); 4 + 1 + 4 (single paratype). The coloration of the presently reported specimen was consistent with that of *E. rhothion* shown in Fricke (1997): head, including snout, lips, cheek, and opercle, and pectoral-fin base black; lateral surface of body with faint bars; first and second dorsal fins black; anal fin pale (without markings). Although the color pattern of the caudal fin (dorsally and ventrally with faint vertical dark streaks; Fricke 1997) is one of the diagnostic characters for the species, such pigmentation was lost in the presently reported specimen after long-term preservation (Fig. 1A).

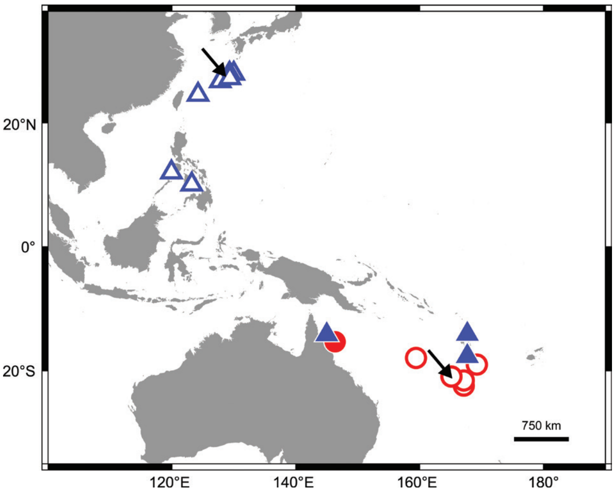

Figure 3. Distributional map of *Enneapterygius rhothion* (*red circles*) and *E. olivaceus* (*blue triangles*). Closed and open symbols indicate localities determined during the presently reported study and previous records, respectively. *Black arrows* indicate type localities of the two species.

Enneapterygius rhothion was originally described based on 129 specimens from New Caledonia and Vanuatu. Subsequently, Fricke (2002) reported the species from Ile des Pins as an additional record of the species from New Caledonia. In addition, Randall (2005) showed a fresh photograph of a female individual of *E. rhothion* in his field guide. The species is one of the common triplefins in New Caledonian waters (Fricke 1997, 2002). In his taxonomic works on triplefins, Fricke (2001, 2002) provided identification keys to the tripterygiid species in New Caledonian waters. Following those keys, the presently reported Australian specimen (AMS I. 5088, male, 32.5 mm SL) was identified as *Enneapterygius rufopileus* (Waite, 1904). However, the keys described the number of symphyseal mandibular pores and the coloration of the second dorsal fin of *E. rhothion* erroneously [symphyseal mandibular pore 1, and second dorsal fin pale (rarely spotted) in males, respectively] (see Fricke 2001, 2002). Although *E. rhothion* is similar to *E. rufopileus* in scale

Table 1. Measurements and counts of *Enneapterygius rhothion*. Means in parentheses.

Character	Australia	New Caledonia and Vanuatu	
	AMS I. 5088 Non-type Male	SMNS 18322 Holotype Male	*n* = 8 Paratypes Males
Morphometric data; absolute value [mm]			
Standard length (SL)	32.5	28.9	23.4–27.8
Morphometric data; relative values [%SL]			
Body depth	20.5	20.0	18.5–20.4 (19.4)
Body width	18.4	18.0	15.6–17.7 (16.8)
Head length	29.3	26.7	28.7–29.8 (29.2)
Snout length	12.5	9.2	9.1–10.1 (9.6)
Orbital tentacle length	1.6	2.1	—
Orbit diameter	8.4	9.6	9.6–10.4 (10.0)
Interorbital width	2.3	2.9	2.4–2.9 (2.7)
Upper-jaw length	11.6	11.4	11.1–11.8 (11.5)
Postorbital length	12.1	12.0	11.6–13.0 (12.5)
Pre-1st-dorsal-fin length	25.4	24.8	25.2–27.3 (26.3)
Pre-2nd-dorsal-fin length	36.5	35.6	35.5–38.6 (37.5)
Pre-3rd-dorsal-fin length	69.2	71.3	69.7–74.6 (72.9)
Pre-anal-fin length	47.0	48.2	48.9–52.8 (50.7)
Anal-fin base length	41.1	42.2	37.6–42.7 (40.4)
Pre-pectoral-fin length	32.2	31.3	29.3–33.1 (31.4)
Pre-pelvic-fin length	21.3	24.4	20.1–24.6 (23.0)
Caudal peduncle length	10.5	10.9	10.9–12.3 (11.6)
Caudal peduncle depth	9.1	8.0	7.6–8.9 (8.2)
1st spine length of 1st dorsal fin	Damaged	9.0	9.8–10.5 (10.1)
2nd spine length of 1st dorsal fin	10.4	8.2	9.2–9.8 (9.4)
3rd spine length of 1st dorsal fin	8.9	7.0	7.8–9.0 (8.1)
1st dorsal-fin base length	5.6	5.6	5.0–6.3 (5.8)
1st spine length of 2nd dorsal fin	14.0	14.2	14.1–15.5 (15.0)
2nd spine length of 2nd dorsal fin	12.5	14.7	14.6–16.6 (15.6)
3rd spine length of 2nd dorsal fin	15.4	14.7	14.5–16.5 (15.5)
2nd dorsal-fin base length	30.5	30.9	29.5–34.9 (31.9)
1st ray length of 3rd dorsal fin	Damaged	16.4	16.1–18.3 (17.0)
2nd ray length of 3rd dorsal fin	Damaged	15.1	16.0–17.1 (16.6)
3rd ray length of 3rd dorsal fin	Damaged	14.9	9.5–16.1 (14.9)
3rd dorsal fin base length	16.4	16.7	14.3–18.1 (16.4)
Pectoral-fin length	Damaged	27.0	29.8–34.8 (32.7)
1st ray length of pelvic fin	16.4	16.0	15.6–19.3 (17.6)
2nd ray length of pelvic fin	Damaged	19.3	22.6–25.1 (24.3)
Meristic data (counts)			
Dorsal-fin rays	III, XIII, 10	III, XIII, 9	III, XIII or XIV, 9 or 10
Anal-fin rays	I, 18	I, 18	I, 17 or 18
Pectoral-fin rays	iii + damaged = 15	ii + 6 + vii = 15	ii–iv + 4–6 + 6 or 7 = 14–16
Scale rows in longitudinal series	33	34	34 or 35
Pored lateral-line scales	16	19	15–17
Notched lateral-line scales	20	19	19–21
Scales above 1st PLL	3	4	4
Scales below 2nd dorsal fin	3	3½	3½ or 4
Scales below 1st NLL	3½	3½	3 or 3½
Scales above last PLL	2½	3	2½ or 3
Mandibular pore formula	3 + 2 + 3	4 + 2 + 4	3 or 4 + 1 or 2 + 3 or 4

counts and overall appearance, the former differs in having the following characters: symphyseal mandibular pore single (vs. double in *E. rufopileus*), head (including maxillary) and pectoral-fin base entirely black (posterior two-thirds of jaws white, pectoral-fin base with black blotch), body with 7 bands (5 bands); first and second dorsal fin black in nuptial males (translucent white); third dorsal fin with black pigmentation in both sexes (not pigmented in either sex); dorsal and ventral parts of caudal fin with vertical streaks in both sexes (caudal fin pale in both sexes) (Fricke 1997; this study).

Enneapterygius rhothion has previously been recorded only from New Caledonia (Chesterfield Islands, Grande Terre, Ile des Pins, and Loyalty Islands) and Vanuatu (Erromango Island), and was considered endemic to those areas (Fricke 1997, 2002). The presently reported specimen represents the first record of the species from Australia, and the new northernmost record.

Enneapterygius olivaceus Dewa, Tashiro, et Motomura, 2023

English name: olive green triplefin

Figs. 3, 4; Table 2

Material examined. 20 specimens (12.1–22.1 mm SL). **AUSTRALIA:** AMS I. 22732-008, male, 22.1 mm SL, Bird Islet, Lizard Island, Queensland, 15°18′00″S, 145°26′59″E, 1981, D. Hoese et al.; AMS I. 30000-001, 9 males and 8 females, 12.1–19.4 mm SL, Lizard Island, 15°19′48″S, 145°28′11″E, 1989. **VANUATU:** AMS I. 6317, 1 of 3 specimens, male, 19.7 mm SL, Vila, Efate, 1903, W.A. Haswell leg.; AMS I. 6451, 1 of 3 specimens, female, 15.9 mm SL, Vanua Lava, Banks Islands, 1903, W.A. Haswell leg.

Description. Counts and measurements given in Table 2. Body moderately elongate, slightly compressed anteriorly, progressively more compressed posteriorly. Dorsal profile of snout straight, moderately steep. Mouth slightly oblique; posterior margin of maxilla reaching to or extending slightly beyond anterior margin of pupil; anterior tip of upper jaw slightly above level of lower margin of orbit (lateral view). Anterior nostril forming membranous tube with short unbranched tentacle, base at level of middle of eye, slightly closer to eye than to upper lip; posterior nostril opening circular, without membranous tube. Eye oriented dorsolaterally; broad leaf-like tentacle on posterodorsal margin, its length longer than nasal tentacle. Interorbital space narrow, its width less than pupil diameter. Opercular margin slightly pointed, reaching to below base of 2nd or 3rd spine of first dorsal fin.

Lateral line discontinuous, with anterior series of pored scales and posterior series of notched scales; pored scale series ending below membrane between 9th and 10th spines of second dorsal fin; notched scale series beginning below second scale from last pored scale, ending at caudal-fin base; Body scales ctenoid; scales absent on head, including maxilla, interorbital space, preopercle and opercle, and pectoral-fin base, undersurface of head, abdomen and pre-dorsal-fin region; all fin membranes, except basal part of caudal fin, scaleless.

First dorsal fin triangular to trapezoid, its origin vertically above preopercular margin or midway between preopercular and opercular margins; 1st spine of first dorsal fin longest, thereafter, becoming shorter posteriorly. Origin of second dorsal fin just above 4th to 6th pored lateral-line scales, 2nd or 3rd spine longest, thereafter, becoming gradually shorter posteriorly, forming rounded

Figure 4. Photographs of preserved specimens of *Enneapterygius olivaceus* (**A**: AMS I. 22732-008, male, 22.1 mm SL, Australia; **B**: AMS I. 6317, male, 19.7 mm SL, Vanuatu; **C**: AMS I. 30000-001, female, 18.0 mm SL, Australia).

Table 2. Measurements and counts of *Enneapterygius olivaceus* collected from Australia and Vanuatu. Means in parentheses.

Character	**Australia**	**Vanuatu**	
	***n* = 18**	**AMS I. 6317**	**AMS I. 6451**
	Males and females	**Male**	**Female**
Morphometric data; absolute value [mm]			
Standard length (SL)	12.1–19.4	19.7	15.9
Morphometric data; relative values [%SL]			
Body depth	20.0–22.1 (21.2)	23.5	20.8
Body width	17.4–20.5 (19.2)	21.4	19.4
Head length	28.9–31.6 (30.4)	32.3	31.9
Snout length	7.8–12.3 (10.4)	12.3	13.6
Orbit diameter	8.2–11.0 (9.6)	9.1	10.4
Interorbital width	1.2–2.4 (1.9)	2.0	1.9
Upper-jaw length	9.3–12.0 (10.5)	11.8	11.4
Postorbital length	12.0–14.6 (13.0)	12.7	11.5
Pre-1st-dorsal-fin length	23.7–27.3 (25.3)	26.2	27.5
Pre-2nd-dorsal-fin length	33.2–38.3 (36.5)	37.9	38.2
Pre-3rd-dorsal-fin length	68.5–73.3 (70.9)	73.8	74.4
Pre-anal-fin length	45.7–53.9 (51.3)	54.1	51.0
Anal-fin base length	38.2–44.0 (41.2)	40.4	38.8
Pre-pectoral-fin length	28.9–35.5 (33.4)	35.6	34.4
Pre-pelvic-fin length	23.6–27.2 (25.6)	28.4	25.1
Caudal peduncle length	9.1–13.7 (11.8)	13.5	11.0
Caudal peduncle depth	7.1–9.2 (8.5)	8.6	8.3
1st spine length of 1st dorsal fin	11.0–15.6 (13.2)	18.2	12.6
2nd spine length of 1st dorsal fin	8.6–11.8 (10.6)	14.3	10.7
3rd spine length of 1st dorsal fin	6.8–9.9 (8.8)	11.2	Damaged
1st dorsal-fin base length	4.3–6.8 (5.2)	5.6	5.0
1st spine length of 2nd dorsal fin	11.9–18.5 (13.5)	14.8	Damaged
2nd spine length of 2nd dorsal fin	12.6–16.6 (14.5)	16.6	Damaged
3rd spine length of 2nd dorsal fin	10.3–18.6 (14.6)	14.9	Damaged
2nd dorsal-fin base length	25.5–30.9 (28.8)	29.4	30.8
1st ray length of 3rd dorsal fin	13.1–19.6 (16.1)	18.6	15.8
2nd ray length of 3rd dorsal fin	13.4–18.2 (15.9)	17.6	12.6
3rd ray length of 3rd dorsal fin	13.6–17.2 (15.4)	15.5	Damaged
3rd dorsal fin base length	13.9–19.5 (17.0)	17.3	15.1
Pectoral-fin length	27.6–34.9 (32.2)	30.9	31.7
1st ray length of pelvic fin	13.4–18.3 (15.6)	19.1	16.3
2nd ray length of pelvic fin	20.6–26.5 (24.0)	30.4	23.9
Meristic data (counts)			
Dorsal-fin rays	III, XI–XIII, 8–10	III, XIII, 9	III, XIII, 8
Anal-fin rays	I, 16 or 17	I, 16	I, 16
Pectoral-fin rays	iii–v + 3–5 + vi–viii = 14–16	3 + damaged = 15	iv + 4 + vii = 15
Scale rows in longitudinal series	29–32	29	30
Pored lateral-line scales	12–14	13	12
Notched lateral-line scales	18–21	20	19
Scales above of 1st PLL	2 (rarely 1)	2	2
Scales below 2nd dorsal fin	2–3	2½	2½
Scales below of 1st NLL	2 or 3	3	2
Caudal peduncle scales	8	8	8
Mandibular pore formula	3 + 1 + 3	3 + 1 + 3	3 + 1 + 3

distal margin. Third dorsal fin semicircular to trapezoid, its origin just above 19th and 20th longitudinal scales, 1st or 2nd ray longest, thereafter becoming gradually shorter posteriorly. Anal-fin membranous margin deeply incised between rays; anal fin origin just below 6th to 8th spine base of second dorsal fin, its posteriormost tip close to caudal-fin base. Pectoral fin relatively long, its posterior tip pointed and slightly beyond or reaching vertical through base of last spine of second dorsal fin; upper and lowermost pectoral-fin base level with bases of 1st spine of second dorsal-fin and 3rd spine of first dorsal fin, respectively. Pelvic fin origin just below vertical through base of 1st spine of first dorsal fin, its tip not reaching anus. Caudal fin rounded; its length similar to head length.

Nuptial male coloration (in preservative). Based on Fig. 4. Body generally yellowish white or brownish. Head, including eye, snout, lips, cheek, and opercle, and pectoral-fin base black or dark brown with melanophores. Pre-pelvic region and undersurface of abdomen black or dark brown with melanophores. Orbital tentacle translucent white, covered by melanophores. Iris greenish white; pupil silver. First dorsal fin black. Second and third dorsal fins generally transparent, with two brown longitudinal bands on fin margin and base, width of former ca. 1/2 length of spines, latter somewhat indistinct. Membranous margin of 1st to 3rd rays of third dorsal fin transparent, without brownish pigmentation. Pectoral fin transparent, membranes between lower 6–8 rays brownish. Pelvic fin white, its basal part brownish. Anal fin brown, fin margin and base whitish. Caudal fin white with faint brownish bars.

Female coloration (in preservative). Body generally yellowish white; lateral surface with A- or X-shaped brownish bars. Faint brownish stripes extending from tip of snout to anterior margin of eye, width subequal to upper lip width. Prepelvic region and undersurface of abdomen whitish. Orbital tentacle translucent white, covered by melanophores. Iris navy, pupil silver. Caudal-fin base with vertical brown band. First dorsal fin transparent, with scattered melanophores. Second and third dorsal fins generally transparent, with 2 or 3 irregular oblique brownish bands. Anal fin white. Pectoral fin translucent white; fin rays broadly flecked with brown pigmentation forming ca. 4 or 5 vertical bands. Pelvic fins translucent white. Caudal fin translucent white with narrow brownish vertical bars.

Distribution. Currently known from Japan (the southern Ryukyu Islands), the Philippines (Talampulan and Negros islands), Australia (Lizard Island), and Vanuatu. (Dewa et al. 2023; this study) (Fig. 3).

Remarks. The morphological characters of the presently reported South Pacific specimens agreed well with the description of *E. olivaceus* provided by Dewa et al. (2023), especially as follows: 11–13 (modally 12) second dorsal-fin spines; 18–21 (modally 20) notched lateral-line scales; mandibular pore formula 3 + 1 + 3; head length 28.9%–32.3% (mean 30.6%) of SL; upper jaw length 9.3%–12.0% (10.6%) of SL; 1st spine of first dorsal fin longer than that of 2nd dorsal-fin, its length 11.0%–18.2% (13.4%) of SL; orbital tentacle broad, leaf-shaped; head, pectoral-fin base and lower part of pectoral fin brownish in nuptial males; caudal fin whitish in nuptial males; pectoral fin with bands in females; anal fin without distinct bars or lines in both sexes. Although the presently reported specimens had fewer longitudinal series scale rows and scales below the 1st notched lateral-line scale compared to the type series of *E. olivaceus* [29–32 (modally 30) and 2 or 3 (3), respectively, in the former vs. 30–32 (31) and 2–3 (2) in the latter], such differences were considered minor and regarded as intraspecific variations.

In Japanese waters, *E. olivaceus* co-occurs with *Enneapterygius minutus* in the Ryukyu Islands (Dewa et al. 2023). Similarly, the two Vanuatu specimens of *E. olivaceus* examined in this study had been collected with *E. minutus* specimens (AMS I. 6317, 2 of 3 specimens, 19.4–20.2 mm SL; AMS I. 6451, 2 of 3 specimens, 16.5–16.7 mm SL). *Enneapterygius olivaceus* is distinguished from *E. minutus* by the following features: orbital tentacle large and leaf-shaped (vs. slender and pointed in *E. minutus*); head long, length 28.4%–33.0% of SL (vs. short, 24.7%–32.4% of SL); upper jaw long, length 9.3%–13.1% of SL (vs. short, 7.4%–11.0% of SL); 1st spine of first dorsal fin relatively long, length 11.0%–18.2% of SL (vs. short, 7.6%–11.4% of SL); black areas in nuptial males restricted to head and all fins, except for caudal fin [body (except nape and all fins) entirely black in nuptial males]; pectoral fin with faint broad bands in females (with distinct narrow bands in females) (Dewa et al. 2023; this study).

Enneapterygius olivaceus was originally described based on 28 specimens from the southern Ryukyu Islands, Japan and Talampulan and Negros islands, the Philippines (Dewa et al. 2023). Accordingly, the presently reported specimens, collected from Australia and Vanuatu, represent the first records of the species from those localities and the Southern Hemisphere.

Acknowledgments

We extend our gratitude to A. Hay, K. Parkinson, S. Reader, Y.-K. Tea and I. Riley (AMS), and R. Fricke (SMNS) for the opportunity to examine specimens. We thank M. Meguro (formerly KAUM) for providing data for type specimens of *E. rhothion*. G. Hardy (Ngunguru, New Zealand) read the manuscript and gave help with English. This study was supported by a 2023/24 Australian Museum Research Institute Visiting Collection Fellowship; Sasakawa Scientific Research Grant from The Japan Science Society Grant Number 2023-4104; JSPS KAKENHI Grant Numbers 20H03311, 21H03651, 23K20304, and 24K02087; the JSPS Core to-core CREPSUM JPJSCCB20200009; and the “Establishment of Glocal Research and Education Network in the Amami Islands” project of Kagoshima University adopted by the Ministry of Education, Culture, Sports, Science and Technology, Japan. This research is a part of the dissertation of the first author. All authors agree with the article publication and dissertation submission.

References

Chiang M-C, Chen I-S (2008) Taxonomic review and molecular phylogeny of the triplefin genus *Enneapterygius* (Teleostei: Tripterygiidae) from Taiwan, with description of two new species. Raffles Bulletin of Zoology Suppl. 19: 183–201.

Dewa Y, Tashiro S, Motomura H (2023) A new species of the genus *Enneapterygius* (Perciformes: Tripterygiidae) from Japan and the Philippines, with a synopsis and synonymy of related species. Zootaxa 5374(3): 333–360. https://doi.org/10.11646/zootaxa.5374.3.2

Fricke R (1994) Tripterygiid fishes of Australia, New Zealand and the Southwest Pacific Ocean (Teleostei). Koeltz Scientific Books, Königstein, Germany, 585 pp.

Fricke R (1997) Tripterygiid fishes of the western and central Pacific (Teleostei). Koeltz Scientific Books, Königstein, Germany, 607 pp.

Fricke R (2001) *Enneapterygius trisignatus*, a new species from northern Grande Terre, with a key to New Caledonian tripterygiid fishes (Teleostei). Stuttgarter Beiträge zur Naturkunde, Serie A (Biologie) 630: 1–9.

Fricke R (2002) Tripterygiid fishes of New Caledonia, with zoogeographical remarks. Environmental Biology of Fishes 65: 175–198. https://doi.org/10.1023/A:1020076906430

Hansen PEH (1986) Revision of the tripterygiid fish genus *Helcogramma*, including descriptions of four new species. Bulletin of Marine Science 38: 313–354.

Hoese DF (2006) Tripterygiidae. Pp. 1517–1528. In: Hoese DF, Bray DJ, Paxton JR, Allen GR (Eds.) Zoological catalogue of Australia. Vol. 35. Fishes. Parts 1–3. CSIRO Publishing, Collingwood, VIC, Australia.

Holleman W (2005) A review of the triplefin fin fish genus *Enneapterygius* (Blennioides: Tripterygiidae) in the western Indian Ocean, with descriptions of four new species. Smithiana Bulletin 5: 1–25.

Motomura H, Harazaki S, Hardy G (2005) A new species of triplefin (Perciformes: Tripterygiidae), *Enneapterygius senoui*, from Japan with a discussion of its in situ colour pattern. Aqua, Journal of Ichthyology and Aquatic Biology 10: 5–14.

Motomura H, Ota R, Meguro M, Tashiro S (2015) *Enneapterygius phoenicosoma*, a new species of triplefin (Tripterygiidae) from the western Pacific Ocean. Species Diversity 20: 1–12. https://doi.org/10.12782/sd.20.1.001

Randall JE (2005) Reef and shore fishes of the South Pacific. New Caledonia to Tahiti and the Pitcairn Islands. University of Hawai'i Press, Honolulu, HI, USA, 720 pp.

Sabaj MH (2020) Codes for natural history collections in ichthyology and herpetology. Copeia 108 (3): 593–669. https://doi.org/10.1643/ASIHCODONS2020

Tashiro S, Motomura H (2018) Redescriptions of two western Pacific triplefins (Perciformes: Tripterygiidae), *Enneapterygius fuscoventer* and *E. howensis*. Ichthyological Research 65 (2): 252–264. https://doi.org/10.1007/s10228-017-0612-5

Acta Ichthyologica et Piscatoria 54, 2024, 269–273 | DOI 10.3897/aiep.54.135133

PENSOFT.

ACTA
ICHTHYOLOGICA
ET PISCATORIA

Length–weight relationships for 11 freshwater fish species (Actinopterygii) from four protected areas, northern Vietnam

Huy Quang NGUYEN[1], Huong Thi Thanh DANG[1], Thuy Thi TA[2], Chi Linh DO[1], Hau Duc TRAN[1]

1 *Faculty of Biology, Hanoi National University of Education, Hanoi, Vietnam*
2 *Faculty of Education, Hanoi Metropolitan University, Hanoi, Vietnam*

https://zoobank.org/90AE8E5E-1FFE-432B-AC7D-F173CB4C205F

Corresponding author: Hau Duc Tran (hautd@hnue.edu.vn)

Academic editor: Rodolfo Reyes ♦ **Received** 20 August 2024 ♦ **Accepted** 14 October 2024 ♦ **Published** 11 November 2024

Citation: Nguyen HQ, Dang HTT, Ta TT, Do CL, Tran HD (2024) Length–weight relationships for 11 freshwater fish species (Actinopterygii) from four protected areas, northern Vietnam. Acta Ichthyologica et Piscatoria 54: 269–273. https://doi.org/10.3897/aiep.54.135133

Abstract

The length–weight relationships (LWRs) of 11 fish species from one national park and three nature reserves, in northern Vietnam, totaling 737 individuals between October 2018 and November 2021, are described in this study. The following species, representing 11 genera and seven families, were studied: *Aphyocypris normalis* Nichols et Pope, 1927, *Barbodes semifasciolatus* (Günther, 1868), *Beaufortia pingi* (Fang, 1930), *Carassius auratus* (Linnaeus, 1758), *Glyptothorax honghensis* Li, 1984, *Hemibarbus medius* Yue, 1995, *Macropodus opercularis* (Linnaeus, 1758), *Neolissochilus benasi* (Pellegrin et Chevey, 1936), *Onychostoma gerlachi* (Peters, 1881), *Opsariichthys minutus* Nichols, 1926, *Rhinogobius duospilus* (Herre, 1935). All regressions were highly significant ($P < 0.001$). Positive allometric growth was seen in six species ($b > 3$, $P < 0.01$) and isometric growth in five species ($b = 3$, $P > 0.05$). This is the first report on the LWRs of six fish species, including *Beaufortia pingi*, *Barbodes semifasciolatus*, *Neolissochilus benasi*, *Opsariichthys minutus*, *Glyptothorax honghensis*, and *Rhinogobius duospilus* from four conservation areas. The presently reported study provides foundational data for future stock assessment works and management initiatives in protected areas, as well as facilities comparisons of LWRs from different habitats.

Keywords

conservation, growth pattern, length–weight relationship, new data

Introduction

Management of aquatic resources requires systematic assessments, integrating accurate data and representative parameters (e.g., abundance, size, and age structures) of fish populations at the local scale (Lou et al. 2005), including the length–weight relationships (LWRs). In fish biology, length–weight relationship is an essential fisheries management technique because they allow the mean weight of fish belonging to a length group to be estimated by establishing a mathematical relationship between length and weight (Beyer 1987). Knowledge of LWRs is essential for characterizing fish growth, body condition, size at first maturity, and life-history phenotypes (Le Cren 1951; Froese 2006).

Mountain regions have high levels of biodiversity and a wide variety of natural habitats due to their varied elevation and topography (Sterling et al. 2017). Bac Me, Nam Xuan Lac, Cham Chu Nature Reserves, and Phia Oac–Phia Den National Park have all been established to safeguard and sustain biodiversity in natural resources, uncommon species, and vulnerable species. Research on species diversity (Ta et al. 2023, 2024; Nguyen et al. 2024), records of new species for the region and for science in recent years have been updated and supplemented in protected areas (Duong et al. 2022; Tran et al. 2023; Dang et al. 2024). Moreover, Dang et al. (2023) presented a study on the extraction and usage of fish resources in these areas, which discovered that fish populations have decreased in certain sites.

Recent taxonomic and ecological work on the fish fauna of northern Vietnam has included an updated checklist summarizing the fauna (Ha et al. 2021), providing a foundation for additional work; however, LWR research on this fauna has been limited to various species of estuarine gobies (e.g., Tran et al. 2021; Ha et al. 2022; Nguyen et al. 2022; Ta et al. 2022). In this study, we present results from the first study of LWRs in primarily freshwater fishes of northern Vietnam, including a total of 11 species, six of which currently have no LWR information publicly available in FishBase (Froese and Pauly 2024). By presenting novel data and results on LWRs of freshwater fishes from protected areas of northern Vietnam, our study provides baseline data for future stock assessment and contributes to a greater understanding of the basic biology and growth patterns of freshwater fishes of conservation concern, which is critical for future conservation and management efforts.

Material and methods

Eight field surveys were conducted to sample freshwater fishes between October 2018 and November 2021 in northern Vietnam (Fig. 1). Fish were collected using hand nets, casting nets, and gillnets. In the field, specimens were first fixed in 10% formalin solution, and in the lab, samples were later preserved in 70% ethanol.

A total of 11 fish species representing 11 genera of 7 families were studied: *Aphyocypris normalis* Nichols et Pope, 1927, *Barbodes semifasciolatus* (Günther, 1868), *Beaufortia pingi* (Fang, 1930), *Carassius auratus* (Linnaeus, 1758), *Glyptothorax honghensis* Li, 1984, *Hemibarbus medius* Yue, 1995, *Macropodus opercularis* (Linnaeus, 1758), *Neolissochilus benasi* (Pellegrin et Chevey, 1936), *Onychostoma gerlachi* (Peters, 1881), *Opsariichthys minutus* Nichols, 1926, *Rhinogobius duospilus* (Herre, 1935).

The total length (TL) and weight (W) of each individual were determined to the nearest 0.01 cm and 0.01 g, respectively. The length–weight relationships

$$W = a\mathrm{TL}^{b}$$

of 11 species were estimated from the following log-transformed equation

$$\mathrm{Log}(W) = \log(a) + b \times \log(\mathrm{TL})$$

where W is the total weight of an individual [g], TL is the total length [cm], a is the intercept, and b is the

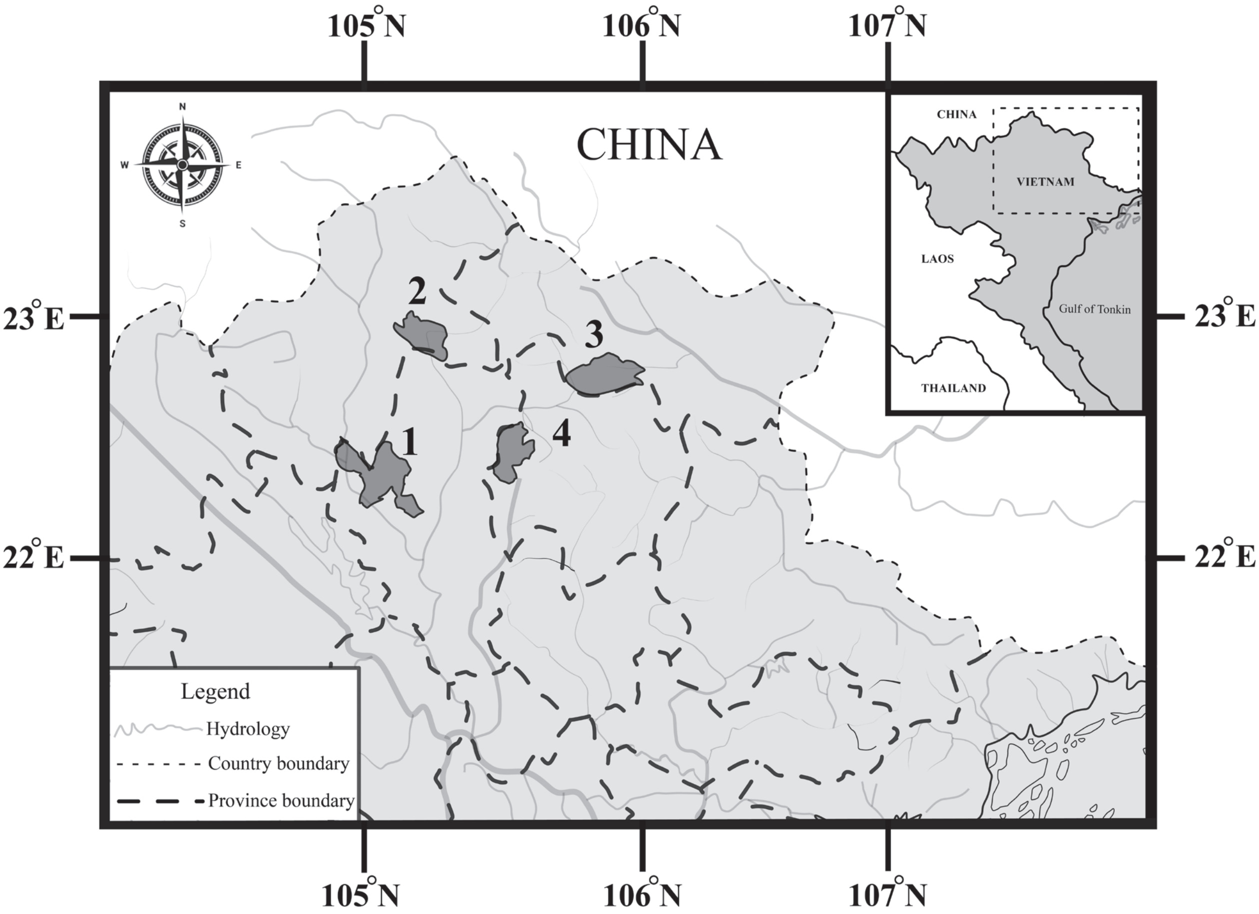

Figure 1. Map of the study area and sampling sites within four protected areas in northern Vietnam. 1. Cham Chu Nature Reserve; 2. Bac Me Nature Reserve; 3. Phia Oac–Phia Den National Park; 4. Nam Xuan Lac Habitat and Species Conservation Area.

slope (Le Cren 1951; Ricker 1973; Froese 2006). In addition, the 95% confidence interval (CI) of the parameters and the statistical significance of the regression relationships (r^2) were calculated statistically. The log-transformed data should be plotted, and obvious outliers should be removed before performing linear regression (Froese et al. 2011). The coefficient b was compared with 3 using Student's t-tests to evaluate the growth pattern. Here, $b = 3$ is generally taken to represent isometric growth, while $b > 3$ indicates positive allometric growth and $b < 3$ indicates negative allometric growth (Froese 2006). Basic functions in R software version 4.1.0 were used to perform all statistical analyses (R Core Team 2024).

Results

A total of 737 specimens were examined in the presently reported study. The LWRs and related statistics for 11 of the species studied are presented in Table 1. The highest number of specimens was measured for *Rhinogobius duospilus* ($n = 294$), while 2 species (*Hemibarbus medius* and *Carassius auratus*) had much smaller sample sizes (17 and 12, respectively). The estimated values of coefficient (a value) from LWRs ranged from 0.004 (*Opsariichthys minutus* and *Aphyocypris normalis*) to 0.012 (*Macropodus opercularis*) while the exponent (b value) ranged from 2.954 (*M. opercularis*) to 3.407 (*A. normalis*). The coefficients of determination r^2 were between 0.952 (for *R. duospilus*) and 0.997 (for *Onychostoma gerlachi* and *A. normalis*). The LWRs of each species were highly significant ($P < 0.001$). The b values of 11 species were significantly higher than or at least equal to three (Table 1).

Discussion

The b values of all species in this study were within the expected range predicted by Froese (2006) and the 95% confidence limits of the Bayesian LWR predicted value at FishBase (Froese et al. 2024), the value of sole b usually falls from 2.50 to 3.50 (Froese 2006). Many factors can affect the parameters of LWR of fish such as different fishing methods, storage techniques, and sample-collecting periods. In addition, the value of slope b could vary mainly due to several environmental (habitat, season), anthropogenic (length type, size range, number of specimens), and biological factors, gonadal maturation, diet, degree of stomach fullness, and growth stage (Hanif et al. 2018). However, the number of specimens for *Carassius auratus* and *Hemibarbus medius* was insufficient to derive an appropriate LWRs equation.

Comparing our results with published LWRs for the focal taxa shows that the slope b of *Hemibarbus gerlachi* (3.096), *Aphyocypris normalis* (3.407), *C. auratus* (3.316) and *H. medius* (3.171) was quite similar (Froese and Pauly 2024). However, *Macropodus opercularis* (2.954) was smaller when compared with the results of Tang et al. (2015). For the range of TL values, *C. auratus* (6.09–12.88 cm) was most similar to the study by Wang et al. (2015); *O. gerlachi* (1.05–17.81 cm) were supplemented with small-sized specimens in our study which conforms with the findings of Que et al. (2014) and He et al. (2023); the range of *A. normalis* was expanded (3.54–10.41 cm); the b-values of *H. medius* and *M. opercularis* were similar or narrower than previous research. Concerning the last six fish species (*Beaufortia pingi*, *Barbodes semifasciolatus*, *Neolissochilus benasi*, *Opsariichthys minutus*, *Glyptothorax honghensis*, and *Rhinogobius duospilus*), no previous data on LWRs were available in FishBase (Froese and Pauly 2024) for these species or areas, hence our study provides the first data on LWRs for them.

Table 1. LWR estimates for 11 species reported from four protected areas in northern Vietnam.

Family and species	n	TL [cm]	W [g]	$W = a\mathrm{TL}^b$					P (t-test) b compared to 3	b FishBase
				a	b	r^2	95% CI of a	95% CI of b		
Balitoridae										
Beaufortia pingi	35	1.06–7.44	0.01–4.25	0.006	3.318	0.991	0.005–007	3.206–3.431	<0.001	—
Cyprinidae										
Barbodes semifasciolatus	74	2.12–7.57	0.10–5.56	0.008	3.294	0.982	0.007–0.010	3.190–3.398	<0.001	—
Carassius auratus	12	6.41–12.88	3.12–35.44	0.005	3.337	0.994	0.004–0.016	3.181–3.566	0.002	2.732–3.336[1]
Neolissochilus benasi	51	2.51–17.86	0.12–71.75	0.008	3.060	0.990	0.006–0.009	2.973–3.147	0.171	—
Onychostoma gerlachi	49	1.05–17.81	0.01–49.80	0.006	3.069	0.997	0.006–0.007	3.023–3.115	0.004	3.060[2]; 3.231[3]
Gobiidae										
Rhinogobius duospilus	294	2.32–5.28	0.12–1.58	0.007	3.201	0.952	0.007–0.008	3.118–3.284	0.020	—
Gobionidae										
Hemibarbus medius	17	7.47–12.49	3.33–16.18	0.006	3.171	0.982	0.003–0.010	2.932–3.410	0.148	3.124[4]; 3.220[3]
Osphronemidae										
Macropodus opercularis	46	3.08–8.12	0.33–5.12	0.012	2.954	0.956	0.009–0.017	2.762–3.146	0.632	3.088[5]
Sisoridae										
Glyptothorax honghensis	39	3.13–13.37	0.35–29.59	0.009	3.068	0.982	0.007–0.012	2.930–3.206	0.327	—
Xenocyprididae										
Aphyocypris normalis	26	3.54–10.41	0.33–12.03	0.004	3.407	0.997	0.004–0.005	3.331–3.483	<0.001	3.103[4]
Opsariichthys minutus	91	2.01–16.92	0.05–47.88	0.004	3.3093.	0.985	0.003–0.005	3.224–3.395	<0.001	—

n = sample size, a = intercept, b = slope, CI = confidence interval, r^2 = coefficient of determination, TL = total length; FishBase references: [1]Froese and Pauly (2024); [2]Que et al. (2014); [3]He et al. (2023); [4]Li et al. (2014); [5]Tang et al. (2015).

In terms of growth type, we found that six species had positive allometric growth ($b > 3$, $P < 0.01$ for all cases), five species had isometric growth ($b = 3$, $P > 0.05$ for all cases), and none had negative allometric growth ($b < 3$). Positive allometric is usually associated with changes in body shape between growth stages, with smaller fish having more elongated or thinner bodies than larger fish. Moreover, smaller individuals have the same body shape and density as larger individuals for isometric growth. In this study, the calculated parameters can be taken as mean values because the data were gathered over a long time and did not indicate any single season. The LWR results give fundamental information for the studied fish and will be valuable for managing and conserving these freshwater fishes.

Acknowledgments

This research was funded by The NEF Bio-ecological Nature Conservation Project in the Mountainous Region of North Vietnam (Nagao Natural Environment Foundation, Japan/Central Institute for Natural Resources and Environmental Studies). Thanks to V.S. Ngo, T.A. Hoang, T.T. Tran, H.V, Pham, and N.T. Nguyen, who assisted in collecting specimens. We thank anonymous reviewers for their comments, which helped improve an earlier version of this manuscript.

References

Beyer JE (1987) On length–weight relationship. Computing the mean weight of the fish of a given length class. Fishbyte 5: 11–13.

Dang TTH, Ta TT, Tran TT (2023) Tình hình khai thác, sử dụng nguồn lợi cá ở một số tỉnh miền núi phía bắc Việt Nam: đề xuất biện pháp bảo tồn và phát triển bền vững. [The exploitation and use of fish resources in some mountainous provinces in northern Vietnam: proposed measures for conservation and sustainable development.] Tap chi Khoa hoc và Cong Nghe – Dai hoc Thai Nguyen = TNU Journal of Science and Technology 229(01): 399–408. [In Vietnamese with English abstract] https://doi.org/10.34238/tnu-jst.8622

Dang TTH, Duong TH, Li F, Nguyen QH, Tran DH (2024) A new loach species of the genus *Vanmanenia* (Actinopterygii: Cypriniformes: Gastromyzontidae) from hill streams of Vietnam. Acta Ichthyologica et Piscatoria 54: 177–187. https://doi.org/10.3897/aiep.54.121328

Duong TH, Tran DH, Dang TTH, Nguyen QH (2022) Mô tả các mẫu vật thuộc giống cá chuôn *Parazacco* (Cypriniformes: Cyprinidae) thu ở Bắc Việt Nam. [Description of specimens of genus *Parazacco* (Cypriniformes: Cyprinidae) collected in Northern Vietnam.] Tap chi Khoa hoc và Cong Nghe – Dai hoc Thai Nguyen = TNU Journal of Science and Technology 227(14): 388–396. [In Vietnamese with English abstract] https://doi.org/10.34238/tnu-jst.6510

Froese R (2006) Cube law, condition factor and weight–length relationships: History, meta-analysis and recommendations. Journal of Applied Ichthyology 22(4): 241–253. https://doi.org/10.1111/j.1439-0426.2006.00805.x

Froese R, Pauly D (Eds.) (2024) FishBase. [Version 04/2024] http://www.fishbase.org

Froese R, Tsikliras AC, Stergiou KI (2011) Editorial note on weight–length relations of fishes. Acta Ichthyologica et Piscatoria 30(4): 11–14. https://doi.org/10.3750/AIP2011.41.4.01

Froese R, Thorson JT, Reyes Jr RB (2014) A Bayesian approach for estimating length–weight relationships in fishes. Journal of Applied Ichthyology 30(1): 78–85. https://doi.org/10.1111/jai.12299

Ha ML, Ta TT, Tran DH (2021) Tương quan chiều dài – khối lượng và hệ số điều kiện ở cá: thực trạng và định hướng nghiên cứu ở miền bắc Việt Nam [Length–weight relationship and condition factor of fish: the research status and orientation for further study in Northern Vietnam.] Tạp chí Nông nghiệp và Phát triển Nông thôn = Science and Technology Journal of Agriculture and Rural Development: 47–56. [In Vietnamese with English abstract]

Ha ML, Tran DH, Nguyen TN, Tran TT, Ta TT, Nguyen TN, Nguyen QH (2022) Length–weight relationship and condition factor of Amur goby *Rhinogobius similis* Gill, 1859 (Actinopteri: Gobiidae) from different areas in Vietnam. Acta Zoologica Bulgarica 74: 559–568.

Hanif MA, Islam MA, Siddik MAB, Chaklader MR (2018) Length–weight relationships of three estuarine fish species from Bangladesh. Journal of Applied Ichthyology 34(4): 1065–1067. https://doi.org/10.1111/jai.13707

He J, Wu Z, Huang L, Li Y, Sun Y, Wang D, Feng J, Lin Y, He A (2023) Length–weight relationships of twenty-nine native fish species from Hongshui River, southern China. Journal of Applied Ichthyology 1–4: 1–4. https://doi.org/10.1155/2023/1744641

Le Cren ED (1951) The length–weight relationship and seasonal cycle in gonad weight and condition in the perch (*Perca fluviatilis*). Journal of Animal Ecology 20(2): 201–219. https://doi.org/10.2307/1540

Li Q, Xu XL, Huang JR (2014) Length–weight relationships of 16 fish species from the Liuxihe national aquatic germplasm resources conservation area, Guangdong, China. Journal of Applied Ichthyology 30(2): 434–435. https://doi.org/10.1111/jai.12378

Lou DC, Mapstone BD, Russ GR, Davies CR, Begg GA (2005) Using otolith weight–age relationships to predict age-based metrics of coral reef fish populations at different spatial scales. Fisheries Research 71(3): 279–294. https://doi.org/10.1016/j.fishres.2004.09.003

Nguyen TN, Ha ML, Nguyen TA, Chu HN, Tran DH, Nguyen PH, Ta TT (2022) Variation in the allometry of morphometric characteristics, growth, and condition factors of wild *Bostrychus sinensis* (Butidae) in Northern Vietnam. Pakistan Journal of Zoology 55(2): 809–818. https://doi.org/10.17582/journal.pjz/20200917140936

Nguyen QH, Dang TTH, Ta TT, Duong TH, Tran DH (2024) Bước đầu ghi nhận về khu hệ cá tại Vườn Quốc gia Phia Oắc-Phia Đén, tỉnh Cao Bằng, Bắc Việt Nam. [Preliminary data on the ichthyofauna in Phia Oac-Phia Den National Park, Cao Bang province, northern Vietnam.] Tap chi Khoa hoc và Cong Nghe – Dai hoc Thai Nguyen = TNU Journal of Science and Technology 229(13): 52–60. [In Vietnamese with English abstract] https://doi.org/10.34238/tnu-jst.10286

Que YF, Pan L, Chen F, Xie S, Liao XL, Zhao N (2014) Length–weight relationships of thirty-seven fish species from the Hongshui River, southwest China. Journal of Applied Ichthyology 31(4): 804–806. https://doi.org/10.1111/jai.12759

R Core Team (2024) A language and environment for statistical computing. R Foundation for Statistical Computing, Vienna, Austria. https://www.R-project.org/

Ricker WE (1973) Linear regressions in fishery research. Journal of the Fisheries Research Board of Canada 30(3): 409–434. https://doi.org/10.1139/f73-072

Sterling EJ, Hurley MM, Minh LD (2017) Vietnam: A natural history. Yale University Press, Princeton, NJ, USA, 426 pp. https://doi.org/10.12987/9780300128215

Ta TT, Chu HN, Nguyen TN, Tran DH, Tran TT, Ha ML, Nguyen TN (2022) Morphometrics and body condition of *Glossogobius olivaceus* in mangrove forests of Northern Vietnam. Journal of Animal and Plant Sciences 32(3): 845–854. https://doi.org/10.36899/JAPS.2022.3.0485

Ta TT, Dang TTH, Nguyen QH, Tran TT, Chu HN, Ngo S Van (2023) Thành phần loài cá ở Khu bảo tồn thiên nhiên Bắc Mê, tỉnh Hà Giang. [Fish species composition in Bac Me Nature Reserve, Ha Giang province.] Tap chi Khoa hoc và Cong Nghe – Dai hoc Thai Nguyen – TNU Journal of Science and Technology 228: 242–250. [In Vietnamese with English abstract] https://doi.org/10.34238/tnu-jst.7708

Ta TT, Duong TH, Dang TTH, Nguyen QH, Nguyen TNM (2024) Species composition and distribution of fish in Nam Xuan Lac species and habitat conservation area, Bac Kan province. Tạp chí Khoa học Tự nhiên = Journal of Natural Sciences 69: 90–102. https://doi.org/10.18173/2354-1059.2024-0009

Tang SK, Zhang TQ, Wang MH, Zhou G, Zhong LQ, Li DM, Pan JL (2015) Length–weight relationships of seven freshwater fishes from the JiangSu province, China. Journal of Applied Ichthyology 31(1): 231–232. https://doi.org/10.1111/jai.12492

Tran DH, Nguyen TA, Chu HN, Nguyen THT, Ta TT, Nguyen PH, Pham VL, Ha ML (2021) Length–weight relations of 11 goby species (Actinopterygii: Gobiiformes) from mangroves along the Ba Lat estuary of the Red River, Vietnam. Acta Ichthyologica et Piscatoria 51(3): 271–274. https://doi.org/10.3897/aiep.51.e64918

Tran DH, Nguyen HD, Dang TTH, Nguyen QH, Nguyen TN (2023) A new species of *Euchiloglanis* Regan, 1907 (Actinopterygii: Sisoridae) from Vietnam. Acta Zoologica Bulgarica 75: 3–11.

Wang LJ, You F, Wang QX, Wu ZH, Liu MX (2015) Length–weight and length–length relationships of 11 fish species from Zhimai River estuary, China. Journal of Applied Ichthyology 31(2): 435–436. https://doi.org/10.1111/jai.12692

Acta Ichthyologica et Piscatoria 54, 2024, 275–282 | DOI 10.3897/aiep.54.131982

ACTA
ICHTHYOLOGICA
ET PISCATORIA

Comparison of the nutrient composition of sludge under aerobic and anaerobic mineralization from African catfish, *Clarias gariepinus* (Actinopterygii: Siluriformes: Clariidae), reared in an intensive recirculating aquaculture system

Rizza Mae GUYAPALE[1], Cleresa DIONELA[1], Fredson HUERVANA[1]

1 *Institute of Aquaculture, College of Fisheries and Ocean Sciences, University of the Philippines Visayas, Miagao, Iloilo, Philippines*

https://zoobank.org/2643A232-96DB-4CA5-9D22-3C604ED106B4

Corresponding author: Fredson Huervana (fhhuervana@up.edu.ph)

Academic editor: Adnan Tokaç ♦ **Received** 3 July 2024 ♦ **Accepted** 7 November 2024 ♦ **Published** 17 December 2024

Citation: Guyapale RM, Dionela C, Huervana F (2024) Comparison of the nutrient composition of sludge under aerobic and anaerobic mineralization from African catfish, *Clarias gariepinus* (Actinopterygii: Siluriformes: Clariidae), reared in an intensive recirculating aquaculture system. Acta Ichthyologica et Piscatoria 54: 275–282. https://doi.org/10.3897/aiep.54.131982

Abstract

One of the major challenges in an intensive recirculating aquaculture system (RAS) is the sustainable management of fish sludge. The sludge contains a significant amount of nutrients that can be utilized by hydroponically grown crops in an integrated system called aquaponics. While this system has promising results, techniques to maximize nutrient recovery still need to be developed. African catfish, *Clarias gariepinus* (Burchell, 1822), can be stocked at very high densities, therefore it produces a substantial amount of sludge. In this study, sludge from African catfish RAS was subjected to different mineralization treatments (T1: anaerobic, T2: aerobic, and T3: aerobic with carbon addition) for nutrient recovery. The supernatant in T3 after mineralization had a statistically significant difference ($P > 0.05$) in their concentrations of N (2700 $\mathrm{mg \cdot L^{-1}}$), P (100 $\mathrm{mg \cdot L^{-1}}$), K (720 $\mathrm{mg \cdot L^{-1}}$), Ca (12 115.6 $\mathrm{mg \cdot L^{-1}}$), and Mg (3391.9 $\mathrm{mg \cdot L^{-1}}$) after 15 days, among the other mineralization methods and untreated sludge. It was then followed by the nutrient recovery performance of T2 and lastly, T1. Moreover, the low pH and warm temperature were observed to improve the solubilization of the nutrients, resulting in a higher nutrient recovery in T3. Hence, among the three mineralization treatments, T3 had the most potential to recover maximum nutrients from African catfish sludge to be used as organic fertilizer for hydroponically grown crops.

Keywords

aerobic mineralization, anaerobic mineralization, catfish aquaculture, decoupled aquaponics, nutrients, organic fertilizer

Introduction

Aquaculture plays a vital role in ensuring the world's food security by providing a stable supply of fish commodities as wild fish stocks steadily decline. However, traditional aquaculture is faced with sustainability issues such as the eutrophication and pollution of the receiving water bodies due to the nutrient-rich effluent from fish farms (Cao et al. 2007). Recent advancements in aquaculture veers toward zero water discharge, giving rise to recirculating aquaculture systems (RAS). RAS is designed to accommodate intensive stocking densities while facilitating the reuse of water within the system using a series of water treatment components (Espinal and Matulić 2019).

Catfish (order Siluriformes) are among the top fish groups being cultured in Asian countries like the Philippines. Catfish culture is an important sector in the aquaculture industry. The production volume in the Philippines increased over time, amounting to 10 849.49 metric tons with a value of Php 1.18 billion (US $20.23 million) yearly contribution in 2022 (PSA 2023). Moreover, the widespread production of catfish can be attributed to an established protocol from breeding up to grow-out culture (Setiadi et al. 2019). The African catfish, *Clarias gariepinus* (Burchell, 1822), was introduced in the Philippines in the early 1990s to aid with the catfish market, with native species declining in number. Since then, the African catfish has been preferred to be cultured. However, catfish are heavy waste producers that, along with the intensification of the stocking density, pose many problems in water quality management. Thus, a more sustainable solution to address nutrient overload and catfish health management must be developed.

The aquaponics system is the integration of raising freshwater aquatic organisms in RAS and cultivating plants in a soilless medium called hydroponics (Delaide et al. 2019). The major role players of aquaponics include cultured fish, plants, and microorganisms, which maintain an ecological balance in the system (Suhl et al. 2016). Nutrients from RAS are derived from fish feces and uneaten feeds that settle at the tank bottom as solid wastes, which are then converted by the microbial community present in the biological filter to make the nutrients available and provide plants with necessary mineral elements that are essential for growth, and thus reducing high nutrient emission in the receiving environments. Moreover, aquaponically-derived nutrients can reduce the reliance of hydroponic crops on inorganic fertilizers that are potentially harmful to the environment. The clean water then moves back to the fish tank for the fish to reuse.

In traditional aquaponics design, the aquaculture and hydroponics components are coupled in a single-loop system. However, this setup results in lesser production yield in fish and plants compared to RAS and hydroponics, respectively, due to the different water parameter requirements of each production unit (Goddek et al. 2015). For instance, the optimum pH for fish and heterotrophic bacteria in the aquaculture component is higher than what is required for most hydroponic crops. In effect, this compromises the availability of nutrients for the plants, resulting in slower growth and longer production cycles. To address these drawbacks, there has been a shift in recent designs towards the decoupling of the compartments such that there is an independent control over each unit. The decoupled aquaponics system has an additional compartment for RAS sludge mineralization to recover particle-bound nutrients to be used as an inorganic nutrient source for plant growth (Goddek et al. 2016).

Sludge mineralization in aquaponics functions as a solid waste reducer and nutrient solubilization enhancer. This process maximizes the nutrient content in the liquid effluent through sludge digestion processes and increases solid organic matter reduction by discharging after activation (Delaide et al. 2018). Several previous studies demonstrated sludge mineralization performance using aerobic and anaerobic methods to reduce solid organic waste in the systems (Goddek et al. 2018) and to evaluate nutrient recovery (Rakocy et al. 2007; Goddek et al. 2016; Panana et al. 2021), with both activation conditions proven to show promising results of on-site mineralization (Delaide et al. 2019).

Despite its high-density tolerance, fast growth rate, and resilience to fluctuating conditions, the African catfish, *C. gariepinus*, in aquaponics is not commonly used or studied. This study sought to evaluate the inorganic macronutrients produced in the mineralization of the fish sludge from African catfish, *C. gariepinus*, RAS when subjected to aerobic and anaerobic mineralization treatments.

Materials and methods

Decoupled aquaponics system. The experiment was conducted in the Freshwater Aquaculture Station of the University of the Philippines Visayas (FAS-UPV), Miagao, Iloilo, Philippines. The decoupled aquaponics system was composed of a catfish RAS unit, a lettuce hydroponic unit, and the experimental mineralization units. The RAS component consisted of a circular fish tank with a diameter of three meters, a height of 1.2 m, and a water depth of 0.8 m. A total of 500 individuals of African catfish, *C. gariepinus*, with mean body weight of 120 g, were stocked in the tank at a high density ($10\ \mathrm{kg} \cdot \mathrm{m}^{-3}$). The fish were fed at 3% body weight daily using commercial catfish feeds containing 34% crude protein. The fish tank water was recirculated through a settling tank (1 × 1 m), a biofilter tank (1 × 1 m), and a sump (1 × 1 m). The biofilter tank contained layers of bio media placed in fishnets and stackable trays. Water recirculation occurred continuously over 24 h, resulting in a total water exchange volume of 400% per day. The hydroponics had three elevated plant boxes (1 × 3 m) with lettuce *Lactuca sativa* in a deep-water culture method with a water depth of 25 cm. Individual plants were placed in each polystyrene cup at 15-cm intervals and held by a stationary raft secured by wire at a fixed level to allow aerial roots to develop. Each plant box contained 150 pieces of lettuce plants. The water was pumped into a separate hydroponics sump for each plant box, which was recirculated within individual units using a pump.

Sludge collection and mineralization treatments. The sludge was collected from the settling tank of the decoupled aquaponics system, where it was allowed to accumulate for seven days. After this period, the sludge was siphoned and allowed to settle for 24 h to concentrate the solids, after which the excess water was removed. This process yielded 10.5 L of concentrated sludge, which was then divided into three mineralization treatments, with each treatment receiving 3.5 L.

The 3.5 L sludge samples were transferred to 20 L buckets for each treatment: T1 (Anaerobic), T2 (Aerobic), and T3 (Aerobic + Molasses). Each sample was diluted to achieve a total solids (TS) concentration of $10\ \mathrm{g \cdot kg^{-1}}$ (Khiari et al. 2019), resulting in a final volume of 17.5 L of diluted sludge per treatment. For T3, commercial molasses was added as a carbon source to assess its potential to accelerate nutrient mineralization. The amount of molasses added was calculated based on the carbon (33%) and nitrogen (5.2%) content of the sludge's dry weight (Strauch et al. 2018; Putra et al. 2019) and the carbon content of the molasses, which was 24% (w/w) (Samocha et al. 2007). To achieve the desired C/N ratio of 20:1, known to enhance nutrient mineralization in African catfish sludge (Rahmatullah et al. 2020), the formula used to compute the required amount of molasses was adapted and modified from Putra et al. (2019):

$$M = \frac{[C_\mathrm{R} \times (\%N_\mathrm{S} \times S)] - (\%C_\mathrm{S} \times S)}{N_\mathrm{R} \times \%C_\mathrm{M}}$$

where M is the required molasses (w/w) [g], C_R is the carbon ratio, $\%N_\mathrm{S}$ is the nitrogen percentage of the sludge, S is the weight (w/w) of the sludge [g], $\%C_\mathrm{S}$ is the carbon percentage of the sludge, N_R is the nitrogen ratio, and $\%C_\mathrm{M}$ is the carbon percentage of the molasses.

T1 was subjected to anaerobic conditions with no aeration and covered with an airtight lid. T1 was not mixed or agitated for the whole duration of the experiment. Meanwhile, T2 and T3 were subjected to aerated conditions with an airstone for each of the buckets added and rested on the bottom to provide vigorous aeration and mixing in the buckets for the duration of the experiment. The diagram of the experimental design is shown in Fig. 1.

Supernatant collection and water analysis. Prior to the start of the experiment, samples were obtained from the liquid fraction of the collected sludge to assess the initial nutrient composition. During the mineralization experiment, samples were collected on Day 5, Day 10, and Day 15. Supernatant samples were collected using 500-mL polyethylene bottles and labeled accordingly. The samples were analyzed for total nitrogen, calcium, and magnesium at the Sugar Regulatory Administration (SRA) Agro-based Laboratory in Bacolod City, Negros Occidental. The Kjeldahl method, utilizing the Foss Tecator Digestion and Foss Kjeltec 8200 Auto Distillation Unit, was employed to determine total nitrogen (AOAC 1990). For calcium and magnesium, the EDTA (ethylenediamine-tetraacetic acid) titrimetric method was used. All analyses were conducted in triplicates.

Phosphorus and potassium analyses were performed at the Regional Organic Soils Laboratory of the Department of Agriculture, Western Visayas (ROSL DA-WV) in Jaro, Iloilo City. The vanadomolybdate method was employed for phosphorus determination, while the flame atomic absorption method was used to determine the potassium concentration. These samples were tested in duplicates. The generated data were analyzed and compared across treatments.

Changes in the concentrations of the nutrients before and after the mineralization treatments are computed as percent change (%) using the formula from Rakocy et al. (2007):

$$\mathrm{PC} = 100\,(C_\mathrm{FN} - C_\mathrm{IN}) \times C_\mathrm{IN}^{-1}$$

where PC is the percent change [%], C_FN is the final concentration of nutrients $[\mathrm{mg \cdot L^{-1}}]$, and C_IN is the initial concentration of nutrients $[\mathrm{mg \cdot L^{-1}}]$.

Water parameters (pH and temperature) for each treatment were monitored daily on-site using a multifunction aquaponics pH meter.

Statistical analysis. The data gathered from the results of the analyses were expressed as means of replicates and were subjected to a one-way analysis of variance (ANOVA). The level of significance at 0.05 was employed. A post-hoc Tukey Test was used if the F-value was less than 0.05 to determine which treatments differed significantly from each other within and between groups. Statistical computations were processed using IBM SPSS version 26 and Microsoft Excel.

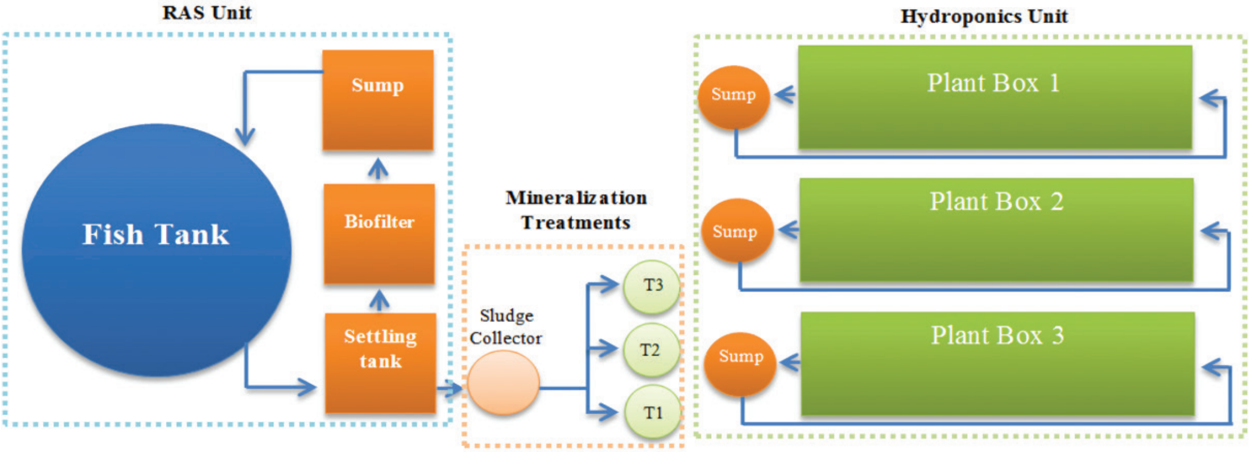

Figure 1. Diagram of the decoupled aquaponics system in FAS-UPV consisting of a RAS unit, hydroponics unit, and the experimental mineralization treatments.

Results

Temperature and pH parameters. During the experiment, the temperature (Fig. 2A) did not have major differences between the treatments, which ranged from 25.6 to 32.6°C. Meanwhile, the pH results (Fig. 2B) revealed that T3 had an acidic pH range of 3.36 to 5.91 compared to T1 and T2, with pH readings ranging from 5.8 to 7.39 and 5.97 to 7.42, respectively.

Sludge supernatant nutrient analysis. In this study, the catfish sludge water prior to mineralization had initial macroelement concentrations of 1060 mg · L^{-1} for nitrogen, 20 mg · L^{-1} for both phosphorus and potassium, 4846.2 mg · L^{-1} for calcium, and less than 170 mg · L^{-1} for magnesium. The performance of the three mineralization treatments, in terms of the concentrations of the five macronutrients essential for plants, namely nitrogen, phosphorus, potassium, calcium, and magnesium, over the 15-day mineralization period, is shown in Fig. 3.

For the total nitrogen, a sudden increase in the concentration was seen in T3 on Day 5 and a minimal increase in the following sampling days, with the maximum concentration at 2700 mg · L^{-1}. A notable increase was seen only after Day 15 in T2, with a final concentration of 2160 mg · L^{-1}, whereas for T1, the N concentration remained stagnant with very little increase (1072 mg · L^{-1}).

The phosphorus concentrations of the samples were tested as phosphate-phosphorus (PO$_4^+$-P) as it is the form that plants assimilate. P increased significantly only on Day 15 in T3, while for T1 and T2, the P concentrations decreased to less than 5 mg · L^{-1} and remained the same for the rest of the mineralization period.

Compared to phosphorus, however, potassium concentration in the sludge supernatant was slightly higher after mineralization as it was easily soluble in water. From the initial K concentration of 20 mg · L^{-1}, the K concentration of samples in T1 only ranged from 20 to 30 mg · L^{-1} and from 10 to 30 mg · L^{-1} for T2. Interestingly, there was a huge increase in the K concentration of the sludge in T3. On Day 5, the K content was recorded at 670 mg · L^{-1} and continued to increase on Day 10 reaching 830 mg · L^{-1}. However, on Day 15, the concentration slightly dropped to 720 mg · L^{-1}.

For calcium concentration after mineralization, T3 attained higher values than those of the samples T1 and T2. The highest Ca concentration of 12 115.6 mg · L^{-1} was recorded for T3 on Day 10 and Day 15. The Ca content for T2 also had a minimal increase on Day 5 with 7269.3 mg · L^{-1} and remained relatively the same for the succeeding days. On the other hand, the Ca concentrations for T1 decreased to 2423.1 mg · L^{-1}, which was half of the initial concentration, and no improvements were observed during the treatment.

Meanwhile, almost the same dynamics were observed for the magnesium concentration, where T3 obtained the highest concentrations. From the initial Mg level of less than 170 mg · L^{-1}, the Mg concentration in this treatment increased to 1695.9 mg · L^{-1} on Days 5 and 10, which doubled on Day 15 to 3391.9 mg · L^{-1}. Meanwhile, for T1 and T2, there is no notable increase in the Mg levels where the concentration remained constant to less than 170 mg · L^{-1}.

Notable changes were observed in the concentrations of the nutrients of the catfish sludge supernatant after subjecting the sludge to different mineralization treatments (Fig. 4). The results showed that among the three treatments, the macronutrients N, P, K, Ca, and Mg from the catfish sludge were best mineralized in T3 with percentage-point changes of 155, 400, 3500, 150, and 1895, respectively.

Discussion

Catfish culture in RAS is an efficient method for stocking catfish at very high densities in a limited space without compromising the water quality (Strauch et al. 2018). Effective wastewater treatment in RAS enables the stocking of African catfish, *C. gariepinus*, at densities up to 200 kg · m^{-3} (Palm et al. 2019). However, this system does not eliminate the risk of increased nutrient loads, as adjustments in feeding occur as the catfish grow. This leads to challenges similar to those faced in traditional intensive systems (Strauch et al. 2018). To address this drawback, nutrients can be recovered and utilized for other purposes, such as integrating a hydroponic compartment to form an aquaponic system. This integration allows nutrient-rich water from the catfish RAS to serve as an organic fertilizer for plant production while purifying the water that returns to the fish tank (Oladimeji et al. 2020).

Traditional single-loop aquaponics designs have several limitations, including reduced independent control over the hydroponic and fish tank units. This compromises the

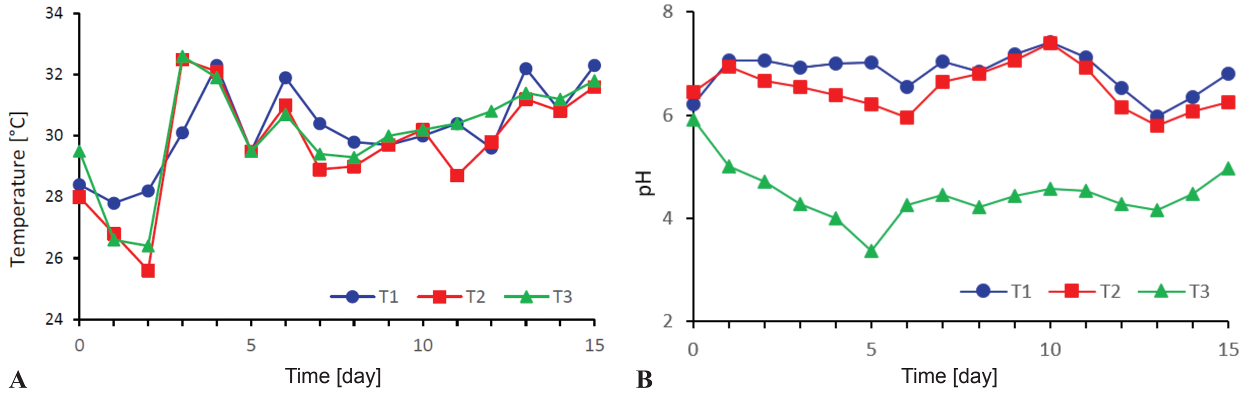

Figure 2. Variation of temperature and pH in the mineralization treatments over the 15-day experimental period. **A** temperature and **B** pH.

specific requirements for optimal growth for both plants and fish (Goddek et al. 2015). In contrast, the decoupled aquaponics system eliminates the loop by entirely separating each compartment. This separation can be achieved by incorporating an additional unit known as a mineralization chamber, which processes fish waste into organic fertilizer. The decoupling allows for complete manipulation of the water parameters including pH, temperature,

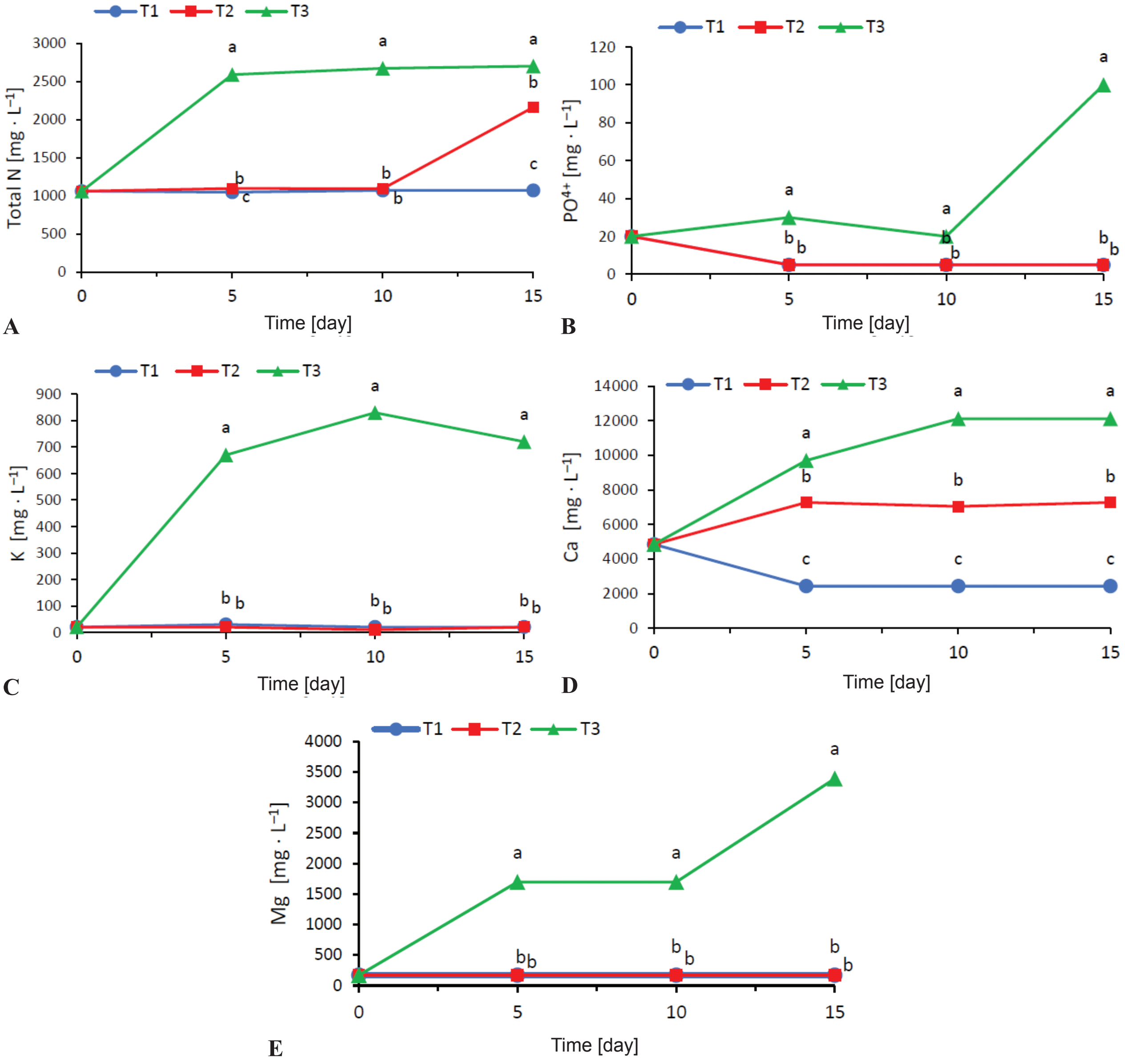

Figure 3. The concentrations of different nutrients over time under different mineralization treatments for 15 days. **A** nitrogen, **B** phosphorous, **C** potassium, **D** calcium, and **E** magnesium. Different lower-case letters indicate significant differences ($P < 0.05$).

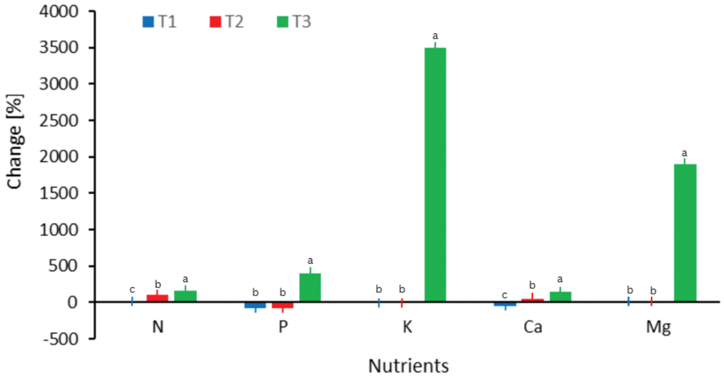

Figure 4. Changes in nutrient concentrations of sludge after subjecting to mineralization treatments for 15 days. Different lower-case letters indicate significant differences ($P < 0.05$).

and nutrient levels required to optimize each compartment without affecting the others (Lucas 2020).

Fish waste and uneaten feed, which contribute to sludge, contain significant amounts of macro and micronutrients essential for plant growth (Delaide et al. 2019). However, these nutrients are often bound in solid particles within the sludge and are not readily available for crops to assimilate, necessitating mineralization to recover these nutrients for use as organic fertilizer. In a decoupled aquaponics system, fish sludge, often discarded as waste, is treated in the mineralization chamber, which recovers nutrients bound in the sludge and reintroduces them into the hydroponics system as fertilizer (Pinho et al. 2021). Furthermore, the water directed to the hydroponics compartment does not recirculate back into the RAS, allowing nutrient concentration in the hydroponics unit for plant use (Lucas 2020).

Both aerobic and anaerobic mineralization methods show promise in recovering particle-bound nutrients, but each has distinct advantages and disadvantages (Delaide et al. 2019; Zhang et al. 2021). For this experiment, catfish sludge from the RAS underwent various on-site mineralization treatments to determine which method would enhance nutrient viability for hydroponically grown lettuce. The initial nutrient concentration in this study was consistent with the sludge water from an intensive African catfish RAS, as reported by Knaus et al. (2020). Applying the appropriate mineralization technique could significantly increase these concentrations, maximizing nutrient availability for the plants.

Noteworthy changes in nutrient concentration in the supernatant were observed after subjecting the catfish sludge to aerobic mineralization with carbon source addition (T3). This indicates that aerating the fish sludge and adding molasses effectively increased macronutrient availability within just 15 days of treatment. This duration is shorter than the prominent increases observed after 29 days in treatments involving simple aeration (Rakocy et al. 2007).

In this study, molasses served as a carbon source for heterotrophic microorganisms, thus accelerating bacterial growth in the system. Reported microorganisms present in aquaculture sludge include genera such as *Rhizobium*, *Flavobacterium*, *Acinetobacter*, *Aeromonas*, and *Pseudomonas* (see Sugita et al. 2005; Munguia-Fragozo et al. 2015). The growth of microbial populations, enhanced by a constant supply of oxygen and carbon sources, increases carbon dioxide production as a byproduct of respiration. Under aerobic mineralization conditions, heterotrophic bacteria break down organic matter, releasing bound nitrogen (N) into the supernatant (Panana et al. 2021). This study observed a marked increase in N concentration on Day 5 for T3, compared to the aerated treatment without a carbon source, which rose on Day 15. Unlike in a biofloc system, where produced bacterial biomass is consumed by cultured aquatic animals, the microbial biomass in the aerobic mineralization treatment with molasses continues to accumulate. This biomass, rich in protein, collectively known as single-celled protein (SCP), can contain up to 85% protein of its dry weight (Sillman et al. 2019). When these bacteria die, their protein becomes part of the organic matter, contributing to N availability in the supernatant.

Additionally, the increase in carbon dioxide from bacterial respiration forms carbonic acid, thereby lowering the pH in the system (Delaide et al. 2019). The drop in pH in T3 correlated with increased concentrations of macronutrients, highlighting the pH's role in solubilizing nutrients from insoluble mineral forms during mineralization. These nutrients became soluble when subjected to acidic conditions, thus increasing their concentrations in the supernatant (Delaide et al. 2019). However, in T2, nitrogen concentration also significantly increased on Day 15, despite a pH above 6.0. This suggests that N solubilization is more reliant on organic matter breakdown, particularly proteins, rather than solely on pH reduction (Panana et al. 2021).

Numerous studies have demonstrated pH's role in leaching nutrients such as phosphorus, potassium, calcium, and magnesium from fish sludge (Jung and Lovitt 2011; Panana et al. 2021). These minerals often become trapped in solid organic molecules within the sludge and are released in their ionic forms after mineralization. However, to maintain their solubilized ionic states, pH must be reduced to an acidic range to prevent nutrient precipitation (Delaide et al. 2019). Macroelements P, Ca, and Mg are effectively solubilized at pH levels below 6.0, facilitating solubilization of bones from fishmeal and minerals that trap these nutrients, like calcium phosphate and struvite (Stewart et al. 2006; Conroy and Couturier 2010). This is further supported by the finding from Goddek et al. (2018), which indicates improved release of P, Ca, and other essential macronutrients when mineralization treatments are acidic. In contrast, Jung and Lovitt (2011) found that adding a carbon source enhanced the fermentation process by anaerobic heterotrophic bacteria, resulting in organic acid production, a drop in pH, and facilitating nutrient leaching. In the presently reported study, although there was a declining trend in the pH of the anaerobic sludge treatment, it did not drop below 6.0, possibly due to the limited presence of hetero-lactic bacteria in the sludge and stagnant conditions of the mineralization setup.

Among the analyzed nutrients, T3 exhibited substantial increases in potassium and magnesium concentrations, with percentage-point increments of 3500 and 1895, respectively. The primary source of potassium in an aquaponics system is fish feeds, which contribute only a minimal amount, resulting in low concentrations in the system (Delaide et al. 2019). Potassium is highly soluble and can be present in the liquid fraction of the sludge even before the mineralization treatments (Panana et al. 2021). The high K concentration in T3 can be attributed to the molasses added during treatment, as it is a source of potassium fertilizer (Otani et al. 2023). Magnesium typically originates from tap water and is also present in trace amounts in fish feeds (Delaide et al. 2019). Under neutral or higher pH conditions, Mg in the system can precipitate into struvite ($NH_4MgPO_4{\cdot}6H_2O$), whereas it can be effectively solubilized in acidic conditions (Zhang et al. 2016). The solubilization of struvite releases both Mg and P, explaining the similar trends for both nutrients in T3, where pH dropped as low as 3.36. Conversely, treatments T1 and T2, which maintained non-acidic pH ranges, exhibited low concentrations or declines in P, K, Ca, and Mg. Higher pH levels facilitate the precipitation of these minerals into insoluble forms, thereby reducing their availability in the supernatant (Zhang et al. 2016; Delaide et al. 2019; Eck et al. 2019).

Overall, fish sludge mineralization through aeration with molasses addition represents a promising approach for nutrient recovery in a decoupled aquaponics system, potentially reducing reliance on inorganic nutrient solutions typically used in hydroponics. Contrary to previous literature suggesting Ca deficiency in coupled aquaponics systems (Seawright et al. 1998; Schmautz et al. 2017), the results indicate that aeration with molasses mineralization can enhance Ca concentrations to levels sufficient for hydroponic lettuce growth. The resulting concentrations of Ca and Mg reached the sufficiency range of 0.8% to 1.2% and 0.2% to 0.7%, respectively, as recommended for hydroponic lettuce growth (Pickens et al. 2022). However, the concentrations of other macronutrients, N, P, and K, remained lower than the optimal levels for hydroponically grown lettuce. This limitation reflects the inherent challenges in controlling nutrient composition derived from biological processes involved in mineralization, which may necessitate supplementary inorganic fertilizers to achieve optimal growth.

Conclusion

A significant amount of nutrients can be recovered from intensive African catfish RAS sludge when subjected to aerobic mineralization with the addition of a carbon source. The results revealed that African catfish sludge treated with aeration and molasses achieved significantly higher concentrations of N, P, K, Ca, and Mg indicating its potential as an organic fertilizer for plants in aquaponics.

Integrating aeration and organic carbon sources into the mineralization of fish sludge in a decoupled aquaponics system offers a sustainable approach to nutrient recovery. This research provides valuable insights into optimizing nutrient availability for plant production while addressing waste management challenges in aquaculture systems.

Acknowledgments

The authors acknowledge the Commission on Higher Education (CHED) Tourism Studies on Island-Based Opportunities for Growth (TSIBOG) in Western Visayas Program, particularly Project 5: UPV Aquaponics Agritourism—Technology Demonstration Farm and Experiment Station for Integrated Farming (Agriculture, Freshwater, and Marine), for funding this study. We also express our gratitude to the Institute of Aquaculture, College of Fisheries and Ocean Sciences, University of the Philippines Visayas, for their technical assistance, provision of facilities, and overall support, which were essential to the completion of this research.

Special appreciation is extended to Dr. Rex Ferdinand M. Traifalgar for his valuable insights and unwavering support, which greatly enriched this study. Furthermore, we sincerely thank the project staff Mr. Carl Luigi M. Cervantes, Ms. Christine N. Fabrigas, Mr. Reynaldo T. Nuñeza, and Mr. Philip C. Nim for their invaluable assistance, which was instrumental in the successful completion of this research.

References

AOAC (1990) Official methods of analysis of the Association of Official Analytical Chemists. 15th edn. Association of Official Analytical Chemists, Arlington, VA, USA.

Cao L, Wang W, Yang Y, Yang C, Yuan Z, Xiong S, Diana J (2007) Environmental impact of aquaculture and countermeasures to aquaculture pollution in China. Environmental Science and Pollution Research International 14(7): 452–462. https://doi.org/10.1065/espr2007.05.426

Conroy J, Couturier M (2010) Dissolution of minerals during hydrolysis of fish waste solids. Aquaculture 298(3–4): 220–225. https://doi.org/10.1016/j.aquaculture.2009.11.013

Delaide B, Goddek SJ, Keesman KM, Jijakli MH (2018) A methodology to quantify the aerobic and anaerobic sludge digestion performance for nutrient recycling in aquaponics. BASE 22 (2): 106–112. https://doi.org/10.25518/1780-4507.16406

Delaide B, Monsees H, Gross A, Goddek S (2019) Aerobic and anaerobic treatments for aquaponic sludge reduction and mineralisation. Pp. 247–266. In: Goddek S, Joyce A, Kotzen B, Burnell GM (Eds.) Aquaponics food production systems: Combined aquaculture and hydroponic production technologies for the future. Springer International Publishing, Cham, Switzerland. https://doi.org/10.1007/978-3-030-15943-6_10

Eck M, Körner O, Jijakli MH (2019) Nutrient cycling in aquaponics systems. Pp. 231–246. In: Goddek S, Joyce A, Kotzen B, Burnell GM (Eds.) Aquaponics food production systems: Combined aquaculture and hydroponic production technologies for the future. Springer International Publishing, Cham, Switzerland. https://doi.org/10.1007/978-3-030-15943-6_9

Espinal CA, Matulić D (2019) Recirculating Aquaculture Technologies. Pp. 35–76. In: Goddek S, Joyce A, Kotzen B, Burnell GM (Eds.) Aquaponics food production systems: Combined aquaculture and hydroponic production technologies for the future. Springer International Publishing, Cham, Switzerland. https://doi.org/10.1007/978-3-030-15943-6_3

Goddek S, Delaide B, Mankasingh U, Ragnarsdottir KV, Jijakli H, Thorarinsdottir R (2015) Challenges of sustainable and commercial aquaponics. Sustainability 7(4): 4199–4224. https://doi.org/10.3390/su7044199

Goddek S, Espinal CA, Delaide B, Jijakli MH, Schmautz Z, Wuertz S, Keesman KJ (2016) Navigating towards decoupled aquaponic systems: A system dynamics design approach. Water 8(7): 303. https://doi.org/10.3390/w8070303

Goddek S, Delaide BPL, Joyce A, Wuertz S, Jijakli MH, Gross A, Eding EH, Bläser I, Reuter M, Keizer LCP, Morgenstern R, Körner O, Verreth J, Keesman KJ (2018) Nutrient mineralization and organic matter reduction performance of RAS-based sludge in sequential UASB-EGSB reactors. Aquacultural Engineering 83: 10–19. https://doi.org/10.1016/j.aquaeng.2018.07.003

Jung IS, Lovitt RW (2011) Leaching techniques to remove metals and potentially hazardous nutrients from trout farm sludge. Water Research 45(18): 5977–5986. https://doi.org/10.1016/j.watres.2011.08.062

Khiari Z, Kaluthota S, Savidov N (2019) Aerobic bioconversion of aquaculture solid waste into liquid fertilizer: Effects of bioprocess parameters on kinetics of nitrogen mineralization. Aquaculture 500: 492–499. https://doi.org/10.1016/j.aquaculture.2018.10.059

Knaus U, Pribbernow M, Xu L, Appelbaum S, Palm HW (2020) Basil (*Ocimum basilicum*) Cultivation in decoupled aquaponics with three hydro-components (grow pipes, raft, gravel) and African catfish (*Clarias gariepinus*) production in northern Germany. Sustainability 12(20): 8745. https://doi.org/10.3390/su12208745

Lucas HL (2020) Analysis of plant biomass production comparing decoupled aquaponics against equivalent single-loop aquaponic and hydroponic systems growing *Lactuca sativa*. MSc Thesis, University of Wisconsin–Milwaukee Milwaukee, WI, USA. [Published in Theses and Dissertations, 2552. https://dc.uwm.edu/etd/2552]

Munguia-Fragozo P, Alatorre-Jacome O, Rico-Garcia E, Torres-Pacheco I, Cruz-Hernandez A, Ocampo-Velazquez RV, Garcia-Trejo JF, Guevara-Gonzalez RG (2015) Perspective for aquaponic systems: "Omic" Technologies for Microbial Community Analysis. BioMed Research International 2015: e480386. https://doi.org/10.1155/2015/480386

Oladimeji SA, Okomoda VT, Olufeagba SO, Solomon SG, Abol-Munafi AB, Alabi KI, Ikhwanuddin M, Martins CO, Umaru J, Hassan A (2020) Aquaponics production of catfish and pumpkin: Comparison with conventional production systems. Food Science and Nutrition 8(5): 2307–2315. https://doi.org/10.1002/fsn3.1512

Otani T, Ando H, Goshima T, Mizuta K, Nii S (2023) Enhanced recovery of potassium from sugarcane molasses for fertilizer. Sugar Tech 25: 820–826. https://doi.org/10.1007/s12355-023-01248-1

Palm HW, Knaus U, Appelbaum S, Strauch SM, Kotzen B (2019) Coupled Aquaponics Systems. Pp. 163–199. In: Goddek S, Joyce A, Kotzen B, Burnell GM (Eds.) Aquaponics food production systems: Combined aquaculture and hydroponic production technologies for the future. Springer International Publishing, Cham, Switzerland. https://doi.org/10.1007/978-3-030-15943-6_7

Panana E, Delaide B, Teerlinck S, Bleyaert P (2021) Aerobic treatment and acidification of pikeperch (*Sander lucioperca* L.) sludge for nutrient recovery. Aquaculture International 29(2): 539–552. https://doi.org/10.1007/s10499-020-00640-y

Pickens J, Wells D, Blanchard C (2022) Greenhouse lettuce production. Alabama Cooperative Extension System. Opelika, AL, USA.

Pinho SM, David LH, Garcia F, Keesman K, Portella MC, Goddek S (2021) South American fish species suitable for aquaponics: a review. Aquaculture International 29: 1427–1449. https://doi.org/10.1007/s10499-021-00674-w

PSA (2023) Aquaculture: Volume of production by species, geolocation, year and quarter. Philippine Statistics Authority (PSA), Quezon City, Philippines.

Putra I, Effendi I, Lukistyowati I, Tang UM (2019) Growth and survival rate of red tilapia (*Oreochromis* sp.) cultivated in the brackish water tank under Biofloc system. Advances in Engineering Research [International Conference of CELSciTech 2019 - Science and Technology track (ICCELST-ST 2019)] 190: 96–99. https://doi.org/10.2991/iccelst-st-19.2019.19

Rahmatullah HD, Prayogo, Rahardja BS (2020) Different addition of molasses on feed conversion ratio and water quality in catfish (*Clarias* sp.) rearing with biofloc-aquaponic system. IOP Conference Series. Earth and Environmental Science 441(1): 012122. https://doi.org/10.1088/1755-1315/441/1/012122

Rakocy JE, Bailey DS, Shultz RC, Danaher JJ (2007) Preliminary evaluation of organic waste from two aquaculture systems as a source of inorganic nutrients for hydroponics. Acta Horticulturae (742): 201–207. https://doi.org/10.17660/ActaHortic.2007.742.27

Samocha TM, Patnaik S, Speed M, Ali A-M, Burger JM, Almeida RV, Ayub Z, Harisanto M, Horowitz A, Brock DL (2007) Use of molasses as carbon source in limited discharge nursery and grow-out systems for *Litopenaeus vannamei.* Aquacultural Engineering 36(2): 184–191. https://doi.org/10.1016/j.aquaeng.2006.10.004

Schmautz Z, Graber A, Jaenicke S, Goesmann A, Junge R, Smits THM (2017) Microbial diversity in different compartments of an aquaponics system. Archives of Microbiology 199(4): 613–620. https://doi.org/10.1007/s00203-016-1334-1

Seawright DE, Stickney RR, Walker RB (1998) Nutrient dynamics in integrated aquaculture–hydroponics systems. Aquaculture 160(3–4): 215–237. https://doi.org/10.1016/S0044-8486(97)00168-3

Setiadi E, Taufik I, Widyastuti YR, Ardi I, Puspaningsih D (2019) Improving productivity and water quality of catfish, *Clarias* sp. cultured in an aquaponic ebb-tide system using different filtration. IOP Conference Series. Earth and Environmental Science 236: e012026. https://doi.org/10.1088/1755-1315/236/1/012026

Sillman J, Nygren L, Kahiluoto H, Ruuskanen V, Tamminen A, Bajamundi C, Nappa M, Wuokko M, Lindh T, Vainikka P, Pitkanen JP, Ahola J (2019) Bacterial protein for food and feed generated via renewable energy and direct air capture of CO2: Can it reduce land and water use? Global Food Security 22(1): 25–32. https://doi.org/10.1016/j.gfs.2019.09.007

Stewart NT, Boardman GD, Helfrich LA (2006) Characterization of nutrient leaching rates from settled rainbow trout (*Oncorhynchus mykiss*) sludge. Aquacultural Engineering 35(2): 191–198. https://doi.org/10.1016/j.aquaeng.2006.01.004

Strauch SM, Wenzel LC, Bischoff A, Dellwig O, Klein J, Schüch A, Wasenitz B, Palm HW (2018) Commercial African catfish (*Clarias gariepinus*) recirculating aquaculture systems: Assessment of element and energy pathways with special focus on the phosphorus cycle. Sustainability 10(6): 1805. https://doi.org/10.3390/su10061805

Sugita H, Nakamura H, Shimada T (2005) Microbial communities associated with filter materials in recirculating aquaculture systems of freshwater fish. Aquaculture 243(1–4): 403–409. https://doi.org/10.1016/j.aquaculture.2004.09.028

Suhl J, Dannehl D, Kloas W, Baganz D, Jobs S, Scheibe G, Schmidt U (2016) Advanced aquaponics: Evaluation of intensive tomato production in aquaponics vs. conventional hydroponics. Agricultural Water Management 178: 335–344. https://doi.org/10.1016/j.agwat.2016.10.013

Zhang X, Hu J, Spanjers H, van Lier JB (2016) Struvite crystallization under a marine/brackish aquaculture condition. Bioresource Technology 218: 1151–1156. https://doi.org/10.1016/j.biortech.2016.07.088

Zhang H, Gao Y, Liu J, Lin Z, Lee CT, Hashim H, Wu W-M, Li C (2021) Recovery of nutrients from fish sludge as liquid fertilizer to enhance sustainability of aquaponics: A review. Chemical Engineering Transactions 83: 55–60. https://doi.org/10.3303/CET2183010

Acta Ichthyologica et Piscatoria 54, 2024, 283–286 | DOI 10.3897/aiep.54.138051

PENSOFT.

ACTA
ICHTHYOLOGICA
ET PISCATORIA

First records of xanthochromism in common snook, *Centropomus undecimalis* (Actinopterygii: Carangiformes: Centropomidae), collected in the Gulf of Mexico

Armando T. WAKIDA-KUSUNOKI[1], Vicente ANISLADO-TOLENTINO[2], Luis Fernando DEL MORAL-FLORES[3], Rodolfo CASTRO-BARBOSA[4]

1 *Centro Regional de Investigación Acuícola y Pesquera de Yucalpetén, Instituto Mexicano de Investigación en Pesca y Acuacultura Sustentables, Yucalpetén, Progreso, YUC, Mexico*
2 *Grupo de Investigadores Libres Sphyrna, Querétaro, QUE, Mexico*
3 *Facultad de Estudios Superiores Iztacala, Universidad Nacional Autónoma de México (UNAM), Tlalnepantla, MEX, Mexico*
4 *Centro Regional de Investigación Acuícola y Pesquera de Ciudad del Carmen, Instituto Mexicano de Investigación en Pesca y Acuacultura Sustentables, Carmen, CAM, Mexico*

https://zoobank.org/1217BB42-4429-419A-A08B-57789786AE0A

Corresponding author: Vicente Anislado-Tolentino (anislado@gmail.com)

Academic editor: Sanja Matić-Skoko ♦ **Received** 28 September 2024 ♦ **Accepted** 13 November 2024 ♦ **Published** 17 December 2024

Citation: Wakida-Kusunoki AT, Anislado-Tolentino V, Del Moral-Flores LF, Castro-Barbosa R (2024) First records of xanthochromism in common snook, *Centropomus undecimalis* (Actinopterygii: Carangiformes: Centropomidae), collected in the Gulf of Mexico. Acta Ichthyologica et Piscatoria 54: 283–286. https://doi.org/10.3897/aiep.54.138051

Abstract

The first case of xanthochromism in a female common snook, *Centropomus undecimalis* (Bloch, 1792), in the southern Gulf of Mexico is described. The specimen supporting this record was caught off the coast of Tabasco, Mexico and it represents the first fish case of this abnormal coloration in the Gulf of Mexico. The analyzed specimen measured 774 mm in total length. Its body was entirely orange with a lighter shade of orange on the belly, while the normal coloration of this fish species is dark to opaque grey with yellow to green tints on the dorsal part, silvery lateral side, white belly, and black lateral line. It is uncertain what caused this abnormality, but it is hypothesized that multiple environmental stressors, natural and anthropogenic, were responsible for the appearance of this particular abnormality and other similar cases in the area. Additional sampling and long-term monitoring are needed to determine the possible causes and their ecological impacts.

Keywords

abnormalities, coloration, southwestern Gulf of Mexico, Tabasco, xanthism

Introduction

Colors and color patterns are particularly rich in fishes. The two primary functions of pigments in animals are to shield them against sunlight and hide from predators (Nüsslein-Volhard and Singh 2017). Color variation is an imperative component of inter- and intra-specific species interactions (e.g., predation, competition, sexual selection, and life stage identification), learning, and communication (Siebeck et al. 2008; Price et al. 2009; Leclercq et al. 2010).

Xanthism or xanthochromism (yellow) is a particular form of hypomelanosis, where bright yellow or orange body coloration becomes prevalent (Jawad et al. 2017). This is recognized as a genetic disorder that reduces the production of black melanin and causes dominance of yellow pigments in certain parts or the whole body of the animal (Colihueque 2010). Cases of total xanthochromism have been identified in several marine and freshwater fish families (Schwartz 1978). There are also many reports in which only body parts are xanthochromic (Jawad and Ibrahim 2018). In marine fishes, specifically, this abnormality has been reported (totally or partially expressed) in a total of 68 species, including seven chondrichthyans and 61 teleosts (Bañón et al. 2023). This article reports the first case of xanthochromism in a common snook, *Centropomus undecimalis*.

Materials and methods

A common snook with an abnormal coloration was landed on 12 May 2021 from a commercial catch of a small-scale fleet in José María Morelos y Pavón, Tabasco, southern Gulf of Mexico (18°25′31″N, 093°8′26″W). The specimen was captured 10 km northeast of José María Morelos y Pavón, Tabasco, Mexico (18°30′13″N, 093°6′54″W; Fig. 1), by a 7.62 m fishing boat with an outboard motor, using gill net with 152.4 mm mesh size, at a maximum depth of 22 m. The depth information was given by the fisherman, and this was estimated using a Garmin fish finder. The taxonomic key of Rivas (1986) was utilized to identify the species. The individual was measured to the nearest 0.1 cm total length (TL) and standard length (SL) following the morphometrics proposed by Rivas (1986). Gutted weight was obtained using a commercial Torrey weight scale. Once the fisherman eviscerated the specimen, the gonads were analyzed to determine sex and maturity stage using the table of macroscopic characteristics of Caballero-Chávez (2011). Since the common snook is a commercial species, after landing, it was transported to the La Viga fish market in Mexico City.

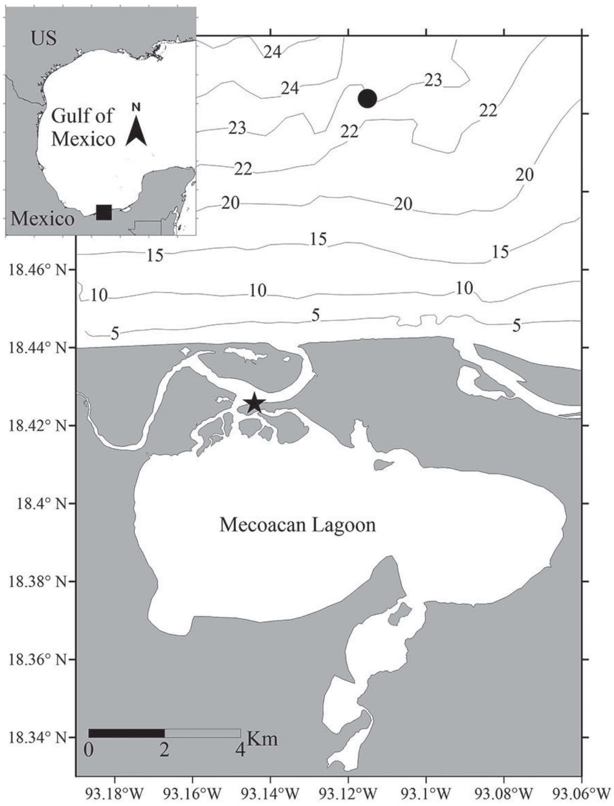

Figure 1. Capture site of a common snook, *Centropomus undecimalis*, with abnormal coloration from the southern Gulf of Mexico. Black circle marks the capture location, and the star indicates the landing site of specimen.

Results

The TL of the female specimen was 774 mm, and the gutted weight was 5 kg. Most of the fish surface, including the fins, lateral line, and dorsal part of the body, was orange, whereas the ventral part was whitish orange (Fig. 2A). The specimen was identified as *Centropomus undecimalis* based on the following combination of characteristics: an anal fin with three spines and six rays; 72 scales in the lateral line; the pectoral fins similar in length to the pelvic fins; and the third dorsal spine higher than the fourth when the fin is extended. Specimens of *C. undecimalis* normally have coloration ranges from dark brown to dull gray with a yellow to green tint on the dorsal surface (Fig. 2B). The lateral surface tends to be silvery, and the ventral surface is generally white. The pectoral fins, pelvic fins, second dorsal fin, and the dorsal lobe of the caudal fin usually are all bright yellow in color, however, some specimens are considerably darker.

Discussion

In Mexico there are four described cases of xanthochromism in fishes representing different families such as Leuciscidae (see Contreras et al. 1985), Epinephelidae (see Irygoyen-Arredondo et al. 2017), Kyphosidae (see Valencia-Méndez et al. 2018), and Pomacentridae (see Palacios-Salgado and Rojas-Herrera 2012). None of these cases were reported from the Gulf of Mexico.

The presently reported, common snook with the abnormal coloration had a normal and clearly healthy appearance (Fig. 2). According to some authors, the survival rate of organisms with xanthochromism is low compared to organisms with normal coloration because they are easier to detect by predators. However, the organisms that have been reported are healthy specimens and capable of reproducing, which could suggest that the abnormality in their coloration does not affect their ability to survive (Endler 1980; Golani et al. 2019; Jawad et al. 2021).

Among the possible causes or triggers of xanthochromism that are mentioned are: nutrition (Leclercq et al. 2010), the mutation of recessive genes (Dunham and Childers 1980; Pawar and Jawad 2017; San Gil-León and Angulo 2021), parasitic infections (Irigoyen-Arredondo et al. 2017), the presence of contaminants (Macieira et al. 2006; Irigoyen-Arredondo et al. 2017), or the presence of wounds caused by other organisms during antagonistic interactions (Colman 1972). The cause of the abnormality of the presently reported specimen is unknown.

According to the fisherman, this is not the first time that the phenomenon has been observed in the area. They mention that cases of xanthochromism had been observed in the common snook (Fig. 3), as well as in other species such as the crevalle jack, *Caranx hippos* (Linnaeus, 1766). On the other hand, cases of color and morphological abnormalities have recently been reported in the common snook and other fish species in the area (Wakida-Kusunoki et al. 2023); this suggests that there is one or more environmental stressors that could be causing these alterations. In this particular area, oil extraction and related activities are intense, so pollution is also a possible cause, although this has not been proven. Therefore, it is necessary to carry out more exhaustive studies and sampling focused on determining the causes of these abnormalities.

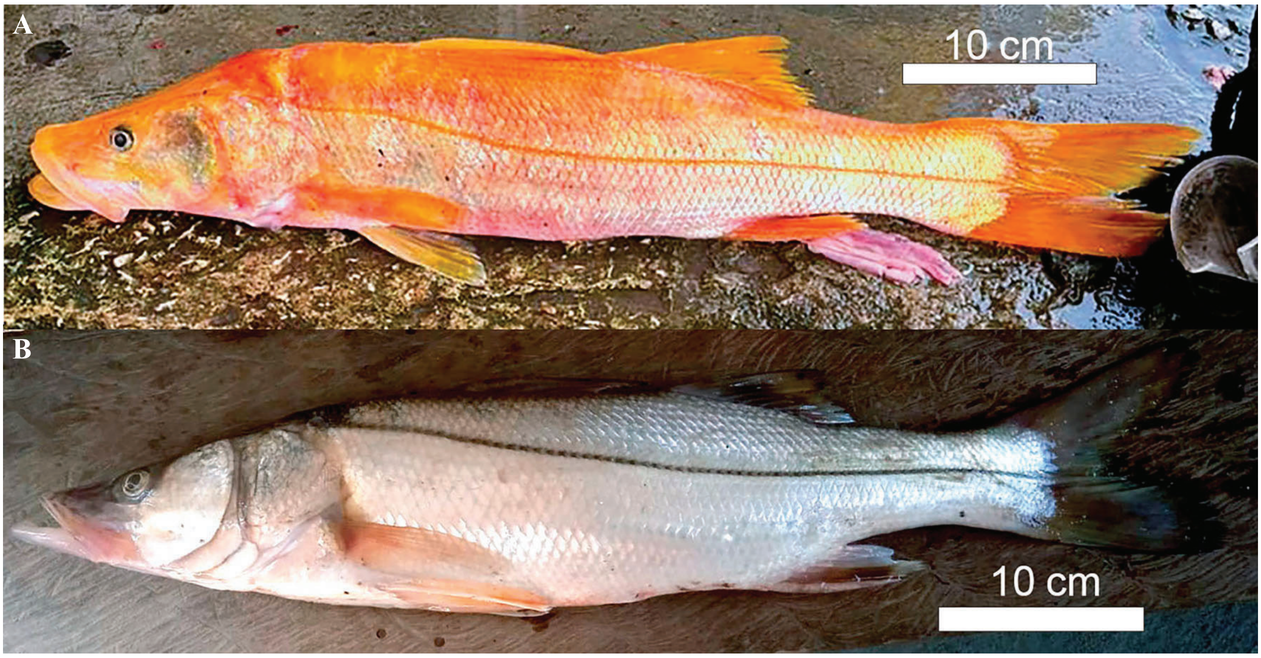

Figure 2. Lateral view of a common snook, *Centropomus undecimalis*, with xanthochromism reported in this study (774 mm TL) (**A**); Lateral view of common snook with normal color, (600 mm TL) (**B**).

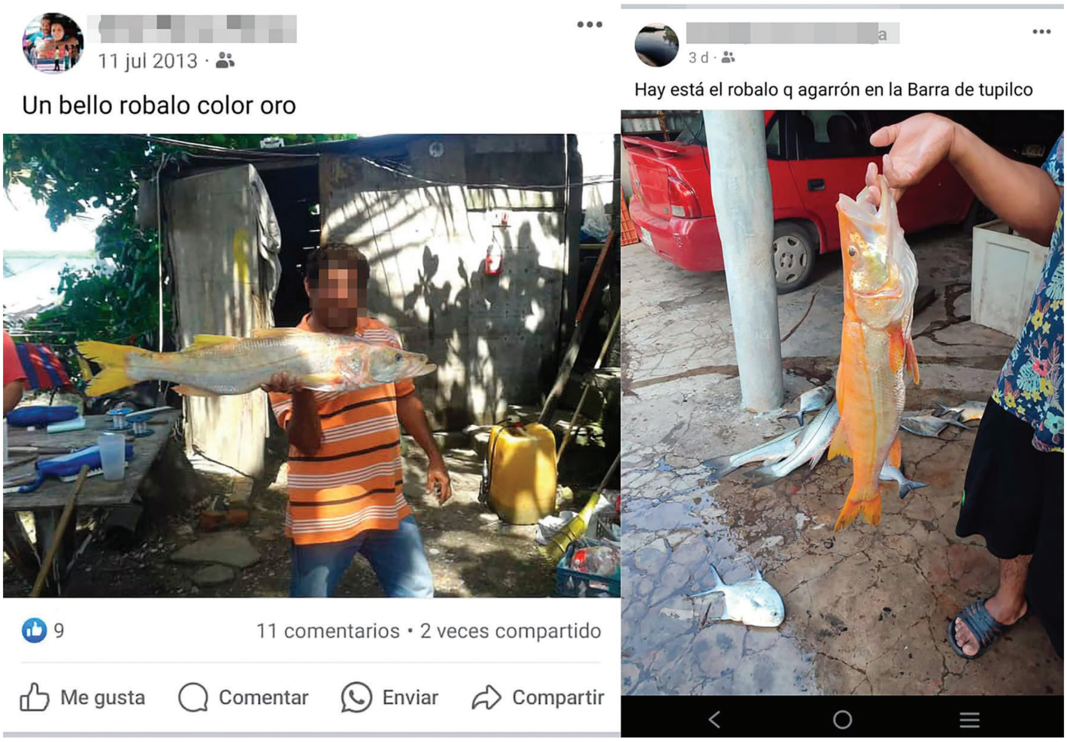
[redacted]

11 jul 2013 ·

Un bello robalo color oro

9

11 comentarios • 2 veces compartido

[redacted]

3 d ·

Hay está el robalo q agarrón en la Barra de tupilco

Figure 3. Photographs of other cases of xanthochromism in common snook, *Centropomus undecimalis*, reported in social networks from the same area.

Acknowledgments

We would like to thank Elain Pérez Pérez, fisherman from José María Morelos y Pavón, Tabasco for providing the information regarding the specimen, as well as the fishing information. We would also like to thank Alejandro Pérez Muñoz for the information provided, anonymous reviewers for suggestions, and the Sistema Nacional de Investigadoras e Investigadores-Consejo Nacional de Humanidades, Ciencia y Tecnología (SNII-CONAHCyT) for financial support.

References

Bañón R, Quigley DTG, Cerdeira D, De Carlos A (2023) A review of xanthochromic malpigmentation in wild marine fishes with the first case in *Diplodus puntazzo* (Walbaum, 1792) (Spariformes: Sparidae). Cybium 47(2): 197–205. https://doi.org/10.26028/cybium/2023-017

Caballero-Chávez V (2011) Reproducción y fecundidad del robalo blanco (*Centropomus undecimalis*) en el suroeste de Campeche. Ciencia Pesquera 19: 35–45.

Colihueque N (2010) Genetics of salmonid skin pigmentation: Clues and prospects for improving the external appearance of farmed salmonids. Reviews in Fish Biology and Fisheries 20(1): 71–86. https://doi.org/10.1007/s11160-009-9121-6

Colman JA (1972) Abnormal pigmentation in the sand flounder. New Zealand Journal of Marine and Freshwater Research 6(1–2): 208–213. https://doi.org/10.1080/00288330.1977.9515419

Contreras S, Contreras A, Torres M, Barajas L (1985) Anomalías de peces mexicanos i. Un gila c. Conspersa xantocromico del río Nazas ii. Un *Astyanax mexicanus* desprovisto de guanina del río San Juan (Pisces: Cyprinidae, Characidae). Publicaciones biológicas – Instituto de Investigaciones Científicas UANL 2(1): 91–104.

Dunham RA, Childers WF (1980) Genetics and implications of the golden color morph in green sunfish. Progressive Fish-Culturist 42(3): 160–163. https://doi.org/10.1577/1548-8659(1980)42[160:GAIOTG]2.0.CO;2

Endler JA (1980) Natural selection on color patterns in *Poecilia reticulata*. Evolution; International Journal of Organic Evolution 34(1): 76–91. https://doi.org/10.2307/2408316

Golani D, Corsini-Foka M, Tikochinski Y (2019) The occurrence of two xanthochromic fish, *Epinephelus marginatus* (Serranidae) and *Diplodus vulgaris* (Sparidae) (Osteichthyes) in the eastern Mediterranean. Zoology in the Middle East 65(3): 215–220. https://doi.org/10.1080/09397140.2019.1627700

Irigoyen-Arredondo MS, Escobar-Sánchez O, Abitia-Cárdenas LA, Moreno-Sánchez XG, Palacios-Salgado DS (2017) Incidence of xanthism in the leopard grouper *Mycteroperca rosacea* (Perciformes: Serranidae) in the Gulf of California. Marine Biodiversity 48(4): 2255–2258. https://doi.org/10.1007/s12526-017-0753-9

Jawad LA, Ibrahim M (2018) First record of abnormal body coloration in fishes obtained from Jubail Area, Arabian Gulf, Saudi Arabia. International Journal of Material Science 7(32): 308–315. https://doi.org/10.5376/ijms.2017.07.0032

Jawad LA, Al-Busaidi HK, Al-Mamary D, Al-Rassadi A, Al-Mamry JM (2017) Malpigmentation in *Diagramma pictum* and *Pardachirus marmoratus* collected from the Arabian sea coasts of Oman. International Journal of Material Science 7(30): 292–296. https://doi.org/10.5376/ijms.2017.07.0030

Jawad LA, Moazzam M, Osmany HB, Rahim A (2021) First records of xanthochromism in four marine fish species collected from the Arabian Sea coasts of Pakistan. Thalassas 37(2): 897–903. https://doi.org/10.1007/s41208-021-00318-z

Leclercq E, Taylor J, Migaud H (2010) Morphological skin colour changes in teleosts. Fish and Fisheries 11(2): 159–193. https://doi.org/10.1111/j.1467-2979.2009.00346.x

Macieira RM, Joyeux JC, Chagas LP (2006) Ambicoloration and morphological aberration in the sole *Achirus declivis* (Pleuronectiformes: Achiridae) and two other cases of color abnormalities in achirid soles from southeastern Brazil. Neotropical Ichthyology 4(2): 287–290. https://doi.org/10.1590/S1679-62252006000200016

Nüsslein-Volhard C, Singh AP (2017) How fish color their skin: A paradigm for development and evolution of adult patterns. BioEssays 39(3): e1600231. https://doi.org/10.1002/bies.201600231

Palacios-Salgado DS, Rojas-Herrera AA (2012) Partial xanthism in a specimen of Acapulco major, *Stegastes acapulcoensis* (Teleostei: Pomacentridae) from the Tropical Eastern Pacific. Pan-American Journal of Aquatic Sciences 7(3): 175–177.

Pawar RT, Jawad LA (2017) First report of a xanthic phenotype of the silver carp, *Hypophthalmichthys molitrix* (Valenciennes, 1844) (Teleostei: Cyprinidae) from Maharashtra Fish Seed Production Centre, India. International Journal of Aquaculture 7(715): 101–105. https://doi.org/10.5376/ija.2017.07.0015

Price AC, Weadick CJ, Shim J, Rodd FH (2009) Pigments, patterns, and fish behavior. Zebrafish 5(4): 297–307. https://doi.org/10.1089/zeb.2008.0551

Rivas LR (1986) Systematic review of the Perciform fishes of the genus *Centropomus*. Copeia 3(3): 579–611. https://doi.org/10.2307/1444940

San Gil-León J, Angulo A (2021) Xantismo en peces cíclidos (Cichliformes: Cichlidae) costarricenses, y variación ontogenética en *Parachromis dovii*. Cuadernos de Investigación UNED 13(1): e3093. https://doi.org/10.22458/urj.v13i1.3093

Schwartz FJ (1978) Xanthochromism in *Epinephelus drummondhayi* (Pisces: Serranidae) caught off North Carolina. Northeast Gulf Science 2(1): 62–64. https://doi.org/10.18785/negs.0201.06

Siebeck UE, Wallis GM, Litherland L (2008) Colour vision in coral reef fish. Journal of Experimental Biology 211(3): 354–360. https://doi.org/10.1242/jeb.012880

Valencia-Méndez O, Domínguez-Domínguez O, López-Pérez A, Martínez-Gómez JE, Ayala-Bocos A (2018) Partial albinism in the Revillagigedo sea chub *Kyphosus sectatrix* (Perciformes: Kyphosidae) from Clarion Island, Mexico. Revista Mexicana de Biodiversidad 89(2): 572–576. https://doi.org/10.22201/ib.20078706e.2018.2.2242

Wakida-Kusunoki AJ, Carrillo-Birkhahn L, Del Moral-Flores LF, Anislado-Tolentino V (2023) Lateral line abnormality in common snook *Centropomus undecimalis* (Bloch, 1792) from the southern Gulf of Mexico. Gulf and Caribbean Research 34(1): SC13–SC19. https://doi.org/10.18785/gcr.3401.18

Acta Ichthyologica et Piscatoria 54, 2024, 287–297 | DOI 10.3897/aiep.54.132489

PENSOFT.

ACTA
ICHTHYOLOGICA
ET PISCATORIA

Distribution and growth of Nga Myin Yinn, *Silonia silondia* (Actinopterygii: Siluriformes: Schilbeidae), in the Ayeyarwady River, Myanmar

Aye Aye MIN[1*], Toe Toe SOE[2*], Thida Lay THWE[2,3], Pwint Thu AYE[2], Than Than LWIN[1], Ye Win THAUNG[1], Tint LWIN[1], Aung Naing OO[1], Wai Lin MAUNG[1], Khin Maung MAW[1], Shota HOSONO[4,5], Hiroyuki MATSUI[4], Shota MITSUI[4,6], Takeshi TERAHARA[4], Masato ENDO[4], Masashi YOKOTA[4], Takeshi KOBAYASHI[4]

1 *Ministry of Agriculture, Livestock and Irrigation, Department of Fisheries, NayPyiTaw, Myanmar*
2 *Department of Zoology, University of Yangon, Yangon, Myanmar*
3 *Department of Zoology, Yangon University of Distance Education, Yangon, Myanmar*
4 *Graduate School of Marine Science and Technology, Tokyo University of Marine Science and Technology, Tokyo, Japan*
5 *Atmosphere and Ocean Research Institute, University of Tokyo, Chiba, Japan*
6 *Marine Biological Research Institute of Japan, Co., Ltd., Tokyo, Japan*

https://zoobank.org/4FF080E5-8ADA-4788-A512-9D34E6B6E457

Corresponding author: Masashi Yokota (yokota@kaiyodai.ac.jp)

Academic editor: Jan Kotusz ♦ **Received** 22 July 2024 ♦ **Accepted** 26 November 2024 ♦ **Published** 20 December 2024

Citation: Min AA, Soe TT, Thwe TL, Aye PT, Lwin TT, Thaung YW, Lwin T, Oo AN, Maung WL, Maw KM, Hosono S, Matsui H, Mitsui S, Terahara T, Endo M, Yokota M, Kobayashi T (2024) Distribution and growth of Nga Myin Yinn, *Silonia silondia* (Actinopterygii: Siluriformes: Schilbeidae), in the Ayeyarwady River, Myanmar. Acta Ichthyologica et Piscatoria 54: 287–297. https://doi.org/10.3897/aiep.54.132489

Abstract

The silond catfish, *Silonia silondia* (Hamilton, 1822), known locally as Nga Myin Yinn, is rare in Myanmar fish markets and can fetch a high price. Efforts are being made to increase the production for domestic demand. We examined the distribution and growth of *S. silondia* based on catches in the Ayeyarwady River and growth records in fish farms near the river. The smaller fish were observed downstream near their nursery and the medium fish were around 1 m total length (TL) were often widespread, whereas the larger fish preferred upstream locations. Estimating the individual age from poorly defined periodic rings on the surface of otolith sections was difficult, but their microchemistry may reflect a shared nursery environment and subsequent migration throughout the entire river region. The growth curve estimates in the farmed population revealed a mean TL of 60 cm at four years, indicating that farmed fish were smaller than commercially captured wild fish. This is one of the first comprehensive studies of the river region, but more detailed surveys are needed to manage the fish resource sustainably.

Keywords

freshwater fisheries, growth, microchemistry, Myanmar, otolith, Silond catfish

---

[*] These authors contributed equally to this work.

Introduction

The silond catfish, *Silonia silondia* (Hamilton, 1822), is a large fish widely distributed in India, Pakistan, Bangladesh, Nepal, and Myanmar (Talwar and Jhingran 1991). It has been known to grow to a length of 183 cm in Nepal, while standard catch sizes are around 1 m (Gupta 2015; Flura et al. 2018; Froese and Pauly 2024). Along with several other catfish species, the silond catfish is a fishery species in the eastern tropical regions of Asia (Talwar and Jhingran 1991; Siddik et al. 2016; Baran et al. 2017). The academic records of this species date back 80 years (Hora 1938), but the known biology of the species is sparse compared with that of other catfish species. The lack of biological knowledge may have derived from the traits exhibited by this species, such as violent, predatory, and exclusive behavior. These traits make studying difficult. In almost all areas bar Myanmar where this species occurs, silond catfish is just one of many fishery species and is not considered outstanding in terms of harvest quantity and price.

The silond catfish, locally known as Nga Myin Yinn (Win et al. 2019), is one of the most economically important species, particularly in Myanmar (Soe et al. 2021). In the domestic market, its price is consistently higher than that of Pangasiidae catfish, a stable commodity from wild and aquaculture fisheries in Southeast Asia (Tran et al. 2019). An economic technology for the aquaculture of silond catfish has not yet been established, and the species is at risk of extinction in wild fisheries because of high fishing pressure over extended periods, resulting in a sharp decline in numbers (Gupta 2015). Therefore, the Myanmar government has regulated a restricted fishing season. In addition, an aquaculture development project has been implemented since 2017 with cooperation from several foreign countries, including Japan (unpublished results by the Department of Fisheries in Myanmar, in Burmese).

Despite being a valuable fish, biological information—such as its distribution, feeding habits, and life history over the past few decades—has been limited to India and Bangladesh (Hora 1938; Gupta 2015; Flura et al. 2018). Similar studies have recently been conducted in the Ayeyarwady River, Myanmar's longest river (Baran et al. 2017), and Soe et al. (2021) showed by mtDNA analysis that the population of *S. silondia* in the Ayeyarwady River is unstructured and singular. In addition, *S. silondia* occurs in India as a single population in every large river (Mandal et al. 2020). The simple genetic structure of *S. silondia* may be attributed to its high mobility, large body, and free migration. However, the inference is based solely on genetic information and has not been confirmed by ecological observations. The ecology of the sympatric Pangasius catfish in the Ayeyarwady is similarly unclear. However, the behavior of *Pangasius krempfi* Fang et Chaux, 1949 in the Mekong River has been observed using otolith microchemistry (Tran et al. 2019, 2021). The migration history of *P. krempfi* was determined by analyzing strontium, such that the concentration of total strontium and of its isotopes in otoliths were correlated with environmental distribution. In Southeast Asia, the aquaculture of several catfish has been successful through reliable knowledge of their biology, to the point that there is enough to support an export business. A similar expansion of ecological and biological knowledge to silond catfish will be essential to develop a food market with this species from both farmed and wild capture.

Our study focuses on silond catfish in the Ayeyarwady River, a target species for freshwater fisheries in Myanmar. The study aimed to gain a deeper understanding of the ecology of silond catfish in the river to support its successful fishery and aquaculture. Here, we present the results of a broad river distribution study based on specimens obtained from local markets and body size records obtained from fishermen. We have assessed biological information about *S. silondia*, such as migration history, by analyzing otolith microstructure and microchemistry. Additionally, we have presented data on the growth rates of fish from the aquaculture development project.

Materials and methods

Collection and measurement of wild fish. In the Ayeyarwady River (Fig. 1), *Silonia silondia* is occasionally captured using drift nets, which are gill nets that are either mobilized or semi-mobilized. Therefore, specimens for this study were available intermittently from August 2017 to September 2019 from fish markets in Yangon or directly from fishermen. While we could know the captured locations of all these specimens, a significant proportion had incomplete bodies after gutting. The other specimens were solely measured in retail fish markets because they were too rare and expensive to be purchased. The total length (TL) of all samples was measured to the nearest 0.1 cm. After samples were wiped with paper towels to remove excess water, their wet body weight (BW) was measured to the nearest 0.1 kg. In addition, TL and BW were measured by local fishermen in every fish market from April to September 2019 before shipping. The sex of each fish was determined by either morphometric characteristics or visual observation of the gonads. Several samples were of unknown sex because of unclear sexual characteristics.

The length–weight relationship was calculated using the allometric equation:

$$\mathrm{BW} = a\mathrm{TL}^{b}$$

where a and b are the regression parameters. The parameters a and b were estimated by linear regression analysis based on natural logarithms:

$$\log\mathrm{BW} = \log a + b\log\mathrm{TL}$$

In addition, the 95% confidence limits of a and b and the coefficient of determination (r^2) were estimated. Basic statistical analyses, analysis of variance (ANOVA), and analysis of covariance (ANCOVA) comparing allometric equations between sexes were all performed using R (R Core Team 2023).

Figure 1. The sampling sites of silond catfish, *Silonia silondia*, in the Ayeyarwady River in Myanmar. The site numbers on the map indicate the location of fishing areas shown in Table 1.

Otolith analysis. A previous age estimation of the channel catfish, *Ictalurus punctatus* (Rafinesque, 1818), was based on the lapilli otoliths—the largest otolith pairs (Long and Stewart 2010). Based on that study, the lapilli in the silond catfish were also examined in the presently reported study. These otoliths were available only from December 2017 to October 2018. After surface observations, otoliths were embedded in ultraviolet-cured resins (Strüssmann et al. 2020) in a round plastic mold and sectioned transversely (including the core) into around 0.7 mm-thick sections. Opaque ring data were determined by transmission light (BX53; Olympus, Tokyo, Japan) using imaging software (Cell Sens; Olympus).

Microchemical analysis was performed using an electron probe microanalyzer (JXA-8230; JEOL, Tokyo, Japan) described by Strüssmann et al. (2020). The otoliths were polished with 6- and 1-µm diamond paste (DP-Paste; Struers, Copenhagen, Denmark) to a mirror finish, and coated with platinum-palladium alloy using an ion sputter (E-1030, Hitachi High-Technologies). Strontium oxide and calcium oxide were used as standards. A line analysis was measured in a transect across the long axis of each otolith from the core to the edge at 3-µm intervals. The electron beam diameter was 2 µm, the accelerating voltage was 15 kV, and the probe current was 200 nA. For an area analysis, maps with a pixel size of 3 µm were generated with a focused beam at an accelerating voltage of 15 kV, a probe current of 500 nA, and a dwell time of 40 ms.

Growth of cultured fish. A technical report on cultured silond catfish provided reliable data on body sizes over cultured time in the developmental fish farm (unpublished results by the Department of Fisheries in Myanmar, in Burmese). The report includes measurements of the TL (nearest 0.5 inches = 1.27 cm) and wet BW (nearest 0.1 kg) of living silond catfish. Because the sexual characteristics of the gonads could not be observed, all living fish were of unknown sex. In addition, 30 fish—12 raised from December 2019 in the Talopehla Fish Farm and 18 fish raised from April 2023 in the Twantay Fish Farm—were captured from the culture ponds. The TL (nearest 0.01 cm) and BW (nearest 0.01 kg) of the fish were measured on 21 and 22 December 2023. The samples were similarly of unknown sex because of immature gonad development.

The von Bertalanffy growth model (von Bertalanffy 1938) was fitted to the observed TL over the rising period

$$\mathrm{TL}_t = \mathrm{TL}_\infty(1 - e^{-kt})$$

where t is the age, TL_∞ is the mean asymptotic TL, and k is the growth coefficient. The parameters were estimated by minimizing the total square of regression between observed and predicted lengths using the Solver function of Microsoft Excel. The cultured fish in Talopehla Fish Farm were all raised from larvae that were 1–4 inches (2.54–10.16 cm) in TL and caught in the Twantay canal (Fig. 1, Site 16) within February and May 2019. Thus, for the growth parameter estimation, we set the birth date of all cultured fish as 1 January 2019.

Ethical approval. Fish sampling was carried out in accordance with the guide for the care and use of laboratory animals from the Tokyo University of Marine Science and Technology. No live animals were used in the experiments performed for this study. All wild fish were procured from commercial catches.

Results

Biological characteristics of wild fish. The TL frequency distributions of *Silonia silondia* among the 356 fish collected and measured from the Ayeyarwady River ranged from 5.6 to 165.0 cm. The distribution had two modes: the most frequent TL mode was around 90 cm, and the more minor TL mode was around 15 cm (Fig. 2). The total length (TL) distributions among fishing sites (Table 1) were significantly different (ANOVA, $P < 0.001$): northern fish captured in the upper region (black or dark bars in Fig. 2) were larger than southern fish captured around the river mouth. Sex was determined in 313 specimens: 184 females (58.8%) and 129 males (41.2%). For males, the regression parameters a and b of the allometric equation

$$\mathrm{BW} = a\ \mathrm{TL}^{b}$$

and coefficients of determination (r^2) were 0.0051 (0.0035–0.0075; 95% confidence limits), 3.13 (3.05–3.22), and 0.93, respectively. For females, a, b, and r^2 were 0.019 (0.0011–0.0034), 2.87 (2.74–2.99), and 0.92, respectively. ANCOVA revealed significant differences between the sexes in the allometric equations ($F_{1,309} = 10.14$, $P = 0.0016$).

Table 1. Principal collection data of silond catfish, *Silonia silondia*, from five regions of the Ayeyarwady River, Myanmar.

Region	Site			*n*	Year	Sample size		
	No.	Name	Code			N_A	N_L	N_S
Mandalay	1	Mandalay	MML	65	2018, 2019	5	2	2
Sagaing	2	Myaung	MMU	1^*	2018			
Mandalay	3	Myingyan	MMG	23	2018, 2019	4	4	3
Magway	4	Pakokku	MPK	4	2017			
Mandalay	5	Nyaung U	MNU	3	2018			
Magway	6	Chauk	MCK	17	2018, 2019	5	3	3
	7	Ye Nan Chaung	MYC	21	2018, 2019	2	2	2
	8	Magway	MGY	30	2018	2		
	9	Aunglan	MAL	12	2018, 2019			
Ayeyarwady	10	Myanaung	MMA	10	2018	7	1	6
	11	Hinthada	MHD	18	2018, 2019	4		2
	12	Danuphyu	MDP	1^*	2018	1		
	13	Nyaungdon	MND	37	2017, 2018, 2019	9	1	8
	14	Pantanaw	MPN	11	2017, 2019	6	2	4
	15	Maubin	MMP	11	2018, 2019			
Yangon	16	Twantay	MTT	66	2017, 2018, 2019	11	7	6
Ayeyarwady	17	Wakema	MWM	25	2017			
	18	Mawgyun	MMK	1^*	2017			
Total				356		56	22	36

n = total number of collected fish and samples used in Fig. 2, N_A = number of samples used for visualized otolith ring analysis, N_L = number of samples used in Figs. 6, 7 for the transect line analysis of microchemistry (Sr/Ca), N_S = number of samples used in Fig. 9 for surface analysis of microchemistry (Sr/Ca). Site number (No.) is given in ascending order from upstream to downstream.

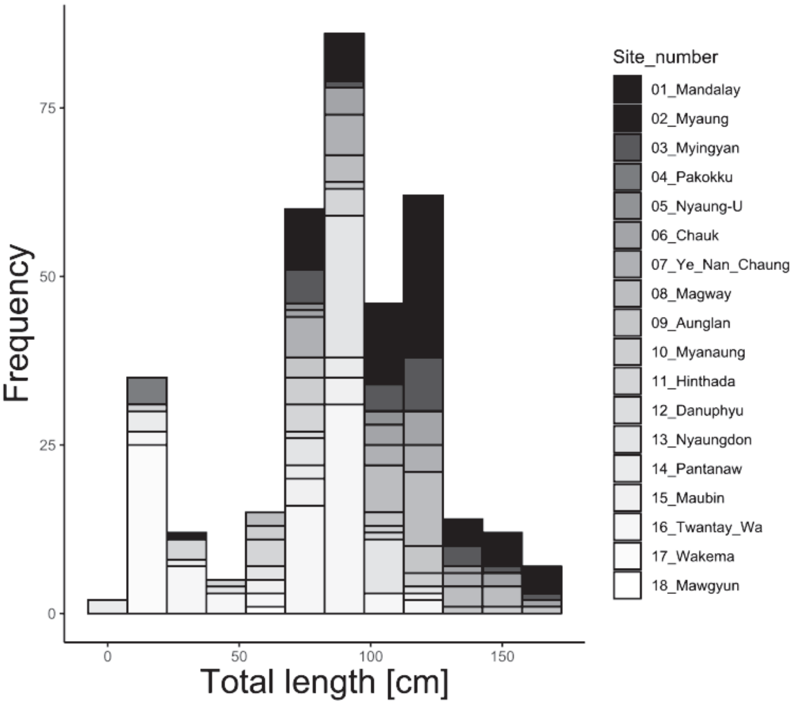

Figure 2. Total-length numerical frequency distributions of silond catfish, *Silonia silondia*, caught from August 2017 to December 2018 in the Ayeyarwady River, Myanmar. The northern and upstream sites show darker bars, while the southern and downstream regions show brighter bars. In the statistical analysis for TL distributions among sites in Fig. 2, one sample represented merged sites 2, 12, and 18 was combined as the northern nearest area, which were sites 1, 11, and 17, respectively, for statistical analysis (site numbers in the map of Fig. 1 and local names in Table 1).

Otolith visualized ring analysis. Lapilli otoliths were extracted from 56 specimens, ranging from 5.6 to 165.0 cm in TL. Not all annuli of otoliths were visible from surface observations. Sectioned otoliths had opaque and translucent zones formed alternately in several parts from the core to the edge, but these zones were unclear in other parts (Fig. 3). Opaque zones on the edges of otoliths could not be measured because of their lack of clarity. According to the classification of opaque types by Katayama (2018), the sectioned otoliths of the two smallest

Figure 3. Photograph of the sectioned otolith (long axis) of the largest female silond catfish, *Silonia silondia*, measured (TL = 165.0 cm) from the Ayeyarwady River, Myanmar. The sectioned sample was prepared using a different embedding material (cold-mounting epoxy resin) and polishing method than the other samples in this study. Scale bar: 2 mm.

fish (TL; 5.6 and 7.0 cm) had type A opaque cores and a translucent zone around the cores. While many areas on sections of larger fish were crystalline, opaque zones of type B or C groove aggregations or blurred black zones were present in several locations. It was difficult to discriminate between the types because of unclassified grooves or cuts and large opaque zones. Forty-three sectioned otoliths (but ignoring those in Fig. 3) were used to count the number of annuli, which were type B or C and opaque from the core to the edge. The other 13 otoliths could not be measured because of the crystallization of nearby zones or the collapse of the core area.

The largest and smallest radii from the core to the edge of the otolith sections were measured under the microscope. The radii ranged from 1348 to 6272 µm for the largest and from 296 to 1534 µm for the smallest. Both radii were significantly linearly correlated, and also significantly correlated with TL (Fig. 4). Counting of periodic rings on the otolith sections proved to be impossible for 14 out of the 43 otoliths. Rings in the remaining 29 otoliths were counted by five readers. The number of periodic rings counted on each otolith differed markedly between the readers, but the combined data were positively correlated with TL (Fig. 5). There was no agreement between all readers on the number of rings in all otoliths, but there were some otoliths for which two or three readers counted the same number of rings.

Microchemistry (Sr/Ca) on otolith sections. From 22 specimens collected at eight sites, otoliths with a detectable core in the sections (Table 1) were used for measuring Sr and Ca concentrations in the transects on the short axis. The Sr/Ca ratio varied greatly through the transect line, and trends differed between specimens (Figs. 6, 7). Individual Sr/Ca profiles illustrate the pattern for all specimens: a slightly higher Sr/Ca ratio near the center of the otolith (around 30 µm from the core) with a decrease before 500 or 600 µm (Figs. 6, 7). After the first decrease around the center, the Sr/Ca ratio exhibited many fluctuations. Some profiles displayed patterns, whereas others displayed no clear features. The Sr/Ca ratios of 10 beam points (30 µm) near the edge in each sample were compared (Fig. 8).

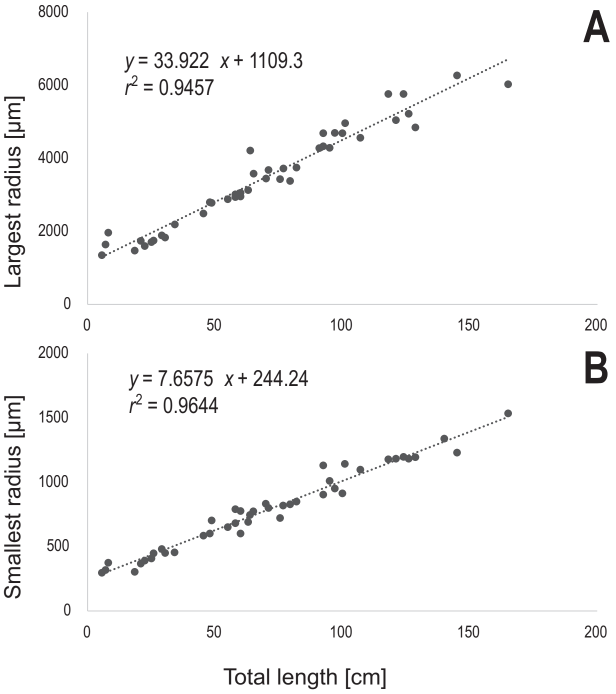

Figure 4. Relationships between TL and (**A**) largest radius and (**B**) smallest radius of silond catfish, *Silonia silondia*, from the Ayeyarwady River, Myanmar.

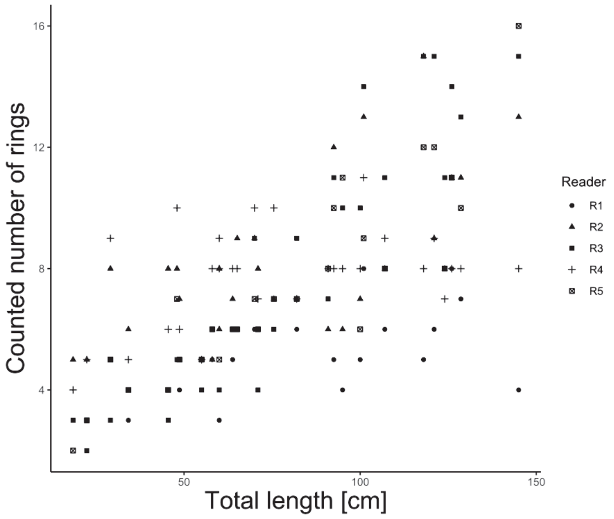

Figure 5. Bias plot with differences in number estimates between five ring readers of otoliths from silond catfish, *Silonia silondia*, from the Ayeyarwady River, Myanmar.

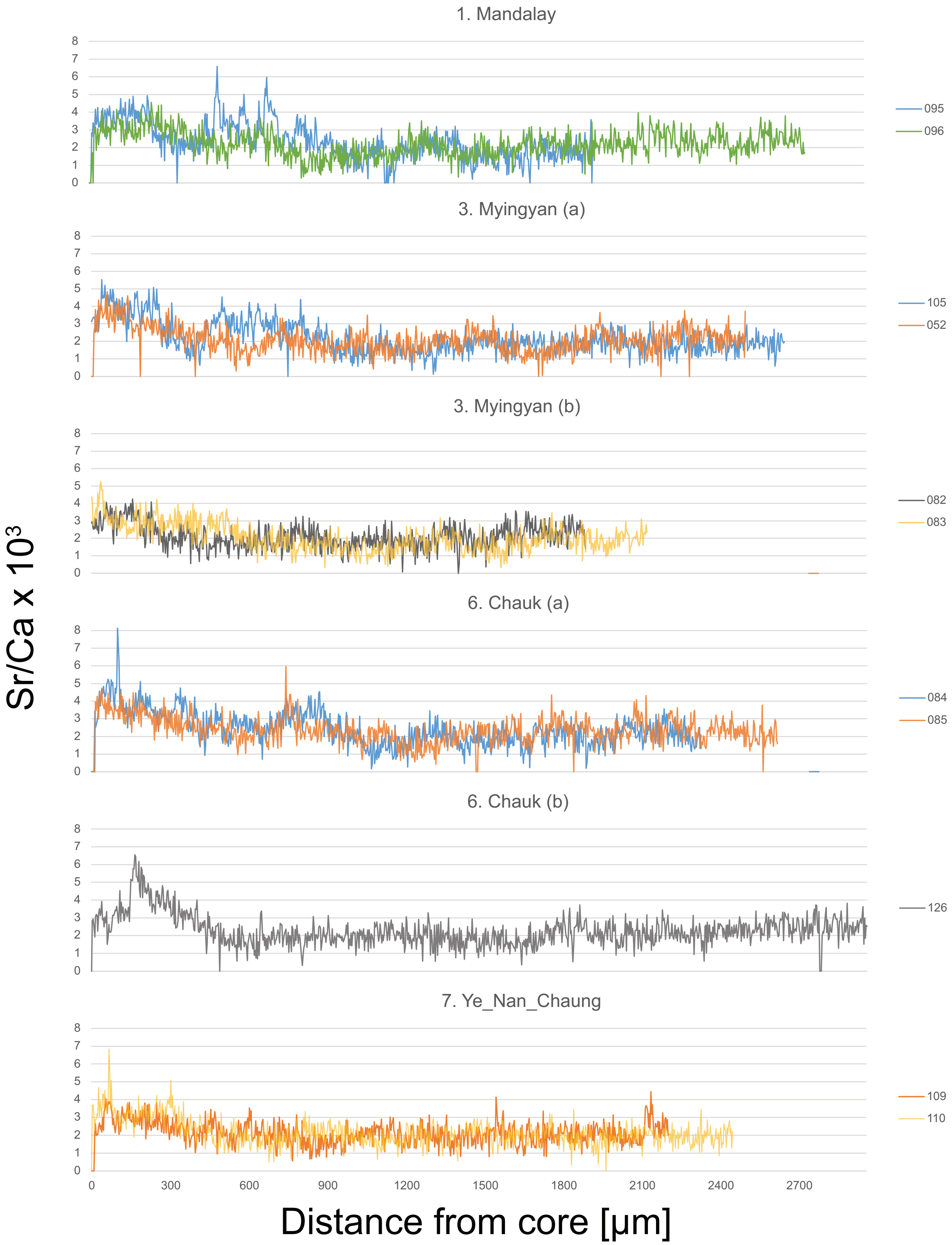

Figure 6. Individual Sr/Ca ratio profiles along an otolith transect of 21 silond catfish, *Silonia silondia*, from the Ayeyarwady River, Myanmar (Sites 1, 3, 6, and 7 in north region).

Although some significant differences between specimens were detected (Tukey's test, $P < 0.05$), no geographical trends in the distribution of sites in the river from north to south were observed. For the map analysis, we measured Sr and Ca concentrations on the section surface of otoliths from 36 specimens collected from nine sites (Table 1). There were some pixels with a Sr/Ca ratio greater than 15×10^{-3} in the surface analysis (Fig. 9), although none

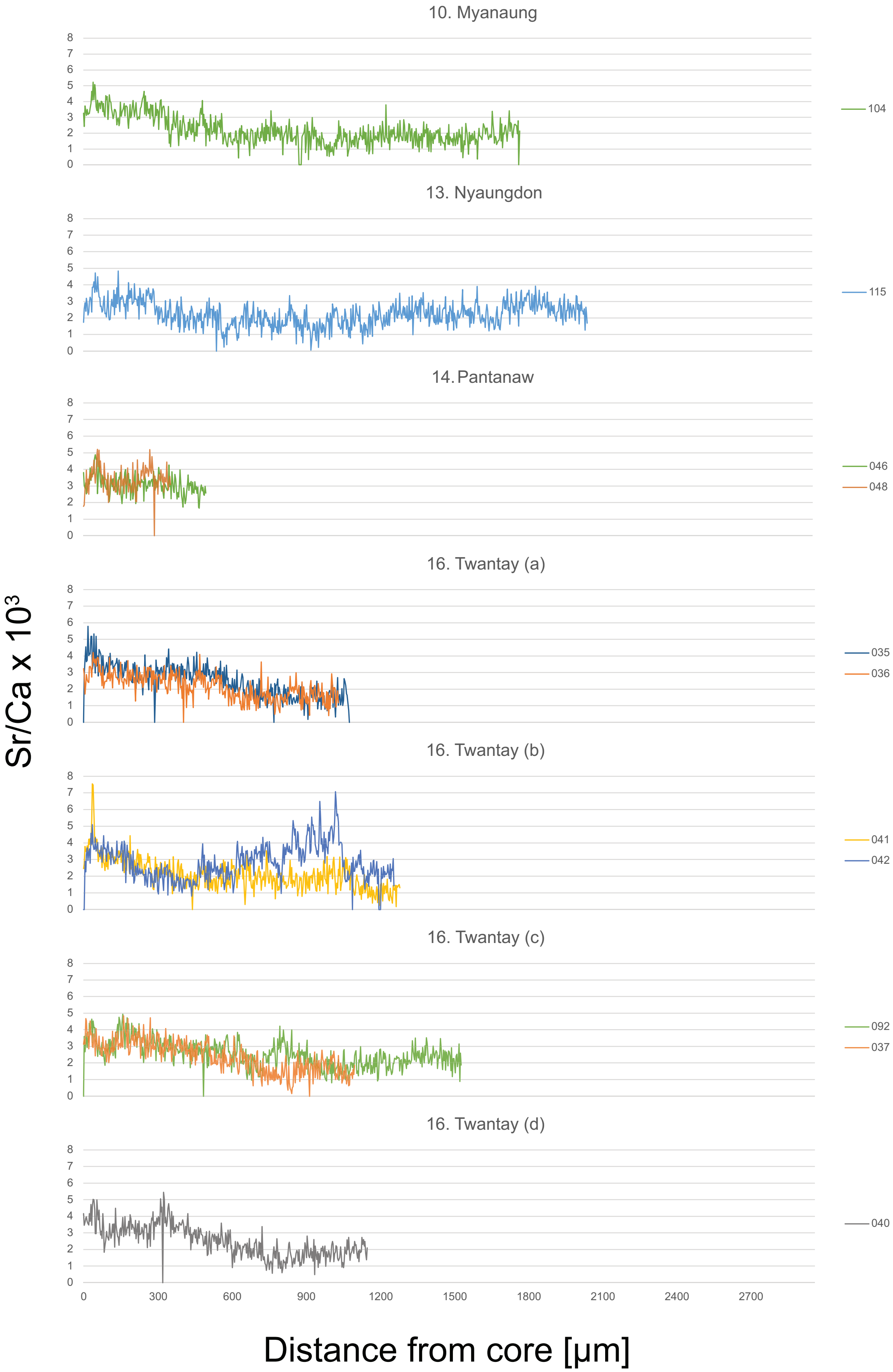

Figure 7. Individual Sr/Ca ratio profiles along an otolith transect of 21 silond catfish, *Silonia silondia*, from the Ayeyarwady River, Myanmar (sites 10, 13, 14, and 16 in south region).

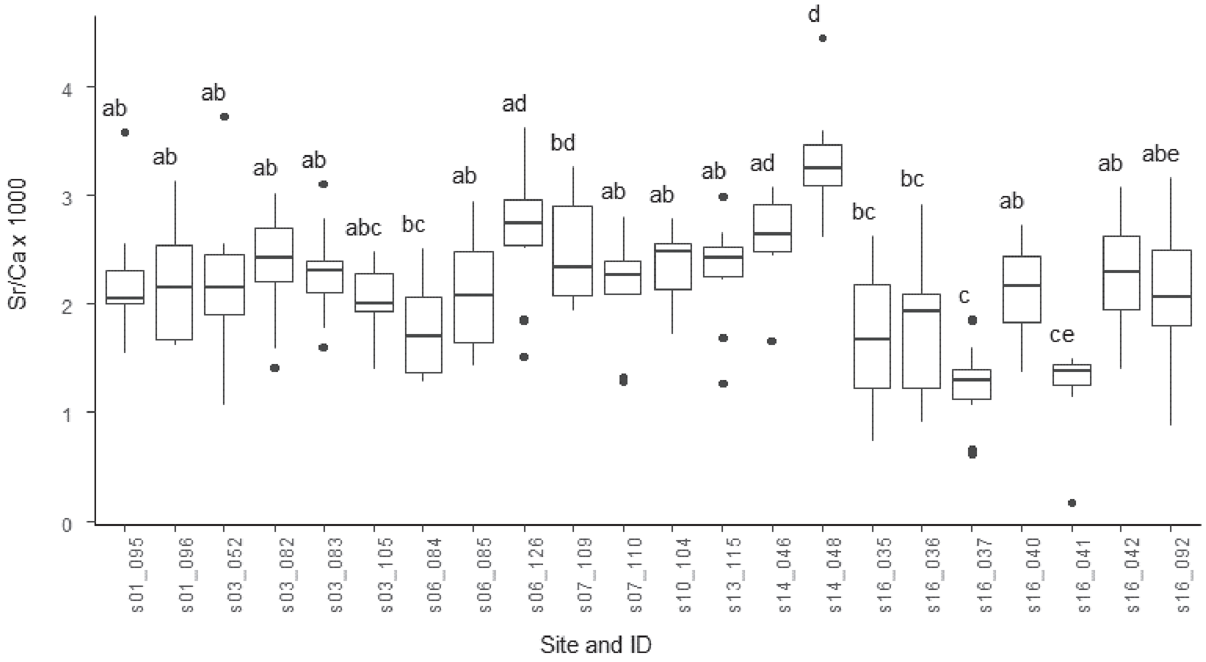

Figure 8. Boxplot of Sr/Ca ratio profiles from 10 measuring points on the otolith edge of the 21 silond catfish, *Silonia silondia*, from the Ayeyarwady River, Myanmar. The thick line in the middle of the box indicates the median. The upper and lower boundaries of the box indicate the 75th and 25th percentile lines, respectively. The bars extend to 1.5 times the box height above and below. Closed circle points outside these limits are plotted. Different letters indicate a statistically significant difference ($P < 0.05$). Two digits after "s" and three after "_" indicate the location number in Table 1 and the identification number, respectively.

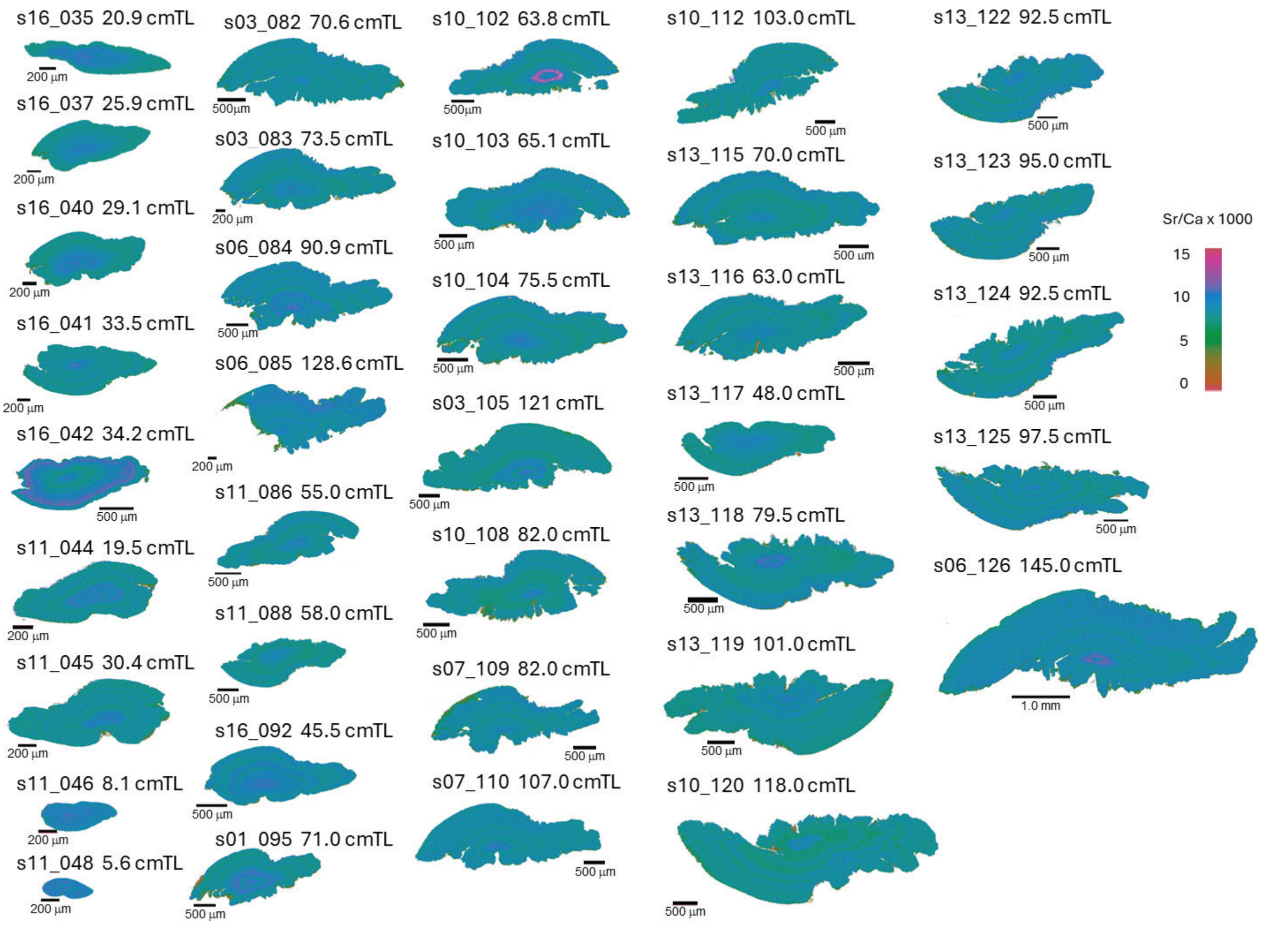

Figure 9. Results of the map analysis of the Sr/Ca ratio in the otoliths (short axis cuts) of the 36 silond catfish, *Silonia silondia*, from the Ayeyarwady River, Myanmar. Two digits after "s" and three after "_" indicate the site number in Table 1 and the identification number, respectively.

were observed in the transect line analysis (Figs. 6, 7). In most cases, the Sr/Ca ratios around the core pixels were relatively higher than those in other areas. Several pixels near the core had a high Sr/Ca ratio, around 10×10^{-3}, but the ratios decreased toward the edge, finally reaching a value of 5×10^{-3}. The periodic increase and decrease of Sr/Ca continued toward the edge of many samples. These periodicities are visible as circular rings on color plots.

Growth of cultured fish. The technical report of Talopehla Fish Farm describes the TL and BW of 114 live silond catfish collected from the ponds on 10 occasions between December 2019 and July 2023. The specimens ranged in size from 18.8 to 81.3 cm TL and BW from 0.05 to 3.5 kg. For specimens measured in December 2023, 12 4-year-oldfish from Talopehla had a TL range from 43.8–72.4 cm (mean = 50.8 cm) and a BW range of 0.33–3.27 kg (1.52 kg). From Twantay Fish Farm, 18 fish under 1 year old had a TL range of 13.8–17.5 cm (15.6 cm) and a BW range of 0.018–0.040 kg (0.028 kg). There were significant differences in TL and BW between 4- and 1-year-old fish ($P < 0.05$). When the TL and BW data from both data sources were combined, the regression parameters a and b of the allometric equation, along with their 95% confidence limits and r^2 values, were 0.0124 (0.0084–0.0184), 2.91 (2.81–3.03), and 0.952, respectively. ANOVA revealed significant allometric equations ($F_{1, 142} = 2810$, $P = 0.000$). The parameters in the growth model were $k = 0.250$ and $L_\infty = 90.3$ cm TL (Fig. 10).

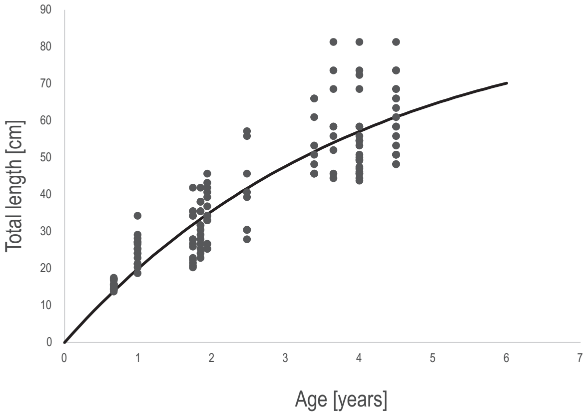

Figure 10. Von Bertalanffy curve of TL as a function of ages in silond catfish, *Silonia silondia*, from fish farm near the Ayeyarwady River, Myanmar.

Discussion

This study focused on several ecological aspects of silond catfish, *Silonia silondia*, in the Ayeyarwady River, such as size distribution in captured wild fish, migration history from otolith analysis, and somatic growth analysis using fish cultured records in the farms.

The size distribution in the total stretch of the river was determined from more than 300 captured individuals. The total length (TL) did not indicate distinct modes associated with age classes, but rather, reflected the migration characteristics of fishing sites in the river (Fig. 2). Thus, relatively larger and smaller fish lived in the upper region and downstream or estuary areas, respectively, while middle fish around 1 m TL appeared in almost every region in the river. The presently reported results suggest that the migration ability and habitat preference of silond catfish depend on body size. Almost all silond fish growing up to 1 m TL could migrate within the entire river drainage basin, whereas larger fish appeared to stay upstream or in the middle stretch.

Regarding the length–weight relationship, the estimated parameter b of the allometric equation was in an acceptable range, between 2.5 and 3.5 (Froese 2006). Our results suggest that the growth of males was positively allometric in the wild, whereas the growth of females was negative. The sexual differences in the allometric equation are likely to have a fundamental biological basis (Le Cren 1951). However, the differences in the b parameter can result from a combination of other factors such as habitat, area, seasonal effect, degree of stomach fullness, gonad maturity, health, preservation techniques, and differences in the observed length ranges of the captured specimens, none of which were considered in this study.

It was difficult to estimate the age of silond fish based on otolith despite the widespread application for many fish. Lapilli, the largest otolith of the fish, had many defects and cracks. Because of its cloudy white opaque state, the core and translucent zones could not be seen from the surface observation. On otolith sections by polishing a few millimeters around the core, periodic rings, like age traits, can be observed. However, it was impossible to distinguish whether periodic rings were real. The number of periodic rings counted from the core to the edge of the otolith section was highly variable among five experienced otolith-ring readers (Fig. 5). Thus, age estimation of this fish using otolith analysis was difficult. Future studies should focus on other hard tissues, such as the spine.

Periodic fluctuations in Sr concentration were observed in the otolith section through surface analysis by electron probe microanalysis. Although fluctuations in the Sr/Ca ratio were not discernible on the line analysis (see Figs. 6, 7), circulars with high Sr/Ca ratios appeared at frequent and some intervals on each otolith surface (see Fig. 9). The intervals of the ring zone exhibiting a high Sr/Ca ratio were unclear on many otolith surfaces. In addition, some circular zones with specific high Sr/Ca ratios, more than 15×10^{-3}, were observed in a few otoliths like s10_102 and s06_126 in Fig. 9. These results indicate that it is challenging to use these Sr/Ca ratio rings to estimate unstable movement between the river's different environments. Nonetheless, the surface analysis revealed a common feature of relatively higher Sr/Ca ratios around the core area. We consider these Sr/Ca ratios resulting from surface analysis may reflect the individual migration history of the adults after leaving any shared nursery area, where the environmental Sr concentration was relatively high. Adult silond catfish might exhibit solitary behavior and migrate freely throughout the entire river region. This inference is only preliminary due to the lack of microchemical information on the river's water quality. However, otolith chemistry remains a valuable tool for assessing water quality during deposition, making it particularly useful for studying migration profiles. Thus, the migration behavior of Pangasius catfish in the Mekong River was detected by Sr profiles on the otolith surface and detailed monitoring data of water quality in each region (Tran et al. 2019). Future microchemical studies might reveal more detailed behavior and habitat information of silond catfish.

Because the growth of wild fish could not be determined from otolith analysis, the growth of farmed fish was analyzed from aquaculture records over four years. The estimated total lengths of the growth curve were 55 cm TL at four years, 65 cm TL at five years, and 90.3 cm TL at infinite time. Whereas several farmed fish reached over 80 cm TL in four years, the maximum size did not even reach 1m TL, the most frequent size in wild specimens. The maximum recorded wild capture body length was 183 cm TL in Nepal (Gupta 2015), and specimens of 165 cm TL were captured in this study. However, we can be confident that fish over 1m TL must be at least 4 years old. The aquaculture results to date are a useful insight into the prolonged raising of this species.

To build on these results, it will be important to optimize the aquaculture environment. Arising from the primary objective of long-term fish growth, the farmed fish have been under significant physiological stress, including frequent transfers between ponds to avoid water pollution and spread of infectious diseases. Additionally, the ponds do not provide sufficient water flow and space because of the shallow pond depth. These conditions differ significantly from those in the wild and appear to have adversely affected growth.

This study has revealed several new aspects of silond biology and developed some new knowledge through the detailed analysis of otolith microstructure. Body sizes from the growing fish for four years have provided reliable information on growth under existing aquaculture conditions. The previous study by Soe et al. (2021) showed that the silond catfish in the Ayeyarwady River was an unstructured and single population. However, with both size distribution and somatic growth, this study revealed that almost all larval and younger fish stay around the downstream and estuary regions. After they grow over 60 cm TL, the fish would freely migrate to the upper side of the large river (Fig. 2). The results from the ecology and migratory behavior of the silond catfish in the river have provided useful information for developing conservation strategies and understanding the population dynamics of this vulnerable species.

Acknowledgments

This research was funded by the Heiwa Nakajima Foundation and the Japan International Corporation Agency (JICA). We are grateful to the members of the Ministry of Agriculture, Livestock and Irrigation, Department of Fisheries, Myanmar for their kind cooperation in collecting the samples and transferring them to Japan. We are grateful to the Rector and Prorectors at the University of Yangon for their support. We are also grateful to the editors and anonymous reviewers for their constructive comments and suggestions.

References

Baran E, Ko WK, Wah ZZ, New KM, Ghataure G, Soe KM (2017) Fisheries in the Ayeyarwady Basin. Ayeyarwady State of the Basin Assessment (SOBA) Report 4.1. National Water Resources Committee (NWRC), Myanmar. https://hdl.handle.net/20.500.12348/696

Flura M, Alam A, Hossain MRA (2018) A review on *Silonia silondia* (Hamilton, 1822) threatened fish of the world: (Siluriformes: Schilbeidae). Research in Agriculture Livestock and Fisheries 5(2): 235–240. https://doi.org/10.3329/ralf.v5i2.38113

Froese R (2006) Cube law, condition factor and weight–length relationships: History, meta-analysis and recommendations. Journal of Applied Ichthyology 22(4): 241–253. https://doi.org/10.1111/j.1439-0426.2006.00805.x

Froese R, Pauly D (Eds.) (2024) FishBase. [Version 04/2024] http://www.fishbase.org

Gupta S (2015) *Silonia silondia* (Hamilton 1822). A threatened fish of Indian Subcontinent. World Journal of Fish and Marine Sciences 7: 362–364. https://doi.org/10.4172/2155-9546.1000400

Hora SL (1938) The game fishes of India. IV. The silond catfish *Silonia silondia.* Journal of the Bombay Natural History Society 40: 137–147.

Katayama S (2018) A description of four types of otolith opaque zone. Fisheries Science 84(5): 735–745. https://doi.org/10.1007/s12562-018-1228-z

Le Cren ED (1951) The length–weight relationship and seasonal cycle in gonad weight and condition in the perch (*Perca fluviatilis*). Journal of Animal Ecology 20(2): 201–219. https://doi.org/10.2307/1540

Long JM, Stewart DR (2010) Verification of otolith identity used by fisheries scientists for aging channel catfish. Transactions of the American Fisheries Society 139(6): 1775–1779. https://doi.org/10.1577/T10-102.1

Mandal S, Singh A, Sah P, Singh RK, Kumar R, Lal KK, Mohindra V (2020) Genetic and morphological assessment of a vulnerable large catfish, *Silonia silondia* (Hamilton, 1822), in natural populations from India. Journal of Fish Biology 98(2): 430–444. https://doi.org/10.1111/jfb.14587

R Core Team (2023) R: A Language and Environment for Statistical Computing. R Foundation for Statistical Computing, Vienna, Austria. https://www.R-project.org/

Siddik MAB, Chaklader MR, Hanif MA, Islam MA, Fotedar R (2016) Length–weight relationships of four fish species from a coastal artisanal fishery, southern Bangladesh. Journal of Applied Ichthyology 32(6): 1300–1302. https://doi.org/10.1111/jai.13181

Soe TT, Thwe TL, Aye PT, Myint KT, Lwin TT, Thaung YW, Min AA, Mitsui S, Terahara T, Endo M, Yokota M, Rahman MM, Kobayashi T (2021) Population structure of Nga Myin Yinn *Silonia silondia* in the Ayeyarwady River, Myanmar, by mitochondrial DNA markers. Fisheries Science 87(3): 311–320. https://doi.org/10.1007/s12562-021-01499-5

Strüssmann CA, Miyoshi K, Mitsui S (2020) A novel, efficient method for otolith specimen preparation using UV-cured resins. North American Journal of Fisheries Management 40(5): 1187–1194. https://doi.org/10.1002/nafm.10484

Talwar PK, Jhingran AG (1991) Inland fishes of India and adjacent countries. Oxford and IBH Publishing Co., New Delhi, India.

Tran NT, Labonne M, Hoang HD, Panfili J (2019) Changes in environmental salinity during the life of *Pangasius krempfi* in the Mekong Delta (Vietnam) estimated from otolith Sr: Ca ratios. Marine and Freshwater Research 70(12): 1734–1746. https://doi.org/10.1071/MF18269

Tran NT, Labonne M, Chung M-T, Wang C-H, Huang K-F, Durand J-D, Grudpan C, Chan B, Hoang HD, Panfili J (2021) Natal origin and migration pathways of Mekong catfish (*Pangasius krempfi*) using strontium isotopes and trace element concentrations in environmental water and otoliths. PLoS One 16(6): e0252769. https://doi.org/10.1371/journal.pone.0252769

von Bertalanffy L (1938) A quantitative theory of organic growth (inquiries on growth laws II). Human Biology 10(2): 181–213.

Win S, Lwin YY, Aye MM, Htay SS, Win SS (2019) Fish species and fish products in Maubin township, Ayeyarwady Region, Myanmar. International Journal of Innovative Science and Research Technology 4(9): 20–23.